UNIVERSITY OF LIVERPOOL

Predicting and modifying response to neoadjuvant therapy in colorectal cancer

This thesis is submitted in accordance with the requirements of the University of Liverpool for the degree of Doctor in Philosophy

By

Paul Anthony Sutton

September 2015

Dedication

To my family. Without your love and support I would not be where I am today.

Declaration

The work presented in this thesis was carried out in the Institute of Translational Medicine, University of Liverpool and was undertaken while working as a research fellow at the Liverpool Cancer Research (UK) Centre. The material contained within this thesis has not been, nor is currently being presented wholly, or in part, for any other degree or qualification.

I declare that all the work presented in this thesis has been carried out by me except where indicated below:

- Cation exchange prior to iTRAQ analysis was performed by Mrs Jane Hamlett
- iTRAQ mass spectrometry was performed by Dr Roz Jenkins
- Assessment of radiological response was performed by Dr G Abbott
- Histopathological assessment of tumour response was performed by Dr M Terlizzo and Dr T Andrews
- Exome sequencing was performed at Genotypic Technology

Paul Sutton

Acknowledgments

I am indebted to the many people who have helped me over the last few years.

First and foremost my supervisors: Professor Dan Palmer, Dr Chris Goldring, Mr Hassan Malik and Mr Dale Vimalachandran. Thank you for your endless support, enthusiasm and patience as I attempted to make the transition from clinician to scientist.

I'd also like to thank my 'room-mate', Dr Neil Kitteringham, who provided endless advice and guidance as well as acting as a sounding board and telling me when I was wrong. I feel extremely lucky to have been trained by you.

One of the most challenging aspects of this work was the bioinformatics analysis, for which I am grateful for the time and assistance of Dr Puthen V Jithesh.

I am also grateful to all the staff in the Medical Research Council Centre for Drug Safety Science who assisted me in the acquisition of laboratory technique, in particular Dr Cliff Rowe and Dr Jo Henry.

The work presented in this thesis required the establishment of a regional network of colorectal surgeons to facilitate the recruitment of patients and collection of clinical samples. As such I am grateful to the following collaborators for their help and support:

Trust	**Principal Investigator**
Royal Liverpool and Broadgreen	Mr Paul Rooney
Aintree University Hospital	Mr Hassan Malik
Countess of Chester Hospital	Mr Dale Vimalachandran
Arrowe Park Hospital	Mr Ciaran Walsh
Clatterbridge Centre for Oncology	Professor Dan Palmer
Mid Cheshire Hospital (Leighton)	Mrs Caroline Bruce
St Helens and Knowsley Hospital	Mr Ajai Samad
Liverpool Heart and Chest Hospital	Mr Michael Shackcloth
Southport and Ormskirk	Mr Tarek Hany

East Cheshire Hospital	Mr Usman Khan
Royal Bolton Hospital	Mr David Smith
North Wales Health Board	Dr Simon Gollins
Warrington and Halton Hospital	Mr Mark Tighe

My fellow surgical trainees have also made the research process much easier, and I wish to thank Mr Rob Jones, Mr Jonathan Evans, Mr Derek McWhirter, Mr David Bowden and Mr Declan Dunne.

I am grateful to Professor John Neoptolemos both for his mentorship, and for affording me this opportunity.

Finally I wish to thank Cancer Research (UK) who funded me and this work.

Contents

Dedication i

Declaration ii

Acknowledgements iii

Contents v

Abstract vii

List of Tables viii

List of Figures xv

Abbreviations xxi

Chapter 1 – General Introduction **1**

1.1 Epidemiology of colorectal cancer 2
1.2 Risk factors for colorectal cancer 3
1.3 Genetics of colorectal cancer 3
1.4 Staging of colorectal cancer 9
1.5 Treatment of colorectal cancer with surgery 18
1.6 Treatment of colorectal cancer with radiotherapy 24
1.7 Chemotherapeutic agents used in colorectal cancer 29
1.8 Treatment of colorectal cancer with chemotherapy 35
1.9 Asssessment of response to chemoradiotherapy 43
1.10 Predictive and prognostic markers in colorectal cancer 49
1.11 Summary 58
1.12 Aims, hypotheses and study plan 59

Chapter 2 - Evaluation of a tissue stabilisation gel (Allprotect^{TM}) to facilitate clinical sampling for translational research in surgical trials **63**

2.1 Introduction 64
2.2 Methods 66
2.3 Results 71
2.4 Discussion 81

Chapter 3 - Exome sequencing of synchronously resected primary colorectal tumours and colorectal liver metastases to inform oncosurgical management **86**

3.1 Introduction 87
3.2 Methods 91
3.3 Results 96
3.4 Discussion 117

Chapter 4 - A global proteomic assessment of patient matched primary and metastatic colorectal tumours **126**

4.1 Introduction 127
4.2 Methods 131
4.3 Results 137
4.4 Discussion 168

Chapter 5 - A global proteomic assessment of serial rectal tumour biopsies **177**

5.1 Introduction 178
5.2 Methods 180
5.3 Results 184
5.4 Discussion 203

Chapter 6 – Targeted analysis of candidate biomarkers in the primary tumour for predicting response to neoadjuvant chemotherapy in colorectal liver metastases **208**

6.1 Introduction 209
6.2 Methods 212
6.3 Results 226
6.4 Discussion 251

Chapter 7 – Concluding Discussion **261**

7.1 Summary of aims and experimental design 262
7.2 Summary of results 263
7.3 Advances in the literature 267
7.4 Study limitations and further work 269
7.5 Review of hypotheses 270
7.6 Conclusions 271

Bibliography 273

Appendix 1 - Lists of single nucleotide variants from exome sequencing 299

Appendix 2 - Genetic variants in colorectal cancer identified by next generation sequencing studies 329

Appendix 3 - Proteomic comparison of metastatic tumour and normal adjacent liver parenchyma 337

Appendix 4 - Proteomic comparison of responders and non-responders in the primary tumour 353

Appendix 5 - Supporting Publications, Presentations, Prizes and Grants 361

Abstract

Background Colorectal cancer is the fourth commonest cancer in the UK, and the second commonest cause of cancer-related death. A knowledge of the biology of colorectal liver metastases would be invaluable to inform clinical decision making; however, deriving this information from the metastatic lesions is not feasible until after resection. We aimed to use proteomic and genomic analysis to establish the degree of biological similarity across disease sites and identify biomarkers in the primary tumour which predict response to neoadjuvant chemotherapy in liver metastases. An identical approach was also used to identify predictors of response to neoadjuvant chemoradiotherapy in rectal cancer.

Methods Fresh tissue from both primary colorectal tumour and liver metastases from 16 patients was subjected to proteomic analysis using isobaric tagging for relative quantification (iTRAQ). Data were analysed with Protein Pilot (Ab Sciex, Framingham, MA, USA), with stratification of patients into those showing low or high response to chemotherapy permitting the identification of potential predictive biomarkers. These markers were subsequently investigated by immunohistochemistry on a tissue microarray of 56 patients, in parallel with a series of *in vitro* studies to investigate the concordance between primary and metastatic tumours of those proteins relevant to the activation and metabolism of 5-FU, irinotecan and oxaliplatin. The therapeutic potential of the identified biomarkers was also investigated by dosing SW480 cells with irinotecan/5FU with or without inhibition (using siRNA or a known competitive inhibitor) of the proteins of interest. Four of the 16 patients studied were resected synchronously, and tissue from these was also used for exome sequencing using the Ion Proton platform. Diagnostic, post-treatment and resection biopsies from 8 patients with rectal cancer were again subjected to iTRAQ with stratification into low or high response to neoadjuvant chemoradiotherapy to investigate potential response biomarkers.

Findings We identified 5766 discrete proteins, of which 2.54% were differentially expressed between primary and metastatic tumours. There were 170 potential response biomarkers in the primary tumour and 27 in the metastases. Two proteins were common to both tissue types and showed consistent dysregulation, including NQO1. Immunostaining of NQ01 in metastases revealed lower expression in patients responding to chemotherapy ($p=0.041$), with a significant correlation between primary and metastatic disease sites ($r=0.44$, $p=0.001$). Knockdown of NQO1 followed by treatment with irinotecan and 5FU reduced the IC50 from 100.1μM to 49.8μM and from 200.1μM to 25.0μM respectively. Pre-treating cells with dicoumarol prior to incubation in irinotecan and 5FU reduced the IC50 from 100.0μM to 50.0μM and from 183.7μM to 49.9μM respectively. Exome sequencing identified 585 non-synonymous missense SNVs of which 215 (36.8%) were unique to the primary tumour, 226 (38.6%) unique to the metastasis and 81 (13.8%) present in patient matched pairs. Aberrations in the ErbB pathway were identified in paired samples (ratio 0.07, $p=5.87\times10^{-7}$), which were validated by Sanger sequencing along with a potential response biomarker in the *CDAN1* gene. Changes to the phenotype of the rectal tumour with chemoradiotherapy were modest, although it is clear that base excision repair (and in particular PARP1) remains of interest, and that acid ceramidase is a potential response biomarker and novel radiosensitiser.

Interpretation Proteomic sequencing of matched metastatic colorectal cancer samples is feasible with high coverage. The high degree of similarity between the primary and secondary tumours suggests that the primary tissue is predictive of the metastatic phenotype. NQO1 expression in the primary tumour predicts response to neoadjuvant chemotherapy in the liver metastases, and inhibition of this protein at both genetic and functional levels improves chemosensitivity.

List of Tables

Table	Legend	Page
1.1	Percentage of cases and 5 year relative survival (%) by Dukes' stage at diagnosis for colorectal cancer patients diagnosed 1996-2002 in England. (Reproduced without permission from Cancer Research (UK)).	2
1.2	Genetics of inherited colorectal tumour syndromes. (Reproduced without permission from Fearon, 2011).	4
1.3	Summary of evidence highlighting complications from percutaneous needle biopsy of colorectal liver metastases. (Reproduced without permission from Cresswell, Welsh and Rees, 2009).	13
1.4	UICC/AJCC TNM staging of colorectal cancer; 7th edition (2010). Available online at https://cancerstaging.org/references-tools/quickreferences/Pages/default.aspx	15
1.5	UICC/AJCC stage groupings for colorectal cancer; 7th edition (2010). Available online at https://cancerstaging.org/references-tools/quickreferences/Pages/default.aspx.	16
1.6	The Jass classification combines a number of patient, histopathological and genetic factors to allocate tumours to a group (1-5). MSI, microsatellite instability; H, high; S, stable; L, low; Dip, diploid; An, aneuploid; Serration, serrated morphology; SP, serrated polyp; AD, adenoma; Circumscribed, circumscribed invasive margin. Reproduced without permission from Jass, 2007.	17
1.7	Summary of recent evidence pertaining to the synchronous management of liver limited metastatic colorectal cancer. Reproduced with permission from Lykoudis *et al* (2014). References: *Martin et al; J Am Coll Surg (2003); 197; 233-241, Chua et al; Dis Colon Rectum (2004); 47; 1310-1316, Capussotti et al; Ann Surg Oncol (2007); 14; 195-201, Capussotti et al, Ann Surg Oncol (2007); 14; 1143-1150, Reddy et al; Ann Surg Oncol (2007); 14; 3481-3491, Thelen et al; Int J Colorectal Dis (2007); 14; 3481-3491, Turrini et al; Eur J Surg Oncol (2007); 33; 735-740, Vassiliou et al; World J Gastroenterol (2007); 13; 1431-1434, Martin et al; J Am Coll Surg (2009); 208; 842-850, Slupski et al; Can J Surg (2009); 52; E241-E244, Brouquet et al, J Am Coll Surg (2010); 210; 934-941, de Haas et al; Br J Surg (2010); 97; 1279-1289, Luo et al; J Gastrointest Surg (2010); 14; 1974-1980, Moug et al; Eur J Surg Oncol (2010); 36; 365-370, Mayo et al; J Am Coll Surg (2013); 216; 707-716.*	23
1.8	The tumour regression grade proposed by Dworak, Keilholz and Hoffmann (1997) extends from 0-4 and includes an assessment of tumour mass as well as the degree of fibrosis and/or vasculopathy. Reproduced without permission from Santos *et al*, 2014.	46
1.9	The Basingstoke Prognostic Index allocates a score (out of 30) based on a number of clinicopathological features. Validated for use in both the pre- and post-operative situations, the score correlates well with outcome.	51
1.10	Prognostic biomarkers identified for colorectal cancer. The table demonstrates the frequency with which these biomarkers are identified, the evidence for its correlation with prognosis and its uptake into routine clinical practice. Reproduced without permission from Pritchard and Grady, 2011.	55
1.11	Predictive biomarkers identified for colorectal cancer. The table demonstrates the frequency with which these biomarkers are identified,	56

	the evidence for its correlation with response to treatment and its uptake into routine clinical practice. EGFR, epidermal growth factor receptor; 5-FU, 5- fluorouracil; LOH, loss of heterozygosity. Reproduced without permission from Pritchard and Grady, 2011.	
2.1	Representative results following DNA extraction from patient 2 (primary tumour). Comparable quality control indices are seen highlighting the suitability of extracted DNA for downstream qPCR analysis. Comparable results following *KRAS* genotyping are seen: the patient is *KRAS* mutant at codon 12 but wild type at codons 13 and 61.	73
3.1	Demographic and clinical features of the four patients from whom tumours were sequenced. IrMdG – Irinotecan and modified de Gramont (5-fluoruracil and folinic acid).	96
3.2	Quality control data from samples undergoing exome sequencing with Ion Proton. Sample ID column identifies samples as follows: SO_2510 relates to project id; 1-4 relate to patient number; A-D relate to tissue type (A – colonic mucosa, B – primary tumour, C – liver parenchyma, D – liver metastasis). All quality control variables and yield were good, with the exception of the colonic mucosa from patient 4. DNA was suboptimal but still adequate for sequencing.	97
3.3	Total number of raw reads through Ion Proton exome sequencing.	98
3.4	Sequencing statistics for all samples. Sample ID (column 1) 1-4 relates to patient number, and A-D tissue type (A: normal mucosa, B: colorectal primary tumour, C: normal liver parenchyma, D: liver metastasis). The report attests to a high number of reads successfully on target, a 1x coverage of 96.58 – 98.07% and 20x coverage of 67.61 – 88.33% of the targeted exome.	99
3.5	Total number of high quality variants identified through Ion Proton exome sequencing.	100
3.6	Total number of somatic, non-synonymous, missense, biologically deleterious SNVs identified in each of the tumour samples.	101
3.7	Pathway analysis for SNVs unique to the primary tumours. P-value is adjusted using Benjamini-Hochberg correction. Ratio identifies the number of focus genes identified (numerator) in the pathway (denominator).	101
3.8	Network analysis for SNVs unique to the primary tumours. The score is derived from a p-value and indicates the probability of the focus genes in a network being found together due to random chance. Focus molecules is the total number of SNVs of interest identified in the respective network.	103
3.9	Pathway analysis for SNVs unique to the metastatic tumours. P-value is adjusted using Benjamini-Hochberg correction. Ratio identifies the number of focus genes identified (numerator) in the pathway (denominator).	103
3.10	Network analysis for SNVs unique to the metastatic tumours. The score is derived from a p-value and indicates the probability of the focus genes in a network being found together due to random chance. Focus molecules is the total number of SNVs of interest identified in the respective network.	105
3.11	Pathway analysis for SNVs present in at least one primary and metastatic tumour pertaining to the same patient. P-value is adjusted using Benjamini-Hochberg correction. Ratio identifies the number of focus genes identified (numerator) in the pathway (denominator).	106
3.12	Network analysis for SNVs present in at least one primary and metastatic tumour pertaining to the same patient. The score is derived from a p-value and indicates the probability of the focus genes in a network being found	108

	together due to random chance. Focus molecules is the total number of SNVs of interest identified in the respective network.	
3.13	Pathway analysis for SNVs unique to the responding tumours. P-value is adjusted using Benjamini-Hochberg correction. Ratio identifies the number of focus genes identified (numerator) in the pathway (denominator)	109
3.14	Network analysis for SNVs unique to the responding tumours. The score is derived from a p-value and indicates the probability of the focus genes in a network being found together due to random chance. Focus molecules is the total number of SNVs of interest identified in the respective network.	110
3.15	Pathway analysis for SNVs unique to the non-responding tumours. P-value is adjusted using Benjamini-Hochberg correction. Ratio identifies the number of focus genes identified (numerator) in the pathway (denominator).	111
3.16	Network analysis for SNVs unique to the non-responding tumours. The score is derived from a p-value and indicates the probability of the focus genes in a network being found together due to random chance. Focus molecules is the total number of SNVs of interest identified in the respective network.	113
3.17	Those SNVs identified for validation with Sanger sequencing.	114
3.18	Summary of the Sanger sequencing for 12 SNVs of interest in 8 samples (matched primary and metastatic tumours from 4 patients). The fields displayed in red highlight the location of SNVs identified through Ion Proton sequencing, with the content of the fields representing the identified base(s) on Sanger sequencing. Those marked undetermined failed due to inability to detect the amplicon.	115
3.19	Summary of next generation sequencing papers published on colorectal cancer.	120
3.20	Some of the ErbB inhibitors currently in clinical use (only ones approved by the Federal Drug Administration are shown). Adapted from Roskoski, 2004.	122
4.1	Clinical, demographic and disease characteristics of the 16 patients recruited to this study. Eleven patients underwent neoadjuvant chemotherapy, the remainder proceeding straight to surgery. Six patients were simultaneously resected. There was considerable variation in location of the primary tumour, disease stage and grade as well as metastatic burden.	139
4.2	Details of neoadjuvant chemotherapy agents and response evaluation. Five patients were chemonaive and 11 underwent neoadjuvant treatment. One of these patients failed to undergo resection of the liver metastasis. Response evaluation data is therefore available for 10 patients, 5 of which had a tumour regression grade of 1-2 (responders) with the remaining 5 having a tumour regression grade of 3-4 (non-responders).	140
4.3	Those proteins differentially expressed between the primary tumour and normal colorectal mucosa. 25 proteins were identified, 6 of which were upregulated (positive values for fold change) and 19 downregulated (negative values for fold change).	142
4.4	Pathway analysis for proteins both upregulated and downregulated in the primary tumour when compared to normal adjacent colorectal mucosa. P-value is adjusted using Benjamini-Hochberg correction. Ratio identifies the number of focus molecules identified (numerator) in the pathway (denominator).	143
4.5	Network analysis for proteins both upregulated and downregulated in the	144

	primary tumour when compared to normal adjacent colorectal mucosa. The score is derived from a p-value and indicates the probability of the focus molecules in a network being found together due to random chance. Focus molecules is the total number of proteins of interest identified in the respective network.	
4.6	Those proteins differentially expressed between the metastatic tumour and normal colorectal mucosa. 53 proteins were identified, 13 of which were upregulated (positive values for fold change) and 40 downregulated (negative values for fold change).	147
4.7	Pathway analysis for proteins both upregulated and downregulated in the metastatic tumour when compared to normal adjacent colorectal mucosa. P-value is adjusted using Benjamini-Hochberg correction. Ratio identifies the number of focus molecules identified (numerator) in the pathway (denominator).	147
4.8	Network analysis for proteins both upregulated and downregulated in the metastatic tumour when compared to normal adjacent colorectal mucosa. The score is derived from a p-value and indicates the probability of the focus molecules in a network being found together due to random chance. Focus molecules is the total number of proteins of interest identified in the respective network.	149
4.9	Pathway analysis for proteins both upregulated and downregulated in the metastatic tumour when compared to normal adjacent colorectal mucosa. P-value is adjusted using Benjamini-Hochberg correction. Ratio identifies the number of focus molecules identified (numerator) in the pathway (denominator).	150
4.10	Network analysis for proteins both upregulated and downregulated in the metastatic tumour when compared to normal adjacent liver parenchyma. The score is derived from a p-value and indicates the probability of the focus molecules in a network being found together due to random chance. Focus molecules is the total number of proteins of interest identified in the respective network.	154
4.11	Those proteins differentially expressed between the metastatic tumour and the primary tumour. 67 proteins were identified, 58 of which were upregulated (positive values for fold change) and 9 downregulated (negative values for fold change).	156
4.12	Pathway analysis for proteins both upregulated and downregulated in the metastatic tumour when compared to the primary tumour. P-value is adjusted using Benjamini-Hochberg correction. Ratio identifies the number of focus molecules identified (numerator) in the pathway (denominator).	157
4.13	Network analysis for proteins both upregulated and downregulated in the metastatic tumour when compared to the primary tumour. The score is derived from a p-value and indicates the probability of the focus molecules in a network being found together due to random chance. Focus molecules is the total number of proteins of interest identified in the respective network.	158
4.14	Pathway analysis for proteins both upregulated and downregulated in the primary tumours of the responders compared to the primary tumours of the non responders. P-value is adjusted using Benjamini-Hochberg correction. Ratio identifies the number of focus molecules identified (numerator) in the pathway (denominator).	159
4.15	Network analysis for proteins both upregulated and downregulated in the	161

	primary tumours of the responders compared to the primary tumours of the non responders. The score is derived from a p-value and indicates the probability of the focus molecules in a network being found together due to random chance. Focus molecules is the total number of proteins of interest identified in the respective network	
4.16	Those proteins differentially expressed between the metastatic tumours of the responders and non-responders. 27 proteins were identified, 17 of which were upregulated (positive values for fold change) and 10 downregulated (negative values for fold change).	163
4.17	Pathway analysis for proteins both upregulated and downregulated in the metastatic tumours of the responders compared to the metastatic tumours of the non responders. P-value is adjusted using Benjamini-Hochberg correction. Ratio identifies the number of focus molecules identified (numerator) in the pathway (denominator).	164
4.18	Network analysis for proteins both upregulated and downregulated in the metastatic tumours of the responders compared to the metastatic tumours of the non responders. The score is derived from a p-value and indicates the probability of the focus molecules in a network being found together due to random chance. Focus molecules is the total number of proteins of interest identified in the respective network.	165
4.19	Summary of predictive biomarkers common to both primary and metastatic tumours.	167
4.20	Summary proteomic data for the 2-group comparisons showing the total number of dysregulated proteins as well as those up/downregulated.	168
5.1	Response evaluation for patients having serial rectal cancer biopsies. The percentage viable tumour is displayed along with corresponding tumour regression grade (TRG). Those patients with TRG 1-2 were considered responders (patients 1, 2, 4 and 6) and patients with TRG 3-4 were considered non-responders (patients 3, 5, 7 and 8).	185
5.2	Clinical and demographic data for patients having serial rectal cancer biopsies. 8 patients were studied, all of which were male ranging in age from 50-78 and Dukes' stage B-D. Two different neoadjuvant chemotherapeutic regimens were used alongside a number of different surgical interventions for formal resection of the rectal tumour	184
5.3	Those proteins differentially expressed between rectal tumours post chemoradiotherapy and diagnostic samples. 18 proteins were identified, 2 of which were downregulated (negative values for fold change) and 16 upregulated (positive values for fold change).	187
5.4	Pathway analysis for proteins both upregulated and downregulated in the rectal tumours post chemoradiotherapy compared to the diagnostic samples. P-value is adjusted using Benjamini-Hochberg correction. Ratio identifies the number of focus molecules identified (numerator) in the pathway (denominator).	188
5.5	Network analysis for proteins both upregulated and downregulated in the rectal tumours post chemoradiotherapy compared to the diagnostic samples. The score is derived from a p-value and indicates the probability of the focus molecules in a network being found together due to random chance. Focus molecules is the total number of proteins of interest identified in the respective network.	189
5.6	Those proteins differentially expressed between rectal tumours at resection and immediately following completion of chemoradiotherapy. 39	191

	proteins were identified, 30 of which were downregulated (negative values for fold change) and 9 upregulated (positive values for fold change).	
5.7	Pathway analysis for proteins both upregulated and downregulated in the rectal tumours at resection compared to immediately following completion of chemoradiotherapy. P-value is adjusted using Benjamini-Hochberg correction. Ratio identifies the number of focus molecules identified (numerator) in the pathway (denominator).	192
5.8	Network analysis for proteins both upregulated and downregulated in the rectal tumours at resection compared to immediately following completion of chemoradiotherapy. The score is derived from a p-value and indicates the probability of the focus molecules in a network being found together due to random chance. Focus molecules is the total number of proteins of interest identified in the respective network.	193
5.9	Those proteins differentially expressed between rectal tumours at resection and at diagnosis. 29 proteins were identified, 10 of which were downregulated (negative values for fold change) and 19 upregulated (positive values for fold change).	195
5.10	Pathway analysis for proteins both upregulated and downregulated in the rectal tumours at resection compared to at diagnosis. P-value is adjusted using Benjamini-Hochberg correction. Ratio identifies the number of focus molecules identified (numerator) in the pathway (denominator).	195
5.11	Network analysis for proteins both upregulated and downregulated in the rectal tumours at resection compared to at diagnosis. The score is derived from a p-value and indicates the probability of the focus molecules in a network being found together due to random chance. Focus molecules is the total number of proteins of interest identified in the respective network.	198
5.12	Those proteins differentially expressed between the primary tumours of the responders and non-responders. 8 proteins were identified, 3 of which were downregulated (negative values for fold change) and 5 upregulated (positive values for fold change).	199
5.13	Pathway analysis for proteins both upregulated and downregulated in the primary tumours of the responders compared to the primary tumours of the non-responders. P-value is adjusted using Benjamini-Hochberg correction. Ratio identifies the number of focus molecules identified (numerator) in the pathway (denominator).	200
5.14	Network analysis for proteins both upregulated and downregulated in the primary tumours of the responders compared to the primary tumours of the non-responders. The score is derived from a p-value and indicates the probability of the focus molecules in a network being found together due to random chance. Focus molecules is the total number of proteins of interest identified in the respective network.	202
5.15	Summary proteomic data for the 2-group comparisons showing the total number of dysregulated proteins as well as those up/downregulated.	203
6.1	Antibody incubation conditions for the proteins of interest with respect to the activation and metabolism of chemotherapeutics.	213
6.2	Preparation of standard controls for mass spectrometry analysis of irinotecan conversion to SN-38 by human CES1/CES2.	214
6.3	Median densitometry values for thymidylate synthase (TS), dihydropyrimidine dehydrogenase (DPYD) and orotate phosphorisobysltransferase (OPRT) expression in patient matched primary	228

	and metastatic tumours. Correlation co-efficients (with Spearman's rank test) showed positive correlations although these did not reach statistical significance.	
6.4	Median densitometry values for carboxylesterase 1 (CES1), carboxylesterase 2 (CES2), topoisomerase I (TOP I), UDP glucuronosyltransferase 1A1 (UGT1A1) and cytochrome P450 3A4 (CYP3A4) expression in patient matched primary and metastatic tumours. Correlation co-efficients (with Spearman's rank test) showed positive correlations, reaching statistical significance in the case of TOP I.	232
6.5	SN38 production in patient matched primary tumour, liver metastasis and liver parenchyma. Of the 12 patients studied there were significant differences between tissue types (by ANOVA) in all except two (highlighted in red). When specifically comparing the primary and metastatic tumours, significant differences (by student's paired t-test) were seen in all except four (also highlighted in red).	235
6.6	*KRAS* (codon 12, 13 and 61), *BRAF* (codon 600 and 601) and microsatellite instability analysis for 16 patients undergoing resection at both sites for liver limited stage IV colorectal cancer. Five patients had *KRAS* codon 12 mutation, one patient had *BRAF* 600/601 mutation and one patient was MSI-Low.	237
6.7	Key clinical and pathological variables in the chemo-naive, responders and non-responders. Continuous data was assessed for significance using ANOVA* and categorical data using the X^2 test$^{\#}$. Only T stage was considerably different between groups, with a greater proportion of T4 tumours in the chemo-naive group.	239
6.8	NQO1 expression in the responders and non-responders grouped by percentage of positively stained cells. No statistically significant difference was observed in the primary tumours (p=0.470) however in the metastases, NQO1 staining is considerably higher in the non-responders compared to the responders (p=0.041, X^2 test).	241

List of Figures

Figure	Legend	Page
1.1	Suggested genetic model for colorectal cancer. In (a) a number of hereditary and sporadic mutations drive the transformation of normal epithelia to an adenomatous lesion and latterly carcinoma. In (b) an inherited or acquired defect in DNA mismatch repair (MMR) function is the initiator for carcinogenesis. (Adapted from Fearon, 2011).	9
1.2	Invasive colonic adenocarcinoma penetrating the muscularis mucosa; stained with haematoxylin and eosin. Photomicrograph taken at x200 magnification.	12
1.3	5-Fluorouracil metabolism – 5-fluorouracil (F-FU) is converted to three main metabolites: fluorodeoxyuridine monophosphate (F-dUMP), fluorodeoxyuridine triphosphate (FUTP) and fluorouridine triphosphate (FUTP). The main mechanism of 5-FU activation is conversion to fluorouridine monophosphate (FUMP) by orotate phosphoribosyltransferase (OPRT). FUMP is then phosphorylated to fluorouridine disphoaphate (FUDP) and again to fluorouridine triphosphate (FUTP). Alternatively, thymidine phosphorylase (TP) can activate 5-FU by catalysing the conversion of 5-FU to fluorodeoxyuridine (FUDR) which is then phosphorylated by thymidine kinase (TK) to FdUMP. FdUMP can be phosphorylated to fluorodeoxyuridine diphosphate (FdUDP) and again to fluorodeoxyuridine triphosphate (FdUTP). 80% of 5-FU is catabolised in the liver by dihydropyrimidine dehydrogenase (DPYD). Adapated from Longley, Harkin and Johnston, 2003.	31
1.4	The metabolism of irinotecan (CPT-11). Irinotecan is converted to the active metabolite SN38 by carboxylesterase (CE), as well as to two other inactive metabolites (NPC and APC) by CYP3A4. NPC can subsequently be converted by SN-38 by CE. Inactivation to SN38-G is predominantly controlled by UGT1A1, however the inactive metabolite can be re-activated to SN38 by β-glucuronidation. Adapted from Mathijssen *et al*, 2001.	33
1.5	Binding of a ligand (EGF, TGFα) to EGFR stimulates receptor dimerisation, tyrosine kinase activation, EGFR autophosphorylation and ultimately initiates signal transduction cascades involved in cell proliferation and survival. Inhibition of EGFR by the monoclonal antibody cetuximab inhibits these downstream events. Adapted from Kirkpatrick, Graham and Muhsin, 2004.	35
1.6	Kaplan-Meir survival curves of patients with colorectal liver metastases treated with neoadjuvant chemotherapy, with greatest survival in those with complete response (a) followed by major response (b) and minor response (c). Reproduced with permission from Blazer *et al*, 2008.	48
1.7	The Cancer Research (UK) roadmap to the discovery, development and validation of a clinically useful biomarker. Available online at http://www.cancerresearchuk.org.	53
2.1	A schematic outline of the stability study. The available tissue was divided into 10 fragments, 5 of which were stabilised immediately in one of the storage conditions shown and the remaining 5 in a similar manner but at the end of the procedure. The study was designed to ask two specific questions: can sampling wait until the end of the procedure, and what is the optimal storage condition?	67
2.2	A schematic outline of the archiving study. The available tissue was divided	68

	into 10 fragments, one of which was immediately snap frozen in liquid nitrogen and transferred to a -80^{o}C freezer (control sample) and one was archived in Allprotect^{TM} for each of the time points shown in the figure.	
2.3	Representative micrographs of H&E stained sections of colorectal liver metastases showing a) tissue snap frozen in liquid nitrogen and b) tissue stabilised in Allprotect^{TM}. Both are clearly identifiable as adenocarcinoma, although contain a degree of clear cell change/vacuolation (X). Histological appearances did not change significantly with the length of the time the sample was exposed to Allprotect^{TM}. Micrographs were taken at 200x magnification.	71
2.4	Cycle threshold (Ct) values for miR-122 in the colorectal liver metastasis from patient 1. All samples are comparable irrespective of the method of tissue stabilisation used, and whether the samples were stabilised immediately following specimen extraction (samples 1-5) or following a delay of 1 hour (samples 6-10). ANOVA with post-hoc Dunnett's test shows that no samples are statistically significant from the current gold standard (sample 1) i.e. tissue snap frozen in liquid nitrogen.	74
2.5	Western blot and corresponding densitometry of HMGB1 expression in primary colorectal cancer samples from patient 1. All samples are comparable irrespective of the method of tissue stabilisation used, and whether the samples were stabilised immediately following specimen extraction (samples 1-5) or following a delay of 1 hour (samples 6-10). ANOVA with post-hoc Dunnett's test shows that no samples are statistically significant from the current gold standard (sample 1) i.e. tissue snap frozen in liquid nitrogen.	75
2.6	Western blot and corresponding densitometry of CES1 expression in colorectal liver metastasis samples from patient 2. All samples are comparable irrespective of the method of tissue stabilisation used, and whether the samples were stabilised immediately following specimen extraction (samples 1-5) or following a delay of 1 hour (samples 6-10). ANOVA with post-hoc Dunnett's test shows that no samples are statistically significant from the current gold standard (sample 1) i.e. tissue snap frozen in liquid nitrogen.	76
2.7	Tissue homogenate was incubated with irinotecan and the production of SN-38 (active metabolite) quantified by liquid-chromatography mass-spectrometry. Data shown is from patient 3 (primary colorectal tumour). All samples are comparable irrespective of the method of tissue stabilisation used, and whether the samples were stabilised immediately following specimen extraction (samples 1-5) or following a delay of 1 hour (samples 6-10). ANOVA with post-hoc Dunnett's test shows that no samples are statistically significant from the current gold standard (sample 1) i.e. tissue snap frozen in liquid nitrogen.	77
2.8	Immunohistochemistry for HMGB1 in samples from patient 3 (primary colorectal tumour): a) Negative control b) Snap frozen in liquid nitrogen c) Allprotect^{TM} at room temperature d) Allprotect^{TM} at 8^{o}C. All sections were scored 3 for coverage (51-74%) and 3 for intensity (moderate). Haemotoxylin counterstain, x400 magnification.	78
2.9	Cycle threshold (Ct) values for miR122 in the liver metastasis from patient 4. Ct values increase with time archived in Allprotect^{TM}, and by 2 weeks there is a statistically significantly difference from the current 'gold standard', i.e. tissue snap frozen in liquid nitrogen (0).	79

2.10	Western blot and corresponding densitometry of HMGB1 expression in primary colorectal cancer samples (patient 1) archived in Allprotect^{TM}. The densitometric panels demonstrate the sharp reduction in protein abundance which occurs between 1 and 3 weeks, by which time it is statistically significantly different from the current 'gold standard', i.e. tissue snap frozen in liquid nitrogen (0).	80
3.1	The sequencing by synthesis of the Ion Proton platform. Sequencing is performed on a semiconductor chip containing small beads with clonally amplified template DNA. DNA polymerase is added with sequentially unmodified A, C, G or T dNTPs which are incorporated if complementary, releasing a hydrogen ion which is results in decreased pH that triggers an ion sensor in the chip. If the nucleotide is not complementary, no reaction takes place within that well. The unmodified dNTPs are then flushed out of the system and the next added. Figure taken from the European Bioinformatic Institute (with permission) http://www.ebi.ac.uk/training/online/course/ebi-next-generation-sequencing-practical-course/what-next-generation-dna-sequencing/ion-torre.	89
3.2	Bioinformatics analysis workflow for exome sequencing of synchronously resected primary colorectal tumours and colorectal liver metastases.	94
3.3	The ErbB signalling pathway was identified as the most statistically significant pathway arising from analysis of the SNVs present in at least one primary and metastatic tumour pertaining to the same patient. The focus genes in which the SNVs have arisen are highlighted in purple.	107
4.1	Samples are reduced and undergo a tryptic digest before being tagged with an isotope labelled molecule. These tags all have the same molecular weight although the reporter and balance moieties vary. After a cation exchange cleanup step the samples undergo nanoLC-MS/MS. The reporter and balance moieties are cleaved from each other and from the peptide to which they are bound, the ratio of which helps determine relative abundance. The peptide is also cleaved into fragment ions used to identify the protein.	129
4.2	Bioinformatics analysis workflow for global proteomic assessment of patient matched primary and metastatic colorectal tumours.	136
4.3	Venn diagram of predictive biomarkers identified in the primary tumour (170), metastatic tumour (27) and common to both (5).	166
5.1	Samples are reduced and undergo a tryptic digest before being tagged with an isotope labelled molecule. These tags all have the same molecular weight although the reporter and balance moieties vary. After a cation exchange cleanup step the samples undergo nanoLC-MS/MS. The reporter and balance moieties are cleaved from each other and from the peptide to which they are bound, the ratio of which helps determine relative abundance. The peptide is also cleaved into fragment ions used to identify the protein.	179
5.2	Bioinformatics analysis workflow for global proteomic assessment of serial rectal tumour biopsies.	183
5.3	The base excision repair (BER) signalling pathway was identified as being highly significant, with this data set suggesting downregulation induced by chemoradiotherapy. Only one of the 12 focus molecules was identified – PARP1 (highlighted in purple).	196
5.4	The ceramide degradation pathway was identified as being the most	200

	significantly downregulated pathway in the diagnostic samples of those primary tumours responding to chemoradiotherapy. Only 1 of the 6 focus molecules was identified – acid ceramidase (highlighted in purple).	
6.1	Antibody optimisation of NQO1 demonstrating the optimal concentration of antibody (1/1000) in the positive controls (left) and negative controls (right) of colonic mucosa (A) and breast cancer (B).	217
6.2	Images from a randomly selected core produced by Tissue Studio v.2.0 (Definiens AG, Munich, Germany), an immunohistochemical scoring package. The stained core as it appears under the light microscope is shown in (A), with the brown regions representing antibody binding and oxidation of DAB by horseradish peroxidase. Cellular identification and localisation is shown in (B), with the nuclei appearing blue and cytoplasm green. The degree of antibody staining is shown in (C) and can be seen to similarly correspond with the appearances on the micrograph (A). Areas shaded white have no antibody staining, yellow have weak antibody binding, orange have moderate antibody staining and brown have intense antibody staining (all considered positive).	218
6.3	Morphology of the SW480 cell line used for this investigation. Micrograph taken at x400 magnification.	219
6.4	Western blot for NQO1 in transfected S480 cells. From the left: DMSO treated cells were used as a control, and the transfection process (scrambled siRNA) had no effect on NQO1 expression. All 4 siRNAs (A-D) offered good knockdown of NQO1 at both concentrations. The optimum knockdown was achieved with siRNA-A at a concentration of 2.5pM.	220
6.5	Wells highlighted in red were transfected with siRNA to knockdown NQO1 and then incubated with irinotecan or 5FU over a range of concentrations. Wells highlighted in blue were transfected with a scrambled siRNA and then similarly treated. Wells highlighted in green were incubated in 0.5% DMSO (vehicle control) and wells highlighted in yellow were incubated in media only.	221
6.6	Wells highlighted in red were transfected with siRNA to knockdown NQO1, pre-treated with dicoumarol and then incubated with the irinotecan or 5FU over a range of concentrations. Wells highlighted in green were transfected but not pre-treated with dicoumarol and wells highlighted in blue were not transfected nor pre-treated. Wells highlighted in yellow were transfected with scrambled siRNA and then pre-treated with 0.5% NaOH and incubated in 0.5% DMSO, and those highlighted in purple were incubated in 0.5% DMSO only.	223
6.7	Wells highlighted in red were pre-treated with dicoumarol and then incubated with irinotecan or 5FU over a range of concentrations. Wells highlighted in blue were not pre-treated but treated with chemotherapy only. Wells highlighted in green were pre-treated with 0.5% NaOH and then incubated in 0.5% DMSO (vehicle control) and wells highlighted in yellow were not pre-treated but incubated in 0.5% DMSO only.	224
6.8	Western blots for thymidylate synthase (TS) in patient matched colonic mucosa (C), primary tumour (P), metastatic tumour (M) and liver parenchyma (L).	226
6.9	Western blots for dihydropyrimidine dehydrogenage (DPYD) in patient matched colonic mucosa (C), primary tumour (P), metastatic tumour (M) and liver parenchyma (L).	227
6.10	Western blots for orotate phosphoribosyltransferase (OPRT) in patient	227

	matched colonic mucosa (C), primary tumour (P), metastatic tumour (M) and liver parenchyma (L).	
6.11	Western blots for human carboxylesterase 1 (CES1) in patient matched colonic mucosa (C), primary tumour (P), metastatic tumour (M) and liver parenchyma (L).	229
6.12	Western blots for human carboxylesterase 2 (CES2) in patient matched colonic mucosa (C), primary tumour (P), metastatic tumour (M) and liver parenchyma (L).	229
6.13	Western blots for human topoisomerase I (TOP I) in patient matched colonic mucosa (C), primary tumour (P), metastatic tumour (M) and liver parenchyma (L).	230
6.14	Western blots for UDP glucuronosyltransferase 1A1 (UGT1A1) in patient matched colonic mucosa (C), primary tumour (P), metastatic tumour (M) and liver parenchyma (L).	230
6.15	Western blots for cytochrome P450 3A4 (CYP3A4) in patient matched colonic mucosa (C), primary tumour (P), metastatic tumour (M) and liver parenchyma (L).	231
6.16	Western blots for DNA polymerase β (DNA POL β) in patient matched colonic mucosa (C), primary tumour (P), metastatic tumour (M) and liver parenchyma (L).	233
6.17	CES1/CES2 activity was measured by SN38 production in patient matched primary tumour, liver metastasis and liver parenchyma. Mean (SD) data are presented for each tissue type for the patients studied.	234
6.18	Mean, SD and 95% confidence interval for SN-38 production in the primary tumours, liver metastases and liver parenchyma. Analysis with ANOVA showed significant differences between groups (p=0.001).	234
6.19	Comparison of protein quantification by western blotting (densitometry iu) and iTRAQ (abundance) for NQO1 demonstrates a high statistically significant relationship (r=0.59; p=0.003).	238
6.20	Correlation between the percentage of cells staining positively for NQO1 in the primary tumour and metastatic tumour. Using Spearman's rank correlation coefficient, r=0.44 (95% CI 0.20 – 0.64, p=0.001).	240
6.21	Dose response analysis for irinotecan in the SW480 cell line. Cells were incubated for 72 hours and cell viability assessed using the MTS assay and presented as a mean (95% CI) percentage of the control (0.5% DMSO). The IC50 is 90.2µM.	241
6.22	Dose response analysis for 5-FU in the SW480 cell line. Cells were incubated for 72 hours and cell viability assessed using the MTS assay and presented as a mean (95% CI) percentage of the control (0.5% DMSO). The IC50 is 202.2µM.	242
6.23	The effect of incubation with irinotecan on NQO1 expression was minimal. No samples were significantly different from the control value (0.5% DMSO).	243
6.24	Dose response analysis for irinotecan in the SW480 cell line with and without knockdown of NQO1 by siRNA transfection. Cells were incubated for 72 hours and cell viability assessed using the MTS assay and presented as a mean (95% CI) percentage of the control (0.5% DMSO). The IC50 is 100.1µM with the scrambled siRNA transfection, and 49.8µM following NQO1 knockdown. Statistical significance was achieved as follows: *p<0.05, **p<0.01, ***p<0.001.	244
6.25	Dose response analysis for 5-FU in the SW480 cell line with and without	245

	knockdown of NQO1 by siRNA transfection. Cells were incubated for 72 hours and cell viability assessed using the MTS assay and presented as a mean (95% CI) percentage of the control (0.5% DMSO). The IC50 is 200.1µM with the scrambled siRNA transfection, and 25.0µM following NQO1 knockdown. Statistical significance was achieved as follows: *p<0.05, **p<0.01, ***p<0.001.	
6.26	Dose response analysis for dicoumarol in the SW480 cell line. Cells were incubated for 4 hours and cell viability assessed using the MTS assay and presented as a mean (95% CI) percentage of the control (media only).	246
6.27	The effect of pre-treating cells with dicoumarol prior to incubation with 100µM irinotecan. Cell viability is expressed as a percentage of control (0.5% NaOH only followed by irinotecan). The maximum effect was achieved at a dicoumarol dose of 100µM.	247
6.28	Dose response analysis for irinotecan in the SW480 cell line firstly showing the effect of NQO1 knockdown by siRNA transfection, and secondly the absence of any additional biological effect following dicoumarol pre-treatment in those cells not expressing NQO1. Cells were incubated for 72 hours and cell viability assessed using the MTS assay and presented as a mean (95% CI) percentage of the control (scrambled siRNA transfection, pre-treatment with 0.5% NaOH and incubation in 0.5% DMSO).	248
6.29	Dose response analysis for irinotecan in the SW480 cell line with and without pre-treatment with dicoumarol. Cells were incubated for 72 hours and cell viability assessed using the MTS assay and presented as a mean (95% CI) percentage of the control (0.5% NaOH followed by 0.5% DMSO). The IC50 is 100.0µM for irinotecan alone, and 50.0µM following NQO1 inhibition with dicoumarol. Statistical significance was achieved as follows: *p<0.05, **p<0.01, ***p<0.001.	250
6.30	Dose response analysis for 5-FU in the SW480 cell line with and without pre-treatment with dicoumarol. Cells were incubated for 72 hours and cell viability assessed using the MTS assay and presented as a mean (95% CI) percentage of the control (0.5% NaOH followed by 0.5% DMSO). The IC50 is 183.7µM for 5-FU alone, and 49.9µM following NQO1 inhibition with dicoumarol. Statistical significance was achieved as follows: *p<0.05, **p<0.01, ***p<0.001.	250
6.31	Nrf2 is bound to Keap1 until pathway activation causes its stabilisation. Nrf2 subsequently translocates to the nucleus where it dimerises with a number of transcription factors and the heterodimer binds to the antioxidant response elements of a number of genes thus activating transcription. Adapted from Bataille and Manautou (2012).	255

Abbreviations

5-FU	5-flourouracil
ACN	acetonitrile
ACTB	β-actin
AJCC	American Joint Committee on Cancer
ANOVA	analysis of variance
APC	adenomatous polyposis coli
APE1	AP endonuclease 1
APER	abdomino-perineal excision of rectum
ARE	anti-oxidant response element
ASCO	American Society of Clinical Oncology
Asf1	anti-silencing function 1
BER	base excision repair
BETA	bevacizumab expanded access trial
bFOL	bolus fluorouracil and low-dose leucovorin with oxaliplatin
BOXER	bevacizumab, oxaliplatin, xeloda in unresectable liver metastases
bp	base pairs
BRiTE	Bevacizumab Regimens: Investigation of Treatment Effects and Safety
BSA	bovine serum albumin
CALGB	Cancer and Leukemia Group B
CapeOXc	apecitabine with oxaliplatin
CDAN1	codanin 1
CEA	carcinoembryonic antigen
CENPE	centromere protein E
CES1	carboxylesterase 1
CES2	carboxylesterase 2
ChIP	chromatin-immunoprecipitation
CI	confidence interval
CIMP	CpG island methylator phenotype
CIN	chromosomal instability
CLASSIC	Conventional versus Laparoscopic-Assisted Surgery in Colorectal Cancer
CoLOR	Colon cancer Laparoscopic or Open Resection
CRC	colorectal cancer

CRM	circumferential resection margin
CRT	chemoradiotherapy
CRUK	Cancer Research United Kingdom
CT	computed tomography
Ct	cycle threshold
CYP3A4	cytochrome P450 3A4
DAB	diaminobenzidine tetrahydrochloride
DACH	diaminocychlohexane
dbSNP	database single nucleotide polymorphisms
DCC	deleted in colorectal carcinoma
DHFU	dihydrofluorouracil
DILI	drug induced liver injury
DMSO	dimethyl sulfoxide
DNA	deoxyribonucleic acid
DNAPOL β	DNA polymerase β
dNTP	deoxynucleotide
DPYD	dihydropyrimidine dehydrogenase
dUTP	deoxyuridine triphosphate
EGF	epidermal growth factor
EGFR	endothelial growth factor receptor
ELISA	enzyme-linked immunosorbent assay
EORTC	European Organisation for Research and Treatment of cancer
EPIC	European Prospective Investigation into Cancer and Nutrition
ErbB	erythroblastic leukemia viral oncogene
ERK	extracellular signal-regulated kinases
FAP	familial adenomatous polyposis
FDA	Food and drug administration
FDG	fluorodeoxyglucose
FdUDP	fluorodeoxyuridine diphosphate
FdUMP	luorodeoxyuridine monophosphate
FdUTP	fluorodeoxyuridine triphosphate
FFPE	formalin-fixed and paraffin-embedded
FOLFIRI	folinic acid, fluorouracil and irinotecan
FOLFIRINOX	folinic acid, fluorouracil, irinotecan and oxaliplatin
FOLFOX	folinic acid, fluorouracil and oxaliplatin

FRL	future remnant liver
FUDP	fluorouridinedisphoaphate
FUTP	fluorouridine triphosphate
H&E	haematoxylin and eosin
HMGB1	high-mobility group protein B1
HNPCC	hereditary nonpolyposis colorectal cancer
HPLC	high pressure liquid chromatography
HPRT1	hypoxanthine phosphoribosyltransferase
HR	hazard ratio
IC50	half maximal inhibitory concentration
Indels	insertions and deletions
IORT	intra-operative radiotherapy
IQR	interquartile range
IRAS	Integrated Research Application System
IrMdG	Irinotecan and modified de Gramont
iTRAQ	isobaric tagging for relative quantification
KEAP1	Kelch-like ECH-associated protein 1
KRAS	Kirsten rat sarcoma
LC-MS/MS	liquid chromatography-mass spectrometry/mass spectrometry
LOH	loss of heterozygosity
Mad2	mitotic arrest deficient 2
MAGIC	Medical Research Council Adjuvant Gastric Infusional Chemotherapy
MAPK	mitogen-activated protein kinase
miRNA	micro ribonucleic acid
MMR	mismatch repair genes
MMTS	methylmethanethiosulfate
MOSAIC	Multicenter Study of Ox/ 5FU-LV in the adjuvant treatment of colon cancer
MRC	Medical Research Council
MRI	magnetic resonance imaging
MRM	multiple reaction monitoring
mRNA	messenger ribonucleic acid
MSH2	MutS protein homolog
MSI	microsatellite instability
MTOR	mammalian target of rapamycin
MW	molecular weight

MWA	microwave ablation
N/A	not applicable
NaOH	sodium hydroxide
NCI	National Cancer Institute
NER	nucleotide-excision repair
NGS	next generation sequencing
NICE	National Institute for Health and Care Excellence
NIH	National Institute Health
NQO1	NAD(P)H dehydrogenase [quinone 1]
NRAS	neuroblastoma RAS viral oncogene homolog
Nrf2	nuclear factor (erythroid-derived 2)
OPRT	orotate phosphoribosyl transferase
OPUS	oxaliplatin and cetuximab in first line treatment of metastatic colon cancer
PAGE	polyacrylamide gel electrophoresis
PARP1	poly(ADP-ribose) polymerase
PCR	polymerase chain reaction
PET	positron emission topography
PETACC-3	Pan-European Trials in Alimentary Cancer
PI3K	phosphatidylinositol-4,5-bisphosphate 3-kinase
PIK3CA	phosphatidylinositol-4,5-bisphosphate 3-kinase, catalytic subunit alpha
PMS2	postmeiotic segregation increased 2
PulMICC	Pulmonary Metastasectomy in Colorectal Cancer
QC	quality control
QUASAR	Quick and Simple and Reliable
R&D	Research and Development
RAF	rapidly accelerated fibrosarcoma
RAS	rat sarcoma
RCRG	Rectal Cancer Regression Grade
REC	Research Ethics Committee
RECIST	Response Evaluation Criteria in Solid Tumours
RFA	radiofrequency ablation
RIN	ribonucleic acid integrity number
RIPA	radioimmunoprecipitation assay
RNA	ribonucleic acid
RPM	revolutions per minute

SCPRT	short-course pre-operative radiotherapy
SD	standard deviation
SDS	sodium dodecyl sulphate
shRNA	short hairpin ribonucleic acid
siRNA	small interfering ribonucleic acid
SN-38	7-Ethyl-10-hydroxy-camptothecin
SNV	single nucleotide variant
TBST	tris buffered saline with tween
TCEP	Tris (2-carboxyethyl) phosphine hydrochloride
TEAB	triethylammonium bicarbonate
TFA	trifluoroacetic acid
TGFα	transforming growth factor α
TK	thymidine kinase
TMA	tissue micro-array
TME	total mesorectal excision
TNM	tumour node metastasis
TOP I	topoisomerase I
TP	thymidine phosphorylase
TP53	tumour protein p53
TRG	tumour regression grade
TS	thymidylate synthase
UGT1A1	UDP glucuronyltransferase 1A1
UICC	Union for International Cancer Control
UK	United Kingdom
UP	uridinephosphorylase
VEGF	vascular endothelial growth factor
vs	versus
WRT	with respect to
WT	Wild type
XRCC1	X-ray repair cross-complementing protein 1

Chapter 1

General Introduction

1.1 Epidemiology of colorectal cancer

The 2011 dataset published by Cancer Research (UK) declares colorectal cancer (CRC) as the fourth commonest cancer in the United Kingdom, with around 41600 people diagnosed in 2011 alone. There is a slight male preponderance for the disease, and it is the third commonest cancer in both men (after prostate and lung), and women (after breast and lung). 95% of cases occur in those over the age of 50, the incidence of which has increased by 6% over the last decade. These figures are representative of disease burden worldwide, with 447 000 new cases diagnosed in Europe and 1.36 million worldwide in 2012. (http://www.cancerresearchuk.org/cancer-info/cancerstats/types/bowel/).

Whilst the fourth commonest cancer, colorectal cancer is the second commonest cause of cancer related death in the UK. The death rate remains high despite a two-fold increase in five year survival over the past 40 years. The UK bowel cancer screening programme has been gradually rolled out since 2006, however it is as yet unclear the effect this will have on survival rates.

Dukes Stage at Diagnosis	Percentage of Cases	Five-Year Survival
A	8.7%	93.2%
B	24.2%	77.0%
C	23.6%	47.7%
D	9.2%	6.6%
Unknown	34.3%	35.4%

Table 1.1 - Percentage of cases and 5 year relative survival (%) by Dukes' stage at diagnosis for colorectal cancer patients diagnosed 1996-2002 in England. (Reproduced without permission from Cancer Research (UK)).

The best known predictor of survival is disease stage, with over 93% of patients with Dukes A disease surviving 5 years compared to less than 7% of those with Dukes D disease (Table 1.1). On separating the disease into tumours of the colon and rectum, survival is comparable. Most recent figures from Cancer Research (UK) show that 1-year survival for men and women with colon cancer is 73.0% and 72.2% respectively, with 5-year survival of

54.4% and 55.1%. In those with rectal cancer 1-year survival for men and women is 78.8% and 78.8% respectively, and 5-year survival 54.6% and 57.5%.

1.2 Risk factors for colorectal cancer

A number of dietary and lifestyle factors have been linked to the development of colorectal cancer, including diets rich in unsaturated fats and red meat, excess alcohol and a sedentary lifestyle (Potter, 1999; Slattery *et al*, 2000; Huxley *et al* 2009). A number of other risk factors have been studied, and a recent review attempted to describe the complex interplay between energy intake, hormone levels, inflammation and gut flora which may lead to colorectal cancer (Slattery and Fitzpatrick, 2009). Smoking is also associated with an increased risk of colorectal cancer (Colangelo *et al*, 2004) as is a preceding diagnosis of inflammatory bowel disease (Choi and Zelig, 1994). Isolated risk factors however have been difficult to define, confounded by the fact that the majority of tumours arise in individuals with poorly defined risk profiles.

1.3 Genetics of colorectal cancer

There are a number of identified gene defects known to predispose to colorectal cancer, as well as a number of somatic mutations that are present in sporadic tumours. These alterations may lead to novel or improved function in oncogenes, or loss of function of tumour suppressor genes. It is estimated that approximately 15-30% of colorectal cancers have a significant hereditary component, of which 5% have a Mendelian cancer syndrome which predisposes to CRC (Lynch and de la Chapelle, 2003; Rustgi, 2007). The majority of these are attributable to hereditary nonpolyposis colorectal cancer (HNPCC) and familial adenomatous polyposis (FAP), with a number of other genetic alterations associated with less common syndromes (Table 1.2).

Syndrome	Common Features	Gene defect(s)
FAP	Multiple adenomatous polyps (>100) and carcinomas of the colon and rectum; duodenal polyps and carcinomas; fundic gland polyps in the stomach; congenital hypertrophy of the retinal pigment epithelium	APC (>90%)
Gardner syndrome	Same as FAP; also, desmoid tumors and mandibular osteomas	APC
Turcot's syndrome	Polyposis and colorectal cancer with brain tumors (medulloblastomas); colorectal cancer and brain tumors (glioblastoma)	APC
		MLH1, PMS2
Attenuated adenomatous polyposis coli	Fewer than 100 polyps, although marked variation in polyp number (from ~5 to > 1,000 polyps) observed in mutation carriers within a single family	APC (precominantly 5' mutations)
Hereditary nonpolyposis colorectal cancer	Colorectal cancer without extensive polyposis; other cancers include endometrial, ovarian and stomach cancer, and occasionally urothelial, hepatobiliary, and brain tumors	MSH2
		MLH1
		PMS2
		GTBP, MSH6
Peutz-Jeghers syndrome	Hamartomatous polyps throughout the GI tract; mucocutaneous pigmentation; increased risk of GI and non-GI cancers	LKB1, STK11 (30-70%)
Cowden disease	Multiple hamartomas involving breast, thyroid, skin, central nervous system and GI tract; increased risk of breast, uterus and thyroid cancers; risk of GI cancer unclear	PTEN (85%)
Juvenile polyposis syndrome	Multiple hemartomatous/juvinile polyps with predominance in colon and stomach: variable increase in colorectal and stomach cancer risk; facial changes	DPC4 (15 %)
		BMPRIa (25 %)
		PTEN (5 %)
MYH - associated polyposis	Mutiple adenomatous GI polyps, autosomal recessive basis; colon	MYH

	polyps often have somatic *KRAS* mutations	

Table 1.2 – Genetics of inherited colorectal tumour syndromes. (Reproduced without permission from Fearon, 2011).

Most tumours arise within dysplastic polyps, and therefore an understanding of the adenoma-carcinoma sequence is crucial. Most polyps are hyperplastic and less than 5mm in diameter, however it is the larger adenomas which have been shown to possess malignant potential (Jass, 2007). An adenoma is a benign lesion of glandular epithelium with a prevalence of approximately 25% by age 50 and 50% by age 70 (Rex *et al*, 1993). Only a small number of polyps progress to malignancy, often over a period of years to decades; polyp surveillance studies have shown that a 1cm polyp has a 10-15% chance of becoming malignant within 10 years (Stryker *et al*, 1987). Adenoma-carcinoma progression was first described by Vogelstein in 1990 as a series of genetic alterations responsible for sporadic CRC, beginning with mutation in the adenomatous polyposis coli (*APC*) gene followed by mutations in the *KRAS* and *TP53* genes. These mutations are positively selected for during carcinogenesis and are intrinsically involved in DNA repair, cell adhesion and proliferation (Wood *et al*, 2007).

1.3.1 Adenomatous polyposis coli

The *APC* tumour suppressor gene encodes for a protein known to regulate cell-adhesion, migration and apoptosis (Fearon and Vogelstein, 1990), and is the genetically defective gene in FAP as well as some of the less common inherited cancer syndromes. The defect is present in over 75% of colorectal cancers, and is widely believed to be an early step in sporadic carcinogenesis due to its reported presence across the adenoma-carcinoma sequence, including microscopic adenomas with a small number of dysplastic glands (Kinzler and Vogelstein, 1996).

The most well understood downstream effect of *APC* mutation is disruption of the WNT pathway. APC targets β-catenin for proteasomal degradation, and therefore mutation results in the nuclear accumulation of β-catenin, increased WNT activity and cellular proliferation (Polakis, 2007).

1.3.2 KRAS/BRAF

The RAS family of proteins (KRAS, HRAS and NRAS) are G-proteins which predominantly fulfil the roles of molecular switches. *KRAS* is a proto-oncogene which, following activation through the endothelial growth factor receptor (EGFR) pathway, triggers downstream signalling through the PI3K/AKT/MTOR and RAF/MEK/ERK pathways resulting in cellular proliferation (Fearon, 2011). Up to 40% of colorectal tumours have a mutated version of the *KRAS* gene, most commonly in codons 12 with smaller subsets affecting codon 13 and rarely codon 61 (Downward, 2003). The mutation is also found in a number of flat colonic epithelial lesions without dysplasia, questioning its role in early carcinogenesis (Pretlow and Pretlow, 2005). However disruption of mutant *KRAS* in advanced CRC has demonstrated that inactivation inhibits tumour growth both *in vitro* and in animal studies, highlighting its role in disease progression (Shirasawa *et al*, 1993).

BRAF is a downstream target of KRAS, exerting its effect through the MEK/ERK pathways. Mutated in approximately 5-10% of colorectal cancers, *BRAF* mutation appears to be independent of *KRAS* mutation, however mutation in either can result in pathway upregulation and activation of relevant downstream transcription factors such as myc (Rajagopalan *et al*, 2002).

1.3.3 TP53

TP53 (p53) is a tumour suppressor gene implicated in a wide range of malignancies, most likely due to its significant role as a regulator of cell-cycle checkpoints, genomic stability, apoptosis and angiogenesis (Vousden and Prives, 2009). Under conditions of DNA damage resulting from cellular stress p53 activates DNA repair proteins, arrests growth by holding the cell cycle at the G1/S regulation point and initiates apoptosis. Over 50% of all tumours have ineffective p53 (Hollstein *et al*, 1991), thought to be a combination of loss of heterogenezity (LOH) of one allelele of 17p and somatic mutation in the other (Fearon and Vogelstein, 1990). This pattern is not observed in most adenomas, highlighting this mutation as a significant event in the transition from adenoma to carcinoma (Baker *et al*, 1990).

1.3.4 Mismatch repair and microsatellite instability

Whilst germline mutations account for a relatively small proportion of tumours they offer a unique opportunity to understand the genetic instability which contributes to the development of CRC. Mismatch repair genes (MMR), for example *MLH1, MSH2, MSH6* and *PMS2*, are responsible for correcting base mismatches and short insertions or deletions which normally occur during DNA replication (Grady and Carethers, 2008). Where these genes are defective, DNA sequences are not faithfully replicated and microsatellites are created - short sections of repeating DNA 1-6 base pairs long.

Germ-line mutations in MMR genes are present in only 2-4% of CRC patients, however 15% of sporadic colorectal cancers exhibit microsatellite instability (MSI). A key mechanism for this is thought to be hypermethylation of the promoter of MLH1 resulting in a loss of function (Aaltonen *et al*, 1993). MSI tumours exhibit a specific phenotype; they tend to be poorly differentiated right colonic tumours with high mucinogens and tumour related lymphyocytes and are less likely to metastasise than microsatellite stable (MSS) tumours (Buecher *et al*, 2013). These pathological features confer a survival advantage, despite a reported resistance to fluorouracil based chemotherapeutic regimens (Ribic *et al*, 2003). Tumours with MSI can be sub-classifed as MSI-Low or MSI-High by the presence of less than or more than 30% unstable loci in a panel of 5-10 points respectively (Boland *et al*, 1998). The distinction of MSI-High/Low is associated with further variations in tumour phenotype and disease characteristics.

1.3.5 Chromosomal instability (CIN)

The chromosomal instability (CIN) phenotype is observed in approximately 70%–85% of CRC. It is widely accepted that most MSS tumours follow the CIN mechanism of tumourigenesis, however the MSI and CIN phenotypes are not mutually exclusive (Lengauer, Kinzler and Vogelstein, 1997).

The cause of chromosomal instability is not known, although it is believed to be due to defects in genes which regulate formation of the mitotic spindle and alignment and segregation of chromosomes at mitosis (Grady, 2004). A small number of specific defects have been suggested, including alterations in Mad2, BubR1, Bub3 and CENPE proteins as well as LOH in chromosome 18q containing the tumour suppressor genes *SMAD2*, *SMAD4,* and *DCC (Barber et al, 2008)*. *APC* mutation is also thought to play a role, but its presence in many other non-CIN tumour phenotypes suggests that the molecular basis for CIN tumours

is more heterogenous than the relationship between MMR genes and microsatellite instability (Alberici and Fodde, 2006).

1.3.6 CpG island methylator phenotype (CIMP)

DNA methylation is thought to serve the biological function of silencing repetitive elements of the genome (Yoder *et al*, 1997), and the significance of hypermethylation resulting in loss of function of *MLH1* has already been discussed. The majority of C-phosphate-G sites have been lost from the human genome during evolution, however hypermethylation of any residual islands, defined as methylation of at least 3 loci from a panel of 5 gene-associated CpG islands, results in the silencing of tumour suppressor or other tumour related genes and ultimately carcinogenesis (Carragher *et al*, 2010). The CPG island methylator phenotype (CIMP) represents a further subset of colorectal cancers with a particular molecular and biological profile. Specifically these tumours have a higher incidence of concurrent mutations in *KRAS/BRAF* but wild type *TP53*, and are more frequently proximal tumours with mucinous and poorly differentiated histopathological features most often presenting in older female patients (Issa*,* 2004). Similarly to MSI, CIMP status of the tumour has been used to infer potential response to chemotherapeutics (Shiovitz *et al*, 2014).

1.3.7 Summary of colorectal cancer genetics

Our understanding of colorectal carcinogenesis has progressed significantly since the model first proffered by Vogelstein in 1990, and is summarised in Figure 1.1.

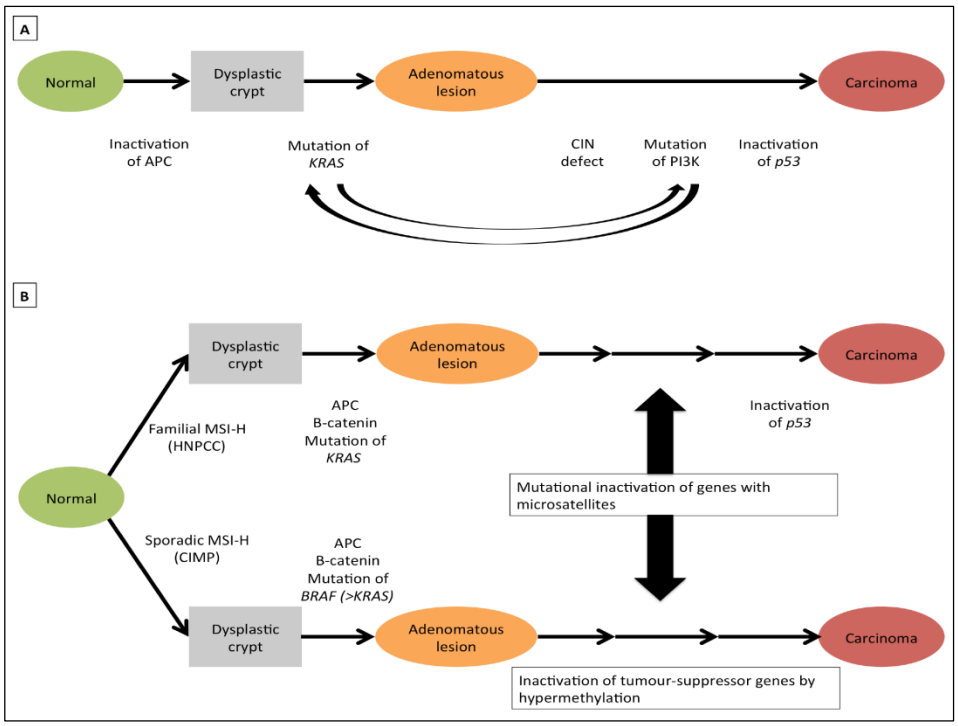

Figure 1.1 – Suggested genetic model for colorectal cancer. In (a) a number of hereditary and sporadic mutations drive the transformation of normal epithelia to an adenomatous lesion and latterly carcinoma. In (b) an inherited or acquired defect in DNA mismatch repair (MMR) function is the initiator for carcinogenesis. (Adapted from Fearon, 2011).

The vast majority of colorectal tumours reflect a series of hereditary and somatic mutations in key genes i.e *APC, KRAS, BRAF* and *TP53*. These mutations are most frequently associated with a CIN phenotype and are often acquired in a different order, although the sequence may be relevant to tumourogenicity. A subset of tumours initiate through inactivation of MMR function, which may be through inherited or, less commonly, somatic mutation, or alternatively epigenetic inactivation through hypermethylation (CIMP) leading to MSI-H. Further cumulative mutations in the *APC/KRAS/BRAF/TP53* genes ultimately lead to carcinogenesis.

1.4 Staging of colorectal cancer

Given the relative immaturity of the Bowel Cancer Screening Programme, the vast majority of patients with colorectal cancer still present symptomatically (Majumdar, Fletcher and Evans, 1999). Lesions in the left side of the colon are associated with alteration in bowel function, rectal bleeding and tenesmus, whereas lesions in the right side of the colon are

associated with abdominal pain and mass, anaemia and systemic symptoms of malignancy such as malaise and anorexia. A timely and accurate diagnosis is imperative to establish the diagnosis, accurately stage the disease and instigate an appropriate management plan.

1.4.1 Clinical assessment

Clinical assessment of the patient includes an understanding of comorbidity relevant to the treatment of the disease as well as an assessment of the disease itself, for example the tumour may be palpable via the abdomen or on *per rectal* examination.

1.4.2 Endoscopic assessment

Colonoscopy allows the visualisation of the entire colonic mucosa whilst also permitting biopsies of any suspicious lesions to be taken as well as delivering therapy, for example polypectomy. This is particularly important given the incidence of synchronous tumours (5%) and concurrent polyps (28%) which may influence management decisions (Langevin and Nivatvongs, 1984). The procedure also permits the marking of lesions with tattoo ink for subsequent localisation during surgery and a better understanding of tumour location and anatomy.

1.4.3 Radiological assessment

Computed tomography (CT) is the most widely used modality for staging local disease, as well as the detection and characterisation of both hepatic and extra-hepatic metastases for which it has a sensitivity of 60-90% (Ong and Leen, 2007). Modern techniques of multi-detector helical scanning combined with rapid infusion of contrast allows visualisation of the liver in a number of different vascular phases. Combined with multi-slice reconstruction this technique has significantly improved lesion characterisation in the liver (Scott *et al*, 2001).

CT scanning is supplemented with magnetic resonance imaging (MRI) in two specific situations. In the local staging of rectal cancer, pre-operative high resolution MRI images provide information previously not normally available until the final surgical specimen had been examined histopathologically. Knowledge of these features in advance of surgery affords the opportunity to downstage disease and therefore influence outcome. On T2-

weighted images taken by a 1.5T system with phased array coils, details of tumour morphology and stage, lymph node status and extramural vascular invasion can all be observed (Taylor *et al*, 2011). Perhaps more importantly, close proximity (within 1mm) of the tumour to the mesorectal fascia on MRI is a very sensitive predictor of circumferential resection margin (CRM) positivity at the time of surgery (MERCURY Study Group, 2006). The widespread adoption of treating these patients with so-called 'threatened margins' with neoadjuvant chemoradiotherapy followed by total mesorectal excision (TME) surgery has led to a significant reduction in margin positivity. Secondly, for indeterminate lesions in the liver, further visualisation with MRI (combined with gadolinium contrast) is considered the most effective imaging modality for accurate characterisation (Kamel and Bluemke, 2003).

Positron emission topography (PET) utilises the increased glucose metabolism in tumour cells to uptake the radiotracer 18-fluorodeoxyglucose (FDG). On uptake the tracer is phosphorylated, thus becoming metabolically inactive and accumulating in cells. Now frequently combined with CT, PET scanning allows for the accurate localisation of small disease deposits, for example extra-hepatic abdominal metastases or local disease recurrence, on the understanding that metabolic changes in cells precede any anatomical variance which may be detected on contrast CT (Arulampalam *et al*, 2004). This additional information has been shown to alter disease management in 29% of patients with colorectal liver metastases (Huebner *et al*, 2000).

1.4.4 Histopathological assessment

As previously discussed, endoscopic examination of the colon permits acquisition of tissue for histopathological analysis. Given that the digestive tract can be considered as a continuum which at all times from mouth to anus is outside the body, biopsies can be taken without fear of seeding tumour into adjacent tumour free tissue.

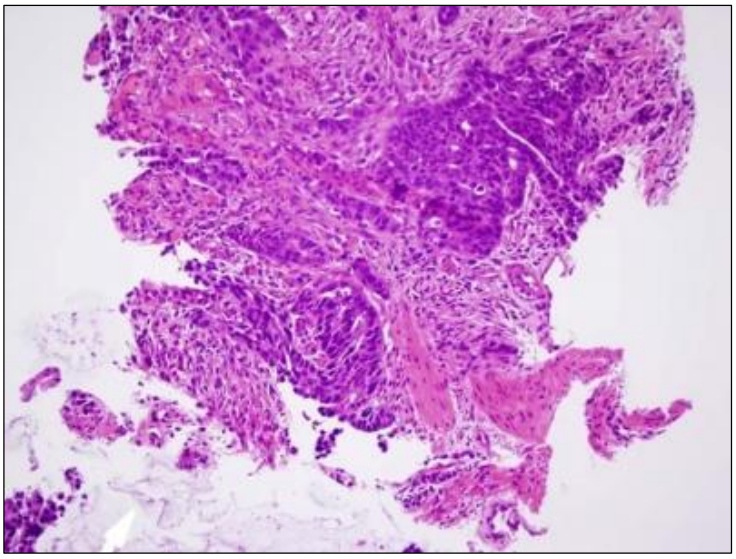

Figure 1.2 - Invasive colonic adenocarcinoma penetrating the muscularis mucosa; stained with haematoxylin and eosin. Photomicrograph taken at x200 magnification.

Tissue for analysis is formalin-fixed and paraffin-embedded (FFPE) and slices for examination are stained with haematoxylin and eosin (H&E). The histological diagnosis of colorectal cancer is based on invasion through the muscularis mucosae into the submucosa (Figure 1.2) and further classification into a number of histopathological subtypes, including: adenocarcinoma, mucinous adenocarcinoma, signet ring cell carcinoma and medullary carcinoma.

Another important element of the histopathological assessment of colorectal cancer is tumour grade; an interpretation of the degree of de-differentation from the morphology of the original tissue assigned on a scale of G1-G4. Assignment of tumour grade considers nuclear features such as pleomorphism, cellular architecture and mitotic count, with G1-2 tumours and G3-4 tumours grouped together for simplicity as low and high grade respectively. Whilst some tumour types have specific grading systems shown to link closely with prognosis, for example the Nottingham index for breast cancer and Gleason score for prostate cancer, none has as yet been developed for colorectal adenocarcinoma.

Biopsy and histopathological assessment of lesions of presumed colorectal origin from outside the gastrointestinal tract, for example in the liver, proves more challenging, with uncertainty amongst clinicians both of its value and safety. Certainly given accurate radiological assessment as previously discussed and the increasing role of serum

biomarkers, the role of needle biopsy of colorectal liver metastases to obtain a diagnosis would seem unnecessary, however obtaining biological information from the metastatic site(s) may provide useful predictive and prognostic information.

The most significant evidence to challenge the practice of biopsying colorectal liver metastases is a case series published by Jones *et al* (2005) comparing two cohorts of patients undergoing surgery for colorectal liver metastases, one of which had pre-operative needle biopsies to confirm diagnosis of adenocarcinoma. The incidence of needle-track tumour deposits was 19%, and whilst operative morbidity in the two groups were similar, the 4-year survival after liver resection was 32.5% in those having pre-operative needle biopsy compared to 46.7% in the group who did not (P=0.008). There are a number of other similar, albeit smaller, studies highlighted in a recent review (Table 1.3) which also goes on to discuss mechanical as well as oncological complications of liver biopsies (Cresswell, Welsh and Rees, 2009). Whilst the overall complication rate is thought to be around 5.9% (Perrault *et al*, 1978), the risk of significant haemorrhage is 0.5% (Knauer, 1978).

Authors	Year	Design	*n*	Findings
Al-Leswas *et al.*	2008	Case report	2	2 cases of implantaion
Jones *et al.*	2005	Retrospective review	17	19% seeding rate; poorer longterm survival after biopsy
Rodgers *et al.*	2003	Retrospective review	7	16% risk of seeding irrespective of route of biopsy
Metcalf e*t al.*	2004	Case report	1	Biopsy added nothing to diagnostic pathway
Ohlsson *et al.*	2002	Case series	5	10% seeding rate
Scheele & Altendorf-Hofmann	1990	Case report	2	Seeding following biopsy of resectable lesion
Ferrucci *et al.*	1979	Case Report	1	First documented case of tract seeding

Table 1.3 – Summary of evidence highlighting complications from percutaneous needle biopsy of colorectal liver metastases. (Reproduced without permission from Cresswell, Welsh and Rees, 2009).

1.4.5 Staging systems

The first staging system for colorectal cancer was described by Dr Cuthbert Dukes in 1932. Applied initially only to rectal cancer, tumours were assigned a classification or Dukes' stage from A-C: Dukes' stage A cancers were confined to the bowel wall, stage B through the bowel wall and stage C where there was lymph node involvement (Dukes, 1932). Duke himself later correlated his pathological grading system with prognosis (Dukes and Bussey, 1958), at which time the subdivision of stages C1 (regional lymph node involvement) and C2 (apical node involvement) were made. Stage D representing distal disease was later added, (Turnbull *et al*, 1967), and the scoring system informally applied to carcinomas arising in the colon.

With significant improvement in both our understanding of disease biology, but perhaps more so the advances in radiological techniques described above, the current standard of care is the use of the Union for International Cancer Control/American Joint Committee for Cancer TNM classification. This classification is a disease specific extension of the original TNM system devised by Denoix *et al* in 1946 whereby the degree of invasion and tumour spread is characterised by a T stage referring to the primary tumour, N stage recording the presence and extent of local lymph node invasion, and M stage describing the presence or absence of distant metastatic disease. The current version in widespread clinical use is the 7th edition published in 2010 (Table 1.4).

TNM Stage	Description
TX	Primary tumour cannot be assessed
T0	No evidence of primary tumour
Tis	Carcinoma in situ: intraepithelial or invasion of lamina propria
T1	Tumour invades submucosa
T2	Tumour invades muscularis propria
T3	Tumour invades through the muscularis propria into pericolorectal tissues
T4a	Tumour penetrates to the surface of the visceral peritoneum
T4b	Tumour directly invades or is adherent to other organs or structures
NX	Regional lymph nodes cannot be assessed
N0	No regional lymph node metastasis
N1	Metastasis in 1-3 regional lymph nodes
N1a	Metastasis in 1 regional lymph node
N1b	Metastasis in 2-3 regional lymph nodes
N1c	Tumour deposit(s) in the subserosa, mesentery, or non peritonealized pericolic or perirectal tissues without regional nodeal metastasis
N2	Metastasis in 4 or more regional lymph nodes
N2a	Metastasis in 4-6 regional lymph nodes
N2b	Metastasis in 7 or more regional lymph nodes
M0	No distant metastasis
M1	Distant metastasis
M1a	Metastasis confined to one organ or site (e.g. Liver, lung, ovary, non regional node)
M1b	Metastases in more than one organ/site or the peritoneum

Table 1.4 – UICC/AJCC TNM staging of colorectal cancer; 7th edition (2010). Available online at https://cancerstaging.org/references-ools/quickreferences/Pages/default.aspx

Given that it is possible to stage disease on a number of parameters at a number of different points along the patient's journey, a number of prefixes to the TNM system have been created to highlight the origin of the information used for staging. These include: c – indicating the stage is given by clinical examination of the patient, p – indicating the stage is given by histopathological examination of a surgical specimen, y – indicating the stage is assessed after chemotherapy and/or radiation therapy (i.e. the patient received neoadjuvant treatment), r – for recurrent tumours with a substantial disease-free period, a

– determined at autopsy (or post mortem examination) and u – determined by ultrasonography.

As can be seen from the table above there are many potential combinations of Tumour, Node and Metastasis stages which the UICC/AJCC have grouped together into stages (Table 1.5) for the benefit of simplifying treatment decisions (Carrato, 2008).

Stage	Description	TNM Stages
0	No tumour	Tis, N0, M0
I	Primary tumour into but not through muscularis propria, and no metastases	T1-2, N0, M0
IIa	Primary tumour grown through to serosa and peritoneal surface but no metastases	T3, N0, M0
IIb		T4a, N0, M0
IIc		T4b, N0, M0
IIIa	Any size of primary tumour with lymph node metastases	T1-2, N1-N1c, M0 / T1, N2a, M0
IIIb		T3-T4a, N1-N1c, M0 *or* T2-T3, N2a, M0 *or* T1-T2, N2b, M0
IIIc		T4a, N2a, M0 *or* T3-T4a, N2b, M0 *or* T4b, N1-2, M0
IVa	Presence of distant metastatic disease	Any T, Any N, M1a
IVb		Any T, Any N, M1b

Table 1.5 - UICC/AJCC stage groupings for colorectal cancer; 7th edition (2010). Available online at https://cancerstaging.org/references-ools/quickreferences/Pages/default.aspx.

Other staging systems have been established to further guide treatment or prognosticate. The best utilised of these systems is the Jass classification (Table 1.6) which combines some of the genetic aberrations previously discussed with a number of macroscopic and microscopic pathological correlates and patient features (Jass, 2007).

Feature	Group 1	Group 2	Group 3	Group 4	Group 5
MSI Status	H	S/L	S/L	S	H
Methylation	+++	+++	++	+/-	+/-
Ploidy	Dip > An	Dip > An	An > Dip	An > Dip	An > Dip
APC	+/-	+/-	+	+++	++
KRAS	-	+	+++	++	++
BRAF	+++	++	-	-	-
TP53	-	+	++	+++	+
Location	R > L	R > L	L > R	L > R	R > L
Gender	F > M	F > M	M > F	M > F	M > F
Precursor	SP	SP	SP/AD	AD	AD
Serration	+++	+++	+	+/-	+/-
Mucinous	+++	+++	+	+	++
Dirty Necrosis	+	+	?	+++	+
Poor differentiation	+++	+++	+	+	++
Circumscribed	+++	+	?	++	++
Tumour budding	+/-	+	?	+++	+
Lymphocytes	+++	+	?	+	+++

Table 1.6 – The Jass classification combines a number of patient, histopathological and genetic factors to allocate tumours to a group (1-5). MSI, microsatellite instability; H, high; S, stable; L, low; Dip, diploid; An, aneuploid; Serration, serrated morphology; SP, serrated polyp; AD, adenoma; Circumscribed, circumscribed invasive margin. Reproduced without permission from Jass, 2007.

Identifying features such as these in classification systems could potentially allow us to gain a greater understanding of causation and pathogenesis. At the very least it acknowledges that colorectal cancer is a complex and multi-pathway disease. The Jass group is often used as a decision tool for those patients with Dukes' Stage B (or Stage II) disease. A study of 183

patients with Dukes' B disease who were also Jass grouped identified that cancer specific mortality was considerably higher in those with Jass group III than I or II. This additional prognostic information may facilitate the selection of patients who are most likely to benefit from adjuvant chemotherapy (Mander *et al*, 2006).

1.5 Treatment of colorectal cancer with surgery

Surgical resection remains the mainstay of oncological treatment for colorectal cancer. The exact oncosurgical strategy to employ and how to incorporate this with other treatment modalities has been the subject of much study in recent years.

1.5.1 Resection of the primary tumour

The surgical approach to colorectal cancer is dependent upon the site and stage of the disease, and in particular is somewhat different for the 37% of tumours present in the rectum.

Small tumours contained within colonic polyps are often removed by polypectomy at the time of colonoscopy, however a significant number of patients undergo formal resection of the diseased segment of colon along with its arterial supply and accompanying lymphatic drainage. For tumours in the right colon a right hemicolectomy is performed. A section of bowel from the terminal ileum to transverse colon is excised, with ligation of the right colic and ileocolic vessels close to their origins in order to ensure maximum lymphatic clearance. For tumours in the transverse colon a more extensive version of this procedure is performed, often referred to as an extended right hemicolectomy. For tumours in the left colon a section of bowel extending from the sigmoid colon for a variable distance along the descending colon, with or without the splenic flexure, is mobilised, and excised following division of the inferior mesenteric artery and vein (usually to obtain full mobility of the colon). In the elective setting of either scenario an anastomosis is usually performed, although this may not be feasible or safe in the emergency setting. The concept of total mesocolic excision and its potential oncological advantages are currently being explored. The procedure consists of three essential components: dissection between the mesenteric plane and the parietal fascia with subsequent removal of the mesentery, a central vascular tie to completely remove all lymph nodes in the central (vertical) direction, and resection of

an adequate length of bowel to remove involved pericolic lymph nodes in the longitudinal direction (West *et al*, 2009).

Tumours in the rectum may be amenable to local or trans-anal excision, with a significant increase in uptake of a number of variations of this technique in recent years (Atallah and Albert, 2013). Formal resection of the diseased segment of bowel however is more frequently performed. In brief tumours of the upper third of the rectum are approached in a similar manner to the operation for tumours in the left colon as previously described. Tumours in the middle and lower thirds of the rectum are now almost universally excised by low anterior resection using a technique known as total-mesorectal excision (TME). Professor Bill Heald popularised this technique in 1982, recognising that the lateral, deep or circumferential margins were much better predictors of local recurrence than distal margin (Heald, Husband and Ryall, 1982). The technique of TME was published in 1988 and the follow up data in 1998 reported a local recurrence rate of between 3-6%, considerably less than the 30% historically quoted (Heald, 1988; Heald *et al*, 1998). It is now well established that involvement of the circumferential resection margin is a good predictor of local recurrence, distant metastasis and also survival (Nagtegaal and Quirke, 2008).

This technique brought about a considerable reduction in the number of abdomino-perineal excision of rectum (APER) procedures, which involves removal of the entirety of the rectum and anal canal. This operation removes the sphincters and results in a permanent stoma, and therefore should be avoided if at all oncologically feasible. Rates of this operation still remain extremely variable, however are universally reducing as combinations of nejoadjuvant chemoradiation, total mesorectal excision, intersphincteric proctectomy and colonic-J pouch to anal anastomosis means that sphincter preservation can be achieved for most patients (Ludwig, 2007).

A number of international multi-centre studies have confirmed the oncological equivalence of laparoscopic colorectal cancer surgery, two of the most significant being the Colon cancer Laparoscopic or Open Resection (CoLOR) trial studying colonic cancer (Veldkamp *et al*, 2005), and the Conventional versus Laparoscopic-Assisted Surgery in Colorectal Cancer (CLASSIC) trial for rectal cancer(Bang *et al*, 2012). Whilst oncological outcomes are comparable, laparoscopic surgery offers reduced wound infection rates, less pain and narcotic use, less overall morbidity and a shorter hospital stay, at the cost of modest increase in operative times (Abraham, Young and Solomon, 2004).

1.5.2 Resection of metastatic disease

Over the past 10-20 years there has been a rapid expansion in potentially curative surgery for colorectal metastases, particularly those confined to the liver. This is in part a result of a more aggressive approach to neoadjuvant chemotherapy combined with improved surgical techniques, bringing an increasing number of patients who were initially thought not to be resectable to resection. Those patients who do undergo resection experience a 10 year survival of 9-69% (Taylor *et al*, 2012).

Prior to this there was a very conservative approach to the management of metastatic disease in the liver, the traditional indications for which were 1-3 unilobar metastases which were resectable with a generous margin. Patients presenting with liver metastases (i.e. those with stage IV disease), those with a rectal primary, multiple diffuse metastases, metastases larger than 5cm, a disease free interval of less than 1 year from the diagnosis of the primary and high serum carcinoembryonic antigen (CEA) were not considered appropriate for curative surgical resection due to poor prognosis (Poston, 2008). The approach to surgical resection in the liver is now more of a consideration of both technical and oncological feasibility.

In order to achieve adequate resection in the liver it must be feasible to remove all macroscopic disease with negative margins, preserve vascular inflow and outflow and leave sufficient future remnant liver (FRL) to ensure adequate hepatic function (Garden *et al*, 2006). The volume of FRL sufficient to ensure adequate hepatic function would clearly depend upon the functional quality of the remaining liver parenchyma, with those patients with cirrhosis, steatosis or, increasingly commonly, drug induced liver injury (DILI), requiring a larger liver remnant than those with normal underlying liver parenchyma. Generally speaking, 25% of the liver volume (approximately two Couinaud segments) is considered adequate. Given the regenerative ability of the liver parenchyma, liver regrowth may allow multi-stage resections (Narita *et al*, 2011).

Removal of all macroscopic and microscopic disease with negative margins is referred to as an R0 resection. Where microscopic disease remains the resection is said to be R1 and where macroscopic disease remains the resection is said to be R2. It has been clearly demonstrated that those patients with R1 resections have better outcomes than those with

R2 (Pawlik *et al*, 2005), and whilst R0 is considered the optimum standard of care, survival in those with R0 and R1 resections is comparable (de Haas, Wicherts and Adam, 2008).

A number of alternatives to surgical resection exist, all of which centre on the concept of tumour ablation. This is now most commonly achieved by radiofrequency ablation (RFA) or microwave ablation (MWA) either at open surgery or percutaneously. Given the considerable variation in local recurrence and overall survival, the role of ablation in the curative setting is unclear. This was highlighted by recent guidelines from the American Society of Clinical Oncology (ASCO) who recommend that resection remains the gold standard of treatment. As such the use of these ablative techniques is often reserved for unfit patients with low volume disease, as an adjunct to formal resection or in the non-curative setting.

Guidance from the National Institute for Health and Care Excellence (NICE) pertaining to the management of colorectal cancer (CG131) now recommends that surgery for metastatic disease in the liver be considered in those patients fit enough for surgery and in whom complete resection can be obtained leaving adequate FRL. The guidance goes on to suggest that liver resection is relatively contra-indicated in those with a non-treatable or recurrent primary tumour, widespread pulmonary and/or metastatic disease, extensive nodal disease or metastases in the bone or central nervous system.

Decision making in the context of extra-hepatic metastases is somewhat more complex, although it is no longer a contra-indication to potentially curative surgery. One of the largest series of pulmonary metastasectomy published by Pfannschmidt *et al* (2003) quotes a five-year survival of 32.4% with number of metastases and lymph node positivity being independently prognostic factors on both multivariate and univariate analysis. The Pulmonary Metastasectomy in Colorectal Cancer (PulMICC) trial is a currently recruiting feasibility study randomising to open/thoracoscopic surgery or active monitoring (no treatment) and will hopefully add further clarity to the role of surgery for metastatic colorectal cancer in the thorax. Extra-hepatic abdominal metastases again are no longer a contra-indication to surgery at other sites, and resection of these sites is associated with a 5-year survival of around 25% (Adam *et al*, 2011).

1.5.3 Surgical management of synchronous disease

The above described strategies apply to those patients who present with a primary tumour, and following a period of disease free survival develop metastastic disease. However, those presenting with a resectable primary tumour and synchronous metastatic disease in the liver, now thought to be approximately 14.5% of patients due to improvements in our ability to detect this radiologically, have a number of surgical options (Manfredi *et al*, 2006). In brief these are: traditional approach (primary first and then liver), reverse approach (liver first and then primary) or to synchronously (often referred to as simultaneously) resect disease at both sites within a single procedure. All of these approaches would require integration with other treatment modalities, in particular peri-operative chemotherapy and, in the case of rectal cancer, neoadjuvant radiotherapy.

It is safe to say the optimal strategy for the management of these patients remains unclear, and there is certainly an absence of level 1 evidence. A recent systematic review identified 18 papers in which 21 comparisons had been performed between at least two of these strategies (Lykoudis *et al*, 2014). A number of other smaller series exist, but for the purpose of the published systematic review only those with patient groups greater than 10 were included (Table 1.7).

Reference	Year	Duration of operation (min)*				Blood loss (ml)*		Transfused patients		Hospital stay (days)*		Morbidity (%)		In-hospital mortality (%)	
		Simultaneous approach	Staged approach												
			Total	Colorectal surgery	Liver surgery	Simultaneous	Staged	Simultaneous	Staged	Simultaneous	Staged	Simultaneous	Staged	Simultaneous	Staged
Cohort studies															
Martin *et al.*	2003	235	411§	n.s.	n.s.	550	1100§	31	38	10	18§	48	68§	2	2
Chua *et al.*	2004	370	392	n.s.	n.s.	600	575	n.s.		10	17§	53	41	0	0
Capussotti *et al.*	2007	n.s.	n.s.	n.s.	n.s.	n.s.		n.s.		n.s.		36	37	Excluded	
Thelen *et al.*	2007	260†	n.s.	n.s.	209[1]	n.s.		35	n.s.	20†	n.s.	18	n.s.	10	n.s.
Turrini *et al.*	2007	325	n.s.	n.s.	256	n.s.		n.s.		18	n.s.	21	n.s.	4	n.s.
Vassiliou *et al.*	2007	260†	340†§	n.s.	n.s.	n.s.		n.s.		12†	20†§	n.s.		0	0
Martin *et al.*	2009	180	235	n.s.	n.s.	300	350	50	45	10	18§	56	55	2	2
Slupski *et al.*	2009	250	290§	90	200	950	1040	n.s.		12	15§	n.s.		0	0
de Haas *et al.*	2010	n.s.	n.s.	n.s.	n.s.	n.s.		n.s.		n.s.		11	25§	0	1
Brouquet *et al.*	2010	n.s.	n.s.	n.s.	n.s.	300	600§	16	13	n.s.		19‡	17‡	n.s.	
Luo *et al.*	2010	255	415§	n.s.	n.s.	400	650§	n.s.		8	14§	47	54	2	2
Mayo *et al.*	2013	n.s.	n.s.	n.s.	n.s.	n.s.		n.s.		n.s.		n.s.		3	3
Martin *et al.*	2003	290	423§	n.s.	n.s.	800	1100§	n.s.		12	18§	60	70§	4	4
Capusotti *et al.*	2007	330	n.s.	n.s.	280	n.s.		42	17¶	14	21§	33	56§	3	0
Reddy *et al.*	2007	n.s.	n.s.	n.s.	n.s.	n.s.		n.s.		9	14§	44	45	n.s.	
Martin *et al.*	2009	202	268	n.s.	n.s.	450	750§	n.s.		12	18§	50	60	0	4
de Haas *et al.*	2010	n.s.	n.s.	n.s.	n.s.	n.s.		n.s.		n.s.		8	31§	0	0
Moug *et al.*	2010	n.s.	n.s.	n.s.	n.s.	475	425	n.s.		12	20§	34	59	0	0

Table 1.7 – Summary of recent evidence pertaining to the synchronous management of liver limited metastatic colorectal cancer. Reproduced with permission from Lykoudis *et al* (2014). References: *Martin et al; J Am Coll Surg (2003); 197; 233-241, Chua et al; Dis Colon Rectum (2004); 47; 1310-1316, Capussotti et al; Ann Surg Oncol (2007); 14; 195-201, Capussotti et al, Ann Surg Oncol (2007); 14; 1143-1150, Reddy et al; Ann Surg Oncol (2007); 14; 3481-3491, Thelen et al; Int J Colorectal Dis (2007); 14; 3481-3491, Turrini et al; Eur J Surg Oncol (2007); 33; 735-740, Vassiliou et al; World J Gastroenterol (2007); 13; 1431-1434, Martin et al; J Am Coll Surg (2009); 208; 842-850, Slupski et al; Can J Surg (2009); 52; E241-E244, Brouquet et al, J Am Coll Surg (2010); 210; 934-941, de Haas et al; Br J Surg (2010); 97; 1279-1289, Luo et al; J Gastrointest Surg (2010); 14; 1974-1980, Moug et al; Eur J Surg Oncol (2010); 36; 365-370, Mayo et al; J Am Coll Surg (2013); 216; 707-716.*

No significant differences in mortality were found between groups. Statistically significant differences were found in: duration of operation, blood loss, transfusion requirements, length of hospital stay and morbidity. Five studies favoured synchronous resection in terms of cumulative procedure duration and blood loss, however no difference was found in either of these variables in 3 and 4 papers respectively. 12 studies examined for length of hospital stay, all of which favoured synchronous resection. Five papers favoured the synchronous approach in terms of overall morbidity, however 8 papers failed to detect any difference. One study found increased transfusion requirements in those undergoing synchronous resection.

The authors conclude that no one strategy is inferior to the others, and that all of them should be considered in patients presenting with synchronous colorectal liver metastases. The clear contra-indication to this approach would be those patients with a symptomatic primary tumour, for example those that are bleeding and requiring transfusion, perforated tumours and those obstructing or with an imminent threat of the same. The biggest question arising from these studies is whether or not it is possible to identify subgroups of patients who would benefit from one particular strategy over another, particularly if considering that those patients presenting with synchronous disease may represent a distinct biological subtype (Silvestrini *et al*, 1990). Unfortunately the evidence is lacking, with a complete absence of prospective data and multiple inadequacies in existing cohort studies, the most appropriate course of management for these patients should be determined on an individual basis by specialty multidisciplinary teams (Abdalla *et al*, 2013).

1.6 Treatment of colorectal cancer with radiotherapy

Radiotherapy is an established adjuvant treatment for the management of colorectal cancer. As with all adjuvant treatments, the majority of patients receiving treatment, along with all the established risks, inconvenience and side-effects, will not actually benefit. This could be either because surgery alone has been curative, or because the disease will ultimately recur regardless of additional treatment received. The decision to treat cohorts of patients with common cancers with adjuvant therapy therefore stems from the concept that altering the outcome in a small proportion of patients will still translate to many hundreds or thousands of lives saved.

1.6.1 Biological effects of radiation

Radiation causes ionisation of atoms, which in turn can affect cell, tissue and organ function. Effects of radiotherapy can be divided into direct and indirect effects. Direct effects occur when, for example, radiation causes ionisation of atoms in DNA molecules, or in other molecules essential to the survival and reproduction of the cell. Given these components make up a relatively small proportion of the cell, most of the radiation will interact with intra-cellular water. The so-called indirect effects of radiation cause fragmentation of water into hydrogen and hydroxyl ions, which may recombine as water or other chemicals more harmful to the cell such as hydrogen peroxide.

The sensitivity of cells to radiation is proportional to its rate of replication. Dividing cells require correct DNA for the progeny to survive, and direct interaction of radiation with DNA may ultimately result in cellular mutation or death. The rapid cell division of a neoplastic lesion is exploited in this manner; tumour cells divide rapidly and are therefore prone to the effects of radiation. Dormant cells, which tend to be relatively hypoxic, are less sensitive to the effects of ionising radiation.

The ability of the tumour to repair damage imparted by radiotherapy is thought at least in part to reflect its resistance and response to treatment. Base excision repair proteins are a key mechanism by which small, non-helix-distorting base lesions are repaired (compared to the nucleotide excision repair pathway which repairs bulky helix-distorting lesions). Base excision repair (BER) mechanisms remove damaged bases that could otherwise cause mutations by mispairing or lead to breaks in DNA during replication. Some of the key proteins involved in this mechanism include AP endonuclease 1 (APE1) which cleaves an AP site for subsequent binding, DNA polymerase β which catalyses short-patch repair (i.e. single nucleotide replacement), and DNA ligase III along with its cofactor XRCC1 which catalyses the nick-sealing step in short-patch BER. The expression of these proteins has been investigated for potential as both biomarkers and therapeutic targets, although as yet there is insufficient evidence for incorporation into clinical practice (Vens and Begg, 2010).

Small bowel epithelia are rapidly dividing cells, and so too are prone to the effects of radiation. The risk of so-called radiation enteritis combined with the relative mobility of the colon within the abdomen poses difficulty for the use of radiation in colon cancer. As such the use of radiation is almost exclusively limited to the treatment of rectal cancer.

1.6.2 Indications for radiotherapy

The most important distinction to be made is between those tumours initially felt to be resectable and those where the planned resection margins are threatened by tumour. Beyond that, the indications for radiotherapy in rectal cancer can be divided into two broad classifications:

- Reducing the risk of local recurrence
- Shrinking locally advanced tumours to facilitate successful surgical resection

1.6.3 Short-course pre-operative radiotherapy (SCPRT)

Where the disease is already felt to be resectable, radiotherapy can be administered either pre- or post-operatively. The main advantage of pre-operative treatment is that pelvic anatomy is undisturbed and therefore toxic doses of radiation to the small bowel are less likely. Conversely, delivering the treatment post-operatively allows for better personalisation of treatment by focusing on those patients with adverse pathological features.

A regimen of irradiation which did not delay definitive surgical treatment became popular, and is now referred to as short-course pre-operative radiotherapy (SCPRT). A typical regimen is the delivery of 25Gy in five 5Gy fractions over 5 days. This approach was supported by a number of early randomised controlled trials (Goldberg *et al*, 1994; Marsh *et al*, 1994; Cedermark *et al*, 1995), the largest and most significant of which being the Swedish Rectal Cancer Trial which demonstrated improved survival and reduced local recurrence rates compared to surgery alone (Swedish Rectal Cancer Trial, 1997).

To further evaluate the role of SCPRT in the post TME era, the Dutch Colorectal Cancer Study Group trial compared SCPRT and TME surgery with TME surgery alone. A total of 1805 patients were randomised to the two groups, and whilst the overall survival at 2 years was comparable, the rate of local recurrence was 2.4% in those receiving SCPRT-TME compared to 8.2% in the group receiving TME alone (Kapiteijn *et al*, 2001). Similarly the Medical Research Council CR07 trial compared SCPRT with selective post-operative chemoradiotherapy (for those patients with CRM involvement). 1350 patients were randomised to the study, the findings of which were a 61% reduction in local recurrence and 6% increase in disease free survival at 3 years in those patients undergoing SCPRT (Sebag-Montefiore *et al*, 2009).

1.6.4 Long-course neoadjuvant chemoradiotherapy

An alternative strategy to SCPRT is the use of a longer course of radiation with a lower dose per fraction. With long-course radiotherapy, 45-50Gy is delivered over 5-6 weeks at 1.8-2.0Gy per fraction. Similarly to SCPRT, there is good evidence for improved local control but no evidence of an increase in survival benefit. Addition of concurrent chemotherapy has been shown to be more effective than radiotherapy alone, with two significant trials (EORTC 222921 and FFCD 9203) both attesting to yet further reductions in local recurrence with this strategy (Bosset *et al*, 2006; Gerard *et al*, 2006).

Only one trial has compared SCPRT and long-course CRT in patients with resectable disease (Bujko *et al*, 2006). Whilst longer courses of radiotherapy were associated with greater tumour down-staging and CRM-negative resections, it was also associated with higher rates of radiation toxicity and no improvement in local recurrence or survival.

Until recently there was doubt as to the optimum timing for long-course CRT, however the recent CAO/ARO/AI0 94 trial compared pre-and post operative chemoradiotherapy in the context of standardised TME surgery and adjuvant chemotherapy. The study reported lower recurrence rates when the radiotherapy is delivered pre-operatively (6% *vs*. 12%), as well as reduced early and late complications (Sauer, 2004).

1.6.5 Radiotherapy in locally advanced rectal cancer

Recognition of the importance of CRM involvement in predicting local recurrence has led to an increase in the use of MRI to accurately stage rectal cancer. This increasingly sophisticated technology is now being used to identify those patients with 'locally advanced disease', defined in many different ways but for the purposes of this discussion should be thought of as being tumour encroaching upon the mesorectal fascia and therefore likely to result in a positive CRM given a satisfactorily performed TME resection (MERCURY, 2006). It is from within this group of patients where the other indications for radiotherapy arises; shrinking tumours to facilitate successful surgical excision.

Given the difficulties of treating these patients with surgery alone, little evidence exists to support this strategy although two trials from the UK have attempted to answer this question. A small trial (284 patients) compared SCPRT with surgery alone, with no

difference in survival benefit or local recurrence, although the authors did perceive a marginal survival benefit in a subgroup analysis of those patients believed by the surgeon to have had a curative resection (Marsh *et al*, 1994). A larger trial with longer follow-up compared long-course CRT with surgery alone, favouring long-course CRT for local recurrence (hazard ratio 0.68), distant recurrence (hazard ratio 0.66) and disease-free survival (hazard ratio 0.76), all of which were statistically significant (Medical Research Council Rectal Cancer Working Party, 1996).

One other potential advantage of neoadjuvant chemoradiotherapy is the potential for converting a planned abomino-perineal resection of the rectum into an anterior resection as a result of tumour shrinkage, thus performing a sphincter-preserving procedure and sparing the patient from a permanent stoma and the morbidity of a significantly more invasive operation. However it would seem that the evidence for this notion is anecdotal, as a recent systematic review of 10 randomised controlled trials comparing neo-adjuvant radiotherapy and surgery with surgery alone failed to find any difference in permanent stoma rates between experimental and control arms (Bujko *et al*, 2006).

1.6.6 Other uses of radiotherapy

Thus far, the role of radiotherapy has only been considered in the curative setting. This may be assumed to be external beam radiotherapy delivered by a linear accelerator, however there are other roles for radiotherapy in patients with rectal cancer.

The application of direct contact radiotherapy, for example using the Papillon system, has been shown to be a safe and effective treatment for early rectal cancers in those patients not suitable for definitive surgical treatment. A study of 220 patients with T1-T3 tumours less than 3cm in diameter was reported from the Clatterbridge Centre of Oncology. The authors report a local control rate of 93% with no significant morbidity in any patient, accepting that their population was highly selective and that close follow-up and plans for salvage surgery are required (Myint *et al*, 2007).

Radiotherapy has also been shown to be advantageous in the palliative setting, be that in those not suitable for surgical intervention or those who have experienced disease recurrence. Radiotherapy at a total dose of 20-60Gy can provide relief of pain and bleeding in 75% of patients for a median duration of 6-9 months (Saltz, 2004). The role of intra-

operative radiotherapy (IORT) for those patients with T4 disease is still under investigation, with the most recent evidence suggesting an improved local recurrence free survival in patients with microscopically involved margins at the time of resection. A study of 409 patients who underwent surgery for locally advanced or recurrent rectal cancer identified 48 with a microscopically involved CRM. Within this cohort those who received IORT (n=31 *vs*. n=17) benefited from a significant difference in cumulative 5-year local recurrence free survival (84% *vs*. 41%; p=0.01) (Alberda *et al*, 2014). No evidence from randomised trials is as yet available and case series remain small, however the results are promising for appropriately selected patients.

1.7 Chemotherapeutic agents used in colorectal cancer

Before 2000, the only agent available for the treatment of metastatic and advanced colorectal cancer was 5-flourouracil (5-FU), which still remains the cornerstone of treatment. Indeed it is still an oral pro-drug of 5-FU (capecitabine) which is used as monotherapy alongside neoadjuvant radiotherapy in the treatment of locally advanced rectal cancer.

The development of alternative agents however has revolutionised our approach to the management of these patients, with combination regimens now considered standard therapy. The most commonly used chemotherapeutic agents in colorectal cancer are 5-fluorouracil and oxaliplatin, which are combined with leucovorin in a regimen known as FOLFOX. An alternative strategy is the combination of fluorouracil and irinotecan with leucovorin (FOLFIRI), or 5-fluorouracil with oxaliplatin, irinotecan and leucovorin (FOLFIRINOX). Our increasing understanding of tumour biology has also led to the development of biological agents, the most common being cetuximab, panitumumab and bevacizumab. These agents are frequently used in combination with existing chemotherapeutic regimens.

Evidence for the use of specific regimens will be discussed, but first we shall consider the mechanism of action of each of these agents individually.

1.7.1 5-fluorouracil (5-FU)

5-FU is a fluropyrimidine anti-metabolite. The drug was designed, synthesized and patented in 1957 as an analogue of uracil, a normal component of RNA. The analogue substitutes a hydrogen for fluorine atom at the C5 position and is a specific competitive antagonist for uracil. Its misincorporation into RNA and DNA arrests RNA synthesis and therefore halts tumour growth.

As well as being incorporated into macromolecules, 5-FU is converted intra-cellularly into a number of active metabolites which disrupt biological function: fluorodeoxyuridine monophosphate (FdUMP), fluorodeoxyuridine triphosphate (FdUTP) and fluorouridine triphosphate (FUTP). It is these active metabolites which inhibit thymidylate synthetase (TS), a nucleotide synthetic enzyme which is thought to be the main target for 5-FU (Figure 1.3). The exact downstream effect of this is unclear, although this action is thought to result in dinucleotide pool imbalances and increased levels of deoxyuridine triphosphate (dUTP), both of which can cause DNA damage (Yoshioka *et al*, 1987).

The drug is predominantly catabolised by dihydropyrimidine dehydrogenase (DPYD), which converts 5-FU to dihydrofluorouracil (DHFU), with around 80% of this occurring in the liver (Diasio and Harris, 1989).

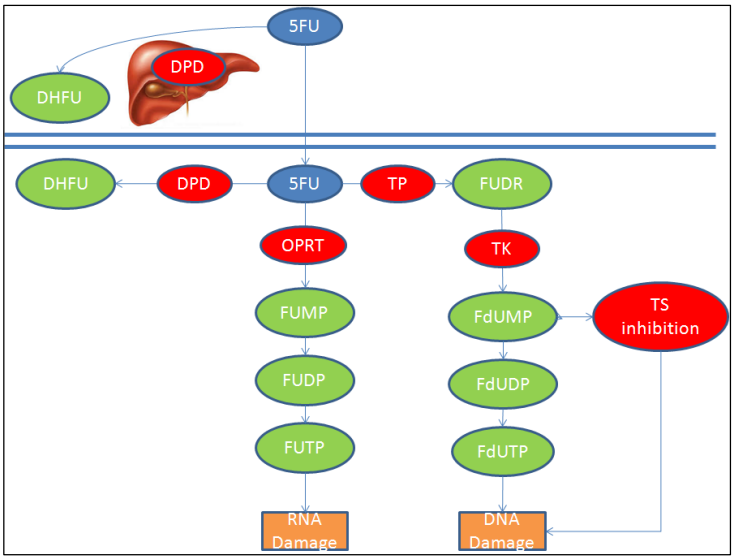

Figure 1.3 – 5-Fluorouracil metabolism – 5-fluorouracil (F-FU) is converted to three main metabolites: fluorodeoxyuridine monophosphate (F-dUMP), fluorodeoxyuridine triphosphate (FUTP) and fluorouridine triphosphate (FUTP). The main mechanism of 5-FU activation is conversion to fluorouridine monophosphate (FUMP) by orotate phosphoribosyltransferase (OPRT). FUMP is then phosphorylated to fluorouridine disphoaphate (FUDP) and again to fluorouridine triphosphate (FUTP). Alternatively, thymidine phosphorylase (TP) can activate 5-FU by catalysing the conversion of 5-FU to fluorodeoxyuridine (FUDR) which is then phosphorylated by thymidine kinase (TK) to FdUMP. FdUMP can be phosphorylated to fluorodeoxyuridine diphosphate (FdUDP) and again to fluorodeoxyuridine triphosphate (FdUTP). 80% of 5-FU is catabolised in the liver by dihydropyrimidine dehydrogenase (DPYD). Adapated from Longley, Harkin and Johnston, 2003.

Common side-effects include nausea, vomiting, diarrhoea, mucositis, headache, myelosuppression, alopecia and photosensitivity.

1.7.2 Leucovorin

High intra-cellular levels of the reduced folate, leucovorin (folinic acid), are required for optimal binding of FdUMP to TS. Leucovorin is transported into cells via the reduced folate transporter, anabolised and polyglutamated. These steps not only increase intra-cellular retention but further help stabilise the complex formed with FdUMP and TS, and as such it

is widely accepted that co-administration of leucovorin increases 5-FU toxicity both *in vitro* and *in vivo* (Wright, 1989).

1.7.3 Capecitabine

An alternative approach to the delivery of 5-FU has been the design of oral pro-drugs which avoid the DPYD mediated catabolism in the liver. Capecitabine is an oral fluoropyrimidine which is absorbed via the gastrointestinal tract and converted in the liver to 5'-deoxy-5-fluorouridine (5'DFUR) by the enzymatic action of carboxylesterase and cytidine deaminase (Johnston and Kaye, 2001). 5-DFUR is ultimately converted to 5-FU by thymidine phosphorylase (TP) and uridine phosphorylase (UP). The higher abundance of these enzymes in tumour tissue is thought to account for the more tumour-specific conversion of capecitabine to 5-FU (Schuller *et al*, 2000).

1.7.4 Irinotecan

Irinotecan is a semi-synthetic analogue of the alkaloid camptothecin. Its mechanism of action is by direct interaction with topoisomerase I (Top I). The role of Top I is uncoiling DNA ready for transcription by inflicting single-strand DNA breaks which ultimately are repaired. Irinotecan binds to the DNA/Top I complex and stabilises these breaks, resulting in DNA fragmentation and cell death.

Irinotecan is a pro-drug, which is converted to its active metabolite, SN-38, by human carboxylesterases CES1 and CES2. Irinotecan can also undergo CYP3A4 mediated oxidative metabolism to form APC and NPC, both of which are inactive however NPC can be further hydrolysed by carboxylesterase to release SN-38 (Mathijssen *et al*, 2001). The biochemistry of the drug is outlined in Figure 1.4.

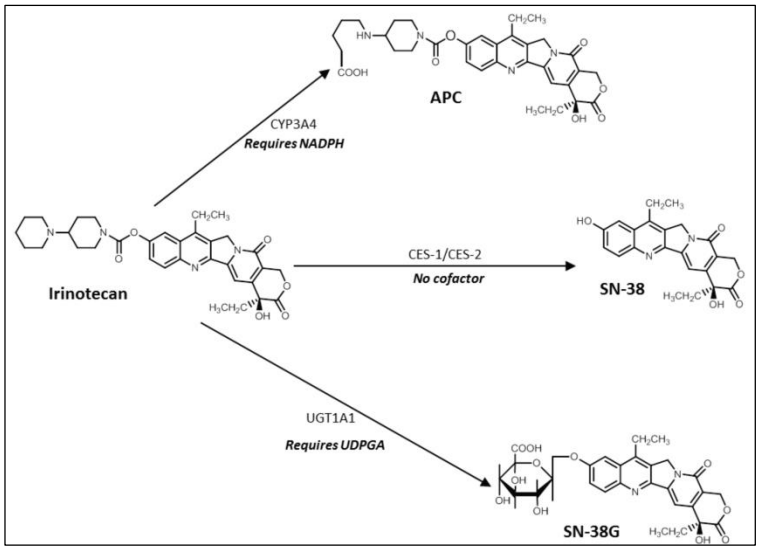

Figure 1.4 – The metabolism of irinotecan (CPT-11). Irinotecan is converted to the active metabolite SN38 by carboxylesterase (CE), as well as to two other inactive metabolites (NPC and APC) by CYP3A4. NPC can subsequently be converted by SN-38 by CE. Inactivation to SN38-G is predominantly controlled by UGT1A1, however the inactive metabolite can be re-activated to SN38 by β-glucuronidation. Adapted from Mathijssen *et al*, 2001.

Irinotecan is conjugated by UDP-glucuronosyl-transferases, the most active form of which is 1A1 (UGT1A1). A common polymorphism in UGT1A1, known as UGT1A1*28, is characterised by the presence of an additional TA repeat in the TATA sequence of the UGT1A1 promoter. Individuals with this polymorphism are at significantly higher risk of developing the most common and severe side effects of irinotecan, diarrhoea and neutropenia (Iyer *et al*, 2002). The glucuronidated product is SN38-G, which can be deglucuronidated by intestinal β–glucuronidase (β-Glu) back to the active metabolite SN38.

1.7.5 Oxaliplatin

Oxaliplatin is a platinum based chemotherapeutic which was discovered in 1976. Its chemical structure features a square planar platinum centre, the bidentate ligand 1,2-diaminocychlohexane (DACH) and a bidentate oxalate group.

Its anti-tumour effects are non-targeted, although oxaliplatin undergoes intra-cellular transformation into a number of active metabolites all of which contain a DACH ring. These

metabolites form inter- and intra-stand cross links in DNA which prevent replication and transcription (Graham, Mushin and Kirkpatrick, 2004).

In a similar way to the patterns of resistance described for radiotherapy, resistance to oxaliplatin is thought to stem from the cell's ability to repair DNA damage. These mechanisms include nucleotide-excision repair (NER) and mismatch repair (MMR), however the major system responsible for the removal of corrupt DNA bases and repair of DNA single strand breaks is the base excision repair (BER) system (Sharma and Dianov, 2007). In particular deficiency in the most significant DNA polymerase, polymerase-β, has been shown to render cells hypersensitive to oxaliplatin therapy (Yang *et al*, 2010).

1.7.6 Biological agents

In recent years significant advances have been made in developing novel small molecule inhibitors of extracellular receptors. Extracellular growth factor receptor (EGFR) is a transmembrane glycoprotein which is a member of the ErbB receptor tyrosine kinase group, mutations in which are known to result in carcinogenesis (Zhang *et al*, 2007).

EGFR is activated by the binding of specific ligands, most commonly epidermal growth factor (EGF) and transforming growth factor α (TGFα). Upon binding EGFR undergoes transformation to an active homodimer stimulating intrinsic intracellular protein-tyrosine kinase activity and a cascade of autophosphorylation resulting in increased signal transduction principally through the PI3K/AKT/MTOR and RAS/RAF/MEK/ERK pathways. This activation activates a number of cell-cell adhesion, DNA synthesis and cell proliferation pathways responsible for carcinogenesis.

Cetuximab is a chimeric mouse/human monoclonal antibody and panitumumab is a fully human monoclonal antibody, both of which target EGFR directly (Figure 1.5). Their use is confined to those tumours who express EGFR and who are *KRAS* wild type, as the key role of this gene in subsequent downstream signalling means that these drugs have little or no effect if the KRAS gene is mutated (Messersmith and Ahnen, 2008). Specifically a mutated *KRAS* will continue to trigger downstream signal activation even following inhibition of EGFR.

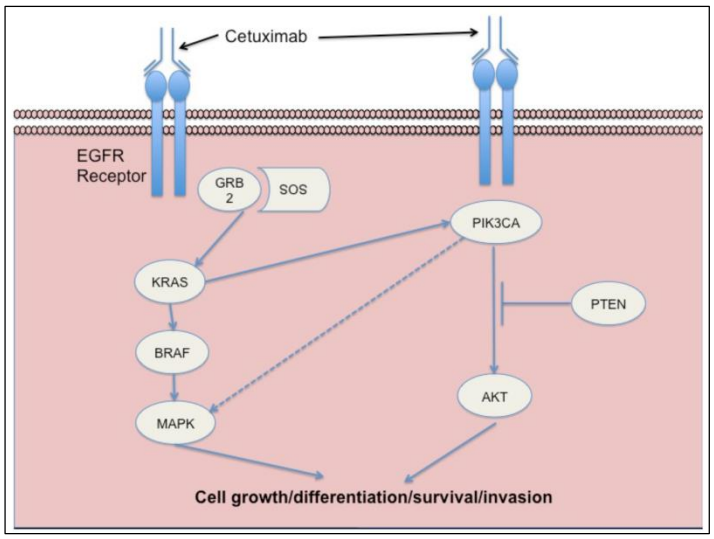

Figure 1.5 – Binding of a ligand (EGF, TGFα) to EGFR stimulates receptor dimerisation, tyrosine kinase activation, EGFR autophosphorylation and ultimately initiates signal transduction cascades involved in cell proliferation and survival. Inhibition of EGFR by the monoclonal antibody cetuximab inhibits these downstream events. Adapted from Kirkpatrick, Graham and Muhsin, 2004.

An alternative approach to inhibiting this pathway is to use small molecule inhibitors, which act on the cytoplasmic side of the receptor to reduce EGFR tyrosine kinase activity. Without this activity, EGFR is unable to autophosphorylate, and therefore downstream signalling is halted and tumour proliferation reduced. Drugs used in this category include gefitinib, erlotinib and lapatanib although none of these are as yet in widespread use for colorectal cancer.

Vascular endothelial growth factor (VEGF) is an important regulator of angiogenic factors crucial for tumour growth and metastasis, activation of which is pro-angiogenic. Bevacizumab is a human monoclonal antibody which binds directly to VEGF and forms a complex which is unable to bind to any other VEGF receptors. This essentially reduces the amount of VEGF available resulting in inhibition of angiogenesis (Los, Roodhart and Voest, 2007).

1.8 Treatment of colorectal cancer with chemotherapy

Chemotherapy regimens with 5-FU as the cornerstone remain a widely used treatment for advanced colorectal cancer, which in the adjuvant setting is thought to confer a 5-10% improvement in absolute survival (Haydon, 2003).

The vast majority of evidence for the use of chemotherapy in colorectal cancer pertains to colon cancer only, with its use in rectal cancer inferred and therefore the subject of much debate. A number of questions remain, including the optimum regimen, route of administration and the potential for combination with other chemotherapeutic or biological agents. Uncertainties still exist around optimum patient selection, in particular the role of chemotherapy in patients with stage II disease.

1.8.1 The evidence for 5-FU

A number of early trials explored the role of 5-FU in advanced colorectal cancer. The quality of these studies was poor, and a meta-analysis performed in 1988 failed to show any survival benefit (Buyse, Zeleniuch-Jacquotte and Chalmers, 1988).

Shortly after this, a large randomised control trial clearly demonstrated a survival benefit following 12 months of 5-FU combined with levamisole (an immunomodulator) when compared to either agent as monotherapy or observation alone (Laurie *et al,* 1989). These findings were confirmed in a subsequent larger trial of 1296 patients (Moertel *et al*, 1990), which led to the recommendation and subsequent adoption of this regimen as standard practice (NIH Consensus Conference, 1990).

Interest subsequently turned to the combination of 5-FU with leucovorin/folinic acid, with one of the most significant trials addressing this being the Quick and Simple and Reliable (QUASAR) study. The trial was a two x two design whereby 4927 patients with colorectal cancer but without residual disease were randomly assigned to receive fluorouracil with high dose or low-dose folinic acid, and either active of placebo levamisole. On an intention to treat analysis for all cause mortality, the inclusion of levamisole in chemotherapy regimens did not improve survival, and high dose folinic acid conferred no additional benefit to low-dose folinic acid (QUASAR Collaborative Group, 2000). Although not randomly allocated, those patients receiving a once weekly bolus regimen suffered less toxicity with equivalent efficacy to those receiving five consecutive days every 4 weeks

(referred to as the 'Mayo regimen'). As a result of this the weekly regimen of 5-FU with low dose folinic acid was widely adopted in the UK.

1.8.2 Combination regimens

Over recent years a number of trials have combined 5-FU with other chemotherapy agents. The MOSAIC trial of 2246 patients compared 5-FU/Folinic Acid with 5-FU/Folinic Acid/Oxaliplatin, and found an increase in 3-year disease free survival from 72.9% to 78.2% (Andre *et al*, 2009). A subgroup analysis within this study also reported a small improvement (72.9% *vs*. 68.3%) in overall survival for stage III but not stage II patients. The NSABP-C07 trial similarly reported 3-year disease free survival rates of 71.8% increasing to 76.1% with the addition of oxalipatin (Kuebler, 2007). Both trials noted the increased disease-free survival came at the cost of significant neurosensory toxicity associated with the use of oxaliplatin, however this regimen was widely adopted across Europe.

Few trials have looked at combining irinotecan in the adjuvant setting. The CALGB 89803 study randomised 1264 patients with completely resected stage III colon cancer to either 5-FU/Leucovorin or 5FU/Leucovorin/Irinotecan, each regimen being delivered by single weekly bolus infusion. Powered for disease free survival and overall survival, no differences were found between groups although significant additional toxicity was reported with the use of irinotecan (Saltz *et al*, 2000). Similar findings were seen in the Pan-European Trials in Alimentary Cancer (PETACC-3) study, with 2094 patients recruited into a similar trial design demonstrating comparable 5-year disease free survival (73.6% *vs.* 71.3%) (Van Cutsem *et al*, 2009). No trials have as yet compared 5-FU/Leucovorin/Oxaliplatin with 5-FU/Leucovorin/Irinotecan for its efficacy in the adjuvant treatment of stage II-III disease.

1.8.3 Adjuvant chemotherapy for colorectal liver metastases

Chemotherapy following resection of colorectal liver metastases (i.e. patients with stage IV disease) aims to maximise survivorship by treating occult residual disease (Chong and Cunningham, 2005). The role of adjuvant chemotherapy in this setting however remains unclear.

The FFCD AURC 9002 trial randomised 171 patients with complete R0 resection of liver metastases to either observation or adjuvant chemotherapy with a 5-FU/Leucovorin

regimen. Whilst the trial failed to recruit to fulfil its primary end-point of overall survival, there was a significant increase (33.5% *vs*. 26.7%) in 5-year disease free survival in the chemotherapy group (Portier *et al*, 2006).The EORTC 0923 trial was a further similarly designed trial which again failed to adequately recruit to demonstrate any potential difference in overall survival (Mitry *et al*, 2008). The authors of this trial went on to pool their data with the FFCD AURC 9002 trial, reporting a median overall survival of 62.2 months *vs*. 47.3 months favouring adjuvant chemotherapy, although this did not reach statistical significance.

The efficacy of combination chemotherapeutic regimens is also unclear. A randomised trial of patients having had R0 resection of colorectal liver metastases comparing 5-FU/Leucovorin with FOLFIRI reported comparable 2-year disease free survival (51% *vs*. 46%) (Ychou *et al*, 2009).

Despite an absence of clear trials evidence for its efficacy, many clinicians still opt to manage this patient group with adjuvant chemotherapy. Decisions like this must take into account the likelihood of disease clearance at the time of surgery, patient preference, perceived efficacy and the burden of morbidity associated with treatment.

1.8.4 Neoadjuvant chemotherapy for colorectal liver metastases

The role of neo-adjuvant chemotherapy for gastrointestinal cancer was initially defined by the MAGIC trial (Cunningham *et* al, 2006) for oesophago-gastric carcinoma. The potential reduction in disease volume may ensure optimum clearance at the resection margin (for example in the primary tumour) or greater sparing of the surrounding parenchyma (for example in the liver and lung). In addition the chemotherapy will treat those micro-metastases not detectable on cross-sectional imaging, which may result in longer disease-free survival. Finally the test of systemic treatment and evaluation of its response provides interesting and clinically useful information about the tumour biology, from which predictive and prognostic information can be inferred.

The safety and tolerability of neoadjuvant chemotherapy was defined in a number of early phase 2 studies. The successful delivery of 99% of scheduled 5-fluorouracil and 99% of scheduled oxaliplatin associated with a 50% post-operative morbidity and 0% mortality (Wein, 2003), and the comparable compliance between neoadjuvant FOLFOX and adjuvant

FOLFIRI associated with a 97% delivery and no operative mortality (Taieb *et al*, 2005) attest to this.

The efficacy of neoadjuvant treatment has also been assessed, although available data is limited. A large retrospective study of 1471 patients compared neoadjuvant chemotherapy (FOLFOX) with surgery alone (Adam *et al*, 2010). Preoperative chemotherapy did not appear to improve overall survival (60% at 5 years in both groups), however adjuvant chemotherapy did (65% *vs*. 55%, p<0.01). Perhaps more concerningly the incidence of postoperative complications was significantly higher in those patients who received neoadjuvant chemotherapy (37.2% *vs*. 24.0%, p=0.006).

The largest trial to investigate this date is the EORTC 40983 study (EPOC trial) which randomised 364 patients with up to four resectable colorectal liver metastases to 12 cycles of peri-operative FOLFOX (half delivered prior to surgery and half after) or surgery alone (Nordlinger *et al*, 2008). Powered for 3-year progression free survival, 152 patients from each arm underwent resection with dropout attributed to disease progression. On an intention to treat basis the median overall survival was 61.3 months in the perioperative chemotherapy group and 54.3 months in the surgery alone group, with 5-year survival of 51.2% and 47.8% respectively (p=0.34). For those who underwent resection, 3-year progression free survival was 36.2% in the perioperative chemotherapy arm compared to 28.1% in the surgery arm (HR 0.77, 95% CI 0.60-1.00; p=0.041). This finding combined with the non-statistically significant trend towards increased survival has led to the uptake of this management strategy in a number of units, however a potential criticism is the exclusion of the higher risk population with more than 4 metastases.

The role of neoadjuvant chemotherapy in the context of non-metastatic disease is even less clear. The FOXTROT trial is currently recruiting patients with colonic T3-4 tumours to be randomised to receive preoperative oxaliplatin, folinic acid, fluorouracil and panitumumab followed by surgery and adjuvant chemotherapy, or surgery and adjuvant chemotherapy combined with panitumumab (Foxtrot Collaborative Group, 2012). The feasibility study has been completed and the trial remains open.

1.8.5 Chemotherapy for irresectable disease

As our ability to accurately stage disease and our understanding of tumour biology improves it is becoming increasingly clear that a significant proportion of patients have irresectable disease. Treatment in this setting with the chemotherapeutic regimens already discussed must be decided in partnership with the patient taking into account co-morbidity, performance status, prognosis and quality of life. Irresectable disease of the primary is unlikely to change significantly with systemic treatment, but it has become apparent that a proportion of patients with colorectal liver metastases will have such a significant treatment effect that their disease may in fact become technically resectable.

The conversion to resectability in the liver is estimated to be around 6-60%, with variation reflecting patient and disease factors, choice of chemotherapeutic regimen, proportion of treatment course completed and local unit approach to surgical resection (Poston, 2008). In the situation where disease is converted to resectability, the 5 year survival is comparable to those patients who underwent resection at the time of presentation – approximately 35-50% (Adam *et al*, 2001). It is not surprising that tumour response to chemotherapy correlates with resection rate; information which should be borne in mind when managing this cohort (Folprecht *et al*, 2005).

NICE currently recommends the use of FOLFOX (with cetuximab if appropriate) as first line treatment for all patients with unresectable liver-limited metastatic colorectal cancer with FOLFIRI reserved for second line treatment. In this setting the efficacy of the two regimens is thought to be comparable (Tournigand *et al*, 2004), although the significant toxicity associated with FOLFIRI may limit its usefulness (Innocenti and Ratain, 2004).

1.8.6 Cetuximab

Extensive trial derived evidence exists for the incorporation of cetuximab into modern chemotherapeutic regimens for selected patients determined by *KRAS* status.

In 2009 the CRYSTAL trial randomised 599 patients to each of FOLFIRI and FOLFIRI plus cetuximab (Van Cutsem *et al*, 2009). All patients had unresectable disease and epidermal growth factor receptor positive tumours. No difference was seen in overall survival between the two groups, however progression-free survival was considerably greater in those receiving cetuximab (hazard ratio 0.85; p=0.048). There was a significant interaction between treatment group and *KRAS* mutation for tumour response, but not progression-

free or overall survival. Resectability rates (irrespective of *KRAS* status) were 7% for FOLFIRI plus cetuximab compared with 3.7% for FOLFIRI alone, with R0 rates of 4.8% *vs*. 1.7% (p=0.002). This increase in tumour response was associated with an increase in skin reactions (19.7% *vs*. 0.2%), infusion-related reactions (2.5% *vs*. 0%) and diarrhoea (15.7% *vs*. 10.5%).

The OPUS trial was again confined to patients with epidermal growth factor-expressing tumours, however here the combination of cetuximab and FOLFOX was compared to FOLFOX alone with treatment continued until disease progression or unacceptable toxicity. A total of 337 patients were randomised, with no statistically significant difference in response rate (46% *vs*. 36%; p=0.06). In those with tissue available for KRAS mutation status (n=233), subgroup analysis showed that in KRAS wild-type tumours the addition of cetuximab to FOLFOX was associated with a significant increase in treatment response (61% *vs*. 37%; p=0.011). In this study cetuximab was generally well tolerated, with no reports of significant adverse events (Bokemeyer *et al*, 2011).

The EPIC trial was a large trial of 1298 patients with metastatic colorectal cancer who had experienced first line failure to 5-fluorouracil and oxaliplatin (Sobrero *et al*, 2008). Patients received either irinotecan monotherapy or irinotecan plus cetuximab. No difference was identified in overall survival (for which the trial was powered), with the authors attributing this to significant variations in post-trial treatment. Cetuximab did however significantly improve both tumour response rate (16.4% *vs*. 4.2%; p=<0.0001) and progression free survival (4.0 *vs*. 2.6 months; p=<0.0001).

A smaller group of patients with irresectable colorectal liver metastases were studied in the CELIM phase 2 trial (Folprecht *et al*, 2010). 114 patients were randomised to receive cetuximab with either FOLFOX or FOLFIRI. Randomisation between groups was stratified by technical resectability and number of metastases as determined by PET scan, as well as epidermal growth factor receptor expression status. Patients were assessed every 8 weeks, and if the locally treating multidisciplinary team deemed the disease to be potentially resectable they were offered surgery. Whilst the trial showed largely comparable response rates and toxicity between groups, a retrospective analysis of response by *KRAS* status showed a partial or complete response in 70% of those with wild-type tumours compared with 41% with *KRAS* mutated tumours (OR 3.42; p=0.008). Further review of the

retrospective data suggested that resectability rates increased from 32% at baseline to 60% following chemotherapy (p<0.0001)

More recently the UK COIN trial (2012) compared continuous oxaliplatin/capecitabine (OxCap) and oxaliplatin/leucovorin/infusional 5-FU (OxFU) with or without cetuximab. The trial reported comparable efficacy between OxFU and OxCap, and the addition of cetuximab to OxFU resulted in less diarrhoea and longer progression free survival than for its combination with OxCap. As a natural progression to the EPOC trial (see Section 1.8.4), New EPOC (2014) compared perioperative treatment with chemotherapy (FOLFOX/FOLFIRI) with chemotherapy plus cetuximab for *KRAS* wild-type patients with resectable colorectal liver metastases, and was halted after an interim analysis reported significantly shorter progression free survival in the chemotherapy plus cetuximab group than in the chemotherapy group alone (14.1 months *vs*. 20.5 months, HR 1.48). The trial authors concluded that further translational investigation is needed to explore the molecular basis for the unexpected interaction.

1.8.7 Bevacizumab

Hurwitz *et al* (2004) reported the first randomised trial of 813 patients with metastatic disease to receive IFL (irinotecan, bolus 5-FU and leucovorin) or IFL plus bevacizumab. Patients receiving bevacizumab benefited from increased median survival (20.3 *vs*. 15.6 months; p=<0.001) and progression free survival (10.6 *vs*. 6.2 months; p=<0.001).The GONO group have also reported their experience of combining FOLFIRINOX with bevacizumab in 57 patients with unresectable metastatic disease (Masi *et al*, 2010). Progression free survival at 10 months was 74% (95% CI 62-85), with similar incidences of adverse events to those previously reported.

The bevacizumab expanded access trial (BEAT) is the largest study documenting the success of this targeted biological agent in patients with unresectable colorectal liver metastases (Van Cutsem *et al*, 2009). Patients were treated with their physician's choice of chemotherapy plus bevacizumab in a non-randomised fashion. The study was predominantly designed to observe safety rather than efficacy, and of the 1914 patients assessed the serious adverse events reported included bleeding (3%), gastrointestinal perforation (2%), arterial thromboembolism (1%), hypertension (5.3%), proteinuria (1%) and wound complications (1%). The sixty-day mortality was 3%, median progression free

survival 10.8 months and overall survival 22.7 months. Overall resection was performed in 7.6% of patients and 15.2% of those with disease confined to the liver, the 2-year survival for which was 89%.

In the United States similar findings were reported in the BRiTE study (Grothey *et al*, 2008). A large observational study of 1445 previously untreated patients with metastatic colorectal cancer classified patients who experienced disease progression into: no treatment post disease progression (n=253), treatment without bevacizumab (n=531) and treatment with bevacizumab (n=642). Baseline factors were well balanced between groups, with reported overall survival rates of 12.6, 19.9 and 31.8 months respectively. Multivariate analyses strongly and independently associated the use of bevacizumab with improved survival (HR 0.48; $p<0.01$), highlighting the role of continued vascular endothelial growth factor inhibition in improving survival following the detection of recurrent disease.

The TREE study randomised patients into three different oxaliplatin/5-fluorouracil regimens – mFOLFOX6 (bolus and infusion fluorouracil and leucovorin with oxaliplatin), bFOL (bolus fluorouracil and low-dose leucovorin with oxaliplatin) or CapeOX (capecitabine with oxaliplatin). A second cohort (referred to as TREE 2) received the above regimens in combination with bevacizumab. For all patients the median overall survival was 18.2 months (95% CI 14.5-21.6) in TREE 1 and 23.7 months (95% CI 21.3-26.8) in TREE 2, highlighting that the addition of bevacizumab to fluoropyrimidine based chemotherapy regimens as first line treatment can significantly improve overall survival (Hochster *et al,* 2008).

Modest improvements in progression free survival attributed to the addition of bevacizumab were also noted in the N016966 phase III randomised trial (9.4 *vs*. 8.0 months; p=0.0023), where FOLFOX was used as the chemotherapeutic backbone (Cassidy *et al*, 2008). The smaller BOXER trial has also reported a conversion rate to resectability of 40% in a cohort of 46 patients receiving neoadjuvant capecitabine, oxaliplatin and bevacizumab (Wong *et al*, 2010).

1.9 Asssessment of response to chemoradiotherapy

There is an extremely variable response to both radiotherapy and chemotherapeutics, irrespective of the setting in which the treatment is delivered. Uncertainty also exists as to

when this response to treatment should be assessed. Radiation, for example, induces an inflammatory reaction such that re-staging the patient immediately after cessation of treatment is likely to result in a considerable under-estimate of tumour response. In addition, the response to radiotherapy continues for several weeks after the completion of treatment. Radiation will initially affect those cells which are actively dividing, however its effects will be latent in those cells which were in the resting (G0) part of the cycle when the tumour was irradiated. As these cells begin the process of cell division it becomes apparent that they will be unable to successfully divide, and therefore upon reaching checkpoints in the cell-cycle are signalled to undergo apoptosis. Patients receiving chemotherapy also exhibit variation in response to their treatment, and individuals with advanced disease are commonly seen to suffer disease progression despite intense combination regimens.

In clinical practice, the response to neoadjuvant treatment is normally achieved with radiological re-staging of the tumour in the manner previously described, i.e. CT scan of the chest, abdomen and pelvis as well as MRI scan of the rectum in the case of rectal cancer (with close attention to the proximity of the tumour to the mesorectal fascia). Alternatively response to treatment can be determined histopathologically following tumour resection.

1.9.1 Radiological response to treatment

Standardisation of response reporting first began in the late 1970s as a collaboration between the International Union Against Cancer and the World Health Organisation (Miller *et al*, 1981). Given the rapid advances in both technology and medicine, an international group consisting of members from the European Organisation for Research and Treatment of cancer (EORTC), the United States National Cancer Institute (NCI) and the Canada Clinical Trials Group set out to refine these response criteria in 1994. The guidelines published are referred to as the Response Evaluation Criteria in Solid Tumours (RECIST) guidelines (Therasse *et al*, 2000).

At baseline, all lesions are originally categorised as either measurable or nonmeasurable. Measurable lesions can be accurately measured in at least one dimension (with the longest dimension to be recorded) as ≥20mm with conventional techniques or as ≥10mm with spiral CT scan. All measurable lesions up to a maximum of 5 lesions per organ and 10 in total are measured with callipers or a rule. These so-called target lesions should be selected on the basis of their size (those with the longest diameter) and suitability for repeated

measurements. The sum of these longest diameters is calculated and referred to as the baseline sum longest diameter. All other lesions are referred to as non-target lesions; measurements are not necessary however their presence or absence during treatment and follow-up should be noted.

The same exercise is repeated following treatment, and an assessment of response allocated to both the target (those previously identified as such) and non-target lesions. In the target lesions: *complete response* is defined as the disappearance of all lesions, *partial response* is at least a 30% reduction in the sum of the longest diameter when compared to the baseline sum longest diameter, *progressive disease* is at least a 20% increase in the sum of the longest diameter and *stable disease* as neither sufficient shrinkage to qualify for progressive disease. In the non-target lesions: *complete response* is the disappearance of all nontarget lesions, *incomplete response/stable disease* as the persistence of one of more non target lesions, and *progressive disease* as the appearance of one or more new lesions and/or unequivocal progression of existing nontarget lesions.

Following widespread adoption in clinical practice and cancer research, these criteria were later modified in 2008 to RECIST v1.1. In brief, the changes made included a reduction in the number of target lesions from 10 to 5, and a maximum of two per organ, an inclusion of pathological lymph nodes as target lesions (assuming a short axis of ≥15mm), and a change to the use of short axis measurements in the sum of lesions for the calculation of tumour response. In addition the definition of disease progression was further clarified, in that in addition to the previously defined 20% increase in the sum of the target lesions, a 5mm absolute increase is also necessary to label the patient as having disease progression (Eisenhauer *et al*, 2008).

1.9.2 Pathological response to treatment

The prequel to the majority of tumour regression grade (TRG) scoring systems originated from an early paper whereby pathological response to treatment was correlated with outcome in oesophageal cancer (Mandard *et al*, 1994). In this paper, TRG was quantified as one of five grades: TRG1 (complete regression) showed absence of residual cancer and fibrosis extending through the oesophageal wall; TRG 2 was characterised by the presence of rare residual cancer cells scattered through the fibrosis; TRG 3 was characterised by an increase in the number of residual cancer cells but fibrosis still predominated; TRG 4

showed residual cancer outgrowing fibrosis; and TRG 5 was characterised by absence of regressive changes. On univariate analysis, tumour size, lymph node status, TRG and oesophageal wall involved correlated with disease free survival, however after multivariate analysis only TRG (at this point dichotomised as 1-3 *vs.* 4-5) remained a significant predictor of disease free survival.

Shortly after this Dworak, Keilholz and Hoffman (1997) published a grading system specifically for the regression of rectal tumours after neoadjuvant chemoradiotherapy, grading regression from GR0-GR4 (Table 1.8) after assessing tumour mass, fibrotic change, irradiation vasculopathy and peri-tumourous inflammatory reaction. Similarly to the original report by Mannard *et al*, this system was later shown to have prognostic value in predicting outcomes in rectal cancer (Losi *et al*, 2006).

Tumour Regression Grade	Description
0	No regression
1	Dominant tumour mass with obvious fibrosis and/or vasculopathy
2	Dominant fibrotic changes with few tumour cells or groups (easy to find)
3	Very few (difficult to find microscopically) tumour cells in fibrotic tissue with or without mucous substance
4	No tumour cells, only fibrotic mass (total regression)

Table 1.8 - The tumour regression grade proposed by Dworak, Keilholz and Hoffmann (1997) extends from 0-4 and includes an assessment of tumour mass as well as the degree of fibrosis and/or vasculopathy. Reproduced without permission from Santos *et al*, 2014.

The publication from Dworak, Keilholz and Hoffman (1997) was followed by a simplified 3 point scale known as the Rectal Cancer Regression Grade (RCRG): RCRG1 – the tumour is either sterilised or only microscopic foci remain; RCRG2 – marked fibrosis but with macroscopic tumour still present; and RCRG3 – little or no fibrosis in the presence of abundant macroscopic tumour. RCRG1 and 2 are considered to represent significant tumour regression (Wheeler *et al*, 2002).

More recently the Royal College of Pathologists have produced a minimum dataset for reporting in colorectal cancer. Originally a 3 tier system was utilised, although a 4 tier

system is now endorsed based on the classification by Ryan *et al* (2005). The 4 tier system allows classification of tumour regression as: 0 – Full tumour regression, no visible tumour cells; 1 – Moderate tumour regression, single cells or scattered groups of cancer cells; 2 – Minimal tumour regression - residual cancer outgrown by fibrosis; 3 – No tumour regression – residual tumour without signs of destroyed tumour cells; 4 – Minimal or no regression (extensive residual tumour). This scoring system has been accepted as the best methodology in the 7th edition of the TNM staging system and has been adopted by the currently recruiting FOXTROT trial (FOXTROT, 2012). A similar grading system (0-3) has also been recommended in the College of American Pathologists guidelines (Washington *et al*, 2009).

Clearly these differing tumour regression grades need to be cross-validated for their predictive and prognostic value and reproducibility in different clinical and research settings. What is true of all of these systems for assessing tumour regression grade is that nodal disease is not considered, however methods of combining these two features are currently under investigation (Huebner *et al*, 2012).

Except in the palliative setting and in the context of synchronous liver metastases, it is unusual for the colonic primary to remain in situ throughout systemic treatment and therefore no system for the assessment of tumour regression exists for colon cancer. A method of evaluating the response of liver metastases to systemic treatment however is clearly needed.

Two types of scoring system exist in this regard, those which quantify remaining viable tumour cells and those similar to the aforementioned strategy of histopathological assessment of regression grade. In a study primarily investigating the effects of bevacizumab, Ribero *et al* (2007) reported a scoring system whereby the area of residual viable tumour cells within each metastatic nodule was estimated as a percentage of the total tumour surface area that included areas of coagulative necrosis, calcification, fibrosis and the associated histiocytes, foreign body giant cells and inflammatory cells. Samples were subsequently grouped into 1-24%, 25-49%, 50-74% and 75% and above for the purposes of analysis. This scoring system was later used to clearly demonstrate the impact of tumour regression on survival following neoadjuvant chemotherapy for colorectal liver metastases (Blazer *et al*, 2008). Cumulative 5-year survival rates were 75% for complete response (no residual cancer cells), 56% for major response (1-49% residual cancer cells)

and 33% for minor response (50% or more residual cancer cells) (Figure 1.6). Multivariate analysis revealed that only surgical margin and pathological response independently predicted survival. The same scoring system has also been used by Kishi *et al* (2010) to report the finding that extended pre-operative chemotherapy (more than 9 cycles) increases the risk of hepatoxicity without improving the pathological response.

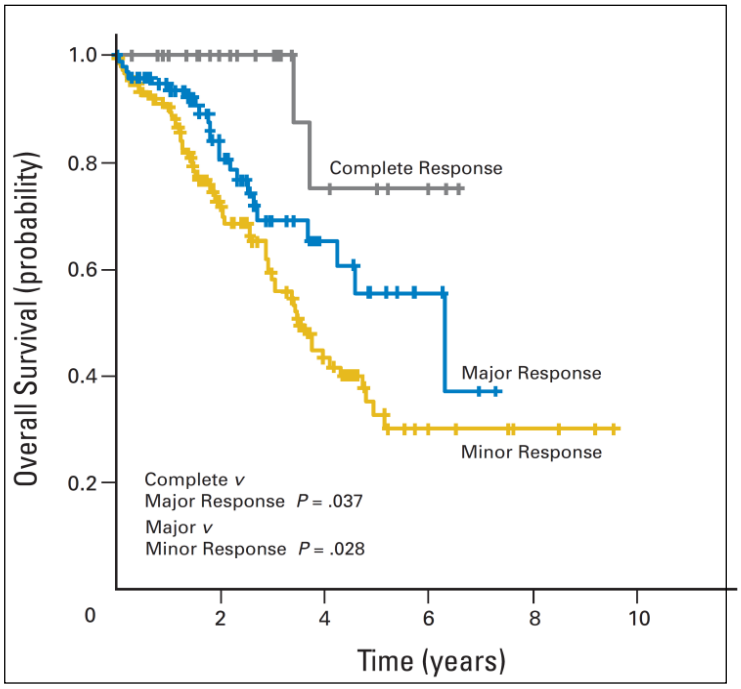

Figure 1.6 – Kaplan-Meir survival curves of patients with colorectal liver metastases treated with neoadjuvant chemotherapy, with greatest survival in those with complete response (a) followed by major response (b) and minor response (c). Reproduced with permission from Blazer *et al*, 2008.

Alternatively the original Mandard tumour regression grade (scored 1-5) has also been used to assess colorectal liver metastases in studies investigating the effects of neoadjuvant chemotherapy (Rubbia-Brandt *et al*, 2007) and more recently the addition of bevacizumab (Klinger *et al*, 2010).

Complete pathological response, whilst oncologically desirable, creates a number of surgical problems (Grothey *et al*, 2008). Correlation between radiological and pathological response is unclear, and up to 80% of lesions showing complete radiological response continue to harbour viable tumour cells (Benoist *et al*, 2006). The optimum method of managing these patients is still under investigation.

1.10 Predictive and prognostic markers in colorectal cancer

The variation in disease and tumour biology coupled with the mode of presentation, rapidity of diagnosis and treatment strategy employed perhaps explains some of the variation in both response to treatment and outcomes. The link between disease stage and outcome has already been discussed however these other factors, and in particular tumour biology, have not yet been incorporated into risk stratification and patient selection for treatment.

The ability to predict response to treatment in the clinical setting would obviously be extremely beneficial. To identify patients, by either patient or tumour factors, who are likely to respond to chemotherapy and/or radiotherapy would allow those individuals to be exposed to a prolonged course of treatment in order to maximise efficacy. It may also be that the approach to managing adverse reactions and events to treatment could differ in those individuals in whom we knew with a degree of certainty would respond to treatment. Taking this one step further if the response to particular chemotherapeutic agents could be predicted up-front prior to commencement then the regimen could be tailored specifically towards the patient – a concept referred to as personalised medicine.

Conversely to identify those patients who are unlikely to respond to treatment is arguably of greater clinical value. In the neoadjuvant setting, for example, failure of a patient with rectal cancer to respond to neoadjuvant chemoradiotherapy commits the patient to retaining their tumour in situ for approximately 4 months. Whilst not accurately studied, it would be reasonable to assume that this confers the risk of tumour growth, dissemination and increases the likelihood of tumour complications such as bleeding, perforation or obstruction.

In the adjuvant setting or indeed in those patients with irresectable disease, the ability to predict response to chemotherapy would allow for personalised treatment, and an open and honest discussion between patient and physician about the appropriateness of aggressive and morbid treatment. In the context of those with irresectable disease it would also provide information to the patient and multidisciplinary team about the likelihood of conversion to resectability.

A cancer diagnosis is clearly a significant life event for any individual, which is handled in any number of different ways. The amount of clinical and prognostic information that people wish to receive is extremely variable, but the option of providing patients with accurate information could potentially assist a proportion of them deal with the psychological impact of the disease.

1.10.1 Clinical prognostic scoring systems

A number of scoring systems are available to assist clinicians classify patients with advanced disease by prognosis, although they are implemented with varying degrees of popularity. The three most commonly used are the Clinical Risk Score (Fong *et al*, 1999), Nordlinger Prognostic Index (Nordlinger *et al*, 1996) and Basingstoke Prognostic Index (Rees *et al*, 2008).

Fong's clinical risk score pertains specifically to the prediction of recurrence after hepatic resection for metastatic colorectal cancer. 1001 consecutive patients were analysed with seven factors found to be significant and independent predictors of poor long-term outcome by multivariate analysis: positive margin, extrahepatic disease, node-positive primary, disease-free interval from primary to detection of metastases of less than 12 months, more than one hepatic tumour, the largest hepatic tumour being greater than 5cm and a carcinoembryonic antigen level (CEA) greater than 200ng/ml. If the last five of these are used pre-operatively, the sum of the number of criteria met was highly predictive of outcome ($p=<0.0001$).

A similar approach was taken by Nordlinger, who identified seven adverse risk factors associated with poor outcome: extension into serosa of primary tumour, lymphatic spread of primary tumour, delay from diagnosis of primary tumour to resection of less than 24 months, number of liver metastases in preoperative imaging, the size of the largest liver metastasis in preoperative imaging greater than or equal to 5cm, preoperatively estimated clearance of normal parenchyma resected with liver metastasis less than 1cm, and age greater than or equal to 60 years.

The Basingstoke Predictive Index was validated for use pre-operatively, given the significant correlation between pre- and post-operative scores in the 929 consecutive patients analysed. Patients are allocated a score based on 7 different risk factors all of which

independents predict poor survival: more than three hepatic metastases, lymph node positivity of the primary tumour, poor differentiation of the primary tumour, the presence of extrahepatic disease, tumour diameter greater than or equal to 5cm, CEA level greater than 60ng/ml and positive resection margins. The first 6 of these criteria were used in a preoperative scoring system and the last 6 in the postoperative setting (Table 1.9), with each criterion multiplied by a weighted constant within a predictive model to give a score out of 30. Patients with a score of 0, 10, 20 and 30 on preoperative scoring had 5-year survival rates of 66%, 35%, 12% and 2% respectively, with comparable scores using the post-operative prediction tool.

Risk Factor	Status	Preoperative	Postoperative
Primary tumour lymph node status	Negative	0	0
	Positive	2	2
Primary tumour differentiation	Well	0	0
	Moderate	3	2
	Poor	5	4
Carcinoembryonic antigen level	<6ng/mL	0	0
	6-60ng/mL	2	1
	>60ng/mL	3	3
Number of hepatic metastases	1-3	0	N/A
	>3	3	3
Largest hepatic tumour diameter	<5cm	0	0
	5-10cm	2	2
	>10cm	8	7
Hepatic resection margin	Negative	N/A	0
	Positive	N/A	11
Extrahepatic disease	No	0	0
	Yes	7	4

Table 1.9 – The Basingstoke Prognostic Index allocates a score (out of 30) based on a number of clinicopathological features. Validated for use in both the pre- and post-operative situations, the score correlates well with outcome.

1.10.2 Biomarkers

A biomarker can be defined as a molecular marker that can be obtained by analysis of mRNA, DNA, protein or circulating tumour cells (or tumour-derived nucleic acids) to stratify

patients for treatment benefit within clinical trials, prognosticate patient outcome or predict and/or monitor response to therapy (Sikorski and Yao, 2010). In more simplistic terms, it is a molecular marker which can in some way be measured upon which predictive or prognostic information can be derived. The measurement can come from blood, urine, or other material such as bile, stomach aspirate or stool. Alternatively biological information can be directly obtained from the tumour itself. Broadly speaking biomarkers can either be prognostic, i.e. provide information regarding patient outcome irrespective of treatment received, or predictive i.e. provide information on the likely effectiveness of therapy in a patient. Alternatively they can be used for early detection and risk stratification, which when applied to the symptomatic and asymptomatic populations are referred to as diagnostic and screening biomarkers respectively.

The previously described benefits of being able to predict response and offer patients prognostic information has led to a significant drive to develop novel biomarkers. To facilitate this, Cancer Research (UK) developed roadmaps to offer guidance as to how this process should be conducted from biomarker discovery, through to assay development, clinical correlation and ultimately application in the clinical setting (Figure 1.7).

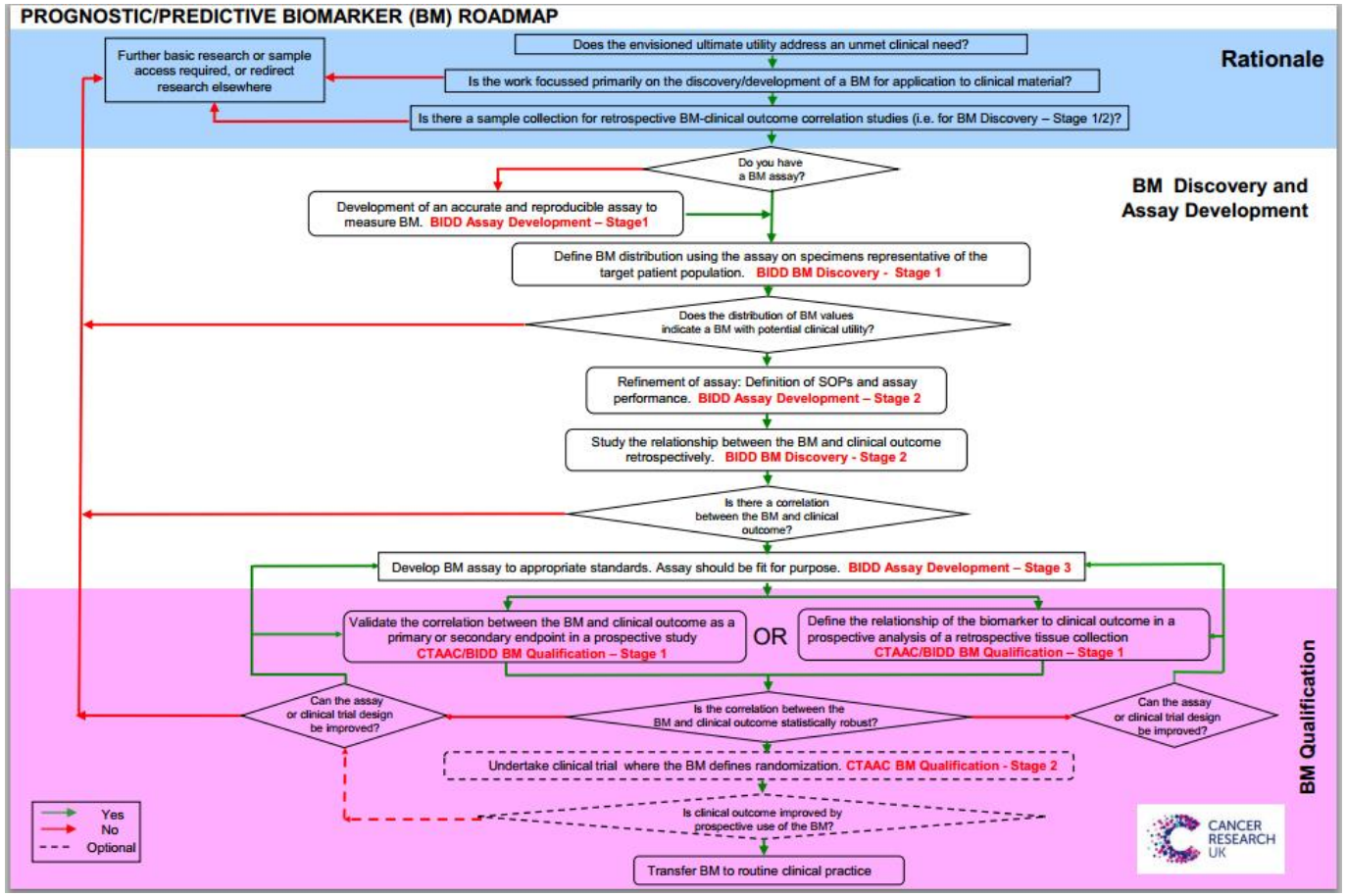

Figure 1.7 – The Cancer Research (UK) roadmap to the discovery, development and validation of a clinically useful biomarker. Available online at http://www.cancerresearchuk.org.

1.10.3 Biomarkers in colorectal cancer

The interest and growth in biomarkers means that the ability to personalise treatment for the individual patient is becoming increasingly close. The best and most well known example of this is the targeting of the use of cetuximab and, to a lesser degree, panitumumab for patients with *KRAS* wild type tumours. This discovery has led to the development of an accurate and cost-effective assay to direct these drugs to appropriate patients.

Most biomarkers studies have focussed on our growing understanding of colorectal carcinogenesis, and in particular the mutations in *KRAS, BRAF, SMAD4, TP53* and *APC* as well as the subsequent downstream pathways previously discussed, as well as markers of microsatellite and chromosomal instability, defects in mismatch repair mechanisms and identification of the CpG island methylator phenotype. The presence of defects in mismatch repair genes (*MLH1, MSH2, MSH6, PMS2*) and microsatellite instability are commonly tested for in the clinical setting in those individuals felt to be at high risk of having Lynch syndrome. Outside of this context routine testing has not yet been adopted, although the presence of a reliable assay to detect MSI status means it is likely to soon be incorporated into clinical practice. To some extent this places the onus on clinicians to update their understanding of colorectal carcinogenesis, and how this may impact on their patients.

Multiple meta-analyses have attempted to assess the value of these factors as prognostic biomarkers, and although conceptually sound very few have actually been validated and used in clinical practice (Pritchard and Grady, 2011). The incorporation of biomarkers as one of multiple, compositive or correlative endpoints in trials is likely to improve the evidence base necessary for further evaluation and adoption. Some of the recently investigated prognostic markers identified are shown in Table 1.10.

Biomarker	Mutation Frequency	Prognosis	Evidence	Status
Microsatellite instability (MSI)	15%	Favourable	Strong	Testing available but not widely used
Chromosome instability (CIN)	70%	Unfavourable	Strong	No readily available test, not in clinical use
18qLOH/*SMAD4* loss	50%	Unfavourable	Moderate	No readily available test, not in clinical use
BRAF V600E mutations	10%	Probably unfavourable	Moderate	Testing available but insufficient evidence to use for prognosis
KRAS codon 12/13 mutations	40%	Probably unfavourable in advanced disease	Limited	Testing widely available but insufficient evidence to use for prognosis
PIK3CA mutations	20%	Possibly unfavourable	Limited	No readily available test, not in clinical use

Table 1.10 – Prognostic biomarkers identified for colorectal cancer. The table demonstrates the frequency with which these biomarkers are identified, the evidence for its correlation with prognosis and its uptake into routine clinical practice. Reproduced without permission from Pritchard and Grady, 2011.

Multiple effective agents now exist for the treatment of colorectal cancer, particularly for stage III and IV disease. The degree of heterogeneity in response to treatment has stimulated interest in predictive biomarkers, a summary of which can be seen in Table 1.11. As might be expected, most relate to the incorporation of relatively new targeted therapies into existing chemotherapeutic regimens.

Biomarker	Mutation Frequency	Drug Selection	Evidence	Status
KRAS codon 12/13 mutations	40%	Predicts resistance to anti-EGFR therapy	Strong	Validated, in routine clinical use
KRAS codon 61/177/146 mutations	1%	Probably predicts resistance to anti-EGFR therapy	Moderate	In clinical use, not fully validated
BRAF V600E mutations	10%	Probably predicts resistance to anti-EGFR therapy, may predict response to BRAF inhibitors	Moderate	In clinical use, not fully validated
PIK3CA mutations	20%	May predict resistance to anti-EGFR therapy	Limited	No readily avaliable test, not in clinical use
PTEN loss	30%	May predict resistance to anti-EGFR therapy	Limited	No readily avaliable test, not in clinical use
Microsatellite instability (MSI)	15%	May predict adverse outcome with 5-FU and improved outcome with Irinotecan	Moderate	Not yet in routine clinical use as a predictive biomarker
18qLOH/*SMAD4* loss	50%	May predict resistance to 5-FU	Moderate	No readily avaliable test, not in clinical use
Topo1 Low	50%	May predice resistance to Irinotecan	Limited	No readily avaliable test, not in clinical use

Table 1.11 – Predictive biomarkers identified for colorectal cancer. The table demonstrates the frequency with which these biomarkers are identified, the evidence for its correlation with response to treatment and its uptake into routine clinical practice. EGFR, epidermal growth factor receptor; 5-FU, 5- fluorouracil; LOH, loss of heterozygosity. Reproduced without permission from Pritchard and Grady, 2011.

Beyond targeted therapies it has been shown that MSI tumours are less likely to respond to 5-fluoruracil based regimens, and in a minority of patients this may even be detrimental (Sargent, 2008). A potential explanation for this is the understanding that an effective MMR system is required for the cytotoxic effect of the drug (Jo and Carethers, 2006), however the finding of chemoresistance to 5-fluouracil in MSI tumours is not uniform (Liang *et al*, 2002). Conversely MSI tumours have been shown to be more response to

chemotherapeutic regimens containing irinotecan (Fallik *et al*, 2003), and therefore it is easy to see how following evaluation of this biomarker on a larger scale that routine testing would be incorporated into clinical practice, particularly for patient selection for adjuvant therapy in stage II-III disease. LOH in 18q has also been shown to be associated with poor response to 5-fluorouracil based therapy (Watanabe *et al*, 2001), with some evidence to suggest this may be due to *SMAD4* located in the 18q21 deleted region (Boulay *et al*, 2002).

The MRC FOCUS trial randomised patients to receive 5-fluorouracil, 5-fluorouracil plus oxaliplatin or 5-fluorouracil with irinotecan. Expression of topoisomerase I, the target for irinotecan, was established by immunohistochemistry and the study demonstrated improved response to irinotecan containing regimens in those patients with high expression of the protein (HR 0.98; 95% CI 0.78-1.22) (Braun *et al*, 2008). Germline polymorphisms which may affect pharmacokinetics and pharmacodynamics have also been studied, for example dihydropyrimidine dehydrogenase and thymidylate synthetase in the metabolism of 5-fluorouracil. Whilst the results appeared promising, there remains insufficient evidence at the current time for its adoption into clinical practice (Ezzeldin and Diasio, 2008). Conversely there is good evidence for the use of the UGT1A1*28 polymorphism previously discussed to predict dose related toxicity to irinotecan, so much so that a commercial genotyping kit was approved by the Food and Drug Administration in 2005 to help guide irinotecan dosing (Palomaki *et al*, 2009).

Biomarker research is challenging, requiring large scale multi-centre randomised trials with good quality clinical material and validated laboratory techniques and reagents. Published studies on biomarkers are often confounding and usually retrospective with small sample sizes. The lack of methodological standardization involved in the detection of biomarkers is perhaps why only the *KRAS* gene has become used routinely in clinical practice. The potential for combining biomarkers in a panel to further increase the sensitivity and specificity is currently being explored, for example the adaptive FOCUS4 trial is stratifying patients by combination of KRAS/BRAF/PIK3CA and other biomarkers to further investigate the role of novel agents.

The Oncotype DX® Recurrence Score® combines a panel of 7 genes (*Ki-67, C-MYC, MYBL2, FAP, BGN, INHBA and GADD45B*) identified through the evaluation of 761 colon cancer related genes in 1851 patients across 4 studies, with 5 housekeeping genes and MSI/MMR status to produce personalised prognostic information for patients with Stage II-III disease.

The score has been shown to correlate with risk of recurrence (p=0.01), disease free survival (p=0.01) and overall survival (p=0.04) using data from the QUASAR study (Kerr *et al*, 2009), however to date no prospective evaluation has been performed. Our understanding of colorectal cancer genetics has evolved significantly over the past 10 years and will continue to evolve over the next 10, and with this increased understanding comes the opportunity to investigate biologically plausible biomarkers in a targeted fashion.

1.11 Summary

In the United Kingdom, colorectal cancer is the fourth commonest cancer and the second commonest cause of cancer related death. Most recent figures from Cancer Research (UK) show that 1-year survival for men and women with colon cancer is 73.0% and 72.2% respectively, with 5-year survival of 54.4% and 55.1%. In those with rectal cancer 1-year survival for men and women is 78.8% and 78.8% respectively, and 5-year survival 54.6% and 57.5%. A number of dietary and lifestyle factors have been linked to the development of colorectal cancer, including diets rich in unsaturated fats and red meat, excess alcohol and a sedentary lifestyle. Smoking and inflammatory bowel disease have also been linked to the development of colorectal cancer.

Over recent years our understanding of the genetics of colorectal carcinogenesis have improved significantly. The vast majority of colorectal tumours reflect a series of hereditary and somatic mutations in key genes i.e *APC, KRAS, BRAF* and *TP53*. These mutations are most frequently associated with a CIN phenotype and are often acquired in a different order. A subset of tumours initiate through inactivation of MMR function, which may be through inherited or, less commonly, somatic mutation, or alternatively epigenetic inactivation through hypermethylation (CIMP) leading to MSI-H.

The evaluation of a patient with colorectal cancer includes clinical, endoscopic, histopathological and radiological assessment, the latter normally consisting of CT, PET and for rectal tumours or further evaluation of liver metastases, MRI. This information can be used to stage the patient and prognosticate outcome. Commonly used staging systems include the Dukes', UICC/AJCC TNM and Jass classifications. Obtaining biological information from the liver metastases is not feasible due to seeding of the cutaneous tract and worse outcomes, and therefore we are limited to information gathered from the primary tumour.

Surgery remains the mainstay of treatment for colorectal cancer, which under normal circumstances would be formal surgical resection of the primary and metastatic tumours. Alternatives exist for the management of liver metastases, in particular radiofrequency ablation or microwave ablation. Radiotherapy is frequently used in the treatment of rectal cancer most commonly as either SCPRT or long course CRT, the aim of which is to reduce the risk of local recurrence and downstage disease in order to reduce the risk of a positive CRM at surgical resection. There remains a significant role for chemotherapy in the neoadjuvant, adjuvant and unresectable settings with 5-fluoruracil (supplemented with leucovorin) remaining the cornerstone of treatment. This is most frequently supplemented with oxaliplatin and/or irinotecan, and increasingly bevacizumab or cetuximab/panitumumab in those known to be *KRAS* wild type.

Response to treatment may be assessed both radiologically and histopathologically, the latter being most commonly performed following surgical resection. Radiological assessment is performed using the RECIST v1.1 guidelines, and histopathological assessment is performed using any of a number of scoring systems which assess the degree of necrosis, fibrosis and viable tumour in a specimen.

Prognostic information is currently derived from clinical and pathological features combined into scoring systems, the three most commonly used being the Clinical Risk Score, Nordlinger Prognostic Index and Basingstoke Prognostic Index. At present there are no reliable prognostic, screening or diagnostic biomarkers in routine clinical use. The sole predictive biomarker in clinical use is *KRAS* status; *KRAS* mutant tumours do not respond to targeted anti-epidermal growth factor receptor treatments such as cetuximab and panitumumab. A number of studies have attempted to correlate the previously discussed genetic aberrations with response to chemotherapy, and germline polymorphisms which may affect pharmacokinetics and pharmacodynamics have also been studied.

1.12 Aims, hypotheses and study plan

From the literature it is clear that there are a number of questions which clinicians face on a daily basis to which there is as yet no satisfactory scientific explanation or rationale for a particular treatment decision. Three of these key questions are:

- In patients with rectal cancer is it possible to predict response to neoadjuvant chemoradiotherapy?
- In patients with colorectal liver metastases is it possible to predict response to neoadjuvant chemotherapy?
- Can biological information from the primary tumour be used to predict response to treatment in colorectal liver metastases?

The aim of this thesis is to begin to address these research questions.

1.12.1 Hypotheses

These research questions can be used to formulate a number of testable hypotheses investigated in this project:

1. Somatic non-synonymous mutations in the primary tumour correlate with those present in the liver metastasis and predict response to treatment.

2. The phenotype of the primary tumour is biologically similar to the liver metastasis, with markers present in the primary tumour which predict the response of the liver metastasis to neoadjuvant chemotherapy.

4. The phenotype of a rectal tumour changes with neoadjuvant chemoradiotherapy, and inter-patient variation in these changes predicts response to treatment.

5. Levels of expression of key proteins involved in the activation and metabolism of chemotherapeutics are comparable between primary and metastatic tumours and predict response to treatment.

6. Levels of expression of DNA base excision repair proteins in rectal tumours vary with treatment, and inter-patient variation in the expression of these proteins predicts response to neoadjuvant chemoradiotherapy.

1.12.2 Study plan

To investigate these hypotheses the following study plan was used:

1. Establish a research network across multiple sites to facilitate the collection of patient matched primary and metastatic tissue, alongside normal liver parenchyma and colonic mucosa, focussing on those receiving neoadjuvant chemotherapy.

2. Establish a research protocol to facilitate the collection of serial temporal biopsies from patients with rectal cancer, acquiring tissue prior to chemoradiotherapy, immediately following chemoradiotherapy and at the time of surgical resection.

3. Investigate alternative strategies to the standard mechanisms of tissue collection (i.e. liquid nitrogen, dedicated research technician and archiving facilities in a -80^{o}C freezer) in order to facilitate 1 and 2.

4. Subject tumour samples (alongside normal adjacent tissue) from patients undergoing synchronous resection to exome sequencing in order to establish the degree of biological similarity between primary and metastatic tumours, specifically to identify whether the presence of somatic non-synonymous mutations in the primary tumour predicts the presence of the same mutations in the liver metastasis.

5. Perform isobaric tagging for relative quantification (iTRAQ) of patient matched primary and metastatic tumours as well as adjacent normal liver parenchyma and colonic mucosa on a discovery set of fresh tissue. Data will be analysed to assess the degree of biological similarity between primary and metastatic tumours, as well as identify potential biomarkers measurable in the primary tumour which will predict the response to chemotherapy in the liver metastases.

6. Validate any potential biomarkers by immunohistochemistry on a larger validation tissue set, with samples combined into a tissue micro-array. Any potential mechanisms for validated biomarkers will be explored.

7. Perform isobaric tagging for relative quantification (iTRAQ) of serial rectal cancer samples on a discovery set of fresh tissue. Data will be analysed to assess how the tumour phenotype changes with treatment, as well as identify potential biomarkers which may predict response of the primary tumour to neoadjuvant chemoradiotherapy.

8. Validate any potential biomarkers by immunohistochemistry on a larger validation tissue set, with samples combined into a tissue micro-array. Any potential mechanisms for validated biomarkers will be explored.

9. Undertake a targeted analysis of the expression and function of key proteins involved in the activation and metabolism of oxaliplatin, 5-fluorouracil and irinotecan in patient matched primary and metastatic tumour samples. Data will be analysed to assess the correlation in expression and function between primary and metastatic tumours as well as how this information may predict response to treatment.

10. Undertake a targeted analysis of the expression of key proteins involved in DNA base excision repair in serial rectal cancer samples. Data will be analysed to assess how levels of expression vary with treatment and how this information may be used to predict response.

Chapter 2

Evaluation of a tissue stabilisation gel (Allprotect^{TM}) to facilitate clinical sampling for translational research in surgical trials

2.1 Introduction

2.1.1 Background

Successful translational research in surgery is dependent upon collaboration between scientists and clinicians. Central to this is the acquisition of tissue samples following surgical or endoscopic resection. In specialties such as thoracic surgery, neurosurgery and some gastrointestinal subspecialties such as hepatopancreaticobiliary, centralisation of services within large trusts or university teaching hospitals has facilitated routine collection of tissue through biobanks. Higher volume specialties performing oncological resections, such as colorectal surgery, have not been centralised. Indeed the majority of colorectal cancer resections are still performed in the non-teaching hospital setting, making the harvest and storage of fresh tissue problematic because of a lack of specialised facilities, such as a ready supply of liquid nitrogen and -80^{o}C storage (Shabihkhani *et al*, 2014). Consequently, most colorectal biobanks contain only formalin-fixed paraffin embedded (FFPE) samples which are of limited use for most bioanalytical applications.

2.1.2 The need for an alternative infrastructure

In order to facilitate the inclusion of high volume non-teaching hospitals in more translational research projects and clinical trials, or for more *ad-hoc* tissue sampling, an alternative method of tissue stabilisation is needed which does not require immediate processing and freezing. Indeed, a system that allowed transfer of samples by post or courier, without the need for specialist shipping conditions, would also increase the potential recruitment of patients for large scale trials and reduce costs associated with on-site processing. Allprotect^{TM} is a new to the market tissue stabilisation gel which according to the manufacturer overcomes the need for liquid nitrogen and -80^{0}C storage, allowing tissue collection and stabilisation to be performed with limited infrastructure (Qiagen, Venlo, Netherlands). As Allprotect^{TM} is a proprietary compound, details of its composition are currently unavailable.

2.1.3 Relevance to this thesis

Clinical samples used for the analysis which has informed later chapters of this thesis will attest to the complex regional infrastructure which was created in order to facilitate the

work. On Merseyside all resections of colorectal liver metastases are performed at Aintree University Hospital, a teaching hospital with a well developed research infrastructure. The hospitals referring patients to this institution however are less well equipped for research, and it is these institutions in which the vast majority of the primary tumours of the patients recruited to these studies were resected. As such, a regional network was established to facilitate the acquisition of patient matched clinical samples and corresponding clinical and demographic data. The work described in this chapter was devised in order to facilitate other translational work presented later in the thesis.

2.1.4 Aims and hypotheses

The aim of this study was to rigorously evaluate the use of Allprotect™ as an alternative to liquid nitrogen for the short and long term storage of clinical samples from patients undergoing surgical resection of colorectal primary and metastatic tumours. Tissue integrity under all storage conditions was assessed across a range of typical biomolecules including DNA, mRNA, microRNA and protein. In addition, retention of protein function following storage in Allprotect™ was determined by enzyme activity measurements. Specifically, we hypothesise that Allprotect™ offers comparable tissue stabilisation to liquid nitrogen for downstream translational research.

2.2 Methods

2.2.1 Sample collection

The study was performed to facilitate an existing translational research project, for which NHS Research Ethics Committee and Research and Development approval had already been obtained (12/NW/0011). Samples were obtained from patients undergoing primary resection for colorectal cancer (n=5). Following delivery of the surgical specimen, the proximal staple line was incised and a linear cut was made down the anti-mesenteric border being cautious to stop either 1cm away from the tumour or upon approaching the mesorectum. Using forceps and a scalpel a peripheral section of tumour was excised. Samples were obtained from a second cohort of patients undergoing resection for colorectal liver metastases (n=5). Following delivery of the surgical specimen an incision was made through the resected surface to the liver metastasis, with care being taken not to breach the liver capsule, and peripheral samples of tumour were obtained as previously described. All tissue sampling was performed in the operating theatre under aseptic conditions.

2.2.2 Stability study

Each sample was cut into 10 discrete sections of approximately 4 mm^3, 5 of which were individually placed into sealed cryodorfs and processed immediately (within 5 minutes of specimen delivery) as follows: 1. Snap frozen in liquid nitrogen and transferred to tissue archiving freezer (-80^{o}C) – control sample. 2. Allprotect^{TM} at room temperature (19^{0}C). 3. Allprotect^{TM} in a fridge (8^{0}C). 4. Allprotect^{TM} in a standard laboratory freezer (-20^{0}C) 5. Allprotect^{TM} in a tissue archiving freezer (-80^{0}C). Those samples processed in Allprotect^{TM} were submerged in a 10:1 ratio by volume as per manufacturer's instructions; samples snap frozen in liquid nitrogen were done so without additives. The remaining 5 sections per sample were left exposed to the environment on a theatre trolley until the end of the procedure (approximately 1 hour for both primary and metastatic resections) in an effort to replicate 'real world' tissue sampling in the absence of a designated research technician. Once the skin had been closed, the remaining samples were processed in an identical manner to that already described. Samples remained under stabilisation conditions for 7 days prior to proceeding with biomolecule extraction. A schematic outline of the study design can be seen in Figure 2.1.

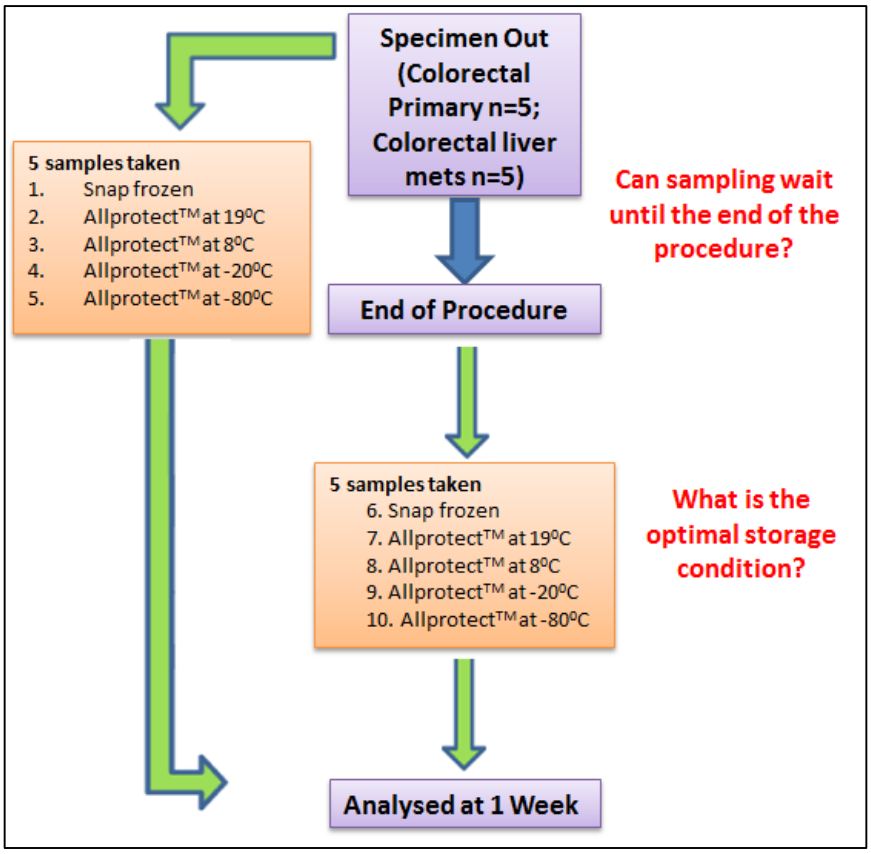

Figure 2.1 – A schematic outline of the stability study. The available tissue was divided into 10 fragments, 5 of which were stabilised immediately in one of the storage conditions shown and the remaining 5 in a similar manner but at the end of the procedure. The study was designed to ask two specific questions: can sampling wait until the end of the procedure, and what is the optimal storage condition?

2.2.3 Archiving study

Further cohorts of patients undergoing resection for primary colorectal cancer (n=5) or liver metastases (n=5) were sampled in the same manner and again tissue was divided into 10 sections. One sample was placed into liquid nitrogen and then transferred to a tissue archiving freezer (-80°C) and the remaining 9 samples were submerged in Allprotect™ and refrigerated (at 8°C). A single sample was removed following storage for 1, 2, 3, 4, 8, 12, 16, 20 and 24 weeks, and processed for biomolecule extraction. A schematic outline of the study design can be seen in Figure 2.2.

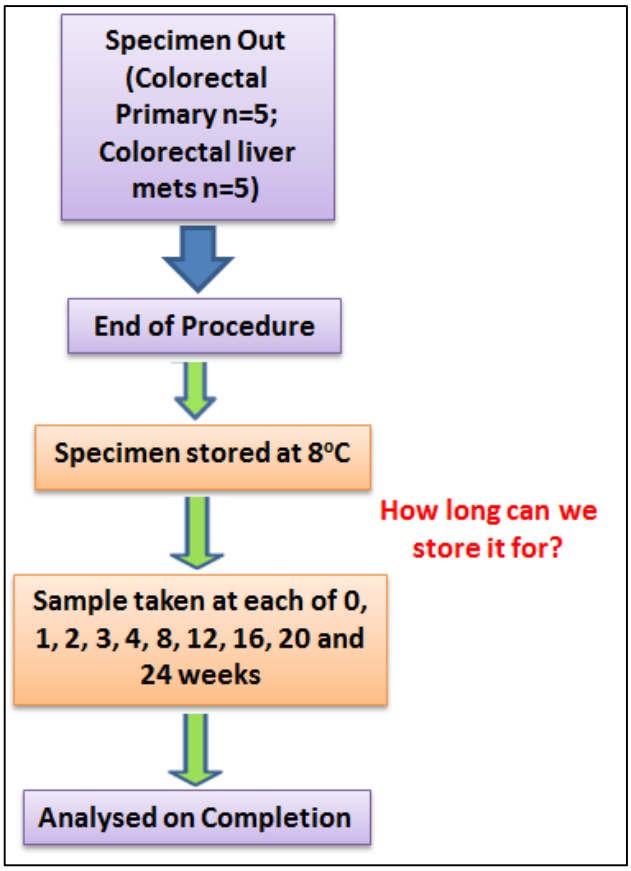

Figure 2.2 – A schematic outline of the archiving study. The available tissue was divided into 10 fragments, one of which was immediately snap frozen in liquid nitrogen and transferred to a -80°C freezer (control sample) and one was archived in Allprotect™ for each of the time points shown in the figure.

2.2.4 Biomolecule extraction

DNA and RNA extraction was performed using the Qiagen miRNeasy Mini Kit and EZ1 DNA Tissue Kit respectively as per manufacturer's instructions (Qiagen, Venlo, Netherlands). Protein extraction was performed by a combination of both mechanical and ultrasonic homogenisation in phosphate-buffered saline. Following centrifugation the protein concentration of the supernatant was established using a Bradford assay (Bradford, 1976). In addition, a section of tissue was taken from each of the samples, fixed in formalin and embedded in paraffin. A slide was stained with haemotoxylin and eosin and reviewed by a pathologist who was blind to the details of the study. Extracted biomolecules were used to perform each of the following assays in triplicate on all samples.

2.2.5 DNA assays

DNA concentration was measured using the NanoDrop™ ND-1000 spectrophotometer (Thermo Scientific, Waltham, USA) and quality assessed using the Human DNAOK! kit (Microzone, Haywards Heath, UK). *KRAS* mutational analysis was performed using an in-house pyrosequencing assay capable of detecting all somatic mutations in codons 12, 13 and 61 of the *KRAS* gene. The lower limit of detection for the assay is 5% of mutated alleles.

2.2.6 RNA Assays

Extracted RNA was initially subjected to quantification and quality control using the Nanodrop™ spectrophotometer and reverse transcription was performed with the RT2 First Strand Kit (Qiagen, Venlo, Netherlands). Further quality control assays were performed using a Bioanalyzer (Agilent, Santa Clara, USA) and the commercially available RT2™ RNA QC PCR Array (SABiosciences, Venlo, Netherlands). In order to assess the functional integrity of the extracted RNA under different storage conditions, RT-PCR was performed on two genes (*HMGB1* and *CES1*) and two microRNAs (mir-122 and let7d) relevant to an on-going translational project conducted within the Medical Research Council Centre for Drug Safety Science. Specific primers were designed for *HMGB1*, *CES1*, miR122 and let7d (Eurofins Scientific, Luxembourg, Luxembourg) and qPCR performed using the ABI-7900 (Applied Bioscience, Foster City, USA).

2.2.7 Protein expression by western blotting

Western blots for HMGB1 and CES1 as representative proteins were performed on both primary colorectal cancer tissue and liver metastases. 10% SDS-PAGE gels were transferred to a nitrocellulose membrane and blocked in 10% milk. Following overnight incubation with the primary antibody (Abcam: ab18256 {HMGB1} or ab45957 {CES1}) membranes were incubated with a LI-COR IRDye 680 LT secondary antibody (Biosciences, Lincoln USA) before semi-quanitative analysis using the Oydssey scanner (LI-COR Biosciences, Lincoln USA).

2.2.8 Protein expression by immunohistochemistry

In order to assess the effect of Allprotect™ on tissue morphology, and the feasibility of fixing tissue previously stabilised in this manner, the expression of HMGB1 in FFPE tissue

was established by immunohistochemistry. 4µm sections were de-waxed in xylene and rehydrated with ethanol solutions of decreasing concentrations. After blocking with 3% hydrogen peroxide in 100% methanol, antigens were retrieved by microwaving for 20 minutes in 10mM citrate buffer and further blocked with 10% goat serum in 0.1% tris-buffered saline with tween. Slides were incubated with the primary antibody (Abcam, ab18256) for 2 hours, and a 1:200 horseradish peroxidase conjugated secondary antibody (Dako UK Ltd, E0432) for 30 minutes. Following incubation with the Vectastain Elite® ABC reporter system (Vectorlabs, Burlingame, USA), slides were developed with diaminobenzidine tetrahydrochloride (DAB) and counterstained with haematoxylin. Slides were reviewed by light microscopy and HMGB1 expression was established using a previously reported scoring system (Liu *et al*, 2012). Two reviewers independently scored five fields at 400x magnification with a total cell count not less than 1000. The proportion of positive cells allowed classification into one of four categories: 1 (<25%), 2 (25-50%), 3 (51-75%) or 4 (>75%). The intensity of nuclear staining was also classified: 1 (no staining/background of negative controls), 2 (weak staining detectable above background), 3 (moderate staining) or 4 (intense staining). The index was then calculated by multiplying the intensity and percentage scores to give a total score out of 16.

2.2.9 Protein function by mass spectrometry

The activity of carboxylesterase was determined with irinotecan as a substrate in order to assess protein function. Tissue homogenate (250µg protein) was incubated with 100nM irinotecan (Sigma Aldrich, Poole, UK) for 30 minutes prior to termination of the reaction using a methanol/acetonitrile solution. The supernatant was subjected to a functional assay optimised to quantify the active metabolite, SN-38, by liquid-chromatography mass-spectrometry (Jones *et al*, 2013).

2.2.10 Statistical analysis

Statistical analysis was based on the comparison of different methods of tissue stabilisation/archiving to the current gold standard, i.e. tissue snap frozen in liquid nitrogen and transferred to a tissue archiving freezer (-80^{o}C). One-way ANOVA with post-hoc Dunnett's test was used to compare each sample in turn to the reference sample. Analysis was performed using Stats Direct 2.7.9 (Stats Direct Ltd, Altrincham, UK).

2.3 Results

2.3.1 Assessment of tissue morphology

All samples were confidently identified as adenocarcinoma on review of the H&E slide, irrespective of the method of tissue stabilisation used or length of time archived in Allprotect™ (Figure 2.3). A degree of clear cell change/vacuolation was seen in all samples which was slightly more apparent in those samples exposed to Allprotect™, although this did not vary significantly with the length of exposure. Tumour sampling did not compromise a complete pathological assessment of the remaining surgical specimen in any of the cases.

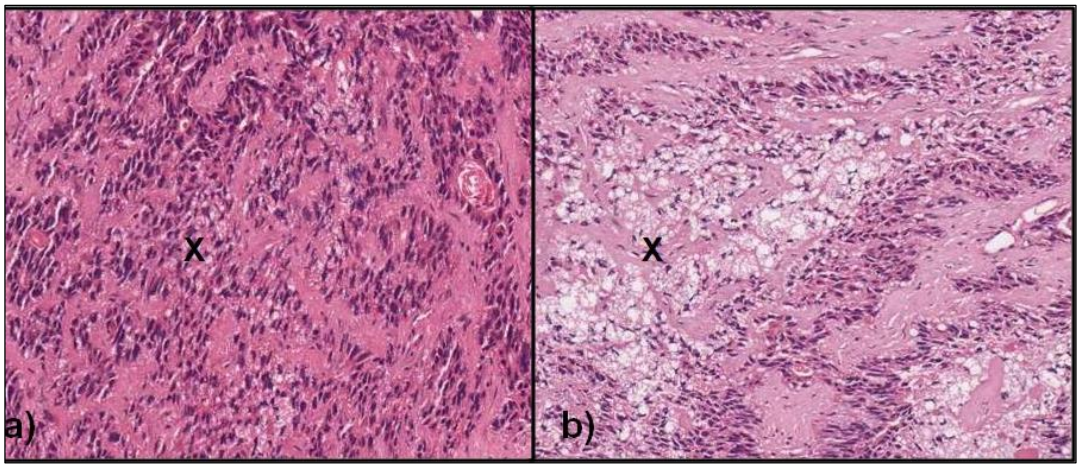

Figure 2.3 – Representative micrographs of H&E stained sections of colorectal liver metastases showing a) tissue snap frozen in liquid nitrogen and b) tissue stabilised in Allprotect™. Both are clearly identifiable as adenocarcinoma, although contain a degree of clear cell change/vacuolation (X). Histological appearances did not change significantly with the length of the time the sample was exposed to Allprotect™. Micrographs were taken at 200x magnification.

2.3.1 Short term (0 - 1 week) maintenance of biomolecule expression and function

DNA

Automated extraction of DNA from the snap frozen and Allprotect™ stabilised samples yielded comparable quantities (2.1-3.3µg/mg tissue) of high quality DNA with 260:280 ratios of 1.8 - 1.9 and 260:230 ratios of 2.0 - 2.4. There was no correlation between the

spectrophotometric quality ratios and the method of stabilisation. The samples immediately stabilised were also comparable to those stabilised after a one hour delay. All samples passed the internal quality control check utilised by the EZ1 Advanced (Qiagen, Venlo, Netherlands). Extracted DNA was successfully utilised for downstream qPCR analysis of *KRAS* status at codons 12, 13 and 61 with 100% concordance between all samples originating from the same biological specimen for all patients and both tissue types (Table 2.1).

Sample	Stabilisation Method	Processing	Concentration (ng/µl)	260/280	260/230	Quality Check	*KRAS* Codon 12	*KRAS* Codon 13	*KRAS* Codon 61
1	Snap frozen (liquid nitrogen)	On specimen extraction	257.24	1.82	2.23	Pass	c.35G>A (p.Gly12Asp) 29.8%	Wild-type	Wild-type
2	Allprotect (room temperature)		259.57	1.86	2.14	Pass	c.35G>A (p.Gly12Asp) 39.9%	Wild-type	Wild-type
3	Allprotect (8^0C)		259.91	1.84	2.22	Pass	c.35G>A (p.Gly12Asp) 33.3%	Wild-type	Wild-type
4	Allprotect (-20^0C)		282.32	1.88	2.08	Pass	c.35G>A (p.Gly12Asp) 10.6%	Wild-type	Wild-type
5	Allprotect (-80^0C)		281.68	1.87	2.10	Pass	c.35G>A (p.Gly12Asp) 30.8%	Wild-type	Wild-type
6	Snap frozen (liquid nitrogen)	At end of procedure	157.3	1.82	2.01	Pass	c.35G>A (p.Gly12Asp) 11.8%	Wild-type	Wild-type
7	Allprotect (room temperature)		230.28	1.82	2.12	Pass	c.35G>A (p.Gly12Asp) 30.1%	Wild-type	Wild-type
8	Allprotect (8^0C)		301.85	1.86	2.18	Pass	c.35G>A (p.Gly12Asp) 34%	Wild-type	Wild-type
9	Allprotect (-20^0C)		256.85	1.86	2.15	Pass	c.35G>A (p.Gly12Asp) 46.4%	Wild-type	Wild-type
10	Allprotect (-80^0C)		284.41	1.87	2.31	Pass	c.35G>A (p.Gly12Asp) 37.2%	Wild-type	Wild-type

Table 2.1 – Representative results following DNA extraction from patient 2 (primary tumour). Comparable quality control indices are seen highlighting the suitability of extracted DNA for downstream qPCR analysis. Comparable results following *KRAS* genotyping are seen: the patient is *KRAS* mutant at codon 12 but wild type at codons 13 and 61.

RNA

The yield of extracted RNA was again comparable between samples (0.41-0.68µg/mg tissue), with 260:280 ratios of 1.9 - 2.1 and RNA Integrity Numbers (RIN) of 7.7 - 8.0. The commercially produced RT2^{TM} Quality Control Array, which is based on a series of housekeeping genes including *ACTB* (β-actin) and *HPRT1* (hypoxanthine phosphoribosyltransferase), confirmed the absence of relevant RNA impurities which would adversely affect reverse transcription or PCR, and whilst there was a small amount of genomic DNA contamination this did not affect PCR results. A minor degree of inter-patient variation can be seen, however cycle threshold (Ct) values did not vary significantly with either a) the method of tissue stabilisation implemented, or b) the timing of stabilisation being either at specimen extraction or after a one hour delay. Figure 2.4 shows the mean Ct values for miR122 in patient 1 (liver metastases). Similar data were seen for let7d and the findings were comparable in the primary tumour, as were mRNA levels for *HMGB1* and *CES1* in both primary and metastatic tissue.

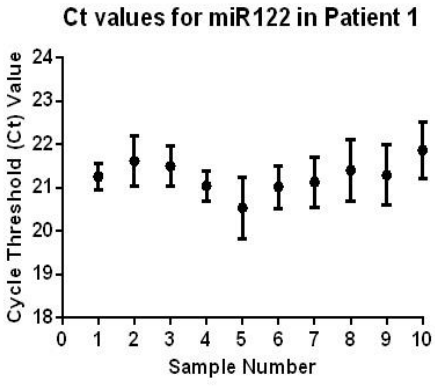

Tissue	Stabilisation Method	Processing	Mean (SD) Cyle Threshold (Ct)	Dunnett's test (wrt Sample 1)
1	Snap frozen (liquid nitrogen)	On specimen extraction	21.26 (0.31)	-
2	Allprotect (room temperature)		21.62 (0.59)	P=0.97
3	Allprotect (8^{0}C)		21.50 (0.47)	P=0.99
4	Allprotect (-20^{0}C)		21.05 (0.35)	P=0.99
5	Allprotect (-80^{0}C)		20.54 (0.71)	P=0.56
6	Snap frozen (liquid nitrogen)	At end of procedure	21.02 (0.49)	P=0.99
7	Allprotect (room temperature)		21.14 (0.58)	P=>0.99
8	Allprotect (8^{0}C)		21.41 (0.70)	P=>0.99
9	Allprotect (-20^{0}C)		21.30 (0.69)	P=>0.99
10	Allprotect (-80^{0}C)		21.87 (0.65)	P=0.56

Figure 2.4 – Cycle threshold (Ct) values for miR-122 in the colorectal liver metastasis from patient 1. All samples are comparable irrespective of the method of tissue stabilisation used, and whether the samples were stabilised immediately following specimen extraction (samples 1-5) or following a delay of 1 hour (samples 6-10). ANOVA with post-hoc Dunnett's test shows that no samples are statistically significant from the current gold standard (sample 1) i.e. tissue snap frozen in liquid nitrogen.

Protein

Protein yield was comparable between all samples (20.3-31.4µg/mg tissue). Coomassie staining confirmed comparable protein coverage and, whilst considerable inter-individual variation was observed, analysis of western blots demonstrated similar densitometry values for both HMGB1 and CES 1 in all samples originating from the same biological specimen for all patients and both tissue types irrespective of the method of tissue stabilisation used. The samples immediately stabilised were also comparable to those stabilised after a one hour delay. Representative data for HMGB1 expression in patient 1 (primary tumour) is shown in Figure 2.5 (0.79 – 1.16iU; P=0.100 - >0.999).

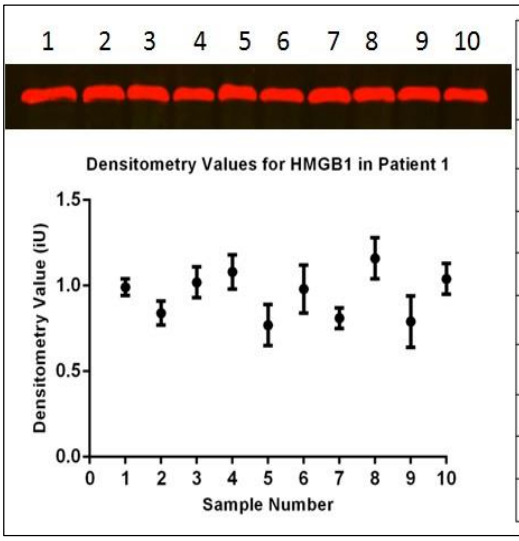

Tissue	Stabilisation Method	Processing	Mean (SD) Densitometry	Dunnett's test (wrt Sample 1)
1	Snap frozen (liquid nitrogen)	On specimen extraction	0.99 (0.05)	-
2	Allprotect (room temperature)		0.84 (0.07)	P=0.46
3	Allprotect (8^{0}C)		1.02 (0.09)	P=>0.99
4	Allprotect (-20^{0}C)		1.08 (0.10)	P=0.85
5	Allprotect (-80^{0}C)		0.77 (0.12)	P=0.10
6	Snap frozen (liquid nitrogen)	At end of procedure	0.98 (0.14)	P=>0.99
7	Allprotect (room temperature)		0.81 (0.06)	P=0.24
8	Allprotect (8^{0}C)		1.16 (0.12)	P=0.29
9	Allprotect (-20^{0}C)		0.79 (0.15)	P=0.16
10	Allprotect (-80^{0}C)		1.04 (0.09)	P=0.99

Figure 2.5 – Western blot and corresponding densitometry of HMGB1 expression in primary colorectal cancer samples from patient 1. All samples are comparable irrespective of the method of tissue stabilisation used, and whether the samples were stabilised immediately following specimen extraction (samples 1-5) or following a delay of 1 hour (samples 6-10). ANOVA with post-hoc Dunnett's test shows that no samples are statistically significant from the current gold standard (sample 1) i.e. tissue snap frozen in liquid nitrogen.

Similar findings were observed for CES1 expression, the data from patient 2 (liver metastases) being displayed in Figure 2.6 (0.41 - 0.62iU; p=0.559 - >0.999).

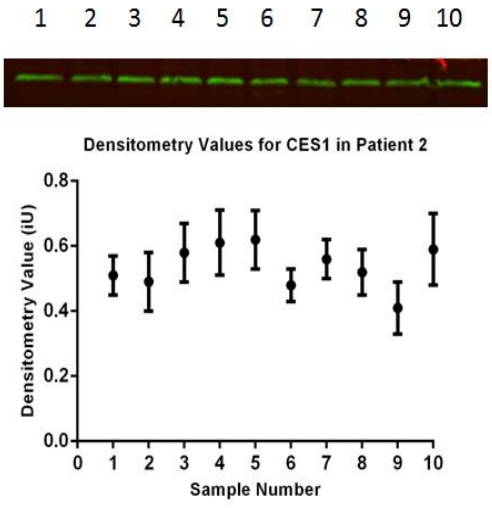

Tissue	Stabilisation Method	Processing	Mean (SD) Densitometry	Dunnett's test (wrt Sample 1)
1	Snap frozen (liquid nitrogen)	On specimen extraction	0.51 (0.06)	-
2	Allprotect (room temperature)		0.49 (0.09)	P=0.99
3	Allprotect (8^{0}C)		0.58 (0.09)	P=0.92
4	Allprotect (-20^{0}C)		0.61 (0.10)	P=0.59
5	Allprotect (-80^{0}C)		0.62 (0.09)	P=0.56
6	Snap frozen (liquid nitrogen)	At end of procedure	0.48 (0.05)	P=0.99
7	Allprotect (room temperature)		0.56 (0.06)	P=0.99
8	Allprotect (8^{0}C)		0.52 (0.07)	P=>0.99
9	Allprotect (-20^{0}C)		0.41 (0.08)	P=0.56
10	Allprotect (-80^{0}C)		0.59 (0.11)	P=0.79

Figure 2.6 – Western blot and corresponding densitometry of CES1 expression in colorectal liver metastasis samples from patient 2. All samples are comparable irrespective of the method of tissue stabilisation used, and whether the samples were stabilised immediately following specimen extraction (samples 1-5) or following a delay of 1 hour (samples 6-10). ANOVA with post-hoc Dunnett's test shows that no samples are statistically significant from the current gold standard (sample 1) i.e. tissue snap frozen in liquid nitrogen.

Mass spectrometry analysis also showed a comparable rate of SN38 production from tissue irrespective of tissue stabilisation method or timing. Representative data for the primary colorectal tumour of patient 3 (4.01-5.58nm/mg tissue/min; p=0.062 - >0.999) can be seen in Figure 2.7, with similar results seen in the liver metastases.

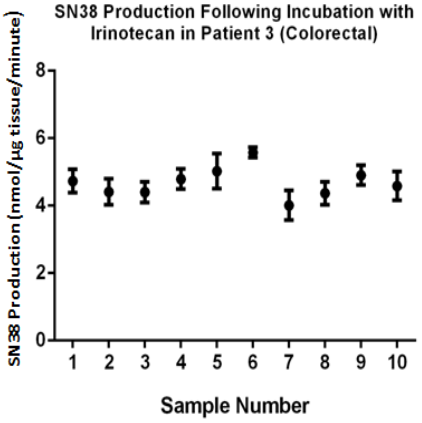

Tissue	Stabilisation Method	Processing	Mean (SD) SN38 Production (nmol/µg/min)	Dunnett's test (wrt Sample 1)
1	Snap frozen (liquid nitrogen)	On specimen extraction	4.73 (0.35)	-
2	Allprotect (room temperature)		4.41(0.39)	P=0.86
3	Allprotect (8^{0}C)		4.40 (0.31)	P=0.85
4	Allprotect (-20^{0}C)		4.79 (0.30)	P=>0.99
5	Allprotect (-80^{0}C)		5.03 (0.52)	P=0.91
6	Snap frozen (liquid nitrogen)	At end of procedure	5.58 (0.15)	P=0.06
7	Allprotect (room temperature)		4.01 (0.44)	P=0.14
8	Allprotect (8^{0}C)		4.37 (0.34)	P=0.77
9	Allprotect (-20^{0}C)		4.90 (0.29)	P=0.99
10	Allprotect (-80^{0}C)		4.59 (0.43)	P=0.99

Figure 2.7 – Tissue homogenate was incubated with irinotecan and the production of SN-38 (active metabolite) quantified by liquid-chromatography mass-spectrometry. Data shown is from patient 3 (primary colorectal tumour). All samples are comparable irrespective of the method of tissue stabilisation used, and whether the samples were stabilised immediately following specimen extraction (samples 1-5) or following a delay of 1 hour (samples 6-10). ANOVA with post-hoc Dunnett's test shows that no samples are statistically significant from the current gold standard (sample 1) i.e. tissue snap frozen in liquid nitrogen.

Immunohistochemistry of sections of primary tumour again revealed no difference in the semi-quantitative scoring of HMGB1 expression. A minor degree of inter-patient variation was seen, however for each patient all sections stained adequately and received identical scores for both coverage and intensity. Figure 2.8 highlights the comparable staining of samples from patient 3 (primary tumour) which scored 3 for coverage (51-74%) and 3 for intensity (moderate). Similar results were seen in colorectal liver metastases.

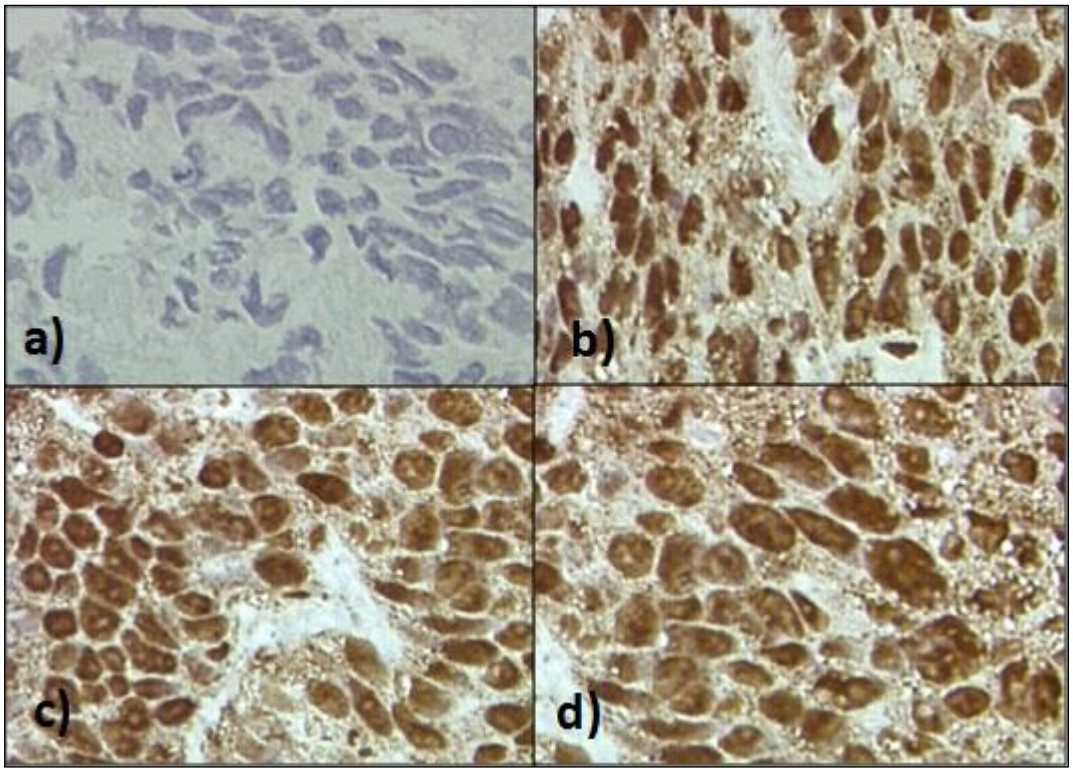

Figure 2.8 – Immunohistochemistry for HMGB1 in samples from patient 3 (primary colorectal tumour): a) Negative control b) Snap frozen in liquid nitrogen c) Allprotect™ at room temperature d) Allprotect™ at 8°C. All sections were scored 3 for coverage (51-74%) and 3 for intensity (moderate). Haemotoxylin counterstain, x400 magnification.

2.3.3 Long term (0 – 24 weeks) maintenance of biomolecule expression and function

DNA

There was insufficient material available to perform DNA analysis on these samples due to a number of smaller tumours in this cohort.

RNA

The yield of extracted RNA was comparable to that observed in the short term study (0.37-0.61µg/mg tissue). All samples had a 260:280 ratio of 1.9 - 2.1, however the RIN fell below 7.0 for those samples archived in Allprotect™ for a period of more than 1 week. The RT2™ Quality Control Array suggested that RNA impurities began to affect both reverse transcription and PCR again after a period of 1 week. Figure 2.9 shows the representative Ct values for miR122 in the liver metastasis of patient 4 clearly demonstrating a progressive

degradation in RNA, which was statistically significant by week 2 (23.60 *vs*. 25.07; p=0.049). Similar data were seen for let7d as well as mRNA levels for *HMGB1* and *CES1* in both primary and metastatic tissue.

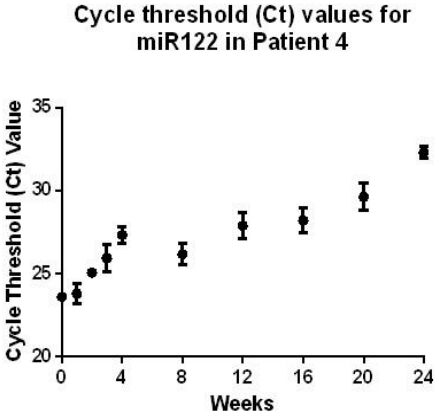

Weeks	Stabilisation Method	Processing	Mean (SD) Cycle Threshold (Ct)	Dunnett's test (wrt 0 weeks)
0	Snap frozen (liquid nitrogen)		23.60 (0.10)	-
1	Allprotect (8ºC)		23.80 (0.61)	P=>0.99
2	Allprotect (8ºC)		25.07 (0.09)	P=<0.05
3	Allprotect (8ºC)		25.93 (0.82)	P=<0.01
4	Allprotect (8ºC)		27.33 (0.52)	P=<0.01
8	Allprotect (8ºC)		26.17 (0.65)	P=<0.01
12	Allprotect (8ºC)		27.90 (0.76)	P=<0.01
16	Allprotect (8ºC)		28.20 (0.77)	P=<0.01
20	Allprotect (8ºC)		29.63 (0.81)	P=<0.01
24	Allprotect (8ºC)	On specimen extraction	32.30 (0.36)	P=<0.01

Figure 2.9 – Cycle threshold (Ct) values for miR122 in the liver metastasis from patient 4. Ct values increase with time archived in Allprotect™, and by 2 weeks there is a statistically significantly difference from the current 'gold standard', i.e. tissue snap frozen in liquid nitrogen (0).

Protein

Protein stability after longer term storage proved much more variable than RNA, with extraction yield ranging from 6.4-30.9 µg/mg tissue and Coomassie staining of polyacrylamide gels identifying progressive degradation of samples with time. Whilst a degree of inter-individual variation was observed in these samples, western blot analysis of HMGB1 showed a marked reduction in protein expression after 2 weeks in Allprotect™. Representative data from patient 1 (primary tumour) is shown in Figure 2.10, which demonstrates that the mean (SD) densitometry of 28.9(0.59)iU achieved by snap freezing the tissue in liquid nitrogen was no longer comparable to tissue archived in Allprotect™ by week 3 (12.43(1.15)iU (p=<0.001), with preservation of expression up until this point. Similar findings were observed for the expression of CES1 and in colorectal liver metastases, and negligible levels of SN-38 were detected in all samples archived in Allprotect™ for periods beyond 2 weeks.

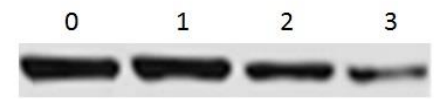

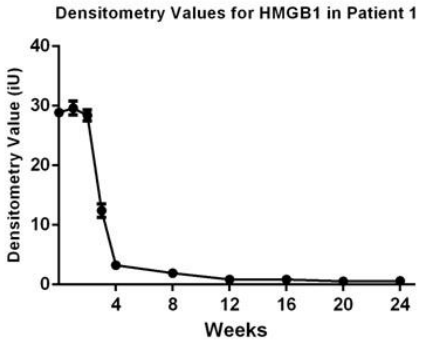

Weeks	Stabilisation Method	Processing	Mean (SD) Densitometry	Dunnett's test (wrt 0 weeks)
0	Snap frozen (liquid nitrogen)	On specimen extraction	28.9 (0.59)	-
1	Allprotect (8ºC)		29.62 (1.16)	P=0.84
2	Allprotect (8ºC)		28.41 (0.93)	P=0.97
3	Allprotect (8ºC)		12.43 (1.15)	P=<0.01
4	Allprotect (8ºC)		3.26 (0.44)	P=<0.01
8	Allprotect (8ºC)		1.91 (0.77)	P=<0.01
12	Allprotect (8ºC)		0.85 (0.53)	P=<0.01
16	Allprotect (8ºC)		0.85 (0.77)	P=<0.01
20	Allprotect (8ºC)		0.55 (0.48)	P=<0.01
24	Allprotect (8ºC)		0.62 (0.69)	P=<0.01

Figure 2.10 – Western blot and corresponding densitometry of HMGB1 expression in primary colorectal cancer samples (patient 1) archived in Allprotect^{TM} . The densitometric panels demonstrate the sharp reduction in protein abundance which occurs between 1 and 3 weeks, by which time it is statistically significantly different from the current 'gold standard', i.e. tissue snap frozen in liquid nitrogen (0).

2.4 Discussion

2.4.1 Summary of aims

The aim of this study was to rigorously evaluate the use of Allprotect™ as an alternative to liquid nitrogen for the short and long term storage of clinical samples from patients undergoing surgical resection of colorectal primary and metatastatic tumours. Tissue integrity under all storage conditions was assessed across a range of typical biomolecules including DNA, mRNA, microRNA and protein. In addition, retention of protein function following storage in Allprotect™ was determined by enzyme activity measurements.

2.4.2 Summary of results

This study has demonstrated that effective tissue stabilisation can be achieved with Allprotect™, and that tissue stabilised in this manner yields high quality DNA, RNA and protein suitable for commonly used laboratory techniques. Comparable protein (by western blot and immunohistochemistry) and mRNA expression for HMGB1 and CES1 in primary colorectal tumour and colorectal liver metastases was observed irrespective of the method of tissue stabilisation employed. Beyond that, the demonstration of comparable production of SN-38, an active metabolite of irinotecan, suggests that protein function (CES1) as well as expression is preserved. miRNA yield was also consistent and all extracted DNA was of sufficient quality for downstream PCR.

Whilst short term tissue stabilisation with Allprotect™ appears to be comparable to liquid nitrogen, its role for long term archiving is less clear. Our study suggests that both protein function and expression are significantly reduced by week 3, and, although densitometry values do not reach statistical significance, visualisation of the western immunoblots suggests that protein degradation may occur even earlier than this. RNA integrity also begins to reduce after one week, with the RIN of samples rapidly falling below 7.0. These findings are confirmed by the RT2 quality control array, and the increasing Ct values seen at qPCR for both mRNA and miRNA. In light of this we have adopted a protocol whereby all samples are removed from Allprotect™ and transferred to a definitive storage facility on a weekly basis.

2.4.3 Current barriers to translational research

Access to good quality clinical material is a fundamental part of translational research (LaBaer, 2012). The standard model for acquisition of clinical material requires a dedicated individual, for example a research nurse or research fellow, being on hand to sample tissue (Magner *et al*, 2007). This in itself has significant cost implications and frequently precludes institutions from being able to contribute their own tissue samples to translational studies (Thasler *et al*, 2013). Following the acquisition of clinical material, the research nurse/fellow would routinely place the sample into a sealed container and snap freeze it in liquid nitrogen. Again, the availability of liquid nitrogen may be variable and there are safety concerns associated with its use. After tissue stabilisation in liquid nitrogen, the final stage is the transfer to a -80^{o}C storage facility which, again, is not available in every institution (Day and Stacey, 2008).

2.4.4 Alternative methods of tissue stabilisation

A number of alternatives to liquid nitrogen have been developed in an attempt to provide lower cost and less resource intense strategies for tissue collection. These tissue stabilisation products also make the transfer of tissue between institutions significantly easier and cheaper. For those institutions with the necessary infrastructure, these approaches would also permit more *ad hoc* tissue sampling; for example, following emergency resections out of hours or unexpected diagnoses on invasive investigations. The best known tissue stabilisation product is RNALater™ (Qiagen, Venlo, Netherlands), but it is often used as an adjunct to liquid nitrogen in an effort to maximise yield rather than as a stabilisation method in its own right (Hatzis *et al*, 2011). The RNA yield of tissue stabilised in RNALater™ and liquid nitrogen are comparable (Khaustova *et al*, 2014), as are those of RNALater™ and an alternative product, PaxGene™ (Qiagen, Venlo, Netherlands) (Weber *et al*, 2010). Allprotect™ offers two key advantages over these existing stabilisation techniques - the ability to preserve DNA and protein structure and function as well as RNA, and the preservation of tissue morphology (Roos-van Groningen *et al*, 2004). In our study, all samples were clearly identifiable as adenocarcinoma with only a minor degree of vacuolation seen in those samples stabilised with Allprotect™. Only two papers have previously investigated the role of Allprotect™. Mee *et al* found lower DNA yield but comparable quality when compared to liquid nitrogen, QIAamp™ (Qiagen, Venlo, Netherlands) and Allprep™ (Qiagen, Venlo, Netherlands), as well as comparable quality RNA and protein yield (Mee *et al*, 2011). Conversely, Staff *et al* were unable to demonstrate preserved antigenicity for immunohistochemical analysis following Allprotect™

stabilisation, and report a mean RIN value of 2.1 (95% CI 0.8 – 3.4) for RNA extracted from 5 patients with benign gynaecological disease (Staff *et al*, 2013). A significant limitation of Allprotect™ is its inability to stabilise DNA, RNA or protein in whole blood or serum, and therefore an alternative strategy would need to be found if this material is also required.

2.4.5 Strengths and limitations of the study

The experimental design was conceived in such a way as to not only determine the feasibility and optimum storage conditions for stabilising tissue in Allprotect™, but also permitted us to ask a further question: Can tissue stabilisation be performed following completion of the surgical procedure? In the 'stability' study, samples 6-10 were all taken at the end of the case, approximately 60 minutes following specimen delivery. The fact that we have demonstrated comparable biomolecule extraction in these samples suggests that an additional member of the research team need not necessarily be available to perform the sampling, and that a member of the surgical team could acquire the tissue at the end of the surgical procedure. Whilst this might not be surprising for protein and DNA retrieval, studies have documented the potential for rapid degradation of RNA from as early as 15 minutes following the onset of tissue ischaemia (Von Euler *et al*, 2005). However Lee *et al* (2013) characterised only a minor reduction in RNA quality which did not affect gene expression levels up to 24 hours following surgical resection. Whilst we have demonstrated comparable RNA quality and yield we would not advocate deliberate delay in the sampling and stabilisation of clinical samples for scientific research, but merely highlight that where this is unavoidable due to institutional constraints, adequate clinical samples can be obtained in this manner.

Whilst our study demonstrates that Allprotect™ offers comparable tissue stabilisation to liquid nitrogen, the panel of biomolecules and laboratory techniques we have studied is narrow. We would therefore advocate that individual research groups validate the use of Allprotect™ for their specific biomolecules and applications of interest. The mere addition of a compound to a clinical sample will inevitably cause biological and chemical differences when compared to samples snap frozen without additive. We have demonstrated no significant difference over the panel we have tested and feel therefore that Allprotect™ is likely to be appropriate for comparison of tissues acquired by the same sampling protocol, however it must be acknowledged that the integration of tissue acquired in this way with an existing tissue bank or comparison to tissue stabilised using an alternative approach may

not be scientifically meaningful. The same argument could however be made for samples acquired across different institutions, all of which will undoubtedly have been sampled, stabilised and processed following slightly different protocols.

2.4.6 Establishing a research infrastructure

This chapter highlights some of the preliminary work performed in order to provide a platform for the remainder of the work contained within this thesis. The collection of patient matched primary and metastatic tissue across multiple sites required the creation of a suitable infrastructrue. In brief this comprised:

- Registration of the project through the Integrated Research Application System (IRAS) to include the completion of Research Ethics Committee (REC) and NHS Research and Development (R&D) proformas
- Responding to queries on the above and provision of patient information sheets, consent forms and notifications to general practitioners
- Attendance at the local meeting of the REC and obtaining final ethical approval
- Attempts to place the study on the NIHR portfolio – failed due to technicalities surrounding the funding stream (at the time Cancer Research (UK) centre awards were ineligible)
- Liaison with NHS R&D co-ordinating centre and global approval of the study
- Establishing a sponsor for the study (Countess of Chester Hospital) and local R&D approval
- The recruitment of a local principal investigator at each of the required trusts
- Following recruitment of a local principal investigator, at each site the following was arranged
    - Site visit and meeting
    - Creation of the site specific information form on IRAS
    - Local research and development approval
    - Letter of access
    - Materials transfer agreement
- After the research sites had been added, the REC responsible for the study was updated and an amendment made to include all research sites
- The completion of ongoing local audit of recruitment figures and research engagement at each of the sites

The infrastructure has since permitted the centralised collection of patient matched primary and metastatic colorectal cancer samples for ongoing translational research in the region. The project was also registered at the Liverpool Tissue Bank.

2.4.7 Conclusion

This study clearly demonstrates that Allprotect™ is appropriate for widening participation in translational research. A major impediment to the recruitment of sampling sites for clinical trials or translational studies is the lack of resources for tissue sampling and storage: this often limits studies to major teaching hospitals simply because the required facilities are not available in smaller hospitals. Foremost in this is the ability to instantly freeze the sample upon collection, prior to transfer or analysis. A method to bypass this bottle-neck could dramatically increase both the scale and recruitment rates of translational studies. In this study, there was no difference between the quality of biological material extracted from tissue samples following storage in Allprotect™ or after snap freezing in liquid nitrogen. Storage for up to one week in Allprotect™ also led to no significant deterioration, meaning that rapid sample retrieval from sampling sites is not required where it may be impractical to accomplish this. After this time period, however, we did detect a significant fall in the quality, and thus it would be imprudent to plan long term storage in this medium.

Across the range of different biomolecules investigated here, there was no evidence that Allprotect™ couldn't play a major role in sample procurement, and this may have profound benefits for the recruitment of smaller or less well-resourced centres for translational research studies.

Chapter 3

Exome sequencing of synchronously resected primary colorectal tumours and colorectal liver metastases to inform oncosurgical management

3.1 Introduction

3.1.1 Genomics of colorectal cancer

Colorectal cancer (CRC) remains the fourth commonest cancer worldwide and the second commonest cause of cancer related death. Like most solid tumours, CRC is a highly complex disorder arising from an interplay between a number of genomic alterations, such as point mutations, rearrangements, gene fusions or copy number alterations (Fearon, 2011) and environmental factors such as diet and lifestyle (Huxley *et al*, 2009). A failure to identify the disease at an early stage of carcinogenesis increases the likelihood of the development of metastases, which, despite significant advances both oncologically and surgically, is still associated with significantly poorer outcomes (Cancer Research UK, 2014).

Our understanding of the development of primary colorectal cancer is improving, with sequential genetic alterations in *APC*, *KRAS*, mismatch repair genes, *TP53* and loss of 18q heterozygosity of great significance. However, how these cells evolve in the process of metastagenesis and the clonal origin and genetic heterogeneity of colorectal liver metastases remains unclear. The initial concept of monoclonal evolution of a tumour, essentially the clonal expansion of dominant tumour clones, has been challenged. The self-feeding polyclonal hypothesis proposes that tumour cells enter the systemic circulation via the tumour vasculature and colonise at a different site therefore establishing a new subpopulation, whereas the mutator phenotype suggests a small population of diverse tumour cells may migrate (Navin and Hicks, 2010). Metastases therefore can be expected to carry similar mutations to their corresponding primary tumour, but also harbour additional mutations acquired after transformation (Siegmund *et al*, 2009). The accrual of these genetic mutations in the metastases results in tumour heterogeneity between sites, presenting problems for treating clinicians. These problems are further confounded in the case of colorectal liver metastases with the knowledge that transcutaneous needle biopsy of the liver lesion is associated with cutaneous seeding and poorer outcomes following surgery (Cresswell, Welsh and Rees, 2009). A thorough understanding of genetic heterogeneity between tumour sites is vital to the development of novel therapeutic agents (Klein, 2009).

3.1.2 Next generation sequencing technology

For many years genomic profiling was conducted using hybridization based micro-array technologies or low-throughput Sanger sequencing. The development of next generation sequencing (NGS) technology has exponentially increased the rapidity and efficacy with which the previously discussed genomic aberrations can be identified and studied.

There are numerous types of next generation sequencing available. Whole genome sequencing uses genomic DNA to identify point mutations, indels, rearrangements and DNA copy number changes; information which is generally detected by paired-end mapping (Chen *et al*, 2009). More focussed exome sequencing can be performed on target regions of genomic DNA which is capable of identifying point mutations and indels. Epigenome sequencing targets genomic DNA to identify sites of DNA methylation and post-translational histone modifications. This can either be achieved using chromatin-immunoprecipitation (ChIP)-based methods (Park, 2009) or DNA methylation sequencing for example using bisulfite-sequencing (Hansen *et al*, 2011). Finally, sequencing of RNA allows for the examination of gene fusions, alternative splicing events, point mutations and indels.

3.1.3 The ion proton platform

There are a number of different platforms available for next generation sequencing studies. The commonest use either pyosequencing (Roche 454, GS FLX Titanium), reversible dye terminators (Illumina HiSeq, Bioscience Heliscope), oligonucleotide chained ligation (Life Technologies SOLiD) or native dNTPs and proton detection (Life Technologies Ion Proton). The selection of an appropriate platform currently relies on a compromise between read length (i.e the number of bases continually read), depth of read (the number of times each section of the library will be read), run time (still a matter of days) and cost (which is extremely variable).

In Ion Proton sequencing the library to be sequenced is a collection of DNA inserts of ~200bp. These are obtained from randomly fragmented genomic DNA of the samples to be sequenced. During sequencing these single stranded inserts function as the template. Such sequencing is referred to as "sequencing by synthesis", during which a complementary strand is built based on the sequence of an adapter ligated template strand. Sequencing is performed on a semiconductor chip containing small beads with clonally amplified template DNA in each microwell. DNA polymerase is added with sequentially unmodified A,

C, G or T dNTPs. Sequencing is based on the detection of hydrogen ions that are released during the polymerization of DNA. If the nucleotide is complementary it is added to the strand. Addition of the nucleotide causes the release of a hydrogen ion, which in turn results in decreased pH that triggers an ion sensor in the chip. The series of electrical pulses transmitted from the chip to a computer is translated into a DNA sequence. If the nucleotide is not complementary, no reaction takes place within that well. The unmodified dNTPs are then flushed out of the system and the next added. This process is repeated 125 times for each base, with no intermediate signal conversion required due to the nucleotide incorporation events being measured directly by the electronics. Signal processing and DNA assembly is carried out using software inbuilt into the platform. Figure 3.1 is a graphical representation of sequencing using the ion torrent platform.

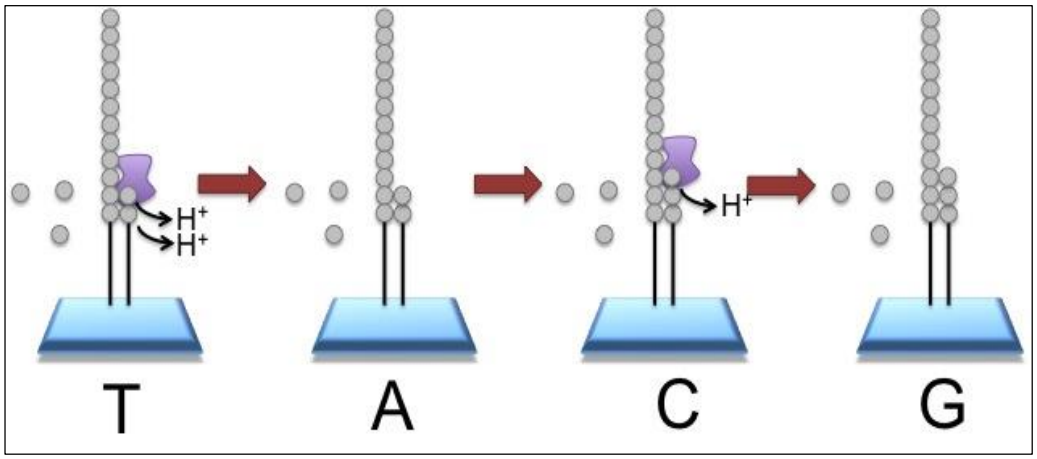

Figure 3.1 – The sequencing by synthesis of the Ion Proton platform. Sequencing is performed on a semiconductor chip containing small beads with clonally amplified template DNA. DNA polymerase is added with sequentially unmodified A, C, G or T dNTPs which are incorporated if complementary, releasing a hydrogen ion which is results in decreased pH that triggers an ion sensor in the chip. If the nucleotide is not complementary, no reaction takes place within that well. The unmodified dNTPs are then flushed out of the system and the next added. Figure taken from the European Bioinformatics Institute (with permission) http://www.ebi.ac.uk/training/online/course/ebi-next-generation-sequencing-practical-course/what-next-generation-dna-sequencing/ion-torre

3.1.4 Aims and hypotheses

The aim of this investigation was to compare and contrast the exome of synchronously resected primary and metastatic colorectal tumours, specifically to identify those genetic aberrations which:

- Are present in the primary tumour but not in the metastasis
- Are present in the metastasis but not in the primary tumour
- Are present in both primary and metastasis (i.e. the primary tumour is predictive of the metastatic genotype)
- May predict response to neoadjuvant therapy

3.2 Methods

3.2.1 Patients and tissue collection

National Health Service Research Ethics Committee and Research and Development approval was obtained for this study. Samples were obtained from four patients undergoing synchronous resection of a primary colorectal tumour and liver metastases. Following delivery of the colorectal specimen the proximal staple line was incised and a linear cut made down the antimesenteric border before excising a peripheral section of tumour using forceps and a scalpel. Following delivery of the liver specimen, an incision was made through the resected surface to the liver metastasis, with care being taken not to breach the liver capsule; a peripheral sample of tumour was obtained. Macroscopically normal adjacent colonic mucosa and liver parenchyma were also obtained, with all tissue sampling performed in the operating theatre under aseptic conditions followed by immediate stabilisation in liquid nitrogen. An additional sample was obtained, formalin fixed and paraffin embedded for concurrent histopathological assessment.

3.2.2 Evaluation of histopathological response

Given all four patients had undergone neoadjuvant treatment, an assessment of histopathological response was made using a scoring system first described by Ribero *et al* (2007), and used for this purpose by Blazer *et al* (2008). The number of residual viable tumour cells within each metastatic nodule was estimated as a percentage of the total tumour surface area that included areas of coagulative necrosis, calcification, fibrosis and the associated histiocytes, foreign body giant cells and inflammatory cells. Samples were subsequently scored as 1 (1-24%), 2 (25-49%), 3 (50-74%) or 4 (>75%) for the purposes of analysis.

3.2.3 DNA extraction, quality control and library preparation

DNA was extracted from harvested material using the DNeasy Blood & Tissue Kit as per manufacturer's instructions (Qiagen, Venlo, Netherlands). Library preparation and sequencing was performed using Ion TargetSeq™ exome enrichment for the Ion Proton™ System (Life Technologies, Carlsbad, USA). Genomic DNA (3.5µg) was fragmented using an ion shear enzyme, and the resulting fragmented DNA cleaned up using Agencourt®

AMPure® XP beads (Beckman Coulter, Brea, USA). The size distribution was checked by running an aliquot of the sample on 2% E-Gel® (Life Technologies, Carlsbad, USA). Adapter ligation was performed using the Ion Plus Fragment Library Kit according to manufacturer's instructions (Life Technologies, Carlsbad, USA). The resulting samples were again cleaned using Agencourt® AMPure® XP beads of 300bp in length using a 2% agarose gel and were eluted using MinElute columns (Qiagen, Venlo, Netherlands). PCR amplification (10 cycles) was subsequently performed to enrich the adaptor-ligated fragments.

3.2.4 Exome sequencing

For capture, 500ng of prepared library was concentrated using a vacuum concentrator and then hybridized with the Ion TargetSeq™ Exome Probe Pool at 47°C for 66 hours. Hybridized library fragments were isolated by magnetic capture using Dynal M-270 streptavidin coated beads (Invitrogen, Carlsbad, USA). PCR amplification (8 cycles) was carried out to amplify the captured library which was again cleaned using Agencourt® AMPure® XP beads. An aliquot of the captured library was run on a High Sensitivity DNA Chip on the Agilent Bioanalyser (Agilent, Santa Clara, USA). Real time PCR validation was performed with pre and post capture libraries to observe the capture efficiency. The purified, exome-enriched library was then used to prepare clonally amplified templated Ion PI™ Ion Sphere™ Particles (ISPs) for sequencing on an Ion PI™ Chip to obtain the necessary data coverage. Sequencing was performed on the Ion Proton™ sequencer at Genotypic Technology's Genomics facility (Bangalore, India).

3.2.5 Variant calling and annotation

Sequenced data was analyzed with Torrent Suite™ v 3.6 (Life Technologies, Carlsbad, USA). Following base calling, raw reads underwent trimming of undesired base calls at the 3' end of the read, the adapter sequence, and low quality 3' ends. The resultant data were filtered of low quality base calls. The raw reads obtained were then aligned to the reference genome (HG19) using the Torrent Mapping Alignment Program for Ion Torrent Data (TMAP) software. Variants were then called and detected using Variant Caller v 4.0, an inbuilt plugin of Torrent Suite v 3.6. These variants were further annotated using Ion Reporter v 1.6 to give location (intronic/exonic/utr), gene name, protein change, function and dbSNP identifier (from the dbSNP database 137).

3.2.6 Somatic variant analysis

Data from tumorous and non-tumorous tissue was compared for each patient. The variants of each sample were compared by chromosome number and position to identify those mutations in the tumour samples which were somatic. The somatic single nucleotide variants (SNVs) identified in both primary and metastatic samples were assessed for functional consequence and biologically deleterious non-synonymous SNVs were selected. The resulting SNVs were compared to identify those present in patient matched primary and metastatic paired samples. Those mutations unique to primary tumour and those unique to liver metastases were subsequently identified. Further analysis was performed to compare and contrast the SNVs present in the responders and non-responders to neoadjuvant systemic therapy.

3.2.7 Ingenuity pathway and network analysis

Genes identified from these lists of SNVs were subjected to pathway analysis using Ingenuity Pathway Analysis (Redwood City, USA). Significant canonical pathways were identified with a threshold p value of <0.05 for significance (after correction). If there are *n* genes in a pathway, and *f* have been identified through sequencing, the p-value is the probability of finding *f* or more genes in a set of *n* genes randomly selected from the global molecular network.

With the aim of reducing the false discovery rate, the Benjamini-Hochberg multiple test correction was used (Benjamini and Hochberg, 1995). In this correction p-values are sorted and ranked, the smallest value receiving 1, second 2 and largest N. Each p-value is then multiplied by N and divided by its assigned rank to give the adjusted p-values.

Ingenuity Pathways Analysis computes a score for each network according to the fit of that network with the identified genes of interest (referred to as the focus genes).The score is derived from a p-value and indicates the probability of the focus genes in a network being found together due to random chance. A score of 2 indicates that there is a 1 in 100 chance that the focus genes are together in a network due to random chance, therefore scores greater than 2 have at least a 99% confidence of not being generated by random chance alone. Analysis must also take into account both the number of focus genes identified and total known genes in each network. A summary of the bioinformatics workflow can be seen in Figure 3.2.

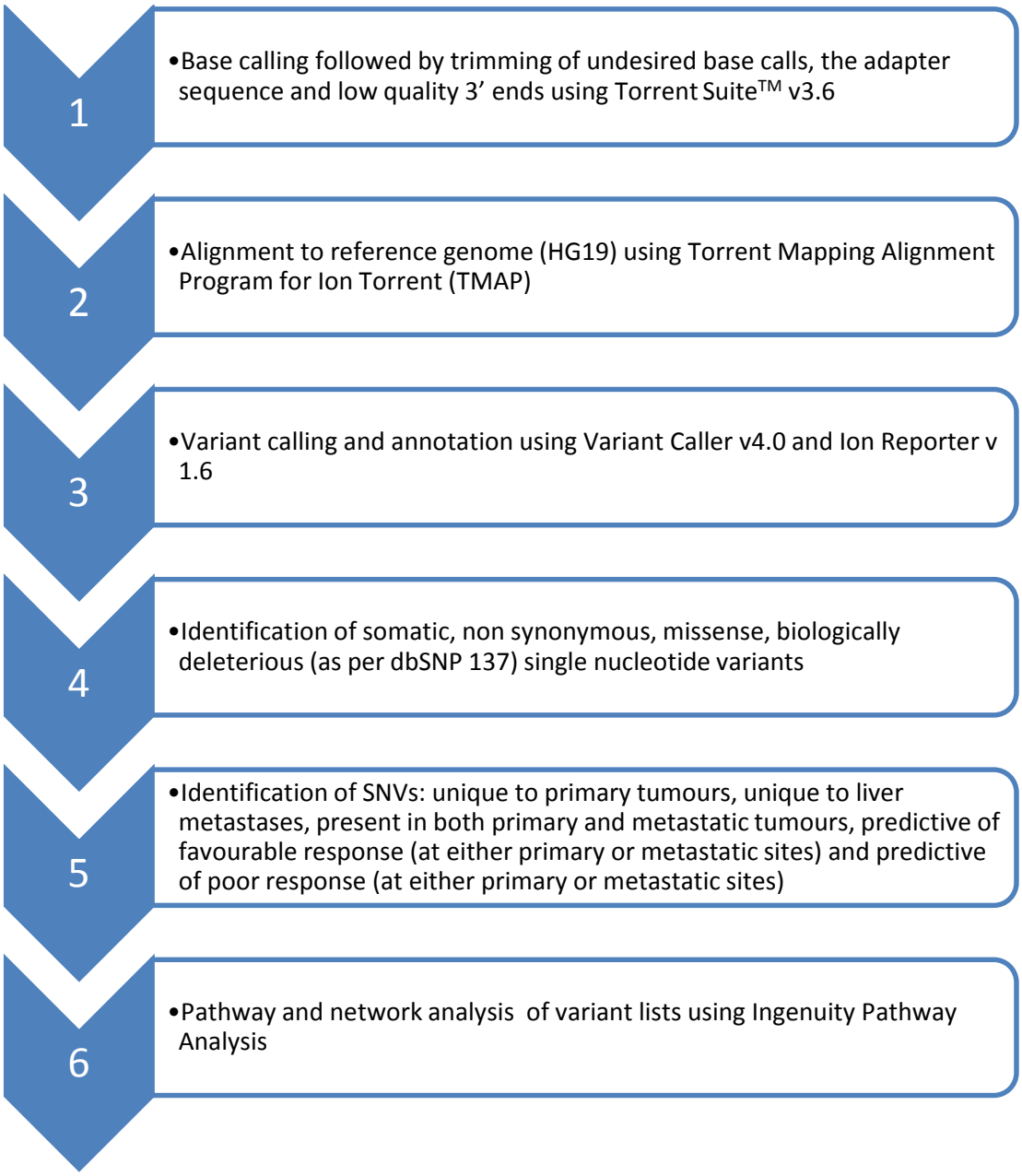

Figure 3.2 – Bioinformatics analysis workflow for exome sequencing of synchronously resected primary colorectal tumours and colorectal liver metastases.

3.2.8 Validation of SNVs by Sanger sequencing

SNVs identified as being of interest during analysis (see Results) were subjected to validation by Sanger sequencing on the same tissue set. Following reconfirmation of DNA quality by agarose gel electrophoresis, samples were cleaned up with an Ultraclean® PCR Clean Up Kit (Mobio, Carlsbad, USA) and quantified using the Nanodrop™ spectrophotometer (Thermo Scientific, Waltham, USA). Targeted forward and reverse

primers were specifically designed and manufactured for each of the SNVs of interest. Sanger sequencing was performed using a BigDye® Terminator v3.1 Cycle Sequencing Kit (Life Technologies, Carlsbad, USA) and 3130XL Genetic Analyser (Life Technologies, Carlsbad, USA), with the resultant FASTA sequence compared with both the reference genome and exome sequencing data to confirm the presence of the previously identified SNVs.

3.3 Results

3.3.1 Clinical information

Demographic and clinical information pertaining to the four patients sequenced is displayed in Table 3.1.

Variable	Patient 1	Patient 2	Patient 3	Patient 4
Age at diagnosis	67	70	59	75
Gender	M	M	F	M
Site of primary	Ascending	Sigmoid	Sigmoid	Sigmoid
T stage	4	3	3	3
N stage	0	0	0	2
Metastatic burden	16 - Bilobar	7 - Bilobar	3 - Bilobar	4 - Unilobar
Neoadjuvant agents	IrMdG	IrMdG	Oxaliplatin, capecitabine, cetuximab	IrMdG
Procedure performed	Right hemicolectomy and multiple segmentectomies	Sigmoid colectomy and multiple segmentectomies	Sigmoid colectomy and multiple segmentectomies	Sigmoid colectomy and left hemi-hepatectomy
Pathological features (primary)	Adenocarcinoma Well differentiated No lymphovascular invasion	Adenocarcinoma Moderately differentiated No lymphovascular invasion	Adenocarcinoma Moderately differentiated No lymphovascular invasion	Adenocarcinoma Poorly differentiated Lymphoid invasion No vascular invasion
Pathological features (liver)	Adenocarcinoma Well differentiated	Adenocarcinoma Moderately differentiated	Adenocarcinoma Moderately differentiated	Adenocarcinoma Poorly differentiated
Tumour regression grade	1	1	3	4

Table 3.1 – Demographic and clinical features of the four patients from whom tumours were sequenced. IrMdG – Irinotecan and modified de Gramont (5-fluoruracil and folinic acid).

All patients underwent 5-fluorouracil based neoadjuvant chemotherapy followed by synchronous resection of a colonic primary and metastatic lesions at a single institution

during the course of the study. All resections were R0 with no significant complications. At the time of writing, all patients were alive with no evidence of recurrent disease.

Two patients (1 and 2) were both scored as having a tumour regression grade of 1. For the purposes of analysis these patients were regarded as the responders to neoadjuvant treatment. Patients 3 and 4 had tumour regression grades of 3 and 4 respectively, and were therefore regarded as the non-responders to neoadjuvant treatment.

3.3.2 Sequencing statistics

All DNA samples passed the necessary quality control steps with adequate 260:280 and 260:230. The colonic mucosa from patient 4 was the only sample regarded as being of suboptimal quality DNA, although still adequate for sequencing (Table 3.2).

		NANODROP QC			QUBIT						
BL No	Sample ID	ng/ul	260/280	260/230	ng/ul	Volume (µl)	QUBIT Yield(ng)	Yield in micro gram	Combined yield (ug)	Minimum Requirement in microgram	QC STATUS
1	SO_2510_1A_1st elution	151.6	1.93	2.1	81.2	90	7308	7.308	10.788	5 microgram by Qbit	Good
2	SO_2510_1A_2nd elution	165.57	1.94	2.42	87	40	3480	3.48		5 microgram by Qbit	
3	SO_2510_1B_1st elution	36.83	1.99	2.61	35.3	90	3177	3.177	4.469	5 microgram by Qbit	Good
4	SO_2510_1B_2nd elution	29.52	2.11	2.71	32.3	40	1292	1.292		5 microgram by Qbit	
5	SO_2510_1C_1st elution	143.2	1.88	1.32	98.8	90	8892	8.892	11.94	5 microgram by Qbit	Good
6	SO_2510_1C_2nd elution	98.29	1.88	1.54	76.2	40	3048	3.048		5 microgram by Qbit	
7	SO_2510_1D_1st elution	77.74	1.96	2.1	69	90	6210	6.21	8.826	5 microgram by Qbit	Good
8	SO_2510_1D_2nd elution	71.21	1.96	2.03	65.4	40	2616	2.616		5 microgram by Qbit	
9	SO_2510_2A_1st elution	640.08	1.89	2	112	90	10080	10.08	14.76	5 microgram by Qbit	Good
10	SO_2510_2A_2nd elution	279.79	1.8	1.52	117	40	4680	4.68		5 microgram by Qbit	
11	SO_2510_2B_1st elution	275.52	1.91	2.34	138	90	12420	12.42	17.22	5 microgram by Qbit	Good
12	SO_2510_2B_2nd elution	136.43	1.94	2.2	120	40	4800	4.8		5 microgram by Qbit	
13	SO_2510_2C_1st elution	120.29	1.83	0.91	54.6	90	4914	4.914	6.374	5 microgram by Qbit	Good
14	SO_2510_2C_2nd elution	126.08	1.68	0.92	36.5	40	1460	1.46		5 microgram by Qbit	
15	SO_2510_2D_1st elution	73.01	2.02	2.15	57.9	90	5211	5.211	6.311	5 microgram by Qbit	Good
16	SO_2510_2D_2nd elution	27.88	2.04	3.39	27.5	40	1100	1.1		5 microgram by Qbit	
17	SO_2510_3A_1st elution	61.61	2	2.33	43.9	90	3951	3.951	5.143	5 microgram by Qbit	Good
18	SO_2510_3A_2nd elution	35.28	1.8	1.79	29.8	40	1192	1.192		5 microgram by Qbit	
19	SO_2510_3D_1st elution	52.22	1.78	0.93	42	90	3780	3.78	4.488	5 microgram by Qbit	Good
20	SO_2510_3D_2nd elution	42.19	1.66	0.87	17.7	40	708	0.708		5 microgram by Qbit	
21	SO_2510_4A_1st elution	65.21	1.8	1.3	28.2	90	2538	2.538	3.162	5 microgram by Qbit	Suboptimal
22	SO_2510_4A_2nd elution	27.54	1.76	1.24	15.6	40	624	0.624		5 microgram by Qbit	
23	SO_2510_4B_1st elution	186.21	1.95	1.95	62.5	90	5625	5.625	8.833	5 microgram by Qbit	Good
24	SO_2510_4B_2nd elution	142.49	1.78	1.35	80.2	40	3208	3.208		5 microgram by Qbit	
25	SO_2510_4C_1st elution	249.45	1.99	1.71	74.5	90	6705	6.705	8.253	5 microgram by Qbit	Good
26	SO_2510_4C_2nd elution	185	1.92	1.65	38.7	40	1548	1.548		5 microgram by Qbit	
27	SO_2510_4D_1st elution	113.68	1.97	1.99	75.3	90	6777	6.777	8.545	5 microgram by Qbit	Good
28	SO_2510_4D_2nd elution	43.51	1.84	1.98	44.2	40	1768	1.768		5 microgram by Qbit	

Table 3.2 – Quality control data from samples undergoing exome sequencing with Ion Proton. Sample ID column identifies samples as follows: SO_2510 relates to project id; 1-4 relate to patient number; A-D relate to tissue type (A – colonic mucosa, B – primary tumour, C – liver parenchyma, D – liver metastasis). All quality control variables and yield were good, with the exception of the colonic mucosa from patient 4. DNA was suboptimal but still adequate for sequencing.

Having established appropriate quality DNA, samples underwent library preparation described above and were sequenced. The total number of reads obtained per sample ranged from ~23-54x10^6 (Table 3.3).

Patient	Sample	Number of Reads
1	Colonic Mucosa	41846478
	Primary Tumour	36382877
	Liver Parenchyma	44525752
	Liver Metastases	50127733
2	Colonic Mucosa	35296569
	Primary Tumour	46092664
	Liver Parenchyma	39611322
	Liver Metastases	54105628
3	Colonic Mucosa	47251410
	Primary Tumour	41224669
	Liver Parenchyma	51992117
	Liver Metastases	48375092
4	Colonic Mucosa	41328946
	Primary Tumour	38052851
	Liver Parenchyma	45159239
	Liver Metastases	22924823

Table 3.3 – Total number of raw reads through Ion Proton exome sequencing.

Further analysis of the sequencing statistics identified that 62.96 - 83.17% of reads were successfully on target areas of the genome, with average base depth per target of 34.68 – 79.63. The result of this coverage has ensured that a minimum of 96.58% of the target (the whole exome) has been sequenced, with 67.61 – 88.33% of targets covered to a depth of at least 20X (Table 3.4).

Sample ID	Coverage Summary							
	Number of mapped reads	Percent reads on target	Average base coverage depth	Uniformity of base coverage	Average base coverage depth per target	Uniformity of base coverage per target	Targets with base coverage at 1x	Targets with base coverage at 20x
Sample 1A	41285283	75.26%	58.05	80.98%	61.45	89.29%	97.71%	82.96%
Sample 1B	35895751	75.42%	47.2	82.12%	51.14	90.57%	97.59%	80.16%
Sample 1C	44061095	75.41%	61.56	81.18%	66.58	88.84%	97.38%	84.49%
Sample 1D	49563231	74.76%	64.91	81.91%	68.54	90.31%	98.07%	85.51%
Sample 2A	34869063	63.20%	40.16	82.50%	43.43	89.10%	96.85%	74.37%
Sample 2B	45538474	63.10%	49.44	82.10%	54	89.78%	96.91%	80.90%
Sample 2C	39037583	64.02%	42.06	83.22%	46.12	91.36%	97.11%	78.40%
Sample 2D	53450361	62.96%	61.54	82.32%	66.68	89.79%	97.28%	84.64%
Sample 3A	46651891	81.06%	68.48	80.55%	74.73	88.21%	97.47%	85.63%
Sample 3B	40603925	81.82%	57.09	82.62%	61.57	90.72%	97.82%	85.19%
Sample 3C	51239767	80.56%	74.47	82.65%	79.63	90.29%	97.92%	88.33%
Sample 3D	47771464	80.82%	72.37	82.07%	77.45	88.48%	97.53%	86.45%
Sample 4A	40903016	81.72%	61.66	80.90%	66.46	88.65%	96.65%	84.51%
Sample 4B	37612651	82.42%	53.85	81.15%	57.93	89.84%	97.42%	82.86%
Sample 4C	44663685	80.48%	66.59	80.18%	72.22	87.23%	96.58%	84.71%
Sample 4D	22694738	83.17%	31.74	81.69%	34.68	90.29%	96.82%	67.61%

Table 3.4 – Sequencing statistics for all samples. Sample ID (column 1) 1-4 relates to patient number, and A-D tissue type (A: normal mucosa, B: colorectal primary tumour, C: normal liver parenchyma, D: liver metastasis). The report attests to a high number of reads successfully on target, a 1x coverage of 96.58 – 98.07% and 20x coverage of 67.61 – 88.33% of the targeted exome.

3.3.3 Variant calling and annotation

The mapped reads described above were subjected to variant calling based on a number of quality control criteria designed to optimise the analysis for high frequency variants and minimal false positive calls. These include minimum coverage criteria and quality scores for the SNV on each strand and a minimum observed allele frequency. The total number of variants identified can be seen in Table 3.5.

Variant Category	Patient 1		Patient 2		Patient 3		Patient 4		Total
	1B	1D	2B	2D	3B	3D	4B	4D	
Synonymous Known	463	738	847	945	650	430	637	452	5162
Synonymous Novel	67	61	65	57	36	47	57	56	446
Synonymous Total	530	799	912	1002	686	477	694	508	5608
Frameshift deletion Known	42	35	67	66	37	37	56	57	397
Frameshift deletion Novel	66	60	85	59	66	58	133	126	653
Frameshift deletion	108	95	152	125	103	95	189	183	1050

Total									
Stop loss Known	3	0	2	3	3	4	4	4	23
Stop loss Novel	0	0	0	0	0	1	0	0	1
Stop loss Total	3	0	2	3	3	5	4	4	24
Nonsense Known	10	5	19	16	9	9	9	7	84
Nonsense Novel	6	9	5	5	0	9	11	3	48
Nonsense Total	16	14	24	21	9	18	20	10	132
Missense Known	514	754	901	1082	673	528	671	455	5578
Missense Novel	129	150	115	89	80	97	131	126	917
Missense Total	643	904	1016	1171	753	625	802	581	6495
Non-Synonymous Known	527	759	922	1101	685	541	684	466	5685
Non-Synonymous Novel	135	159	120	94	80	107	142	129	966
Non-Synonymous Total	662	918	1042	1195	765	648	826	595	6651
Somatic Known	1693	2288	2973	3414	2072	1714	2134	1449	17737
Somatic Novel	463	458	429	369	321	353	532	517	3442
Somatic Total	2156	2746	3402	3783	2393	2067	2666	1966	21179
Total Variants	**26881**	**28762**	**28303**	**29009**	**28768**	**29498**	**27562**	**23442**	**222225**

Table 3.5 – Total number of high quality variants identified through Ion Proton exome sequencing

Called variants were subjected to the analysis workflow outlined in Section 3.2.6. This workflow was designed to remove germline mutations and identify somatic SNVs that are non-synonymous, missense and biologically deleterious. It is these SNVs which have been used for subsequent bioinformatics analysis, the numbers of which were identified in each of the samples can be seen in Table 3.6. A total of 585 unique SNVs were identified.

Patient	Sample	Number of SNVs
1	Primary Tumour	94
	Liver Metastases	110
2	Primary Tumour	106
	Liver Metastases	120
3	Primary Tumour	93
	Liver Metastases	88
4	Primary Tumour	98
	Liver Metastases	85

Table 3.6 – Total number of somatic, non-synonymous, missense, biologically deleterious SNVs identified in each of the tumour samples.

3.3.4 Variants unique to the primary tumours

This analysis identified all those eligible SNVs present in one or more of the primary tumours but not present in any of the metastases. A total of 215 SNVs were identified across 177 genes spanning all autosomes and the X chromosome. The complete list of variants can be seen in Appendix 1 – Lists of single nucleotide variants from exome sequencing Table 1: Single nucleotide variants exclusive to the primary tumours.

Ingenuity core analysis of direct and indirect relationships revealed the significant canonical pathways in this group to be: α-tocopherol degradation, vitamin C transport, glycine biosynthesis III, GDP-L fructose biosynthesis I and TCA cycle II. Statistics for these identified pathways can be seen in Table 3.7.

Pathway	p-value	Ratio
α-tocopherol degradation	5.36E-04	2/4 (0.5)
Vitamin-c transport	7.64E-03	2/14 (0.143)
Glycine biosynthesis	1.90E-02	1/2 (0.5)
GDP-L-fucose biosynthesis I	1.90E-02	1/2 (0.5)
TCA cycle II (eukaryotic)	2.01E-02	2/23 (0.087)

Table 3.7 – Pathway analysis for SNVs unique to the primary tumours. P-value is adjusted using Benjamini-Hochberg correction. Ratio identifies the number of focus genes identified (numerator) in the pathway (denominator).

Further analysis of all (unfiltered) biological pathways identified 5 networks with scores greater than 2 pertaining to: connective tissue disorders, drug metabolism, infectious diseases, cell cycle and molecular transport. The focus genes and statistics pertinent to these networks can be seen in Table 3.8.

ID	Molecules in Network	Score	Focus Molecules	Top Diseases and Functions
1	26s Proteasome,ADAMTS1,Akt,APOB,C5orf22,CHRNA5,CLDN3,COL15A1,COL6A2,CTBP2,DROSHA,DUOX2,E2f,ELP2,ERK1/2,estrogen receptor,FGFR3,FSH,GALNT2,GDNF,GLB1,Hsp70,INF2,KRT18,MUC4,MUC16,NCOR1,NFkB (complex),PABPC1,PI3K (complex),PRKRA,PTPRS,TCF3,TNS1,USPL1	44	25	Connective Tissue Disorders, Developmental Disorder, Skeletal and Muscular Disorders
2	AGTR1,AURKA,CBX5,CDC27,CNN2,CTNNB1,CYP2C8,CYP2D6,DCLK1,DHTKD1,FUT11,Histone h3,HIVEP3,HNF4A,KIFC1,MAGI1,MSH6,NFATC2IP,NR1I2,NUPR1,PABPC3,PAK7,PPP1R2,RAB11FIP5,RB1,RNF123,RPL19,SDHA,SOX7,SPATS2L,SRRM2,TFAP2A,TNFRSF14,TNIK,TRAF2	22	15	Drug Metabolism, Small Molecule Biochemistry, Cellular Assembly and Organization
3	ADD1,CCL5,CCRN4L,CD93,CD300C,CSRNP1,CX3CR1,CYP4F2,DMTN,EHD1,F2,F9,FERMT1,FMN2,HSPG2,KCNJ12,KHSRP,KRT34,LILRA5,MAPK1,MT-CYB,PHF11,PI3,RELA,SAMHD1,SERPINB8,SERPINB10,SQLE,SREK1IP1,TDRD7,TGM2,TNF,TPMT,TPSD1,ZNF318	20	14	Infectious Disease, Hematological System Development and Function, Organismal Functions
4	ABCC5,BMP2K,CDKN1A,CELF1,CHAT,COL5A3,COTL1,CSAD,ESR1,ESRRA,FAM102A,FKBPL,GPR6,HAMP,HSF1,IFI16,Interferon alpha,KLF16,KRT13,LOC100996763/NOTCH2NL,MAZ,MINOS1,MSR1,NDUFS2,NFYA,PAK2,Pkc(s),PLEKHG2,POU2F1,PTGS2,RASA4,SEC14L3,SMARCA4,TGM1,UBALD1	20	14	Cell Cycle, Nervous System Development and Function, Organ Morphology
5	ABCC3,ACSL3,ADA,AMOTL2,ARPC1B,CASP1,DOCK7,EVL,HIST4H4,IL13,IL3RA,KIF24,KLK10,KMT2C,MLH1,NAA30,NLRC4,PFKP,PIEZO1,PRDM5,S100A2,SETD8,SKIV2L,SLC16A1,SLC25A5,SLC2A1,SLC43A3,SLC5A8,SYVN1,TMSB10/TMSB4X,TNFRSF10B,TP53,TPT1,WNT10B,YLPM1	18	13	Molecular Transport, Cell Death and Survival, Developmental Disorder

Table 3.8 - Network analysis for SNVs unique to the primary tumours. The score is derived from a p-value and indicates the probability of the focus genes in a network being found together due to random chance. Focus molecules is the total number of SNVs of interest identified in the respective network.

3.3.5 Variants unique to the liver metastases

This analysis identified all those eligible SNVs present in one or more of the metastatic tumours but not present in any of the primaries. A total of 226 SNVs were identified across 199 genes spanning all autosomes and the X chromosome. The complete list of variants can be seen in Appendix 1 – Lists of single nucleotide variants from exome sequencing Table 2: Single nucleotide variants exclusive to the metastatic tumours.

Ingenuity core analysis of direct and indirect relationships revealed the significant canonical pathways in this group to be: AMPK signalling, rennin-angiotensin signalling, role of NANOG in mammalian embryonic stem cell pluripotency, basal cell carcinoma signalling and PEDF signalling. Statistics for these identified pathways can be seen in Table 3.9.

Pathway	p-value	Ratio
AMPK signalling	5.84E-04	7/132 (0.053)
Renin-angiotensin signalling	6.36E-03	5/108 (0.046)
Role of NANOG in mammalian embryonic stem cell pleuripotency	6.61E-03	5/109 (0.046)
Basal cell carcinoma signalling	6.62E-03	4/69 (0.058)
PEDF signalling	7.32E-03	4/71 (0.056)

Table 3.9 – Pathway analysis for SNVs unique to the metastatic tumours. P-value is adjusted using Benjamini-Hochberg correction. Ratio identifies the number of focus genes identified (numerator) in the pathway (denominator).

Further analysis of all (unfiltered) biological pathways identified 8 networks with scores greater than 2 pertaining to: Cancer, respiratory disease, dermatological disease and conditions, infectious disease, DNA replication, recombination and repair, endocrine system disorders, gastrointestinal disease, metabolic disease, cellular development, haematological system development and function, haematopoiesis, developmental disorder, organismal injury and abnormalities, inflammatory response, cellular movement,

cardiac infarction, cell cycle. The focus genes and statistics pertinent to these networks can be seen in Table 3.10.

ID	Molecules in Network	Score	Focus Molecules	Top Diseases and Functions
1	26s Proteasome,A4GALT,APOBEC3G,CALCA,calpain,caspase,CD1A,CHRNA3,CTBP2,DSG1,DUOX2,E2f,EP400,FANCA,FES,GATA3,Hsp27,Hsp90,HSPD1,Interferon alpha,KMT2C,KRT14,NOTCH1,P38 MAPK,p70 S6k,PABPC1,PI3K (complex),Pkc(s),POU4F2,RBBP5,SETD8,STK17A,TH,TLR2,TP53	39	23	Cancer, Respiratory Disease, Dermatological Diseases and Conditions
2	ACTN2,ASPM,ATXN1,BNIP3L,CLCN4,CORO1C,DNA2,DNAJC15,DPH6,ELMOD1,EME1,ERCC2,ERCC5,FLVCR1,GHR,ING2,ITIH1,KAT5,KCNJ12,MKL2,MPG,NAV1,NR3C1,NUPR1,PARN,PARP4,PDLIM2,PLK3,PRUNE2,PTX3,RAG1,RELA,SERF1A/SERF1B,SERTAD2,ZC3HAV1	24	16	Infectious Disease, Respiratory Disease, DNA Replication, Recombination, and Repair
3	ADRA2A,ADRB3,AHSP,Akt,ALDH3B2,CDH8,CDH13,CFTR,ERK,ERK1/2,estrogen receptor,FUT3,Histone h3,Histone h4,HNF1A,HRAS,IgG,IL36A,INS,IRS,Jnk,Mapk,MBD1,NFkB (complex),NHLRC1,NOD1,NUP98,PACSIN2,PAK2,PI3Kγ,PPL,PRKRA,RALGDS,SYT6,TRPM2	22	16	Endocrine System Disorders, Gastrointestinal Disease, Metabolic Disease
4	ACTR1A,ASUN,BMP4,C21orf119,CCT8,CDK8,CDKN1A,COL5A3,E2F1,FAM86C1,FRG1,GZMM,HSD17B14,IFI30,KMT2E,LRBA,LUM,MUC16,NFYA,PARP1,PTPRCAP,PTPRU,RAB33A,RRN3,SALL2,SLC22A16,SMARCA4,TAL1,TBP,TCF3,TMEFF1,TMEM180,TYR,WNT16,ZP3	17	14	Cellular Development, Hematological System Development and Function, Hematopoiesis
5	ACE,ADORA1,ALG1,BCAS3,CHTOP,CNN2,CTNNB1,DDX54,DYNLL2,ERG,ESR1,GPR64,KMT2D,LAMA5,MAGI1,MUC6,NCOA4,NRCAM,NUP88,NUP214,PDZK1,PRSS1,PTEN,RANBP2,RBFOX2,RNF31,RYR3,TACC1,TFF1,TGFBR2,TMEM74,TNRC6A,TRIM65,WNT2,WNT11	15	12	Cancer, Developmental Disorder, Organismal Injury and Abnormalities
6	ACACB,ADIPOQ,AGTR1,AZU1,CCRL2,CD300C,CEACAM3,COL4A3,CP,CXCL16,DCD,EHD1,EMR2,FCGR1B,GNAQ,H	12	10	Inflammatory Response, Cellular Movement, Cardiac

	SP,HSPA1A/HSPA1B,IFNG,ITGB3,LGALS9,LILRA5,LRP1B,MAGEA3/MAGEA6,MARCKSL1,MORC2,MYO9B,PABPC3,PLA2G5,PTGDR,SACS,Sod,STAR,TGM2,TNF,VIPR1			Infarction
7	ANAPC7,BRCA1,CCNA2,CCNB1,CDC16,CDC20,CDC27,CDK2,CEBPD,CHUK,ERBB3,FOXM1,GADD45A,GRB2,HDAC1,HNRNPA1,HNRNPH1,HNRNPK,Hsp90,HSP90AB1,MAD2L1,NCAPG,NCL,NPM1,PCDHA9,PLEC,PLK1,RB1,RBMX,Rnr,SBDS,SOD2,SPTAN1,TERT,TNXB	4	5	Cell Cycle, Cancer, Organismal Injury and Abnormalities
8	KCNB1,KCNG4	4	2	Cancer, Organismal Injury and Abnormalities, Reproductive System Disease

Table 3.10 - Network analysis for SNVs unique to the metastatic tumours. The score is derived from a p-value and indicates the probability of the focus genes in a network being found together due to random chance. Focus molecules is the total number of SNVs of interest identified in the respective network.

3.3.6 Paired variants

This analysis identified all those eligible SNVs present in at least one primary and metastatic tumour pertaining to the same patient. A total of 81 SNVs were identified across 67 genes spanning the X chromosome and all autosomes except 22. The complete list of variants can be seen in Appendix 1 – Lists of single nucleotide variants from exome sequencing Table 3: Single nucleotide variants present in paired samples.

Ingenuity core analysis of direct and indirect relationships revealed the significant canonical pathways in this group to be: ErbB signalling, germ cell-sertoli cell junction signalling, endothelin-1 signalling, antiproliferative role of somatostatin receptor 2, and rening-angiotensin signalling. Statistics for these identified pathways can be seen in Table 3.11.

Pathway	p-value	Ratio
ErbB signalling	5.87E-07	6/85 (0.071)
Germ cell-sertoli cell junction signalling	1.40E-06	7/156 (0.045)
Endothelin-1 signalling	2.20E-06	7/167 (0.042)
Antiproliferative role of somatostatin receptor 2	2.37E-06	5/60 (0.083)
Renin angiotensin signalling	2.41E-06	6/108 (0.056)

Table 3.11 – Pathway analysis for SNVs present in at least one primary and metastatic tumour pertaining to the same patient. P-value is adjusted using Benjamini-Hochberg correction. Ratio identifies the number of focus genes identified (numerator) in the pathway (denominator).

The ErbB signalling pathway was identified as the most significant pathway arising from the analysis of SNVs meeting these criteria (Figure 3.3). Whilst only 6 (*KRAS, MAP2K3, PAK2, PIK3C2G, PLCG2, RRAS*) of the 85 genes contained SNVs (ratio 0.07), the likelihood of this combination of SNVs occurring due to chance alone is $<5.87 \times 10^{-7}$. The identified genes are well known, i.e. *KRAS, RRAS* and a number of associated downstream kinases.

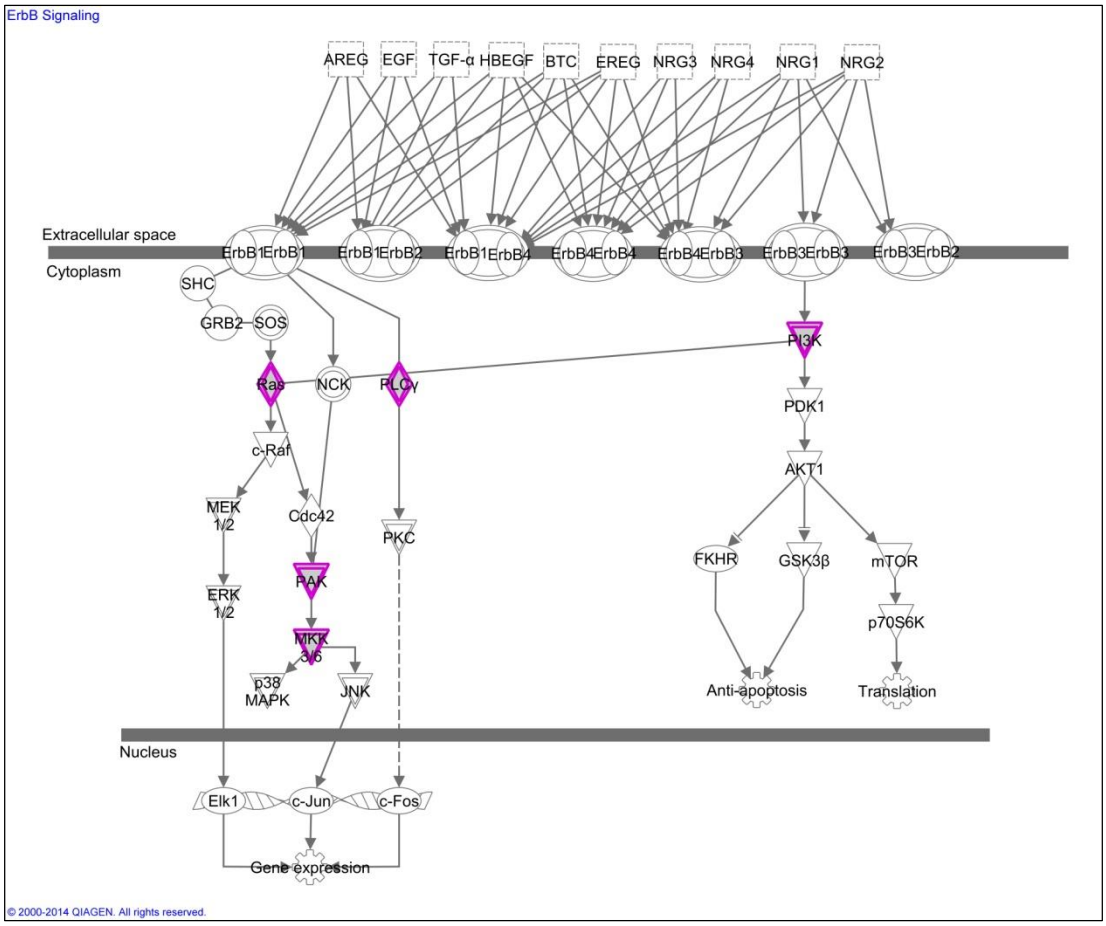

Figure 3.3 – The ErbB signalling pathway was identified as the most statistically significant pathway arising from analysis of the SNVs present in at least one primary and metastatic tumour pertaining to the same patient. The focus genes in which the SNVs have arisen are highlighted in purple.

Further analysis of all (unfiltered) biological pathways identified 3 networks with scores greater than 2 pertaining to: endocrine system disorders, gastrointestinal disease, inflammatory disease, cellular development, nervous system development and function, tissue development, free radical scavenging, molecular transport and cellular growth and proliferation. The focus genes and statistics pertinent to these networks can be seen in Table 3.12.

ID	Molecules in Network	Score	Focus Molecules	Top Diseases and Functions
1	A2M,ABLIM,ADCY7,Akt,ARPC1A,ATP9A,BRAF,C1QTNF9,COL18A1,Cyclin A,DUSP3,ERK,ERK1/2,FSH,GNLY,GNRH,IgG,KRAS,KRT18,LGALS3,Lh,MAP2K3,NCOA1,NFkB (complex),PAK2,PDXK,PLCG2,PLIN3,POP5,PRKX,PRSS1,PRSS3,PTPRN,TLK1,USPL1	23	13	Endocrine System Disorders, Gastrointestinal Disease, Inflammatory Disease
2	ACAA1,ACSS2,ANAPC5,CCND1,CDC27,CDK5RAP2,CINP,CREB1,CTNNB1,DBN1,DPEP1,EPHB3,ERG,GFRA3,LAMB1,MAGI1,MAML1,MGEA5,MINK1,MYO5A,NME1,NOS1,NRP2,PABPC1,PPARA,RB1,STARD4,SVIL,TCF7,TUBA4A,UTRN,VENTX,WNT2,WNT11,ZMIZ2	16	10	Cellular Development, Nervous System Development and Function, Tissue Development
3	ACTN2,AGTR1,AKAP13,BNIP3L,CYP3A4,DIABLO,DRD5,EPB41L3,G3BP2,GCH1,KCNJ12,LTB,MAP3K7,NOD2,NR3C1,NRIP1,PABPC3,PAWR,PLD1,PPP1R13L,PTCH1,RELA,RGS2,RIPK2,RRAS,SDHA,SH,SNX1,SPTBN1,TADA3,TP53BP2,TRAF5,TRAF3IP2,WDR26,YWHAH	12	8	Free Radical Scavenging, Molecular Transport, Cellular Growth and Proliferation

Table 3.12 - Network analysis for SNVs present in at least one primary and metastatic tumour pertaining to the same patient. The score is derived from a p-value and indicates the probability of the focus genes in a network being found together due to random chance. Focus molecules is the total number of SNVs of interest identified in the respective network.

3.3.7 Predictors of favourable response

This analysis identified all those eligible SNVs present in one or more of the primary or metastatic tumours which exhibited favourable response to neoadjuvant chemotherapy (i.e. patient 1 and 2), which were not also present in those exhibiting unfavourable response (i.e. patient 3 and 4). A total of 268 SNVs were identified across 228 genes spanning all autosomes and the X chromosome. The complete list of variants can be seen in Appendix 1 – Lists of single nucleotide variants from exome sequencing Table 4: Single nucleotide variants exclusive to the responders.

Ingenuity core analysis of direct and indirect relationships revealed the significant canonical pathways in this group to be: thyroid cancer signalling, regulation of the epithelial-mesenchymal transition pathway, ovarian cancer signalling, acute myeloid leukemia signalling, and colorectal cancer metastasis signalling. Statistics for these identified pathways can be seen in Table 3.13.

Pathway	p-value	Ratio
Thyroid cancer signalling	7.32E-06	6/39 (0.154)
Regulation of the epithelial-mesenchymal transition pathway	1.55E-05	11/182 (0.06)
Ovarian cancer signalling	3.21E-05	9/130 (0.069)
Acute myeloid leukaemia signalling	4.00E-05	7/76 (0.092)
Colorectal cancer metastasis signalling	1.35E-04	11/231 (0.048)

Table 3.13 – Pathway analysis for SNVs unique to the responding tumours. P-value is adjusted using Benjamini-Hochberg correction. Ratio identifies the number of focus genes identified (numerator) in the pathway (denominator).

Further analysis of all (unfiltered) biological pathways identified 7 networks with scores greater than 2 pertaining to: cancer, gastrointestinal disease, respiratory disease, organismal development, connective tissue disorders, dermatological diseases and conditions, cellular assembly and organisation, cellular function and maintenance, drug metabolism, cellular movement, haematological system development and function, immune cell trafficking, cellular movement, cell-to-cell signalling and interaction and inflammatory response. The focus genes and statistics pertinent to these networks can be seen in Table 3.14.

ID	Molecules in Network	Score	Focus Molecules	Top Diseases and Functions
1	26s Proteasome,BRAF,CALCA,CD3,CD1A,CHRNA3,CHRNA5,CTBP2,Cyclin A,DCLK1,EP400,ERK,ERK1/2,GATA3,Histone h3,Histone h4,HSPD1,IFI16,INS,KMT2C,KRAS,LGALS3,MBD1,MSH6,MUC16,NOTCH1,PI3K (complex),Pka,Pkc(s),SETD8,TCF3,TH,TLR2,TP53,ZP3	40	25	Cancer, Gastrointestinal Disease, Respiratory Disease
2	A2M,Akt,ALDH3B2,APOB,C5orf22,CLDN3,DSC1,E2f,ELP2,estrogen	31	21	Organismal Development,

	receptor,GALNT2,GHR,HNF1A,Hsp70, Hsp90,HSPG2,IgG,Interferon alpha,Jnk,KRT14,LDL,LDL-cholesterol,MAP2K3,Mek,NFkB (complex),NOD1,NOS1,NUP98,P38 MAPK,PLCG2,PLEC,PRKRA,SACS,SYT6,TGM1			Connective Tissue Disorders, Dermatological Diseases and Conditions
3	ADD1,AGTR1,APP,ARHGAP17,ATXN1,CD81,CNN2,CTNNB1,CYP2B6,CYP2C8,CYP2D6,DNM1,DVL1,EPB41L3,ERG,GNAQ,HNF4A,IGSF8,ITGB1,LAMA5,MAGI1, MYO5A,NAA10,NOTCH4,NR1I2,NRCAM,PABPC3,PAK7,ROCK2,RPL19,RRAS,RYR3,VANGL2,WNT2,WNT11	19	15	Cellular Assembly and Organization, Cellular Function and Maintenance, Drug Metabolism
4	Aldose Reductase,ATXN10,AZU1,CCND1,CCT8,CDC27,CEACAM3,CHAT,CP,CXCL16,FCGR1B,GGT1,GZMM,HSP,IFNG,IL17RB,KIF26B,MAGEA3/MAGEA6,MARCKSL1, MYO9B,NQO1,PARP1,Pkc(s),PLA2G5,PTGDR,SERPINB8,SERPINB10,SLC25A5,Sod,TNF,TNFRSF10B,TYMP,TYR,VIPR1,YLPM1	17	14	Cellular Movement, Hematological System Development and Function, Immune Cell Trafficking
5	ABCC5,ACSS2,CD93,CDCA7,COL4A3,COL5A3,CPE,CSAD,CX3CR1,ESR1,ESRRA, FAM102A,FBP1,FERMT1,FMN2,ITGB3,ITIH1,KRT13,LAMB1,MGEA5,MINOS1,NAV1,NFYA,PDLIM2,PHKB,PNRC1,POU2F1,PTX3,RELA,SLC7A2,TGM2,TMEM74, UBALD1,WNT11,YPEL3	16	13	Cellular Movement, Cell-To-Cell Signaling and Interaction, Inflammatory Response
6	ABHD2,ACTN2,ACTR1A,ALDH3A1,CDKN1A,CELF1,CORO1C,DEDD2,DNASE1L3,E2F1,FOXG1,HNRNPA3,HSF1,IFI30,JMJD6,LOC100996763/NOTCH2NL,LUM, MT1L,NDUFS2,NPAT,NR3C1,NRP2,PAK2,PBRM1,POLA2,RIMS1,RRM1,RRN3,SALL2,SMARCA4,SRSF2,SWI-SNF,TAF1B,TBP,WNT16	14	12	Cell Cycle, Connective Tissue Development and Function, Cellular Assembly and Organization
7	ASPM,ATF3,ATR,AURKA,CASP3,CCND1,CHUK,CXCL8,DHTKD1,DPH6,EREG,FLVCR1,Histone h3,KAT5,KIF2C,MKL2,MYC,NUPR1,PARP1,PLK1,PPP1R2,RAG1,SCN2A,TP53	9	8	Cancer, DNA Replication, Recombination, and Repair, Cell Cycle

Table 3.14 - Network analysis for SNVs unique to the responding tumours. The score is derived from a p-value and indicates the probability of the focus genes in a network being found together due to random chance. Focus molecules is the total number of SNVs of interest identified in the respective network.

3.3.8 Predictors of poor response

This analysis identified all those eligible SNVs present in one or more of the primary or metastatic tumours which exhibited poor response to neoadjuvant chemotherapy (i.e. patient 3 and 4), which were not also present in those exhibiting favourable response (i.e. patient 1 and 2). A total of 226 SNVs were identified across 187 genes spanning all autosomes and the X chromosome. The complete list of variants can be seen in Appendix 1 – Lists of single nucleotide variants from exome sequencing Table 5: Single nucleotide variants exclusive to the non-responders.

Ingenuity core analysis of direct and indirect relationships revealed the significant canonical pathways in this group to be: regulation of cellular mechanics by calpain protease, renal cell carcinoma signalling, PEDF signalling, thyroid cancer signalling, and UVC-induced MAPK signalling. Statistics for these identified pathways can be seen in Table 3.15.

Pathway	p-value	Ratio
Regulation of cellular mechanics by calpain protease	2.43E-03	4/55 (0.073)
Renal cell carcinoma signalling	5.31E-03	4/69 (0.058)
PEDF signalling	5.87E-03	4/71 (0.056)
Thyroid cancer signalling	7.18E-03	3/39 (0.077)
UVC-induced MAPK signalling	8.82E-03	3/42 (0.071)

Table 3.15 – Pathway analysis for SNVs unique to the non-responding tumours. P-value is adjusted using Benjamini-Hochberg correction. Ratio identifies the number of focus genes identified (numerator) in the pathway (denominator).

Further analysis of all (unfiltered) biological pathways identified 7 networks with scores greater than 2 pertaining to: cancer, endocrine system disorders, organismal injury and abnormalities, cellular development, cell-to-cell signalling and interaction, cellular assembly and organisation, cell cycle, cellular growth and proliferation, cellular movement, cell signalling, haematological disease, lipid metabolism, molecular transport, small molecule biochemistry and inflammatory response. The focus genes and statistics pertinent to these networks can be seen in Table 3.16.

ID	Molecules in Network	Score	Focus Molecules	Top Diseases and Functions
1	26s Proteasome,A4GALT,Akt,APOBEC3G,CDH8,CFTR,COL18A1,COL6A2,CTBP2,Cyclin A,estrogen receptor,FANCA,FGFR3,GDNF,GLB1,HRAS,Hsp90,INF2,Interferon alpha,Jnk,KMT2E,KRAS,KRT18,MUC4,NCOA1,NCOR1,NFkB (complex),PABPC1,PI3K (complex),PRKRA,PTPRS,SEC14L3,TCF7,TNS1,VWF	46	26	Cancer, Endocrine System Disorders, Organismal Injury and Abnormalities
2	AIM1,ALG1,BCAS3,BMP2K,BTF3,CNN2,COTL1,CTNNA3,CTNNB1,DDX54,DNA2,ERCC2,FASTK,FUT3,GPR6,HAMP,IgG,IL17RB,MC4R,MINK1,MUC6,MYC,PERP,PLEKHG2,PLS3,PPL,RANBP2,RASA4,RGS3,SMARCA4,SNRK,TACSTD2,TFAP2A,TFF1,ZMIZ2	16	12	Cellular Development, Cell-To-Cell Signaling and Interaction, Cellular Assembly and Organization
3	ABLIM,ADAMTS1,ADCY7,ARPC1A,ATP9A,CCNB1,CDC27,COL15A1,CTDSP2,CYP4F2,DOCK7,DUSP3,F2,FSH,GNLY,GNRH,Lh,MAPK1,PDXK,PHF11,PI4K2A,PLIN3,POP5,PPFIA4,PRKX,PRSS3,PTPRN,RB1,RBMX,SMAD1,SOX7,STK17A,TGFB1,TLK1,TPSD1	16	12	Cell Cycle, Cellular Growth and Proliferation, Cell-To-Cell Signaling and Interaction
4	ADCYAP1,ALPPL2,BAI1,C1QTNF9,CCL21,CRIP2,CSPG4,DISP1,DROSHA,DUOX2,E2f,EFNA1,ENO3,ERK,ERK1/2,GMFG,GPR183,Histone h3,HOXC6,HPSE,ITSN1,KMT2B,KMT2C,KMT2D,LGALS1,NANOG,NHLRC1,PAGR1,PAK2,PAXIP1,RBBP5,RNF41,SCRIB,TRPM2,VRK2	14	11	Cellular Movement, Cancer, Cell Signaling
5	ACTN2,AMOTL2,CDK11B,CLCN4,DAPK3,DNAJC15,EBAG9,GLIPR1,GRIN1,HIST4H4,KIF24,NR3C1,PARN,PDLIM2,PHLDA3,PPP1R13L,PRDM5,PRUNE2,SCARA3,SETD8,SKIV2L,SLC25A5,SLC2A1,SLC43A3,SON,STOM,SYVN1,TNFRSF14,TNFRSF10B,TNS4,TP53,TRAF2,TRIM24,WNT10B,ZC3HAV1	14	12	Hematological Disease, Cancer, Organismal Injury and Abnormalities
6	ABCC3,ACAA1,ACACB,ACE,APOA1,APOA4,APOA5,APOC2,APOC3,CD163,CPT1A,DIABLO,DSG1,FABP2,HDL,HDL-cholesterol,Hsp27,IL6R,KCNJ12,KHSRP,LIPG,LPL,MSR1,MVP,NR1D1,NR1H3,NR1H4,PLA2G2A,POU4F2,PPARA,PTX3,SERPINB10,SREK1IP1,TAC1,TNF	12	10	Lipid Metabolism, Molecular Transport, Small Molecule Biochemistry

Table 3.16 - Network analysis for SNVs unique to the non-responding tumours. The score is derived from a p-value and indicates the probability of the focus genes in a network being found together due to random chance. Focus molecules is the total number of SNVs of interest identified in the respective network.

3.3.9 Selection of SNVs for validation

The primary purpose of the study was to identify whether biological information from a primary tumour is predictive of the metastatic genotype, and if this information could potentially be used to predict response to neoadjuvant treatment. To that end, the list of all those eligible SNVs present in at least one primary and metastatic tumour pertaining to the same patient (i.e. paired) were combined with those SNVs exclusive to either the responders or the non-responders. The resulting lists of variants can be seen in Appendix 1 – Lists of single nucleotide variants from exome sequencing Table 6: Single nucleotide variants present in paired samples and exclusive to the responders, and Table 7: Single nucleotide variants present in paired samples and exclusive to the non-responders.

In order to rationalise the use of resource, the following decisions were made for SNV validation:

1. Those paired predictors of favourable response present in 3 or more samples would be validated.
2. All paired predictors of poor response were only present in 2 samples. As such those novel SNVs (as per dbSNP) would be validated.
3. Given its potential significance to the aim of the study, those SNVs identified in the ErBb signalling pathway would be validated.

The resulting SNVs subjected to Sanger sequencing for validation can therefore be seen in Table 3.17.

Paired predictors of favourable response (present in 3 or more samples)					
Annotation	**Gene**	**Chromosome**	**Location**	**Substituted Amino Acid**	**New Amino Acid**
CDAN1_15_43020983_G/A	CDAN1	15	43020983	G	A
LGALS3_14_55604935_C/A	LGALS3	14	55604935	C	A
PANK3_5_167988433_T/A	PANK3	5	167988433	T	A
CTDSP2_12_58220811_G/T	CTDSP2	12	58220811	G	T
Paired predictors of poor response (novel only)					
Annotation	**Gene**	**Chromosome**	**Location**	**Substituted Amino Acid**	**New Amino Acid**
ABCA13_7_48390326_G/A	ABCA13	7	48390326	G	A
CDC27_17_45214551_G/A	CDC27	17	45214551	G	A
ErbB signalling pathway (identified through pathway analysis)					
Annotation	**Gene**	**Chromosome**	**Location**	**Substituted Amino Acid**	**New Amino Acid**
KRAS_12_25398284_C/A	KRAS	12	25398284	C	A
MAP2K3_17_21207834_C/T	MAP2K3	17	21207834	C	T
PAK2_3_196529982_A/G	PAK2	3	196529982	A	G
PIK3C2G_12_18650667_A/T	PIK3C2G	12	18650667	A	T
PLCG2_16_81888178_C/T	PLCG2	16	81888178	C	T
RRAS_19_50140130_G/A	RRAS	19	50140130	G	A

Table 3.17 – Those SNVs identified for validation with Sanger sequencing

3.3.9 Sanger sequencing

Sanger sequencing was attempted for 12 SNVs (above) in 8 samples (primary tumour and liver metastases from 4 patients). Eighty-eight of the 96 runs were successful; in 8 samples there was failure to detect the amplicon. A summary of the Sanger sequencing results can be seen in Table 3.18.

Annotation	Count	Patient 1		Patient 2		Patient 3		Patient 4	
		Primary	Metastasis	Primary	Metastasis	Primary	Metastasis	Primary	Metastasis
Paired predictors of favourable response									
CDAN1_15_43020983_G/A	3	G and A	G and A	G and A	G and A	G	G	G	G
LGALS3_14_55604935_C/A	4	C	C	C	C	C	C	C	C
PANK3_5_167988433_T/A	3	Undetermined	Undetermined	T	T	T	Undetermined	T	T
CTDSP2_12_58220811_G/T	3	G	G	G	G	G	G	G	G
Paired predictors of poor response									
ABCA13_7_48390326_G/A	2	G	G	G	G	G	G	G	G
CDC27_17_45214551_G/A	2	G and C	G and C	G and C	G and C	G and C	G and C	G and C	G and C
ErbB signalling pathway									
KRAS_12_25398284_C/A	2	C	Undetermined	Undetermined	C	C	C	C	C and A
MAP2K3_17_21207834_C/T	2	C and T	C and T	C and T	C and T	C	C	C	C
PAK2_3_196529982_A/G	3	A	A	A	A	A	A	A	Undetermined
PIK3C2G_12_18650667_A/T	2	A and T	A and T	A	A and T	A	A	A	A
PLCG2_16_81888178_C/T	2	C and T	C and T	Undetermined	C	C	C	C	C
RRAS_19_50140130_G/A	2	G and A	G and A	G	Undetermined	G	G	G	G

Table 3.18 – Summary of the Sanger sequencing for 12 SNVs of interest in 8 samples (matched primary and metastatic tumours from 4 patients). The fields displayed in red highlight the location of SNVs identified through Ion Proton sequencing, with the content of the fields representing the identified base(s) on Sanger sequencing. Those marked undetermined failed due to inability to detect the amplicon.

For those paired predictors of favourable response, only the SNV occurring in the *CDAN1* gene was validated by Sanger sequencing. The table shows the presence of both G and A nucleotides in all samples from the responders (patient 1 and 2), including the primary tumour from patient 1 which was not seen on exome sequencing. Conversely only the G nucleotide is present in the non-responders (patient 3 and 4). The remainder of the Sanger sequencing failed to identify any of the substituted nucleotides seen on exome sequencing. Where the amplicon was detected, the nucleotide identified was the same in all samples.

For the paired predictors of poor response, no SNVs were validated. The SNV observed in the *ABCA13* gene was not identified in any of the samples, whereas in the *CDC27* gene a substitution from G to C was seen in all samples rather than the expected G to A.

When considering the ErbB pathway, the SNV:

- in the *KRAS* gene was confirmed in 1 of 2 expected samples and no others
- in the *MAP2K3* gene was confirmed in 2 of 2 expected samples and two others (from the same patient)
- in the *PAK2* gene was not confirmed in any sample
- in the *PIK3C2G* gene was confirmed in 2 of 2 expected samples and one other
- in the *PLCG2* gene was confirmed in 2 of 2 expected samples and no others
- in the *RRAS* gene was confirmed in 2 of 2 expected samples and no others

3.4 Discussion

3.4.1 Summary of aims

In this study, a comprehensive exome analysis of four synchronously resected patient matched primary and metastatic tumours was performed. Analysis of acquired data focussed solely on the identified somatic, non-synonymous missense biologically deleterious SNVs. The aims were to identify those genetic aberrations that:

- Are present in the primary tumour but not in the metastasis
- Are present in the metastasis but not in the primary tumour
- Are present in both primary and metastasis (i.e. the primary tumour is predictive of the metastatic genotype)
- May predict response to neoadjuvant therapy

3.4.2 Summary of results

Of the 585 unique non-synonymous, missense SNVs identified 215 (36.8%) were unique to the primary tumour, 226 (38.6%) unique to the metastasis and 81 (13.8%) present in at least one primary and metastatic tumour pertaining to the same patient. The remaining 63 (10.8%) were neither unique to a tissue type or present in a pair of samples from the same patient. Two hundred and sixty-eight (45.8%) predicted favourable response, whilst 226 (38.6%) predicted poor response. Of those, 43 and 23 respectively were present in patient matched samples. The remaining 91 (15.6%) were neither unique to responders or non-responders.

Pathway analysis identified putative pathways in those variants unique to the primary tumour (α-tocopherol degradation, vitamin C transport, glycine biosynthesis III, GDP-L fructose biosynthesis I and TCA cycle II), unique to the metastatic tumour (AMPK signalling, rennin-angiotensin signalling, role of NANOG in mammalian embryonic stem cell pluripotency, basal cell carcinoma signalling and PEDF signalling), present in at least one primary and metastatic tumour pertaining to the same patient (ErbB signalling, germ cell-sertoli cell junction signalling, endothelin-1 signalling, antiproliferative role of somatostatin receptor 2, and rening-angiotensin signalling), unique to the responders (thyroid cancer signalling, regulation of the epithelial-mesenchymal transition pathway, ovarian cancer

signalling, acute myeloid leukemia signalling, and colorectal cancer metastasis signalling) and unique to the non-responders (regulation of cellular mechanics by calpain protease, renal cell carcinoma signalling, PEDF signalling, thyroid cancer signalling, and UVC-induced MAPK signalling).

The ErbB signalling pathway was identified as the most significant pathway arising from the analysis of SNVs in paired patient samples, with 6 (*KRAS, MAP2K3, PAK2, PIK3C2G, PLCG2, RRAS*) of the 85 pathway genes containing SNVs (Ratio 0.07, $p=5.87x10^{-7}$).

Sanger sequencing validated the CDAN1_15_43020983_G/A SNV as a potential predictor of favourable response where the primary tumour is predictive of the metastatic genotype. For the 6 SNVs of interest in the ErbB pathway, 4 showed absolute concordance between the primary and metastatic genotype (those in *MAP2K3, PIK3C2G, PLCG2 and RRAS*) thus validating the results of the Ion Proton exome sequencing.

3.4.3 Next generation sequencing of colorectal cancer

For decades our understanding of the genetics of colorectal carcinogenesis has gone unchallenged, however a complete catalogue of oncogenic drivers has yet to be determined.

The largest published study to date remains The Cancer Genome Atlas Network (2012) of 276 colorectal samples subjected to exome sequencing, 97 of which also underwent whole genome sequencing. This paper demonstrated that colon and rectal cancers had similar patterns of genomic alteration, and that most of the 24 genes found to be significantly mutated were known cancer-related genes such as *APC, TP53, KRAS, PIK3CA and SMAD4*.

A number of studies, published both before and after, have attempted to improve our understanding of the genomic aberrations in colorectal cancer with three main aims: identifying clinically actionable targets for personalised therapy, improving pathway-level understanding of carcinogenesis, and identifying novel features or mutation types. A summary of these papers can be seen in Table 3.19, and a complete list of accompanying variants from these papers can be found in Appendix 2 – Genetic variants in colorectal cancer identified by next generation sequencing studies.

Paper	Number of Patients	Comparing	Summary
The Cancer Genome Atlas Network *Nature, 2012*	276	Tumour and normal mucosa	Implicated pathways included WNT, RAS-MAPK, PI3K, TGF-B, P53, and DNA mismatch repair.
The consensus coding sequences of human breast and colorectal cancers *Science, 2006*	11	Tumour and normal mucosa	Sanger sequencing study identifying 189 genes, most of which not known to be implicated in carcinogenesis
Patterns of somatic mutation in human cancer genomes *Nature, 2007*	28	Tumour and normal mucosa	44 mutations identified, many of which were protein kinases
Somatic mutation profiles of MSI and MSS colorectal cancer identified by whole exome next generation sequencing and bioinformatics analysis *PLOS One, 2010*	2 (1 MSI-S, 1 MSI-H)	Tumour and normal mucosa	359 significant mutations for the MSI tumour and 45 for the MSS, all with predicted altered protein function
Exome capture sequencing of adenoma reveals genetic alterations in multiple cellular pathways at the early stage of colorectal tumorigenesis *PLOS One, 2013*	1	Tumour, adenoma and normal mucosa	12 variants were identified in the adenoma and 42 in the adenocarcinoma
Chromothripsis is a common mechanism driving genomic rearrangements in primary and metastatic colorectal cancer *Genome Biology, 2011*	4	Primary tumour, normal mucosa, liver metastasis and liver parenchyma	24 genes suggesting the relevance of chromothripsis to metastagenesis
Genomic sequencing of colorectal adenocarcinomas identifies a recurrent VTI1A-TCF7L2 fusion *Nature Genetics, 2011*	9	Tumour and normal mucosa	Eleven rearrangements encode predicted in-frame fusion proteins, including a fusion of TVI1A and TCF7L2 found in 3 out of 9 patients
Exome sequencing reveals frequent inactivating mutations in ARID1A, ARID1B, ARID2 and ARID4 in microsatellite unstable colorectal cancer *International Journal of Cancer, 2013*	21	Tumour and normal mucosa	Analysis focussed to ARID genes only which were frequently mutated (13-39%)
Comprehensive genomic analysis of a metastatic colon cancer to the lung by whole exome sequencing and gene expression analysis *International Journal of Oncology, 2014*	1	Metastatic lung tumour and normal lung	8 of the 71 variants identified pertain to the 'metastatic colorectal cancer signalling' or 'phospholipase C signalling' pathways

Targeted sequencing of cancer related genes in colorectal cancer using next generation sequencing *PLOS One, 2013*	60	Tumour and normal mucosa	183 genes selected for analysis from COSMIC database (study designed to validate new platform)

Table 3.19 – Summary of next generation sequencing papers published on colorectal cancer.

As can be seen, at the time of writing only one paper includes the sequencing of colorectal liver metastases: Kloosterman *et al* (2011) demonstrated that chromothripsis is a widespread phenomenon in colorectal primary and metastatic tumours with considerable variation between sites, and that in the 24 genes they identified (including *APC*, *KRAS*, *SMAD4* and *PIK3CA)* considerable variation was seen between primary and metastatic tumours. This will no doubt rapidly change, and as the technology grows the challenge will increasingly be how to exploit this to better our understanding of the mechanisms underlying colorectal carcinogenesis.

3.4.4 The ErbB receptor tyrosine kinases and pathway

The epidermal growth factor receptor (EGFR) family consists of 4 members, ErbB1-4. These receptors consist of a glycosylated extracellular domain and an intracellular domain with a juxtamembrane segment, protein kinase domain and carboxylterminal tail. ErbB1, ErbB3 and ErbB4 all have 7 biologically occurring ligands (EGF, EPG, TGFα, AR, BTC, HB-EGFEPR), whereas Erb2 has none (Roskoski, 2004).

Downstream signalling of ErbB activation is by 3 integrated pathways: the phosphatidylinositol 3-kinase/Akt (PKB) pathway, the Ras/Raf/Mek/ERK pathway and the phospholipase C pathway (See Section 1.7.6). Many tumours besides colorectal tumours are associated with mutation or increased expression of the gene family, which have a number of designations: *EGFR/ERBB1/HER1, ERBB2/HER2/NEU, ERBB3/HER3 and ERBB4/HER4*. These mutations results in aberrant activity of downstream pathways (Miettinen *et al*, 1995).

Given their importance in a number of cell functions, including regulation of apoptosis, cell cycle progression, cytoskeletal rearrangement, differentiation and development (Manning *et al*, 2002), and their biological implication in colorectal cancer (Yao *et al*, 2013), the ErbB

family and downstream pathways have become a commonly utilised drug target (Table 3.20).

Small Molecule Inhibitors	Manufacturer	Target	Year	Application
Afatinib/Gilotrif®	Boehringer Ingelheim	ErbB1	2013	First-line treatment of non small cel lung cancer with exom-19 deletions
Erlotinib/Tarceva®	Genentech/OSI	ErbB1	2004	(i) First-line treatment of non small cel lung cancer with exom-19 deletions (ii) second-line treatment following cytotoxic therapy and (iii) first-line treatment of pancreatic cancer in combination with gemcitabine
Gefitinib/Iressa®	Astra Zeneca	ErbB1	2003	Second-line treatment of non small cell lung cancer after cytotoxic therapies
Lapatinib/Tykerb®	Glaxo SmithKline	ErbB1/2	2007	Second-line treatment of patients with capecitabine for ErbB2 positive breast cancer who have previously received cytotoxic chemotherapy or trastuzumab
Monoclonal Antibodies	**Manufacturer**	**Target**	**Year**	**Application**
Ado-trastuzumab emtansine/Kadcyla®	Genentech/OSI	ErbB2	2013	ErbB2 positive metastatic breast cancer previously treated with trastuzumab
Cetuximab/Erbitux®	ImClone	ErbB1	2004	(i) Wildtype KRAS colorectal cancer in combination with cytotoxic therapies and (ii) head and neck cancers in combination with radiation therapy or cytotoxic chemotherapy
Panitumumab/Vectibix®	Genentech/OSI	ErbB1	2006	Second-line treatment for metastatic colorectal cancer following cytotoxic therapies
Pertuzumab/Omnitarg®	Abgenix	ErbB2	2012	ErbB2 positive metastatic breast cancer in combination with trastuzumab and docetaxel in patients who have not received prior anti-ErbB2 therapy or chemotherapy

				for metastatic disease
Trastuzumab/Herceptin®	Genentech	ErbB2	1998	ErbB2 positive breast, gastric and gastro-oesophageal cancer

Table 3.20 – Some of the ErbB inhibitors currently in clinical use (only ones approved by the Federal Drug Administration are shown). Adapted from Roskoski, 2004.

The efficacy of cetuximab in relation to *KRAS* status, and concordance of the primary and metastatic genotype in this regard has been discussed in Section 1.7.6. Given the inter-relation of the *RAS/RAF* pathway with other downstream effectors of ErbB signalling, our study raises the question of whether the concordance seen in the case of *KRAS* can be extrapolated to other members of the ErbB pathways. As our understanding of the role of these genes in treatment response improves, this concordance could be exploited to create personalised treatment regimens. Such a move would have the potential for improved treatment efficacy as well as a reduction in unwanted off-target effects.

3.4.5 The CDAN1 gene

Codanin 1 (*CDAN1*) is located at 15q15.2 and codes for a protein which appears to play a role in nuclear envelope integrity, possibly through microtubule attachments. Mutation of this gene is known to cause the clinical condition congenital dyserythropoietic anaemia type I, a rare autosomal recessive disorder resulting in morphological abnormalities of erythroblasts, ineffective erythropoiesis, macrocytic anaemia and secondary haemochromatosis (Tamary *et al*, 2005). The genetic variants responsible for this condition have been well reported (Dgany *et al*, 2002), although their potential role in cancer and treatment response have not yet been investigated.

The mechanism of action of the codanin 1 protein remains to be elucidated, however in an immunofluorescence study of HeLa cells, Noy-Lotan *et al* (2009) localised it to heterochromatin in interphase cells, found high levels in the S-phase of the cell cycle, and noted its phosphorylation and exclusion from condensed chromosomes during mitosis. As such they concluded that the protein is cell-cycle regulated and active during the S-phase.

Ask *et al* (2012) suggest that the function of the protein is direct interaction with the histone chaperone anti-silencing function 1 (Asf1) complex, sequestering it in the cytoplasm, blocking histone delivery and arresting S-phase progression.

A potential mechanism of action for carcinogenesis and treatment response could therefore be hypothesised, however given the paucity of information in the literature it would be prudent to first validate the presence of this SNV in a larger cohort of cancer samples.

3.4.6 Study strengths and limitations

This study represents the first genomic sequencing of synchronously resected patient matched primary colorectal tumour and colorectal liver metastases in the literature. As such it is complementary to the paper by Kloosterman *et al* (2011), in which the patients were metachronously resected. The significance of this is the exclusion of confounding factors introduced by metachronous resection, be that merely the passage of time, other neoadjuvant treatments or the stress response to the first operation.

Given the aims of this study clearly the numbers we have used are inadequate to draw any firm conclusions. Our desire to perform exome sequencing is in part related to later chapters of this thesis in which we perform a global proteomic analysis on the same (and other) tissue sets. Focussing on the non-synonymous missense SNVs has allowed us to make potentially more meaningful correlations between the datasets, but in doing so has left little regard for the potential for significant findings in both the SNVs not meeting these criteria as well as indels.

We opted to validate the SNVs of interest in the same tissue set but using an alternative technology, specifically Sanger sequencing. The preferred alternative would have been validation on a larger, different tissue set using either the same or a different platform. The precious nature of these difficult to acquire samples meant that this was not feasible, as synchronous resections are a relatively recent development in hepatobiliary surgery. The incorporation of metachronous resections into the tissue set would have increased numbers (and cost) at the expense of losing the novelty and scientific value we have achieved with this study.

The final limitation is the inherent heterogeneity in the study population. Differences existed in terms of patient age, gender, TNM stage, burden and distribution of metastases, and the presence of adverse pathological features. It is advantageous that all of the primary tumours were confined to the colon (rather than including rectal cancers also), although there were primary tumours from both the right and left colon. It is now widely accepted that right and left colonic tumours are to be regarded as different biological entities, particularly where genomic aberrations are concerned (Zhu, 2013). Given the study partly attempted to review SNVs which may account for differences in response to neoadjuvant treatment, again there was heterogeneity between patients. All patients received a 5-fluorouracil based regimen, although one patient received this as capecitabine. The same patient (3) was the only patient to receive an EGFR inhibitor. As such the biomarkers identified are likely to relate to the cellular response to chemotherapy, rather than the mechanism of action of the specific agents involved. Indeed as the tumours have been treated with chemotherapy, those cells remaining available for biopsy may represent those that are particularly chemoresistant. Intra-tumoural heterogeneity has also already been briefly discussed and is a key limitation of this study. Given that all patients had received neoadjuvant therapy it is possible that only chemo-resistant cells remained for sampling and analysis. This concept is explored further in Section 4.4.4.

3.4.7 Conclusion

Approximately one third of mutations identified in this study are present exclusively in the primary tumour, one third are present exclusively in the metastases and one third are present in tumours at both sites. In this cohort, only 13.8% of mutations were present in patient matched samples, i.e. only 13.8% of the metastatic genotype can be predicted by the genotype of the primary tumour.

We have identified a SNV in the *CDAN1* gene which has potential to serve as a predictive biomarker, with the presence of the SNV in the primary tumour predicting the metastatic genotype. Further validation on a micro-array of multiple patient matched samples with corresponding response and outcome data would assist with further evaluation.

SNVs identified in the ErbB pathway appear to be concordant between primary and metastatic tumours. As our understanding of the relevance of this pathway (and genetic variants within) to response to treatment with chemotherapy and targeted agents grows,

treatment decisions may increasingly be made on the basis of other genetic abberations beyond the currently used *KRAS* status. This genotypic information can be acquired from the primary tumour given its concordance with the metastatic genotype.

Chapter 4

A global proteomic assessment of patient matched primary and metastatic colorectal tumours

4.1 Introduction

4.1.1 Background

The role of neoadjuvant therapy has already been discussed in some detail (Section 1.8.4). In the context of colorectal liver metastases, neoadjuvant chemotherapy is often used to downstage borderline resectable patients to facilitate safe and effective surgery with the survival benefit we now know that it confers.

The ability to establish prospectively the likely response to neoadjuvant therapy would be of tremendous benefit to clinicians. Those patients who are identifiable as likely to respond could be subjected to potentially more effective systemic therapy, whilst conversely those less likely to respond could be saved the unnecessary morbidity of systemic treatment and the delay to surgical intervention necessary with the use of neoadjuvant treatments.

Access to the colon and rectum to obtain tumour samples for biological analysis is feasible and safe by means of endoscopic assessment. In the context of metastatic disease in the liver, studies have shown that pre-operative needle biopsy is associated with seeding of the cutaneous tract and a considerable increase in morbidity (Cresswell, Welsh and Rees, 2009). As such we are limited to the primary tumour for biological information to help us guide the treatment of the liver metastases. This is observed in current clinical practice with the genotyping of *KRAS* performed on the archived primary tumour tissue to establish the potential benefit of the inclusion of cetuximab alongside other systemic agents.

4.1.2 Proteomics

Proteomics is defined as the large scale study of proteins, and in particular their structure and function. The term was first coined in 1997 to draw a parallel with the increasing interest in genomics (James, 1997). The proteome is the entire set of proteins produced or modified by an organism or system which varies with time and distinct requirements of the cell or organism (Wilkins *et al*, 1996).

The study of proteomics is arguably more complicated than the genomics described in Chapter 3. Firstly, an individual's genome remains more or less constant, however the proteome can vary between cells and over time. Secondly, modification of the translated

protein, for example by phosphorylation or glycosylation, is common and can have a significant impact on protein function. Thirdly, many proteins form complexes with other proteins, and only exert their biological effect as part of this complex. Fourthly, protein degradation plays a significant part in any attempt at quantification. Finally, as a combination of the above factors, reproducibility between experimental runs, with alternative equipment and in different laboratories can prove challenging (Peng *et al*, 2003). These challenges however represent an opportunity to help us understand the complexities of tumour biology, which is critical in helping us develop the most effective diagnostic tools and treatment strategies for the future (Ceciliani *et al*, 2014).

The investigation of protein expression, structure and protein-protein interactions is all feasible. Proteomic data can also be used to enhance gene annotations, with parallel genomic studies assisting to further characterise post-translational modifications and proteolytic events (Gupta *et al*, 2007). Monitoring these post-translational modifications is critical, as for many cellular events protein abundance does not change rather their function is altered by these modifications. A current area of significant method development is the advancement of quantitative proteomics, data from which would permit a more detailed analysis of cell systems and biological functions (Yin *et al*, 2013).

4.1.3 Isobaric tagging for relative (and absolute) quantification

Isobaric tagging for relative and absolute quantification (iTRAQ) is a quantitative proteomics technique designed to determine the absolute or relative amount of proteins from a number of different samples within a single experiment. Samples are prepared by reducing and alkylating cysteine residues and subjecting them to an overnight tryptic digest, whereby proteins are cleaved at the carboxyl side of the amino acids lysine and arginine (except when either is followed by proline) to produce peptides.

Each sample is incubated with a specific isotope labelled molecule which covalently binds to the N-terminus and side chains of all peptides within the sample. The iTRAQ tag consists of a reporter moiety which is used for quantification during analysis and a balance moiety. All tags have the same total mass of 145Da, however the reporter moieties in each tag are different in mass. When each tag binds to a peptide that is present in all eight samples, all eight iTRAQ labelled peptides should have the same mass.

For ease of mass spectrometry, samples first undergo a ‘clean up’ step where the peptides are separated into fractions of certain ionic charge by cation exchange. During mass spectrometry, the peptides within a particular fraction are separated by mass and ionised thus producing parent ion molecules. Each parent ion is represented by a single peak and is isolated and directed to a collision chamber where the peptides are bombarded with a collision gas causing the tagged peptides to fragment. During fragmentation, the reporter and balance moieties are cleaved from each other and from the peptide to which they are bound. The peptide itself is also cleaved into fragment ions and these ions are used to identify the protein that this peptide represents by cross-referencing with a known database. The released reporter molecules, which should be a combination of the eight varying masses, are used to quantify the relative abundance of the peptide to which they were bound in each of the original samples by calculating the ratios of the reporter molecules. The abundance is compared to a common pool of a number of samples, use of which across multiple runs allows for efficient and accurate multiplexing (Zieske, 2006). Figure 4.1 is a schematic representation of this laboratory technique as applied to the experimental design.

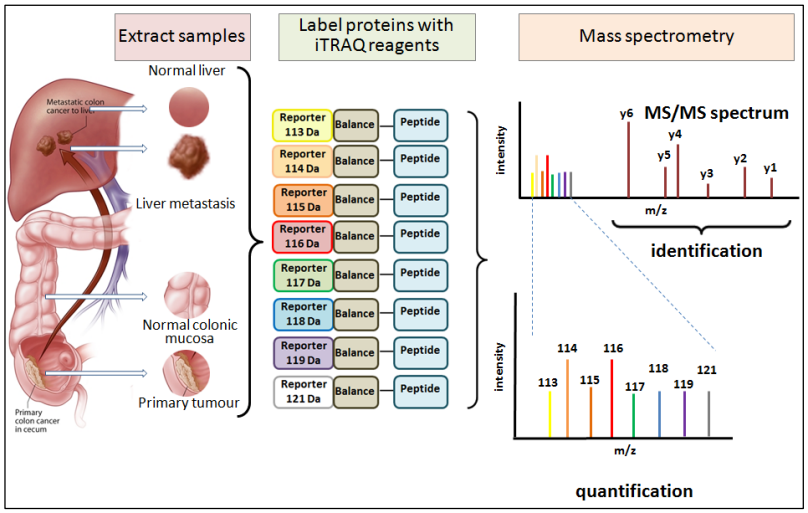

Figure 4.1 – Samples are reduced and undergo a tryptic digest before being tagged with an isotope labelled molecule. These tags all have the same molecular weight although the reporter and balance moieties vary. After a cation exchange cleanup step the samples undergo nanoLC-MS/MS. The reporter and balance moieties are cleaved from each other and from the peptide to which they are bound, the ratio of which helps determine relative abundance. The peptide is also cleaved into fragment ions used to identify the protein.

4.1.4 Study aim

The aim of this investigation is to compare the proteomic profile of the primary and metastatic tumours, both with each other and with their normal adjacent tissue, to establish the degree of similarity and identify potential response biomarkers present in the primary tumour which may predict response to neoadjuvant therapy in the liver metastasis.

4.2 Methods

National Health Service Research Ethics Committee and Research and Development approval was obtained for this study and informed consent obtained from each of the study participants.

4.2.1 Patient recruitment and tissue collection

Samples were obtained from consecutive patients undergoing synchronous or staged resection of a primary colorectal tumour and liver metastases at any of the institutions within the research infrastructure constructed to facilitate this study.

Following delivery of the colorectal specimen the proximal staple line was incised and a linear cut made down the antimesenteric border before excising a peripheral section of tumour using forceps and a scalpel. Following delivery of the liver specimen, an incision was made through the resected surface to the liver metastasis, with care being taken not to breach the liver capsule; a peripheral sample of tumour was obtained as described previously. Macroscopically normal adjacent colonic mucosa and liver parenchyma were also obtained, with all tissue sampling performed in the operating theatre under aseptic conditions followed by immediate stabilisation in liquid nitrogen and transfer to a -80^{o}C storage facility.

4.2.2 Exclusion criteria

For this study, the exclusion criteria were:

- Recent (last 12 months) personal history of malignancy at another site
- Patients under the age of 18
- Patients without capacity to provide informed consent
- Patients identified by the multidisciplinary team as being at significant risk of emotional distress by additional hospital visits and/or procedures that may be required

4.2.3 Evaluation of histopathological response to treatment

Additional tumour samples were obtained for the purposes of formalin fixation and embedding in paraffin. All samples were reviewed by a consultant histopathologist to verify the diagnosis of adenocarcinoma.

For those patients who had received neoadjuvant chemotherapy the histopathological response to treatment was assessed. The number of residual viable tumour cells within each sample was estimated as a percentage of the total tumour surface area that included areas of coagulative necrosis, calcification, fibrosis and the associated histiocytes, foreign body giant cells and inflammatory cells. Samples were subsequently scored as tumour regression grade 1 (1-24%), 2 (25-49%), 3 (50-74%) or 4 (>75%) for the purposes of analysis. This scoring system was first described by Ribero *et al* (2007), and used for this purpose by Blazer *et al* (2008).

4.2.4 Sample preparation

Protein was extracted from sampled tissue by mechanical dissolution and sonication in 500mM triethylammonium bicarbonate (TEAB) with 0.1% sodium dodecyl sulphate (SDS). After centrifugation at 4^{o}C at 2000 g for 15 minutes, the supernatant was removed and protein concentration determined by Bradford assay (Bradford, 1976).

4.2.5 Protein quantification

Standard protein concentrations of bovine serum albumin (BSA) (Sigma Aldrich) were prepared at 0.1, 0.2, 0.4, 0.8, 1.0 and 1.4mg/ml and 20µl placed in triplicate on a 96 well plate. Serial dilutions of each sample were made at concentrations of 1:10, 1:20, 1:50 and 1:100, and 20µl placed in triplicate on the same 96 well plate. Bradford reagent (BioRad) was diluted 1:5 with dH_2O and 180µl placed in each of the wells and then mixed. Absorbance at 570nm was measured using the Dynex MRXe plate reader (Magellan Biosciences, Chelmsford, UK), and protein concentration of the sample calculated by comparison to the standard curve.

4.2.6 Creation of a reference pool

In order to infer relative protein abundance between samples, a reference pool was created for each study. For each sample to be quantified 100µg of protein was combined

together in a common pool i.e. 100µg of each of normal mucosa, primary tumour, liver metastasis and liver parenchyma for each patient in the study. Once the reference pool had been created it was re-quantified as above and prepared in an identical fashion to the other samples as follows.

4.2.7 Allocation across and within experimental runs

iTRAQ reagents are available in 4-plex and 8-plex formats, thus restricting the number of samples to 8 per run. Inclusion of the reference pool as a sample further limits each experimental run to 7. Given some of the inherent difficulties in reproducibility with proteomics discussed in Section 4.1.2, all samples to be analysed were randomly allocated across all experimental runs in a stratified fashion thus ensuring even distribution of tissue types and patients. In order to facilitate rigorous bioinformatics analysis across sample runs the same reference pool was included. Within experimental runs allocation to iTRAQ label was performed on a purely random basis.

4.2.8 iTRAQ labelling

Labelling with iTRAQ reagents was carried out according to the Applied Biosystems protocol for an 8-plex procedure (Life Technologies, Paisley, UK). In brief, 100µg of protein from each sample was reduced with Tris (2-carboxyethyl) phosphine hydrochloride (TCEP) and capped with methylmethanethiosulfate (MMTS), before overnight digestion with trypsin (Promega, Southampton, UK). Peptides were then labelled with isobaric tags and pooled and diluted to 5ml with 10mM potassium dihydrogen phosphate/25% acetonitrile (ACN) and acidified to <pH3 with phosphoric acid.

4.2.9 Cation exchange

Samples were fractionated on a Polysulfoethyl A strong cation-exchange column (200 × 4.6mm, 5µm, 300Å; Poly LC, Columbia, MD) at 2ml/minute using a gradient from 10mM potassium dihydrogen phosphate/25% ACN (w/v) to 0.5M potassium chloride/10mM potassium dihydrogen phosphate/25% ACN (w/w/v) in 75 minutes. Fractions of 2ml were collected and dried by centrifugation under vacuum (SpeedVac, Eppendorf UK Ltd, Stevenage, UK). Fractions were reconstituted in 1ml of 0.1% trifluoroacetic acid (TFA) and were desalted using a mRP Hi Recovery protein column 4.6 x 50mm (Agilent, Berkshire UK)

on a Vision Workstation (Applied Biosystems/Life Technologies, Paisley, UK) prior to mass spectrometric analysis.

4.2.10 Mass spectrometry

Desalted fractions were reconstituted in 40µl 0.1% formic acid and 5µl aliquots were delivered into a Triple TOF 5600 (AB Sciex, Warrington, UK) via an Eksigent NanoUltra cHiPLC System (AB Sciex) mounted with a microfluidic trap and analytical column (15 cm × 75 µm) packed with ChromXP C_{18}−CL 3 µm. A NanoSpray III source was fitted with a 10µm inner diameter PicoTip emitter (New Objective, Woburn, USA). The trap column was washed with 2% ACN/0.1% formic acid for 10 minutes at 2µL/minute before switching in-line with the analytical column. A gradient of 2−50% ACN/0.1% formic acid (v/v) over 90 minutes was applied to the column at a flow rate of 300nl/min. Spectra were acquired automatically in positive ion mode using information-dependent acquisition powered by Analyst TF 1.5.1. software (AB Sciex). Up to 25 MS/MS spectra were acquired per cycle (approximately 10Hz) using a threshold of 100 counts per second and with dynamic exclusion for 12 seconds. The rolling collision energy was increased automatically by selecting the iTRAQ check box in Analyst, and manually by increasing the collision energy intercepts by 5.

4.2.11 Protein identification and quantification

Data were searched using ProteinPilot 4.2 and the Paragon algorithm (AB Sciex) against the latest version of the SwissProt database, with MMTS as a fixed modification of cysteine residues and biological modifications allowed. The data were also searched against a reversed decoy database and only proteins lying within a 1% global false discovery rate (FDR) were taken forward for analysis. Quantitation of proteins was relative to the common pooled sample present in each iTRAQ-MS experiment. iTRAQ data for proteins identified by 2 or more peptides with at least 90% confidence of correct sequence assignment, or by a single peptide with at least 99% confidence were log2 transformed, batch corrected and included in subsequent analyses.

4.2.12 Bioinformatics analysis

Proteins present in at least 50% of all samples were taken forward for bioinformatics analysis. A number of direct two group comparisons were made using Partek® (St Louis,

USA) to identify proteins significantly different between the groups. A two-way Analysis of Variance (ANOVA) was employed to identify the differential proteins whilst accounting for batch effect. With the aim of reducing the false discovery rate, the Benjamini-Hochberg multiple test correction was used (Benjamini and Hochberg, 1995). In this correction p values are sorted and ranked, the smallest value receiving 1, second 2 and largest N. Each p value is then multiplied by N and divided by its assigned rank to give the adjusted p-values. Statistical significance was taken as log2 fold change >2 with an adjusted p value of <0.05.

Those proteins identified as statistically significantly different were subjected to analysis with Ingenuity Pathway Analysis (Redwood City, USA). Ingenuity Pathways Analysis computes a score for each network according to the fit of that network with the identified proteins of interest (referred to as the focus proteins). The score is derived from a p-value and indicates the probability of the focus proteins in a network being found together due to random chance. A score of 2 indicates that there is a 1 in 100 chance that the focus proteins are together in a network due to random chance, therefore scores greater than 2 have at least a 99% confidence of not being generated by random chance alone. Analysis must also take into account both the number of focus proteins identified and total known proteins in each network. Significant canonical pathways were identified with a threshold p value of <0.05 (after correction). If there are *n* proteins in a pathway, and *f* have been identified through iTRAQ, the p-value is the probability of finding *f* or more proteins in a set of *n* proteins randomly selected from the global molecular network.

In addition, the lists of single nucleotide variants identified in Chapter 3 will be combined with the proteomic dataset to identify those proteins in which SNVs have also been found. A summary of the bioinformatics workflow can be seen in Figure 4.2.

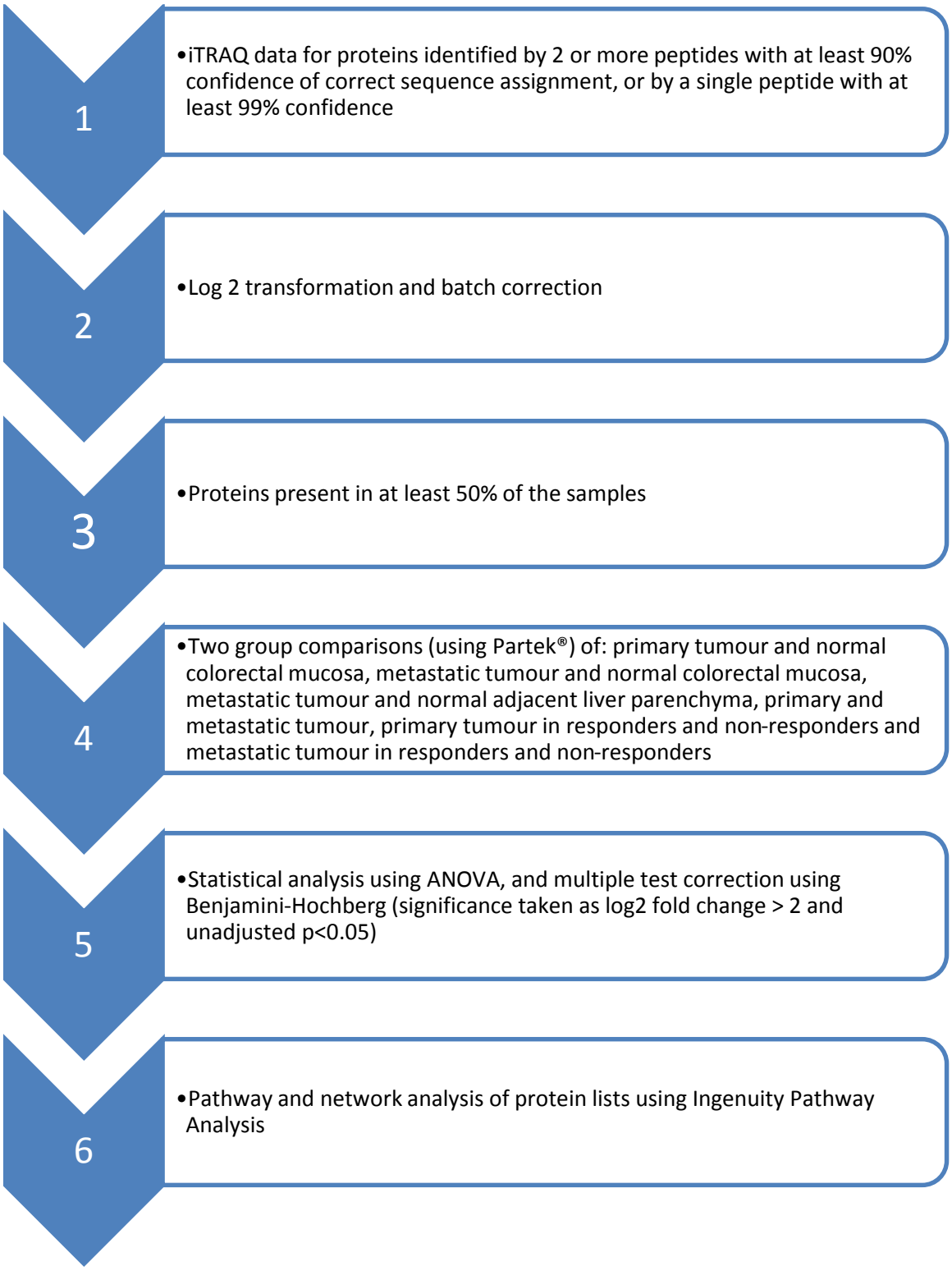

Figure 4.2 – Bioinformatics analysis workflow for global proteomic assessment of patient matched primary and metastatic colorectal tumours.

4.3 Results

4.3.1 Clinical and demographic data

Sixteen patients presenting with liver limited stage IV disease were recruited to this study. Of these patients, 12 were male and 4 female ranging in age from 59-84 years at the time of diagnosis. Eleven patients underwent neoadjuvant chemotherapy, with 5 proceeding straight to surgery. Six patients underwent simultaneous resection of disease at both sites, with the remainder undergoing staged resections. The distribution of disease across the colon ranged from the rectum through to the caecum, with T-stage varying from 2-4 and a mixture of node positive and negative disease. Similarly 1-17 liver metastases were identified in one or both lobes of the liver and there was variation in tumour grade at both sites. All patients with the exception of patient 14 underwent resection at both sites. In this particular case the liver metastasis was unresectable due to its proximity to major vascular structures. A summary of the clinical and demographic data can be seen in Table 4.1.

Patient	Age at Diagnosis	Sex	Neoadjuvant Chemotherapy	Synchronously Resected	Location of Primary	Primary Histology	T Stage	N Stage	Number of Mets	Distribution of Mets	Mets Histology
1	66	M	Y	N	Rectum	Moderately differentiated	3	1	4	Unilobar	Moderately differentiated
2	73	M	N	N	Sigmoid	Poorly differentiated	3	1	2	Unilobar	Moderately differentiated
3	64	F	Y	Y	Caecum	Moderately differentiated	2	0	5	Bilobar	Moderately differentiated
4	84	M	N	N	Rectum	Moderately differentiated	3	1	2	Unilobar	Moderately differentiated
5	75	F	Y	N	Rectum	Poorly differentiated	3	0	2	Unilobar	Moderately differentiated
6	76	M	N	N	Sigmoid	Moderately differentiated	3	1	1	Unilobar	Moderately differentiated
7	73	F	N	N	Sigmoid	Moderately differentiated	4	0	1	Unilobar	Moderately differentiated
8	81	M	N	N	Sigmoid	Moderately differentiated	4	0	2	Unilobar	Moderately differentiated
9	79	M	Y	N	Caecum	Moderately differentiated	4	0	3	Bilobar	Moderately differentiated
10	62	M	Y	N	Caecum	Moderately differentiated	3	1	1	Unilobar	Moderately differentiated
11	76	M	Y	N	Rectum	Moderately differentiated	3	1	2	Bilobar	Moderately differentiated

12	70	M	Y	Y	Sigmoid	Moderately differentiated	3	0	7	Bilobar	Moderately differentiated
13	67	M	Y	Y	Ascending	Well differentiated	4	0	16	Bilobar	Well differentiated
14	70	M	Y	Y	Caecum	Moderately differentiated	2	0	1	Unilobar	*Unavailable*
15	59	F	Y	Y	Sigmoid	Moderately differentiated	3	0	3	Bilobar	Moderately differentiated
16	75	M	Y	Y	Sigmoid	Poorly differentiated	3	2	4	Unilobar	Poorly differentiated

Table 4.1 – Clinical, demographic and disease characteristics of the 16 patients recruited to this study. Eleven patients underwent neoadjuvant chemotherapy, the remainder proceeding straight to surgery. Six patients were simultaneously resected. There was considerable variation in location of the primary tumour, disease stage and grade as well as metastatic burden.

4.3.2 Response evaluation

Eleven of the 16 patients recruited underwent neoadjuvant chemotherapy, for which there was considerable variation in the regimen. One of these 11 patients did not undergo resection of the liver metastasis. As such, response evaluation data is available for 10 patients (Table 4.2).

Patient	Neoadjuvant Chemotherapy	Agents	Viable Tumour (%)	Tumour Regression Grade	Responder
1	Y	Oxaliplatin and capecitabine	60	3	No
2	N				
3	Y	IrMdG	60	3	No
4	N				
5	Y	FOLFOX	20	1	Yes
6	N				
7	N				
8	N				
9	Y	FOLFOX	20	1	Yes
10	Y	IrMdG	90	4	No
11	Y	FOLFOX	40	2	Yes
12	Y	IrMdG	25	2	Yes
13	Y	IrMdG	40	2	Yes
14	Y	Irinotecan and capecitabine			
15	Y	Oxaliplatin, capecitabine and cetuximab	80	4	No
16	Y	IrMdG	80	4	No

Table 4.2 – Details of neoadjuvant chemotherapy agents and response evaluation. Five patients were chemonaive and 11 underwent neoadjuvant treatment. One of these patients failed to undergo resection of the liver metastasis. Response evaluation data is therefore available for 10 patients, 5 of which had a tumour regression grade of 1-2 (responders) with the remaining 5 having a tumour regression grade of 3-4 (non-responders).

There was considerable variation (20-80%) in histopathological response to neoadjuvant treatment. Five patients had a tumour regression grade of 1-2 and five patients had a tumour regression grade of 3-4. For the purposes of analysis these two groups are referred to as responders and non-responders respectively.

4.3.3 Overview of iTRAQ data

A total of 5766 unique proteins were identified. Of these, 2637 were present in at least half of the samples and therefore taken forwards for analysis. The data were acquired over 12 experimental runs, with a mean (SD) of 10.2 (3.3) peptides used to identify the proteins of origin. This corresponds to a mean (SD) coverage of 21.04% (8.92%) for identified proteins.

4.3.4 Comparison of primary tumour and normal colorectal mucosa

This analysis identified all those proteins dysregulated in the primary tumour compared to the normal colorectal mucosa. A total of 25 proteins were identified, 6 of which were upregulated in the tumour and 19 downregulated (Table 4.3).

Accession Number	Name	p Value	Log2 Fold-Change (Primary/Mucosa)
Q8NHM4	Putative trypsin-6	2.39E-04	-187.923
P10645	Chromogranin-A	6.22E-05	-11.296
P07585	Decorin	1.73E-04	-10.715
Q8WWA0	Intelectin-1	2.00E-04	-6.680
P22676	Calretinin	6.62E-04	-4.223
P00403	Cytochrome c oxidase subunit 2	6.86E-05	-4.215
P00488	Coagulation factor XIII A chain	2.57E-04	-3.765
P21397	Amine oxidase [flavin-containing] A	6.66E-04	-3.351
P09669	Cytochrome c oxidase subunit 6C	3.13E-04	-2.990
P14406	Cytochrome c oxidase subunit 7A2, mitochondrial	1.97E-04	-2.928
P06576	ATP synthase subunit beta, mitochondrial	6.97E-05	-2.812
P25705	ATP synthase subunit alpha, mitochondrial	6.28E-05	-2.662
Q99795	Cell surface A33 antigen	1.41E-04	-2.540
P48047	ATP synthase subunit O, mitochondrial	2.32E-05	-2.458
P56470	Galectin-4	1.06E-05	-2.281
P50224	Sulfotransferase 1A3/1A4	5.97E-04	-2.231
Q53EL6	Programmed cell death protein 4	1.39E-04	-2.158
P19404	NADH dehydrogenase [ubiquinone] flavoprotein 2, mitochondrial	4.19E-04	-2.077
P31930	Cytochrome b-c1 complex subunit 1, mitochondrial	1.45E-04	-2.075
Q96D15	Reticulocalbin-3	1.01E-04	2.064
P06733	Alpha-enolase	2.57E-05	2.108
P50454	Serpin H1	2.34E-04	2.360
P80188	Neutrophil gelatinase-associated lipocalin	4.48E-04	2.385
P05109	Protein S100-A8	4.01E-04	2.668
P06702	Protein S100-A9	1.58E-04	2.780

Table 4.3 – Those proteins differentially expressed between the primary tumour and normal colorectal mucosa. 25 proteins were identified, 6 of which were upregulated (positive values for fold change) and 19 downregulated (negative values for fold change).

Analysing those proteins upregulated separately from those downregulated, Ingenuity core analysis of direct and indirect relationships revealed the significant upregulated canonical pathways in this group to be: Role of IL-17A in psoriasis, differential regulation of cytokine production in intestinal epithelial cells by IL-17A and IL-17F, glycolysis I, gluconeogenesis I and IL-17A signalling in fibroblasts. Similarly the downregulated canonical pathways were: Mitochondrial dysfunction, oxidative phosphorylation, melatoning degradation II, phenylalanine degradation IV and extrinsic prothrombin activation pathway. Statistics for these identified pathways can be seen in Table 4.4.

Upregulated Pathways	**p-value**	**Ratio**
Role of IL-17A in psoriasis	7.10E-06	2/13 (0.154)
Differential regulation of cytokine production in intestinal epithelial cells	7.59E-03	1/23 (0.043)
Glycolysis I	7.91E-03	1/24 (0.042)
Gluconeogenesis I	8.24E-03	1/25 (0.04)
IL-17A signalling in fibroblasts	1.15E-02	1/35 (0.029)
Downregulated Pathways	**p-value**	**Ratio**
Mitochondrial dysfunction	7.35E-15	9/165 (0.055)
Oxidative phosphorylation	2.07E-14	8/104 (0.077)
Melatonin degradation II	3.74E-03	1/4(0.25)
Phenylalanine degradation IV	1.30E-02	1/14 (0.071)
Extrinsic prothrombin activation pathway	1.49E-02	1/16 (0.062)

Table 4.4 – Pathway analysis for proteins both upregulated and downregulated in the primary tumour when compared to normal adjacent colorectal mucosa. P-value is adjusted using Benjamini-Hochberg correction. Ratio identifies the number of focus molecules identified (numerator) in the pathway (denominator).

Further analysis of all (unfiltered) biological pathways identified 1 upregulated network with a score greater than 2 pertaining to: cellular movement, haematological system development and function and immune cell trafficking. Similarly 5 downregulated networks were identified pertaining to: Cellular development, haematological system development and function, haematopoiesis, cell morphology, cell death and survival, cell-to-cell signalling and interaction, cancer, cellular growth and proliferation and cellular assembly and organisation. The focus molecules and statistics pertinent to these networks can be seen in Table 4.5.

Upregulated Networks				
ID	**Molecules in Network**	**Score**	**Focus Molecules**	**Top Diseases and Functions**
1	A4GALT,APOC2,CCL11,CTSS,ENO1,GSTA1,HEXA,HEXB,HIF1A,HLA-DQ,HSF2,HTR4,HTR7,IL25,IL37,IL1B,LAMA3,LCN2,LILRA5,lymphotoxin-alpha1-beta2,MMP8,MMP12,PGF,PLA2G3,PLA2G5,POPDC2,PROK2,S100A8,S100A9,SERPINB9,SERPINH1,SHH,Sod,TAB3,TNF	13	5	Cellular Movement, Haematological System Development and Function, Immune Cell Trafficking
Downregulated Networks				
1	AGTR1,ATP5A1,ATP5B,C10orf10,CALB2,CHGA,CHST2,COA3,COX5A,COX6C,CTNNAL1,CTNNB1,DCD,DCN,estrogen receptor,F13A1,HSPE1,IFNE,IL6,IL10,IL13,LGALS4,LILRA5,MAOA,MKK3/6,MT-CO2,NID1,PDCD4,PDGFC,SEMA3C,SLC8A1,STAT1,SURF1,TIMP4,TNF	26	11	Cellular Development, Hematological System Development and Function, Hematopoiesis
2	GPA33,KLF4	3	1	Cellular Development, Hematopoiesis, Cell Morphology
3	ITLN1,LTF	3	1	Cell Death and Survival, Cell Morphology, Cell-To-Cell Signaling and Interaction
4	NDUFV2,RBM5	3	1	Cancer, Cellular Development, Cellular Growth and Proliferation
5	RTN4,UQCRC1	3	1	Cell Death and Survival, Cell Morphology, Cellular Assembly and Organization

Table 4.5 - Network analysis for proteins both upregulated and downregulated in the primary tumour when compared to normal adjacent colorectal mucosa. The score is derived from a p-value and indicates the probability of the focus molecules in a network being found together due to random chance. Focus molecules is the total number of proteins of interest identified in the respective network.

4.3.5 Comparison of metastatic tumour and normal colorectal mucosa

This analysis identified all those proteins dysregulated in the metastatic tumour compared to the normal colorectal mucosa. A total of 53 proteins were identified, 13 of which were upregulated in the tumour and 40 downregulated (Table 4.6).

Accession Number	Name	p Value	Log2 Fold-Change (Metastasis/Mucosa
Q8NHM4	Putative trypsin-6	2.21E-04	-231.682
P20774	Mimecan	5.66E-04	-67.140
Q03135	Caveolin-1	3.51E-04	-20.544
P10645	Chromogranin-A	2.75E-05	-12.934
P02511	Alpha-crystallin B chain	1.50E-03	-10.484
P07585	Decorin	1.63E-04	-10.388
O60844	Zymogen granule membrane protein 16	7.41E-04	-9.924
Q8WWA0	Intelectin-1	2.20E-05	-9.843
P43121	Cell surface glycoprotein MUC18	9.46E-04	-8.682
Q96BQ1	Protein FAM3D	2.90E-04	-7.850
A8K7I4	Calcium-activated chloride channel regulator 1	8.23E-04	-5.347
Q9Y6R7	IgGFc-binding protein	1.35E-03	-4.591
Q96A26	Protein FAM162A	1.30E-03	-4.281
Q02952	A-kinase anchor protein 12	1.37E-04	-4.268
P22676	Calretinin	9.49E-04	-4.166
Q09666	Neuroblast differentiation-associated protein AHNAK	4.27E-05	-4.085
Q9NR45	Sialic acid synthase	3.98E-04	-3.972
P00403	Cytochrome c oxidase subunit 2	1.14E-04	-3.839
O75489	NADH dehydrogenase [ubiquinone] iron-sulfur protein 3, mitochondrial	1.73E-04	-3.469
P23946	Chymase	2.27E-04	-3.391
O00159	Myosin-Ic	2.81E-04	-3.185
P14406	Cytochrome c oxidase subunit 7A2, mitochondrial	7.69E-05	-3.171
Q9Y639	Neuroplastin	1.24E-04	-3.166
P09669	Cytochrome c oxidase subunit 6C	1.66E-04	-3.146
P56470	Galectin-4	2.42E-07	-2.95662

Q99795	Cell surface A33 antigen	5.44E-05	-2.950
P00488	Coagulation factor XIII A chain	1.27E-03	-2.910
P09936	Ubiquitin carboxyl-terminal hydrolase isozyme L1	1.36E-03	-2.888
Q99798	Aconitate hydratase, mitochondrial	1.21E-03	-2.602
P05023	Sodium/potassium-transporting ATPase subunit alpha-1	6.41E-05	-2.590
P25705	ATP synthase subunit alpha, mitochondrial	7.71E-05	-2.567
Q53EL6	Programmed cell death protein 4	1.46E-05	-2.523
P50224	Sulfotransferase 1A3/1A4	1.43E-04	-2.504
P06576	ATP synthase subunit beta, mitochondrial	2.10E-04	-2.490
P19404	NADH dehydrogenase [ubiquinone] flavoprotein 2, mitochondrial	6.70E-05	-2.362
P48047	ATP synthase subunit O, mitochondrial	3.48E-05	-2.344
O95571	Protein ETHE1, mitochondrial	3.86E-07	-2.202
P01877	Ig alpha-2 chain C region	2.59E-04	-2.185
Q14651	Plastin-1	1.21E-04	-2.165
Q9P2B2	Prostaglandin F2 receptor negative regulator	1.01E-03	-2.098
P34897	Serine hydroxymethyltransferase, mitochondrial	5.92E-05	2.038
P17096	High mobility group protein HMG-I/HMG-Y	8.96E-04	2.072
P06733	Alpha-enolase	2.08E-05	2.107
Q53H82	Beta-lactamase-like protein 2	1.11E-03	2.114
P50454	Serpin H1	6.50E-04	2.130
Q96HE7	ERO1-like protein alpha	4.37E-04	2.212
P08195	4F2 cell-surface antigen heavy chain	1.56E-03	2.398
Q06787	Fragile X mental retardation 1 protein	5.60E-04	2.667
P13797	Plastin-3	4.66E-05	3.007
P19971	Thymidine phosphorylase	4.73E-04	3.656
P40261	Nicotinamide N-	1.21E-03	4.242

	methyltransferase		
P05181	Cytochrome P450 2E1	1.12E-03	6.000
P05177	Cytochrome P450 1A2	7.07E-04	32.731

Table 4.6 – Those proteins differentially expressed between the metastatic tumour and normal colorectal mucosa. 53 proteins were identified, 13 of which were upregulated (positive values for fold change) and 40 downregulated (negative values for fold change).

Analysing those proteins upregulated separately from those downregulated, Ingenuity core analysis of direct and indirect relationships revealed the significant upregulated canonical pathways in this group to be: bupronion degradation, acetone degradation I, estrogen biosynthesis, nicotine degradation III and melatonin degradation I. Similarly the downregulated canonical pathways were: oxidative phosphorylation, mitochondrial dysfunction, CMP-N-acetylneuramine biosynthesis I, extrinsic prothrombin activation pathway and Parkinson's signalling. Statistics for these identified pathways can be seen in Table 4.7.

Upregulated Pathways	**p-value**	**Ratio**
Bupropion degradation	1.34E-04	2/24 (0.083)
Acetone degradation I	1.41E-04	2/25 (0.08)
Estrogen biosynthesis	2.95E-04	2/36 (0.056)
Nicotine degradation III	4.41E-04	2/44 (0.045)
Melatonin degradation I	5.03E-04	2/47 (0.043)
Downregulated Pathways	**p-value**	**Ratio**
Oxidative phosphorylation	3.77E-11	8/104 (0.077)
Mitochondrial dysfunction	4.46E-11	9/165 (0.055)
CMP-N-acetylneuraminate biosynthesis I	1.04E-02	1/5 (0.2)
Extrinsic prothrombin activation pathway	3.30E-02	1/16 (0.062)
Parkinson's signalling	3.30E-02	1/16)0.062)

Table 4.7 – Pathway analysis for proteins both upregulated and downregulated in the metastatic tumour when compared to normal adjacent colorectal mucosa. P-value is adjusted using Benjamini-Hochberg correction. Ratio identifies the number of focus molecules identified (numerator) in the pathway (denominator).

Further analysis of all (unfiltered) biological pathways identified 3 upregulated networks with a score greater than 2 pertaining to: cellular assembly and organisation, drug metabolism, energy production, post-translational modification, protein folding, cardiovascular disease, cellular movement, inflammatory disease, and nervous system development and function. Similarly 2 downregulated networks were identified pertaining to: cardiovascular system development and function, cell-to-cell signalling and interaction, tissue development, cellular compromise, tissue morphology and cellular growth and proliferation. The focus molecules and statistics pertinent to these networks can be seen in Table 4.8.

Upregulated Networks				
ID	**Molecules in Network**	**Score**	**Focus Molecules**	**Top Diseases and Functions**
1	C9orf3,CDK5R1,CTNNB1,CYP1A2,CYP2E1,DVL3,DYNLL1,ENO1,EPHB2,FAF1,FMR1,GFER,GLI2,HAS3,Hat,HIF1AN,HMGA1,LTBP2,mir-24,MYC,NFkB (complex),PI3K (complex),PLS3,RAB31,RGS3,SERPINH1,SFRP1,SHMT2,SLC3A2,SNRK,ST3GAL1,TDG,TGFB1,TYMP,ZMIZ2	24	10	Cellular Assembly and Organization, Drug Metabolism, Energy Production
2	ERO1L,PDIA2	3	1	Post-Translational Modification, Protein Folding, Cardiovascular Disease
3	CHI3L1,EIF2AK2,NNMT	3	1	Cellular Movement, Inflammatory Disease, Nervous System Development and Function
Downregulated Networks				
1	ACO2,AGTR1,Akt,ANXA9,ATP5A1,ATP5B,CALB2,CAV1,CD44,CDH13,CMA1,COA3,COX5A,COX6C,DCN,estrogen receptor,F12,FAT1,IL6,IL1B,LGALS4,LILRA5,MAP1B,MAP3K14,MCAM,MT-CO2,MYO1C,ORM1,PDCD4,PIK3R2,RPL6,RPL35A,RPS11,S1PR2,SURF1	26	13	Cardiovascular System Development and Function, Cell-To-Cell Signaling and Interaction, Tissue Development
2	AHNAK,AIM1,AKAP12,APP,ATP1A1,CD81,CHGA,CLCA1,CLEC4A,CRYAB,CTNNAL1,CTNNB1,DVL1,ERK1/2,ETHE1,F13A1,FAM162A,GPR183,IL13,MAPK8IP1,MN1,MT1L,MUC5AC,PERP,PLS1,PPP3CA,PTGFRN,RAD23A,SEMA3C,SMARCA4,SORT1,STXBP1,TP53,tyrosine kinase,UCHL1	23	12	Cellular Compromise, Tissue Morphology, Cellular Growth and Proliferation

Table 4.8 - Network analysis for proteins both upregulated and downregulated in the metastatic tumour when compared to normal adjacent colorectal mucosa. The score is derived from a p-value and indicates the probability of the focus molecules in a network being found together due to random chance. Focus molecules is the total number of proteins of interest identified in the respective network.

4.3.6 Comparison of metastatic tumour and normal adjacent liver parenchyma

This analysis identified all those proteins dysregulated in the metastatic tumour compared to the normal liver parenchyma. A total of 444 proteins were identified, 164 of which were upregulated in the tumour and 280 downregulated. The data set can be found in Appendix 3 – Proteomic comparison of metastatic tumour and normal adjacent liver parenchyma.

Analysing those proteins upregulated separately from those downregulated, Ingenuity core analysis of direct and indirect relationships revealed the significant upregulated canonical pathways in this group to be: acute phase response signalling, LXR/RXR activation, FXR/RXR activation, complement system and coagulation system. Similarly the downregulated canonical pathways were: serotonin degradation, LPS/IL mediated inhibition of RXR, fatty acid β-oxidation I, noradrenaline and adrenaline degradation and xenobiotic metabolism signalling. Statistics for these identified pathways can be seen in Table 4.9.

Upregulated Pathways	**p-value**	**Ratio**
Acute phase response signalling	6.23E-30	29/168 (0.173)
LXR/RXR activation	2.10E-26	24/121 (0.198)
FXR/RXR activation	1.56E-24	23/125 (0.184)
Complement system	2.15E-19	13/32 (0.406)
Coagulation system	2.22E-13	10/35 (0.286)
Downregulated Pathways	**p-value**	**Ratio**
Serotonin degradation	4.85E-27	22/52 (0.423)
LPS/IL mediated inhibition of RXR	8.04E-27	35/208 (0.168)
Fatty acid β-oxidation I	2.31E-24	17/29 (0.586)
Noradrenaline and adrenaline degradation	2.42E-23	17/32 (0.531)
Xenobiotic metabolism signalling	1.52E-21	33/256 (0.129)

Table 4.9 – Pathway analysis for proteins both upregulated and downregulated in the metastatic tumour when compared to normal adjacent colorectal mucosa. P-value is adjusted using Benjamini-Hochberg correction. Ratio identifies the number of focus molecules identified (numerator) in the pathway (denominator).

Further analysis of all (unfiltered) biological pathways identified 8 upregulated networks with a score greater than 2 pertaining to: cell-to-cell signalling and interaction, haematological system development and function, immune cell trafficking, cellular movement, cancer, digestive system development and function, developmental disorder,

haematological disease, cellular movement, organismal injury and abnormalities, dermatological diseases and conditions, hereditary disorder, organismal survival, cellular development, embryonic development, organismal development and gene expression. Similarly 10 downregulated networks were identified pertaining to: lipid metabolism, small molecule biochemistry, vitamin and mineral metabolism, energy production, molecular transport, endocrine system development and function, drug metabolism, nucleic acid metabolism, amino acid metabolism, infectious disease, carbohydrate metabolism, cancer, organismal injury and abnormalities, reproductive system disease, antimicrobial response, metabolic disease, neurological disease and psychological disorders. The focus molecules and statistics pertinent to these networks can be seen in Table 4.10.

Upregulated Networks				
ID	**Molecules in Network**	**Score**	**Focus Molecules**	**Top Diseases and Functions**
1	Alpha Actinin,ANXA1,APOA1,APOA2,APOA4,APOB,APOE,APOH,C3,C5,C7,C9,CFB,CLU,Creb,EPCAM,Fibrinogen,HDL,HDL-cholesterol,HPX,ITGAM,ITGB2,KNG1,LCN2,LDL,LTF,MPO,NFkB (complex),PLG,PLTP,PRELP,PRTN3,S100A12,TES,TSPAN8	49	27	Cell-To-Cell Signaling and Interaction, Hematological System Development and Function, Immune Cell Trafficking
2	Akt,Ap1,ATP1B3,AZGP1,CAPG,CD9,CFH,CFL1,CLDN3,COL12A1,DCN,estrogen receptor,FSH,GPRC5A,GSTP1,HMGA1,Hsp90,IgG,Jnk,KRT19,LGALS3,LGALS3BP,MYH14,PADI4,PDGF BB,PI3K (family),POSTN,S100A4,S100A6,SDCBP,SLC12A2,TF,TFRC,THBS1,VIM	44	26	Cellular Movement, Cancer, Digestive System Development and Function
3	A2M,Alp,ANXA2,CD44,COL1A1,Cyclin A,ERK,ERK1/2,F2,FGA,FGB,FGG,FLNA,FN1, Focal adhesion kinase,GC,Igm,IL12 (complex),Iti,ITIH1,ITIH2,MVP,MYH11,P38 MAPK,PI3K (complex),Pkc(s),S100A10,SERPINC1,SERPIND1,SET,SFN,TIMP1,TNC,Vegf,VTN	37	22	Cellular Movement, Developmental Disorder, Hematological Disease
4	ABCC5,CDH17,CHMP4B,CHMP4C,COL1A2,CTNNB1,EFEMP1,ESR1,FBLN2,FBN1,GJB1,GTSE1,HIST1H1B,KIFC1,KRT20,LDHB,MAGI1,NUPR1,PDCD6IP,PKM,PPARG,RAD23A,S100P,SEMA3C,SLC2A1,SLC2A12,SLC39A8,TAGLN2,TCF4,TMEM97,TMSB10/TMSB4X,TP53,UNC5B,VEGFA,VENTX	18	14	Cellular Movement, Cancer, Organismal Injury and Abnormalities
5	ACTC1,AGTR1,AHSG,ANXA3,APCS,ASPN,C1R,C1S,C4BPA,CDX2,CKAP4,CLDN7,CLIC1,	18	14	Organismal Injury and

	DEPTOR,F5,F11,GLS,HNF1A,IFI44,LAMA4,LBR,LIPA,MAPK1,MEP1A,MT1X,MUC13,MX2,PLA1A,SERPINB1,SERPING1,SMAD3,SOAT2,TCR,UGT1A9 (includes others),YWHAZ			Abnormalities, Dermatological Diseases and Conditions, Hereditary Disorder
6	Actin,AGR2,ALDOA,BGN,CDKN1A,CSF2,CX3CR1,CYP4F3,EPHB2,FFAR2,FSTL3,GSN,HEXB,HIF1A,HSPH1,LOXL2,Ltbp,LUM,MAPK13,mir-145,NOV,OLFM4,PBRM1,S100A8,S100A9,S100A11,SERPINH1,SLPI,SMARCA4,SPAG4,TAGLN,TEC,TGFB1,TGFBI,TGM2	16	13	Cancer, Organismal Survival, Cellular Movement
7	AIF1,APOL1,AUTS2,C8A,CABP7,CAV1,CP,DSG2,EFCAB6,ELAVL1,EMID1,HMOX1,HSP,IFNG,IGHM,IGLL1/IGLL5,IL6,Interferon alpha,MARCKSL1,miR-146a-5p (and other miRNAs w/seed GAGAACU),MORC2,ORM1,PCOLCE,PGLYRP2,PIGR,PTMA,RTDR1,SLC2A11,SMC1B,THBS2,TNF,TRIL,TRIOBP,TTC28,TTR	16	13	Cellular Development, Embryonic Development, Organismal Development
8	26s Proteasome,BCL2,CCND1,CEACAM1,CEACAM5,CTNNB1,CXCL8,DICER1,DPEP1,GFI1,IGHG1,IL2,IL6,IL1A,IRS1,ITGB3,KLK2,MAPT,MGEA5,MYC,SERPINA1,SERPINA3,SERPINF1,SP1,STAT3,TCF,TGFB1,TNF	8	7	Cellular Development, Cancer, Gene Expression
Downregulated Networks				
1	ABLIM,AIFM1,ALDH1A1,ALDH3A2,CAT,CRAT,CYP2E1,CYP3A4,CYP4F2,CYP8B1,DHCR7,ENO3,FASN,FSH,GOT1,GPT,GSTA2,Histone h3,HSD11B1,HSD17B2,IDH1,Jnk,Lh,MGST1,MTTP,NFkB (complex),NQO2,PGRMC1,POR,RNA polymerase II,Rxr,SLC27A2,SOD2,SULT2A1,TCF	41	26	Lipid Metabolism, Small Molecule Biochemistry, Vitamin and Mineral Metabolism
2	AADAC,ACADS,ACADVL,ADH1A,AK4,AKR1C4,AKR1C1/AKR1C2,BHMT2,CCDC87,CDKN1A,CYB5A,CYP3A5,DECR1,DYNC1I2,FH,GLUD1,HADHA,HADHB,HNF1A,LDL-cholesterol,LOH12CR1,MAT1A,MCCC1,mediator,MTORC1,PCK2,SKIV2L2,SREBF1,TAL1,TFR2,TFRC,TUBB6,TXLNG,UGT2B15,ZFC3H1	28	21	Energy Production, Lipid Metabolism, Small Molecule Biochemistry
3	ABCB11,ACAA1,ACAA2,ACOX1,ACSL1,ACSM2B,ADH1B,APOA5,APOC3,APOM,CPT2,CPT1A,CYP3A4,CYP4A11,CYP7A1,DDX20,FABP2,FABP6,G6PC,GLYATL1,HADH,HMGCS2,KNG1,mir-21,mir-27,miR-124-3p (and other miRNAs w/seed	17	15	Lipid Metabolism, Small Molecule Biochemistry, Molecular Transport

	AAGGCAC),NR1H4,PPARA,Rxr,RXRA,RXRG,SLC10A2,SUCLG2,TCF7,UGT2B4			
4	ACAT1,ACAT2,ALDH2,ALDH5A1,ALOX15,APOBEC3B,AQP9,CA2,CSRNP1,DAPK2,ELMOD1,EPB41L4A-AS1,FANCC,H6PD,ING2,KYNU,LILRA5,LSS,NCKIPSD,NPPB,NR3C1,NUPR1,P4HB,PAX3,PEBP1,PRDX3,RAF1,SAMD4A,SLC25A20,SRGAP2,TGM2,TNF,UGT2B7,WDR3,YWHAG	15	13	Endocrine System Development and Function, Lipid Metabolism, Small Molecule Biochemistry
5	ACADM,AGTR1,ATP5B,CYP1A2,CYP2A6 (includes others),CYP2C8,CYP2C9,CYP7A1,ENO1,ESRRA,FOXA3,GFER,HNRNPA2B1,HNRNPM,HSD17B4,mir-122,MUT,NR1I2,NR1I3,P110,p85 (pik3r),PIPOX,PPARGC1A,PPIA,RPL6,RPS2,SDHA,SDHB,SEC14L2,SEMA3B,SULT1A2,TDGF1,TMPO,TUBA1A,ZNF217	15	13	Drug Metabolism, Endocrine System Development and Function, Energy Production
6	ACSM3,BDH1,BRD4,CDC45,CDC42EP5,CDCA7L,CDK4,CES1,DCTPP1,ENO1,ENPP2,EPAS1,FOSL2,GCDH,GYS2,HAMP,IL17RB,IQGAP2,LAMP2,MC4R,miR-145-5p (and other miRNAs w/seed UCCAGUU),MTHFD1,MYC,PBLD,PIM2,PNN,RGS3,SERINC3,SHMT1,SHMT2,SORD,SOX5,TMPRSS6,TYMS,UGP2	13	12	Nucleic Acid Metabolism, Small Molecule Biochemistry, Amino Acid Metabolism
7	ABCD3,ABLIM1,ACO1,ADAP1,CRYL1,DAK,DHX58,DRD3,ERP29,FBP1,FLNA,GATM,ICK,IFI44,IFIH1,ITGB7,KHK,LBR,MAPK1,MGEA5,MMP14,MX2,NIPSNAP1,NNT,NREP,OASL,PAK1,PECR,PFKM,PGM1,SLC2A3,SOX11,TCR,TGFBR2,TUBA1A	13	13	Infectious Disease, Carbohydrate Metabolism, Small Molecule Biochemistry
8	AKR1C3,ALDH6A1,AR,ASGR1,ASS1,CDH1,COMT,ENTPD5,EPHX1,ESR1,ESR2,FKBP4,FKBPL,FMN1,FOXA1,GREB1,HSD17B6,Hsp90,IDH2,KDM4B,LTBP1,MAOA,MARC2,MGAT3,NCOA4,NEUROG1,NFATC4,PRKCD,RPRM,SIAH2,SOD1,SOST,TMEM74,TMOD1,VAV3	13	12	Cancer, Organismal Injury and Abnormalities, Reproductive System Disease
9	ADH5,AIM2,ARG1,CBS/LOC102724560,CCNG2,CLEC4M,CSNK2A1,CTH,CYP17A1,DDB2,ECHDC3,EIF2AK2,EPHX2,FAM213A,GBP1,HAS1,HEBP1,HRH2,IFI27,IL18RAP,Interferon alpha,ISG20,MAOB,MAPKAPK2,miR-483-3p (miRNAs w/seed CACUCCU),MKNK1,NF1,OAS1,P38 MAPK,SMAD4,SP1,TRIB1,UGDH,UNC93B1,USP18	12	11	Amino Acid Metabolism, Small Molecule Biochemistry, Antimicrobial Response
10	ACTB,APBA2,APOE,APP,ASL,ATP5A1,CCN	10	12	Metabolic

	D1,CEP55,CES2,DDT,GART,GSTO1,HSD17B10,HSPA1L,ITM2B,MLH1,MYBL1,PDX1,PFAS,PFKP,PHGDH,Pp2b,PPAT,PPP3CA,PRDX6,RFC1,RNF219,SCP2,SLC2A2,SNRK,SNRNP70,TAGLN2,TMSB15A,TP53,UCHL1			Disease, Neurological Disease, Psychological Disorders

Table 4.10 - Network analysis for proteins both upregulated and downregulated in the metastatic tumour when compared to normal adjacent liver parenchyma. The score is derived from a p-value and indicates the probability of the focus molecules in a network being found together due to random chance. Focus molecules is the total number of proteins of interest identified in the respective network.

4.3.7 Comparison of primary and metastatic tumours

This analysis identified all those proteins significantly differentially expressed in the metastatic tumour compared to the primary tumour. A total of 67 proteins were identified, 58 of which were more abundant in the metastatic tumour and 9 were less abundant (Table 4.11).

Accession Number	Name	p Value	Log2 Fold-Change (Metastasis/Primary)
P08311	Cathepsin G	6.05E-03	-5.220
P48539	Purkinje cell protein 4	1.46E-02	-4.063
P24158	Myeloblastin	5.40E-03	-3.844
P84157	Matrix-remodeling-associated protein 7	3.21E-02	-2.579
P25815	Protein S100-P	2.50E-02	-2.505
P06702	Protein S100-A9	1.05E-03	-2.077
P05106	Integrin beta-3	3.78E-02	-2.068
P23142	Fibulin-1	9.89E-03	-2.040
Q02952	A-kinase anchor protein 12	1.55E-02	-2.037
P01019	Angiotensinogen	4.10E-02	2.012
P13671	Complement component C6	4.65E-02	2.032
P04114	Apolipoprotein B-100	1.28E-02	2.048
P15153	Ras-related C3 botulinum toxin substrate 2	2.02E-02	2.152
O14773	Tripeptidyl-peptidase 1	1.69E-02	2.212
Q9BX68	Histidine triad nucleotide-binding protein 2, mitochondrial	1.93E-02	2.260
P42765	3-ketoacyl-CoA thiolase,	4.04E-02	2.292

	mitochondrial		
P36269	Gamma-glutamyltransferase 5	4.61E-03	2.360
P08571	Monocyte differentiation antigen CD14	1.10E-03	2.364
P02792	Ferritin light chain	3.17E-02	2.385
P07858	Cathepsin B	2.86E-03	2.388
P40261	Nicotinamide N-methyltransferase	1.59E-02	2.437
P19971	Thymidine phosphorylase	4.02E-03	2.438
P02787	Serotransferrin	1.55E-02	2.469
P01834	Ig kappa chain C region	1.42E-02	2.477
P01857	Ig gamma-1 chain C region	3.23E-02	2.482
P34896	Serine hydroxymethyltransferase, cytosolic	2.06E-02	2.494
P05177	Cytochrome P450 1A2	3.40E-03	2.557
P21695	Glycerol-3-phosphate dehydrogenase [NAD+], cytoplasmic	3.34E-02	2.578
P08123	Collagen alpha-2(I) chain	3.97E-02	2.743
P51884	Lumican	3.26E-02	2.779
Q00796	Sorbitol dehydrogenase	1.43E-02	2.839
Q8IUX7	Adipocyte enhancer-binding protein 1	5.60E-03	2.872
P15104	Glutamine synthetase	4.91E-02	2.994
Q9UJS0	Calcium-binding mitochondrial carrier protein Aralar2	1.94E-02	3.037
Q7Z4W1	L-xylulose reductase	3.03E-02	3.065
Q4G0N4	NAD kinase domain-containing protein 1	6.71E-03	3.146
Q16719	Kynureninase	3.73E-02	3.158
P01011	Alpha-1-antichymotrypsin	2.36E-03	3.186
P22307	Non-specific lipid-transfer protein	3.28E-02	3.235
P00367	Glutamate dehydrogenase 1, mitochondrial	1.95E-02	3.410
P02749	Beta-2-glycoprotein 1	3.82E-02	3.589
P28845	Corticosteroid 11-beta-dehydrogenase isozyme 1	2.32E-02	3.649
P28332	Alcohol dehydrogenase 6	1.30E-02	3.674
P01033	Metalloproteinase inhibitor 1	6.73E-03	3.685
P09467	Fructose-1,6-bisphosphatase 1	2.75E-02	3.972
P35442	Thrombospondin-2	4.00E-03	4.321

P02649	Apolipoprotein E	5.18E-03	4.333
P04196	Histidine-rich glycoprotein	1.27E-02	4.599
P10620	Microsomal glutathione S-transferase 1	4.56E-02	4.652
P04004	Vitronectin	1.25E-02	4.721
P32754	4-hydroxyphenylpyruvate dioxygenase	5.36E-03	6.385
Q06828	Fibromodulin	2.79E-03	6.766
P11498	Pyruvate carboxylase, mitochondrial	1.17E-02	7.180
P00167	Cytochrome b5	3.30E-02	7.915
P05089	Arginase-1	3.85E-02	9.069
P05181	Cytochrome P450 2E1	3.98E-04	9.526
P00325	Alcohol dehydrogenase 1B	3.47E-02	12.136
P33121	Long-chain-fatty-acid--CoA ligase 1	4.67E-02	14.035
P24752	Acetyl-CoA acetyltransferase, mitochondrial	2.70E-02	15.347
P51888	Prolargin	7.03E-03	17.972
P05062	Fructose-bisphosphate aldolase B	4.04E-02	22.005
P50440	Glycine amidinotransferase, mitochondrial	2.12E-02	34.116
O75891	Cytosolic 10-formyltetrahydrofolate dehydrogenase	4.02E-02	34.809
P31513	Dimethylaniline monooxygenase [N-oxide-forming] 3	2.52E-02	36.361
P30038	Delta-1-pyrroline-5-carboxylate dehydrogenase, mitochondrial	2.68E-02	54.551
P08319	Alcohol dehydrogenase 4	3.35E-02	253.897
Q06520	Bile salt sulfotransferase	4.40E-03	954.271

Table 4.11 – Those proteins differentially expressed between the metastatic tumour and the primary tumour. 67 proteins were identified, 58 of which were upregulated (positive values for fold change) and 9 downregulated (negative values for fold change).

Analysing those proteins upregulated separately from those downregulated, Ingenuity core analysis of direct and indirect relationships revealed the significant upregulated canonical pathways in this group to be: FXR/RXR activation, ethanol degradation II, LXR/RXR activation, LPS/IL-I mediated inhibition of RXR and noradrenaline and adrenaline

degradation. Similarly the downregulated canonical pathways were: role of IL-17A in psoriasis, glioma invasiveness signalling, agrin interactions at neuromuscular junction, macropinocytosis signalling and caveolar-mediated endocytosis signalling. Statistics for these identified pathways can be seen in Table 4.12.

Upregulated Pathways	p-value	Ratio
FXR/RXR activation	5.06E-09	8/125 (0.064)
Ethanol degradation II	3.44E-08	5/30 (0.167)
LXR/RXR activation	9.91E-08	7/121 (0.058)
LPS/IL-I mediated inhibition of RXR	2.67E-07	8/208 (0.038)
Noradrenaline and adrenaline degradation	2.95E-06	4/32 (0.125)
Downregulated Pathways	**p-value**	**Ratio**
Role of IL-17A in psoriasis	5.72E-03	1/13 (0.077)
Glioma invasiveness signalling	2.49E-02	1/57 (0.018)
Agrin interactions at neuromuscular junction	2.92E-02	1/67 (0.015)
Macropinocytosis signalling	2.96E-02	1/68 (0.015)
Caveolar-mediated endocytosis signalling	3.13E-02	1/72 (0.014)

Table 4.12 – Pathway analysis for proteins both upregulated and downregulated in the metastatic tumour when compared to the primary tumour. P-value is adjusted using Benjamini-Hochberg correction. Ratio identifies the number of focus molecules identified (numerator) in the pathway (denominator).

Further analysis of all (unfiltered) biological pathways identified 3 upregulated networks with a score greater than 2 pertaining to: lipid metabolism, small molecule biochemistry, vitamin and mineral metabolism, cellular movement, haematological system development and function and immune cell trafficking. Similarly, 1 downregulated network was identified pertaining to: cell-to-cell signalling and interaction, haematological system development and function and immune cell trafficking. The focus molecules and statistics pertinent to these networks can be seen in Table 4.13.

Upregulated Networks				
ID	**Molecules in Network**	**Score**	**Focus Molecules**	**Top Diseases and Functions**
1	ABHD2,ACAT1,ACSL1,ADH4,AIM1,AKAP13,CTNNB1,CTSB,CYB5A,CYP1A2,CYP2E1,DYNLL1,DYNLL2,GFER,GLA,GLUL,HNF1A,HSD11B1,HSD17B2,IGHG1,LUM,MGST1,MSX2,MT1L,NFIC,NR3C1,PGR,PTP4A1,S100P,SERPINA5,SMARCA4,TFEB,TNS4,TPP1,VTN	26	16	Lipid Metabolism, Small Molecule Biochemistry, Vitamin and Mineral Metabolism
2	ACPP,APOB,APOE,ARG1,CDCA7L,Cg,DHCR7,EIF2AK2,FBP1,FDFT1,FMOD,FTL,GLIPR1,HMGCS1,LAMP2,LOC102724788/PRODH,LSS,MGEA5,MYC,NAP1L1,NNMT,PERP,PFKM,Pp2b,S100A2,SCP2,SHC1,SHMT1,SNRK,SULT2A1,TAF5L,TIMP1,TMSB10/TMSB4X,TP53,TPD52L1	19	12	Lipid Metabolism, Small Molecule Biochemistry, Vitamin and Mineral Metabolism
3	ABCC3,AFP,AGT,APOH,C3,CASP3,CD14,CFB,COL1A2,CYP27A1,FCGR1B,FGA,GMFG,HMOX1,HSPE1,IL6,IL17D,KYNU,LGALS4,LILRA4,LILRA5,MMP8,PRELP,RAC2,S100A10,SCAVENGER receptor CLASS A,SERPINA3,SIRT6,SREBF1,TF,THBS2,TNF,TNFRSF18,TNIP3,TYMP	19	11	Cellular Movement, Hematological System Development and Function, Immune Cell Trafficking
Downregulated Networks				
1	AKAP12,BCAN,CCL5,CDKN3,CELSR2,CTSG,ENPP1,ESR1,FBLN1,Fibrin,FN1,GUSB,HEXA,IL1B,ITGB3,ITPA,MAPK12,mir-224,miR-224-5p (miRNAs w/seed AAGUCAC),miR-24-3p (and other miRNAs w/seed GGCUCAG),PCP4,PPIF,PRIM1,PRTN3,S100A9,S100P,SEMA3A,SERPINH1,SLC39A8,Sod,SQLE,TGFB1,TMEM97,TOP2B,TP53	21	7	Cell-To-Cell Signaling and Interaction, Hematological System Development and Function, Immune Cell Trafficking

Table 4.13 - Network analysis for proteins both upregulated and downregulated in the metastatic tumour when compared to the primary tumour. The score is derived from a p-value and indicates the probability of the focus molecules in a network being found together due to random chance. Focus molecules is the total number of proteins of interest identified in the respective network.

4.3.8 Predictive biomarkers in the primary tumours

Patients from whom matched primary and metastatic tissue had been obtained and neoadjuvant chemotherapy had been given(n=10) were classified as being responders or non-responders to chemotherapy on the basis of histopathological assessment (Section 4.2.3). Proteins differentially expressed between responders and non-responders (log2 fold change >2, unadjusted p<0.05) were again identified and subjected to pathway and network analysis.

A total of 170 proteins were differentially expressed between the primary tumours of the responders and the primary tumours of the non-responders. 59 proteins were upregulated in the responders, and 111 downregulated. Details of these can be seen in Appendix 4 – Proteomic comparison of responders and non-responders in the primary tumour.

Analysing those proteins upregulated separately from those downregulated, Ingenuity core analysis of direct and indirect relationships revealed the significant upregulated canonical pathways in this group to be: TR/RXR activation, Huntington's disease signalling, role of PI3K/AKT signalling, cell cycle: G1/S checkpoint regulation and IL4 signalling . Similarly the downregulated canonical pathways were: mitochondrial dysfunction, fatty acid β-oxidation I, oxidative phosphorylation, serotonin degradation and glutaryl-CoA degradation. Statistics for these identified pathways can be seen in Table 4.14.

Upregulated Pathways	**p-value**	**Ratio**
TR/RXR activation	1.68E-04	4/85 (0.047)
Huntington's disease signalling	8.33E-04	5/226 (0.022)
Role of PI3K/AKT signalling	1.03E-03	3/61 (0.049)
Cell cycle: G1/S checkpoint regulation	1.13E-03	3/63 (0.048)
IL-4 signalling	1.73E-03	3/73 (0.041)
Downregulated Pathways	**p-value**	**Ratio**
Mitochondrial dysfunction	6.22E-07	9/165 (0.055)
Fatty acid β-oxidation I	7.23E-07	5/29 (0.172)
Oxidative phosphorylation	2.89E-06	7/104 (0.067)
Serotonin degradation	1.42E-05	5/52 (0.096)
Glutaryl-CoA degradation	3.27E-05	3/11 (0.273)

Table 4.14 – Pathway analysis for proteins both upregulated and downregulated in the primary tumours of the responders compared to the primary tumours of the non responders. P-value is adjusted using Benjamini-Hochberg correction. Ratio identifies the number of focus molecules identified (numerator) in the pathway (denominator).

Further analysis of all (unfiltered) biological pathways identified 4 upregulated networks with a score greater than 2 pertaining to: cellular movement, haematological system development and function, immune cell trafficking, cancer, dermatological diseases and conditions, immunological disease, hematological disease, organismal injury and abnormalities, cell cycle, lipid metabolism, small molecule biochemistry and vitamin and mineral metabolism. Similarly 5 downregulated networks were identified pertaining to: cellular assembly and organization, cellular function and maintenance, cell death and survival, energy production, lipid metabolism, small molecule biochemistry, cell-to-cell signalling and interaction, infectious disease, amino acid metabolism, cell signalling, molecular transport, lymphoid tissue structure and development, cancer and organismal injury and abnormalities. The focus molecules and statistics pertinent to these networks can be seen in Table 4.15.

Upregulated Networks				
ID	**Molecules in Network**	**Score**	**Focus Molecules**	**Top Diseases and Functions**
1	ANXA1,AQP9,ATM,CLEC11A,DPY30,ENO3, ERK1/2,FANCC,FKBP5,Histone h3,Hsp90,IDH1,IL36A,KPNA3,LSP1,MAPK10,miR-491-5p (and other miRNAs w/seed GUGGGGA),MT-TY,MTOR,MYL1,MYO1E,NFKB1,NFkB (complex),P2RY6,PPP1R18,PPP1R16B,RLN2,SH3GLB2,SLC52A1,SSRP1,TGM2,TOP1,TPCN1,TPM3,UGT2B7	20	12	Cellular Movement, Hematological System Development and Function, Immune Cell Trafficking
2	ABHD2,ACAT1,ARFGEF1,ARFGEF2,BCOR,CDC34,CDCA7L,COTL1,DYNLL1,ENO1,GLIPR1,HEXB,HLA-DRA,Hla-Drb,HSD11B1,IRF1,MT1L,MTHFD1,MXD1,MYC,NFIC,NFKBIA,NR3C1,ODC1,PERP,PRKAC,PRKACB,PRKAR1A,PSME1,ROCK1,SERPINE2,SH3KBP1,SKP1,SMARCA4,THY1	18	11	Cancer, Dermatological Diseases and Conditions, Immunological Disease
3	AIMP1,C4BPA,CCT5,CCT6A,CDKN2AIP,COL6A3,CTNNB1,CTSD,GNAI2,GNL3,GRB2,GRIN1,HINT1,HNF1A,HNMT,HSD17B2,ITGA1,mir-224,miR-224-5p (miRNAs w/seed AAGUCAC),miR-24-3p (and other miRNAs w/seed GGCUCAG),PDE6B,PRIM1,RAD23A,RPL8,RPL23,RPL26,RPL7A,RPS7,RPS4X,SEMA3C,SLC2A12,SLC39A8,SP1,TGFB1,TP53	18	12	Hematological Disease, Organismal Injury and Abnormalities, Cell Cycle
4	AP2M1,APOB,BST2,CD74,COL14A1,Cpla2, CXCL5,CYP27A1,EFEMP1,EIF2S1,HLA-DRB4,HSPG2,IGFBP2,LDL,LGALS3,LIPG,MCTS1,MHC Class II	16	11	Lipid Metabolism, Small Molecule Biochemistry,

	(complex),NBN,Nr1h,NR1H3,OSCAR,PCK2,PCSK9,PLA2G4A,PON1,PPA1,PTAFR,PTGS2,RPLP0,SMC1A,SREBF1,TF,TNF,TRAF1			Vitamin and Mineral Metabolism
Downregulated Networks				
1	AIFM1,ANXA2,ATP1B1,BAX,calpain,caspase,CAST,CD3,CLTC,CSK,CYP27A1,DSP,ERK1/2,ERP29,estrogen receptor,Hsp90,IgG,INF2,IRF6,Jnk,KRT7,KRT17,KRT18,KRT19,MVP,MYH14,NFkB (complex),P38 MAPK,PHB,PHB2,PPP2R1A,PPP2R2A,SERPINB5,VDAC2,XIAP	47	24	Cellular Assembly and Organization, Cellular Function and Maintenance, Cell Death and Survival
2	ACAA2,ACADS,ACADVL,ACP1,ATM,CCNA2,CDKN2AIP,CHMP4C,CNOT1,COPG2,CTTN,E4F1,ETHE1,FDPS,GRB2,GSR,HADH,HIST1H4A,HSD17B4,KIF24,LPIN1,MAT1A,PDCD6IP,PLEC,RGS6,RPL13,RPL23,RPL26,RPL7A,RPS7,RXRG,SREBF1,SYK,TP53,TUFM	25	16	Energy Production, Lipid Metabolism, Small Molecule Biochemistry
3	ABLIM,ADCY7,AKR1B10,AKT1,ARPC1A,ATP9A,CASK,CRYL1,DUSP3,ETV5,FANCC,FH,FSH,GNLY,GNRH,LAD1,Lh,MAPK1,MMP2,MYO6,MYRF,NQO1,NR3C1,PDXK,PKP2,PKP3,PLIN3,PPIH,PRKX,PRPF4B,PTPRN,RAB5A,S100A14,TLK1,VCL	17	12	Cell-To-Cell Signaling and Interaction, Infectious Disease, Amino Acid Metabolism
4	ABCC3,ACAA1,ACOX1,ALDH2,APOB,CHST2,EHD1,EPB41L1,ERMAP,G0S2,HDAC10,Histone h3,Hsp90,IL13,KDM5B,KLHDC10,LIMCH1,LONP1,MKK3/6,MT-CO2,MT-CYB,NID1,PDIA3,PDIA4,PLXNC1,PPARA,RNA polymerase II,SLC8A1,SORT1,SPTA1,SWAP70,SYNPO,TAF10,TNF,TPM3	15	10	Cell Signaling, Molecular Transport, Small Molecule Biochemistry
5	AQP3,BCL6,CCND1,CCR6,CD72,EPB41L2,FCGRT,FES,FOLR1,FUT7,HNF1A,HNF1B,HNMT,HNRNPA2B1,KIF20A,KLK1,PBLD,PBX1,PCBP1,PLD2,SEL1L,SKIV2L,SPI1,STOM,SULT1A1,SYVN1,TARS,TLE1,TNFRSF14,TUBA3C/TUBA3D,UGT2B17,UQCRC2,USP5,UTRN,VIL1	12	10	Lymphoid Tissue Structure and Development, Cancer, Organismal Injury and Abnormalities

Table 4.15 – Network analysis for proteins both upregulated and downregulated in the primary tumours of the responders compared to the primary tumours of the non responders. The score is derived from a p-value and indicates the probability of the focus molecules in a network being found together due to random chance. Focus molecules is the total number of proteins of interest identified in the respective network.

4.3.9 Predictive biomarkers in the metastatic tumours

A total of 27 proteins were differentially expressed between the metastatic tumours of the responders and the metastatic tumours of the non-responders. 17 proteins were upregulated in the responders, and 10 downregulated. Details of these can be seen in Table 4.16.

Accession Number	Name	p Value	Log2 Fold-Change (Responders/Non-Responders)
P01719	Ig lambda chain V-V region DEL	2.27E-02	-78.793
P13760	HLA class II histocompatibility antigen, DRB1-4 beta chain	4.63E-03	-67.649
Q7L5L3	Glycerophosphodiester phosphodiesterase domain-containing protein 3	2.56E-03	-15.402
P15559	NAD(P)H dehydrogenase [quinone] 1	4.09E-02	-3.767
Q9Y6D6	Brefeldin A-inhibited guanine nucleotide-exchange protein 1	4.24E-02	-3.112
O76003	Glutaredoxin-3	2.77E-02	-2.284
P02745	Complement C1q subcomponent subunit A	1.84E-02	-2.271
Q29865	HLA class I histocompatibility antigen, Cw-18 alpha chain	1.64E-02	-2.239
P15311	Ezrin	2.85E-02	-2.132
Q99439	Calponin-2	3.85E-02	-2.060
Q99735	Microsomal glutathione S-transferase 2	3.69E-02	2.034
P51570	Galactokinase	6.66E-03	2.210
Q9Y2S2	Lambda-crystallin homolog	3.12E-02	2.358
P43155	Carnitine O-acetyltransferase	2.42E-02	2.365
O14773	Tripeptidyl-peptidase 1	2.50E-02	3.401
Q14508	WAP four-disulfide core domain protein 2	3.12E-02	3.850
P04040	Catalase	4.62E-02	4.088
P01880	Ig delta chain C region	4.16E-02	4.671
Q02252	Methylmalonate-semialdehyde dehydrogenase [acylating], mitochondrial	4.81E-02	4.898
Q08257	Quinone oxidoreductase	2.95E-02	6.470
Q02318	Sterol 26-hydroxylase, mitochondrial	3.47E-02	13.663
P05089	Arginase-1	4.61E-02	32.760
P51888	Prolargin	4.08E-02	61.579

P80404	4-aminobutyrate aminotransferase, mitochondrial	3.90E-02	66.207
P07099	Epoxide hydrolase 1	4.46E-02	100.906
O75891	Cytosolic 10-formyltetrahydrofolate dehydrogenase	2.07E-02	397.163
Q08AH3	Acyl-coenzyme A synthetase ACSM2A, mitochondrial	4.51E-02	56001.100

Table 4.16 – Those proteins differentially expressed between the metastatic tumours of the responders and non-responders. 27 proteins were identified, 17 of which were upregulated (positive values for fold change) and 10 downregulated (negative values for fold change).

Analysing those proteins upregulated separately from those downregulated, Ingenuity core analysis of direct and indirect relationships revealed the significant upregulated canonical pathways in this group to be: β-alanine degradation I, valine degradation I, LPS/IL-1 mediated inhibition of RXR, xenobiotic metabolism signalling and D-glucuronate degradation I. Similarly the downregulated canonical pathways were: antigen presentation pathway, allograft rejection signalling, OX40 signalling pathway, communication between innate and adaptive immune cells and crosstalk between dendritic cells and natural killer cells. Statistics for these identified pathways can be seen in Table 4.17.

Upregulated Pathways	p-value	Ratio
β-alanine degradation I	7.30E-07	2/2 (1)
Valine degradation I	1.11E-04	2/18 (0.111)
LPS/IL-1 mediated inhibition of RXR	7.46E-04	3/208 (0.014)
Xenobiotic metabolism signalling	1.36E-03	3/256 (0.012)
D-glucuronate degradation I	2.64E-03	1/3 (0.333)
Downregulated Pathways	**p-value**	**Ratio**
Antigen presentation pathway	1.44E-04	2/37 (0.054)
Allograft rejection signalling	2.44E-04	2/48 (0.042)
OX40 signalling pathway	3.09E-04	2/54 (0.037)
Communication between innate and adaptive immune cells	7.12E-04	2/82 (0.024)
Crosstalk between dendritic cells and natural killer cells	8.38E-04	2/89 (0.022)

Table 4.17 – Pathway analysis for proteins both upregulated and downregulated in the metastatic tumours of the responders compared to the metastatic tumours of the non responders. P-value is adjusted using Benjamini-Hochberg correction. Ratio identifies the number of focus molecules identified (numerator) in the pathway (denominator).

Further analysis of all (unfiltered) biological pathways identified 5 upregulated networks with a score greater than 2 pertaining to: infectious disease, organismal injury and abnormalities, neurological disease, cell-to-cell signalling and interaction, tissue development, increased levels of potassium, DNA replication, recombination and repair, drug metabolism, cancer, cellular assembly and organization, developmental disorder, hereditary disorder, lipid metabolism, molecular transport and small molecule biochemistry. Similarly 1 downregulated network was identified pertaining to: cell death and survival, cell cycle, and cell-to-cell signalling and interaction. The focus molecules and statistics pertinent to these networks can be seen in Table 4.18.

Upregulated Networks				
ID	**Molecules in Network**	**Score**	**Focus Molecules**	**Top Diseases and Functions**
1	ABCC3,ALDH6A1,APLN,ARG1,C3,CAT,CFB,CYP27A1,EPHX1,ESR1,FCGR1B,FGA,FMN1,FOXA1,GMFG,GREB1,HSPE1,IL6,IL17D,LGALS4,LILRA4,LILRA5,PRELP,PRSS23,RPRM,S100A10,SCAVENGER receptor CLASS A,SIRT6,Sod,TM4SF1,TMEM74,TNF,TNFAIP2,TNFRSF18,TNIP3	13	7	Infectious Disease, Organismal Injury and Abnormalities, Neurological Disease
2	CRYL1,MAPK1	3	1	Cell-To-Cell Signaling and Interaction, Tissue Development, Increased Levels of Potassium
3	CRYZ,REXO4	3	1	DNA Replication, Recombination, and Repair, Drug Metabolism, Cancer
4	TFEB,TPP1	3	1	Cellular Assembly and Organization, Developmental Disorder, Hereditary Disorder
5	CRAT,CTNNB1,TCF	3	1	Lipid Metabolism, Molecular Transport, Small Molecule Biochemistry
Downregulated Networks				
1	ARFGEF1,C1QA,CDKN1A,CEACAM3,CNN2,CTNNB1,CXCL16,EZR,FCGR1B,Ferritin,GLRX3,HLA-C,HLA-DRB4,HSP,IFNG,IL17RB,KIR,KIR2DL1/KIR2DL3,KIR2DS4 (includes others),LAIR1,MAGEA3/MAGEA6,MARCKSL1,NQO1,PLA2G5,PRKAR2A,PTGDR,SEMA3C,SERPINA5,SOAT1,Sod,TNF,TYMP,U1 snRNP,ULBP1,VIPR1	21	8	Cell Death and Survival, Cell Cycle, Cell-To-Cell Signaling and Interaction

Table 4.18 – Network analysis for proteins both upregulated and downregulated in the metastatic tumours of the responders compared to the metastatic tumours of the non responders. The score is derived from a p-value and indicates the probability of the focus molecules in a network being found together due to random chance. Focus molecules is the total number of proteins of interest identified in the respective network.

4.3.10 Predictive biomarkers common to primary and metastatic tumours

170 proteins in the primary tumours were significantly differentially expressed between responders and non-responders. In the metastases 22 proteins were identified. 5 proteins were common to both primary and metastatic tissues, none of which were significantly differentially expressed between the two tissue types (Figure 4.3).

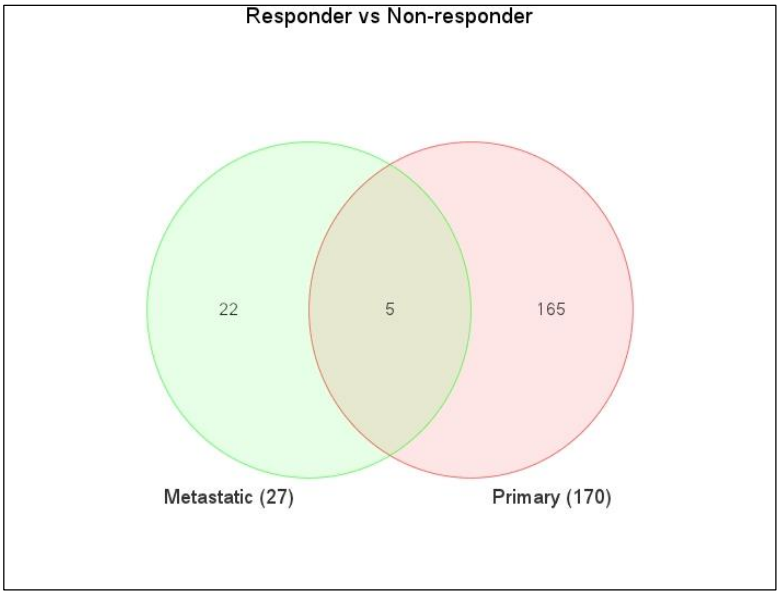

Figure 4.3 – Venn diagram of predictive biomarkers identified in the primary tumour (170), metastatic tumour (27) and common to both (5).

The 5 proteins identified as predictors of response alongside the P value and log2 fold change for both tissue types are shown in Table 4.19. Of these 5, 2 proteins were upregulated in the primary tumour but downregulated in the metastasis and 1 was downregulated in the primary tumour but upregulated in the metastasis. Only 2 proteins had consistent dysregulation between primary and metastatic tissue: NAD(P)H dehydrogenase [quinone 1] and lambda-crystallin homolog were both downregulated in the primary and metastatic tumours of those patients responding to neoadjuvant chemotherapy.

Accession Number	Name	Primary		Metastasis	
		p Value	Log2 Fold Change	p Value	Log2 Fold Change
P13760	HLA class II histocompatibility antigen, DRB1-4 beta chain	5.91E-03	88.035	4.63E-03	-67.649
P15559	NAD(P)H dehydrogenase [quinone] 1	2.64E-04	-9.918	4.09E-02	-3.767
Q02318	Sterol 26-hydroxylase, mitochondrial	6.70E-03	-2.114	3.47E-02	13.663
Q9Y2S2	Lambda-crystallin homolog	3.25E-03	-2.085	3.25E-03	-2.085
Q9Y6D6	Brefeldin A-inhibited guanine nucleotide-exchange protein 1	7.37E-03	4.595	4.24E-02	-3.112

Table 4.19 – Summary of predictive biomarkers common to both primary and metastatic tumours.

4.3.11 Phenotypic anchoring of exome sequencing

Of the 5766 proteins identified through iTRAQ, SNVs were identified in the protein coding region of 2627. For 3 of these proteins the SNV was present in 14 samples, for 10 it was present in 10 samples, 9 present in 9, 3 present in 7, 8 present in 6, 16 present in 5, 92present in 4, 93 present in 9, 498 present in 2 and 1895 present in 1.

4.4 Discussion

4.4.1 Summary of aims

In this study a comprehensive proteomic analysis of paired primary and metastatic samples from 16 patients was performed. The aim of this investigation was to compare the proteomic profile of the primary and metastatic tumours, both with each other and with their normal adjacent tissue, to establish the degree of similarity and identify potential response biomarkers present in the primary tumour which may predict response to neoadjuvant therapy in the liver metastasis.

4.4.2 Summary of results

Matched primary and metastatic tissue from 16 patients was subjected to iTRAQ. Eleven patients had undergone neoadjuvant chemotherapy, 10 of which achieved resection. Five of these patients had a tumour regression grade of 1-2 and the remaining 5 had a tumour regression grade of 3-4. A total of 5766 proteins were identified, of which 2637 were taken forwards for bioinformatics analysis. A summary of the proteomic data is shown in Table 4.20.

Comparison	Total Dysregulated	Upregulated	Downregulated
Primary Tumour / Colonic Mucosa	25	6	19
Metastatic Tumour / Colonic Mucosa	53	13	40
Metastastic Tumour / Liver Parenchyma	444	164	280
Metastatic Tumour / Primary Tumour	67	58	9
Responders / Non Responders (Primary)	170	59	111
Responders / Non Responders (Metastasis)	27	17	10

Table 4.20 - Summary proteomic data for the 2-group comparisons showing the total number of dysregulated proteins as well as those up/downregulated.

Comparing primary tumour with normal colon, 25 proteins were significantly differentially expressed (6 upregulated and 19 downregulated) and for metastatic tumour compared with normal colon there were 53 (13 upregulated and 40 downregulated). Comparison of the metastatic tumour with liver parenchyma identified 444 proteins differentially

expressed, 164 of which were upregulated and 280 downregulated. Only 67 of the 2637 (2.54%) proteins studied were significantly different between primary and metastatic tissue, with 58 upregulated in the metastatic tumour and 9 downregulated. One hundred and seventy proteins were identified in the primary tumour which were significantly differentially expressed between responders and non-responders with 59 upregulated and 111 downregulated in the responders. In the metastases there were 27 (17 upregulated and 10 downregulated). Five proteins were common to both tissue types, only two of which showed consistent dysregulation between responders and non-responders (NAD(P)H dehydrogenase [quinone 1] and lambda-crystallin homolog). Of the 5766 proteins identified by iTRAQ, SNVs were previously identified in the protein coding region of 2627. Further bioinformatics analysis of these comparator groups revealed putative pathways and networks involved in carcinogenesis.

4.4.3 iTRAQ for evaluation of tumour biology

Proteomic studies using techniques such as iTRAQ offer a significant advantage over genomic approaches to similar questions. The level of transcription of a gene only gives an estimate of its level of translation into a protein, as an mRNA produced in abundance may be degraded rapidly or translated inefficiently. Other proteomics approaches may help to investigate post-translational modification of proteins, investigate alternative splicing, evaluate the formation of protein complexes and account for protein degradation by providing quantitative data, although the technique we have adopted for this study is currently unable to provide such insight.

A number of studies have attempted to use iTRAQ to further our understanding of tumour biology. Lin *et al* (2014) characterised the profile of the human colon adenocarcinoma cell line HCT-116 with its metastatic derivative E1. A total of 547 proteins were identified with 31 differentially expressed including translationally controlled tumour protein 1, A-kinase anchor protein 12 and Drebrin (DBN1). Western blotting subsequently validated these findings.

In 2014, Liu *et al* characterised the cancer stroma expression profile of muscle-invasive bladder cancer. 30 clinical samples of 3 different metastatic risk groups were profiled to identify differentially expressed proteins. A total of 1049 differentially expressed proteins were identified by paired comparisons (high risk *vs*. median risk, low risk and normal;

median risk *vs*. low risk and normal, low risk *vs*. normal group), with 510, 549 and 548 proteins significantly altered respectively. On pathway analysis the differentially expressed proteins were mainly located in the focal adhesion pathway, systemic lupus erythematosus pathway and ECM-receptor interaction pathway. This group also identified several candidate biomarkers (EXOC4, MYH10 and MMP-9) of invasion.

Wang *et al* (2012) compared the proteome of ovarian cancer tissues and normal ovarian epithelium. One thousand two hundred and fifty-nine unique proteins were identified, with 205 differentially expressed between ovarian cancer and normal ovarian tissue. A number of these proteins were validated by western blotting, RT-PCR or immunohistochemistry. Similarly pancreatic adenocarcinoma tissues of varying histological differentiation were sequenced by Wang *et al* in 2013. A total of 1623 proteins were identified of which 15 were differentially expressed. Myoferlin was validated initially by western blotting and latterly by immunohistochemistry in a further 154 samples. The authors conclude that iTRAQ identified this protein as correlating with histological expression, and evaluation against corresponding clinical data suggests its expression is an independent prognostic factor for survival.

Similarly to this study, Leong *et al* (2012) attempted to identify predictors of response to chemotherapy in breast cancer. To focus their assessment on apoptosis, iTRAQ of enriched mitochondria and endoplasmic reticulum cells was performed leading to the identification of several differentially abundant proteins in breast cancer cells treated with doxorubicin. Pathway analysis suggested cellular assembly and organization, molecular transport, oxidative stress, cell motility, cell death, and cancer were key pathways upregulated with treatment. In another *in vitro* study, Nishimura *et al* (2014) investigated four human tumour derived cell lines: cisplatin-sensitive UM-SCC-23, UM-SCC-23-CDDPR with acquired cisplatin resistance, naturally cisplatin-resistant UM-SCC-81B, and UM-SCC-23/WR with acquired 5-fluorouracil resistance. In total, 13 multiple drug resistance proteins were identified with a further 7 specifically associated with resistance to cisplatin.

Perhaps of most clinical interest is a translational study reported by Rehman *et al* in 2012. Pooled serum samples were analysed from 4 groups of patients characterised as benign prostatic hyperplasia, localised cancer, apparently localised cancer but with biochemical suggestion of spread and advanced disease. Only 122 proteins were identified, although 25 were differentially abundant in those with progressive disease. The authors reported

eukaryotic translation elongation factor 1 alpha 1 (eEF1A1) as significantly upregulated in osteoblasts adjacent to metastatic tumour cells compared with osteoblasts in control bone ($p = 0.035$). This study highlights the potential use of iTRAQ in identifying serum biomarkers rather than those dependent upon the evaluation of tumour tissue.

What is apparent from these studies is that the level of protein coverage we have obtained with our samples is significantly higher than has been obtained in tumour derived cell lines or serum/tissue from cancer patients. The implication of this is that a greater degree of coverage will assist in formulating a better understanding of tumour biology and an increased likelihood of identifying relevant biomarkers. Similar study designs have not been reported.

4.4.4 Tumour heterogeneity

One of the largest challenges facing the delivery of tumour biomarkers to clinical practice is the issue of tumour heterogeneity. Whilst inter-individual variation is to be expected, intra-tumour heterogeneity has also been shown in a number of studies, for example in metastasis-initiating cells in pancreatic cancer (Campbell *et al*, 2010). Carcinogenesis is an evolutionary process of naturally selected cells which have acquired a selective advantage, which may also explain drug resistance during systemic therapy (Gerlinger and Swanton, 2010). Whilst most tumours are thought to arise from a monoclonal population, its expansion combined with the acquisition of further mutations creates subclones and heterogeneity. Phylogenetic trees constructed from sequencing data are increasingly being used to demonstrate the relationships between subclones (Campbell *et al*, 2008). A recent study from Gerlinger *et al* (2002) used this phylogenetic approach to analyse next generation sequencing data and report the branched evolutional tumour growth in a renal cell carcinoma and its associated metastatic sites, with 63-69% of all somatic mutations not detectable across every tumour region.

This heterogeneity clearly has significant implications for biomarker studies such as this which rely on a single tumour biopsy sample to be representative of the whole tumour phenotype (Poste, 2011). Despite this it remains clear that some mutations are common between tumours and across tumour sites, located in the so-called ‘trunk’ of the phylogenetic tree, and it is perhaps these which offer the most potential to serve as reliable clinical biomarkers. It may be that the analysis of circulating tumour cells or DNA allows for

more comprehensive, accurate and translatable biomarker studies, although this is based on the assumption that cancer cells are shed into the circulation in a manner proportional to their clonal frequency.

A small number of studies comparing the genotype of primary and metastatic colorectal tumours have already been discussed in Chapter 3, and the concordance of KRAS status between primary and metastatic tumours is now widely accepted (Paligioannis *et al*, 2014). With respect to global proteomic studies, none have compared the phenotype of the primary and metastatic lesions of any tumour type. Some groups have however attempted to correlate specific proteins of interest, for example in 2013, Laird *et al* characterised the correlation of Ki67, p53 and VEGF between primary renal cell carcinomas, renal vein thrombus and metastasis. Similarly Gao *et al* (2013) compared the protein expression of VEGF, HIF-1α, Met, P53, TGF-β1, Cox-2 and TNF-α by immunohistochemistry in eleven patients who had received resection of lung cancers and distant metastases, finding no statistical significance between primary cancers and matched metastases for the expression of these selected biomarkers.

Our data suggests a high degree of biological similarity (97.46%) between the primary and secondary tumours, which will require further analysis and validation. Combined with this evidence in the literature, it may be feasible that despite the issues of tumour heterogeneity and clonal selection, the phenotype of the primary tumour is sufficiently similar to the metastasis to derive useful biological information in order to inform treatment strategy.

4.4.5 NAD(P)H dehydrogenase [quinone 1]

NQO1 encodes the cytosolic flavoenzyme NAD(P)H dehydrogenase [quinone 1], which is involved in the 2-electron reduction of a broad range of substrates including quinones to hydroquinones (Sarbia *et al*, 2003). This 2-electron reduction of the quinone to hydroquinone prevents the generation of semiquinone free radicals and reactive oxygen species, thus protecting cells from oxidative damage (Rauth, Goldberg and Misra, 1996). NQO1 also acts as an antioxidant enzyme which is of significant importance during the detoxification of environmental carcinogens (Ross *et al*, 2000).

The importance of NQO1 activity in carcinogenesis was demonstrated by a study which reported that the effects of chemical carcinogens on skin cells were more likely to result in skin cancer in NQO1 knockout mice than their wild type control group (Long *et al*, 2001). Other studies have shown that NQO1 expression increases with disease progression in colorectal cancer (Mikami *et al*, 1998). In 2006 a case-control study conducted by Beglieter *et al* demonstrated an association between NQO1 polymorphism and the development of colorectal cancer. Within this study serum blood samples were taken from 298 patients with colon cancer and 349 healthy control subjects. They were able to demonstrate that polymorphisms of the NQO1 gene which lead to a loss of function were statistically higher in patients with colorectal cancer. Contradictory to this, a case-control study by Hart *et al* (2000) investigated serum blood samples for polymorphic mutation of NQO1 in 323 patients with colorectal cancer and 205 healthy volunteers, failing to demonstrate any association with colorectal cancer risk.

NQO1 has been of specific interest for the design of many new chemotherapeutic agents due to its high levels of expression in many tumours (Winski *et al*, 2001). Its involvement in the bioactivation of quinones such as β-lapachone and 17-AAG has highlighted its potential use as a predictive biomarker when considering cancer treatment with these therapies. Testing for the NQO1*2 polymorphism, which leads to null NQO1 individuals, provides an indicator of poor response to quinones thus suggesting the avoidance of these therapies (Siegel, Yan and Ross, 2012).

Our study has suggested that low NQO1 levels are associated with favourable response to chemotherapy, and that levels in the primary tumour may be predictive of the metastatic phenotype. NQO1 loss and the resultant loss of cyto-protection has already been linked to carcinogenesis, although given the agents used in our study are not quinones the currently suggested mechanism of 2-electron reduction may not be relevant. Further evaluation is needed both to establish the role of NQO1 as a predictive biomarker and also as a therapeutic target.

4.4.6 Lambda-crystallin homolog

Lambda-crystallin homolog was identified during bioinformatic analysis as a potential biomarker. Specifically levels appeared to be reduced in the responders to neoadjuvant chemotherapy, and expression between primary and metastasis not significantly different.

The protein is a cytosolic enzyme known to have greatest expression in the liver and kidney (Chen *et al*, 2003). The corresponding CRYL-1 gene is located at 13q12.11, and codes for an enzyme which catalyzes the dehydrogenation of L-gulonate into dehydro-L-gulonate in the uronate cycle. The enzyme requires NAD(H) as a cofactor, and is inhibited by inorganic phosphate (Bando *et al*, 2006). Very little information exists on this protein in the literature, with the overwhelming majority of references focusing on the structural role of this protein in the rabbit lens (Mulders *et al*, 1998). The only discernable reference to malignancy was the incidental finding of downregulation in 58% of 60 hepatocellular carcinomas in a Chinese population (Chen *et al*, 2003). With little understood about its exact role beyond an enzyme in the uronate cycle, it would be challenging to explore the functional potential of this biomarker. Investigation in a larger tissue set to confirm these findings before embarking upon further work would therefore be prudent.

4.4.7 Study strengths and limitations

This study represents the first attempt to characterise the proteome of primary and metastatic colorectal tumours with a view to establishing biological similarity and identifying novel predictive biomarkers.

The relative merits and difficulties of a proteomic approach to these questions have already been discussed, but it should be remembered that a number of factors can contribute to difficulties in reproducibility between experimental runs, with alternative equipment and in different laboratories (Peng *et al*, 2003).

As with most clinical studies there is inherent heterogeneity in the study population. Differences exist in terms of patient age, gender, TNM stage, location of the primary tumour, burden and distribution of metastases and the presence of adverse pathological features. Ten of the 16 patients were metachronously resected, 5 of which received neoadjuvant chemotherapy prior to resection of the liver metastases. In this cohort, considerable variation should be expected between the chemonaive primary tumour and chemotherapy treated liver metastases. Furthermore the differences in neoadjuvant therapies received limit the conclusions we can draw to issues of sensitivity to treatment rather than allowing us to explore mechanisms *per se*. That said, all patients received a 5-fluorouracil based regimen.

The study we have designed and performed utilises biological material obtained from patients at the time of resection. If the intent is to look for up-front predictive biomarkers of response it would be necessary to assay the levels in the diagnostic biopsy. By the very nature of these biopsies there is little biological material available, and therefore obtaining them from clinical institutions (i.e. outside of the context of a clinical trial) is not feasible. To address this, *in vitro* studies to demonstrate that observed changes in protein expression are likely to be a biological feature of the tumour rather than a treatment effect would be necessary. Direct comparison of the proteome of those tumours which are chemonaive with those tumours treated with neoadjuvant chemotherapy may also assist with identifying which protein changes are induced by chemotherapy and which are biological features of the tumour i.e. present pre-treatment and expressed in the diagnostic samples.

The analyses were constructed in such a way that a protein could feature in a list of dysregulated proteins even if the relationship was identified in a single sample. For example, the analysis of primary tumour and colonic mucosa was performed by compiling pooled lists of proteins dysregulated in one or more sample in one tissue type with respect to the other. Whilst statistical attempts were made to reduce the false discovery rate, this approach does risk over-fitting of the data. An alternative approach of quantifying the number of sample pairs in which the dysregulation was observed could have helped minimise that risk and provide further insight into the extent of the differences between the proteomes.

The yield of our mass spectrometry in terms of confidently identified and accurately mapped proteins is excellent, and considerably more (often many fold) than many other oncology based proteomic studies. The tissue resources we have collected are high value and the research questions are novel.

4.4.8 Conclusion

This study has evaluated the biological similarity of primary and metastatic tumours, and found that only 2.54% of proteins quantified are significantly differentially expressed between primary and metastatic tissues. As such, it may be feasible to utilise biological information from the primary tumour to predict the phenotype of the metastasis.

Bioinformatic analysis of proteins significantly differentially expressed between tissue types identified putative pathways of carcinogenesis. Of the two biomarkers identified, NQO1 shows both biological plausibility and a part-understood role in cancer making it a suitable candidate for further validation and exploration of relevant mechanisms.

Chapter 5

A global proteomic assessment of serial rectal tumour biopsies

5.1 Introduction

5.1.1 Background

The role of neoadjuvant therapy has already been discussed in some detail (Section 1.8.4). Patients with rectal cancer who have threatened margins on initial MRI are frequently subjected to long-course neoadjuvant chemoradiotherapy in an attempt to downstage disease and reduce the risk of a positive margin at resection.

The ability to establish prospectively the likely response to neoadjuvant therapy would be of tremendous benefit to clinicians. Those patients who are identifiable as likely to respond could be subjected to potentially more aggressive systemic therapy, whilst conversely those less likely to respond could be saved the unnecessary morbidity of systemic treatment and the delay to surgical intervention necessary with the use of neoadjuvant treatments.

One final quandary still remains with the neoadjuvant treatment of rectal cancer with chemoradiotherapy, which is the continued downstaging seen for many weeks following cessation of treatment. One potential explanation for this is the fact that radiation only has its desired effect on actively dividing cells, not those with slow cell turnover or that remain in the G0 (rest) phase. The treatment effect is dependent on the amount and type of radiation reaching the cell and the speed of cell growth, and as such it may take several days or weeks for the treatment effect to manifest (Willet *et al*, 1995).

5.1.2 Proteomics and iTRAQ

Proteomic assessment of tumours and the technique of iTRAQ have already been discussed in Sections 4.1.2 and 4.1.3 respectively. This investigation applies the previously described approach to the study design shown in Figure 5.1.

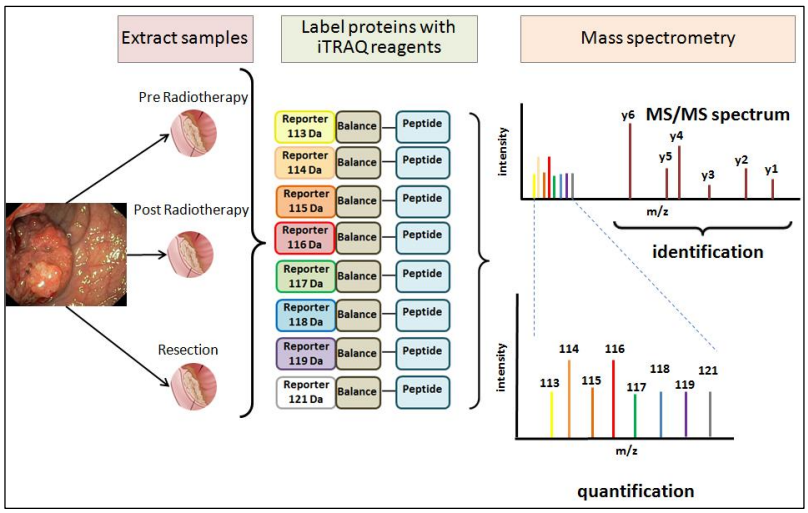

Figure 5.1 – Samples are reduced and undergo a tryptic digest before being tagged with an isotope labelled molecule. These tags all have the same molecular weight although the reporter and balance moieties vary. After a cation exchange cleanup step the samples undergo nanoLC-MS/MS. The reporter and balance moieties are cleaved from each other and from the peptide to which they are bound, the ratio of which helps determine relative abundance. The peptide is also cleaved into fragment ions used to identify the protein.

5.1.3 Aims

The aim of this investigation is to compare the proteomic profile of serial rectal cancer biopsies taken at diagnosis, immediately after long course neoadjuvant chemoradiotherapy and at resection, to establish how this profile changes with treatment and identify potential response biomarkers that are detectable and measurable on the initial diagnostic biopsy.

5.2 Methods

National Health Service Research Ethics Committee and Research and Development approval was obtained for this study and informed consent obtained from each of the study participants.

5.2.1 Patient recruitment and tissue collection

Patients recently having received a diagnosis of rectal cancer and who had been identified by the multidisciplinary team as requiring long course chemoradiotherapy were approached for inclusion in the study. Those agreeing to participate in the study were invited back to the endoscopy unit at the Countess of Chester Hospital for a repeat limited flexible sigmoidoscopy and biopsy. Three 'double bites' of a standard endoscopic forcep (approximately $3mm^3$ tissue in total) of peripheral tumour was biopsied, with deliberate attempts to avoid the area of necrotic tissue in the centre of the tumour.

Patients were contacted one week after cessation of their chemoradiotherapy and invited to return for a further limited flexible sigmoidoscopy and biopsy. On the day of resection, a sample of tumour and normal adjacent mucosa were obtained. Following delivery of the colorectal specimen the proximal staple line was incised and a linear cut made down the antimesenteric border before excising a peripheral section of tumour using forceps and a scalpel. All samples were placed in individually labelled cryodorfs, snap frozen in liquid nitrogen and transferred to a -80^{o}C storage facility.

5.2.2 Exclusion criteria

For this study the exclusion criteria were:

- Recent (last 12 months) personal history of malignancy at another site
- Patients under the age of 18
- Patients without capacity to provide informed consent
- Patients identified by the multidisciplinary team as being at significant risk of emotional distress by additional hospital visits and/or procedures that may be required

5.2.3 Evaluation of histopathological response to treatment

Additional tumour samples were obtained for the purposes of formalin fixation and embedding in paraffin. All samples were reviewed by a consultant histopathologist to verify the diagnosis of adenocarcinoma. Histopathological response was assessed in the resection specimens and recorded as described in Section 4.2.3.

5.2.4 Evaluation of radiological response to treatment

The radiological response to treatment was also assessed and noted. Pre-treatment and 10 week post-treatment MRI scans were reviewed by a consultant radiologist, and response determined in line with the RECIST v1.1 guidelines (Eisenhauer *et al*, 2009). In brief, this comprises an initial assessment of tumour burden and documentation of target and non-target lesions, followed by an allocation to one of four response groups as follows:

- Complete response – Disappearance of all target lesions. Any pathological lymph nodes must have reduction in short axis to <10mm.
- Partial response – At least a 30% decrease in the sum of diameters of target lesions, taking as reference the baseline sum diameters.
- Progressive disease – At least a 20% increase in the sum of diameters of target lesions, taking as reference the smallest sum on study.
- Stable disease – Neither sufficient shrinkage to qualify for partial response nor sufficient increase to qualify for progressive disease, taking as reference the smallest sum diameters on study.

5.2.5 Sample preparation

Sample preparation was performed as described in Section 4.2.4.

5.2.6 Protein quantification

Protein quantification was performed as described in Section 4.2.5.

5.2.7 Creation of a reference pool

In order to infer relative protein abundance between samples, a reference pool was

created as described in Section 4.2.6. For each time point from every patient, 100µg of protein was added to the reference pool. Once the reference pool had been created it was re-quantified and prepared in an identical fashion to the other samples as follows.

5.2.8 Allocation across and within experimental runs

Allocation across and within experimental runs was performed as described in Section 4.2.7.

5.2.9 iTRAQ labelling

iTRAQ labelling was performed as described in Section 4.2.8.

5.2.10 Cation exchange

Cation exchange was performed as described in Section 4.2.9.

5.2.11 Mass spectrometry

Mass spectrometry was performed as described in Section 4.2.10.

5.2.12 Protein identification and quantification

Protein identification and quantification was performed as described in Section 4.2.11.

5.2.13 Bioinformatics analysis

Bioinformatics analysis was performed as described in Section 4.2.12. Proteins differentially expressed (log2 fold change >1.5, unadjusted $p<0.05$) were identified and subjected to pathway and network analysis. A summary of the bioinformatics analysis can be seen in Figure 5.2.

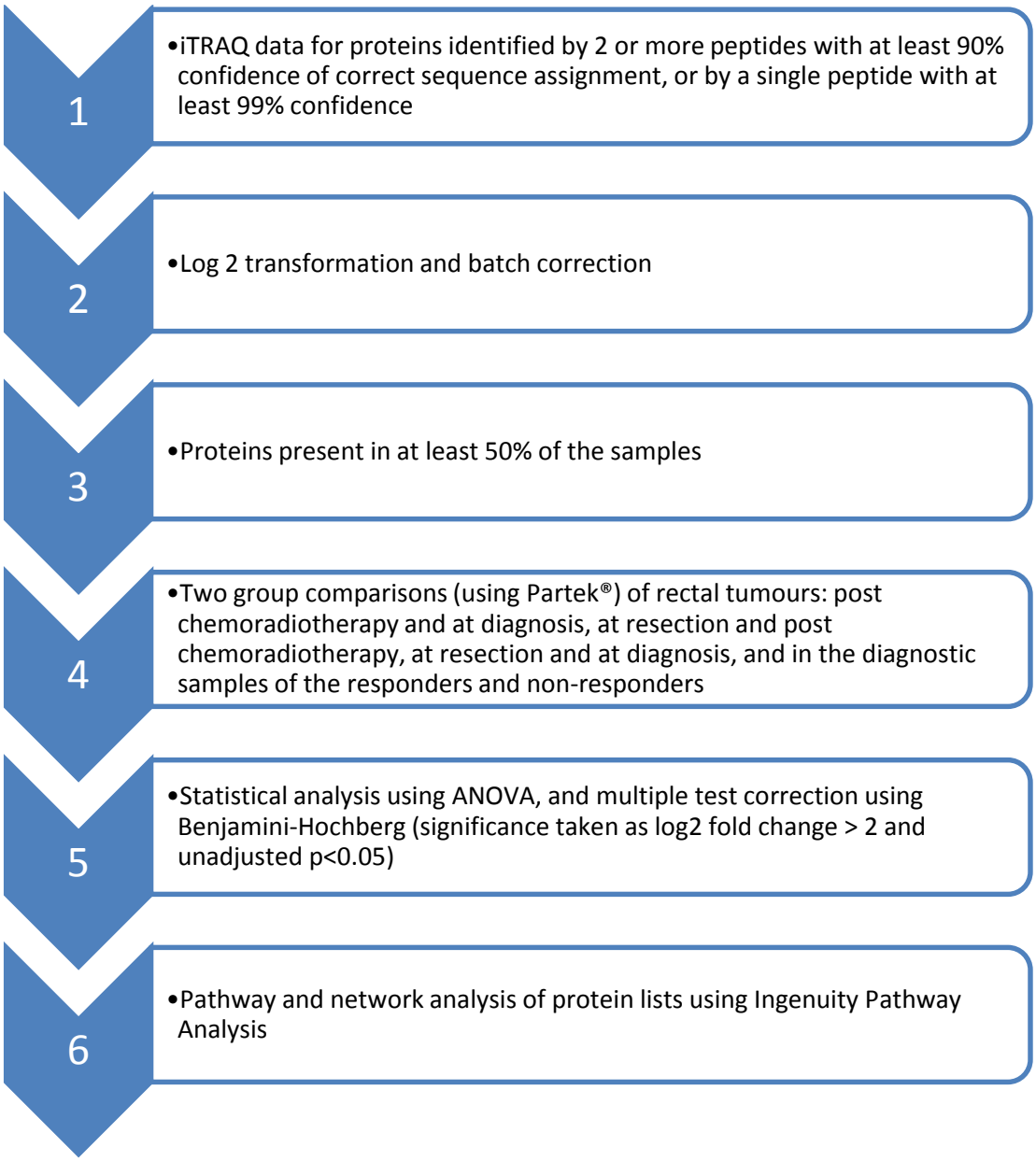

Figure 5.2 – Bioinformatics analysis workflow for global proteomic assessment of serial rectal tumour biopsies.

5.3 Results

5.3.1 Clinical and demographic data

Eight patients were recruited to this study, all of which were male with an age range of 50-78 years at the time of diagnosis. Dukes' Stage of the tumours ranged from B-D with variation in T (2-4), N (0-1) and M (0-1) stage seen. Patients received oral capecitabine plus either 45Gy in 25 fractions or 50.4Gy in 28 fractions at the discretion of the treating radiation oncologist. Following this, participants underwent formal excision of the rectum in a manner appropriate for both the patient and the tumour (Table 5.1).

5.3.2 Response evaluation

Response evaluation can be seen in Table 5.2. For the purposes of analysis, responders were those with a histopathological tumour regression grade of 1-2 (n=4) and non responders those with a tumour regression grade of 3-4 (n=4). Given the small numbers of patients recruited, radiological response was noted but not used for analysis.

Patient Number	Radiological Response	Viable Tumour (%)	Tumour Regression Grade	Responder
1	PR	5	1	Yes
2	SD	10	1	Yes
3	SD	55	3	No
4	PR	40	2	Yes
5	SD	60	3	No
6	PR	45	2	Yes
7	PD	55	3	No
8	PD	75	4	No

Table 5.2 – Response evaluation for patients having serial rectal cancer biopsies. The percentage viable tumour is displayed along with corresponding tumour regression grade (TRG). Those patients with TRG 1-2 were considered responders (patients 1, 2, 4 and 6) and patients with TRG 3-4 were considered non-responders (patients 3, 5, 7 and 8).

Patient	Sex	Age at Diagnosis	Dukes' Stage	Nodes Harvested	Nodes Involved	T Stage	N Stage	M Stage	Histology	Neoadjuvant Treatment	Procedure
1	M	77	C2	1	1	3	1	0	Moderately differentiated	Capecitabine plus 45Gy in 25 fractions	Open low anterior resection
2	M	50	B	9	0	2	0	0	Moderately differentiated	Capecitabine plus 50.4Gy in 28 fractions	Laparoscopic low anterior resection
3	M	77	C1	36	1	3	1	0	Moderately differentiated	Capecitabine plus 45Gy in 25 fractions	Open low anterior resection
4	M	77	B	10	0	3	0	0	Moderately differentiated	Capecitabine plus 50.4Gy in 28 fractions	Ultra-low Hartmann's
5	M	63	D	20	2	3	1	1	Moderately differentiated	Capecitabine plus 50.4Gy in 28 fractions	Laparoscopic low anterior resection
6	M	71	B	2	0	4	0	0	Moderately differentiated	Capecitabine plus 50.4Gy in 28 fractions	Laparoscopic low anterior resection
7	M	57	B	21	0	3	0	0	Moderately differentiated	Capecitabine plus 50.4Gy in 28 fractions	Laparoscopic low anterior resection
8	M	78	B	17	0	3	0	0	Moderately differentiated	Capecitabine plus 45Gy in 25 fractions	APER

Table 5.1 – Clinical and demographic data for patients having serial rectal cancer biopsies. 8 patients were studied, all of which were male ranging in age from 50-78 and Dukes' stage B-D. Two different neoadjuvant chemotherapeutic regimens were used alongside a number of different surgical interventions for formal resection of the rectal tumour.

5.3.3 Overview of iTRAQ data.

A total of 3359 unique proteins were identified, all of which were present in at least half of the samples and therefore taken forwards for analysis. The data were acquired over 3 experimental runs, with a mean (SD) of 7 (21.2) peptides used to identify the proteins of origin. This corresponds to a mean (SD) coverage of 15.18% (15.72%) for identified proteins.

5.3.4 Comparison of rectal tumours post chemoradiotherapy with diagnostic samples

A total of 18 proteins were differentially expressed in the tumours after chemoradiotherapy compared with the initial diagnostic samples. Of these proteins, 2 were downregulated and 16 upregulated (Table 5.3).

Accession Number	Name	P Value	Log2 Fold-Change (Post chemoradiotherapy/diagnostic)
P12109	Collagen alpha-1(VI) chain	1.34E-02	-1.953
P12429	Annexin A3	9.71E-03	-1.757
Q1KMD3	Heterogeneous nuclear ribonucleoprotein U-like protein 2	3.76E-02	1.521
P51648	Fatty aldehyde dehydrogenase	1.11E-02	1.525
Q13162	Peroxiredoxin-4	1.84E-02	1.572
Q96PD5	N-acetylmuramoyl-L-alanine amidase	3.04E-02	1.686
P02652	Apolipoprotein A-II	1.02E-02	1.758
Q9BY50	Signal peptidase complex catalytic subunit SEC11C	1.69E-02	1.760
Q9Y6R7	IgGFc-binding protein	3.22E-03	1.761
P01023	Alpha-2-macroglobulin	1.54E-02	1.783
P01859	Ig gamma-2 chain C region	2.67E-02	1.801
Q8NBS9	Thioredoxin domain-containing protein 5	1.17E-02	1.823
P01591	Immunoglobulin J chain	2.57E-02	1.861
O75795	UDP-glucuronosyltransferase 2B17	3.03E-02	1.946
P02765	Alpha-2-HS-glycoprotein	2.18E-02	2.105
P01275	Glucagon	2.77E-04	2.381
P04114	Apolipoprotein B-100	1.75E-02	2.429
P10645	Chromogranin-A	6.10E-03	3.357

Table 5.3 – Those proteins differentially expressed between rectal tumours post chemoradiotherapy and diagnostic samples. 18 proteins were identified, 2 of which were downregulated (negative values for fold change) and 16 upregulated (positive values for fold change).

Analysing those proteins upregulated separately from those downregulated, Ingenuity core analysis of direct and indirect relationships revealed the significant upregulated canonical pathways in this group to be: LXR/RXR activation, FXR/RXR activation, acute phase response signalling, serotonin degradation and phenylethylamine degradation I. Similarly the

downregulated canonical pathways were: hepatic fibrosis/hepatic stellate cell activation. Statistics for these identified pathways can be seen in Table 5.4.

Upregulated Pathways	p-value	Ratio
LXR/RXR activation	1.24E-04	3/121 (0.025)
FXR/RXR activation	1.37E-04	3/125 (0.024)
Acute phase response signalling	3.27E-04	3/168 (0.018)
Serotonin degradation	8.27E-04	2/52 (0.038)
Phenylethylamine degradation I	3.30E-03	1/4 (0.25)
Downregulated Pathways	**p-value**	**Ratio**
Hepatic fibrosis/hepatic stellate cell activation	2.15E-02	1/196 (0.005)

Table 5.4 – Pathway analysis for proteins both upregulated and downregulated in the rectal tumours post chemoradiotherapy compared to the diagnostic samples. P-value is adjusted using Benjamini-Hochberg correction. Ratio identifies the number of focus molecules identified (numerator) in the pathway (denominator).

Further analysis of all (unfiltered) biological pathways identified 5 upregulated networks with a score greater than 2 pertaining to: lipid metabolism, molecular transport, small molecule biochemistry, cancer, cell-to-cell signalling and interaction, cell-mediated immune response, cellular function and maintenance, cellular growth and proliferation, haematological system development and function, cell death and survival, cell cycle, cell morphology, cardiovascular system development and function, carbohydrate metabolism and post-translational modification. Similarly 2 downregulated networks were identified pertaining to: cancer, organismal injury and abnormalities, reproductive system disease, hereditary disorder, skeletal and muscular disorders and connective tissue disorders. The focus molecules and statistics pertinent to these networks can be seen in Table 5.5.

Upregulated Networks				
ID	**Molecules in Network**	**Score**	**Focus Molecules**	**Top Diseases and Functions**
1	26s Proteasome,A2M,ABCC2,AHSG,ALDH3A2, APOA2,APOB,AQP3,CCND1,CDC73,CHGA, CTNNA2,CTNNB1,EPCAM,GCG,GPLD1,HN F1A,HSD17B2,KIF20A,LRP,MAML1,MTTP, PCDH11Y,PKM,PSMD14,RAD23A,RB1CC1, SLCO1B1,SNRK,SP4,TMSB15A,TSPAN8,UG T2B17,VENTX,ZMIZ2	18	8	Lipid Metabolism, Molecular Transport, Small Molecule Biochemistry

2	CD40,IGHG2	3	1	Cancer, Cell-To-Cell Signaling and Interaction, Cell-mediated Immune Response
3	miR-146a-5p (and other miRNAs w/seed GAGAACU),PGLYRP2	3	1	Cellular Function and Maintenance, Cellular Growth and Proliferation, Hematological System Development and Function
4	BLM,HNRNPUL2,MDC1	3	1	Cell Death and Survival, Cell Cycle, Cell Morphology
5	MGEA5,PRDX4,SRXN1	3	1	Cardiovascular System Development and Function, Carbohydrate Metabolism, Post-Translational Modification
Downregulated Networks				
1	ANXA3,CLDN7	3	1	Cancer, Organismal Injury and Abnormalities, Reproductive System Disease
2	CHI3L1,COL6A1,COL6A2,COL6A3,estrogen receptor,HR,SPDEF	3	1	Hereditary Disorder, Skeletal and Muscular Disorders, Connective Tissue Disorders

Table 5.5 – Network analysis for proteins both upregulated and downregulated in the rectal tumours post chemoradiotherapy compared to the diagnostic samples. The score is derived from a p-value and indicates the probability of the focus molecules in a network being found together due to random chance. Focus molecules is the total number of proteins of interest identified in the respective network.

5.3.5 Comparison of rectal tumours at resection with post chemoradiotherapy samples

A total of 39 proteins were differentially expressed in the tumours at resection compared with the samples taken immediately following completion of chemoradiotherapy. Of these proteins, 30 were downregulated and 9 upregulated (Table 5.6).

Accession Number	Name	P Value	Log2 Fold-Change (Resection/Post chemoradiotherapy)
P10645	Chromogranin-A	1.12E-02	-3.430
P04114	Apolipoprotein B-100	2.22E-02	-2.630
P01275	Glucagon	4.03E-04	-2.562
P12532	Creatine kinase U-type, mitochondrial	3.62E-02	-2.427
O75795	UDP-glucuronosyltransferase 2B17	2.21E-02	-2.293
Q9Y5M8	Signal recognition particle receptor subunit beta	3.61E-02	-2.226
Q9Y6R7	IgGFc-binding protein	1.62E-03	-2.095
P01833	Polymeric immunoglobulin receptor	3.21E-02	-2.078
P01591	Immunoglobulin J chain	2.99E-02	-1.992
Q07654	Trefoil factor 3	9.92E-03	-1.952
P21397	Amine oxidase [flavin-containing] A	4.66E-02	-1.882
P17931	Galectin-3	3.48E-02	-1.830
Q16836	Hydroxyacyl-coenzyme A dehydrogenase, mitochondrial	1.91E-02	-1.787
P00966	Argininosuccinate synthase	2.71E-02	-1.757
Q96EY8	Cob(I)yrinic acid a,c-diamide adenosyltransferase, mitochondrial	9.12E-03	-1.726
Q8NBS9	Thioredoxin domain-containing protein 5	3.23E-02	-1.725
P31930	Cytochrome b-c1 complex subunit 1, mitochondrial	3.25E-02	-1.714
P38117	Electron transfer flavoprotein subunit beta	2.28E-02	-1.691
P19075	Tetraspanin-8	3.31E-02	-1.686
O75874	Isocitrate dehydrogenase [NADP] cytoplasmic	3.49E-02	-1.682
P80303	Nucleobindin-2	4.17E-02	-1.661
Q96FQ6	Protein S100-A16	1.44E-02	-1.648
Q9HAT2	Sialate O-acetylesterase	9.52E-03	-1.626
P17980	26S protease regulatory	2.19E-02	-1.624

	subunit 6A		
Q1KMD3	Heterogeneous nuclear ribonucleoprotein U-like protein 2	3.93E-02	-1.614
P51648	Fatty aldehyde dehydrogenase	1.33E-02	-1.596
P15880	40S ribosomal protein S2	4.52E-02	-1.583
Q13510	Acid ceramidase	1.35E-02	-1.568
O96000	NADH dehydrogenase [ubiquinone] 1 beta subcomplex subunit 10	2.29E-03	-1.538
P30049	ATP synthase subunit delta, mitochondrial	1.15E-03	-1.537
Q16658	Fascin	7.94E-03	1.628
P61106	Ras-related protein Rab-14	2.03E-02	1.706
Q9H4M9	EH domain-containing protein 1	2.25E-02	1.769
P08572	Collagen alpha-2(IV) chain	4.48E-02	2.006
P12429	Annexin A3	6.90E-03	2.009
P98160	Basement membrane-specific heparan sulfate proteoglycan core protein	2.73E-02	2.021
P12109	Collagen alpha-1(VI) chain	1.45E-02	2.136
P13674	Prolyl 4-hydroxylase subunit alpha-1	9.64E-03	2.569
P24821	Tenascin	3.63E-02	3.329

Table 5.6 – Those proteins differentially expressed between rectal tumours at resection and immediately following completion of chemoradiotherapy. 39 proteins were identified, 30 of which were downregulated (negative values for fold change) and 9 upregulated (positive values for fold change).

Analysing those proteins upregulated separately from those downregulated, Ingenuity core analysis of direct and indirect relationships revealed the significant upregulated canonical pathways in this group to be: hepatic fibrosis/stellate cell activation, inhibition of angiogenesis by TSP1, inhibition of matrix metalloproteases, crosstalk between dendritic cells and natural killer cells and dendritic cell maturation. Similarly the downregulated canonical pathways were: serotonin degradation, mitochondrial dysfunction, phenylalanine degradation IV, tryptophan degradation and putrescine degradation. Statistics for these identified pathways can be seen in Table 5.7.

Upregulated Pathways	p-value	Ratio
Hepatic fibrosis/hepatic stellate cell activation	3.98E-03	2/196 (0.01)
Inhibition of angiogenesis by TSP1	1.58E-02	1/32 (0.031)
Inhibition of matrix metalloproteases	1.87E-02	1/38 (0.026)
Crosstalk between dendritic cells and natural killer cells	4.33E-02	1/89 (0.011)
Dendritic cell maturation	8.08E-02	1/169 (0.006)
Downregulated Pathways	**p-value**	**Ratio**
Serotonin degradation	7.71E-05	3/52 (0.058)
Mitochondrial dysfunction	1.31E-05	4/165 (0.024)
Phenylalanine degradation IV	2.22E-04	2/14 (0.143)
Tryptophan degradation	2.92E-04	2/16 (0.125)
Putrescine degradation	2.92E-04	2/16 (0.125)

Table 5.7 – Pathway analysis for proteins both upregulated and downregulated in the rectal tumours at resection compared to immediately following completion of chemoradiotherapy. P-value is adjusted using Benjamini-Hochberg correction. Ratio identifies the number of focus molecules identified (numerator) in the pathway (denominator).

Further analysis of all (unfiltered) biological pathways identified 2 upregulated networks with a score greater than 2 pertaining to: organismal injury and abnormalities, connective tissue disorders, dermatological diseases and conditions, cancer and reproductive system disease. Similarly 1 downregulated network was identified pertaining to: tissue development, cell death and survival and dermatological diseases and conditions. The focus molecules and statistics pertinent to these networks can be seen in Table 5.8.

Upregulated Networks				
ID	**Molecules in Network**	**Score**	**Focus Molecules**	**Top Diseases and Functions**
1	AFP,BGN,CDH11,CLDN4,COL4A1,COL4A2,COL5A1,COL6A1,COL6A2,COL6A3,COL7A1,EHD1,estrogen receptor,FGA,FSCN1,HEXA,HEXB,HIF1A,HSPG2,KRT7,KRT15,LAMC2,LOXL2,LTBP2,mir-31,MMP12,NOV,P4HA1,SPAG4,TGFB1,TNC,TNF,TYMP,WISP1,WNT5B	17	7	Organismal Injury and Abnormalities, Connective Tissue Disorders, Dermatological Diseases and Conditions
2	ANXA3,CLDN7	3	1	Cancer, Organismal Injury and Abnormalities, Reproductive System Disease
Downregulated Networks				
1	AIM1,AJAP1,Akt,ALDH3A2,CDH1,CHGA,CNN2,CRAT,CTNNB1,CXCL8,DEFA5,DPEP1,EDN3,F13A1,GAD1,GCG,GPX2,HSD17B2,IDH1,IHH,IL4,KLK3,LGALS3,MAOA,MUC6,PCCA,PIGR,QPCT,RCN1,SLC26A2,TCF,TFF3,TOB2,TSPAN8,UGT2B17	20	9	Tissue Development, Cell Death and Survival, Dermatological Diseases and Conditions

Table 5.8 – Network analysis for proteins both upregulated and downregulated in the rectal tumours at resection compared to immediately following completion of chemoradiotherapy. The score is derived from a p-value and indicates the probability of the focus molecules in a network being found together due to random chance. Focus molecules is the total number of proteins of interest identified in the respective network.

5.3.6 Comparison of rectal tumours at resection with diagnostic samples

A total of 29 proteins were differentially expressed in the tumours at resection compared with the samples taken at diagnosis. Of these proteins, 10 were downregulated and 19 upregulated (Table 5.9).

Accession Number	Name	P Value	Log2 Fold-Change (Resection/Diagnostic)
O95881	Thioredoxin domain-containing protein 12	3.98E-02	-2.779
P16444	Dipeptidase 1	3.35E-02	-2.740
Q13228	Selenium-binding protein 1	2.03E-02	-2.013
P05783	Keratin, type I cytoskeletal 18	3.44E-02	-1.835
Q9BY42	UPF0549 protein C20orf43	2.97E-02	-1.732
P09874	Poly [ADP-ribose] polymerase 1	5.82E-03	-1.599
O96008	Mitochondrial import receptor subunit TOM40 homolog	8.41E-03	-1.566
Q9NX63	Coiled-coil-helix-coiled-coil-helix domain-containing protein 3, mitochondrial	4.29E-02	-1.548
P11940	Polyadenylate-binding protein 1	4.44E-02	-1.530
P05455	Lupus La protein	3.78E-02	-1.525
P07099	Epoxide hydrolase 1	4.17E-02	1.504
O14773	Tripeptidyl-peptidase 1	1.17E-02	1.590
Q99536	Synaptic vesicle membrane protein VAT-1 homolog	2.76E-02	1.644
Q92930	Ras-related protein Rab-8B	1.03E-02	1.690
Q9H4M9	EH domain-containing protein 1	1.24E-02	1.714
Q9UJ70	N-acetyl-D-glucosamine kinase	1.59E-02	1.737
P08758	Annexin A5	2.30E-02	1.770
P53004	Biliverdin reductase A	1.61E-02	1.842
P04271	Protein S100-B	4.74E-02	1.882
P02765	Alpha-2-HS-glycoprotein	3.26E-02	1.896
Q9BUF5	Tubulin beta-6 chain	4.44E-02	2.002
P01824	Ig heavy chain V-II region WAH	1.80E-02	2.073
P13674	Prolyl 4-hydroxylase subunit alpha-1	1.06E-02	2.141
B9A064	Immunoglobulin lambda-like polypeptide 5	2.80E-02	2.249
P01860	Ig gamma-3 chain C region	4.99E-02	2.271
P08603	Complement factor H	4.15E-02	2.310
P01008	Antithrombin-III	2.61E-02	2.317
P01834	Ig kappa chain C region	4.25E-02	2.731
P10909	Clusterin	4.97E-02	4.945

Table 5.9 – Those proteins differentially expressed between rectal tumours at resection and at diagnosis. 29 proteins were identified, 10 of which were downregulated (negative values for fold change) and 19 upregulated (positive values for fold change).

Analysing those proteins upregulated separately from those downregulated, Ingenuity core analysis of direct and indirect relationships revealed the significant upregulated canonical pathways in this group to be: primary immunodeficiency signalling, haematopoiesis from pluripotent stem cells, haem degradation, N-acetylglucosamine degradation II and CMP-N-acetylneuraminate biosynthesis I. Similarly the downregulated canonical pathways were: glutathione redox reactions II, BER pathway, DNA double-strand break repair by non-homologous end joining, leukotriene biosynthesis and granzyme B signalling. Statistics for these identified pathways can be seen in Table 5.10.

Upregulated Pathways	**p-value**	**Ratio**
Primary immunodeficiency signalling	1.21E-05	3/46 (0.065)
Haematopoiesis from pluripotent stem cells	8.59E-04	2/44 (0.045)
Haem degradation	3.96E-03	1/4 (0.25)
N-acetylglucosamine degradation II	3.96E-03	1/4 (0.25)
CMP-N-acetylneuraminate biosynthesis I	4.95E-03	1/5 (0.2)
Downregulated Pathways	**p-value**	**Ratio**
Glutathione redox reactions II	1.49E-03	1/3 (0.333)
BER pathway	5.94E-03	1/12 (0.083)
DNA double-strand break repair by non-homologous end joining	6.93E-03	1/14 (0.071)
Leukotriene biosynthesis	6.93E-03	1/14 (0.071)
Granzyme B signalling	7.91E-03	1/16 (0.062)

Table 5.10 – Pathway analysis for proteins both upregulated and downregulated in the rectal tumours at resection compared to at diagnosis. P-value is adjusted using Benjamini-Hochberg correction. Ratio identifies the number of focus molecules identified (numerator) in the pathway (denominator).

The base excision repair (BER) signalling pathway was identified as being highly significant, with this data set suggesting downregulation induced by chemoradiotherapy (Figure 5.3).

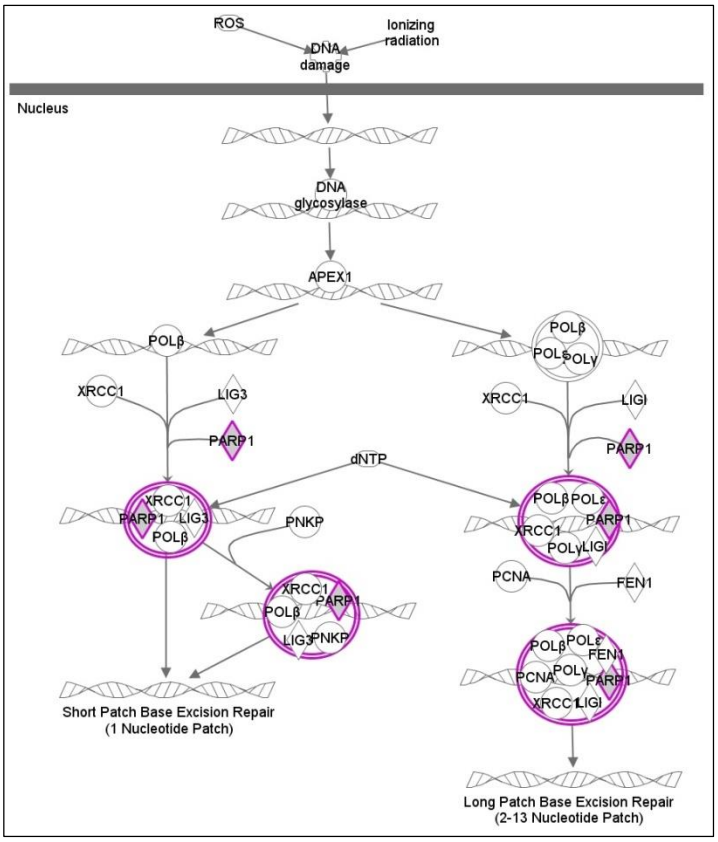

Figure 5.3 – The base excision repair (BER) signalling pathway was identified as being highly significant, with this data set suggesting downregulation induced by chemoradiotherapy. Only one of the 12 focus molecules was identified – PARP1 (highlighted in purple).

Further analysis of all (unfiltered) biological pathways identified 6 upregulated networks with a score greater than 2 pertaining to: cell death and survival, tissue morphology, cellular development, gastrointestinal disease, hepatic system disease, organismal injury and abnormalities, cell-to-cell signalling and interaction, cellular assembly and organization, cellular function and maintenance, cancer, carbohydrate metabolism, endocrine system disorders, cell morphology, developmental disorder and hereditary disorder. Similarly 3 downregulated networks were identified pertaining to: cancer, organismal injury and abnormalities, reproductive system disease, cell death and survival, energy production, nucleic acid metabolism, cardiovascular system development and function, endocrine system disorders and gastrointestinal disease. The focus molecules and statistics pertinent to these networks can be seen in Table 5.11.

Upregulated Networks				
ID	**Molecules in Network**	**Score**	**Focus Molecules**	**Top Diseases and Functions**
1	ANXA5,BMP2,BMP4,CDC25B,CDC25C,CDKN1A,CHRNA3,CLU,GDF15,HMGB1,HRAS,ID1,IL1R1,JAG1,LTF,NFkB (complex),NUMBL,NUP98,PLAA,PP2A,PYCARD,RASSF5,RBPJ,REL,RNF34,S100B,SERPINB2,SNW1,SOD2,TCP1,TFRC,TNFSF13,USP11,VHL,XRCC5	5	3	Cell Death and Survival, Tissue Morphology, Cellular Development
2	BLVRA,IL13	3	1	Gastrointestinal Disease, Hepatic System Disease, Organismal Injury and Abnormalities
3	miR-30a-3p (and other miRNAs w/seed UUUCAGU),RAB8B	3	1	Cell-To-Cell Signaling and Interaction, Cellular Assembly and Organization, Cellular Function and Maintenance
4	AHSG,HNF1A	3	1	Cancer, Carbohydrate Metabolism, Endocrine System Disorders
5	CD24,NAGK	3	1	Cell Morphology, Cellular Function and Maintenance, Carbohydrate Metabolism
6	TFEB,TPP1	3	1	Cellular Assembly and Organization, Developmental Disorder, Hereditary Disorder
Downregulated Networks				
1	APH1B,BRCA1,CASP3,CSTF1,EMILIN2,KRT18,MIR585,mir-95,mir-128,mir-182,mir-183,mir-188,mir-191,mir-193,mir-224,mir-320,mir-330,mir-486,mir-500,miR-125b-5p (and other miRNAs w/seed CCCUGAG),miR-17-3p (and other miRNAs w/seed CUGCAGU),miR-330-3p (and other miRNAs w/seed CAAAGCA),miR-378a-3p (and other miRNAs w/seed CUGGACU),miR-486-5p	12	5	Cancer, Organismal Injury and Abnormalities, Reproductive System Disease

	(and other miRNAs w/seed CCUGUAC),miR-501-5p (miRNAs w/seed AUCCUUU),PABPC1,PARP1,PARP2,PEBP4, PINK1,PPT1,SSB,TEP1,TOMM40,TP53			
2	CHCHD3,CHCHD6	3	1	Cell Death and Survival, Energy Production, Nucleic Acid Metabolism
3	CTNNB1,DPEP1,MGEA5,TCF	3	1	Cardiovascular System Development and Function, Endocrine System Disorders, Gastrointestinal Disease

Table 5.11 - Network analysis for proteins both upregulated and downregulated in the rectal tumours at resection compared to at diagnosis. The score is derived from a p-value and indicates the probability of the focus molecules in a network being found together due to random chance. Focus molecules is the total number of proteins of interest identified in the respective network.

5.3.7 Predictive biomarkers in the diagnostic samples

A total of 8 proteins were differentially expressed between the initial diagnostic samples of the responders and non-responders. Of these proteins, 3 were downregulated and 5 upregulated (Table 5.12).

Accession Number	Name	P Value	Log2 Fold-Change (Responders/Non-responders)
Q9NZM1	Myoferlin	4.35E-02	-1.633
Q13510	Acid ceramidase	1.17E-02	-1.526
P09525	Annexin A4	1.93E-02	-1.524
P41219	Peripherin	2.13E-02	1.583
P12109	Collagen alpha-1(VI) chain	3.61E-02	1.800
P80748	Ig lambda chain V-III region LOI	4.82E-02	1.866
P07602	Proactivator polypeptide	5.90E-04	1.943
P01860	Ig gamma-3 chain C region	2.74E-02	2.549

Table 5.12 – Those proteins differentially expressed between the primary tumours of the responders and non-responders. 8 proteins were identified, 3 of which were downregulated (negative values for fold change) and 5 upregulated (positive values for fold change).

Analysing those proteins upregulated separately from those downregulated, Ingenuity core analysis of direct and indirect relationships revealed the significant upregulated canonical pathways in this group to be: hepatic fibrosis/stellate cell activation, inhibition of angiogenesis by TSP1, inhibition of matrix metalloproteases, crosstalk between dendritic cells and natural killer cells and dendritic cell maturation. Similarly the downregulated canonical pathways were: serotonin degradation, mitochondrial dysfunction, phenylalanine degradation IV, tryptophan degradation and putrescine degradation. Statistics for these identified pathways can be seen in Table 5.13.

Upregulated Pathways	p-value	Ratio
Lipid antigen presentation by CD1	5.28E-03	1/24 (0.042)
Autoimmune thyroid disease signalling	9.23E-03	1/42 (0.024)
Haematopoiesis from pleuripotent stem cells	9.67E-03	1/44(0.024)
Primary immunodeficiency signalling	1.01E-02	1/46 (0.022)
Allograft rejection signalling	1.05E-02	1/48 (0.021)
Downregulated Pathways	**p-value**	**Ratio**
Ceramide degradation	9.92E-04	1/6 (0.167)
Sphingosine and sphingosine-1-phosphate metabolism	1.32E-03	1/8 (0.125)
Sphingosine-1-phosphate signalling	1.78E-02	1/108 (0.009)

Table 5.13 – Pathway analysis for proteins both upregulated and downregulated in the primary tumours of the responders compared to the primary tumours of the non-responders. P-value is adjusted using Benjamini-Hochberg correction. Ratio identifies the number of focus molecules identified (numerator) in the pathway (denominator).

The ceramide degradation pathway was identified as being the most significantly downregulated pathway in those tumours responding to chemoradiotherapy (Figure 5.4). This is based on the significantly lower levels of acid ceramidase identified in the diagnostic samples.

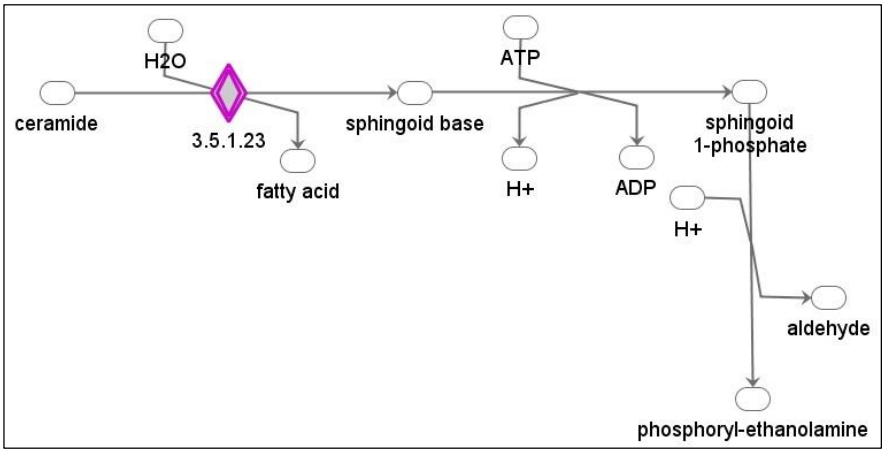

Figure 5.4 – The ceramide degradation pathway was identified as being the most significantly downregulated pathway in the diagnostic samples of those primary tumours responding to chemoradiotherapy. Only 1 of the 6 focus molecules was identified – acid ceramidase (highlighted in purple).

Further analysis of all (unfiltered) biological pathways identified 4 upregulated networks with a score greater than 2 pertaining to: cancer, cell cycle, cell morphology and haematological disease, hereditary disorder, immunological disease, lipid metabolism, small molecule biochemistry, molecular transport, skeletal and muscular disorders and connective tissue disorders. Similarly 2 downregulated networks were identified pertaining to: cancer, cell cycle, cell death and survival, cardiovascular system development and function, tissue morphology and cell death and survival. The focus molecules and statistics pertinent to these networks can be seen in Table 5.14.

Upregulated Networks				
ID	**Molecules in Network**	**Score**	**Focus Molecules**	**Top Diseases and Functions**
1	CCND1,PRPH	3	1	Cancer, Cell Cycle, Cell Morphology
2	CD40,FCGR2C,IGHG3	3	1	Hematological Disease, Hereditary Disorder, Immunological Disease
3	CDKN1A,GBA,mir-19,PSAP,TFEB	3	1	Lipid Metabolism, Small Molecule Biochemistry, Molecular Transport
4	CHI3L1,COL6A1,COL6A2,COL6A3,estrogen receptor,HR,SPDEF	3	1	Hereditary Disorder, Skeletal and Muscular Disorders, Connective Tissue Disorders
Downregulated Networks				
1	ANXA4,PLAA,TP53	3	1	Cancer, Cell Cycle, Cell Death and Survival
2	FANCC,KDR,MYOF,SYVN1,TGFBR2	3	1	Cardiovascular System Development and Function, Tissue Morphology, Cell Death and Survival

Table 5.14 – Network analysis for proteins both upregulated and downregulated in the primary tumours of the responders compared to the primary tumours of the non-responders. The score is derived from a p-value and indicates the probability of the focus molecules in a network being found together due to random chance. Focus molecules is the total number of proteins of interest identified in the respective network.

5.4 Discussion

5.4.1 Summary of aims

In this study a comprehensive proteomic analysis of serial rectal cancer biopsies from 8 patients was performed. The aim of this investigation was to compare the proteomic profile of serial rectal cancer biopsies taken at diagnosis, immediately after long course neoadjuvant chemoradiotherapy and at resection, to establish how this profile changes with treatment and identify potential response biomarkers which are detectable and measurable on the initial diagnostic biopsy.

5.4.2 Summary of results

Serial rectal cancer biopsies were obtained at 3 time points (diagnosis, post chemoradiotherapy and resection) from 8 patients which were dichotomised by histopathological response into responders and non-responders. 3359 proteins were identified, all of which were subjected to bioinformatics analysis. A summary of the proteomic data is shown in Table 5.15.

Comparison	Total Dysregulated	Upregulated	Downregulated
Post chemoradiotherapy / Diagnosis	18	16	2
Resection / Post chemoradiotherapy	39	9	30
Resection / Diagnosis	29	19	10
Responder / Non-responder (Diagnosis)	8	5	3

Table 5.15 - Summary proteomic data for the 2-group comparisons showing the total number of dysregulated proteins as well as those up/downregulated.

When comparing the post chemoradiotherapy samples with the diagnostic biopsies 18 proteins were significantly dysregulated, 2 of which were downregulated and 16 upregulated. Comparing the samples at resection with post chemoradiotherapy samples identified 39 proteins dysregulated, 30 of which were downregulated and 9 upregulated. Similarly a comparison of the resection and diagnostic samples identified 29 proteins, 10 of which were downregulated and 19 upregulated. The base excision repair pathway was the most significantly downregulated pathway in this analysis as a result of a reduction in

PARP1 abundance with treatment. Eight candidate biomarkers were identified in the primary tumours which appeared to predict response to chemoradiotherapy, 3 of which were downregulated and 5 upregulated. The most statistically significantly downregulated pathway was ceramide degradation as a result of low expression of acid ceramidase in those patients responding favourably to chemoradiotherapy. Again, further bioinformatic analysis of these comparator groups revealed putative pathways and networks involved in carcinogenesis.

5.4.3 iTRAQ for evaluation of tumour biology

The use of iTRAQ for the evaluation of tumour biology has previously been discussed (Section 4.4.3). Again this study reports protein coverage greater than that commonly seen in the literature and a novel study design. No other studies have attempted to characterise how the phenotype of any tumour changes with treatment.

5.4.4 Base excision repair

Base excision repair proteins are a key mechanism by which small, non-helix-distorting base lesions are repaired (compared to the nucleotide excision repair pathway which repairs bulky helix-distorting lesions). Base excision repair (BER) mechanisms remove damaged bases that could otherwise cause mutations by mispairing or lead to breaks in DNA during replication. Some of the key proteins involved in this mechanism include AP endonuclease 1 (APE1) which cleaves an AP site for subsequent binding, DNA polymerase β which catalyses short-patch repair (i.e. single nucleotide replacement), and DNA ligase III along with its cofactor XRCC1 which catalyses the nick-sealing step in short-patch BER. The expression of these proteins has been investigated for potential as both biomarkers and therapeutic targets, although as yet there is insufficient evidence for incorporation into clinical practice (Vens and Begg, 2010).

The BER pathway was one of the most significantly downregulated pathways identified between the initial diagnostic samples and resection, and was identified due to the decreased abundance in poly(ADP-ribose) polymerase (PARP1) at resection. PARP1 modifies nuclear proteins by poly ADP-ribosylation and is therefore relevant to differentiation, proliferation and tumour transformation, predominantly by repairing single stranded DNA breaks. Failure to repair these breaks, for example in the case of absent

PARP1, leads to an increase in the frequency of double-strand DNA breaks which are subsequently repaired by homologous recombination. Cells lacking PARP1 therefore exhibit a compensatory hyper-recombinagenic phenotype (Schultz *et al*, 2003). Interestingly the BRCA1 and BRCA2 genes are required for the adequate function of the homologous recombination pathway. BRCA mutated tumours are therefore highly sensitive to PARP1 loss (Farmer *et al*, 2005).

This knowledge has led investigators to consider the potential for PARP1 inhibition as a radiosensitiser. In an *in vitro* study of Ewing sarcoma cell lines, Lee *et al* (2013) demonstrated that inhibiting *PARP1* with shRNA amplified both the level and duration of DNA damage caused by radiotherapy which ultimately resulted in increased apoptosis and cell death. Wang *et al* (2012) considered the effects of PARP1 inhibition with an inhibitor currently in phase 1 clinical trials (MK-4827) in lung and breast cancer xenografts, demonstrating improved chemosensitivity irrespective of p53 status.

Only one pre-clinical study is reported for colorectal cancer. Shelton *et al* (2013) investigated the radiosensitisation of ABT-888, an orally available inhibitor of PARP1, compared to and in combination with other chemotherapeutics (5-FU, irinotecan, oxaliplatin). In the HCT116 and HT26 colorectal tumour derived cell lines ABT-888 radiosensitised at higher levels than the chemotherapeutics and acted synergistically with these when assessed by clonogenic assays.

When considering the findings from this investigation in light of the literature it is clear that the role of PARP-1 requires further investigation both as a biomarker and potential chemosensitiser for rectal cancer. What remains unclear is why we may be observing a reduction in abundance following chemoradiotherapy in our samples.

5.4.5 Acid ceramidase

Acid ceramidase is a sphingolipid - a group of biomolecules known to be responsible for important signalling functions in the control of cell growth and differentiation (Garcia-Barros *et al*, 2014). Importantly, a recent study from Mahdy *et al* (2009) has convincingly demonstrated that downregulation of the corresponding gene with siRNA in a prostate cancer cell line confers radiosensitivity. This *in vitro* study in PPC-1 cells assessed radiation response by clonogenic and cytotoxic assays, and also demonstrated that upregulation of

acid ceramidase decreased sensitivity to radiation and created cross-resistance to chemotherapy. The small molecule acid ceramidase inhibitor, LCL385, was also sufficient to sensitize PPC-1 cells to radiation. These data support our finding of low levels of acid ceramidase in those tumours responding to radiotherapy, with our data suggesting the potential for its use as an up-front predictive biomarker of response. Further evaluation in a larger patient cohort is clearly required however.

Carmofur, in common to the widely used radiosensitiser capecitabine, is a fluorouracil analogue currently in widespread clinical use in the US in the adjuvant setting for colorectal cancer. In addition to its presumed primary mode of action as a thymidylate synthetase inhibitor it has also independently been shown to inhibit acid ceramidase in the human tumour derived cell lines SW403 (colorectal) and LNCaP (prostate), a property not shared by fluorouracil or capecitabine (Realini *et al*, 2013). In light of our study, further work is needed to compare the radiosensitisation of capecitabine (thymidylate synthase inhibition) and carmofur (thymidylate synthase and acid ceramidase inhibition).

5.4.6 Study strengths and limitations

The relative merits and difficulties of a proteomic approach to these questions have already been discussed (Peng *et al*, 2003). As with most clinical studies there is inherent heterogeneity in the study population; differences exist in terms of patient age, TNM stage and tumour grade as well as the total dose of radiation received. That said, all patients received oral capecitabine as a radiosensitiser.

One of the clear strengths of the study (in contrast with that described in Chapter 4) is the utilisation of fresh tissue taken prior to treatment to prospectively identify novel response biomarkers. In addition, the yield of our mass spectrometry in terms of confidently identified and accurately mapped proteins is excellent, and considerably more (often many fold) than many other oncology based proteomic studies. The tissue resources we have collected are high value and the research questions are novel.

Given the aims of this study the numbers we have used are inadequate to draw any firm conclusions. This combined with the heterogeneity in the study sample, and the issue of tumour heterogeneity previously discussed (Section 4.4.4) mandates a degree of caution in the interpretation of the results and validity of any conclusions.

5.4.7 Conclusion

This study has evaluated the changes to the phenotype of a rectal tumour with chemoradiotherapy. Whilst the changes we have seen are modest in absolute figures, it is clear that base excision repair (and in particular PARP1) remains of interest in both carcinogenesis and treatment response. We have also identified acid ceramidase as a potential response biomarker, which complements existing understanding of its role in radiosensitisation.

Chapter 6

Targeted analysis of candidate biomarkers in the primary tumour for predicting response to neoadjuvant chemotherapy in colorectal liver metastases

6.1 Introduction

6.1.1 Background

Previous chapters in this thesis have described a global approach to both genomic and proteomic analysis of patient matched primary and metastatic colorectal tumours. The biological similarity of the tumours has been discussed at both a genomic and proteomic level, and the issues surrounding the problems of tumour heterogeneity and clonal selection on biomarker studies such as this have also been explored. Further necessary targeted work has been identified to explore these findings in more detail.

6.1.2 Pharmacology of chemotherapeutics

The bioinformatics analyses described have identified a number of potential pathways and networks involved in metastagenesis and treatment response. Accepting that for all patients the cornerstone of neoadjuvant therapy received has been 5-FU, the treatments have been heterogenous and as such any conclusions drawn relate to chemosensitivity of the tumour rather than a precise understanding of the mechanism of action of the chemotherapeutic agents received. The global proteomic study failed to confidently identify, in sufficient samples to make any meaningful interpretation, those proteins most relevant to the metabolism and biological effect of:

- 5-FU – dihydropyrimidine dehydrogenase (DPYD), thymidylate synthase (TS), orotate phosphoribosyl transferase (OPRT)
- Irinotecan – carboxylesterase 1 (CES1), carboxylesterase 2 (CES2), topoisomerase I (TOP I), UDP glucuronyltransferase 1A1 (UGT1A1) and cytochrome P450 3A4 (CYP3A4)
- Oxaliplatin – DNA polymerase β (DNAPOL β)

Therefore, a more targeted approach to their investigation is required.

As yet the focus has purely been on protein expression, however the potential for post-translational modification affecting protein function is well understood. To characterise the similarity in protein function (in addition to expression) between primary and metastatic tumours would provide further insight into the potential for using biomarkers from the

primary tumour to target therapy in the liver metastases. A mass-spectrometry assay of irinotecan conversion to SN-38 by action of human CES1 and CES2 has already been described (Section 2.2.9), however such an assay does not exist for 5-FU. It is however well-established that MSI-H tumours are less likely to respond to 5-fluoruracil-based regimens, and in a minority of patients, treatment may even be detrimental (Sargent, 2008). As such, establishing MSI status in these patients may provide further useful insight. In addition, given the increasing use of EGFR inhibitors evaluating the concordance of *KRAS* and *BRAF* status in our patients would also add to the existing body of knowledge in this regard.

6.1.3 Biomarker validation (NQO1)

The bioinformatics analysis of patient-matched primary and metastatic tumours identified 5 potential response biomarkers, two of which were similarly dysregulated in the primary and metastatic tumours and one of these (NQO1) appeared biologically plausible and worthy of further investigation.

The original discovery tissue set was the 16 patients from which fresh tissue was obtained. Validation of the iTRAQ findings on the same samples by another laboratory technique, for example western blotting, would be necessary before any further work could be undertaken. Beyond that the next step would be validation in a larger tissue set to further evaluate the potential for the use of this protein as a predictive biomarker. In addition the nature of the dysregulation, i.e. reduced abundance in the responders, raises the question about the potential for this protein to be used as a therapeutic target.

6.1.4 Aims and hypotheses

The aim of this investigation was to further explore the potential for utilising biological information from the primary tumour to inform and predict response to treatment for the liver metastases using a targeted approach of previously-identified markers of interest.

Specifically we hypothesise that:

1. Expression of those proteins known to be relevant to the activation and metabolism of chemotherapeutics (DPYD, TS, OPRT, CES1, CES2, TOP I, UGT1A1, CYP3A4 and DNAPOL β) in

the primary tumour correlate with expression in the liver metastases and predict response to treatment.

2. Activity of CES1/CES2 (and therefore conversion of irinotecan to SN-38) in the primary tumour correlates with CES1/CES2 activity in the metastasis and predicts response to treatment.

3. MSI status in the primary tumour predicts status in the metastasis (and therefore likely response to 5-FU).

4. *KRAS* and *BRAF* status in the primary tumour predicts status in the metastasis (and therefore likely response to EGFR inhibitors).

5. NQO1 expression by western blot confirms the validity of the iTRAQ data.

6. Immunohistochemical analysis of NQO1 expression in a larger patient cohort confirms its status as a predictive biomarker to (5FU based) neoadjuvant chemotherapy.

7. Inhibition of NQO1 in an *in vitro* model (by siRNA and/or use of a known competitive inhibitor) improves chemosensitivity.

6.2 Methods

6.2.1 Western blotting of proteins relevant to the activation and metabolism of chemotherapeutics

Fresh frozen samples of 16 patients undergoing synchronous or staged resection of metastatic colorectal cancer were collected as previously described (Section 4.2.1). Those samples with sufficient remaining material were used for this study. Protein extraction was performed by a combination of both mechanical and ultrasonic homogenisation in phosphate-buffered saline.

Following centrifugation the protein concentration of the supernatant was established using a Bradford assay (Bradford, 1976). Standard protein concentrations of bovine serum albumin (BSA) (Sigma Aldrich) were prepared at 0.1, 0.2, 0.4, 0.8, 1.0 and 1.4mg/ml and 20µl placed in triplicate on a 96 well plate. Serial dilutions of each sample were made at concentrations of 1:10, 1:20, 1:50 and 1:100, and 20µl placed in triplicate on the same 96 well plate. Bradford reagent (BioRad) was diluted 1:5 with dH_2O and 180µl placed in each of the wells and then mixed. Absorbance at 570nm was measured using the Dynex MRXe plate reader (Magellan Biosciences, Chelmsford, UK), and protein concentration of the sample calculated by comparison to the standard curve.

Samples containing 20µg total protein were prepared with 2X Laemmli buffer (BioRad), boiled at 100^{o}C for 10 minutes and run on 10% SDS-PAGE gels at 110V for 1 hour. A rainbow molecular marker (Sigma Aldrich, Poole, UK) was used to assist with the analysis of the molecular weight of protein samples.

After electrophoresis, membranes were washed in transfer buffer (1 x running buffer with 20% methanol) and transferred to a Hybond nitrocellulose membrane (GE Lifescience) within a blotting sandwich in a transfer unit containing transfer buffer at 230A for 1 hour. Membranes were washed briefly in 1x TBST (20mM Tris-Cl pH 7.6, 150mM NaCl, 0.1% Tween 20) and the quality of transfer assessed with Ponceau S stain. The stain was removed with TBST and the membrane blocked overnight in 10% Marvel milk in TBST with constant agitation.

The optimum conditions for antibody incubation were determined by experimentation, with the final conditions used shown in Table 5.1. All primary antibodies were diluted in 2% Marvel milk with TBST and incubated overnight with constant agitation in a cold room (4^{o}C).

Primary Antibody	Manufacturer	Reference	Dilution	Secondary Antibody	Molecular Weight (kDA)
TS	Abcam	ab3145	1:100	Mouse	35
DPYD	Abcam	ab54797 1	1:1000	Mouse	111
OPRT	Abcam	ab155763	1:2500	Rabbit	55
CES1	Abcam	ab64867 1	1:1000	Rabbit	58
CES2	Abcam	ab64867 1	1:1000	Rabbit	58
TOP I	Abcam	ab109374 1	1:2500	Rabbit	91
UGT1A1	Abcam	ab170858	1:2500	Rabbit	55
CYP3A4	Sigma	1400064	1:2500	Mouse	50
DNA POL β	Kind gift from Dr J Parsons	N/A	1:2500	Rabbit	33
β-Actin	Abcam	ab6726	1:5000	Mouse	42

Table 6.1 – Antibody incubation conditions for the proteins of interest with respect to the activation and metabolism of chemotherapeutics.

After incubation, membranes were washed with TBST for 3 x 10 minutes and then incubated with the appropriate LI-COR IRDye 680 LT secondary antibody (Biosciences, Lincoln USA) as shown in Table 6.1. The incubation was performed at a concentration of 1/20000 at room temperature for 1 hour with constant agitation in a light-tight box. Semi-quantitative analysis was performed using the Odyssey scanner (LI-COR Biosciences, Lincoln USA), with the same intensity adjustments used for all membranes being blotted for the same protein. Densitometry measurements were taken at the time of first scanning.

To permit inter-gel comparisons the same reference sample was included on all blots which were performed and analysed in triplicate with β-actin used as a loading control. Data were normalised to the reference sample.

6.2.2 CES1/CES2 activity assessment by mass spectrometry

The activity of CES1/CES2 was determined with irinotecan as a substrate in order to assess protein function. Tissue homogenate (250µg protein) from all patients with sufficient remaining primary and metastatic tumour was incubated with 200nM irinotecan (Sigma

Aldrich, Poole, UK) in dH_20 at 37°C on a bench top rocker for 30 minutes. Given the high abundance of CES1 and CES2 in the liver and the significance of this to irinotecan activation (Jones *et al*, 2013), matched liver parenchyma was also studied. The reaction was terminated by protein precipitation following the addition of the same volume of a 50% acetonitrile / 50% methanol and 0.005% formic acid solution. This solution also contained the internal standard – 80nM camptothecin (Sigma Aldrich, Poole, UK), chosen due to its structural similarity to the analytes of interest and ready availability. The terminated reaction was centrifuged at 14000rpm for 20 minutes at 4°C. 300µl of supernatant was then filtered through a Millipore Multiscreen Solvinert 96 well filter plate, which had been pre-wetted using 100µl of water. Samples were collected in a clean 96 well plate, after which 100µL was transferred to a 200µl Chromacol glass autosampler vial and sealed with a cap. 20 µL was injected onto the LC-MS/MS system, the final concentration of which was 100nM irinotecan and 40nM camptothecin.

Two sets of parallel controls were prepared, one containing no tissue homogenate and one without irinotecan. A series of standard controls containing irinotecan, SN-38 (Sigma Aldrich, Poole, UK) and camptothecin were also prepared as shown in Table 6.2.

Standard Control	SN38 (nM)	Irinotecan (nM)	Camptothecin (nM)
0	0	0	40
20	20	20	40
50	50	50	40
100	100	100	40
200	200	200	40
400	400	400	40

Table 6.2 – Preparation of standard controls for mass spectrometry analysis of irinotecan conversion to SN-38 by human CES1/CES2.

The standard controls, control samples and protein samples underwent high pressure liquid chromatography mass spectrometry analysis to quantify the active metabolite, SN-38 (Jones *et al*, 2013). The assay used has previously been developed and validated in line with the US Department of Health & Human Services Food and Drug Administration guidelines, as outlined in Bioanalytical Method Validation; Guidance for Industry (FDA, 2001).

Sample separation was performed on a Dionex HPLC stack using an Ultimate 3000 system and an Altima c18 (150 x 2.1mm, 5µM) column. A dual-buffer technique of an aqueous buffer A (LC-MS grade H_20 with 0.25% formic acid) and organic buffer B (LC-MS grade acetonitrile with 0.25% formic acid) was used with a run time of 15 minutes. The elution time of SN38 was 5.5 minutes with a clearly detectable peak and m/z of 393.2. Conditions for optimal detection of SN-38 were based on existing literature (Chen *et al*, 2012) and a multiple reaction monitoring (MRM) method implemented. All samples were run in triplicate. The concentration of SN-38 in the samples was calculated by reference to the standard curve, normalised to the internal standard by peak area ratio and a rate of production (nmol/µg protein/minute) calculated.

6.2.3 Microsatellite instability analysis and KRAS/BRAF pyrosequencing

DNA extraction was performed using the Qiagen EZ1 DNA Tissue Kit as per manufacturer's instructions (Qiagen, Venlo, Netherlands). DNA concentration was measured using the NanoDrop™ ND-1000 spectrophotometer (Thermo Scientific, Waltham, USA) and quality assessed using the Human DNAOK! kit (Microzone, Haywards Heath, UK). *KRAS* mutational analysis was performed on the PyroMark Q96 ID (Qiagen, Venlo, Netherlands) using an in-house pyrosequencing assay capable of detecting all somatic mutations in codons 12, 13 and 61 of the *KRAS* gene with a lower limit of detection of 5% mutated alleles. *BRAF* mutational analysis for codons 600 and 601 with a lower limit of detection of 10% mutated alleles was similarly performed. The MSI Analysis System v1.2 (Promega) was used, with samples subsequently run on the Applied Biosystems 3130XL genetic analyser and data analysed using GeneMapper® (Life Technologies).

6.2.4 Validation of iTRAQ data

Western blotting for NQO1 was performed on all samples with sufficient remaining material. A mouse monoclonal antibody for NQO1 (Abcam, ab28947) was used at a dilution of 1:500. An anti-mouse LI-COR IRDye 680 LT secondary antibody (Biosciences, Lincoln USA) was used to detect a protein with a molecular weight of 30kDa. All conditions were otherwise as described in Section 6.2.1. Densitometry values were normalised to a common sample to allow inter-gel comparisons and the correlation between densitometry on western blotting and protein expression by iTRAQ was established.

6.2.5 Tissue micro-array construction

Archived samples of formalin-fixed paraffin embedded patient matched primary and metastatic colorectal cancer tissues were obtained from the contributing research sites within the Merseyside and Cheshire cancer network (n=56). Where available, normal adjacent colonic mucosa and liver parenchyma were also obtained. Blocks and corresponding haematoxylin and eosin (H&E) stained slides were reviewed and marked by a consultant pathologist in order to identify representative areas of both tumour and normal tissue. The H&E slides of the liver metastases of those patients who had received neoadjuvant chemotherapy were also reviewed and scored for histopathological response to treatment as previously described (Blazer *et al*, 2008).

The method of tissue micro-array (TMA) construction is described in full elsewhere (Kononen *et al,* 1998). TMAs were constructed using a tissue microarrayer (Beecher Instruments Inc) with 0.6mm cores retrieved from donor blocks and transferred into the recipient master paraffin block in triplicate. Triplicate samples of breast and tonsillar tissue were also transferred to each TMA to act as controls. Samples of primary tumour, normal colon, normal liver and colorectal liver metastases were randomised over four TMAs which were produced in duplicate to ensure sufficient material for immunohistochemical staining. To allow inter-array comparisons, a sample set consisting of all four sample types from a single patient were placed on each of the 4 TMAs. TMAs were incubated at 37°C overnight, placed on ice and then 5µm sections were cut on a rocking microtome. Sections were then placed onto coated glass slides.

6.2.6 Immunohistochemical analysis of NQO1

To establish optimal conditions three dilutions of the primary antibody were used on a series of test slides with concentrations centred around that suggested by the manufacturer (1/100, 1/500, 1/1000). Appropriate positive controls (breast tumour and colonic mucosa) identified using Protein Atlas (www.proteinatlas.org) were included alongside these samples. Antibody diluent only and a mouse IgG1 isotype control (Abcam, ab91353) were used as negative controls to assess for background staining.

Sections were de-waxed in xylene and rehydrated with ethanol solutions of decreasing concentrations. After blocking with 3% hydrogen peroxide in 100% methanol, antigens were retrieved by microwaving for 20 minutes in 10mM citrate buffer and further blocked with 10% goat serum in 0.1% TRIS-buffered saline with tween. Slides were incubated with

the primary antibody for 2 hours (Abcam, ab28947) followed by a 1:200 horseradish peroxidase conjugated secondary antibody for 30 minutes (Dako UK Ltd, E0433). Following incubation with the Vectastain Elite® ABC reporter system (Vectorlabs, Burlingame, USA), slides were developed with diaminobenzidine tetrahydrochloride (DAB) and counterstained with haematoxylin. The optimisation slides and positive/negative controls were reviewed by a consultant histopathologist who confirmed the appropriateness of the staining and advised the optimum concentration to be used (1/1000). The control slides can be seen in Figure 6.1.

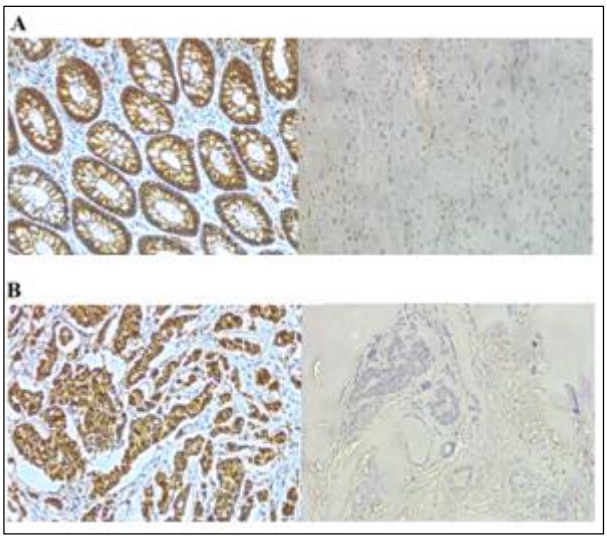

Figure 6.1 – Antibody optimisation of NQO1 demonstrating the optimal concentration of antibody (1/1000) in the positive controls (left) and negative controls (right) of colonic mucosa (A) and breast cancer (B).

After optimisation, sections of the TMAs were taken and stained in triplicate using the previously described methodology. Stained sections of the TMA were initially reviewed by light microscopy, and slides then scanned using the Aperio Scanscope (Leica Biosystems). Semi-quantification of protein expression was performed using Tissue Studio v.2.0 (Definiens AG, Munich, Germany). Prior to quantification the system required programming. In brief this consisted of nuclear and cell membrane identification to enable the recognition of cells, followed by setting the intensity thresholds for negative and positive (weak, moderate and intense) staining. Minor adjustments were made until concordance with a 10% sample similarly scored by eye had been achieved and then the TMA slides were scored (Figure 6.2).

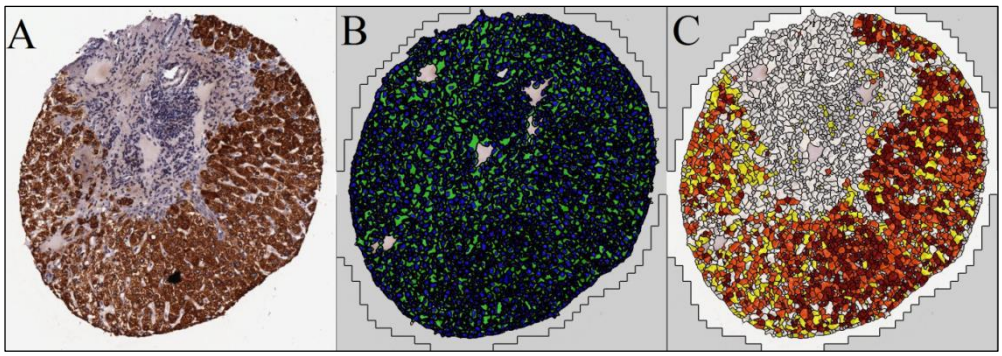

Figure 6.2 - Images from a randomly selected core produced by Tissue Studio v.2.0 (Definiens AG, Munich, Germany), an immunohistochemical scoring package. The stained core as it appears under the light microscope is shown in (A), with the brown regions representing antibody binding and oxidation of DAB by horseradish peroxidase. Cellular identification and localisation is shown in (B), with the nuclei appearing blue and cytoplasm green. The degree of antibody staining is shown in (C) and can be seen to similarly correspond with the appearances on the micrograph (A). Areas shaded white have no antibody staining, yellow have weak antibody binding, orange have moderate antibody staining and brown have intense antibody staining (all considered positive).

The data generated by Tissue Studio allowed a scoring system to be implemented based on that previously used by Yang *et al* (2014). A score was allocated for the proportion of positively stained cells as follows: 1 (<25%), 2 (25-50%), 3 (51-75%) or 4 (>75%).

6.2.7 Cell culture of the SW480 cell line and dose response analysis

The SW480 cell line is an immortal colorectal tumour derived cell line originating from a Dukes B adenocaricnoma of the colon. The cells were provided as a kind gift from the Department of Molecular and Clinical Cancer Medicine, University of Liverpool.

Cells were maintained in Dulbecco's Modified Eagle Medium (Sigma), 10% foetal bovine serum (Sigma) and 1% Penicillin/Streptomycin (Sigma). Cells were kept incubated at 37^{o}C and their morphology/confluence observed every 3-4 days at which time the media was changed (Figure 6.3). Upon establishing confluence, cells were trypsinised with 0.25% trypsin-EDTA (Sigma), filtered through a sterile needle and syringe, passaged in a 1:20 ratio and subcultured in the same media. Where the experimental intent was to establish cell viability, cells were cultured in 96-well plates at 5000 cells/well. Where sufficient material was needed for western blot analysis, 12-well plates were seeded with 3x10^{5} cells/well.

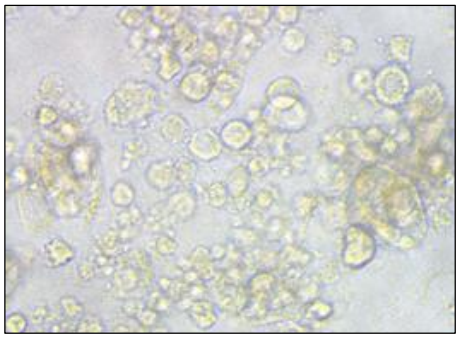

Figure 6.3 – Morphology of the SW480 cell line used for this investigation. Micrograph taken at x400 magnification.

Initially, the toxic effect of irinotecan and 5-FU on the cell lines was determined. A 160mM stock concentration of each of the drugs was made by dissolving 4.2mg of 5FU (MW 130.10Da) in 200µl of dimethyl sulfoxide (DMSO) and 5.0mg of irinotecan (MW 623.14Da) in 50µl DMSO. A series of 7 1:2 dilutions were then performed with DMSO. 7.5µl of each of these solutions combined with 1493µl of media produced solutions of 800 µM, 400µM, 200µM, 100µM, 50µM, 25µM, 12.5µM and 6.25µM each with 0.5% DMSO. The control sample (0.5% DMSO) was prepared by diluting 25µl of DMSO in 4975µl of media. Wells were dosed in triplicate with 100µl of each of the prepared solutions with the control samples and media-only controls also placed in triplicate on the same 96 well plate. Cells were incubated at 37^{o}C for 72 hours before assessing cell viability. The experiment was repeated in triplicate for both irinotecan and 5FU.

An MTS [3-(4,5-dimethylthiazol-2-yl)-5-(3-carboxymethoxyphenyl)-2-(4-sulfophenyl)-2H-tetrazolium, inner salt] assay was used to assess cell viability. The assay utilises MTS tetrazolium which is reduced into a formazan-coloured product by viable cells. The solubility of the product reduces the need for detergents, and the rapid colour change and ease of storage make it desirable for studies such as this (Buttke *et al*, 1993). 20µL MTS reagent (Promega) was introduced to all wells and the plates incubated for 2 hours at 37°C. A microplate reader (Multiskan, Thermo Labsystems, Ventaa, Finland) was used to measure optical density at 490nm. Cell viability was expressed as a percentage of control cells.

6.2.8 Effect of chemotherapy on NQO1 expression

The experiment described in 6.2.7 was repeated in 12 well plates. Following a 72 hour incubation period at 37°C, cells were lysed with 50µL of radioimmunoprecipitation assay

(RIPA) buffer and incubated at room temperature for 5 minutes. Cells were scraped from the wells and the lysate centrifuged at 15,000 RPM for 15 minutes at 4°C. The resulting supernatant was quantified using the Bradford assay and underwent western blotting for NQO1 as previously described.

6.2.9 siRNA transfection of NQO1

A set of four human NQO1 siGENOME siRNAs (Thermoscientific) each targeting different coding regions of the gene was obtained and reconstituted according to manufacturer's instructions. Twelve well plates with each well containing 3 X 10^5 cells in 1ml media were seeded and incubated overnight prior to transfection with one of the four siRNAs. Lipofectamine® RNAimax (Invitrogen) and opti-MEM® (Life technologies) were combined with the siRNA as per manufacturer's instructions and incubated for 10 minutes prior to application of 15µl to the 85µl of media already placed in the wells. Each siRNA was used at two different concentrations (1.25pM and 2.5pM) and placed in triplicate. As a negative control, a non-targeting scrambled human siRNA was used to transfect the cells.

Following a 48 hour incubation period at 37°C, cells were lysed with 50µL of RIPA buffer and incubated at room temperature for 5 minutes. Cells were scraped from the wells and the lysate centrifuged at 15,000 RPM for 15 minutes at 4°C. The resulting supernatant was quantified using the Bradford assay and underwent western blotting for NQO1 as previously described. The blot was examined to identify the siRNA (and concentration) conferring the best knockdown of NQO1 (Figure 6.4)

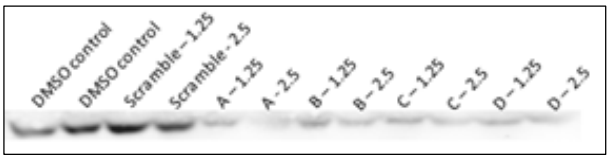

Figure 6.4 – Western blot for NQO1 in transfected S480 cells. From the left: DMSO treated cells were used as a control, and the transfection process (scrambled siRNA) had no effect on NQO1 expression. All 4 siRNAs (A-D) offered good knockdown of NQO1 at both concentrations. The optimum knockdown was achieved with siRNA-A at a concentration of 2.5pM.

As can be seen, the transfection process (scrambled siRNA) had no effect on NQO1 expression. All 4 siRNAs (A-D) offered good knockdown of NQO1 at both concentrations. The optimum knockdown was achieved with siRNA-A at a concentration of 2.5pM. Transfecting the cells with this siRNA alone produced no reduction in cell viability at 72 hours, and therefore this was used for subsequent experimental work.

6.2.10 Effect of NQO1 knockdown on chemosensitivity

The experiment described in section 6.2.7 was repeated in NQO1 knocked down cells following siRNA transfection as previously described. 96 well plates were seeded, incubated overnight and transfected in triplicate for each drug dose to be used. After a 48 hour incubation period, the media was removed and cells dosed in triplicate with irinotecan at concentrations of 800µM, 400µM, 200µM, 100µM, 50µM, 25µM, 12.5µM or 6.25µM. Scrambled siRNA followed by irinotecan dosing was used as the control arm. Further sets of 0.5% DMSO and media only controls were included. Cells were incubated for 72 hours at 37°C before assessing cell viability with an MTS assay as previously described. The experiment was repeated using 5-FU, and each plate was run in triplicate. A plate plan for this experiment is shown in Figure 6.5.

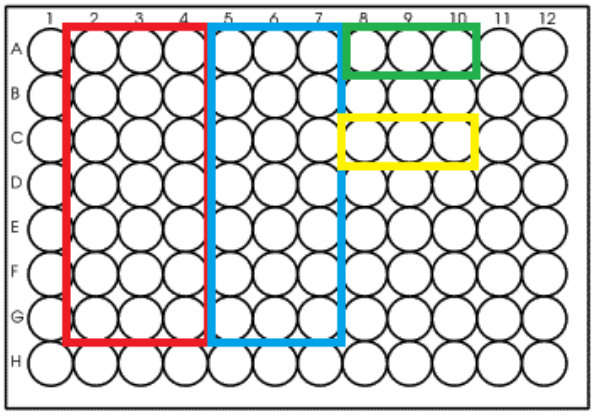

Figure 6.5 – Wells highlighted in red were transfected with siRNA to knockdown NQO1 and then incubated with irinotecan or 5FU over a range of concentrations. Wells highlighted in blue were transfected with a scrambled siRNA and then similarly treated. Wells highlighted in green were incubated in 0.5% DMSO (vehicle control) and wells highlighted in yellow were incubated in media only.

6.2.11 Evaluating dicoumarol as an inhibitor of NQO1 and chemosensitiser

Dicoumarol, a coumarin currently in clinical use, has been shown to competitively inhibit the action of NQO1 (Tsvetkov *et al*, 2005). Dicoumarol competes with NAD(P)H for the binding of NQO1, thus inhibiting the transfer of electrons from NAD(P)H to the FAD cofactor and ultimately preventing the substrate from being reduced (Asher *et al*, 2006).

The effects of dicoumarol on SW480 cells

Firstly the effect of dicoumarol on SW480 cells was established. A 1mM stock concentration was made by dissolving 3.6mg of dicoumarol (MW 336.3) in 10ml NaOH and performing a series of dilutions as previously described to produce 500µM, 250µM, 100µM, 50µM, 25µM and 10µM solutions of dicoumarol in 0.5% NaOH. A control sample (0.5% NaOH) was prepared by diluting 25µl of NaOH in 4975µl of media and a media only control also used. Wells were dosed in triplicate with 100µl of each of the prepared solutions with the control samples also placed in triplicate on the same 96 well plate. Cells were incubated at 37^{o}C for 4 hours (the intended duration of pre-treating for future studies) before assessing cell viability using the MTS assay as previously described. The experiment was repeated in triplicate.

Establishing the optimum concentration of dicoumarol

A 96 well plate was seeded and incubated overnight before pre-treating triplicate wells with each of the dicoumarol concentrations described above. After 4 hours the media was removed and the cells dosed with 100µM irinotecan (the closest dose to the IC50). The control wells were incubated with 0.5% NaOH for 4 hours (vehicle control for dicoumarol) followed by irinotecan. Plates were incubated at 37^{o}C for 72 hours before assessing cell viability using the MTS assay as previously described. The experiment was repeated in triplicate and again for 5FU at a concentration of 200µM (the closest dose to the IC50). The maximal effective concentration (lowest concentration to exert the full biological effect) was identified and used for the remainder of the experiments.

Attributing the effects of dicoumarol to NQO1 activity

The optimum scientific strategy would be the correlation of any biological effect seen by the addition of dicoumarol with cellular NQO1 activity. However, without access to a well-validated activity assay for NQO1 we adopted an alternative strategy. Given the well established knock down already demonstrated with siRNA it would perhaps be reasonable

to assume that if dicoumarol were exerting its biological effect through NQO1 inhibition, then the addition of dicoumarol to cells in which NQO1 had already been knocked down would not result in any further effect than that already achieved with siRNA. This would provide at least some circumstantial evidence to confirm that dicoumarol is exerting its biological effect through NQO1 inhibition and not another pathway or mechanism.

A 96 well plate was seeded and incubated overnight before transfecting 6 wells for each dose of chemotherapy to be used. After transfection, half of those cells were pre-treated with dicoumarol at a dose of 100µM (as previously determined), and the media changed in the remainder. After 4 hours all media was removed and the transfected wells, transfected and dicoumarol pre-treated wells, and a parallel set of wells which had not been transfected or treated were dosed with irinotecan at the range of concentrations previously described. The control samples were transfected with scrambled siRNA, incubated for 4 hours in 0.5% NaOH (vehicle control for dicoumarol) and then incubated for 72 hours in 0.5% DMSO (vehicle control for irinotecan). A further set of 0.5% DMSO only controls were also included. Plates were incubated at 37^{o}C for 72 hours before assessing cell viability using the MTS assay. The experiment was repeated using 5-FU, and each plate was run in triplicate. A plate plan for this experiment is shown in Figure 6.6.

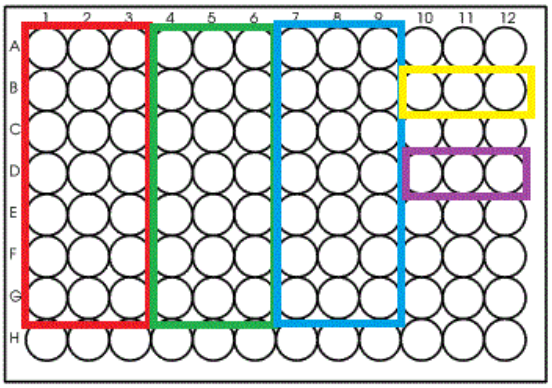

Figure 6.6 - Wells highlighted in red were transfected with siRNA to knockdown NQO1, pre-treated with dicoumarol and then incubated with the irinotecan or 5FU over a range of concentrations. Wells highlighted in green were transfected but not pre-treated with dicoumarol and wells highlighted in blue were not transfected nor pre-treated. Wells highlighted in yellow were transfected with scrambled siRNA and then pre-treated with 0.5% NaOH and incubated in 0.5% DMSO, and those highlighted in purple were incubated in 0.5% DMSO only.

Effect of NQO1 inhibition on chemosensitivity by pre-treating cells with dicoumarol

The experiment described in section 6.2.7 was repeated in cells pre-treated with dicoumarol as previously described. 96 well plates were seeded, incubated overnight and pre-treated with 100µM dicoumarol in triplicate for each drug concentration to be used. A parallel set of wells within the same plate were not pre-treated with dicoumarol. After a 4 hour incubation period, the media was removed and cells dosed in triplicate with irinotecan at concentrations of 800µM, 400µM, 200µM, 100µM, 50µM, 25µM, 12.5µM or 6.25µM. Pre-treatment with 0.5% NaOH followed by incubation with 0.5% DMSO (the vehicle control for irinotecan), and 0.5% DMSO only wells were used as controls. Cells were incubated for 72 hours at 37°C before assessing cell viability with an MTS assay as previously described. The experiment was repeated using 5-FU, and each plate was run in triplicate. A plate plan for this experiment is shown in Figure 6.7.

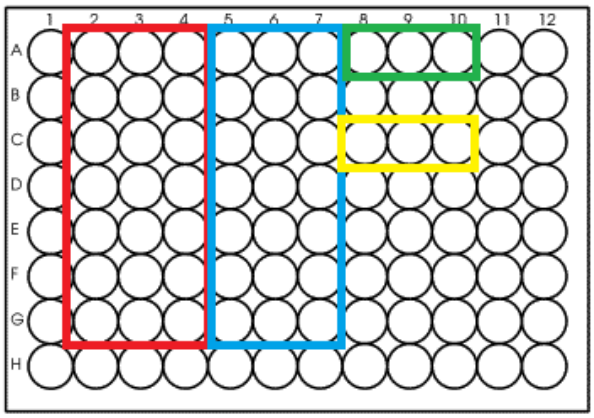

Figure 6.7 – Wells highlighted in red were pre-treated with dicoumarol and then incubated with irinotecan or 5FU over a range of concentrations. Wells highlighted in blue were not pre-treated but treated with chemotherapy only. Wells highlighted in green were pre-treated with 0.5% NaOH and then incubated in 0.5% DMSO (vehicle control) and wells highlighted in yellow were not pre-treated but incubated in 0.5% DMSO only.

6.2.12 Statistical analysis

Protein expression in primary and metastatic tumours by western blotting was compared using Spearman's rank correlation co-efficient. SN38 production was compared between primary and metastatic tumours using the student's paired t-test, and between all three groups (primary, metastasis and liver parenchyma) using one-way ANOVA. Correlation

between densitometry on immunoblot and iTRAQ expression was established using Pearson's rank correlation co-efficient.

With respect to the immunohistochemistry, key clinicopathological variables were compared between groups using ANOVA for continuous data and the X^2 test for categorical data. Spearman's rank correlation coefficient was used to assess for correlation in the percentage of positively stained cells in the primary and metastatic tumours, with a two-way test for significance. The X^2 test was used to compare the positively stained cells in the responders and non-responders.

For the *in vitro* work data were normalised to the experimental control and experimental arms compared using the student's un-paired t-test. Where multiple testing across doses was used, the Bonferroni correction was applied.

6.3 Results

6.3.1 Western blotting of proteins relevant to the activation and metabolism of chemotherapeutics

For this investigation samples were available from 12 patients: 1, 2, 3, 5, 7, 9, 10, 11, 12, 13, 15 and 16. After optimisation of the laboratory technique, western blotting demonstrated a band at the expected molecular weight for each target protein. Wide variation was seen in protein expression both in different tissue types and also across individuals. Given the small number of patients for whom samples were available and the heterogeneity between chemotherapeutic regimens received, correlation between expression and treatment response would not have been scientifically meaningful. The expression between primary and metastatic tumours however was compared.

Proteins relevant to 5-FU

Western blots for TS, DPYD and OPRT are shown in Figures 6.8, 6.9 and 6.10 respectively.

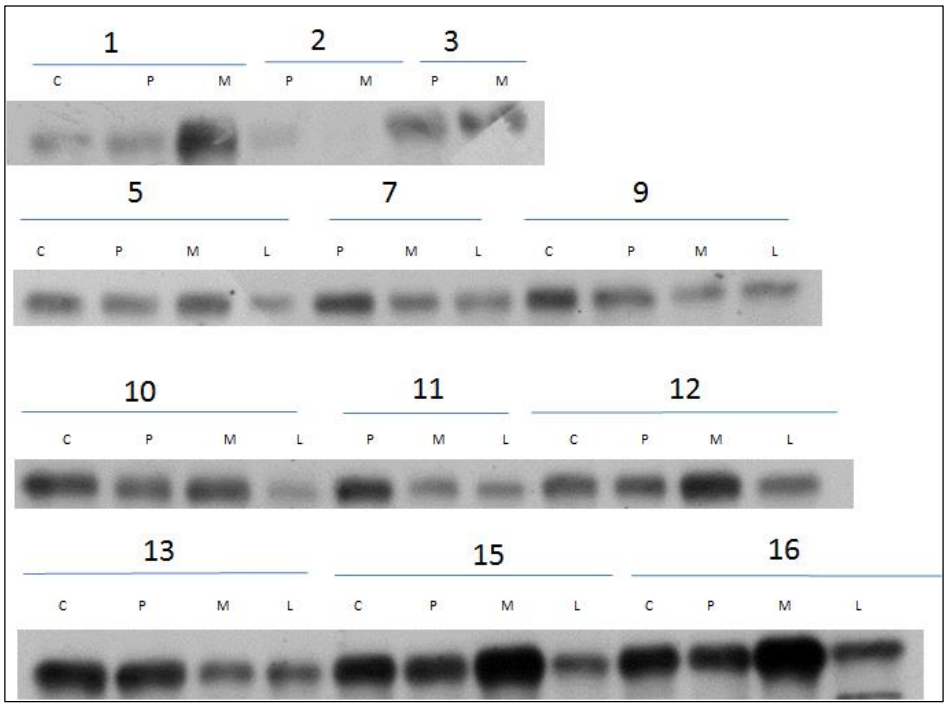

Figure 6.8 - Western blots for thymidylate synthase (TS) in patient matched colonic mucosa (C), primary tumour (P), metastatic tumour (M) and liver parenchyma (L).

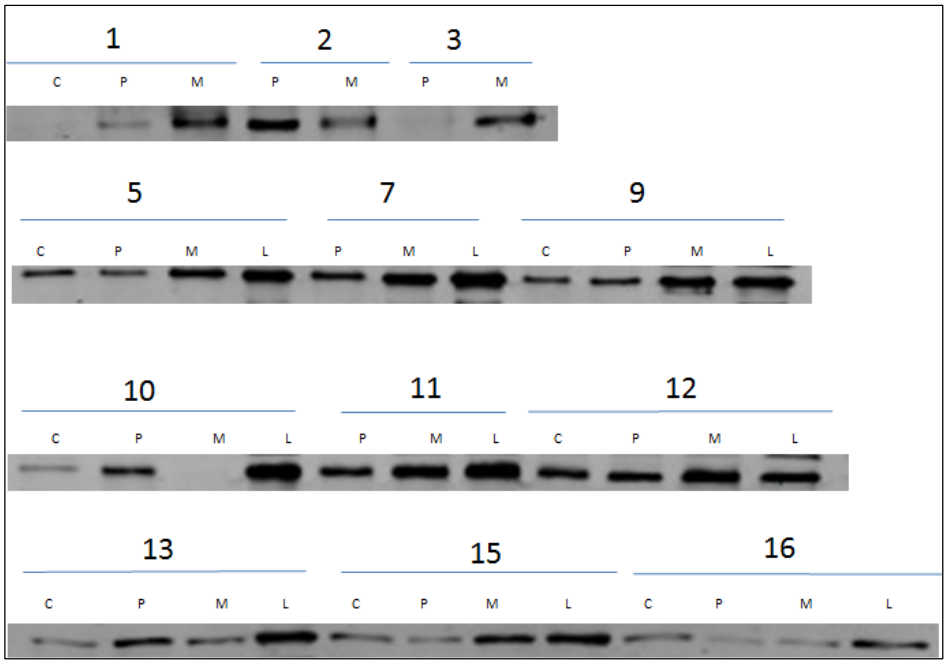

Figure 6.9 - Western blots for dihydropyrimidine dehydrogenage (DPYD) in patient matched colonic mucosa (C), primary tumour (P), metastatic tumour (M) and liver parenchyma (L).

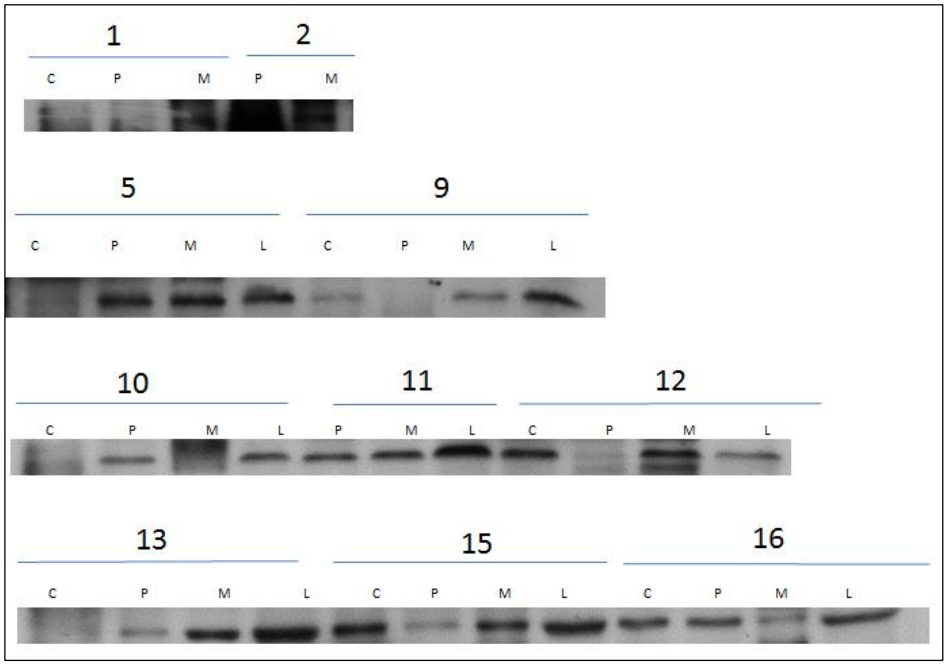

Figure 6.10 - Western blots for orotate phosphoribosyltransferase (OPRT) in patient matched colonic mucosa (C), primary tumour (P), metastatic tumour (M) and liver parenchyma (L).

Densitometry values were normalised to a common sample included on all gels to allow inter-gel comparisons and the correlation between primary and metastatic tumour samples were compared using Spearman's rank test (Table 6.3). Whilst a positive correlation was seen for all proteins, this did not reach statistical significance.

Protein	Median (IQR) primary tumour densitometry	Mean (SD) metastatic tumour densitometry	Correlation co-efficient	p value
TS	830.05 (630.89 – 1245.12)	597.04 (509.60 – 1798.08)	0.64	0.054
DPYD	5.52 (4.56 – 7.11)	11.21 (7.82 – 17.34)	0.63	0.054
OPRT	17.50 (10.31 – 24.10)	32.40 (24.67 – 39.75)	0.05	0.882

Table 6.3 – Median densitometry values for thymidylate synthase (TS), dihydropyrimidine dehydrogenase (DPYD) and orotate phosphorisobysltransferase (OPRT) expression in patient matched primary and metastatic tumours. Correlation co-efficients (with Spearman's rank test) showed positive correlations although these did not reach statistical significance.

Proteins relevant to irinotecan

Western blots for CES1, CES2, TOP I, UGT1A1 and CYP3A4 are shown in Figures 6.11, 6.12, 6.13, 6.14 and 6.15 respectively.

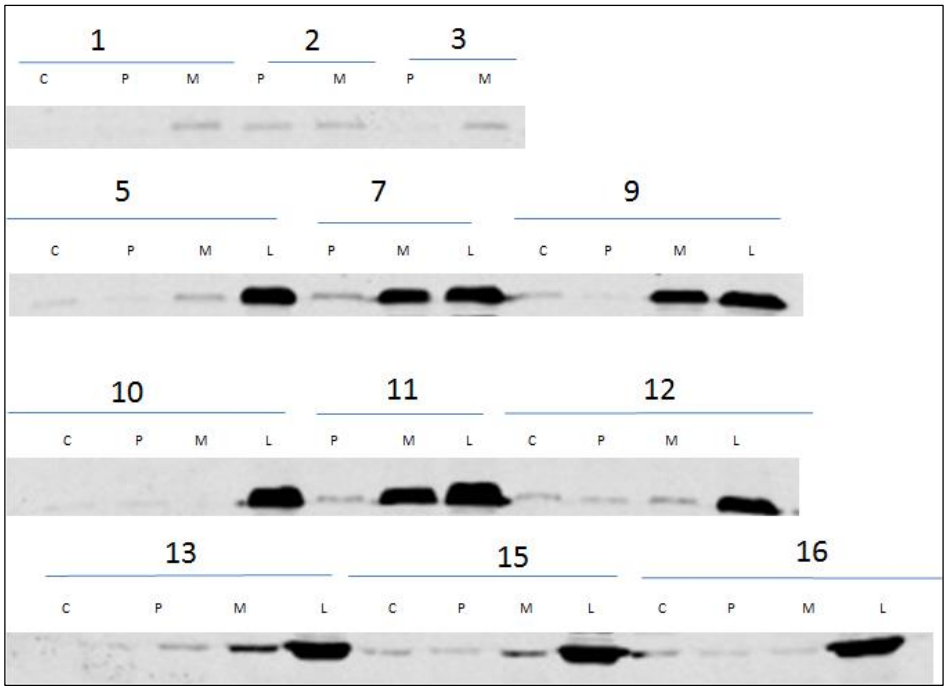

Figure 6.11 - Western blots for human carboxylesterase 1 (CES1) in patient matched colonic mucosa (C), primary tumour (P), metastatic tumour (M) and liver parenchyma (L).

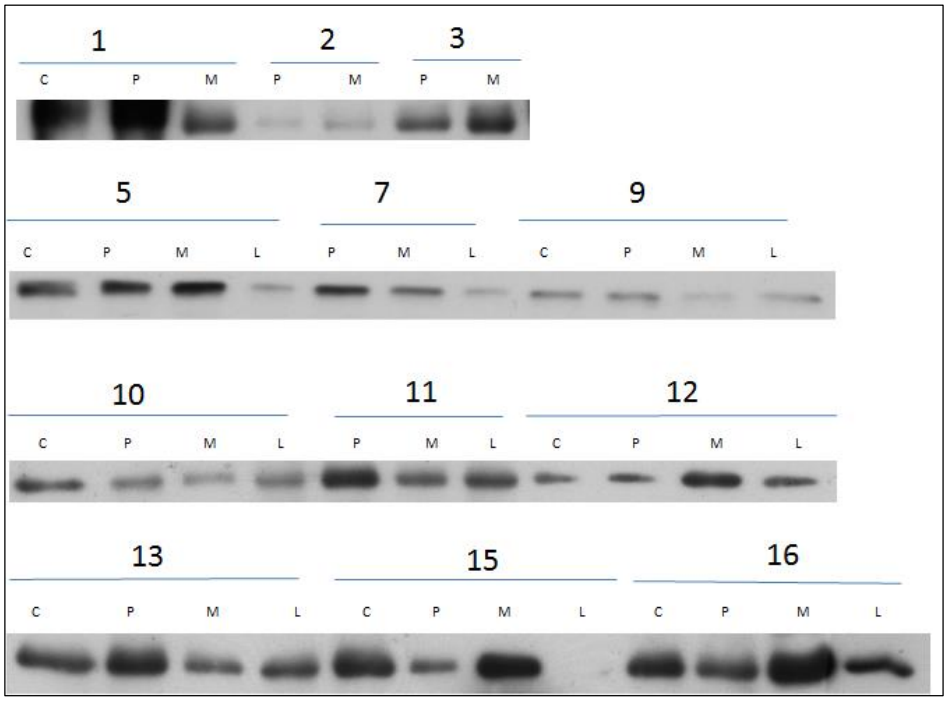

Figure 6.12 - Western blots for human carboxylesterase 2 (CES2) in patient matched colonic mucosa (C), primary tumour (P), metastatic tumour (M) and liver parenchyma (L).

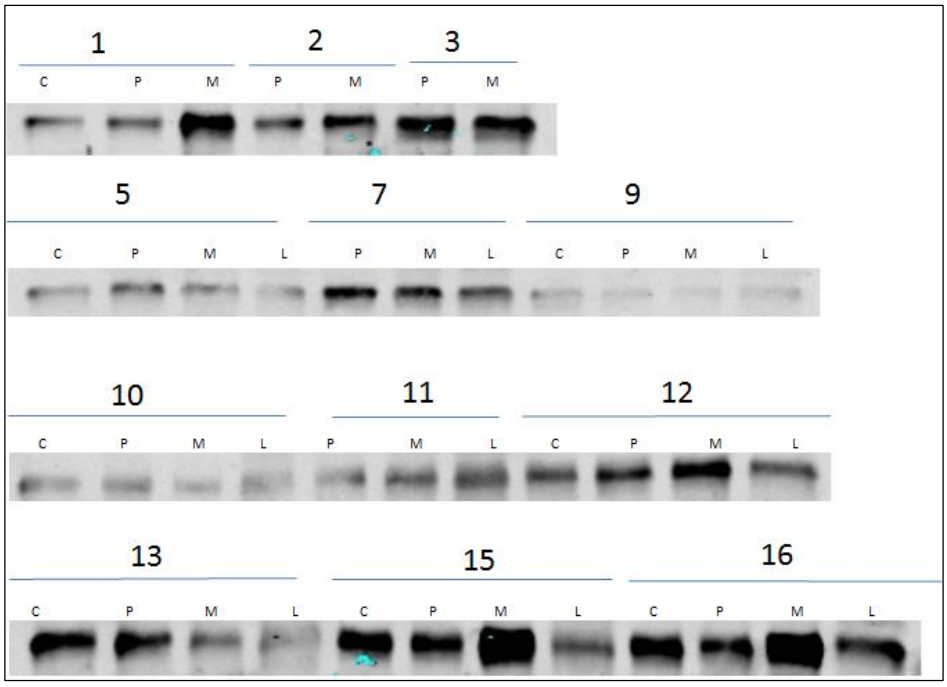

Figure 6.13 - Western blots for human topoisomerase I (TOP I) in patient matched colonic mucosa (C), primary tumour (P), metastatic tumour (M) and liver parenchyma (L).

Figure 6.14 - Western blots for UDP glucuronosyltransferase 1A1 (UGT1A1) in patient matched colonic mucosa (C), primary tumour (P), metastatic tumour (M) and liver parenchyma (L).

Figure 6.15 - Western blots for cytochrome P450 3A4 (CYP3A4) in patient matched colonic mucosa (C), primary tumour (P), metastatic tumour (M) and liver parenchyma (L).

Densitometry values were normalised to a common sample included on all gels to allow inter-gel comparisons and the correlation between primary and metastatic tumour samples were compared using Spearman's rank test (Table 6.4). A positive correlation was seen for all proteins, reaching statistical significance for TOP I (r=0.79; P=0.009).

Protein	Median (IQR) primary tumour densitometry	Mean (SD) metastatic tumour densitometry	Correlation co-efficient	p value
CES1	4.28 (1.59 - 7.30)	15.23 (6.47 – 37.75)	0.41	0.248
CES2	363.04 (219.33 – 498.44	518.55 (255.42 – 837.22)	0.50	0.144
TOP I	7.89 (5.05 – 12.80)	8.50 (5.38 – 17.75)	0.79	0.009
UGT1A1	2.54 (1.89 – 4.45)	29.20 (4.51 – 55.57)	0.09	0.811
CYP3A4	520.23 (465.13 – 645.98)	543.80 (356.28 – 1288.73)	0.26	0.470

Table 6.4 – Median densitometry values for carboxylesterase 1 (CES1), carboxylesterase 2 (CES2), topoisomerase I (TOP I), UDP glucuronosyltransferase 1A1 (UGT1A1) and cytochrome P450 3A4 (CYP3A4) expression in patient matched primary and metastatic tumours. Correlation co-efficients (with Spearman's rank test) showed positive correlations, reaching statistical significance in the case of TOP I.

Proteins relevant to oxaliplatin

Western blots for DNA POL β are shown in Figure 6.16.

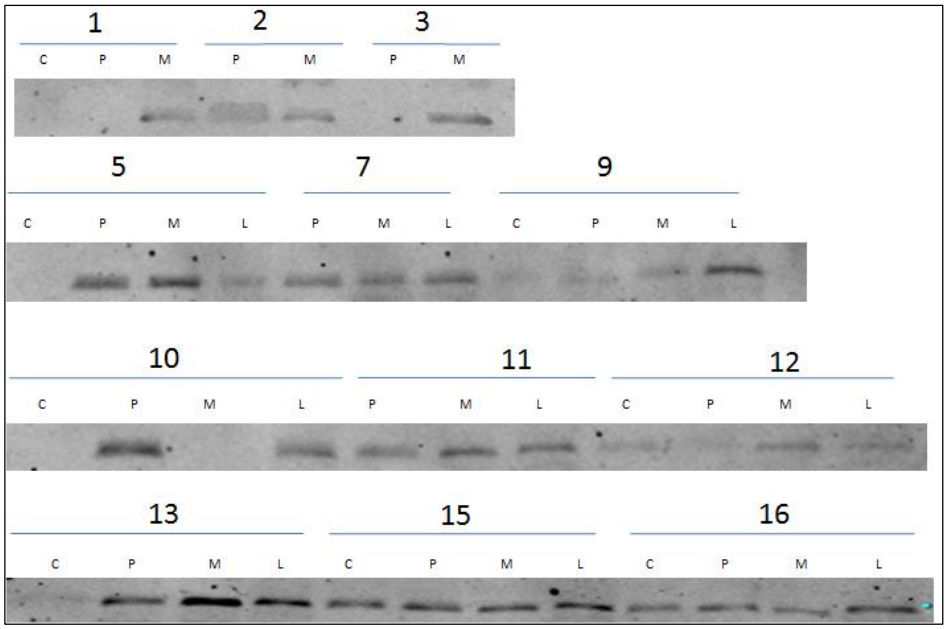

Figure 6.16 - Western blots for DNA polymerase β (DNA POL β) in patient matched colonic mucosa (C), primary tumour (P), metastatic tumour (M) and liver parenchyma (L).

Densitometry values were normalised to a common sample included on all gels to allow inter-gel comparisons and the correlation between primary and metastatic tumour samples were compared using Spearman's rank test. The median (IQR) densitometry values in the primary and metastatic tumours were 4.21 (1.47 – 5.01) and 4.52 (3.07 – 8.32) respectively. Spearman rank correlation was 0.58 (p=0.088).

6.3.2 CES1/CES2 activity assessment by mass spectrometry

Patient matched primary tumour, liver metastasis and liver parenchyma were available for patients 1, 2, 3, 5, 7, 9, 10, 11, 12, 13, 15 and 16. SN-38 production in these samples ranged from 0.77-5.36 nmol/µg protein/minute (Figure 6.17).

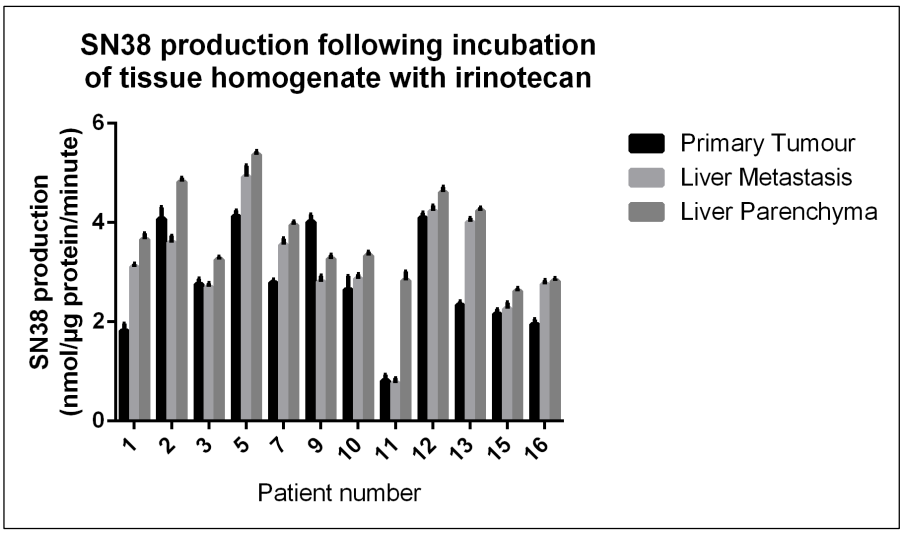

Figure 6.17 - CES1/CES2 activity was measured by SN38 production in patient matched primary tumour, liver metastasis and liver parenchyma. Mean (SD) data are presented for each tissue type for the patients studied.

When considering the variation in SN38 production across tissue types, the mean (SD) rate was 2.80 (0.13) nmol/µg protein/minute in the primary tumours, 3.13 (0.11) nmol/µg protein/minute in the metastatic tumours, and 3.73 (0.08) nmol/µg protein/minute in the liver parenchymal samples (Figure 6.18). Comparison across groups with one-way ANOVA showed a statistically significant difference (p=0.001).

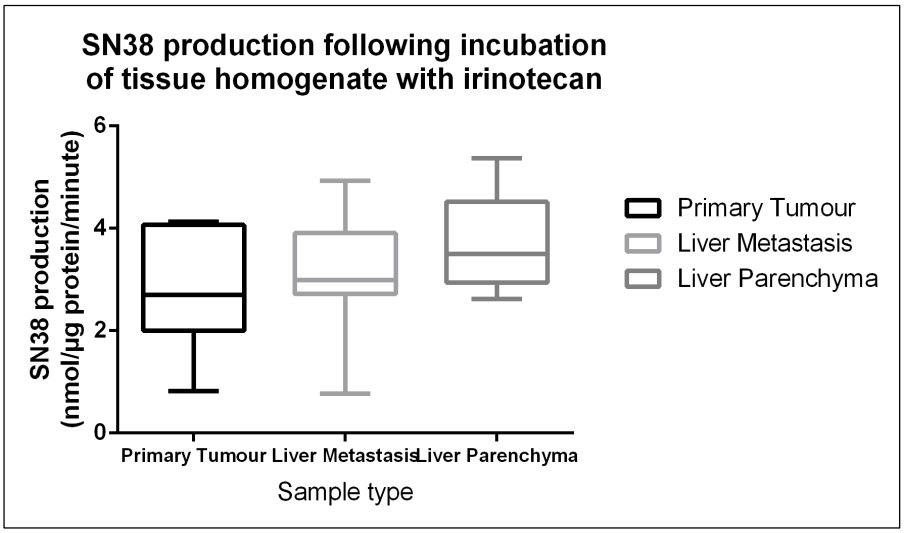

Figure 6.18 – Mean, SD and 95% confidence interval for SN-38 production in the primary tumours, liver metastases and liver parenchyma. Analysis with ANOVA showed significant differences between groups (p=0.001).

Having identified significant differences between tissue types, patients were analysed on an individual basis both across all three tissue types (using ANOVA) and in light of the specific hypothesis the rate of production was compared between the primary and metastatic tumours (using student's paired t-test). Of the 12 patients studied, there were significant differences between tissue types in all except two. When comparing primary and metastatic tumours, significant differences were seen in all except four (Table 6.5). As such the activity of carboxylesterase in the primary tumour does not predict that in the metastasis, and neither correlate well with activity in the liver parenchyma.

Sample	Mean (SD) Primary	Mean (SD) Metastasis	Mean (SD) Liver	All Groups (ANOVA)	Primary *vs*. Mets (Paired t-test)
1	1.82 (0.14)	3.11 (0.06)	3.66 (0.12)	0.006	0.003
2	4.08 (0.23)	3.60 (0.13)	4.82 (0.08)	0.018	0.051
3	2.76 (0.11)	2.70 (0.08)	3.26 (0.05)	0.003	0.055
5	4.13 (0.11)	4.93 (0.22)	5.37 (0.07)	0.003	0.024
7	2.79 (0.06)	3.56 (0.12)	3.95 (0.07)	0.004	0.001
9	4.02 (0.14)	2.81 (0.12)	3.27 (0.08)	0.002	0.000
10	2.65 (0.27)	2.87 (0.09)	3.34 (0.07)	0.052	0.112
11	0.82 (0.10)	0.77 (0.09)	2.84 (0.17)	0.001	0.029
12	4.10 (0.10)	4.23 (0.11)	4.61 (0.11)	0.039	0.175
13	2.34 (0.07)	4.01 (0.08)	4.24 (0.06)	0.002	0.001
15	2.16 (0.09)	2.27 (0.12)	2.62 (0.06)	0.061	0.228
16	1.95 (0.10)	2.76 (0.08)	2.83 (0.05)	0.003	0.000

Table 6.5 – SN-38 production in patient matched primary tumour, liver metastasis and liver parenchyma (nmol/µg protein/minute). Of the 12 patients studied there were significant differences between tissue types (by ANOVA) in all except two (highlighted in red). When specifically comparing the primary and metastatic tumours, significant differences (by student's paired t-test) were seen in all except four (also highlighted in red).

6.3.3 KRAS/BRAF pyrosequencing and microsatellite instability analysis

With the exception of patient 14, sufficient material was available for analysis of primary and metastatic tumours from all patients. Corresponding colonic mucosa and liver parenchyma was also sequenced where available. Five patients (3, 6, 10, 12, and 16) had mutations in *KRAS* codon 12, with 100% concordance between primary and metastatic

tumours and the mutations not present in the normal adjacent colonic mucosa from which the tumour had arisen. No mutations were detected in *KRAS* codon 13 or 61. One patient (13) had *BRAF* mutations in codons 600 and 601 and again this mutation was present in both primary and metastatic tumour. All patients were microsatellite-stable except patient 16 who was microsatellite instability low (MSI-L) in the colonic mucosa, primary tumour, liver metastasis and liver parenchyma. Results and mutational frequencies can be seen in Table 6.6.

Patient	Tissue	KRAS Codon 12	KRAS Codon 13	KRAS Codon 61	BRAF Codon 600 and 601	MSI Status
1	Colon	WT	WT	WT	WT	Stable
	Primary	WT	WT	WT	WT	Stable
	Metastasis	WT	WT	WT	WT	Stable
2	Primary	WT	WT	WT	WT	Stable
	Metastasis	WT	WT	WT	WT	Stable
3	Primary	c.35G>T (p.Gly12Val) 25%	WT	WT	WT	Stable
	Metastasis	c.35G>T (p.Gly12Val) 25%	WT	WT	WT	Stable
4	Primary	WT	WT	WT	WT	Stable
	Metastasis	WT	WT	WT	WT	Stable
	Liver	WT	WT	WT	WT	Stable
5	Colon	WT	WT	WT	WT	Stable
	Primary	WT	WT	WT	WT	Stable
	Metastasis	WT	WT	WT	WT	Stable
	Liver	WT	WT	WT	WT	Stable
6	Colon	WT	WT	WT	WT	Stable
	Primary	c.35G>C (p.Gly12Ala) 20%	WT	WT	WT	Stable
	Metastasis	c.35G>C (p.Gly12Ala) 20%	WT	WT	WT	Stable
	Liver	WT	WT	WT	WT	Stable
7	Colon	WT	WT	WT	WT	Stable
	Primary	WT	WT	WT	WT	Stable
	Metastasis	WT	WT	WT	WT	Stable
	Liver	WT	WT	WT	WT	Stable
8	Primary	WT	WT	WT	WT	Stable
	Metastasis	WT	WT	WT	WT	Stable
	Liver	WT	WT	WT	WT	Stable
9	Colon	WT	WT	WT	WT	Stable

	Primary	WT	WT	WT	WT	Stable
	Metastasis	WT	WT	WT	WT	Stable
	Liver	WT	WT	WT	WT	Stable
10	Colon	WT	WT	WT	WT	Stable
	Primary	c.34G>T (p.Gly12Cys) 35%	WT	WT	WT	Stable
	Metastasis	c.34G>T (p.Gly12Cys) 20%	WT	WT	WT	Stable
	Liver	WT	WT	WT	WT	Stable
11	Colon	WT	WT	WT	WT	Stable
	Primary	WT	WT	WT	WT	Stable
	Metastasis	WT	WT	WT	WT	Stable
	Liver	WT	WT	WT	WT	Stable
12	Colon	WT	WT	WT	WT	Stable
	Primary	c.35G>A (p.Gly12Asp) 20%	WT	WT	WT	Stable
	Metastasis	c.35G>A (p.Gly12Asp) 30%	WT	WT	WT	Stable
	Liver	WT	WT	WT	WT	Stable
13	Colon	WT	WT	WT	WT	Stable
	Primary	WT	WT	WT	c.1799T>A (p.Val600Glu) 23%	Stable
	Metastasis	WT	WT	WT	c.1799T>A (p.Val600Glu) 44%	Stable
	Liver	WT	WT	WT	WT	Stable
15	Colon	WT	WT	WT	WT	Stable
	Primary	WT	WT	WT	WT	Stable
	Metastasis	WT	WT	WT	WT	Stable
	Liver	WT	WT	WT	WT	Stable
16	Colon	WT	WT	WT	WT	MSI-Low
	Primary	c.35G>T (p.Gly12Val) 50%	WT	WT	WT	MSI-Low
	Metastasis	c.35G>T (p.Gly12Val) 50%	WT	WT	WT	MSI-Low
	Liver	WT	WT	WT	WT	MSI-Low

Table 6.6 – *KRAS* (codon 12, 13 and 61), *BRAF* (codon 600 and 601) and microsatellite instability analysis for 16 patients undergoing resection at both sites for liver limited stage IV colorectal cancer. Five patients had *KRAS* codon 12 mutation, one patient had *BRAF* 600/601 mutation and one patient was MSI-Low. WT = wild type.

With respect to *KRAS/BRAF* mutation, as only patient received cetuximab (Table 4.2) it is not possible to make any further comment on patient selection or treatment response. Although all patients undergoing neoadjuvant chemotherapy received 5-FU, only one patient had microsatellite instability and therefore again no comment on patient selection or treatment response can be made.

6.3.4 Validation of iTRAQ data

Data acquired by iTRAQ were validated by western immunoblotting for NQO1. Evaluation of protein expression was directly comparable (Figure 6.19), with a Pearson correlation co-efficient of 0.59 (95% CI 0.47 – 0.69; p=0.003).

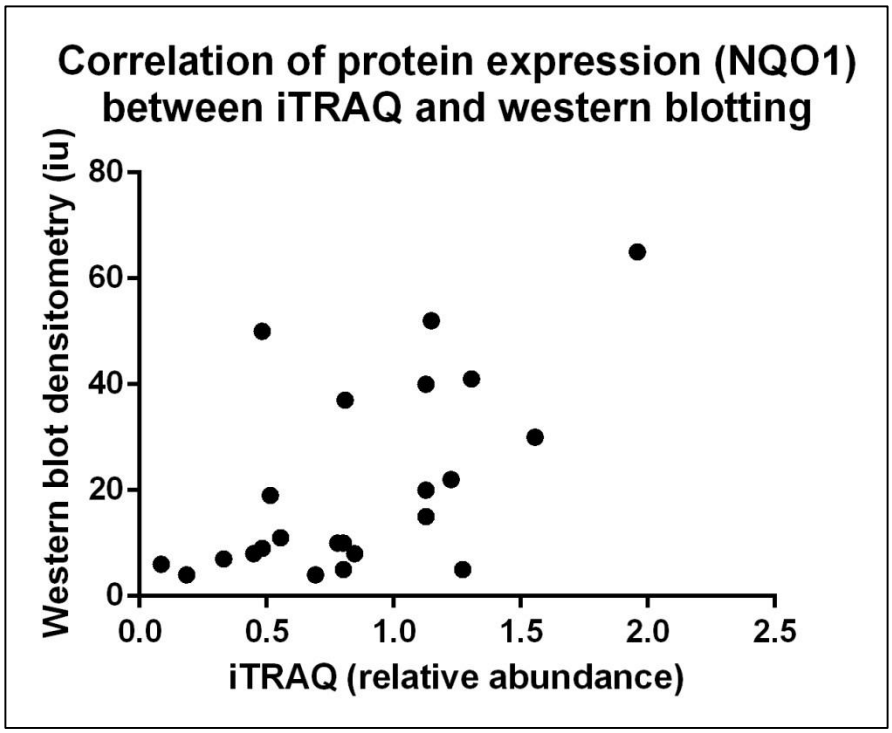

Figure 6.19 – Comparison of protein quantification by western blotting (densitometry iu) and iTRAQ (abundance) for NQO1 demonstrates a high statistically significant relationship (r=0.59; p=0.003).

6.3.5 Immunohistochemical analysis of NQO1

A tissue micro-array of 56 patient matched primary and metastatic tumour samples was assembled. Where available, normal colonic mucosa and liver parenchyma were also included. Of the 56 patients, 37 had received neoadjuvant treatment and 19 were chemo-

naive. As discussed in previous chapters, there was again considerable variation in the agents and regimens received. Of the 37 patients, 14 (37.8%) had a tumour regression grade of I-II (the responders), and 23 (62.2%) had a tumour regression grade of III-IV. Key clinical and pathological characteristics between these groups were compared (Table 6.7).

Variable		Responders	Non-responders	Chemo-naive	P value
Median age (range)		66.1 (49-80)	61.8 (37-77)	67.2	0.363*
Sex (%)	Male	10 (71.4)	17 (73.9)	13 (68.4)	0.926#
	Female	4 (28.6)	6 (26.1)	6 (31.6)	
Simultaneous resection (%)		3 (21.4)	2 (8.7)	2 (10.5)	0.617#
Location of primary (%)	Rectum	5 (35.7)	6 (26.1)	3 (15.8)	0.506#
	Left	8 (57.1)	11 (47.8)	11 (57.9)	
	Right	1 (7.1)	6 (26.1)	5 (26.3)	
T stage	1	0 (0.0)	0 (0.0)	0 (0.0)	**0.017#**
	2	4 (28.6)	8 (34.8)	5 (26.3)	
	3	9 (64.3)	14 (60.9)	6 (31.6)	
	4	1 (7.1)	1 (4.3)	8 (42.1)	
N stage	0	4 (28.6)	11 (47.8)	12 (63.2)	0.118#
	1	5 (35.7)	10 (43.5	5 (26.3)	
	2	5 (35.7)	(35.7)	2 (10.5)	
Differentiation	Poor	1 (7.1)	0 (0.0)	1 (5.3)	0.444#
	Moderate	8 (57.1)	15 (65.2)	15 (78.9)	
	Well	5 (35.7)	8 (34.8)	3 (15.8)	
Mean (SD) number of metastases		2.2 (1.2)	2.4 (1.9)	3.0 (4.3)	0.756*
Total patients		**14**	**23**	**19**	**N/A**

Table 6.7 – Key clinical and pathological variables in the chemo-naive, responders and non-responders. Continuous data was assessed for significance using ANOVA* and categorical data using the X^2 test#. Only T stage was considerably different between groups, with a greater proportion of T4 tumours in the chemo-naive group.

Continuous data was assessed for significance using ANOVA and categorical data using the X^2 test. Only T stage was considerably different between groups, with a greater proportion of T4 tumours in the chemo-naive group (42.1% *vs* 7.1% in the responders and 4.3% in the non-responders, P=0.017). This discrepancy is most likely to be explained by the 'straight to surgery' approach usually taken with T4 tumours given their tendency to be symptomatic and at high risk of obstruction and perforation.

The percentage of positive cells stained was calculated as previously described. To establish the correlation between primary and metastatic tumour expression, the raw data were plotted as x and y variables (Figure 6.20).

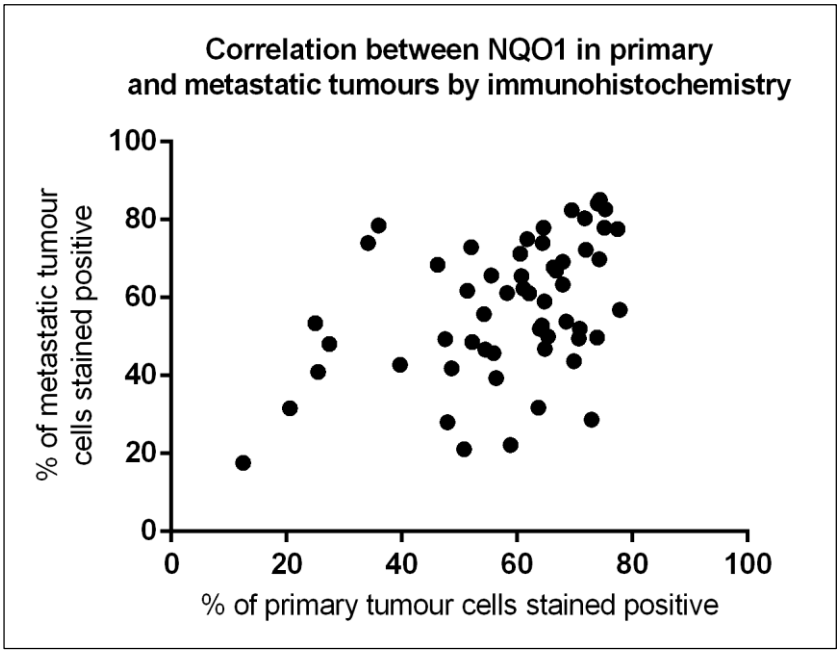

Figure 6.20 – Correlation between the percentage of cells staining positively for NQO1 in the primary tumour and metastatic tumour. Using Spearman's rank correlation coefficient, r=0.44 (95% CI 0.20 – 0.64, p=0.001).

Given the skewed appearance towards high expression, correlation was assessed statistically using Spearman's rank correlation coefficient. A moderate positive association reaching statistical significance was seen: r=0.44 (95% CI 0.20 – 0.64, p=0.001).

NQO1 expression in the responders and non-responders grouped by percentage of positively stained cells (Section 6.2.6) can be seen in Table 6.8. X^2 test applied to the primary tumour scores was not significant (p=0.470) however analysis of the metastases showed that NQO1 staining is considerably higher in the non-responders compared to the responders (p=0.041).

Cell Staining	Primary		Metastasis	
	Responders	Non responders	Responders	Non responders
1 (<25%)	1	1	2	0
2 (25-50%)	3	3	7	6
3 (51-75%)	10	19	5	12
4 (>75%)	0	0	0	5

Table 6.8 - NQO1 expression in the responders and non-responders grouped by percentage of positively stained cells. No statistically significant difference was observed in the primary tumours (p=0.470) however in the metastases, NQO1 staining is considerably higher in the non-responders compared to the responders (p=0.041, X^2 test).

6.3.6 Cell culture of the SW480 cell line and dose response analysis

Dose-response data for irinotecan in the SW480 cell line is shown in Figure 6.21.

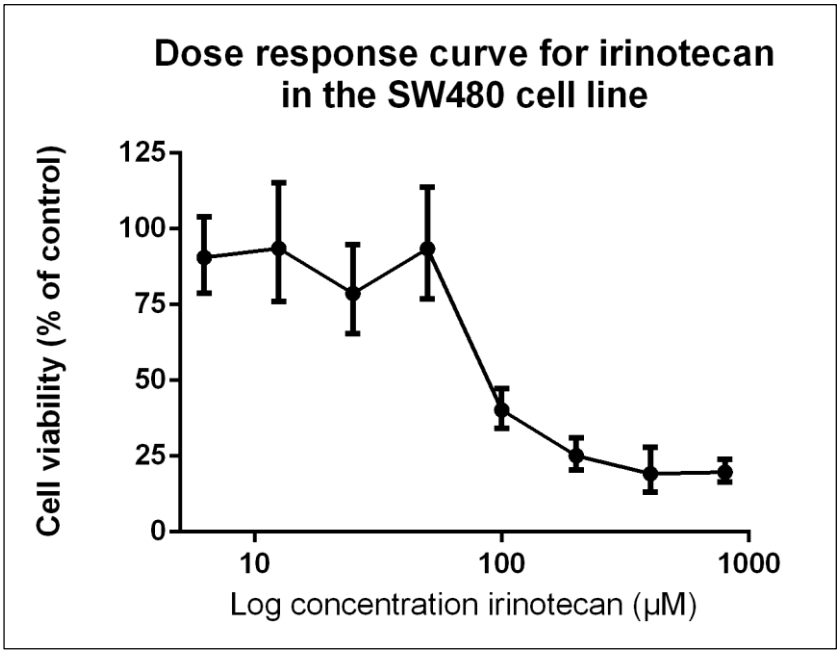

Figure 6.21 – Dose response analysis for irinotecan in the SW480 cell line. Cells were incubated for 72 hours and cell viability assessed using the MTS assay and presented as a mean (95% CI) percentage of the control (0.5% DMSO). The IC50 is 90.2µM.

As can be seen, doses up to ~50µM have little toxic effect, after which a sharp reduction in cell viability is seen. At 800µM, less than 20% of cells were viable at 72 hours. The IC50

(concentration of drug required to render 50% of cells non-viable) under these experimental conditions is 90.2µM.

Dose-response data for 5-FU in the SW480 cell line is shown in Figure 6.22.

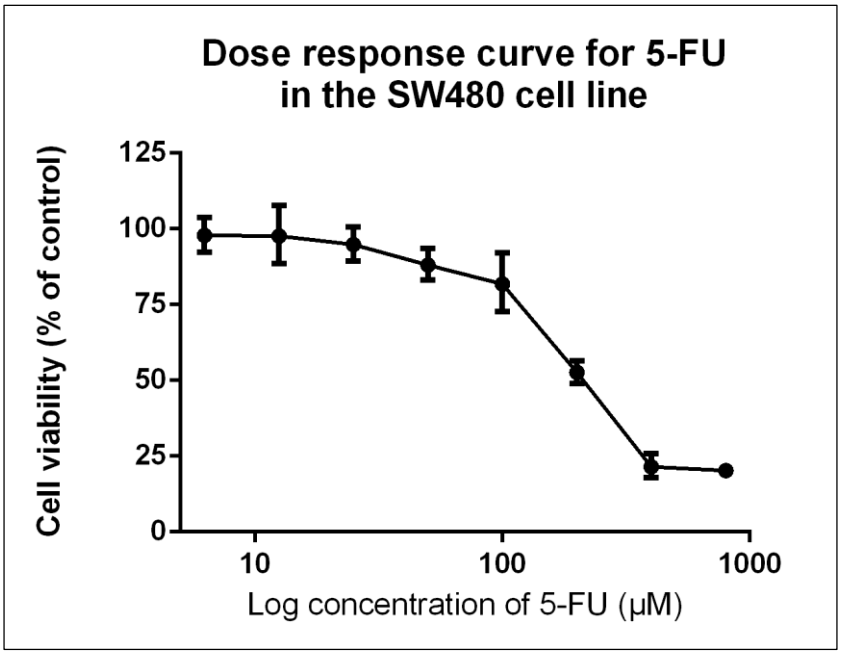

Figure 6.22 – Dose response analysis for 5-FU in the SW480 cell line. Cells were incubated for 72 hours and cell viability assessed using the MTS assay and presented as a mean (95% CI) percentage of the control (0.5% DMSO). The IC50 is 202.2µM.

As can be seen, doses up to ~100µM have little toxic effect, after which a sharp reduction in cell viability is seen. At 800µM, less than 20% of cells were viable at 72 hours. The IC50 (concentration of drug required to render 50% of cells non-viable) under these experimental conditions is 202.2µM.

6.3.7 Effect of chemotherapy on NQO1 expression

To establish the effect of the chemotherapy agents on NQO1 expression, western blots were performed on cell lysates following incubation with the drug for 72 hours. The blot and corresponding densitometry values for irinotecan can be seen in Figure 6.23. The effect was negligible, did not reach statistical significance and was similarly observed following incubation with 5-FU.

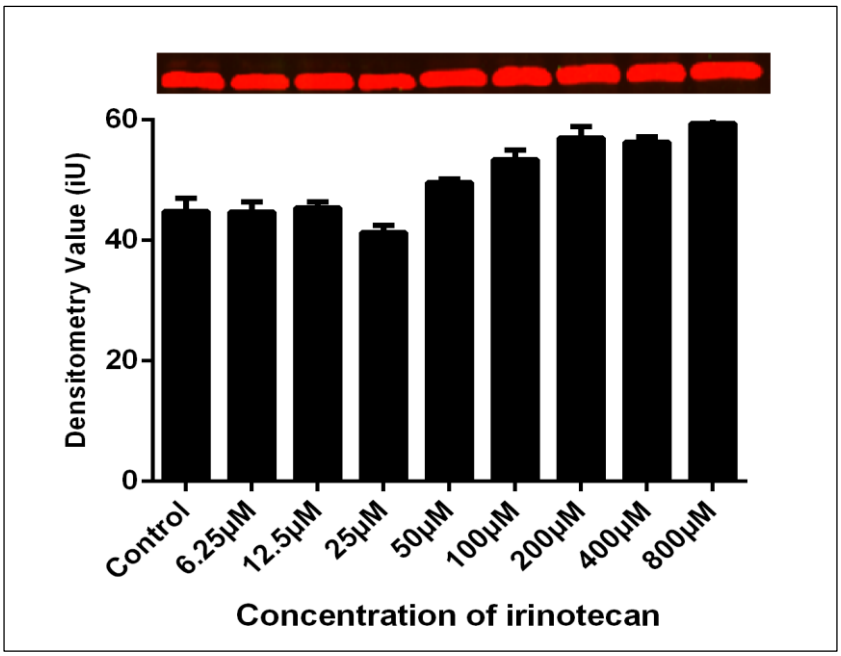

Figure 6.23 – The effect of incubation with irinotecan on NQO1 expression was minimal. No samples were significantly different from the control value (0.5% DMSO).

6.3.8 Effect of NQO1 knockdown on chemosensitivity

The effect of NQO1 knockdown by siRNA transfection on chemosensitivity to irinotecan can be seen in Figure 6.24.

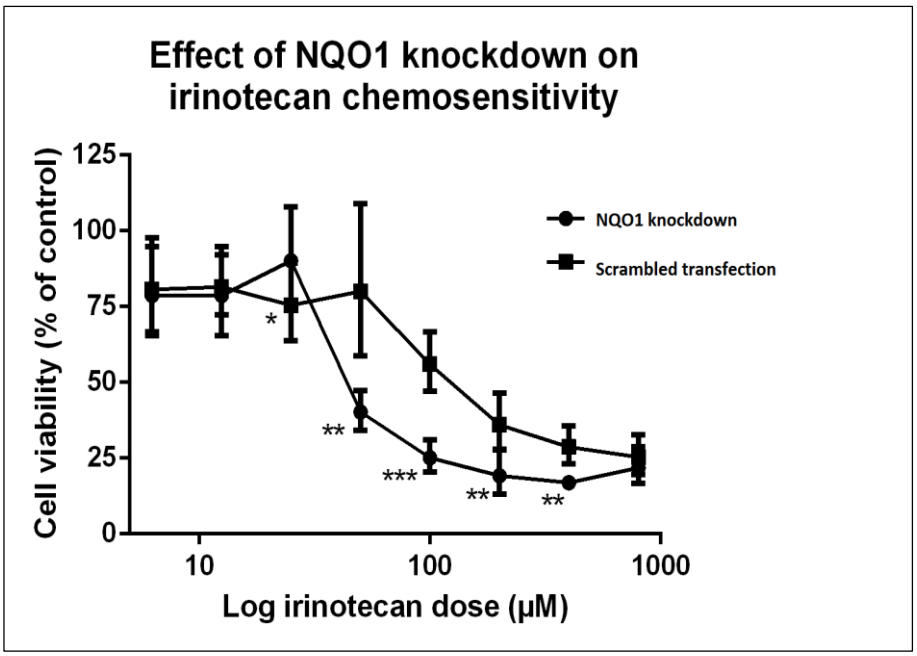

Figure 6.24 – Dose response analysis for irinotecan in the SW480 cell line with and without knockdown of NQO1 by siRNA transfection. Cells were incubated for 72 hours and cell viability assessed using the MTS assay and presented as a mean (95% CI) percentage of the control (0.5% DMSO). The IC50 is 100.1µM with the scrambled siRNA transfection, and 49.8µM following NQO1 knockdown. Statistical significance was achieved as follows: *p<0.05, **p<0.01, ***p<0.001.

An increase in chemosensitivity was seen following knockdown of NQO1 when compared to the scramble siRNA transfection, reaching statistical significance at 25µM (p=0.038), 50µM (p=0.002), 100µM (p=<0.001), 200µM (p=0.004) and 400µM (p=0.001) doses of irinotecan. The IC50 is 100.1µM with the scrambled siRNA transfection, and 49.8µM following NQO1 knockdown.

The effect of NQO1 knockdown by siRNA transfection on chemosensitivity to 5-FU can be seen in Figure 6.25.

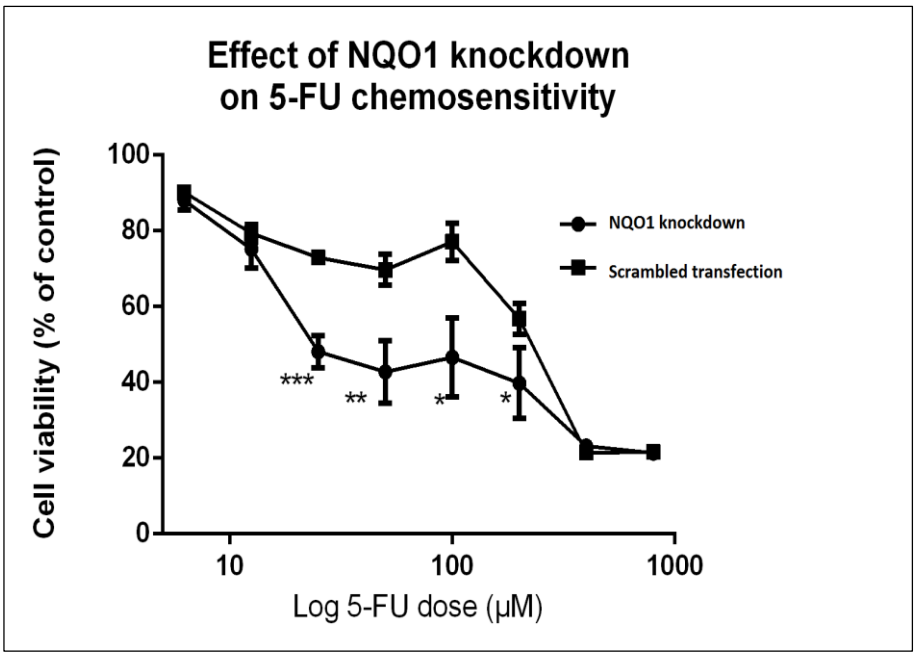

Figure 6.25 – Dose response analysis for 5-FU in the SW480 cell line with and without knockdown of NQO1 by siRNA transfection. Cells were incubated for 72 hours and cell viability assessed using the MTS assay and presented as a mean (95% CI) percentage of the control (0.5% DMSO). The IC50 is 200.1µM with the scrambled siRNA transfection, and 25.0µM following NQO1 knockdown. Statistical significance was achieved as follows: *p<0.05, **p<0.01, ***p<0.001.

An increase in chemosensitivity was seen following knockdown of NQO1 when compared to the scramble siRNA transfection, reaching statistical significance at 25µM (p=<0.001), 50µM (p=0.007), 100µM (p=0.010) and 200µM (p=0.044) doses of 5-FU. The IC50 is 200.1µM with the scrambled siRNA transfection, and 25.0µM following NQO1 knockdown.

6.3.9 Evaluating dicoumarol as an inhibitor of NQO1 and chemosensitiser

The effect of dicoumarol on SW480 cell viability

The effect of dicoumarol alone on cell viability can be seen in Figure 6.26. The effects are negligible, with no significant difference between doses.

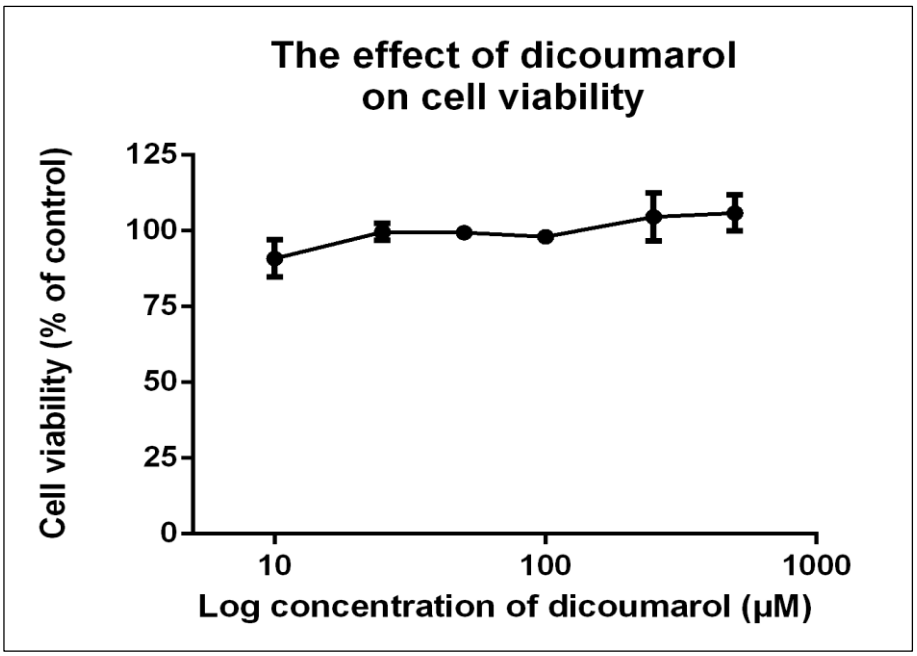

Figure 6.26 - Dose response analysis for dicoumarol in the SW480 cell line. Cells were incubated for 4 hours and cell viability assessed using the MTS assay and presented as a mean (95% CI) percentage of the control (media only).

Establishing the optimum concentration of dicoumarol

The maximal effective concentration for dicoumarol was calculated by pre-treating cells for 4 hours prior to incubation in irinotecan for 72 hours (Figure 6.27).

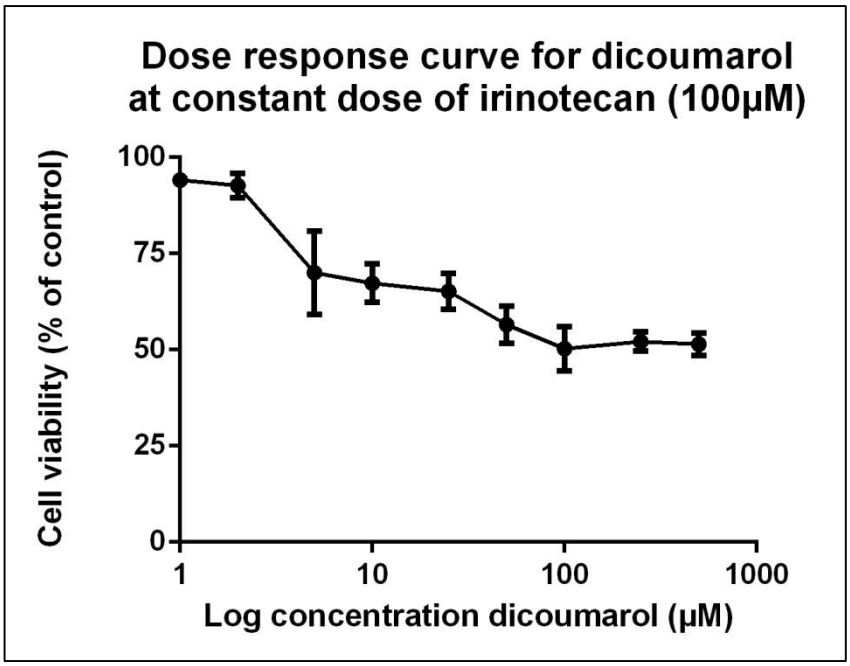

Figure 6.27 – The effect of pre-treating cells with dicoumarol prior to incubation with 100µM irinotecan. Cell viability is expressed as a percentage of control (0.5% NaOH only followed by irinotecan). The maximum effect was achieved at a dicoumarol dose of 100µM.

In these experimental conditions, the maximal effective concentration was ~100µM, and therefore this dose was used for subsequent investigations. Similar data were also seen following incubation with 5-FU.

Attributing the effects of dicoumarol to NQO1 activity

Treatment with dicoumarol following siRNA knockdown of NQO1 was performed to establish whether dicoumarol may be exerting its pharmacological effect via another pathway.

The results for irinotecan dosing can be seen in Figure 6.28. When comparing the NQO1 knockdown with irinotecan only, similar data to that previously described are seen. Negligible differences are seen between the 'knockdown' and 'knockdown and dicoumarol' experimental arms, and analysis with the student's un-paired t-test showed no significant difference at any data points. As such, dicoumarol does not appear to have any effect on chemosensitivity in cells not-expressing NQO1. Similar data were also seen following 5-FU incubation.

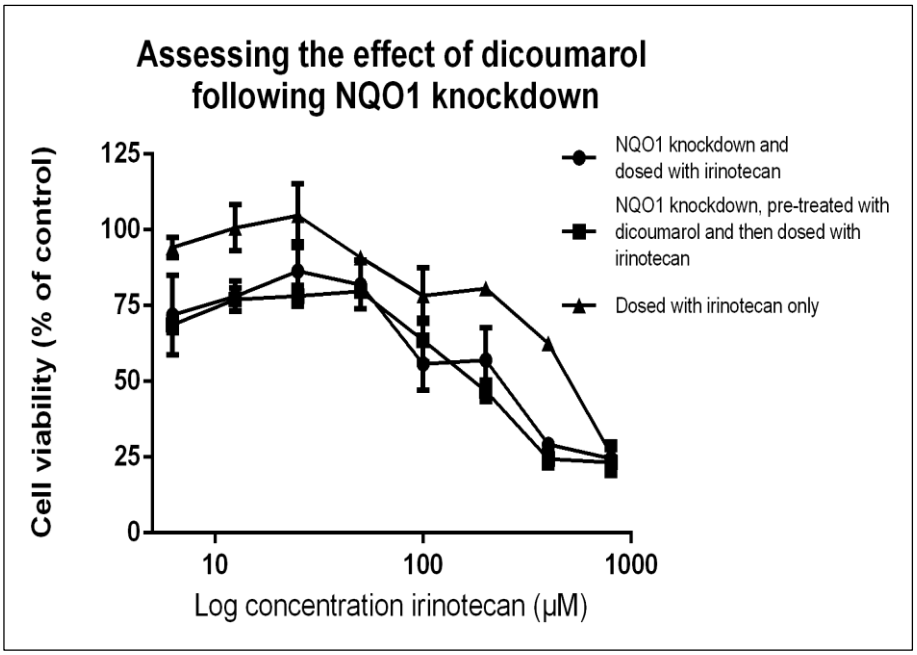

Figure 6.28 - Dose response analysis for irinotecan in the SW480 cell line firstly showing the effect of NQO1 knockdown by siRNA transfection, and secondly the absence of any additional biological effect following dicoumarol pre-treatment in those cells not expressing NQO1. Cells were incubated for 72 hours and cell viability assessed using the MTS assay and presented as a mean (95% CI) percentage of the control (scrambled siRNA transfection, pre-treatment with 0.5% NaOH and incubation in 0.5% DMSO).

Effect of NQO1 inhibition on chemosensitivity by pre-treating cells with dicoumarol

To establish the effect of NQO1 inhibition with dicoumarol on chemosensitivity, cells were pre-treated with 100µM dicoumarol prior to being dosed with irinotecan. Results are shown in Figure 6.29.

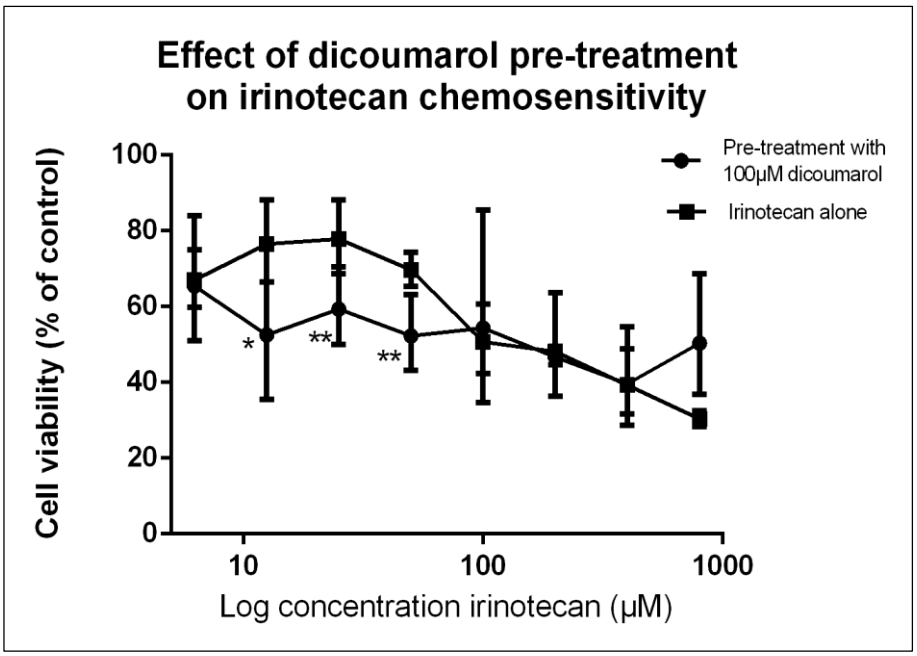

Figure 6.29 – Dose response analysis for irinotecan in the SW480 cell line with and without pre-treatment with dicoumarol. Cells were incubated for 72 hours and cell viability assessed using the MTS assay and presented as a mean (95% CI) percentage of the control (0.5% NaOH followed by 0.5% DMSO). The IC50 is 100.0µM for irinotecan alone, and 50.0µM following NQO1 inhibition with dicoumarol. Statistical significance was achieved as follows: *p<0.05, **p<0.01, ***p<0.001.

An increase in chemosensitivity was seen following inhibition of NQO1 with dicoumarol compared to the control, reaching statistical significance at 12.5µM (p=0.013), 25µM (p=0.005), and 50µM (p=0.002) doses of irinotecan. The IC50 is 100.0µM for irinotecan alone, and 50.0µM following NQO1 inhibition with dicoumarol. The experiment was repeated with 5-FU, with the results shown in Figure 6.30.

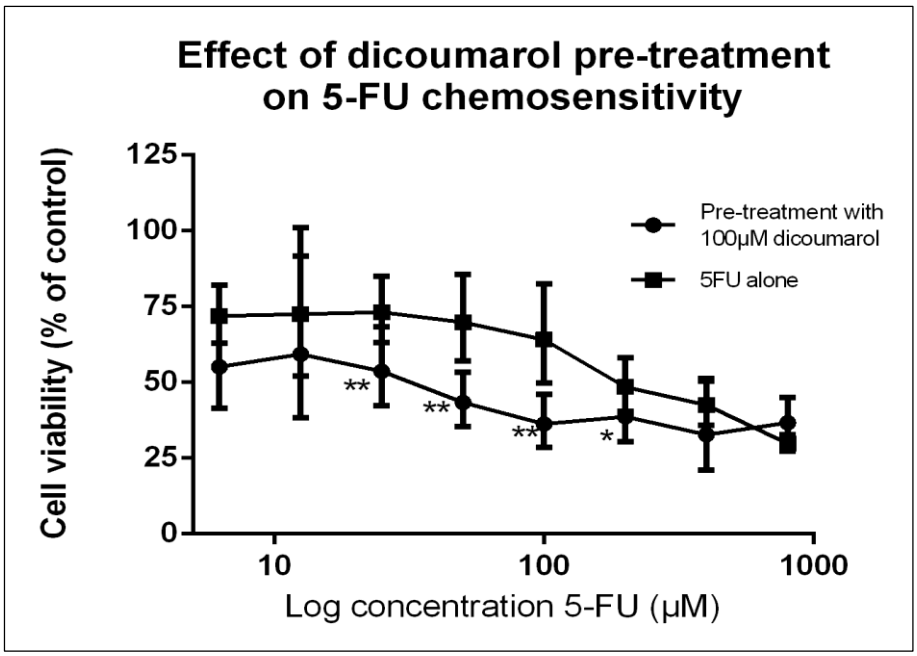

Figure 6.30 – Dose response analysis for 5-FU in the SW480 cell line with and without pre-treatment with dicoumarol. Cells were incubated for 72 hours and cell viability assessed using the MTS assay and presented as a mean (95% CI) percentage of the control (0.5% NaOH followed by 0.5% DMSO). The IC50 is 183.7µM for 5-FU alone, and 49.9µM following NQO1 inhibition with dicoumarol. Statistical significance was achieved as follows: *p<0.05, **p<0.01, ***p<0.001.

An increase in chemosensitivity was seen following inhibition of NQO1 with dicoumarol compared to the control, reaching statistical significance at 25µM (p=0.008), 50µM (p=0.002), 100µM (p=0.003) and 200µM (p=0.030) doses of 5-FU. The IC50 is 183.7µM for 5-FU alone, and 49.9µM following NQO1 inhibition with dicoumarol.

6.4 Discussion

6.4.1 Summary of aims

The aim of this investigation was to further explore the potential for utilising biological information from the primary tumour to inform and predict response to treatment for the liver metastases using a targeted approach of previously identified markers of interest. Specific hypotheses were formulated relating to protein expression and activity levels of proteins relevant to the activation and metabolism of chemotherapeutics as well as the concordance between primary and metastatic tumours of *KRAS, BRAF* and MSI status.

The main objective of this investigation, however, was to validate the findings of the proteomic work previously undertaken and progress our understanding of the role of NQO1 as a predictive biomarker of treatment response. This entailed a direct comparison of the iTRAQ data by western blotting and validation of these findings in a larger tissue set. The finding that NQO1 levels are reduced in those tumours responding to chemotherapy also prompted the investigation of its role as a potential drug target.

6.4.2 Summary of results – patient matched clinical samples

Western blotting for the proteins of interest with respect to the activation and metabolism of key chemotherapeutics (TS, DPYD, OPRT, CES1, CES2, TOPI, UGT1A1, CYP3A4 and DNA POL β) all showed a positive correlation in expression between primary and metastatic tumours, although this only reached statistical significance for TOP I ($p=0.009$). Given the variation in neoadjuvant treatment regimens received by these patients no response analysis was considered feasible.

Mass spectrometry analysis of CES1/CES2 activity (by irinotecan conversion to SN-38) showed significant differences across primary tumour, metastatic tumour and liver parenchyma ($p=0.001$). When analyses were made for individual patients, all except 2 had statistically significant differences in the CES1/CES2 activity in the primary tumour, metastatic tumour and liver parenchyma. When interrogating the data pertaining to the primary and metastatic tumour only, all patients except 4 had statistically significant differences between protein activity levels at the two disease sites. As such the activity of

carboxylesterase in the primary tumour does not predict that in the metastasis, and neither correlate well with activity in the liver parenchyma.

Pyrosequencing for *KRAS* and *BRAF* mutations identified the *KRAS* codon 12 mutation in 5 patients with 100% concordance between primary and metastatic tumours and no mutation similarly detected in the adjacent normal colonic mucosa. No mutations were seen in codons 13 or 61. One patient had *BRAF* mutation in both codons (600 and 601) again with concordance between primary and metastatic tumours. One patient had microsatellite instability, which was detected in the colonic mucosa as well as the primary and metastatic tumours. Given the low numbers of mutations detected and the heterogeneity in the neoadjuvant treatment regimens received, no analysis of correlation with response was feasible.

Western blotting for NQO1 was used to validate the iTRAQ proteomic data reported in Chapter 4. Correlation of protein expression by western blotting densitometry and iTRAQ abundance data showed a statistically significant positive correlation ($r=0.59$, $p=0.003$). Having confirmed the validity of the original proteomic data the investigation was expanded to validate these findings in a larger tissue set.

Of the 56 patients for whom patient matched primary and metastatic FFPE blocks were available, 37 received neoadjuvant treatment. Fourteen of these patients responded to chemotherapy (TRG1-2), 23 did not (TRG3-4). Comparing clinicopathological features between groups revealed a higher proportion of T4 tumours in the chemonaive group ($p=0.017$), most likely reflecting a clinical preference for prompt surgery in this patient cohort. No other potentially confounding variables were different between groups. A statistically significant positive correlation between immunohistochemical protein expression in the primary and metastatic tumours was seen ($r=0.44$, $p=0.001$). NQO1 expression in the primary tumour was not statistically significantly different between responders and non-responders ($p=0.470$), however expression in the metastases was considerably lower in those patients responding to chemotherapy ($p=0.041$), mirroring the conclusion of the proteomic data.

6.4.3 Summary of results – in vitro model of colorectal cancer

Under the experimental conditions studied, the IC50 for irinotecan and 5-FU in the SW480 cell line was 90.2μM and 202.2μM respectively. Western blotting for NQO1 after treating cells with chemotherapy demonstrated no effect on protein expression. Knockdown of NQO1 with siRNA had no direct effect on cell viability. Knockdown of NQO1 followed by treatment with irinotecan reduced the IC50 from 100.1μM to 49.8μM, with statistically significant differences at doses between 25-400μM. Similarly with respect to 5-FU, NQO1 knockdown reduced the IC50 from 200.1μM to 25.0μM, with statistically significant differences at doses between 25-200μM.

Dosing cells with dicoumarol alone had no effect on cell viability. When cells were pre-treated with dicoumarol over a range of doses prior to incubation with a chemotherapeutic, a reduction in cell viability was seen which reached its maximal effectiveness at ~100μM. Cells in which NQO1 had been knocked down with siRNA experienced no further reduction in viability by the addition of dicoumarol, suggesting this drug is acting by inhibition of NQO1 rather than through an alternative pathway. Pre-treating cells with dicoumarol prior to incubation in irinotecan reduced the IC50 from 100.0μM to 50.0μM, with statistically significant differences at irinotecan doses between 12.5-50μM. Similarly with respect to 5-FU, inhibition of NQO1 with dicoumarol reduced the IC50 from 183.7μM to 49.9μM, with statistically significant differences at 5FU doses between 25-200μM.

6.4.4 NQO1 as a chemosensitiser

The role of the NQO1 protein as a biomarker has already been discussed in Section 4.4.5. Two polymorphisms of NQO1 however have been well defined and characterised. The NQO1*2 polymorphism is a C609T substitution (on 16q) resulting in a proline to serine substitution at amino acid 187. The resulting protein is inactive, and therefore homozygotes (up to 40% of the population) are NQO1 null with heterozygotes demonstrating reduced activity (Traver *et al*, 1992). The less common (0.05%) NQO1*3 polymorphism is a C465T substitution resulting in an arginine to tryptophan amino acid change. This variant however is similar to the wildtype and is catalytically active but with major differences in the rate of metabolism of quinone substrates (Pan *et al*, 1995). Given that NQO1 activity and protein expression could potentially be rapidly induced by a host of dietary and other factors, genotyping patients for the NQO1*2 polymorphism may be more clinically beneficial than immunostaining if it were to be further considered as a predictive biomarker.

The *in vitro* data from this study confirms the likelihood that the NQO1 expression levels seen in the proteomic study are determined by the phenotype of the tumour rather than an effect of treatment with chemotherapy. Furthermore, the immunohistochemical analysis suggests that the primary tumour is predictive of the metastatic phenotype and confirms the findings of reduced expression in chemo-responsive metastases. Knockdown of this protein alone (with siRNA or dicoumarol) had no effect on cell viability, and therefore its potential therapeutic role is as a chemosensitiser rather than a cytotoxic.

In common with many other cytoprotective proteins, NQO1 is transcriptionally regulated through the Keap1-Nrf2 pathway. Under normal conditions Nrf2 (nuclear factor (erythroid-derived 2)) is sequestered in the cytoplasm physically bound to Keap1 (Kelch-like ECH-associated protein 1). Inducers of the pathway, which may be endogenous or exogenous, interact with cysteine residues of Keap1 rendering it unable to target Nrf2 for degradation. Consequently Nrf2 is stabilised and subsequently translocates to the nucleus (Figure 6.31). Here it dimerises with a number of transcription factors and the heterodimer binds to the antioxidant response elements (ARE) of a number of genes thus activating transcription (Bataille and Manautou, 2012).

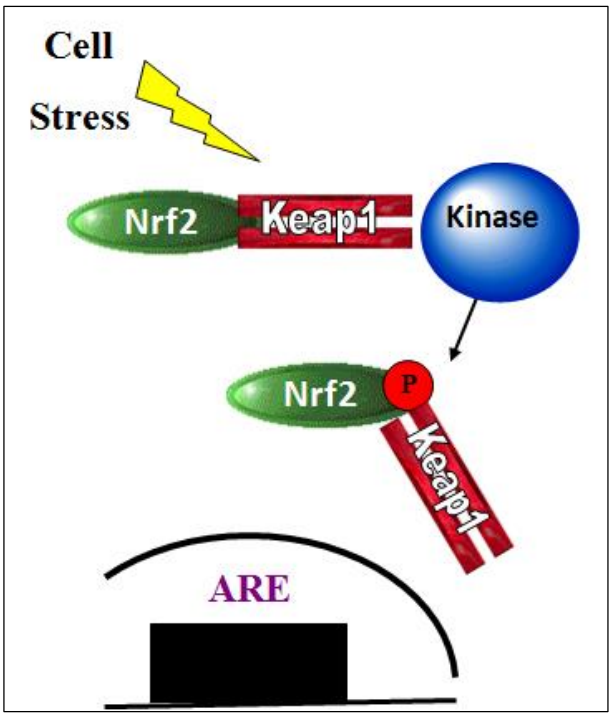

Figure 6.31 - Nrf2 is bound to Keap1 until pathway activation causes its stabilisation. Nrf2 subsequently translocates to the nucleus where it dimerises with a number of transcription factors and the heterodimer binds to the antioxidant response elements of a number of genes thus activating transcription. Adapted from Bataille and Manautou (2012).

NQO1 is a multifunctional antioxidant enzyme and exceptionally versatile cytoprotector. The cytosolic enzyme catalyses the beneficial two-electron reduction of quinines to hydroquinones, reducing the formation of reactive oxygen species (Lind *et al*, 1990). This mechanism of action explains the reductive activation of chemotherapeutic quinines such as mitomycins and aziridinyl-benzoquinones, but not those studied in this investigation (Siegel *et al*, 1990). The hydroquinones derived from these agents are more chemically reactive and produce reactive species which kill malignant cells, and therefore if acting through this or a similar mechanism we would expect to see high levels of NQO1 in patients responding to chemotherapy.

So if inhibition of NQO1 is not directly increasing the efficacy of the chemotherapeutic agent by biochemical modulation, it may be inhibiting the cytoprotective features of the cells and rendering them more susceptible to chemotherapy through a mechanism other than its enzymatic activity. NQO1 appears to exert cytoprotective effects through another

mechanism, by regulating the proteasomal degradation of specific proteins. NQO1 has been shown to regulate the ubiquitin-independent 20S proteasomal degradation of p73α (Asher *et al*, 2005), p33 (Garate *et al*, 2008) and perhaps of most relevance p53. In 2001, Asher *et al* reported that NQO1 inhibits the degradation of p53 in HCT-116 cells, and exposure to an inhibitor of NQO1 enhances p53 proteasomal degradation. This degradation appears to be most prominent under conditions of oxidative stress, and independent of both Mdm-2 and ubiquitin (Gong *et al*, 2007).

We report low levels of NQO1 in chemoresponsive tumours, both in clinical samples and following manipulation in *in vitro* studies, potentially therefore associated with enhanced degradation of p53. Whilst some studies have reported that p53 is necessary for efficient execution of the death programme following treatment with chemotherapeutics and that increased expression causes chemosensitivity by promoting apoptosis (Lowe *et al*, 1993), others have suggested that p53 inhibition actually improves response to chemotherapy. If apoptosis is suppressed, a frequent finding in tumour cells, the residual functions of p53 (growth arrest at cell cycle checkpoints and modulation of DNA repair) may contribute to cells surviving anticancer treatment (Xu, Mymryk and Cairncross, 2005). Browder *et al* (2000) treated p53-null and p53-WT mouse xenografts with a chemotherapeutic regimen, demonstrating increased efficacy in the p53-null mice and concluding that p53 is playing a protective role. A similar protective role is observed in the epithelium of the small intestine following γ irradiation, where p53 is suggested to allow cells to reside in a growth arrested state thus reducing the risk of a mitotic catastrophe (Gudkov and Komarova, 2003).

Whether or not the observed effects of NQO1 inhibition are a result of its catalytic activity, p53 stabilisation, regulation of the proteasomal degradation of another protein or an entirely different mechanism has not been answered by this investigation and should be the subject of further study.

6.4.5 Topoisomerase I

A large randomised control trial comparing 5FU with 5FU and irinotecan demonstrated that high expression of TOP I measured by immunohistochemistry correlated with responsiveness to treatment (HR 0.98; 95% CI 0.78 – 1.22) (Braun *et al*, 2008). A similar trial from Dutch Colorectal Cancer Group however failed to replicate these findings, with no association seen between TOP I expression and response to irinotecan (Koopman *et al*,

2007). The concordance we have found between expression at different disease sites is novel, and contradictory to the evidence presented by Boonsong *et al* (2002) who found no concordance between the expression in primary tumour and lymph node metastases. There is clearly conflicting evidence both in terms of concordance of expression across disease sites and the potential for its use as a biomarker, however it is clear that TOP I is worthy of further investigation.

6.4.6 Strengths and limitations of the study

Undertaking investigations on clinical samples has brought the known challenges of small numbers and a diverse patient population, resulting in difficulty drawing accurate scientific conclusions. The issues surrounding the relevance of tumour heterogeneity and clonal selection on biomarker studies such as these have already been discussed in previous chapters.

The *in vitro* cancer model used shares the same advantages and disadvantages of all in vitro experimental models. The complexities of an organism are simplified to basic functions, allowing the investigator to focus on and manipulate a small number of conditions (Vignais, 2010). In this study, for example, it has allowed the manipulation of a single protein's expression using siRNA which would prove challenging in alternative models of cancer. Conversely, investigators must be wary about their conclusions and the potential difficulties in extrapolating data back to the intact organism. This is particularly true for drug-based studies such as these where issues of drug formulation and delivery, pharmacokinetics and toxicity have not been studied (De Clercq, 2005).

The strengths of this study, and in particular the work examining NQO1, is that it has arisen from, validates and builds on the iTRAQ proteomic data described in Chapter 4. NQO1 was identified through an unbiased shotgun proteomic screen and has now been validated in a larger tissue set as a predictive biomarker of chemoresponsiveness. Moreover, investigations into its potential use as a novel drug target have begun. The quality of the western blot for NQO1 protein and the well-demonstrated knockdown achieved with siRNA lead us to a degree of confidence in these findings.

6.4.7 Future work

With respect to the analysis of patient matched tissues for expression of proteins involved in the activation and metabolism of chemotherapeutics, very little can be conclusively stated given the small number of patients studied and also the heterogeneity of the treatment regimens received by the patients. To address the hypothesis of whether protein expression in the primary tumour predicts the metastatic phenotype, a sensible next step would be immunostaining the TMA constructed within this study for these proteins. To answer questions related to the potential use of these proteins as response biomarkers, a more homogenous population would need to be defined and studied. Given the difficulty in acquiring primary and metastatic tissue which was encountered for this study, the most efficient way to accomplish this is likely to be its incorporation as a translational arm in a clinical trial.

Similarly with regards to protein activity, a larger and more homogenous population is required. The mass spectrometry assay used for this study is reliant upon tissue homogenate, and therefore a method of extracting protein from FFPE blocks which is suitable for other proteomic studies besides immunohistochemistry is required. This work has already commenced with a comparison of two techniques, one reported by Scicchitano *et al* (2009) and the commercially available Qproteome FFPE tissue kit (Qiagen, Venlo, Netherlands).

Cancer Research UK published a roadmap to assist clinicians and scientists in bringing biomarker studies to a clinically useful endpoint. As such, the next steps to further evaluate NQO1 as a predictive biomarker would be:

- Developing and refining a reproducible assay
- Defining biomarker distribution in the target population and subsequently validating the assay
- Studying the relationship between the biomarker and clinical outcome retrospectively
- Defining the relationship of the biomarker to clinical outcome in a prospective analysis of a retrospective tissue collection
- Validating the correlation between the biomarker and clinical outcome as a primary or secondary endpoint in a prospective study
- Undertaking a clinical trial where the biomarker defines randomisation

To some extent this study has addressed many of these issues, although to drive this work forwards there would be need for the early development of an alternative strategy for assaying the protein or exploring the option for genotyping. As previously discussed, incorporating this work as a translational arm into a prospective clinical trial would address many of the problems encountered in this study.

The work presented in this thesis confidently identifies NQO1 as a therapeutic target, although the evidence for the use of dicoumarol as a competitive inhibitor is somewhat lacking. This is largely a result of difficulties encountered in attributing the effect of dicoumarol to NQO1 inhibition. As previously discussed the approach taken with the complementary siRNA inhibition provides some circumstantial evidence, although this is insufficient. Since the commencement of this project, Mitosciences® (Oregon, USA) released a series of microplate kits which are essentially a sandwich-ELISA for immunocapture of the protein combined with a measurement of substrate/product turnover to generate specific activity data. One of these plates is for NQO1, the activity of which is determined following the simultaneous reduction of menadione (with NADH as a cofactor) and WST1 (a cell proliferation reagent) which leads to increased absorbance at 440nm. This would be the essential next step in determining whether dicoumarol is exerting the observed effects via this pathway, although it would be unhelpful unless the cytoprotective effects we are inhibiting are related to the enzymatic activity of the protein. Other *in vitro* work which would potentially be of interest would be the co-incubation of dicoumarol with the chemotherapeutic rather than the pre-treatment approach opted for in this study, and repeating the investigation in a p53-deficient cell line.

Beyond establishing reduced NQO1 activity, to further evaluate the chemosensitising effects of NQO1 inhibition it would be necessary to transfer to an *in vivo* model. A simple xenograft model would provide useful scientific information and allow tumour measurements to be compared into two animal cohorts: chemotherapeutic drug(s) *vs.* chemotherapeutic drug(s) and dicoumarol. To properly test the hypothesis in the metastatic setting however the most suitable model would be surgical orthotopic implantation, reported to reliably produce liver metastases in 100% of mice after 11 passages (Sun *et al*, 1999).

6.4.8 Conclusion

We have convincingly demonstrated concordance between the primary and metastatic tumour for Topoisomerase I expression. *KRAS, BRAF* and MSI status also appear concordant although numbers of mutations detected in this regard were small.

Western blotting for NQO1 validated the proteomic data set and the conclusions drawn in Chapter 4. Immunohistochemical analysis has demonstrated that with respect to NQO1 the primary tumour is predictive of the metastatic phenotype. Furthermore, NQO1 expression in the metastatic tumour is lower in those patients responding favourably to neoadjuvant chemotherapy.

In vitro work has suggested that this finding is a biological feature of the tumour rather than a phenomenon seen as a result of treatment with chemotherapeutics. Knockdown of this protein alone had no effect on cell viability, and therefore the potential therapeutic role of NQO1 is as a chemosensitiser rather than a cytotoxic. Indeed knockdown of NQO1 with siRNA considerably improved chemosensitivity to both irinotecan and 5-FU in an *in vitro* model.

Dicoumarol, a known inhibitor of NQO1, has shown potential for its use in this regard. Pre-treatment of cells with dicoumarol again improved chemosensitivity to both irinotecan and 5-FU in the same *in vitro* model, although evidence to suggest it is exerting the observed effect through NQO1 inhibition is circumstantial.

Further evaluation of these findings in a larger and more homogenous population, for example in the context of a clinical trial, is necessary. Attributing the effects of dicoumarol to NQO1 inhibition is also necessary prior to any further translational work, the next step for which would be transfer to an *in vivo* model.

Chapter 7

Concluding Discussion

7.1 Summary of aims and experimental design

The starting point for the thesis was the identification of three key questions faced by clinicians treating patients with colorectal cancer on a daily basis, which as yet have no satisfactory scientific explanation or rationale for the selection of one particular course of action. These questions are:

- In patients with rectal cancer is it possible to predict response to neoadjuvant chemoradiotherapy?
- In patients with colorectal liver metastases is it possible to predict response to neoadjuvant chemotherapy?
- Can biological information from the primary tumour be used to predict response to treatment in colorectal liver metastases?

In order to investigate these research questions, the following study plan was implemented:

1. Establish a research network across multiple sites to facilitate the collection of patient matched primary and metastatic tissue, as well as serial biopsies of rectal tumours. Establish a research protocol and a satisfactory means of tissue collection.

2. Subject tumour samples (alongside normal adjacent tissue) from patients undergoing synchronous resection to exome sequencing, in order to establish the degree of biological similarity between primary and metastatic tumours, and specifically to identify whether the presence of somatic non-synonymous mutations in the primary tumour predicts the presence of the same mutations in the liver metastasis.

3. Perform an unbiased assessment of the proteome of patient-matched primary and metastatic tumours, as well as adjacent normal liver parenchyma and colonic mucosa on a discovery set of fresh tissue. Analyse data to assess the degree of biological similarity between primary and metastatic tumours, as well as identify potential biomarkers measurable in the primary tumour which may predict the response to chemotherapy in the liver metastases.

4. Validate any potential biomarkers by immunohistochemistry on a larger validation tissue set, with samples combined into a tissue micro-array. Explore any potential mechanisms for validated biomarkers.

5. Perform an unbiased assessment of the proteome of serial rectal cancer samples on a discovery set of fresh tissue. Analyse data to assess how the tumour phenotype changes with treatment, as well as identify potential biomarkers which may predict response of the primary tumour to neoadjuvant chemoradiotherapy.

6. Validate any potential biomarkers by immunohistochemistry on a larger validation tissue set, with samples combined into a tissue micro-array. Explore any potential mechanisms for validated biomarkers.

7. Undertake a targeted analysis of the expression and function of key proteins involved in the activation and metabolism of oxaliplatin, 5-fluorouracil and irinotecan in patient matched primary and metastatic tumour samples. Analyse data to assess the correlation in expression and function between primary and metastatic tumours and establish how this information may predict response to treatment.

8. Undertake a targeted analysis of the expression of key proteins involved in DNA base excision repair in serial rectal cancer samples. Data will be analysed to assess how levels of expression vary with treatment and how this information may be used to predict response.

The experimental plan was followed and completed with the exception of steps 6 and 8, the further evaluation of biomarkers and DNA base excision repair proteins in rectal cancer. These steps were purely omitted due to time constraints and remain valid lines of enquiry to address the research questions described above. Given the small numbers of samples collected, response analysis was not feasible for step 7.

7.2 Summary of results

Chapter 2 evaluated the use of a novel tissue stabilisation gel, Allprotect^{TM}. The study demonstrated that effective tissue stabilisation was achieved with Allprotect^{TM}, and that

tissue stabilised in this manner yields high quality DNA, RNA and protein suitable for commonly used laboratory techniques. Comparable protein (by western blot and immunohistochemistry) and mRNA expression for HMGB1 and CES1 in primary colorectal tumour and colorectal liver metastases was observed irrespective of the method of tissue stabilisation employed. Beyond that, the demonstration of comparable production of SN-38, an active metabolite of irinotecan, suggested that protein function (CES1) as well as expression is preserved. miRNA yield was also consistent and all extracted DNA was of sufficient quality for downstream PCR.

Whilst short term tissue stabilisation with Allprotect^{TM} appeared to be comparable to liquid nitrogen, its role for long term archiving was less clear. Our study suggested that both protein function and expression were significantly reduced by week 3, and, although densitometry values did not reach statistical significance, visualisation of the western immunoblots suggested that protein degradation may occur even earlier than this. RNA integrity also began to reduce after one week, with the RIN of samples rapidly falling below 7.0. These findings were confirmed by the RT2 quality control array, and the increasing Ct values seen by qPCR for both mRNA and miRNA.

Chapter 3 reported the exome sequencing of 4 simultaneously resected primary and metastatic tumours alongside normal colonic mucosa and liver parenchyma. Of the 585 unique non-synonymous, missense SNVs identified, 215 (36.8%) were unique to the primary tumour, 226 (38.6%) unique to the metastasis, and 81 (13.8%) present in at least one primary and metastatic tumour pertaining to the same patient. The remaining 63 (10.8%) were neither unique to a tissue type nor present in a pair of samples from the same patient. 268 (45.8%) predicted favourable response, whilst 226 (38.6%) predicted poor response. Of those, 43 and 23 respectively were present in patient-matched samples. The remaining 91 (15.6%) were neither unique to responders nor non-responders.

The ErbB signalling pathway was identified as the most significant pathway arising from the analysis of SNVs in paired patient samples, with 6 (*KRAS, MAP2K3, PAK2, PIK3C2G, PLCG2, RRAS*) of the 85 pathway genes containing SNVs (Ratio 0.07, $p=5.87 \times 10^{-7}$). Sanger sequencing validated the CDAN1_15_43020983_G/A SNV as a potential predictor of favourable response, where the primary tumour is predictive of the metastatic genotype. For the 6 SNVs of interest in the ErbB pathway, 4 showed absolute concordance between

the primary and metastatic genotype (those in *MAP2K3, PIK3C2G, PLCG2 and RRAS*) thus validating the results of the Ion Proton exome sequencing.

Chapter 4 reported the results of the isobaric tagging for relative quantification in patient matched primary and metastatic tissues. Of the 16 patients sampled, 11 had undergone neoadjuvant chemotherapy 10 of which achieved resection. Five of these patients had a tumour regression grade of 1-2 and the remaining 5 had a tumour regression grade of 3-4. A total of 5766 proteins were identified, of which 2637 were taken forwards for bioinformatics analysis. Comparing primary tumour with normal colon, 25 proteins were significantly differentially expressed (6 upregulated and 19 downregulated) and for metastatic tumour compared with normal colon there were 53 differentially expressed (13 upregulated and 40 downregulated). Comparison of the metastatic tumour with liver parenchyma identified 444 proteins differentially expressed, 164 of which were upregulated and 280 downregulated. Only 67 of the 2637 (2.54%) proteins studied were significantly different between primary and metastatic tissue, with 58 upregulated in the metastatic tumour and 9 downregulated. One hundred and seventy proteins were identified in the primary tumour which were significantly differentially expressed between responders and non-responders with 59 upregulated and 111 downregulated in the responders. In the metastases, there were 27 differentially expressed (17 upregulated and 10 downregulated). Five proteins were common to both tissue types, only two of which showed consistent dysregulation between responders and non-responders (NAD(P)H dehydrogenase [quinone 1] and lambda-crystallin homolog). Of the 5766 proteins identified by iTRAQ, SNVs were previously identified in the protein coding region of 2627.

Chapter 5 reported the results of the isobaric tagging for relative quantification in serial rectal cancer biopsies. A total of 3359 proteins were identified all of which were subjected to bioinformatics analysis. When comparing the post chemoradiotherapy samples with the diagnostic biopsies 18 proteins were significantly dysregulated, 2 of which were downregulated and 16 upregulated. Comparing the samples at resection with post chemoradiotherapy samples identified 39 proteins dysregulated, 30 of which were downregulated and 9 upregulated. Similarly a comparison of the resection and diagnostic samples identified 29 proteins, 10 of which were downregulated and 19 upregulated. The base excision repair pathway was the most significantly downregulated pathway in this analysis as a result of a reduction in PARP1 abundance with treatment. Eight candidate biomarkers were identified in the primary tumours which appeared to predict response to

chemoradiotherapy, 3 of which were downregulated and 5 upregulated. The most statistically significantly downregulated pathway was ceramide degradation as a result of low expression of acid ceramidase in those patients responding favourably to chemoradiotherapy.

Chapter 6 reported the targeted analysis of previously identified biomarkers of interest. Western blotting of those proteins relevant to the activation and metabolism of key chemotherapeutics (TS, DPYD, OPRT, CES1, CES2, TOPI, UGT1A1, CYP3A4 and DNA POL β) all showed a positive correlation in expression between primary and metastatic tumours, although this only reached statistical significance for TOP I (P=0.009). Mass spectrometry analysis of CES1/CES2 activity (by irinotecan conversion to SN-38) showed significant differences across primary tumour, metastatic tumour and liver parenchyma (p=0.001). All patients except 4 had statistically significant differences between protein activity levels at the primary and metastatic disease sites.

Pyrosequencing for *KRAS* and *BRAF* mutations identified the *KRAS* codon 12 mutation in 5 patients with 100% concordance between primary and metastatic tumours and no mutation similarly detected in the adjacent normal colonic mucosa. No mutations were seen in codons 13 or 61. One patient had *BRAF* mutation in both codons (600 and 601) again with concordance between primary and metastatic tumours. One patient had microsatellite instability, which was detected in the colonic mucosa as well as the primary and metastatic tumours.

Western blotting for NQO1 was used to validate the iTRAQ proteomic data reported in Chapter 4. Correlation of protein expression by western blotting densitometry and iTRAQ abundance data showed a statistically significant positive correlation (r=0.59, p=0.003), and therefore the findings were investigated by immunohistochemistry. Of the 56 patients for whom patient matched primary and metastatic FFPE blocks were available, 37 received neoadjuvant treatment. Fourteen of these patients responded to chemotherapy (TRG1-2), 23 did not (TRG3-4). Comparing clinicopathological features between groups revealed a higher proportion of T4 tumours in the chemo-naive group (p=0.017), most likely reflecting a clinical preference for prompt surgery in this patient cohort. No other potentially confounding variables were different between groups. A statistically significant positive correlation between immunohistochemical protein expression in the primary and metastatic tumours was seen (r=0.44, p=0.001). NQO1 expression in the primary tumour

was not statistically significantly different between responders and non-responders (p=0.470), however expression in the metastases was considerably lower in those patients responding to chemotherapy (p=0.041), mirroring the conclusion of the proteomic data.

Functional investigation of these findings in an *in vitro* model demonstrated that treating cells with chemotherapy had no effect on protein expression, and that knockdown of NQO1 with siRNA had no direct effect on cell viability. Knockdown of NQO1 followed by treatment with irinotecan reduced the IC50 from 100.1μM to 49.8μM, with statistically significant differences at doses between 25-400μM. Similarly with respect to 5-FU, NQO1 knockdown reduced the IC50 from 200.1μM to 25.0μM, with statistically significant differences at doses between 25-200μM. Dosing cells with dicoumarol alone had no effect on cell viability. When cells were pre-treated with dicoumarol over a range of doses prior to incubation with a chemotherapeutic, a reduction in cell viability was seen which reached its maximal effectiveness at ~100μM. Cells in which NQO1 had been knocked down with siRNA experienced no further reduction in viability by the addition of dicoumarol, suggesting this drug is acting by inhibition of NQO1 rather than through an alternative pathway. Pre-treating cells with dicoumarol prior to incubation in irinotecan reduced the IC50 from 100.0μM to 50.0μM, with statistically significant differences at irinotecan doses between 12.5-50μM. Similarly with respect to 5-FU, inhibition of NQO1 with dicoumarol reduced the IC50 from 183.7μM to 49.9μM, with statistically significant differences at 5FU doses between 25-200μM.

7.3 Advances in the literature

Since the commencement of this thesis the only significant developments in the literature have been the publication of 3 papers in 2014 reporting next generation sequencing of patient matched primary and metastatic colorectal tumours. This reflects the significant increase in the availability of this technology coupled with the associated reduction in cost.

Xie *et al* (2014) performed whole genome sequencing of patient matched primary and metastatic colorectal tumours. Comparing the data to germline DNA they characterised somatic alterations including single nucleotide variants, insertions and deletions, copy number aberrations and structural alterations. The focus of the analysis was to identify those novel mutations in the metastasis which may be drivers of disease progression, as both patients were chemo-naive and simultaneously resected. In both patients clones and

subclones of mutational clusters were identified. In one patient 75% of the mutations in the primary tumour were present in the metastasis, whereas the other patient had 95% of mutations also present in the metastasis. Having attempted to model clonal evolution, the authors conclude that this discrepancy occurred as a result of temporal differences in metastatic dissemination with respect to the evolution of the founding clone at the primary site. The proportion of somatic SNVs shared between primary tumour and liver metastasis were 68.4% and 52.8%, compared to 13.8% in our study. The authors focus their discussion on the concordance of TP53, APC and KRAS and highlight aberrations in FBXW7, DCLK1, FAT2 and PHF6 as being functional and exclusive to the metastases.

Brannon *et al* (2014) performed targeted sequencing of 230 key genes in 69 matched primary and metastatic tumours, alongside whole genome sequencing of 4 patients. Overall, 434 distinct non-synonymous somatic mutations were identified, with 79% concordance between primary and metastatic tumour. The analysis differs to the one we performed in that indels were also included. The authors focus their discussion on the absolute concordance of APC, KRAS, NRAS and BRAF mutations in their samples, concluding that these early carcinogenic mutations persist through tumour evolution. The authors attempted to correlate mutational concordance with key clinicopathological features but found no such association. The whole genome sequencing in this study was used to validate the concordance demonstrated by the capture-based assay used (IMPACT), and as such the two concordant samples were also concordant on whole genome sequencing (80% and 83%)and vice versa for the non-concordant samples (38% and 25%).

Lee *et al* (2014) performed exome sequencing of 15 patient matched micro-satellite stable primary and metastatic tumours. In total, 1079 and 4366 mutations were identified in the primary and metastatic tumours respectively. 60.8% of those mutations in the primary tumour were non-synonymous compared to 54.9% in the metastases. Whilst the data is available in supplementary information, the authors merely state that the findings were consistent with previous observations (Greenman *et al*, 2007) and not significantly different between primary and metastatic samples. No analysis is provided to justify this conclusion, and the remainder of the paper focuses on the parallel somatic copy-number alteration (SCNA) analyses.

Our data are complementary to these publications, and the finding of concordance in the SNVs within the ErbB family remains novel. The discrepancy in the proportion of mutations

concordant between primary and metastatic tumours may possibly be explained by the biopsy of clones/subclones within a tumour, but also the inclusion of other genetic aberrations (for example indels) included in the reported figures.

7.4 Study limitations and further work

The limitations of specific investigations and experimental techniques have been discussed throughout the thesis, however there are two key themes. Firstly the acquisition of fresh material from patient matched primary and metastatic tumours, as well as serial rectal tumour samples, was conducted prospectively within the study resulting in small numbers. Given the nature of the disease and the complexities involved in its management, there was also considerable heterogeneity both in clinicopathological features and treatment received. Secondly, whilst most tumours are thought to arise from a monoclonal population, its expansion combined with the acquisition of further mutations creates subclones and tumour heterogeneity. This heterogeneity clearly has significant implications for biomarker studies such as this which rely on a single tumour biopsy sample to be representative of the whole tumour (Poste, 2011). The first limitation could be addressed by incorporating this work as a translational arm in a clinical trial. The second is more challenging to address, and even though alternative (but non-translatable) strategies such as laser capture microdissection or the acquisition of circulating tumour cells may remove stromal contamination, they still fail to address this crucial problem (Curran *et al*, 2000).

The exome sequencing study has generated two lines of enquiry. The potential role of the SNV identified in the *CDAN1* gene should be explored by characterisation in a larger dataset, in parallel with an analysis of the ErbB pathway genes. The co-analysis of the exome and proteome datasets performed thus far has been rudimentary, and further integration would require super-specialist bioinformatic support.

By their very nature, studies which include sequencing of any form, proteomic or genomic, generate large amounts of data. In order to handle such volumes of data it is necessary to approach the analysis with a clear series of questions. The disadvantage of this approach is the potential to overlook key findings in the data. In this study for example the numerous pathway and network analyses are likely to provide key insights into carcinogenesis, disease progression and treatment response, however it has been necessary to select only a small number of findings from these preliminary studies for further analysis. Revisiting these

pathway and network analyses in conjunction with a literature review would very likely generate a number of research questions worthy of further work.

Evaluation of the base excision repair proteins relevant to radiotherapy response (PARP1, APE1, DNAPOL β and XRCC1) and the potential for the use of acid ceramidase as a biomarker and/or chemosensitiser requires further work and validation, although this proved unfeasible within the time constraints of this study. The next steps in the further evaluation of NQO1 as a biomarker have been recently highlighted in a roadmap by Cancer Research UK. Prior to exploring its role as a drug target in an *in vivo* model, further *in vitro* work to establish whether the effects seen by inhibiting NQO1 relate to its enzymatic activity, protein stabilisation function or another mechanism are necessary.

7.5 Review of hypotheses

A number of testable hypotheses were generated at the commencement of the thesis.

1. Somatic non-synonymous mutations in the primary tumour correlate with those present in the liver metastasis and predict response to treatment.

Disproved – only 13.8% of single nucleotide variants identified were concordant between primary and metastatic tumours in the small number of samples we studied.

2. The phenotype of the primary tumour is biologically similar to the liver metastasis, with markers present in the primary tumour which predict the response of the liver metastasis to neoadjuvant chemotherapy.

Proved - Only 67 of the 2637 (2.54%) proteins studied were significantly different between primary and metastatic tissue. NQO1 and lambda-crystallin homolog appeared to predict response to treatment. NQO1 levels in the primary tumour predict the metastatic phenotype, and low protein abundance in the metastatic tumour is associated with favourable treatment response. Inhibiting the protein (with siRNA or a competitive inhibitor) improved chemosensitivity in an *in vitro* model.

3. The phenotype of a rectal tumour changes with neoadjuvant chemoradiotherapy, and inter-patient variation in these changes predicts response to treatment.

Partially Proved – Only minor changes in tumour phenotype were detected with neoadjuvant chemoradiotherapy. The most statistically significantly downregulated pathway in those patients responding favourably to chemoradiotherapy was ceramide degradation as a result of low expression of acid ceramidase.

4. Levels of expression of key proteins involved in the activation and metabolism of chemotherapeutics are comparable between primary and metastatic tumours and predict response to treatment.

Partially Proved – All proteins studied had a positive correlation although this was only statistically significant for Topoisomerase I.

5. Levels of expression of DNA base excision repair proteins in rectal tumours vary with treatment, and inter-patient variation in the expression of these proteins predicts response to neoadjuvant chemoradiotherapy.

Inconclusive – This hypothesis was incompletely tested due to time constraints. iTRAQ data of serial rectal cancer samples did however suggest that base excision repair (and in particular PARP1) remains of interest in both carcinogenesis and treatment response.

7.6 Conclusions

This thesis has generated a number of lines of enquiry and ideas for further work as well as providing sufficient evidence to conclude the following:

- *AllprotectTM confers comparable tissue stabilisation* to liquid nitrogen for up to 1 week for the extraction and downstream laboratory analysis of DNA, RNA and protein.
- *Approximately one third of single nucleotide mutations identified are present exclusively in the primary tumour, one third are present exclusively in the metastases and one third are present in tumours at both sites.* In our data, only 13.8% of mutations were present in patient matched samples.
- *A SNV in the CDAN1 gene has potential to serve as a predictive biomarker*, with the presence of the SNV in the primary tumour predicting the metastatic genotype.

- SNVs across the *ErbB pathway appear to be concordant between primary and metastatic tumours*, and not limited to KRAS alone.
- *Only 2.54% of proteins are significantly differentially expressed between primary and metastatic tumours*. As such, it may be feasible to utilise biological information from the primary tumour to predict the phenotype of the metastasis.
- *Phenotypic changes induced by chemoradiotherapy in rectal cancers are modest*. Base excision repair (and in particular PARP1) remains of interest in both carcinogenesis and treatment response, and acid ceramidase is a potential novel response biomarker.
- *Topoisomerase I expression in the primary tumour correlates significantly with expression in colorectal liver metastases*. A positive correlation was also seen in other proteins responsible for the activation and metabolism of chemotherapeutics, as well as *KRAS, BRAF* and MSI status.
- *NQO1 expression in the primary tumour is predictive of the metastatic phenotype*, and expression in the metastatic tumour is lower in those patients responding favourably to neoadjuvant chemotherapy.
- *Inhibition of NQO1 with siRNA is not directly therapeutic but enhances the cytotoxic effect of irinotecan and 5-FU*. The NQO1 inhibitor dicoumarol has similar potential, although requires further evaluation.

Bibliography

Aaltonen, L., Peltomäki, P., Leach, F., Sistonen, P., Pylkkanen, L., Mecklin, J., Jarvinen, H., Powell, S., Jen, J., Hamilton, S., et al. (1993). Clues to the pathogenesis of familial colorectal cancer. *Science*, **260**(1509), 812-166.

Abdalla, E., Bauer, T., Chun, Y., D'Angelica, M., Kooby, D. and Jarnagin, W. (2013) Locoregional surgical and interventional therapies for advanced colorectal cancer liver metastases: expert consensus statements. *HPB* (Oxford), **15**(2), 119-130.

Abraham, N., Young, J. and Solomon, M. (2004) Meta-analysis of short-term outcomes after laparoscopic resection for colorectal cancer. *British Journal of Surgery*, **91**(9), 1111–1124

Adam, R., Avisar, E., Ariche, A., Giachetti, S.,Azoulay, D., Castaing, D., Kunstilinger, F. and Bismuth, F. (2001). Five year survival following hepatic resection after neoadjuvant therapy for nonresectable colorectal disease. *Annals of Surgical Oncology*, **8**(4), 347-353.

Adam, R., Bhangui, P., Poston, G., Mirza, D., Nuzzo, G., Barroso, E., Ijzermans, J., Hubert, C., Ruers, T., Capussotti, L., Ouellet, J., Laurent, C., Cugat, E., Colombo, P. and Milicevic, M. (2010). Is perioperative chemotherapy useful for solitary, metachronous, colorectal liver metastases? *Annals of Surgical Oncology*, **252**(5), 774-787.

Adam, R., de Haas, R., Wicherts, D., Vibert, E., Salloum, C., Azoulay, D. and Castaing, D. (2011). Concomitant extrahepatic disease in patients with colorectal liver metastases: when is there a place for surgery? *Annals of Surgical Oncology*, **253**(2), 349-359.

Alberda, W., Verhoef, C., Nuyttens, J., van Meerten, E., Rothbarth, J., de Wilt, J. and Burger, J. (2014). Intraoperative radiation therapy reduces local recurrence rates in patients with microscopically involved circumferential resection margins after resection of locally advanced rectal cancer. *International Journal of Radiation Oncology*, *Biology, Physics*, **88**(5), 1032-1040.

Alberici, P. and Fodde, R. (2006). The role of the APC tumor suppressor in chromosomal instability. *Genome Dynamics*, **1**,149-170.

Andre, T., Boni, C., Navarro, M., Tabernero, J., Hickish, T., Topham, C., Bonetti, A., Clingan, P., Bridgewater, J., Rivera, F. and de Gramont, A. (2009). Improved overall survival with oxaliplatin, fluoruracil and leucovorin as adjuvant treatment in stage II or III colon cancer in the MOSAIC trial. *Journal of Clinical Oncology*, **27**(19), 3109-3116.

Anwar, A., Dehn, D., Siegel, D., Kepa, J., Tang, L., Pietenpol, J. and Ross, D. (2003). Interaction of human NAD(P)H: quinone oxidoreductase 1 (NQO1) with the tumor suppressor protein p53 in cells and cell-free systems. *Journal of Biological Chemistry*, **278**(12), 10368 – 10373.

Arulampalam, T., Francis, D., Visvikis, D., Taylor, I. and Ell, P. (2004). FDG-PET for the pre-operative evaluation of colorectal liver metastases. *European Journal of Surgical Oncology*, **30**(3), 286-291.

Asher, G., Dym, O., Tsvetkov, P., Adler, J. and Shaul, Y. (2006). The crystal structure of NAD (P) H quinone oxidoreductase 1 in complex with its potent inhibitor dicoumarol. *Biochemistry*, **45**(20), 6372-6378.

Asher, G., Lotem, J., Cohen, B., Sachs, L. and Shaul, Y. (2001). Regulation of p53 stability and p53-dependent apoptosis by NADH quinone oxidoreductase 1. *Proceedings of the National Academy of Science of the United States of America*, **98**(3), 22559-22564.

Asher, G., Tsvetkov, P., Kahana, C. and Shaul, Y. (2005). A mechanism of ubiquitin-independent proteasomal degradation of the tumor suppressors p53 and p73. *Genes and Development*, **19**(3), 316-321.

Ask, K., Jasencakova, Z., Menard, P., Feng, Y., Almouzni, G. and Groth, A. (2012). Codanin-1, mutated in the anaemic disease CDAI, regulates Asf1 function in S-phase histone supply. *EMBO Journal*, **31**(8), 2013-2023.

Atallah, S. and Albert, R. (2013). Transanal minimally invasive surgery (TAMIS) versus transanal endoscopic microsurgery (REM): is one better than the other? *Surgical Endoscopy*, **27**(12), 4750-4751.

Bakalakos, E., Burak, W., Young, D. and Martin, E. (1999). Is carcino-embryonic antigen useful in the follow-up management of patients with colorectal liver metastases? *The American Journal of Surgery*, **177**(1), 2-6.

Baker, S., Preisinger, A., Jessup, J., Paraskeva, C., Markowitz, S., Wilson, J., Hamilton, S. and Vogelstein, B.(1990). p53 gene mutations occur in combination with 17p allelic deletions as late events in colorectal tumorigenesis. *Cancer Research*, **50**(23), 7717-7722.

Bando, M., Oka, M., Kawai, K., Obazawa, H., Kobayashi, S. and Takehana, M. (2006). NADH binding properties of rabbit lens lambda-crystallin. *Molecular Vision*, **12**, 692-697.

Bang, Y., Kim, Y., Yang, H., Chung, H., Park, Y., Lee, K., Lee, K., Kim, Y., Noh, S., Cho, J., Mok, Y., Kim, Y., Ji, J., Yeh, T., Button, P., Sirzén, F. and Noh, S. (2012). Adjuvant capecitabine and oxaliplatin for gastric cancer after D2 gastrectomy (CLASSIC): a phase 3 open-label, randomised controlled trial. *Lancet*, **379**(9813), 315-321.

Barber, T., McManus, K., Yuen, K., Reis, M., Parmigiani, G., Shen, D.,Barrett, I., Nouhi, Y., Spencer, F.,Markowitz, S., Velculescu, V., Kinzler, K., Vogelstein, B., Lengauer, C. and Hieter, P.(2008). Chromatid cohesion defects may underlie chromosome instability in human colorectal cancers. *Proceedings of the National Academy of Sciences of the United States of America*, **105**(9), 3443-3448.

Bass, A., Lawrence, M., Brace, L., Ramos, A., Drier, Y., Cibulskis, K., Sougnez, C., Voet, D., Saksena, G., Sivachenko, A., Jing, R., Parkin, M., Pugh, T., Verhaak, R., Stransky, N., Boutin, A., Barretina, J., Solit, D., Vakiani, E., Shao, W., Mishina, Y., Warmuth, M., Jimenez, J.,

Chiang, D., Signoretti, S., Kaelin, W., Spardy, N., Hahn, W., Hoshida, Y., Ogino, S., Depinho, R., Chin, L., Garraway, L., Fuchs, C., Baselga, J., Tabernero, J., Gabriel, S., Lander, E., Getz, G. and Meyerson, M. (2011). Genomic sequencing of colorectal adenocarcinomas identifies a recurrent VTI1A-TCF7L2 fusion. *Nature Genetics*, **43**(10), 964-968.

Bataille, A. and Manautou, J. (2012). Nrf2: A Potential Target for New Therapeutics in Liver Disease. *Clinical Pharmacology & Therapeutics*, **92** (3), 340-348.

Begleiter, A., Hewitt, D., Maksymiuk, A., Ross, D. and Bird, R. (2006). A NAD (P) H: quinone oxidoreductase 1 polymorphism is a risk factor for human colon cancer. *Cancer Epidemiology Biomarkers & Prevention*, **15** (12), 2422-2426.

Benjamini, Y. and Hochberg, Y. (1995). Controlling the False Discovery Rate: A Practical and Powerful Approach to Multiple Testing. *Journal of the Royal Statistical Society, Series B (Methodological)*, **57**(1), 289-300.

Benoist, S., Brouquet, A., Penna, C., Julie, C., El Hajjam, M., Chagnon, S., Mitry, E., Rougier, P. and Nordlinger, B. (2006). Complete response of colorectal liver metastases after chemotherapy: does it mean cure? *Journal of Clinical Oncology*, **24**(24), 3939-3945.

Blazer, D., Kishi, Y., Maru, D., Kopetz, S., Chun, Y., Overman, M., Fogelman, D., Eng, C., Chang, D., Wang, H., Zorzi, D., Ribero, D., Ellis, L., Glover, K., Wolff, R., Curley, S., Abdalla, E. and Vauthey, J. (2008). Pathologic response to preoperative chemotherapy: a new outcome end point after resection of hepatic colorectal metastases. *Journal of Clinical Oncology*, **26**(33), 5344-5351.

Bokemeyer, C., Bondarenko, I., Hartmann, J., de Braud, F., Schuch, G., Zubel, A., Celik, I., Schlichting, M. and Koralewski, P. (2011). Efficacy according to biomarker status of Cetuximab plus FOLFOX-4 as first-line treatment for metastatic colorectal cancer: the OPUS study. *Annals of Oncology*, **22**(7), 1535-1546.

Bokemeyer, C., Bondarenko, I., Makhson, A., Hartman, J., Aparicio, J., de Braud, F., Donea, S., Ludwig, H., Schuch, G., Stroh, C., Loos, A., Zubel, A. and Koralewski, P. (2009). Fluorouracil, leucovorin, and oxaliplatin with and without Cetuximab in the first-line treatment of metastatic colorectal cancer. *Journal of Clinical Oncology*, **27**(5), 663-671.

Boland, C., Thibodeau, S., Hamilton, S., Sidransky, D., Eshleman, J., Burt, R., Meltzer, S., Rodriguez-Bigas, M., Fodde, R., Ranzani, G. and Srivastava, S. (1998). A National Cancer Institute Workshop on Microsatellite Instability for cancer detection and familial predisposition: development of international criteria for the determination of microsatellite instability in colorectal cancer. *Cancer Research*, **58**(22), 5248-5257.

Boonsong, A., Curran, S., McKay, J., Cassidy, J., Murray, G. and McLeod, H. (2002) Topoisomerase I protein expression in primary colorectal cancer and lymph node metastases. *Human Pathology*, **33**(11), 1114-1119.

Bosslet, K., Straub, R., Blumrich, M., Czech, J., Gerken, M., Specker, B., Kroemer, H., Gesson, J., Koch, M. and Monneret, C. (1998). Elucidation of the mechanism enabling tumor selective prodrug monotherapy. *Cancer Research*, **58**(6), 1195-1201.

Boulay, J., Mild, G., Lowy, A., Reuter, J., Lagrange, M., Terracciano, L., Laffer, U., Herrmann, R. and Rochilitz, C. (2002). SMAD4 is a predictive marker for 5-Fluorouracil-based chemotherapy in patients with colorectal cancer. *British Journal of Cancer*, **87**(6), 630-634.

Bradford, M. (1976). A rapid and sensitive method for the quantificationof microgram quantities of protein utilizing the principle of protein-dye binding. *Analytical Biochemistry*, **7**(72), 248-254.

Braun, M., Richman, S., Quirke, P., Daly, C., Adlard, J., Elliott, F., Barrett, J., Selby, P., Meade, A., Stephens, R., Parmar, M. and Seymour, M. (2008). Predictive biomarkers of chemotherapy efficacy in colorectal cancer: results from the UK MRC FOCUS trial. *Journal of Clinical Oncology*, **26**(16), 2690-2698.

Browder, T., Butterfield, C., Kraling, B., Shi, B., Marshall, B., O'Reilly, M. and Folkman, J. (2000). Antiangiogenic scheduling of chemotherapy improves efficacy against experimental drug-resistant cancer. *Cancer Research*, **60**(7), 1878–1886.

Buecher, B., Cacheux, W., Rouleau, E., Dieumegard, B., Mitry, E. and Lièvre, A. (2013). Role of microsatellite instability in the management of colorectal cancers. *Digestive Liver Disease*, **45**(6), 441-449.

Bujko, K., Nowacki, M., Nasierowska-Guttmejer, A., Michalski, W., Bebenek, M. and Kryj, M. (2006). Long-term results of a randomized trial comparing preoperative short-course radiotherapy with preoperative conventionally fractionated chemoradiation for rectal cancer. *British Journal of Surgery*, **93**(10), 1215-1223.

Buttke, T. and Sandstrom, P. (1994). Oxidative stress as a mediator of apoptosis. *Immunology Today*. **15**(1), 7-10.

Buttke, T., McCubrey, J. and Owen, T. (1993). Use of an aqueous soluble tetrazolium/formazan assay to measure viability and proliferation of lymphokine-dependent cell lines. *Journal of Immunological Methods*, **157**(1-2), 233–240.

Buyse, M., Zeleniuch-Jacquotte, A. and Chalmers, T. (1988). Adjuvant therapy of colorectal cancer. Why we still don't know. *JAMA*, **259**(24), 3571-3578.

Campbell, P. and Pleasance, E. (2008). Subclonal phylogenetic structures in cancer revealed by ultra-deep sequencing. *Proceedings of the National academy of Sciences of the USA*, **105**(35), 13081-13086.

Campbell, P., Yachida, S., Mudie, L., Stephens, P., Pleasance, E., Stebbings, L., Morsberger, L., Latimer, C., McLaren, S., Lin, M., McBride, D., Varela, I., Nik-Zainal, S., Leroy, C., Jia, M., Menzies, A., Butler, A., Teague, J., Griffin, C., Burton, J., Swerdlow, H., Quail, M., Stratton, M., Iacobuzio-Donahue, C. and Futreal, P. (2010). The patterns and dynamics of genomic instability in metastatic pancreatic cancer. *Nature*, **467**(7319), 1109-1113.

Cancer Research UK (2012) *Cancer Research UK Prognostic/Predictive Biomarker Development Roadmap.* Available at: http://www.cancerresearchuk.org/prod_consump/groups/cr_common/@fre/@fun/documents/generalcontent/cr_027486.pdf [Accessed 23 October 2014].

Cancer Research UK. 2012. *Bowel Cancers Statistics* [on-line]. Available at: http://www.cancerresearchuk.org/cancer-info/cancerstats/types/bowel [Accessed 29 September 2014].

Carragher, L., Snell, K., Giblett, S., Aldridge, V., Patel, B. and Cook, S. (2010). V600EBraf induces gastrointestinal crypt senescence and promotes tumour progression through enhanced CpG methylation of p16INK4a. *EMBO Molecular Medicine*, **2**(11), 458-471.

Carrato, A. (2008). Adjuvant treatment of colorectal cancer. *Gastrointestinal Cancer Research*, **2**(4), S42-S46.

Cassidy, J., Clarke, S., Díaz-Rubio, E., Scheithauer, W., Figer, A., Wong, R., Koski, S., Lichinitser, M., Yang, T., Rivera, F., Couture, F., Sirzén, F. and Saltz, L. (2008).Randomized phase III study of capecitabine plus oxaliplatin compared with fluorouracil/folinic acid plus oxaliplatin as first-line therapy for metastatic colorectal cancer. *Journalof Clinical Oncology*, **26**(12), 2006-2012.

Ceciliani, F., Eckersall, D., Burchmore, R. and Lecchi, C. (2014). Proteomics in veterinary medicine: applications and trends in disease pathogenesis and diagnostics. *Veterinary Pathology*, **51**(2), 351–362.

Cedermark, B., Johansson, H., Rutqvist, L. and Wilking, N. (1995). The Stockholm I trial of preoperative short term radiotherapy in operable rectal carcinoma. A prospective randomized trial. Stockholm Colorectal Cancer Study Group.*Cancer*, **75**(9), 2269-2275.

Center for Drug Evaluation and Research (CDER), Centre for Veterinary Medicine (CVM). (2001). *Guidance for industry: bioanalytical method validation*. Rockville, MD: CDER.

Chen, J., Yu, L., Li, D., Gao, Q., Wang, J., Huang, X., Bi, G., Wu, H. and Zhao, S. (2003).Human CRYL1, a novel enzyme-crystallin overexpressed in liver and kidney and downregulated in 58% of livercancer tissues from 60 Chinese patients, and four new homologs from other mammalians. *Gene*, **302**(1-2), 103-113.

Chen, K., Wallis, J., McLellan, M., Larson, D., Kalicki, J., Pohl, C., McGrath, S., Wendl, M., Zhang, Q., Locke, D., Shi, X., Fulton, R., Ley, T., Wilson, R., Din, L. and Mardis, E. (2009). Break Dancer: an algorithm for high-resolution mapping of genomic structural variation. *Nature Methods*, **6**(9), 677-681.

Choi, P. and Zelig, M. (1994). Similarity of colorectal cancer in Crohn's disease and ulcerative colitis: implications for carcinogenesis and prevention. *Gut*, **35** (7), 950-954.

Chong, G., Cunningham, D. (2005). Improving long-term outcomes for patients with liver metastases from colorectal cancer. *Journal of Clinical Oncology*, **23**(36), 9063-9066.

Choti, M., Sitzmann, J., Tiburi, M., Sumetchotimetha, W., Rangsin, R., Schulick, R., Lillemoe, K., Yeo, C. and Cameron, J. (2002). Trends in long-term survival following liver resection for hepatic colorectal metastases. *Annals of Surgery*, **235**(6), 759-766.

Colangelo, L., Gapstur, S., Gann, P. and Dyer, A. (2004). Cigarette smoking and colorectal carcinoma mortality in a cohort with long-term follow-up. *Cancer*, **100**(2), 288-293.

Creswell, A., Welsh, F. and Rees, M. (2009). A diagnostic paradigm for resectable liver lesions: to biopsy or not to biopsy? *HPB (Oxford)*, **11**(7), 533-540.

Cunningham, D., Allum, W., Stenning, S., Thompson, J., Van de Velde, C., Nicolson, M., Scarffe, J., Lofts, F., Falk, S., Iveson, T., Smith, D., Langley, R., Verma, M., Weeden, S., Chua, Y. and MAGIC Trial Participants. (2006). Perioperative chemotherapy versus surgery alone for resectable gastroesophageal cancer. *New England Journal of Medicine*. **355**(1), 11-20.

Curran, S., McKay, J., McLeod, H. and Murray, G. (2005). Laser capture microscopy. *Molecular Pathology*, **53**(2), 64-68.

Day, J. and Stacey, G. (2008). Biobanking. *Molecular Biotechnology*, **40**(2), 202-213.

De Clercq, E. (2005). Recent highlights in the development of new antiviral drugs. *Current Opinion in Microbiology*, **8** (5), 552-560.

de Haas, R., Wicherts, D. and Adam, R. (2008). Resection of colorectal liver metastases with extrahepatic disease. *Digestive Surgery*, **25**(6), 461-466.

Denoix, P. (1946). Enquete permanent dans les centres anticancereaux. *Bulletin de l'Institut national d'hygiene*, **1**, 70–75.

Dgany, O., Avidan, N., Delaunay, J., Krasnov, T., Shalmon, L., Shalev, H., Eidelitz-Markus, T., Kapelushnik, J., Cattan, D., Pariente, A., Tulliez, M., Cretien, A., Schischmanoff, P.-O., Iolascon, A., Fibach, E., Koren, A., Roessler, J., Le Merrer, M. and Tamary, H. (2002). Congenital dyserythropoietic anemia type I is caused by mutations in codanin-1. *American Journal of Human Genetics*, **71**(6), 1467-1474.

Diasio, R. and Harris, B. (1989). Clinical pharmacology of 5-fluorouracil. *Clinical Pharmacokinetics*, **16**(4), 215-237.

Downward, J. (2003). Targeting RAS signalling pathways in cancer therapy. *Nature Reviews Cancer*, **3**(1), 11-22.

Dukes, C. (1932). The classification of cancer of the rectum. *The Journal of Pathology and Bacteriology*, **35**(3), 323-332.

Dukes, C. and Bussey, H. (1958). The spread of rectal cancer and its effect on prognosis. *British Journal of Cancer*, **12**(3), 309-320.

Dworak, O., Keilholz, L. and Hoffmann, A.(1997). Pathological features of rectal cancer after preoperative radiochemotherapy. *International Journal of Colorectal Disease*, **12**(1), 19-23.

Eisenhauer, E., Therasse, P., Bogaerts, J., Schwartz, L., Sargent, D., Ford, R., Dancey, J., Arbuck, S., Gwyther, S., Mooney, M., Rubinstein, L., Shankar, L., Dodd, L., Kaplan, R., Lacombe, D. and Verweil, J. (2009). New response evaluation criteria in solid tumours: revised RECIST guideline (version 1.1). *European Journal of Cancer*, **45**(2), 228-247.

Ezzeldin, H. and Diasio, R. (2008). Predicting fluorouracil toxicity: can we finally do it? *Journal of Clinical Oncology*, **26**(12), 2080-2082.

Fallik, D., Borrini, F., Boige, V., Viguier,J., Jacob, S., Miquel, C., Sabourin, J., Ducreux, M. and Praz, F. (2003) Microsatellite instability is a predictive factor of the tumor response to irinotecan in patients with advanced colorectal cancer. *Cancer Research*, **63**(18), 5738-5744.

Fang, L., Lee, S., Choi, H., Kim, H., Jew, G., Kang, H., Chen, L., Jablons, D. and Kim, I. (2014). Comprehensive genomic analyses of a metastatic colon cancer to the lung by whole exome sequencing and gene expression analysis. *International Journal of Oncology*, **44**(1), 211-221.

Farmer, H., McCabe, N., Lord, C., Tutt, A., Johnson, D., Richardson, T., Santarosa, M., Dillon, K., Hickson, I., Knights, C., Martin, N., Jackson, S., Smith, G. and Ashworth, A. (2005). Targeting the DNA repair defect in BRCA mutant cells as a therapeutic strategy. *Nature*, **434**(7035), 917–921.

Fearon, E. (2011). Molecular genetics of colorectal cancer. *Annual Review of Pathology*,**6**, 479-507.

Fearon, E. and Vogelstein, B. (1990). A genetic model for colorectal tumorigenesis. *Cell*, **61**(5), 759-767.

Folprecht, G., Grothey, A., Alberts, S., Raab, H. and Kohne, C. (2005). Neoadjuvant treatment of unresectable colorectal liver metastases: correlation between tumour response and resection rates. *Annals of Oncology*, **16**(8), 1311-1319.

Folprecht, G., Gruenberger, T., Bechstein, W., Raab, H., Lordick, F., Hartman, J., Lang, H., Frilling, A., Stoehlmacher, J., Weitz, J., konopke, R., Stroszcynski, C., Liersch, T., Ockert, D., Herrmann, T., Goekkurt, E., Parisi, F and Kohne, C. (2010). Tumour response and secondary resectability of colorectal liver metastases following neoadjuvant chemotherapy with Cetuximab: the CELIM randomised phase 2 trial. *The Lancet Oncology*, **11**(1), 38-47.

Fong, Y., Fortner, J., Sun, R., Brennan, M. and Bulmgart, L. (1999). Clinical score for predicting recurrence after hepatic resection for metastatic colorectal cancer: analysis of 1001 consecutive cases. *Annals of Surgery*, **230**(3), 309-318; discussion 318-321.

Gao, D., Zhang, T., Li, S., Liu, Q. and Du, J. (2013). A comparison on expression of selected biomarkers between primary lung cancers and matched metastases. *Medical Oncology*, **30**(4), 742.

Garate, M., Wong, R., Campos, E., Wang, Y. and Li, G. (2008) NAD(P)H quinone oxidoreductase 1 inhibits the proteasomal degradation of the tumour suppressor p33(ING1b). *EMBO Reports*, **9**(6) 576-581.

García-Barros, M., Coant, N., Truman, J., Snider, A. and Hannun, Y. (2014). Sphingolipids in colon cancer. *Biochimica et Biophysica Acta*, **1841**(5), 773-782.

Garden, O., Rees, M., Poston, G., Mirza, D., Saunders, M., Leaderman, J., Primrose, J. and Parks, R. (2006). Guidelines for resection of colorectal cancer liver metastases. *Gut*, **55** (3), iii 1-8.

Gérard, J., Conroy, T., Bonnetain, F., Bouché, O., Chapet, O., Closon-Dejardin, M., Untereiner, M., Leduc, B., Francois, E., Maurel, J., Seitz, J., Buecher, B., Mackiewicz, R., Ducreux, M. and Bedenne, L. (2006)Preoperative radiotherapy with or without concurrent fluorouracil and leucovorin in T3-4 rectal cancers: results of FFCD 9203. *Journal of Clinical Oncology*, **24**(28), 4620-4625.

Gerlinger, M. and Swanton, C. (2010).
How Darwinian models inform therapeutic failure initiated by clonal heterogeneity in cancer medicine. *British Journal of Cancer*, **103**(8), 1139-1143.

Goldberg, P., Nicholls, R., Porter, N., Love, S. and Grimsey, J. (1994). Long-term results of a randomised trial of short-course low-dose adjuvant pre-operative radiotherapy for rectal cancer: reduction in local treatment failure. *European Journal of Cancer*, **30A**(11), 1602-1606.

Gong, X., Kole, L. Iskander, K. and Jaiswal, A. (2007). NRH:quinone oxidoreductase 2 and NAD(P)H: quinone oxidoreductase 1 protect tumor suppressor p53 against 20s proteasomal degradation leading to stabilization and activation of p53. *Cancer Research*, **67**(11), 5380 – 5388.

Grady, W. and Carethers, J. (2008). Genomic and epigenetic instability in colorectal cancer pathogenesis. *Gastroenterology*, **135** (4), 1079-1099.

Grady, W. (2004). Genomic instability and colon cancer. *Cancer Metastasis Review*, **23**(1-2), 11-27.

Graham, J., Mushin, M. and Kirkpatrick, P. (2004). "Oxaliplatin". *Nature Reviews Drug Discovery*, **3** (1), 11–12.

Greenman, C., Stephens, P., Smith, R., Dalgliesh, G., Hunter, C., Bignell, G., Davies, H., Teague, J., Butler, A., Stevens, C., Edkins, S., O'Meara, S., Vastrik, I., Schmidt, E., Avis, T., Barthorpe, S., Bhamra, G., Buck, G., Choudhury, B., Clements, J., Cole, J., Dicks, E., Forbes, S., Gray, K., Halliday, K., Harrison, R., Hills, K., Hinton, J., Jenkinson, A., Jones, D., Menzies, A., Mironenko, T., Perry, J., Raine, K., Richardson, D., Shepherd, R., Small, A., Tofts, C., Varian, J., Webb, T., West, S., Widaa, S., Yates, A., Cahill, D., Louis, D., Goldstraw, P., Nicholson, A., Brasseur, F., Looijenga, L., Weber, B., Chiew, Y., DeFazio, A., Greaves, M., Green, A., Campbell, P., Birney, E., Easton, D., Chenevix-Trench, G., Tan, M., Khoo, S., Teh, B., Yuen, S., Leung, S., Wooster, R., Futreal, P. and Stratton, M. (2007). Patterns of somatic mutation in human cancer genomes. *Nature*, **446**(7132), 153–158.

Grothey, A., Hedrick, E., Mass, R., Sarkar, S., Suzuki, S., Ramanathan, R., Hurwitz, H., Goldberg, R. and Sargent, D. (2008). Response-independent survival benefit in metastatic colorectal cancer: a comparative analysis of N9741 and AVF2107. *Journal of Clinical Oncology*, **26**(2), 183-189.

Gudkov, A. and Komarova, E. (2003). The role of p53 in determining sensitivity to radiotherapy. *Nature Reviews Cancer*, **3**(2), 117–129.

Gupta, N., Tanner, S., Jaitly, N., Adkins, J., Lipton, M., Edwards, R., Romine, M., Osterman, A., Bafna, V., Smith, R. and Pevzner, P.(2007). Whole proteome analysis of post-translational modifications: applications of mass-spectrometry for proteogenomic annotation. *Genome Research*, **17**(9), 1362–1377.

Hansen, K., Timp, W., Bravo, H., Sabunciyan, S., Langmead, B., McDonald, O., Wen, B., Wu, H., Liu, Y., Diep, D., Briem, E., Zhang, K., Irizarry, R. and Feinberg, A. (2011). Increased methylation variation in epigenetic domains across cancer types. *Nature Genetics*, **43**(8), 768-775.

Harth, V., Donat, S., Ko, Y., Abel, J., Vetter, H. and Brüning, T. (2000). NAD (P) H quinone oxidoreductase 1 codon 609 polymorphism and its association to colorectal cancer. *Archives of Toxicology*, **73**(10-11), 528-531.

Hatzis, C., Sun, H., Yao, H., Hubbard, R., Meric-Bernstam, F., Babiera, G., Wu, Y., Pusztai, L. and Symmans, W. (2011). Effects of tissue handling on RNA integrity and microarray measurements from resected breast cancers. *Journal of the National Cancer Institute*, **103**(24), 1871-1883.

Haydon, A. (2003). Adjuvant chemotherapy in colon cancer: what is the evidence? *Internal Medicine Journal*, **33**(3), 119-124.

Heald, R. (1988). The 'Holy Plane' of rectal surgery.Journal of the *Royal Society of Medicine*, **81**(9), 503-508.

Heald, R., Husband, E. and Ryall, R. (1982). The mesorectum in rectal cancer surgery-the clue to pelvic recurrence? *British Journal of Surgery*, **69**(10), 613-616.

Heald, R., Moran, B., Ryall, R., Sexton, R. and MacFarlane, J. (1998). Rectal cancer: the Basingstoke experience of total mesorectal excision, 1978-1997.*Archives of Surgery*, **133**(8), 894-899.

Hochster, H., Hart, L., Ramanathan, R., Childs, B., Hainsworth, J., Cohn, A., Wong, L., Fehrenbacher, L.,Abubakr, Y., Saif, M., Schwartzberg, L. and Hedrick, E. (2008). Safety and efficacy of oxaliplatin and fluropyrimidine regimens with or without bevacizumab as first line treatment of metastatic colorectal cancer: results of the TREE Study. *Journal of Clinical Oncology*, **26**(21), 3523-3529.

Hollstein, M., Sidransky, D., Vogelstein, B. and Harris, C. (1991). p53 mutations in human cancers. *Science*, **253**(5015), 49-53.

Huebner, M., Wolff, B., Smyrk, T., Aakre, J. and Larson, D. (2012). Partial pathologic response and nodal status as most significant prognostic factors for advanced rectal cancer treated with preoperative chemoradiotherapy. *World Journal of Surgery*, **36**(3), 675-683.

Huebner, R., Park, K., Shepherd, J., Schwimmer, J., Czernin, J., Phelps, M. and Gambhir, S. (2000). A meta-analysis of the literature for whole-body FDG PET detection of recurrent colorectal cancer. *Journal of Nuclear Medicine*, **41**(7), 1177-1189.

Hurwitz, H., Fehrenbacher, L., Novotny, W., Cartwright, T., Hainsworth, J., Heim, W., Berlin, J., Baron, A., Griffing, S., Holmgren, E., Ferrara, N., Fyfe, G., Rogers, B., Ross, R and Kabbinavar, F. (2004). Bevacizumab plus irinotecan, fluorouracil, and leucovorin for metastatic colorectal cancer. *New England Journal of Medicine*, **350**(23), 2335-2342.

Huxley, R., Ansary-Moghaddam, A., Clifton, P., Czernichow, S., Parr, C. and Woodward, M. (2009).The impact of dietary and lifestyle risk factors on risk of colorectal cancer: a quantitative overview of the epidemiological evidence. *International Journal of Cancer*, **125**(1), 171-180.

Innocenti, F. and Ratain, M.(2004). "Irinogenetics" and UGT1A: from genotypes to haplotypes. *Clinical Pharmacology and Therapeutic*, **75**(6), 495-500.

Innocenti, F., Undevia, S., Iyer, L., Chen, P., Das, S., Kocherginsky, M., Karrison, T., Janisch, L., Ramirez, J., Rudin, C., vokes, E. and Ratain, M. (2004). Genetic variants in the UDP-glucuronosyltransferase 1A1 gene predict the risk of severe neutropenia of irinotecan. *Journal of Clinical Oncology*, **22** (8), 1382-1388.

Issa, J. (2004).CpG island methylator phenotype in cancer. *National Review of Cancer*, **4**(12), 988-993.

Iyer, L., Das, S., Janisch, L., Wen, M., Ramirez, J., Karrison, T., Fleming, G., Vokes, E., Schilsky, R. and Ratain, M. (2002). UGT1A1*28 polymorphism as a determinant of irinotecan disposition and toxicity. *The Pharmacogenomics Journal*, **2**(1), 43-47.

Iyer, L., Ramírez, J., Shepard, D., Bingham, C., Hossfeld, D., Ratain, M. and Mayer, U. (2002). Biliary transport of irinotecan and metabolites in normal and P-glycoprotein-deficient mice. *Cancer Chemotherapy and Pharmacology*, **49** (4), 336-341.

James, P. (1997). Protein identification in the post-genome era: the rapid rise of proteomics. *Quarterly reviews of biophysics*, **30**(4), 279–331.

Jass, J. (2007). Classification of colorectal cancer based on correlation of clinical, morphological and molecular features. *Histopathology*, **50**(1), 113-130.

Jo, W. and Carethers, J. (2006). Chemotherapeutic implications in microsatellite unstable colorectal cancer. *Cancer Biomarkers*, **2**(1-2), 51-60.

Johnston, P. and Kaye, S. (2001). Capecitabine: a novel agent for the treatment of solid tumors. *Anticancer Drugs*, **12**(8), 639-646.

Jones, R., Sutton, P., Greensmith, R., Santoyo-Castelazo, A., Carr, D., Jenkins, R., Rowe, C. Hamlett, J., Park, B., Terlizzo, M., O'Grady, E., Ghaneh, P., Fenwick, S., Malik, H., Poston, G. and Kitteringham, N. (2013). Hepatic activation of irinotecan predicts tumour response in patients with colorectal liver metastases treated with DEBIRI: exploratory findings from a phase II study. *Cancer Chemotherapy and Pharmacology*, **72**(2), 359-368.

Jones, O., Rees, M., John, T., Bygrave, S. and Plant, G. (2005). Biopsy of resectable colorectal liver metastases causes tumour dissemination and adversely affects survival after liver resection. *British Journal of Surgery*, **92**(9), 1165-1168.

Kamel, I. and Bluemke, D. (2003). MR imaging of liver tumors. *Radiologic Clinics of North America*, **41**(1), 51-65.

Kapiteijn, E., Marijnen, C., Nagtegaal, I., Putter, H., Steup, W., Wiggers, T., Rutten, H., Pahlman, L., Glimelius, B., van Krieken, J., Leer, J., van de Velde, C. and The Dutch Colorectal Cancer Group. (2001). Preoperative radiotherapy combined with total mesorectal excision for resectable rectal cancer. *New England Journal of Medicine*, **345**(9), 638-646.

Kerr, D., Gray, R., Quirke, P., Watson, D., Yothers, G., Lavery, I.C., Lee, M., O'Connell, M.J., Shak, S., and Wolmark, N. (2009). A quantitative multigene RT-PCR assay for prediction of recurrence in stage II colon cancer: selection of the genes in four large studies and results of the independent, prospectively designed QUASAR validation study. *Journal of Clinical Oncology*, **27**(15S), 4000.

Khaustova, N., Makeeva, D., Kondrashina, O., Fedotov, N., Savelov, N., Grinevich, V., Maltseva, D., Galatenko, V. and Shkurnikov, M. (2014). Comparison of the results of PCR analysis of gene expression in breast cancer tissue specimens stabilized in formalin and RNAlater. *Bulletin of Experimental Biology and Medicine*, **156**(4), 486-490.

Kinzler, K. and Vogelstein, B. (1996). Lessons from hereditary colorectal cancer. *Cell*, **87**(2), 159-170.

Kirkpatrick, P., Graham, J. and Muhsin, M.(2004). Cetuximab. *Nature Reviews Drug Discovery*, **3** (7), 549-550.

Kishi, Y., Zorzi, D., Contreras, C., Maru, D., Kopetz, S., Ribero, D., Motta, M., Ravarino, N., Risio, M., Curley, S.,Abdalla, E., Capussotti, L. and Vauthey, J. (2010). Extended preoperative chemotherapy does not improve pathologic response and increases postoperative liver insufficiency after hepatic resection for colorectal liver metastases. *Annals of Surgical Oncology*, **17**(11), 2870-2876.

Klein, C. (2009). Parallel progression of primary tumours and metastases. *Nature Reviews Cancer*, **9**(4), 302-312.

Klinger, M., Tamandl, D., Eipeldauer, S., Hacker, S., Herberger, B., Kaczirek, K., Dorfmeister, M., Gruenberger, B. and Gruenberger, T. (2010). Bevacizumab improves pathological response of colorectal cancer liver metastases treated with XELOX/FOLFOX. *Annals of Surgical Oncology*, **17**(8), 2059-2065.

Kloosterman, W., Hoogstraat, M., Paling, O., Tavakoli-Yaraki, M., Renkens, I., Vermaat, J., van Roosmalen, M., van Lieshout, S., Nijman, I., Roessingh, W., van 't Slot, R., van de Belt, J., Guryev, V., Koudijs, M., Voest, E. and Cuppen, E. (2011). Chromothripsis is a common mechanism driving genomic rearrangements in primary and metastatic colorectal cancer. *Genome Biology*, **12**(10), R103.

Knauer, C. (1978). Percutaneous biopsy of the liver as a procedure for outpatients. *Gastroenterology*, **74**(1), 101–102.

Kononen, J., Bubendorf, L., Kallionimeni, A., Bärlund, M., Schraml, P., Leighton, S., Torhorst, J., Mihatsch, M., Sauter, G. and Kallionimeni, O. (1998). Tissue microarrays for high-throughput molecular profiling of tumor specimens. *Nature medicine*, **4**(7), 844-847.

Koopman, M., Antonini, N., Douma, J., Wals, J., Honkoop, A., Erdkamp, F., de Jong, R., Rodenburg, C., Vreugdenhil, G., Loosveld, O., van Bochove, A., Sinnige, H., Creemers, G., Tesselaar, M., Slee, P., Werter, M., Mol, L., Dalesio, O. and Punt, C. (2007). Sequential *vs*. combination chemotherapy with capecitabine, irinotecan, and oxaliplatin in advanced colorectal cancer (CAIRO): a phase III randomised controlled trial. *Lancet*, **370**(9582), 135–142.

Kuebler, J., Wieand, H., O'Connell, M., Smith, R., Colangelo, L., Yothers, G., Petrelli, N., Findlay. M,, Seay, T., Atkins, J., Zapas, J., Goodwin, J., Fehrenbacher, L., Ramanathan, R., Conley. B,, Flynn, P., Soori, G., Colman, L., Levine, E., Lanier, K. and Wolmark, N. (2007). Oxaliplatin combined with weekly bolus fluorouracil and leucovorin as surgical adjuvant chemotherapy for stage II and III colon cancer: results from NSABP C-07. *Journal of Clinical Oncology*, **25**(16), 2198-2204.

LaBaer, J. (2012) Improving international research with clinical specimens: 5 achievable objectives. *Journal of Proteome Research*, **11**(12), 5592-5601.

Lancet (2000). Comparison of fluorouracil with additional levamisole, higher-dose folinic acid, or both, as adjuvant chemotherapy for colorectal cancer: a randomised trial. QUASAR Collaborative Group, **355**(9215), 1588-1596.

Langevin, J. and Nivatvongs, S. (1984). The true incidence of synchronous cancer of the large bowel. A prospective study. *American Journal of Surgery*, **147**(3), 330-333.

Laurie, J., Moertel, C., Fleming, T., Wieand, H., Leigh, J., Rubin, J., McCormack, G., Gerstner, J., Krook, J., Malliard, J,. et al. (1989). Surgical adjuvant therapy of large-bowel carcinoma: an evaluation of levamisole and the combination of levamisole and fluorouracil. The North Central Cancer Treatment Group and the Mayo Clinic. *Journal of Clinical Oncology,* **7**(10), 1447-1456.

Lee, H., Yoon, C., Schmidt, B., Park do, J., Zhang, A., Erkizan, H., Toretsky, J., Kirsch, D. and Yoon, S. (2013). Combining PARP-1 inhibition and radiation in Ewing sarcoma results in lethal DNA damage. *Molecular Cancer Therapeutics*, **12**(11), 2591-2600.

Lee, S., Schelcher, C., Gashi, S., Schreiber, S., Thasler, R., Jauch, K and Thasler, W. (2013). RNA stability in human liver: comparison of different processing times, temperatures and methods. *Molecular Biotechnology*, **53**(1), 1-8.

Lengauer, C., Kinzler, K. and Vogelstein, B. (1997). Genetic instability in colorectal cancers. *Nature*, **386**(6625), 623-627.

Leong, S., Nunez, A., Lin, M., Crossett, B., Christopherson, R. and Baxter, R.(2012). AQ-based proteomic profiling of breast cancer cell response to doxorubicin and TRAIL. *Journal of Proteome Research*, **11**(7), 3561-3572.

Liang, J., Huang, K., Lai, H., Lee, P., Cheng, Y., Hsu, H., Cheng, A., Hsu, C., Yeh, K., Wang, S., Tang, C and Chang, K. (2002). High-frequency microsatellite instability predicts better chemosensitivity to high-dose 5-fluorouracilplus leucovorin chemotherapy for stage IV sporadic colorectal cancer after palliative bowel resection. *International Journal of Cancer*, **101**(6), 519-525.

Lin, Q., Tan, H., Lim, T., Khoo, A., Lim, K. and Chung, M. (2014). iTRAQ analysis of colorectal cancer cell lines suggests Drebrin (DBN1) is overexpressed during liver metastasis. *Proteomics*, **14**(11), 1434-1443.

Lind, C., Cadenas, E., Hochstein, P. and Ernster, L. (1990). DT-diaphorase. Purification, properties and function. *Methods in Enzymology*, **186**, 287-301.

Liu, F., Zhang, Y., Peng, Z., Gao, H., Xu, L. and Chen, M. (2012). High expression of high mobility group box 1 (HMGB1) predicts poor prognosis for hepatocellular carcinoma after curative hepatectomy. *Journal of Translational Medicine*, **10**, 135.

Liu, P., Wang, Y., Cao, Y., Jiang, H., Yang, X., Wang, X. and Niu, H. (2014). Far from resolved: stromal cell-based iTRAQ research of muscle-invasive ladder cancer regarding heterogeneity. *Oncology Reports*, **32**(4),1489-1496.

Long, D., Waikel, R., Wang, X.-J., Roop, D. and Jaiswal, A. (2001). NAD (P) H: quinone oxidoreductase 1 deficiency and increased susceptibility to 7, 12-dimethylbenz [a]-anthracene-induced carcinogenesis in mouse skin. *Journal of the National Cancer Institute*, **93**(15), 1166-1170.

Longley, D., Harkin, D. and Johnston, P. (2003). 5 Fluorouracil: mechanisms of action and clinical strategies. *Nature Reviews Cancer*, **3**(5), 330-338.

Los, M., Roodhart, J. and Voest, E. (2007). Target Practice: Lessons from Phase III Trials with Bevacizumab and Vatalanib in the Treatment of Advanced Colorectal Cancer. *The Oncologist*, **12**(4), 443–450.

Losi, L., Luppi, G., Gavioli, M., Iachetta, F., Bertolini, F., D'Amico, R., Jovic, G., Bertoni, F., Falchi, A. and Conte, P. (2006). Prognostic value of Dworak grade of regression (GR) in patients with rectal carcinoma treated with preoperative radiochemotherapy. *International Journal of Colorectal Disease*, **21**(7), 645-651.

Lowe, S., Ruley, H., Jacks, T. and Housman, D. (1993). p53-dependent apoptosis modulates the cytotoxicity of anticancer agents. *Cell*, **74**(6), 957-967.

Ludwig, K. (2007). Sphincter-sparing resection for rectal cancer. *Clinics in Colon and Rectal Surgery*, **20**(3), 203-212.

Lykoudis, P., O'Reilly, D., Nastos, K. and Fusai, G. (2014). Systematic review of surgical management of synchronous colorectal liver metastases. *British Journal of Surgery*, **101**(6), 605-612.

Lynch, H. and de la Chapelle, A. (2003). Hereditary colorectal cancer. *The New England Journal of Medicine*, **348**(10), 919-932.

Mager, S., Oomen, M., Morente, M., Ratcliffe, C., Knoxa, K., Kerr, D., Pezzella, F. and Riegman, P. (2007). Standard operating procedure for the collection of fresh frozen tissue samples. *European Journal of Cancer*, **43**(5), 828–834.

Mahdy, A., Cheng, J., Li, J., Elojeimy, S., Meacham, W., Turner, L., Bai, A., Gault, C., McPherson, A., Garcia, N., Beckham, T., Saad, A., Bielawska, A., Bielawski, J., Hannun, Y., Keane, T., Taha, M., Hammouda, H., Norris, J. and Liu, X. (2009). Acid ceramidase upregulation in prostate cancer cells confers resistance to radiation: AC inhibition, a potential radiosensitizer. *Molecular Therapy*, **17**(3), 430-438.

Majumdar, S., Fletcher, R. and Evans, A. (1999). How does colorectal cancer present? Symptoms, duration, and clues to location. *American Journal of Gastroenterology*, **94**(10), 3039-3045.

Mandard, A., Dalibard, F., Mandard, J., Marnay, J., Henry-Amar, M., Petiot, J., Roussel, A., Jacob, J., Segol, P., Samama, G., et al. (1994). Pathologic assessment of tumor regression after preoperative chemoradiotherapy of esophageal carcinoma. Clinicopathologic correlations. *Cancer,* **73**(11),2680-2686.

Mander, B., Carney, L., Scott, H. and Donaldson, D. (2006). Jass staging is a predictor of outcome following "curative" resection of Dukes' B colorectal carcinoma. *The Surgeon,* **4**(4), 227-230.

Manfredi, S., Lepage, C., Hatem, C., Coatmeur, O., Faivre, J. and Bouvier, A.(2006). Epidemiology and management of liver metastases from colorectal cancer. *Annals of Surgery*, **244**(2), 254-259.

Manning, G., Whyte, D., Martinez, R., Hunter, T. and Sudarsanam, S. (2002). The protein kinase complement of the human genome. *Science*, **298**(5600), 1912-1934.

Masi, G., Loupakis, F., Salvatore, L., fornaro, L., Cremolini, C., Cupini, S., Ciarlo, A., Del Monte, F., Cortesi, E., Amoroso, D., Granetto, C., Fontanono, G., Sennsi, E., Lupi, C., Andreuccetti, M and Falcone, A. (2010). Bevacizumab with FOLFOXIRI (irinotecan, oxaliplatin, fluorouracil, and folinate) as first-line treatment for metastatic colorectal cancer: a phase 2 trial. *The Lancet Oncology*, **11**(9), 845-852.

Mathijssen, R., van Alphen, R., Verweij, J., Loos, W., Nooter, K., Stoter, G. and Sparreboom, A. (2001). Clinical pharmacokinetics and metabolism of irinotecan (CPT-11). *Clinical Cancer Research*, **7**(8), 2182-2194.

Mee, B., Carroll, P., Donatello, S., Connolly, E., Griffin, M., Dunne, B., Burke, L., Flavin, R., Rizkalla, H., Ryan, C., Hayes, B., D'Adhemar, C., Banville, N., Faheem, N., Muldoon, C. and Gaffney, E. (2011). Maintaining Breast Cancer Specimen Integrity and Individual or Simultaneous Extraction of Quality DNA, RNA, and Proteins from Allprotect-Stabilized and Nonstabilized Tissue Samples. *Biopreservation and Biobanking*, **9**(4), 389-398.

Madi, A., Fisher, D., Wilson, R.H., Adams, R.A., Meade, A.M., Kenny, S.L., Nichols, L.L., Seymour, M.T., Wasan, H., Kaplan, R., Maughan, T.S. and the COIN Research Group. (2012). Oxaliplatin/capecitabine *vs*. oxaliplatin/infusional 5-FU in advanced colorectal cancer: the MRC COIN trial. *British Journal of Cancer*, **107**(7), 1037-1043.

MERCURY Study Group. (2006). Diagnostic accuracy of preoperative magnetic resonance imaging in predicting curative resection of rectal cancer: prospective observational study. *British Medical Journal*, **333**(7572), 779.

Messersmith, W. and Ahnen, D. (2008). Targeting EGFR in colorectal cancer. *New England Journal of Medicine*, **359**(17), 1834–1836.

Miettinen, P., Berger, J., Meneses, J., Phung, Y., Pederson, R., Werb, Z. and Derynck, R. (1995). Epithelial immaturity and multiorgan failure in mice lacking epidermal growth factor receptor. *Nature*, **376**(6538), 337-341.

Mikami, K., Naito, M., Ishiguro, T., Yano, H., Tomida, A., Yamada, T., Tanaka, N., Shirakusa, T. and Tsuruo, T. (1998). Immunological Quantitation of DT-Diaphorase in Carcinoma Cell Lines and Clinical Colon Cancers: Advanced Tumors Express Greater Levels of DT-Diaphorase. *Cancer Science*, **89**(9), 910-915.

Miller, A,, Hoogstraten, B., Staquet, M. and Winkler, A. (1981). Reporting results of cancer treatment. *Cancer*, **47**(1), 207-214.

Mitry, E., Fields, A., Bleiberg, H., Labianca, R., Portier, G., Tu, D., Nitti, D., Torri, V., Elias, D., O'Callaghan, C., Langer, B., Martigoni, G., Bouche, O., Lazorthes, F., Van Cutsem, E., Bedenne, L., Moore, M. and Rougier, P. (2008). Adjuvant chemotherapy after potentially curative resection of metastases from colorectal cancer: a pooled analysis of two randomized trials. *Journal of Clinical Oncology,* **26** (30), 4906-4911.

Moertel, G., Fleming, T., Macdonald, J., Haller, D., Laurie, J., Goodman, P., Ungerleider, J., Emerson, W., Tormey, D., Glick, J., Veeder, M., and Milliard, J. (1990). Levamisole and fluorouracil for adjuvant therapy of resected colon carcinoma. *New England Journal of Medicine*, **322**(6), 352-358.

Mulders, J., Hendriks, W., Blankesteijn, W., Bloemendal, H. and De Jong, W. (1988). Lambda-crystallin, a major rabbit lens protein, is related to hydroxyacyl-coenzyme a dehydrogenases. *The Journal of Biological Chemistry*, **263**(30), 15462–15466.

Nagtegaal, I. and Quirke, P. (2008). What is the role for the circumferential margin in the modern treatment of rectal cancer? *Journal of Clinical Oncology*, **2**, 303-312.

Narita, M., Oussoultzoglou, E., Jaeck, D., Fuchschuber, P., Rosso, E., Pessaux, P., Marzano, E. and Bachellier, P. (2011). Two-stage hepatectomy for multiple bilobar colorectal liver metastases. *British Journal of Surgery*, **98** (10), 1463-1475.

Navin, N. and Hicks, J. (2010). Tracing the tumor lineage. *Molecular Oncology*, **4**(3), 267-283.

New England Journal of Medicine. (1997) Improved survival with preoperative radiotherapy in resectable rectal cancer. Swedish Rectal Cancer Trial. **336**(14), 980-987.

Nishimura, K., Tsuchiya, Y., Okamoto, H., Ijichi, K., Gosho, M., Fukayama, M., Yoshikawa, K., Ueda, H., Bradford, C., Carey, T. and Ogawa, T. (2014). Identification of chemoresistant factors by protein expression analysis with iTRAQ for head and neck carcinoma. *British Journal of Cancer*, **111**(4), 799-806.

Nordlinger, B., Guiguet, M., Vaillant, J., Balladur, P., Boudjema, K., Bachellier, P. and Jaeck, D. (1996). Surgical resection of colorectal carcinoma metastases to the liver. A prognostic scoring system to improve case selection, based on 1568 patients. Association Française de Chirurgie. *Cancer*, **77** (7), 1254-1262.

Nordlinger, B., Sorbye, H., Glimelius, B., Poston, G., Schlag, P., Rougier, P., Bechstein, W., Primrose, J.,Walpole, E., Finch-Jones, M., Jaeck, D., Mirza, D., Parks, R., Collette, L., Praet, M., Bethe, U., Van Cutsem, E.,Scheithauer, W., Gruenberger, T., EORTC Gastro-Intestinal Tract Cancer Group, Cancer Research UK, Arbeitsgruppe Lebermetastasen und-tumoren in der Chirurgischen Arbeitsgemeinschaft Onkologie (ALM-CAO), Australasian Gastro-Intestinal Trials Group (AGITG), Fédération Francophone de Cancérologie Digestive (FFCD).(2008). Perioperative chemotherapy with FOLFOX4 and surgery versus surgery alone for resectable liver metastases from colorectal cancer (EORTC Intergroup trial 40983): a randomised controlled trial. *The Lancet*, **371**(9617), 1007-1016.

Noy-Lotan, S., Dgany, O., Lahmi, R., Marcoux, N., Krasnov, T., Yissachar, N., Ginsberg, D., Motro, B., Resnitzky, P., Yaniv, I., Kupfer, G. and Tamary, H. (2009). Codanin-1, the protein encoded by the gene mutated in congenital dyserythropoietic anemia type I (CDAN1), is cell cycle-regulated. *Haematologica*, **94**(5), 629-637.

Ong, K. and Leen, E. (2007). Radiological staging of colorectal liver metastases. *Surgical Oncology*, **16**(1),7-14.

Paliogiannis, P., Cossu, A., Tanda, F., Palmieri, G. and Palomba, G. (2014). KRAS mutational concordance between primary and metastatic colorectal adenocarcinoma. *Oncology Letters*, **8**(4), 1422-1426.

Palomaki, G., Bradley, L., Douglas, M., Kolor, K. and Dotson, W. (2009). Can UGT1A1 genotyping reduce morbidity and mortality in patients with metastatic colorectal cancer treated with irinotecan? An evidence-based review. *Genetic Medicine*, **11**(1), 21-34.

Pan, S., Forrest, G., Akman, S. and Hu, L. (1995). NAD(P)H:quinone oxidoreductase expression and mitomycin C resistance developed by human colon cancer HCT166 cells. *Cancer Research*, **55** (2), 330-335.

Park, P. (2009). ChIP-seq: advantages and challenges of a maturing technology. *Nature Reviews, Genetics*, **10**(10), 669-680.

Pawlik, T., Scoggins, C., Zorzi, D., Abdalla, E., Andres, A., Eng, C., Curley, S.Loyer, E., Muratore, A., Mentha, G., Capussotti, L. and Vauthey, J. (2005). Effect of surgical margin status on survival and site of recurrence after hepatic resection for colorectal metastases. *Annals of Surgery*, **241** (5), 715-722, discussion 722-724.

Peng, J., Elias, J., Thoreen, C., Licklider, L. and Gygi, S. (2003). Evaluation of multidimensional chromatography coupled with tandem mass spectrometry (LC/LC-MS/MS) for large-scale protein analysis: The yeast proteome. *Journal of Proteome Research*, **2**(1), 43–50.

Perrault, J., McGill, D., Ott, B., and Taylor, W. (1978). Liver biopsy: complications in 1000 inpatients and outpatients. *Gastroenterology*, **74**(1), 103–106.

Pfannschmidt, J., Muley, T., Hoffmann, H. and Dienemann, H. (2003). Prognostic factors and survival after complete resection of pulmonary metastases from colorectal carcinoma: experiences in 167 patients. *The Journal of Thoracic and Cardiovascular Surgery*, **126** (3), 732-739.

Polakis, P. (2007). The many ways of Wnt in cancer. *Current Opinion in Genetics and Development*, **17**(1), 45-51.

Portier, G., Elias, D., Bouche, O., Rougier, P., Bosset, J., Saric, J., Belghiti, J., Piedbois, P., Guimbaud, R., Nordlinger, B., Bugat, R., Lazorther, F. and Bedenne, L. (2006). Multicenter randomized trial of adjuvant fluorouracil and folinic acid compared with surgery alone after resection of colorectal liver metastases: FFCD ACHBTH AURC 9002 trial. *Journal of Clinical Oncology*, **24** (31), 4976-4982.

Poste, G. (2011). Bring on the biomarkers. *Nature*, **469**(7329), 156-157.

Poston, G. (2008). Staging of advanced colorectal cancer. *Surgical Oncology Clinics of North America*, **17**(3), 503-517, viii.

Potter, J. (1999). Colorectal cancer: molecules and populations. *Journal of the National Cancer Institute*, **91**(11), 916-932.

Pretlow, T. P. and Pretlow, T.G. (2005). Mutant KRAS in aberrant crypt foci (ACF): initiation of colorectal cancer? *Biochimica et Biophysica Acta*, **1756**(2), 83-96.

Primrose, J., Falk, S., Finch-Jones, M., Valle, J., O'Reilly, D., Siriwardena, A., Hornbuckle, J., Peterson, M., Rees, M., Iveson, T., Hickish, T., Butler, R., Stanton, L., Dixon, E., Little, L., Bowers, M., Pugh, S., Garden, O., Cunningham, D., Maughan, T. and Bridgewater, J. (2014).

Systemic chemotherapy with or without cetuximab in patients with resectable colorectal liver metastasis: the New EPOC randomised controlled trial. *The Lancet*, **15** (1), 601-611.

Pritchard, C. and Grady, W.(2011). Colorectal cancer molecular biology moves into clinical practice. *Gut*, **60** (1), 116-129.

Rajagopalan, H., Bardelli, A., Lengauer, C., Kinzler, K., Vogelstein, B. and Velculescu, V. (2002). Tumorigenesis: RAF/RAS oncogenes and mismatch-repair status. *Nature*, **418**(6901), 934.

Rauth, A., Goldberg, Z. and Misra, V. (1996). DT-diaphorase: possible roles in cancer chemotherapy and carcinogenesis. *Oncology Research*, **9**(6-7), 339-349.

Raymond, E., Boige, V., Faivre, S., Sanderink, G., Rixe, O., Vernillet, L., Jacques, C., Gatineau, M., Ducreux, M. and Armand, J. (2002). Dosage adjustment and pharmacokinetic profile of irinotecan in cancer patients with hepatic dysfunction. *Journal of Clinical Oncology*, **20**(21), 4303-4312.

Realini, N., Solorzano, C., Pagliuca, C., Pizzirani, D., Armirotti, A., Luciani, R., Costi, M., Bandiera, T. and Piomelli, D. (2013). Discovery of highly potent acid ceramidase inhibitors with in vitro tumor chemosensitizing activity. *Scientific Reports*, **3**, 1035.

Rees, M., Tekkis, P., Welsh, F., O'Rourke, T. and John, T. (2008). Evaluation of long-term survival after hepatic resection for metastatic colorectal cancer: a multifactorial model of 929 patients. *Annals of Surgery*, **247**(1), 125-135.

Rehman, I., Evans, C., Glen, A., Cross, S., Eaton, C., Down, J., Pesce, G., Phillips, J., Yen, O., Thalmann, G., Wright, P. and Hamdy, F. (2012). iTRAQ identification of candidate serum biomarkers associated with metastatic progression of human prostatecancer. *PLoS One*, **7**(2), e30885.

Rex, D., Lehman, G., Ulbright, T., Smith, J., Pound, D., Hawes, R., Helper, D., Wiersema, M., Langefeld, C and Li, W. (1993). Colonic neoplasia in asymptomatic persons with negative fecal occult blood tests: influence of age, gender, and family history. *American Journal of Gastroenterology*, **88**(6), 825-831.

Ribero, D., Wang, H., Donadon, M., Zorzi, D., Thomas, M., Eng, C., Chang, D., Curley, S., Abdalla. E., Ellis, L. and Vauthey, J. (2007). Bevacizumab improves pathologic response and protects against hepatic injury in patients treated with oxaliplatin-based chemotherapy for colorectal liver metastases. *Cancer*, **110**(12), 2761-2767.

Ribic, C., Sargent, D., Moore, M., Thibodeau, S., French, A., Goldberg, R., Hamilton, S., Laurent-Puig, P., Gryfe, R., Shepherd, L., Tu, D., Redston, M. and Gallinger, S. (2003). Tumor microsatellite-instability status as a predictor of benefit from fluorouracil-based adjuvant chemotherapy for colon cancer. *New England Journal of Medicine*, **349**(3), 247-257.

Roos-van Groningen, M., Eikmans, M., Baelde, H., Baelde, H., de Heer, E. and Bruijn, J. (2004). Improvement of extraction and processing of RNA from renal biopsies. *Kidney International*, **65**(1), 97-105.

Rose, C. and Wu, H. (2010). Morphologic Criteria of Invasive Colonic Adenocarcinoma on Biopsy Specimens. *The Internet Journal of Pathology,* **12** (1), 1.

Roskoski, R. (2014). The ErbB/HER family of protein-tyrosine kinases and cancer. *Pharmacological Research*, **79**, 34-74.

Ross, D., Kepa, J., Winski, S., Beall, H., Anwar, A. and Siegel, D. (2000). NAD (P) H: quinone oxidoreductase 1 (NQO1): chemoprotection, bioactivation, gene regulation and genetic polymorphisms. *Chemico-biological interactions*, **129**(1-2), 77-97.

Rubbia-Brandt, L., Giostra, E., Brezault, C., Roth, A., Andres, A., Sartoretti, P., Dousset, B., Majno, P., Soubrane, O., Chaussade, S., Mentha, G. and Terris, B. (2007). Importance of histological tumor response assessment in predicting the outcome in patients with colorectal liver metastases treated with neo-adjuvant chemotherapy followed by liver surgery. *Annals of Oncology*, **18** (2), 299-304.

Rustgi, A. K. (2007). The genetics of hereditary colon cancer. *Genes and Development*, **21**(20), 2525-2538.

Ryan, R., Gibbons, D., Hyland, J., Treanor, D., White, A., Mulcahy, H., O'Donoghue, D., Moriarty, M., Fennelly, D. and Sheahan, K. (2005). Pathological response following long-course neoadjuvant chemoradiotherapy for locally advanced rectal cancer. *Histopathology*, **47**(2), 141-146.

Saltz, L. (2004). Palliative management of rectal cancer: the roles of chemotherapy and radiation therapy. *Journal of Gastrointestinal Surgery*, **8** (3), 274–276.

Saltz, L., Cox, J., Blanke, C., Rosen, L., Fehrenbacher, L., Moore, M., Maroun, J., Ackland, S., Locker, P., Pirotta, N., Elfring, G. and Miller, L. (2000). Irinotecan plus fluorouracil and leucovorin for metastatic colorectal cancer. Irinotecan Study Group. *New England Journal of Medicine*, **343**(13), 905-914.

Santos, M., Silva, C., Rocha, A., Matos, E., Nogueira, C. and Lopes, C. (2014). Prognostic value of mandard and dworak tumor regression grading in rectal cancer: study of a single tertiary centre. *ISRN Surgery*, **310542**, 1-8.

Sarbia, M., Bitzer, M., Siegel, D., Ross, D., Schulz, W., Zotz, R., Kiel, S., Geddert, H., Kandemir, Y. and Walter, A. (2003). Association between NAD (P) H: quinone oxidoreductase 1 (NQO1) inactivating C609T polymorphism and adenocarcinoma of the upper gastrointestinal tract. *International Journal of Cancer*, **107**(3), 381-386.

Sargent, D. (2008). Advances in defective mismatch repair colon cancer. *Clinical Advances in Hematology and Oncology*, **6**(9), 639-641.

Sauer, R., Fietkau, R., Wittekind, C., Rödel, C., Martus, P., Hohenberger, W., Tschmelitsch, J., Sabitzer, H., Karstens, J., Becker, H., Hess, C., Raab, R. and The German Rectal Cancer Group. (2003). Adjuvant *vs*. neoadjuvant radiochemotherapy for locally advanced rectal cancer: the German trial CAO/ARO/AIO-94. *Colorectal Disease*, **5**(5), 406-415.

Schüller, J., Cassidy, J., Dumont, E., Roos, B., Durston, S., Banken, L., Utoh, M., Mori, K., Weidekamm, E. and Reigner, B. (2000). Preferential activation of capecitabine in tumor following oral administration to colorectal cancer patients. *Cancer Chemotherapy and Pharmacology*, **45**(4), 291-297.

Schultz, N., Lopez, E., Saleh-Gohari, N. and Helleday, T. (2003). Poly(ADP-ribose) polymerase (PARP-1) has a controlling role in homologous recombination. *Nucleic Acids Research*, **31**(17), 4959–4964.

Scicchitano, M., Dalmas, D., Boyce, R., Thomas, H. and Frazier, K. (2009). Protein Extraction of Formalin-fixed, Paraffin-embedded Tissue Enables Robust Proteomic Profiles by Mass Spectrometry. *Journal of Histochemistry and Cytochemistry*, **57**(9),849-860.

Scott, D., Guthrie, J., Arnold, P., Ward, J., Atchley, J., Wilson, D. and Robinson, P. (2001). Dual phase helical CT versus portal venous phase CT for the detection of colorectal liver metastases: correlation with intra-operative sonography, surgical and pathological findings. *Clinical Radiology*, **56**(3), 235-242.

Sebag-Montefiore, D., Stephens, R., Steele, R., Monson, J., Grieve, R., Khanna, S., Quirke, P., Couture, J., de Metz, C., Myint, A., Bessell, E., Griffiths, G., Thompson, L. and Parmar, M. (2009). Preoperative radiotherapy versus selective postoperative chemoradiotherapy in patients with rectal cancer (MRC CR07 and NCIC-CTG C016): a multicentre, randomised trial. *Lancet*, **373**(9666), 811-820.

Shabihkhani, M., Lucey, G., Wei, B., Mareninov, S., Lou, J., Vinters, H., Singer, E., Cloughesy, T. and Yong, W. (2014). The procurement, storage, and quality assurance of frozen blood and tissue biospecimens in pathology, biorepository, and biobank settings. *Clinical Biochemistry*, **47**(4), 258-266.

Sharma, R. and Dianov, G. (2007). Targeting base excision repair to improve cancer therapies. *Molecular Aspects of Medicine*, **28**(3-4), 345-374.

Shelton, J., Waxweiler, T., Landry, J., Gao, H., Xu, Y., Wang, L., El-Rayes, B., Shu, H. (2013). In vitro and in vivo enhancement of chemoradiation using the oral PARP inhibitor ABT-888 in colorectal cancer cells. *International Journal of Radiation Oncology, Biology and Physics*, **86**(3), 469-476.

Shiovitz, S., Bertagnolli, M., Renfro, L., Nam, E., Foster, N., Dzieciatkowski, S., Luo, Y., Lao, V., Monnat, R. Jr, Emond, M., Maizels, N., Niedzwiecki, D., Goldberg, R., Saltz, L., Venook, A., Warren, R., Grady, W. amd The Alliance for Clinical Trials in Oncology. (2014). CpG island methylator phenotype is associated with response to adjuvant irinotecan-based therapy for stage III colon cancer. *Gastroenterology*, **147**(3), 637-645.

Shirasawa, S., Furuse, M., Yokoyama, N. and Sasazuki, T. (1993). Altered growth of human colon cancer cell lines disrupted at activated Ki-ras. *Science*, **260**(5104), 85-88.

Siegel, D. Gibson N., Preusch, P. and Ross, D. (1990). Metabolism of mitomycin C by DT-diaphorase: Role in mitomycin C-induced DNA damage and cytotoxicity in human colon carcinoma cells. *Cancer Research*, **50**(23), 7483-7489.

Siegel, D., Yan, C. and Ross, D. (2012). NAD (P) H: quinone oxidoreductase 1 (NQO1) in the sensitivity and resistance to antitumor quinones. *Biochemical pharmacology*, **83**(8), 1033-1040.

Siegmund, K., Marjoram, P., Tavare, S. and Shibata, D. (2009). Many colorectal cancers are "flat" clonal expansions. *Cell Cycle*, **8**(14), 2187-2193.

Sikorski, R. and Yao, B. (2010). Visualizing the landscape of selection biomarkers in current phase III oncology clinical trials. *Science Translational Medicine*, **2**(34), 34 ps 27.

Silvestrini, R., Costa, A., Gennari, L., Doci, R., Bombardieri, E. and Bombelli, L. (1990). Cell kinetics of hepatic metastases as a prognostic marker in patients with advanced colorectal carcinoma. *HPB Surgery*, **2**(2), 135-143.

Sjöblom, T., Jones, S., Wood, L., Parsons, D., Lin, J., Barber, T., Mandelker, D., Leary, R., Ptak, J., Silliman, N., Szabo, S., Buckhaults, P., Farrell, C., Meeh, P., Markowitz, S., Willis, J., Dawson, D., Willson, J., Gazdar, A., Hartigan, J., Wu, L., Liu, C., Parmigiani, G., Park, B., Bachman, K., Papadopoulos, N., Vogelstein, B., Kinzler, K. and Velculescu, V. (2006). The consensus coding sequences of human breast and colorectal cancers. *Science*, **314**(5797), 268-274.

Slattery, M. and Fitzpatrick,F. (2009). Convergence of hormones, inflammation, and energy-related factors: a novel pathway of cancer etiology. *Cancer Prevention Research (Philadelphia)*, **2**(11), 922-930.

Slattery, M., Curtin, K., Anderson, K., Ma, K., Ballard, L., Edwards, S., Schaffer, D., Potter, J., Leppert, M. and Samowitz, W. (2000). Associations between cigarette smoking, lifestyle factors, and microsatellite instability in colon tumors. *Journal of the National Cancer Institute*, **92**(22), 1831-1836.

Sobrero, A., Maurel, J., Fehrenbacher, L., Scheithauer, W., Abubakr, Y., Lutz, M., Vega-Villegas, M., Eng, C.,Steinhauer. E., Prausova, J., Lenz, H., Borg, C., Middleton, G., Kröning, H., Luppi, G., Kisker, O., Zubel, A., Langer, C., Kopit, J. and Burris, H. 3rd. (2008). EPIC: phase III trial of cetuximab plus irinotecan after fluoropyrimidine and oxaliplatin failure in patients with metastatic colorectal cancer. *Journal of Clinical Oncology*, **26**(14), 2311-2319.

Staff, S., Kujala, P., Karhu, R., Rokman, A., Ilvesaro, J., Kares, S. and Isola, J. (2013). Preservation of nucleic acids and tissue morphology in paraffin-embedded clinical samples: comparison of five molecular fixatives. *Journal of Clinical Pathology*, **66**(9), 807-810.

Stryker, S., Wolff, B., Culp, C., Libbe, S., Ilstrup, D. and MacCarthy, R. (1987). Natural history of untreated colonic polyps. *Gastroenterology*, **93** (5), 1009-1013.

Sun Myint, A., Grieve, R., McDonald, A., Levine, E., Ramani, S., Perkins, K., Wong, H., Makin, C. and Hershman, M.(2007). Combined modality treatment of early rectal cancer: the UK experience. *Clinical Oncology*, **19**(9), 674-681.

Sun, F., Sasson, A., Jiang, P., An, Z., Gamagami, R., Li, L., Moossa, A. and Hoffman, R. (1999). An ultra-metastatic model of human colon cancer in nude mice. *Clinical and Experimental Metastasis*, **17**(1), 41– 48.

Taïeb, J., Artru, P., Paye, F., Louvet, C., Perez, N., Andre, T., Gayet, B., Hebbar, M., Goebel, F., Tournigand, C., Parc, R. and de Gramont, A. (2005). Intensive systemic chemotherapy combined with surgery for metastatic colorectal cancer: results of a phase II study. *Journal of Clinical Oncology*, **23**(3), 502-509.

Tamary, H., Dgany, O., Proust, A., Krasnov, T., Avidan, N., Eidelitz-Markus, T., Tchernia, G., Geneviève, D., Cormier-Daire, V., Bader-Meunier, B., Ferrero-Vacher, C., Munzer, M., Gruppo, R., Fibach, E., Konen, O., Yaniv, I. and Delaunay, J. (2005). Clinical and molecular variability in congenital dyserythropoietic anaemia type I. *British Journal of Haematology*, **130**(4), 628-634.

Taylor, A., Kanas, G., Primrose, J., Langeberg, W., Kelsh, M., Mowat, F., AAlexander, D., Choti, M. and Poston, G.(2012) Survival after liver resection in metastatic colorectal cancer; review and meta-analysis of prognostic factors. *Clinical Epidemiology*, **4**(1), 283-301.

Taylor, F., Quirke, P., Heald, R., Moran, B., Blomqvist, L., Swift, I., Sebag-Montefiore, D., Tekkis, P., Brown, G. and MERCURY study group. (2011). Preoperative high-resolution magnetic resonance imaging can identify good prognosis stage I, II, and III rectal cancer best managed by surgery alone: a prospective, multicenter, European study. *Annals of Surgery*, **253**(4), 711-719.

Thasler, W., Thasler, R., Schelcher, C. and Jauch, K. (2013). Biobanking for research in surgery: are surgeons in charge for advancing translational research or mere assistants in biomaterial and data preservation? *Langenbecks Archives of Surgery*, **398**(4), 487-499.

Therasse, P., Arbuck, S., Eisenhauer, E., Wanders, J., Kaplan, R., Rubinstein, L., Verweij, J., Van Glabbeke, M., van Oosterom, A., Christian, M and Gwyther, S. (2000). New guidelines to evaluate the response to treatment in solid tumors. European Organization for Research and Treatment of Cancer, National Cancer Institute of the United States, National Cancer Institute of Canada. *Journal of the National Cancer Institute*, **92**(3), 205-216.

Timmermann, B., Kerick, M., Roehr, C., Fischer, A., Isau, M., Boerno, S., Wunderlich, A., Barmeyer, C., Seemann, P., Koenig, J., Lappe, M., Kuss, A., Garshasbi, M., Bertram, L., Trappe, K., Werber, M., Herrmann, B., Zatloukal, K., Lehrach, H. and Schweiger, M. (2010). Somatic Mutation Profiles of MSI and MSS Colorectal Cancer Identified by Whole Exome Next Generation Sequencing and Bioinformatics Analysis. *PLoS One*, **5**(12), e15661.

Tournigand, C., André, T., Achille, E.,Lledo, G., Flesh, M., Mery-Mignard, D., Quinaux, E., Couteau, C., Buyse M,Ganem, G., Landi, B., Colin, P., Louvet, C. and de Gramont,

A.(2004). FOLFIRI followed by FOLFOX6 or the reverse sequence in advanced colorectal cancer: a randomized GERCOR study. *Journal of Clinical Oncology*, **22**(2), 229-237.

Traver, R., Horikoshi, T., Danenberg, K., Stadlbauer, T., Danenberg, P., Ross, E. and Gibson, N. (1992). NADPH:quinone oxidoreductase gene expression in human colon carcinoma cells: characterisation of a mutation which modules DT-diaphorase activity and mitomycin sensitivity. *Cancer Research*, **52**(4), 797-802.

Tsvetkov, P., Asher, G., Reiss, V., Shaul, Y., Sachs, L. and Lotem, J. (2005). Inhibition of NAD (P) H: quinone oxidoreductase 1 activity and induction of p53 degradation by the natural phenolic compound curcumin. *Proceedings of the National Academy of Sciences of the United States of America*, **102** (15), 5535-5540.

Turnbull, R. Jr, Kyle, K., Watson, F. and Spratt, J. (1967) Cancer of the colon: the influence of the no-touch isolation technic on survival rates. *Annals of Surgery*, **166**(3), 420-427.

Van Cutsem, E., Köhne, C., Hitre, E., Zaluski, J., Chang Chien, C., Makhson, A., D'Haens, G., Pintér, T., Lim, R.,Bodoky, G., Roh, J., Folprecht. G., Ruff, P., Stroh, C., Tejpar. S., Schlichting, M., Nippgen, J. and Rougier, P.(2009).Cetuximab and chemotherapy as initial treatment for metastatic colorectal cancer. *New England Journal of Medicine*, **360**(14), 1408-1417.

Van Cutsem, E., Labianca, R.,Bodoky, G., Barone, C., Aranda, E., Nordlinger, B., Topham, C., Tabernero, J., Andre, T., Sobrero, A., Mini, E., Greil, R., Di Constanzo, F., Colette, L., Cisar, L., Zhang, X., Kayat, D., Bokemeyer, C., Roth, A. and Cunningham, D. (2009). Randomized phase III trial comparing biweekly infusional fluouracil/leucovorin alone or with irinotecan in the adjuvant treatment of stage III colon cancer: PETACC-3. *Journal of Clinical Oncology*, **27**(19), 3117-3125.

Van Cutsem, E., Rivera, F., Berry, S.,Kretzschmar, A., Michael, M., DiBartolomeo, M., Mazier, M., Canon, J.,Georgoulias, V., Peeters, M., Bridgewater, J., Cunningham, D. and First BEAT investigators. (2009). Safety and efficacy of first-line bevacizumab with FOLFOX, XELOX, FOLFIRI and fluoropyrimidines in metastatic colorectal cancer: the BEAT study. *Annals of Oncology*, **20** (11), 1842-1847.

Veldkamp, R., Kuhry, E., Hop, W., Jeekel, J., Kazemier, G., Bonjer, H., Haglind, E., Påhlman, L., Cuesta, M., Msika, S., Morino, M, and Lacy, A. (2005). Laparoscopic surgery versus open surgery for colon cancer: short-term outcomes of a randomised trial. Colon cancer Laparoscopic or Open Resection Study Group (COLOR). *Lancet Oncology*, **6**(7), 477-484.

Vens, C. and Begg, A. (2010).Targeting base excision repair as a sensitization strategy in radiotherapy. *Seminars in Radiation Oncology*, **20**(4), 241-249.

Vignais, P. M. and Vignais, P. (2010). *Discovering Life, Manufacturing Life: How the experimental method shaped life sciences.* Berlin: Springer.

Von Euler, H., Khoshnoud, R., He, Q., Khoshnoud, A., Fornander, T., Rutqvist, L. and Skog, S. (2005). Time-dependent RNA degradation affecting cDNA array quality in spontaneous

canine tumours sampled using standard surgical procedures. *International Journal of Molecular Medicine*, **16**(6), 979-985.

Vousden, K. and Prives, C. (2009). Blinded by the Light: The Growing Complexity of p53. *Cell*, **137**(3), 413-431.

Wang, L., Mason, K., Ang, K., Buchholz, T., Valdecanas, D., Mathur, A., Buser-Doepner, C., Toniatti, C. and Milas, L. (2012). MK-4827, a PARP-1/-2 inhibitor, strongly enhances response of human lung and breast cancer xenografts to radiation. *Investigational New Drugs*, **30**(6), 2113-2120.

Wang, L., Tong, S., Hu, H., Ye, F., Li, S., Ren, H., Zhang, D., Xiang, R. and Yang, Y.(2012). Quantitative proteome analysis of ovarian cancer tissues using a iTRAQ approach. *Journal of Cell Biochemistry*, **113**(12), 3762-3772.

Wang, W., Liu, X., Liu, L., Lou, W., Jin, D., Yang, P. and Wang, X.(2013). iTRAQ-based quantitative proteomics reveals myoferlin as a novel prognostic predictor in pancreatic adenocarcinoma. *Journal of Proteomics*, **91**, 453-465.

Washington, M., Berlin, J., Branton,P.,Burgart, L., Carter, D., Fitzgibbons, P., Halling, K., Frankel, W., Jessup, J., Kakar, S., Minsky, B., Nakhleh, R., Compton, C. and Members of the Cancer Committee, College of American Pathologists. (2009). Protocol for the examination of specimens from patients with primary carcinoma of the colon and rectum. *Archives of Pathology and Laboratory Medicine*, **133**(10), 1539-1551.

Watanabe, T., Wu, T., Catalano, P., Ueki, T., Satriano, R., Haller, D., Benson, A. 3rd, and Hamilton, S. (2001). Molecular predictors of survival after adjuvant chemotherapy for colon cancer. *New England Journal of Medicine*, **344**(16), 1196-1206.

Weber, D., Casjens, S., Rozynek, P., Lehnert, M., Zilch-Schoneweis, S., Bryk, O., Taeger, D., Gomolka, M., Kreuzer, M., Otten, H., Pesch, B., Johnen, G. and Brüning, T. (2010). Assessment of mRNA and microRNA stabilization in peripheral human blood for multicenter studies and biobanks. *Biomarker Insights*, **5**, 95-102.

West, N., Hohenberger, W., Weber, K., Perrakis, A., Finan, P. and Quirke, P. (2010). Complete mesocolic excision with central vascular ligation produces an oncologically superior specimen compared with standard surgery for carcinoma of the colon. *Journal of Clinical Oncology*, **28**(2), 272-278.

Wheeler, J., Warren, B., Mortensen, N., Ekanyaka, N., Kulacoglu, H., Jones, A., George, B. and Kettlewell, M. (2002) Quantification of histologic regression of rectal cancer after irradiation: a proposal for a modified staging system. *Diseases of the Colon and Rectum*, **45**(8), 1051–1056.

Wilkins, M., Pasquali, C., Appel, R., Ou, K., Golaz, O., Sanchez, J-J., Yan, J., Gooley, A., Hughes, G., Humphery-Smith, I., Williams, K. and Hochstrasser, D. (1996). From Proteins to Proteomes: Large Scale Protein Identification by Two-Dimensional Electrophoresis and Arnino Acid Analysis. *Nature Biotechnology*, **14**(1), 61–65.

Willett, C., Warland, G., Coen, J., Shellito, P. and Compton, C. (1995). Rectal cancer: the influence of tumor proliferation on response to preoperative irradiation. *International Journal of Radiation Oncology, Biology and Physics*, **32**(1), 57-61.

Winski, S., Swann, E., Hargreaves, R., Dehn, D., Butler, J., Moody, C. and Ross, D. (2001). Relationship between NAD (P) H: quinone oxidoreductase 1 (NQO1) levels in a series of stably transfected cell lines and susceptibility to antitumor quinones. *Biochemical pharmacology*, **61**(12), 1509-1516.

Wong, S., Mangu, P., Choti, M., Crocenzi, T., Dodd, G. 3rd, Dorfman, G., Eng, C., Fong, Y., Giusti, A., Lu D,Marsland, T., Michelson, R., Poston, G., Schrag, D., Seidenfeld, J. and Benson, A. 3rd. (2010). American Society of Clinical Oncology 2009 clinical evidence review on radiofrequency ablation of hepatic metastases from colorectal cancer. *Journal of Clinical Oncology*, **28**(3), 493-508.

Wood, L., Parsons, D.,Jones, S., Lin, J., Sjöblom, T., Leary, R., Shen, D., Boca, S., Barber, T., Ptak, J., Silliman, N., Szabo, S., Dezso, Z., Ustyanksky, V., Nikolskaya, T., Nikolsky, Y., Karchin, R., Wilson, P., Kaminker, J., Zhang, Z., Croshaw, R., Willis, J., Dawson, D., Shipitsin, M., Willson, J., Sukumar. S., Polyak, K., Park, B., Pethiyagoda, C., Pant, P., Ballinger, D., Sparks, A., Hartigan, J., Smith, D., Suh, E., Papadopoulos, N., Buckhaults, P., Markowitz, S., Parmigiani, G., Kinzler, K., Velculescu, V. and Vogelstein, B. (2007). The genomic landscapes of human breast and colorectal cancers. *Science*, **318**(5853), 1108-1113.

Wright, J., Dreyfuss, A., el-Magharbel, I., Trites, D., Jones, S., Holden, S., Rosowsky, A. and Frei, E. 3rd. (1989). Selective expansion of 5,10-methylenetetrahydrofolate pools and modulation of 5-fluorouracil antitumor activity by leucovorin in vivo. *Cancer Research*, **49**(10), 2592-2596.

Xu, G., Mymryk, J. and Cairncross, J. (2005). Inactivation of p53 sensitizes astrocytic glioma cells to BCNU and temozolomide, but not cisplatin. *Journal of Neuro-oncology*, **74**(2), 141–149.

Yang, J., Parsons, J., Nicolay, N., Caporali, S., Harrington, C., Singh, R., Finch, D., D'Atri, S., Farmer, P., Johnston, P., McKenna, W., Dianov, G. and Sharma, R.(2010) Cells deficient in the base excision repair protein, DNA polymerase beta, are hypersensitive to oxaliplatin chemotherapy. *Oncogene*, **29**(3), 463-468.

Yang, Y., Zhang, Y., Wu, Q., Cui, X., Lin, Z., Liu, S. and Chen L. (2014). Clinical implications of high NQO1 expression in breast cancers. *Journal of Experimental & Clinical Cancer Research*, **33**(1), 14.

Yao, Y., Shao, J., Zhang, C., Wu, J., Zhang, Q., Wang, J. and Zhu, W. (2013). Proliferation of colorectal cancer is promoted by two signaling transduction expression patterns: ErbB2/ErbB3/AKT and MET/ErbB3/MAPK. *PLoS One*, **8**(10), e78086.

Ychou, M., Hohenberger, W., Thezenas, S., Navarro, M., Maurel, J., Bokemeyer, C., Shacham-Shmueli, E., Rivera, F., Kwok-Keung Choi, C. and Santoro, A. (2009). A

randomized phase III study comparing adjuvant 5-fluorouracil/folinic acid with FOLFIRI in patients following complete resection of liver metastases from colorectal cancer. *Annals of Oncology*, **20**(12), 1964-1970.

Yin, H., Zhang, L., Xie, L., Huang, L., Xu, Y., Cai, S., Yang, P. and Lu, H. (2013). Hyperplex-MRM: a hybrid multiple reaction monitoring method using mTRAQ/iTRAQ labeling for multiplex absolute quantification of human colorectal cancer biomarker. *Journal of Proteome Research*, **12**(9), 3912-3919.

Yoder, J., Soman, N., Verdine, G. and Bestor, T. (1997). DNA (cytosine-5)-methyltransferases in mouse cells and tissues. Studies with a mechanism-based probe. *Journal of Molecular Biology*, **270**(3), 385-395.

Yoshioka, A., Tanaka, S., Hiraoka, O., Koyama, Y., Hirota, Y., Ayusawa, D., Seno, T., Garrett, C. and Wataya, Y. (1987). Deoxyribonucleoside triphosphate imbalance. 5-Fluorodeoxyuridine-induced DNA double strand breaks in mouse FM3A cells and the mechanism of cell death. *Journal of Biological Chemistry*, **262**(17), 8235-8241.

Zhang, H., Berezov, A., Wang, Q., Zhang, G., Drebin, J., Murali, R. and Greene,M. (2007). ErbB receptors: from oncogenes to targeted cancer therapies. *Journal of Clinical Investigation*, **117**(8), 2051–2058.

Zhou, D., Yang, L., Zheng, L., Ge, W., Li, D., Zhang, Y., Hu, X., Gao, Z., Xu, J., Huang, Y., Hu, H., Zhang, H., Zhang, H., Liu, M., Yang, H., Zheng, L. and Zheng, S. (2013). Exome Capture Sequencing of Adenoma Reveals Genetic Alterations in Multiple Cellular Pathways at the Early Stage of Colorectal Tumorigenesis. *PLoS One*, **8**(1), e53310.

Zhu, H., Wu, T., Chen, W., Zhou, L., Wu, Y., Zeng, L. and Pei, H. (2013). Screening for differentially expressed genes between left- and right-sided colon carcinoma by microarray analysis. *Oncology Letters*, **6**(2), 353-358.

Zieske, L. (2006). A perspective on the use of iTRAQ reagent technology for protein complex and profiling studies. *Journal of Experimental Botany*, **57**(7), 1501–1508.

Appendix 1

Lists of single nucleotide variants from exome sequencing

Table 1 – Single nucleotide variants exclusive to the primary tumours

Annotation	Gene	Chromosome	Location	Substituted Amino Acid	New Amino Acid
ABCC3_17_48761053_G/A	ABCC3	17	48761053	G	A
ACAD11_3_132338346_T/G	ACAD11	3	132338346	T	G
ACADL_2_211060050_T/G	ACADL	2	211060050	T	G
ADAMTS1_21_28212761_G/A	ADAMTS1	21	28212761	G	A
ADD1_4_2916762_C/G	ADD1	4	2916762	C	G
AGXT_2_241808314_C/T	AGXT	2	241808314	C	T
ALPP_2_233243586_C/T	ALPP	2	233243586	C	T
APOB_2_21250914_G/A	APOB	2	21250914	G	A
ARHGEF19_1_16532498_G/A	ARHGEF19	1	16532498	G	A
BAIAP3_16_1394822_C/T	BAIAP3	16	1394822	C	T
BMP2K_4_79832411_A/G	BMP2K	4	79832411	A	G
C18orf25_18_43796346_G/C	C18orf25	18	43796346	G	C
C2orf43_2_20974689_C/T	C2orf43	2	20974689	C	T
C5orf22_5_31532534_G/C	C5orf22	5	31532534	G	C
CACNA1H_16_1254369_C/T	CACNA1H	16	1254369	C	T
CACNA1H_16_1268376_G/A	CACNA1H	16	1268376	G	A
CADM4_19_44130960_A/G	CADM4	19	44130960	A	G
CCDC136_7_128454762_G/A	CCDC136	7	128454762	G	A
CCDC78_16_774760_T/C	CCDC78	16	774760	T	C
CCRN4L_4_139966431_C/T	CCRN4L	4	139966431	C	T
CCT6B_17_33269648_C/G	CCT6B	17	33269648	C	G
CD93_20_23065209_G/A	CD93	20	23065209	G	A
CDC27_17_45214615_G/C	CDC27	17	45214615	G	C
CDC27_17_45214617_G/C	CDC27	17	45214617	G	C
CEP135_4_56819375_A/G	CEP135	4	56819375	A	G
CHAT_10_50835687_C/T	CHAT	10	50835687	C	T
CHRNA5_15_78880752_G/A	CHRNA5	15	78880752	G	A
CHRND_2_233398698_C/T	CHRND	2	233398698	C	T
CHST15_10_125769672_G/A	CHST15	10	125769672	G	A
CLCNKA_1_16356501_G/A	CLCNKA	1	16356501	G	A
CLCNKB_1_16371067_G/T	CLCNKB	1	16371067	G	T
CLDN3_7_73183979_G/A	CLDN3	7	73183979	G	A
CNGA4_11_6265242_G/C	CNGA4	11	6265242	G	C
CNN2_19_1036211_C/T	CNN2	19	1036211	C	T
CNN2_19_1037715_T/C	CNN2	19	1037715	T	C
CNN2_19_1037716_G/A	CNN2	19	1037716	G	A
CNN2_19_1037718_G/T	CNN2	19	1037718	G	T
COL15A1_9_101778346_C/G	COL15A1	9	101778346	C	G
COL5A3_19_10085054_G/A	COL5A3	19	10085054	G	A

COL6A2_21_47551942_G/A	COL6A2	21	47551942	G	A
CPAMD8_19_17025292_G/A	CPAMD8	19	17025292	G	A
CTBP2_10_126681824_G/A	CTBP2	10	126681824	G	A
CTBP2_10_126681831_C/G	CTBP2	10	126681831	C	G
CTBP2_10_126681838_C/G	CTBP2	10	126681838	C	G
CTBP2_10_126681848_T/A	CTBP2	10	126681848	T	A
CTBP2_10_126683099_G/A	CTBP2	10	126683099	G	A
CTBP2_10_126683111_C/T	CTBP2	10	126683111	C	T
CTBP2_10_126683132_A/T	CTBP2	10	126683132	A	T
CTBP2_10_126683243_C/T	CTBP2	10	126683243	C	T
CTBP2_10_126683244_C/G	CTBP2	10	126683244	C	G
CTBP2_10_126686629_G/A	CTBP2	10	126686629	G	A
CTBP2_10_126691552_T/G	CTBP2	10	126691552	T	G
CTDSP2_12_58217770_G/C	CTDSP2	12	58217770	G	C
CX3CR1_3_39307162_G/A	CX3CR1	3	39307162	G	A
CYP2C8_10_96818119_G/C	CYP2C8	10	96818119	G	C
CYP2D6_22_42526694_G/A	CYP2D6	22	42526694	G	A
CYP4F12_19_15784377_C/T	CYP4F12	19	15784377	C	T
CYP4F2_19_15989696_G/C	CYP4F2	19	15989696	G	C
D2HGDH_2_242690675_G/A	D2HGDH	2	242690675	G	A
DCLK1_13_36686139_G/C	DCLK1	13	36686139	G	C
DHTKD1_10_12143122_C/T	DHTKD1	10	12143122	C	T
DIS3L2_2_233127938_C/G	DIS3L2	2	233127938	C	G
DLAT_11_111916647_G/A	DLAT	11	111916647	G	A
DNAH17_17_76456017_C/G	DNAH17	17	76456017	C	G
DOCK7_1_62993881_T/C	DOCK7	1	62993881	T	C
DROSHA_5_31508739_C/T	DROSHA	5	31508739	C	T
DUOX2_15_45393014_G/C	DUOX2	15	45393014	G	C
EFCAB8_20_31480028_A/T	EFCAB8	20	31480028	A	T
EHBP1_2_63176139_A/C	EHBP1	2	63176139	A	C
ELP2_18_33736498_C/T	ELP2	18	33736498	C	T
ESRRA_11_64083320_T/C	ESRRA	11	64083320	T	C
ESRRA_11_64083328_C/T	ESRRA	11	64083328	C	T
ESRRA_11_64083331_C/T	ESRRA	11	64083331	C	T
EXTL3_8_28575417_T/C	EXTL3	8	28575417	T	C
FAM70B_13_114504663_G/A	FAM70B	13	114504663	G	A
FAM8A1_6_17606159_C/A	FAM8A1	6	17606159	C	A
FCGBP_19_40376675_G/A	FCGBP	19	40376675	G	A
FERMT1_20_6088265_G/A	FERMT1	20	6088265	G	A
FGFR3_4_1806629_C/T	FGFR3	4	1806629	C	T
FMN2_1_240370985_C/T	FMN2	1	240370985	C	T
FOXN4_12_109725707_G/A	FOXN4	12	109725707	G	A
FRG1_4_190876196_G/A	FRG1	4	190876196	G	A
FRG1_4_190883039_T/C	FRG1	4	190883039	T	C

GALNT2_1_230391032_G/A	GALNT2	1	230391032	G	A
GDNF_5_37816112_G/A	GDNF	5	37816112	G	A
GGT2_22_21576218_G/A	GGT2	22	21576218	G	A
GLB1_3_33138549_G/A	GLB1	3	33138549	G	A
GLIS2_16_4385158_A/G	GLIS2	16	4385158	A	G
GLOD4_17_685752_G/A	GLOD4	17	685752	G	A
GSTT1_22_24379402_T/G	GSTT1	22	24379402	T	G
HEXDC_17_80391684_A/G	HEXDC	17	80391684	A	G
HMCN1_1_186101539_A/G	HMCN1	1	186101539	A	G
HMCN2_9_133294224_C/T	HMCN2	9	133294224	C	T
HSPG2_1_22179244_C/T	HSPG2	1	22179244	C	T
IFI16_1_159024668_A/T	IFI16	1	159024668	A	T
IL3RA_X_1471083_C/G	IL3RA	X	1471083	C	G
INF2_14_105180785_C/T	INF2	14	105180785	C	T
INPP5B_1_38329999_C/G	INPP5B	1	38329999	C	G
IQSEC3_12_247544_C/T	IQSEC3	12	247544	C	T
IRX4_5_1878325_C/T	IRX4	5	1878325	C	T
IRX6_16_55362942_T/C	IRX6	16	55362942	T	C
KCNH8_3_19574945_A/G	KCNH8	3	19574945	A	G
KCNJ12_17_21319523_C/T	KCNJ12	17	21319523	C	T
KCNJ12_17_21319786_G/A	KCNJ12	17	21319786	G	A
KIAA1958_9_115422069_G/A	KIAA1958	9	115422069	G	A
KIF24_9_34254413_G/C	KIF24	9	34254413	G	C
KIF26B_1_245848798_C/T	KIF26B	1	245848798	C	T
KLHL33_14_20897676_T/C	KLHL33	14	20897676	T	C
KLK10_19_51519365_C/G	KLK10	19	51519365	C	G
KRT18_12_53343225_C/T	KRT18	12	53343225	C	T
KRT18_12_53343231_G/C	KRT18	12	53343231	G	C
KRT32_17_39616430_G/T	KRT32	17	39616430	G	T
KRT40_17_39135089_G/A	KRT40	17	39135089	G	A
KRT40_17_39137154_C/G	KRT40	17	39137154	C	G
LYPD2_8_143833856_C/T	LYPD2	8	143833856	C	T
MATN2_8_98943447_G/C	MATN2	8	98943447	G	C
MLL3_7_151935866_G/A	MLL3	7	151935866	G	A
MLL3_7_151935871_C/A	MLL3	7	151935871	C	A
MPPED1_22_43831057_G/T	MPPED1	22	43831057	G	T
MSH6_2_48027136_A/G	MSH6	2	48027136	A	G
MSR1_8_16026181_T/C	MSR1	8	16026181	T	C
MTCH2_11_47640398_T/C	MTCH2	11	47640398	T	C
MTCH2_11_47660334_C/T	MTCH2	11	47660334	C	T
MUC16_19_8999530_C/T	MUC16	19	8999530	C	T
MUC4_3_195495916_G/C	MUC4	3	195495916	G	C
MYH3_17_10542257_A/G	MYH3	17	10542257	A	G
MYOM3_1_24409191_C/T	MYOM3	1	24409191	C	T

NAGLU_17_40696233_C/G	NAGLU	17	40696233	C	G
NCOR1_17_16097825_T/G	NCOR1	17	16097825	T	G
NCOR1_17_16097870_C/A	NCOR1	17	16097870	C	A
NDUFS2_1_161183191_C/G	NDUFS2	1	161183191	C	G
NOTCH2NL_1_145281408_C/T	NOTCH2NL	1	145281408	C	T
NPBWR1_8_53852871_A/T	NPBWR1	8	53852871	A	T
NPEPPS_17_45669359_T/G	NPEPPS	17	45669359	T	G
PABPC1_8_101719138_C/T	PABPC1	8	101719138	C	T
PABPC1_8_101719201_A/G	PABPC1	8	101719201	A	G
PABPC1_8_101725003_C/A	PABPC1	8	101725003	C	A
PABPC1_8_101727714_G/A	PABPC1	8	101727714	G	A
PABPC1_8_101727716_C/T	PABPC1	8	101727716	C	T
PABPC3_13_25671195_A/G	PABPC3	13	25671195	A	G
PAK2_3_196509577_C/G	PAK2	3	196509577	C	G
PANK3_5_167986134_T/C	PANK3	5	167986134	T	C
PCDHB4_5_140502343_C/T	PCDHB4	5	140502343	C	T
PCDHB4_5_140502344_C/T	PCDHB4	5	140502344	C	T
PCDHGB6_5_140788491_T/G	PCDHGB6	5	140788491	T	G
PHF11_13_50095041_A/G	PHF11	13	50095041	A	G
PHKB_16_47732476_C/T	PHKB	16	47732476	C	T
PIEZO1_16_88787673_G/A	PIEZO1	16	88787673	G	A
PIEZO1_16_88791458_G/A	PIEZO1	16	88791458	G	A
PIEZO2_18_10731428_C/T	PIEZO2	18	10731428	C	T
PLEKHG2_19_39913519_C/G	PLEKHG2	19	39913519	C	G
PLVAP_19_17471595_T/G	PLVAP	19	17471595	T	G
POU2F1_1_167343528_G/A	POU2F1	1	167343528	G	A
PPP1R2_3_195269788_T/C	PPP1R2	3	195269788	T	C
PRDM7_16_90126993_A/G	PRDM7	16	90126993	A	G
PRKRA_2_179300979_A/T	PRKRA	2	179300979	A	T
PSMD9_12_122353796_A/G	PSMD9	12	122353796	A	G
PTPRS_19_5258067_C/T	PTPRS	19	5258067	C	T
RAB26_16_2203334_G/A	RAB26	16	2203334	G	A
RASA4_7_102235769_T/C	RASA4	7	102235769	T	C
RC3H1_1_173952595_C/T	RC3H1	1	173952595	C	T
RNF123_3_49759490_G/A	RNF123	3	49759490	G	A
RPL19_17_37360846_C/T	RPL19	17	37360846	C	T
RPL19_17_37360863_A/T	RPL19	17	37360863	A	T
RSPH4A_6_116950734_G/A	RSPH4A	6	116950734	G	A
SBNO1_12_123805023_C/A	SBNO1	12	123805023	C	A
SDHA_5_236649_C/T	SDHA	5	236649	C	T
SDHA_5_236676_G/A	SDHA	5	236676	G	A
SDHA_5_236678_G/A	SDHA	5	236678	G	A
SDK2_17_71426656_G/T	SDK2	17	71426656	G	T
SEC14L3_22_30864610_A/G	SEC14L3	22	30864610	A	G

SERPINB10_18_61582751_T/G	SERPINB10	18	61582751	T	G
SERPINB10_18_61600384_C/T	SERPINB10	18	61600384	C	T
SERPINB8_18_61654463_A/G	SERPINB8	18	61654463	A	G
SETD8_12_123892186_T/C	SETD8	12	123892186	T	C
SKIV2L_6_31931747_G/A	SKIV2L	6	31931747	G	A
SLC15A1_13_99337138_A/G	SLC15A1	13	99337138	A	G
SLC25A5_X_118604030_T/C	SLC25A5	X	118604030	T	C
SLC25A5_X_118604399_C/G	SLC25A5	X	118604399	C	G
SLC25A5_X_118604428_T/C	SLC25A5	X	118604428	T	C
SLC2A1_1_43393457_T/C	SLC2A1	1	43393457	T	C
SLC44A4_6_31846741_C/A	SLC44A4	6	31846741	C	A
SLC46A3_13_29292117_C/T	SLC46A3	13	29292117	C	T
SLC6A7_5_149578877_C/T	SLC6A7	5	149578877	C	T
SMPD4_2_130930380_A/G	SMPD4	2	130930380	A	G
SOX7_8_10683685_A/G	SOX7	8	10683685	A	G
SPNS1_16_28990588_G/A	SPNS1	16	28990588	G	A
SREK1IP1_5_64020269_T/C	SREK1IP1	5	64020269	T	C
STAB2_12_104048454_C/A	STAB2	12	104048454	C	A
SYT8_11_1857751_C/G	SYT8	11	1857751	C	G
TAS2R46_12_11214025_A/T	TAS2R46	12	11214025	A	T
TAS2R46_12_11214080_G/A	TAS2R46	12	11214080	G	A
TCF3_19_1650228_A/G	TCF3	19	1650228	A	G
TEKT4_2_95541427_G/T	TEKT4	2	95541427	G	T
TEKT4_2_95541447_C/T	TEKT4	2	95541447	C	T
TFAP2A_6_10410556_C/T	TFAP2A	6	10410556	C	T
TGM1_14_24729863_G/A	TGM1	14	24729863	G	A
TIAM2_6_155561796_C/T	TIAM2	6	155561796	C	T
TNFRSF14_1_2488153_A/G	TNFRSF14	1	2488153	A	G
TNS1_2_218713282_G/A	TNS1	2	218713282	G	A
TPSD1_16_1306986_C/T	TPSD1	16	1306986	C	T
TPTE_21_10943003_C/T	TPTE	21	10943003	C	T
TSPAN32_11_2325427_T/C	TSPAN32	11	2325427	T	C
TSTA3_8_144697051_T/C	TSTA3	8	144697051	T	C
TXNRD2_22_19907099_C/A	TXNRD2	22	19907099	C	A
USP40_2_234394477_A/G	USP40	2	234394477	A	G
WDR33_2_128525866_A/G	WDR33	2	128525866	A	G
WDR72_15_53907948_G/A	WDR72	15	53907948	G	A
WNT10B_12_49364239_C/T	WNT10B	12	49364239	C	T
YLPM1_14_75248652_C/G	YLPM1	14	75248652	C	G
ZNF404_19_44377669_G/A	ZNF404	19	44377669	G	A
ZNF527_19_37879853_C/T	ZNF527	19	37879853	C	T
ZNF544_19_58774094_C/T	ZNF544	19	58774094	C	T
ZNF717_3_75790880_A/G	ZNF717	3	75790880	A	G
ZNF730_19_23329194_A/G	ZNF730	19	23329194	A	G

Table 2 – Single nucleotide variants exclusive to the metastatic tumours

Annotation	Gene	Chromosome	Location	Substituted Amino Acid	New Amino Acid
A4GALT_22_43089654_C/T	A4GALT	22	43089654	C	T
ABCA9_17_67017930_T/C	ABCA9	17	67017930	T	C
ABCB5_7_20762646_G/T	ABCB5	7	20762646	G	T
ABCC9_12_22017410_C/T	ABCC9	12	22017410	C	T
ACACB_12_109650663_A/G	ACACB	12	109650663	A	G
ACE_17_61568577_C/T	ACE	17	61568577	C	T
ACTN2_1_236902618_G/A	ACTN2	1	236902618	G	A
ACTR1A_10_104241913_C/T	ACTR1A	10	104241913	C	T
ADNP2_18_77895325_T/G	ADNP2	18	77895325	T	G
AK2_1_33478931_G/C	AK2	1	33478931	G	C
ALDH3B2_11_67433662_C/T	ALDH3B2	11	67433662	C	T
ALG1_16_5128817_G/A	ALG1	16	5128817	G	A
ALPPL2_2_233271669_C/T	ALPPL2	2	233271669	C	T
AMY2A_1_104163266_G/A	AMY2A	1	104163266	G	A
ANKK1_11_113269792_C/A	ANKK1	11	113269792	C	A
ANKRD36_2_97860487_T/C	ANKRD36	2	97860487	T	C
APOBEC3G_22_39482396_C/A	APOBEC3G	22	39482396	C	A
ARHGEF19_1_16534255_C/G	ARHGEF19	1	16534255	C	G
ARSD_X_2836002_C/T	ARSD	X	2836002	C	T
ASPM_1_197070442_G/T	ASPM	1	197070442	G	T
ASPM_1_197070697_T/C	ASPM	1	197070697	T	C
ATP11A_13_113530199_G/A	ATP11A	13	113530199	G	A
ATP13A4_3_193209178_T/C	ATP13A4	3	193209178	T	C
ATP6V0D2_8_87151837_A/T	ATP6V0D2	8	87151837	A	T
ATXN1_6_16306751_G/A	ATXN1	6	16306751	G	A
AZU1_19_830841_G/A	AZU1	19	830841	G	A
BCHE_3_165491184_A/C	BCHE	3	165491184	A	C
BMP3_4_81967150_G/A	BMP3	4	81967150	G	A
BPI_20_36954670_G/A	BPI	20	36954670	G	A
C16orf96_16_4625938_A/T	C16orf96	16	4625938	A	T
C3orf39_3_43121884_G/C	C3orf39	3	43121884	G	C
CACNA1B_9_140777306_C/G	CACNA1B	9	140777306	C	G
CALCA_11_14991511_A/G	CALCA	11	14991511	A	G
CCBL2_1_89448608_G/A	CCBL2	1	89448608	G	A
CCDC138_2_109408208_G/A	CCDC138	2	109408208	G	A
CCT8_21_30439894_C/A	CCT8	21	30439894	C	A
CD1A_1_158226621_G/T	CD1A	1	158226621	G	T
CDC27_17_45214523_A/C	CDC27	17	45214523	A	C
CDC27_17_45214531_G/A	CDC27	17	45214531	G	A

CDC27_17_45214606_G/T	CDC27	17	45214606	G	T
CDC27_17_45214623_G/A	CDC27	17	45214623	G	A
CDC27_17_45214690_G/A	CDC27	17	45214690	G	A
CDC27_17_45219296_G/C	CDC27	17	45219296	G	C
CDC27_17_45219332_T/G	CDC27	17	45219332	T	G
CDC27_17_45247298_A/G	CDC27	17	45247298	A	G
CDH8_16_61859047_T/C	CDH8	16	61859047	T	C
CELA1_12_51740416_C/G	CELA1	12	51740416	C	G
CFTR_7_117188750_C/T	CFTR	7	117188750	C	T
CHRNA3_15_78894026_C/T	CHRNA3	15	78894026	C	T
CHRNE_17_4806020_G/A	CHRNE	17	4806020	G	A
CLCN4_X_10176599_T/C	CLCN4	X	10176599	T	C
CLEC18C_16_70211379_C/T	CLEC18C	16	70211379	C	T
CNGB1_16_57996933_C/A	CNGB1	16	57996933	C	A
CNN2_19_1037756_G/A	CNN2	19	1037756	G	A
CNN2_19_1037766_G/A	CNN2	19	1037766	G	A
COL24A1_1_86512536_C/T	COL24A1	1	86512536	C	T
COL4A3_2_228135631_C/T	COL4A3	2	228135631	C	T
COL5A3_19_10071347_C/T	COL5A3	19	10071347	C	T
CORO1C_12_109094907_A/G	CORO1C	12	109094907	A	G
COSM45060_17_7577581_A/G	COSM45060	17	7577581	A	G
CP_3_148916235_T/A	CP	3	148916235	T	A
CTBP2_10_126691979_C/G	CTBP2	10	126691979	C	G
CTDSP2_12_58217770_G/T	CTDSP2	12	58217770	G	T
CYP21A2_6_32006387_A/T	CYP21A2	6	32006387	A	T
DISP1_1_223116472_G/A	DISP1	1	223116472	G	A
DNA2_10_70191724_C/G	DNA2	10	70191724	C	G
DNAH9_17_11651057_A/G	DNAH9	17	11651057	A	G
DSG1_18_28909921_G/T	DSG1	18	28909921	G	T
DUOX2_15_45392075_G/A	DUOX2	15	45392075	G	A
EME1_17_48457758_C/G	EME1	17	48457758	C	G
EMR2_19_14875388_G/A	EMR2	19	14875388	G	A
ENOX2_X_129837156_G/A	ENOX2	X	129837156	G	A
EP400_12_132445675_G/A	EP400	12	132445675	G	A
EPPK1_8_144944226_G/A	EPPK1	8	144944226	G	A
ESPNL_2_239039981_A/G	ESPNL	2	239039981	A	G
FAM126A_7_23016393_C/G	FAM126A	7	23016393	C	G
FAM136A_2_70524515_T/A	FAM136A	2	70524515	T	A
FAM136A_2_70524576_C/G	FAM136A	2	70524576	C	G
FAM136A_2_70524606_G/A	FAM136A	2	70524606	G	A
FAM65C_20_49209710_C/T	FAM65C	20	49209710	C	T
FANCA_16_89857935_G/A	FANCA	16	89857935	G	A
FCRLB_1_161697072_G/C	FCRLB	1	161697072	G	C
FES_15_91433090_A/G	FES	15	91433090	A	G
FLVCR1_1_213068595_C/T	FLVCR1	1	213068595	C	T

FNDC1_6_159655103_T/G	FNDC1	6	159655103	T	G
FRG1_4_190876293_C/A	FRG1	4	190876293	C	A
FRG1_4_190878563_C/A	FRG1	4	190878563	C	A
FRG1_4_190878569_T/C	FRG1	4	190878569	T	C
FUT3_19_5843784_A/T	FUT3	19	5843784	A	T
GATA3_10_8100641_G/A	GATA3	10	8100641	G	A
GHR_5_42719239_A/C	GHR	5	42719239	A	C
GNAQ_9_80537112_T/A	GNAQ	9	80537112	T	A
GPATCH2_1_217604654_T/C	GPATCH2	1	217604654	T	C
GPRC6A_6_117130544_A/C	GPRC6A	6	117130544	A	C
GXYLT1_12_42499825_A/C	GXYLT1	12	42499825	A	C
GZMM_19_548612_G/A	GZMM	19	548612	G	A
HIP1R_12_123345509_G/T	HIP1R	12	123345509	G	T
HMGXB3_5_149390148_G/A	HMGXB3	5	149390148	G	A
HNF1A_12_121435427_G/A	HNF1A	12	121435427	G	A
HRAS_11_533880_G/A	HRAS	11	533880	G	A
HSD17B11_4_88278497_C/T	HSD17B11	4	88278497	C	T
HSPD1_2_198363406_C/T	HSPD1	2	198363406	C	T
IFI30_19_18285944_G/A	IFI30	19	18285944	G	A
INS_11_2181060_T/G	INS	11	2181060	T	G
ITIH1_3_52820981_A/T	ITIH1	3	52820981	A	T
ITSN2_2_24435599_G/A	ITSN2	2	24435599	G	A
KCNB1_20_47991468_G/A	KCNB1	20	47991468	G	A
KCNG4_16_84256410_C/T	KCNG4	16	84256410	C	T
KCNH6_17_61615545_A/G	KCNH6	17	61615545	A	G
KCNJ12_17_21319230_G/C	KCNJ12	17	21319230	G	C
KCNJ16_17_68128332_G/A	KCNJ16	17	68128332	G	A
KCNK13_14_90651135_G/T	KCNK13	14	90651135	G	T
KCNV1_8_110984553_G/A	KCNV1	8	110984553	G	A
KIAA0141_5_141309824_G/A	KIAA0141	5	141309824	G	A
KIAA0753_17_6513329_G/A	KIAA0753	17	6513329	G	A
KIF19_17_72340981_G/A	KIF19	17	72340981	G	A
KRT14_17_39742807_C/T	KRT14	17	39742807	C	T
KRT36_17_39643340_T/G	KRT36	17	39643340	T	G
LAMA5_20_60889385_G/T	LAMA5	20	60889385	G	T
LDHAL6B_15_59500180_C/G	LDHAL6B	15	59500180	C	G
LRP1B_2_141459344_C/T	LRP1B	2	141459344	C	T
LRRC17_7_102574920_G/C	LRRC17	7	102574920	G	C
MASP2_1_11090916_C/A	MASP2	1	11090916	C	A
MBD1_18_47800179_G/C	MBD1	18	47800179	G	C
MGAT2_14_50089014_A/C	MGAT2	14	50089014	A	C
MKL2_16_14341144_A/G	MKL2	16	14341144	A	G
MLL2_12_49430947_T/C	MLL2	12	49430947	T	C
MLL3_7_151927021_C/A	MLL3	7	151927021	C	A
MLL3_7_151927067_T/C	MLL3	7	151927067	T	C

MLL3_7_151935910_C/T	MLL3	7	151935910	C	T
MLL5_7_104717522_A/G	MLL5	7	104717522	A	G
MLPH_2_238449007_T/C	MLPH	2	238449007	T	C
MOGAT1_2_223559089_T/C	MOGAT1	2	223559089	T	C
MTCH2_11_47663951_A/G	MTCH2	11	47663951	A	G
MTCH2_11_47663986_C/T	MTCH2	11	47663986	C	T
MTCH2_11_47663996_C/T	MTCH2	11	47663996	C	T
MTMR11_1_149906167_T/G	MTMR11	1	149906167	T	G
MUC16_19_9002597_C/T	MUC16	19	9002597	C	T
MUC6_11_1027811_C/T	MUC6	11	1027811	C	T
MYH4_17_10355371_C/T	MYH4	17	10355371	C	T
MYO1H_12_109872909_C/T	MYO1H	12	109872909	C	T
MYO9B_19_17213218_G/A	MYO9B	19	17213218	G	A
MZT2B_2_130948087_C/T	MZT2B	2	130948087	C	T
NAV1_1_201754444_G/C	NAV1	1	201754444	G	C
NHLRC1_6_18122258_C/T	NHLRC1	6	18122258	C	T
NIN_14_51202311_G/C	NIN	14	51202311	G	C
NOD1_7_30492237_C/T	NOD1	7	30492237	C	T
NOTCH1_9_139412350_G/A	NOTCH1	9	139412350	G	A
NUP88_17_5289554_T/C	NUP88	17	5289554	T	C
NUP98_11_3744435_C/G	NUP98	11	3744435	C	G
OGDHL_10_50950976_G/A	OGDHL	10	50950976	G	A
OLFM1_9_138011540_T/C	OLFM1	9	138011540	T	C
OR51G1_11_4945199_C/T	OR51G1	11	4945199	C	T
PABPC1_8_101730043_G/C	PABPC1	8	101730043	G	C
PABPC1_8_101730064_G/A	PABPC1	8	101730064	G	A
PABPC1_8_101730110_A/C	PABPC1	8	101730110	A	C
PABPC3_13_25670868_G/A	PABPC3	13	25670868	G	A
PABPC3_13_25670877_G/A	PABPC3	13	25670877	G	A
PABPC3_13_25670955_C/T	PABPC3	13	25670955	C	T
PAK2_3_196529902_G/C	PAK2	3	196529902	G	C
PARN_16_14576574_A/C	PARN	16	14576574	A	C
PARP4_13_25016762_G/A	PARP4	13	25016762	G	A
PCDHA9_5_140228164_C/A	PCDHA9	5	140228164	C	A
PEX6_6_42935117_G/A	PEX6	6	42935117	G	A
PIK3C2G_12_18649057_C/T	PIK3C2G	12	18649057	C	T
PLEC_8_144995494_C/T	PLEC	8	144995494	C	T
POTED_21_14987871_G/T	POTED	21	14987871	G	T
POU4F2_4_147561758_C/T	POU4F2	4	147561758	C	T
PPIAL4G_1_143767544_T/A	PPIAL4G	1	143767544	T	A
PPIAL4G_1_143767547_G/A	PPIAL4G	1	143767547	G	A
PPL_16_4935985_C/G	PPL	16	4935985	C	G
PPP1R9A_7_94540527_G/A	PPP1R9A	7	94540527	G	A
PRKRA_2_179309165_G/A	PRKRA	2	179309165	G	A
PRR23C_3_138762854_G/T	PRR23C	3	138762854	G	T

PRSS1_7_142458451_A/T	PRSS1	7	142458451	A	T
PRUNE2_9_79320847_G/C	PRUNE2	9	79320847	G	C
PSAPL1_4_7435721_C/T	PSAPL1	4	7435721	C	T
RAB40B_17_80615774_T/G	RAB40B	17	80615774	T	G
RAG1_11_36597313_A/G	RAG1	11	36597313	A	G
RANBP2_2_109382348_T/C	RANBP2	2	109382348	T	C
RBBP5_1_205068225_T/C	RBBP5	1	205068225	T	C
RBMX_X_135958704_G/C	RBMX	X	135958704	G	C
RRN3_16_15162102_G/A	RRN3	16	15162102	G	A
RRP7A_22_42912136_G/T	RRP7A	22	42912136	G	T
RYR3_15_33954652_C/T	RYR3	15	33954652	C	T
SACS_13_23905771_C/A	SACS	13	23905771	C	A
SALL2_14_21991626_C/G	SALL2	14	21991626	C	G
SETD8_12_123889492_A/C	SETD8	12	123889492	A	C
SIGLEC11_19_50463982_T/G	SIGLEC11	19	50463982	T	G
SLC25A5_X_118603958_G/A	SLC25A5	X	118603958	G	A
SLC25A5_X_118604006_A/G	SLC25A5	X	118604006	A	G
SLC25A5_X_118604467_C/T	SLC25A5	X	118604467	C	T
SLC25A5_X_118605017_C/T	SLC25A5	X	118605017	C	T
SLC35E2_1_1666175_C/T	SLC35E2	1	1666175	C	T
SLC39A12_10_18270341_A/G	SLC39A12	10	18270341	A	G
SNCAIP_5_121761114_C/T	SNCAIP	5	121761114	C	T
SRMS_20_62174830_C/T	SRMS	20	62174830	C	T
SRPK3_X_153047251_A/G	SRPK3	X	153047251	A	G
STK17A_7_43659260_T/C	STK17A	7	43659260	T	C
SYT6_1_114641758_A/G	SYT6	1	114641758	A	G
TBX10_11_67402362_T/G	TBX10	11	67402362	T	G
TGM4_3_44929287_G/C	TGM4	3	44929287	G	C
TH_11_2190951_C/T	TH	11	2190951	C	T
TIMM23_10_51620361_G/C	TIMM23	10	51620361	G	C
TLR2_4_154625951_C/A	TLR2	4	154625951	C	A
TMEM41B_11_9308058_A/G	TMEM41B	11	9308058	A	G
TMEM74_8_109796955_G/A	TMEM74	8	109796955	G	A
TMPRSS13_11_117789345_G/C	TMPRSS13	11	117789345	G	C
TNRC6A_16_24834859_T/C	TNRC6A	16	24834859	T	C
TNXB_6_32010272_T/A	TNXB	6	32010272	T	A
TP53_17_7577139_G/A	TP53	17	7577139	G	A
TP53_17_7579472_G/C	TP53	17	7579472	G	C
TPD52L3_9_6328947_T/C	TPD52L3	9	6328947	T	C
TROAP_12_49724370_G/A	TROAP	12	49724370	G	A
TRPM2_21_45825813_G/C	TRPM2	21	45825813	G	C
TYR_11_89017961_G/A	TYR	11	89017961	G	A
USP32_17_58285542_G/A	USP32	17	58285542	G	A
VWA3B_2_98928429_C/G	VWA3B	2	98928429	C	G
WNT16_7_120969745_G/T	WNT16	7	120969745	G	T

WWC3_X_10090689_G/T	WWC3	X	10090689	G	T
ZBTB9_6_33423004_C/G	ZBTB9	6	33423004	C	G
ZCWPW1_7_100017260_T/C	ZCWPW1	7	100017260	T	C
ZNF717_3_75790837_C/A	ZNF717	3	75790837	C	A
ZNF813_19_53995266_C/T	ZNF813	19	53995266	C	T
ZNF880_19_52888071_G/T	ZNF880	19	52888071	G	T
ZP3_7_76071228_A/G	ZP3	7	76071228	A	G

Table 3 – Single nucleotide variants present in paired samples

Annotation	Gene	Chromosome	Location	Substituted Amino Acid	New Amino Acid
A2M_12_9262564_G/T	A2M	12	9262564	G	T
ABCA13_7_48390326_G/A	ABCA13	7	48390326	G	A
ABCA7_19_1045173_G/A	ABCA7	19	1045173	G	A
ACAA1_3_38167095_A/G	ACAA1	3	38167095	A	G
ACTN2_1_236911005_G/A	ACTN2	1	236911005	G	A
ADCY2_5_7789872_C/A	ADCY2	5	7789872	C	A
AK2_1_33478888_C/T	AK2	1	33478888	C	T
AK2_1_33478900_T/A	AK2	1	33478900	T	A
BRAF_7_140453136_A/T	BRAF	7	140453136	A	T
C1orf109_1_38151996_A/C	C1orf109	1	38151996	A	C
C1QTNF9_13_24895805_G/A	C1QTNF9	13	24895805	G	A
CDAN1_15_43020983_G/A	CDAN1	15	43020983	G	A
CDC27_17_45214551_G/A	CDC27	17	45214551	G	A
CDC27_17_45214648_G/C	CDC27	17	45214648	G	C
CDC27_17_45214654_C/T	CDC27	17	45214654	C	T
CDC27_17_45247317_A/G	CDC27	17	45247317	A	G
CDC27_17_45247338_T/G	CDC27	17	45247338	T	G
CDC27_17_45258951_A/G	CDC27	17	45258951	A	G
CDC27_17_45258954_A/G	CDC27	17	45258954	A	G
COL18A1_21_46911188_C/G	COL18A1	21	46911188	C	G
CTDSP2_12_58217698_G/T	CTDSP2	12	58217698	G	T
CTDSP2_12_58220784_A/T	CTDSP2	12	58220784	A	T
CTDSP2_12_58220811_G/T	CTDSP2	12	58220811	G	T
DRD5_4_9784542_A/C	DRD5	4	9784542	A	C
EPB41L3_18_5398020_C/G	EPB41L3	18	5398020	C	G
KCNJ12_17_21319285_C/T	KCNJ12	17	21319285	C	T
KRAS_12_25398284_C/A	KRAS	12	25398284	C	A
KRAS_12_25398284_C/T	KRAS	12	25398284	C	T
KRT18_12_53343209_G/A	KRT18	12	53343209	G	A
KRT32_17_39619115_G/A	KRT32	17	39619115	G	A
KRT40_17_39137387_C/T	KRT40	17	39137387	C	T
LAMB1_7_107594098_C/A	LAMB1	7	107594098	C	A
LGALS3_14_55604935_C/A	LGALS3	14	55604935	C	A
MAP2K3_17_21207834_C/T	MAP2K3	17	21207834	C	T
MDGA2_14_47770622_G/A	MDGA2	14	47770622	G	A
MEOX2_7_15725874_C/G	MEOX2	7	15725874	C	G
MINK1_17_4797305_G/A	MINK1	17	4797305	G	A
MTCH2_11_47660294_C/T	MTCH2	11	47660294	C	T
MTCH2_11_47660295_A/G	MTCH2	11	47660295	A	G

MTCH2_11_47663948_C/T	MTCH2	11	47663948	C	T
MYO5A_15_52664445_C/T	MYO5A	15	52664445	C	T
NCOA1_2_24888632_G/A	NCOA1	2	24888632	G	A
NOS1_12_117669907_G/A	NOS1	12	117669907	G	A
NRP2_2_206610510_G/A	NRP2	2	206610510	G	A
PABPC1_8_101721705_G/T	PABPC1	8	101721705	G	T
PABPC1_8_101721709_T/A	PABPC1	8	101721709	T	A
PABPC3_13_25671015_A/G	PABPC3	13	25671015	A	G
PAK2_3_196529982_A/G	PAK2	3	196529982	A	G
PANK3_5_167988433_T/A	PANK3	5	167988433	T	A
PAPPA2_1_176679244_G/T	PAPPA2	1	176679244	G	T
PCDHB8_5_140558628_T/C	PCDHB8	5	140558628	T	C
PHACTR1_6_13283706_G/A	PHACTR1	6	13283706	G	A
PIGT_20_44048972_A/C	PIGT	20	44048972	A	C
PIK3C2G_12_18650667_A/T	PIK3C2G	12	18650667	A	T
PKHD1L1_8_110457064_G/T	PKHD1L1	8	110457064	G	T
PLCG2_16_81888178_C/T	PLCG2	16	81888178	C	T
PPIAL4G_1_143767513_A/T	PPIAL4G	1	143767513	A	T
PRSS1_7_142460744_G/C	PRSS1	7	142460744	G	C
PRSS3_9_33797951_A/C	PRSS3	9	33797951	A	C
PTCH1_9_98209594_G/A	PTCH1	9	98209594	G	A
RIMS1_6_73016976_A/T	RIMS1	6	73016976	A	T
RRAS_19_50140130_G/A	RRAS	19	50140130	G	A
SCN2A_2_166245924_G/C	SCN2A	2	166245924	G	C
SCN4A_17_62041068_T/C	SCN4A	17	62041068	T	C
SDHA_5_236628_C/T	SDHA	5	236628	C	T
SDR16C5_8_57228812_G/A	SDR16C5	8	57228812	G	A
SIPA1L1_14_72054755_C/A	SIPA1L1	14	72054755	C	A
SLC25A5_X_118604911_C/A	SLC25A5	X	118604911	C	A
SLC25A5_X_118604935_T/C	SLC25A5	X	118604935	T	C
SLC45A4_8_142228160_C/T	SLC45A4	8	142228160	C	T
SLCO5A1_8_70617423_C/G	SLCO5A1	8	70617423	C	G
SVIL_10_29779847_A/C	SVIL	10	29779847	A	C
TAS2R31_12_11183066_A/T	TAS2R31	12	11183066	A	T
TCF7_5_133451683_C/A	TCF7	5	133451683	C	A
TIMM23_10_51623147_C/T	TIMM23	10	51623147	C	T
TRPV5_7_142625304_C/T	TRPV5	7	142625304	C	T
TSPAN31_12_58139552_G/T	TSPAN31	12	58139552	G	T
TTPAL_20_43117986_C/T	TTPAL	20	43117986	C	T
VANGL2_1_160388913_G/A	VANGL2	1	160388913	G	A
WDR62_19_36577616_G/C	WDR62	19	36577616	G	C
WNK2_9_96021312_G/A	WNK2	9	96021312	G	A

Table 4 – Single nucleotide variants exclusive to the responders

Annotation	Gene	Chromosome	Location	Substituted Amino Acid	New Amino Acid
A2M_12_9262564_G/T	A2M	12	9262564	G	T
ABCA7_19_1045173_G/A	ABCA7	19	1045173	G	A
ABCA9_17_67017930_T/C	ABCA9	17	67017930	T	C
ABCB5_7_20762646_G/T	ABCB5	7	20762646	G	T
ABCC9_12_22017410_C/T	ABCC9	12	22017410	C	T
ACTN2_1_236911005_G/A	ACTN2	1	236911005	G	A
ACTR1A_10_104241913_C/T	ACTR1A	10	104241913	C	T
ADCY2_5_7789872_C/A	ADCY2	5	7789872	C	A
ADD1_4_2916762_C/G	ADD1	4	2916762	C	G
ALDH3B2_11_67433662_C/T	ALDH3B2	11	67433662	C	T
ANKK1_11_113269792_C/A	ANKK1	11	113269792	C	A
APOB_2_21250914_G/A	APOB	2	21250914	G	A
ARHGEF19_1_16532498_G/A	ARHGEF19	1	16532498	G	A
ARHGEF19_1_16534255_C/G	ARHGEF19	1	16534255	C	G
ARSD_X_2836002_C/T	ARSD	X	2836002	C	T
ASPM_1_197070442_G/T	ASPM	1	197070442	G	T
ATP11A_13_113530199_G/A	ATP11A	13	113530199	G	A
ATP13A4_3_193209178_T/C	ATP13A4	3	193209178	T	C
ATXN1_6_16306751_G/A	ATXN1	6	16306751	G	A
AZU1_19_830841_G/A	AZU1	19	830841	G	A
BAIAP3_16_1394822_C/T	BAIAP3	16	1394822	C	T
BCHE_3_165491184_A/C	BCHE	3	165491184	A	C
BMP3_4_81967150_G/A	BMP3	4	81967150	G	A
BPI_20_36954670_G/A	BPI	20	36954670	G	A
BRAF_7_140453136_A/T	BRAF	7	140453136	A	T
C16orf96_16_4625938_A/T	C16orf96	16	4625938	A	T
C1orf109_1_38151996_A/C	C1orf109	1	38151996	A	C
C5orf22_5_31532534_G/C	C5orf22	5	31532534	G	C
CACNA1B_9_140777306_C/G	CACNA1B	9	140777306	C	G
CACNA1H_16_1268376_G/A	CACNA1H	16	1268376	G	A
CADM4_19_44130960_A/G	CADM4	19	44130960	A	G
CALCA_11_14991511_A/G	CALCA	11	14991511	A	G
CCDC136_7_128454762_G/A	CCDC136	7	128454762	G	A
CCDC138_2_109408208_G/A	CCDC138	2	109408208	G	A
CCDC78_16_774760_T/C	CCDC78	16	774760	T	C
CCT6B_17_33269648_C/G	CCT6B	17	33269648	C	G
CCT8_21_30439894_C/A	CCT8	21	30439894	C	A
CD1A_1_158226621_G/T	CD1A	1	158226621	G	T
CD93_20_23065209_G/A	CD93	20	23065209	G	A

CDAN1_15_43020983_G/A	CDAN1	15	43020983	G	A
CDC27_17_45214606_G/T	CDC27	17	45214606	G	T
CDC27_17_45214648_G/C	CDC27	17	45214648	G	C
CDC27_17_45214654_C/T	CDC27	17	45214654	C	T
CDC27_17_45214690_G/A	CDC27	17	45214690	G	A
CDC27_17_45214699_T/C	CDC27	17	45214699	T	C
CELA1_12_51740416_C/G	CELA1	12	51740416	C	G
CHAT_10_50835687_C/T	CHAT	10	50835687	C	T
CHRNA3_15_78894026_C/T	CHRNA3	15	78894026	C	T
CHRNA5_15_78880752_G/A	CHRNA5	15	78880752	G	A
CHRND_2_233398698_C/T	CHRND	2	233398698	C	T
CLCNKA_1_16356501_G/A	CLCNKA	1	16356501	G	A
CLDN3_7_73183979_G/A	CLDN3	7	73183979	G	A
CLEC18C_16_70211379_C/T	CLEC18C	16	70211379	C	T
CNGB1_16_57996933_C/A	CNGB1	16	57996933	C	A
CNN2_19_1037715_T/C	CNN2	19	1037715	T	C
CNN2_19_1037716_G/A	CNN2	19	1037716	G	A
CNN2_19_1037718_G/T	CNN2	19	1037718	G	T
CNN2_19_1037756_G/A	CNN2	19	1037756	G	A
CNN2_19_1037766_G/A	CNN2	19	1037766	G	A
COL24A1_1_86512536_C/T	COL24A1	1	86512536	C	T
COL4A3_2_228135631_C/T	COL4A3	2	228135631	C	T
COL5A3_19_10071347_C/T	COL5A3	19	10071347	C	T
CORO1C_12_109094907_A/G	CORO1C	12	109094907	A	G
CP_3_148916235_T/A	CP	3	148916235	T	A
CPAMD8_19_17025292_G/A	CPAMD8	19	17025292	G	A
CTBP2_10_126683058_T/G	CTBP2	10	126683058	T	G
CTBP2_10_126683099_G/A	CTBP2	10	126683099	G	A
CTBP2_10_126683111_C/T	CTBP2	10	126683111	C	T
CTBP2_10_126683132_A/T	CTBP2	10	126683132	A	T
CTBP2_10_126683244_C/G	CTBP2	10	126683244	C	G
CTBP2_10_126686629_G/A	CTBP2	10	126686629	G	A
CTBP2_10_126691979_C/G	CTBP2	10	126691979	C	G
CTDSP2_12_58220784_A/T	CTDSP2	12	58220784	A	T
CTDSP2_12_58220811_G/T	CTDSP2	12	58220811	G	T
CX3CR1_3_39307162_G/A	CX3CR1	3	39307162	G	A
CYP21A2_6_32006387_A/T	CYP21A2	6	32006387	A	T
CYP2C8_10_96818119_G/C	CYP2C8	10	96818119	G	C
CYP2D6_22_42526694_G/A	CYP2D6	22	42526694	G	A
CYP4F12_19_15784377_C/T	CYP4F12	19	15784377	C	T
D2HGDH_2_242690675_G/A	D2HGDH	2	242690675	G	A
DCLK1_13_36686139_G/C	DCLK1	13	36686139	G	C
DHTKD1_10_12143122_C/T	DHTKD1	10	12143122	C	T
DIS3L2_2_233127938_C/G	DIS3L2	2	233127938	C	G

DLAT_11_111916647_G/A	DLAT	11	111916647	G	A
DNAH9_17_11651057_A/G	DNAH9	17	11651057	A	G
EFCAB8_20_31480028_A/T	EFCAB8	20	31480028	A	T
EHBP1_2_63176139_A/C	EHBP1	2	63176139	A	C
ELP2_18_33736498_C/T	ELP2	18	33736498	C	T
EP400_12_132445675_G/A	EP400	12	132445675	G	A
EPB41L3_18_5398020_C/G	EPB41L3	18	5398020	C	G
EPPK1_8_144944226_G/A	EPPK1	8	144944226	G	A
ESRRA_11_64083320_T/C	ESRRA	11	64083320	T	C
ESRRA_11_64083328_C/T	ESRRA	11	64083328	C	T
ESRRA_11_64083331_C/T	ESRRA	11	64083331	C	T
FAM136A_2_70524515_T/A	FAM136A	2	70524515	T	A
FAM136A_2_70524576_C/G	FAM136A	2	70524576	C	G
FAM136A_2_70524606_G/A	FAM136A	2	70524606	G	A
FAM65C_20_49209710_C/T	FAM65C	20	49209710	C	T
FAM70B_13_114504663_G/A	FAM70B	13	114504663	G	A
FCRLB_1_161697072_G/C	FCRLB	1	161697072	G	C
FERMT1_20_6088265_G/A	FERMT1	20	6088265	G	A
FLVCR1_1_213068595_C/T	FLVCR1	1	213068595	C	T
FMN2_1_240370985_C/T	FMN2	1	240370985	C	T
FRG1_4_190878563_C/A	FRG1	4	190878563	C	A
FRG1_4_190878569_T/C	FRG1	4	190878569	T	C
GALNT2_1_230391032_G/A	GALNT2	1	230391032	G	A
GATA3_10_8100641_G/A	GATA3	10	8100641	G	A
GGT1_22_25011031_C/T	GGT1	22	25011031	C	T
GHR_5_42719239_A/C	GHR	5	42719239	A	C
GNAQ_9_80537112_T/A	GNAQ	9	80537112	T	A
GPRC6A_6_117130544_A/C	GPRC6A	6	117130544	A	C
GZMM_19_548612_G/A	GZMM	19	548612	G	A
HIP1R_12_123345509_G/T	HIP1R	12	123345509	G	T
HMCN1_1_186101539_A/G	HMCN1	1	186101539	A	G
HMCN2_9_133294224_C/T	HMCN2	9	133294224	C	T
HMGXB3_5_149390148_G/A	HMGXB3	5	149390148	G	A
HNF1A_12_121435427_G/A	HNF1A	12	121435427	G	A
HSD17B11_4_88278497_C/T	HSD17B11	4	88278497	C	T
HSPD1_2_198363406_C/T	HSPD1	2	198363406	C	T
HSPG2_1_22179244_C/T	HSPG2	1	22179244	C	T
IFI16_1_159024668_A/T	IFI16	1	159024668	A	T
IFI30_19_18285944_G/A	IFI30	19	18285944	G	A
INPP5B_1_38329999_C/G	INPP5B	1	38329999	C	G
INS_11_2181060_T/G	INS	11	2181060	T	G
ITIH1_3_52820981_A/T	ITIH1	3	52820981	A	T
ITSN2_2_24435599_G/A	ITSN2	2	24435599	G	A
KCNB1_20_47991468_G/A	KCNB1	20	47991468	G	A

KCNH8_3_19574945_A/G	KCNH8	3	19574945	A	G
KCNJ16_17_68128332_G/A	KCNJ16	17	68128332	G	A
KCNK13_14_90651135_G/T	KCNK13	14	90651135	G	T
KCNV1_8_110984553_G/A	KCNV1	8	110984553	G	A
KIAA0141_5_141309824_G/A	KIAA0141	5	141309824	G	A
KIF19_17_72340981_G/A	KIF19	17	72340981	G	A
KIF26B_1_245848798_C/T	KIF26B	1	245848798	C	T
KLHL33_14_20897676_T/C	KLHL33	14	20897676	T	C
KRAS_12_25398284_C/T	KRAS	12	25398284	C	T
KRT14_17_39742807_C/T	KRT14	17	39742807	C	T
KRT32_17_39616430_G/T	KRT32	17	39616430	G	T
LAMA5_20_60889385_G/T	LAMA5	20	60889385	G	T
LAMB1_7_107594098_C/A	LAMB1	7	107594098	C	A
LGALS3_14_55604935_C/A	LGALS3	14	55604935	C	A
MAP2K3_17_21207813_T/G	MAP2K3	17	21207813	T	G
MAP2K3_17_21207834_C/T	MAP2K3	17	21207834	C	T
MASP2_1_11090916_C/A	MASP2	1	11090916	C	A
MBD1_18_47800179_G/C	MBD1	18	47800179	G	C
MEOX2_7_15725874_C/G	MEOX2	7	15725874	C	G
MKL2_16_14341144_A/G	MKL2	16	14341144	A	G
MLL3_7_151935871_C/A	MLL3	7	151935871	C	A
MOGAT1_2_223559089_T/C	MOGAT1	2	223559089	T	C
MSH6_2_48027136_A/G	MSH6	2	48027136	A	G
MTCH2_11_47640398_T/C	MTCH2	11	47640398	T	C
MTCH2_11_47660334_C/T	MTCH2	11	47660334	C	T
MTMR11_1_149906167_T/G	MTMR11	1	149906167	T	G
MUC16_19_8999530_C/T	MUC16	19	8999530	C	T
MUC16_19_9002597_C/T	MUC16	19	9002597	C	T
MYO5A_15_52664445_C/T	MYO5A	15	52664445	C	T
MYO9B_19_17213218_G/A	MYO9B	19	17213218	G	A
NAGLU_17_40696233_C/G	NAGLU	17	40696233	C	G
NAV1_1_201754444_G/C	NAV1	1	201754444	G	C
NDUFS2_1_161183191_C/G	NDUFS2	1	161183191	C	G
NOD1_7_30492237_C/T	NOD1	7	30492237	C	T
NOS1_12_117669907_G/A	NOS1	12	117669907	G	A
NOTCH1_9_139412350_G/A	NOTCH1	9	139412350	G	A
NOTCH2NL_1_145281408_C/T	NOTCH2NL	1	145281408	C	T
NOTCH4_6_32188383_T/C	NOTCH4	6	32188383	T	C
NPEPPS_17_45669359_T/G	NPEPPS	17	45669359	T	G
NRP2_2_206610510_G/A	NRP2	2	206610510	G	A
NUP88_17_5289554_T/C	NUP88	17	5289554	T	C
NUP98_11_3744435_C/G	NUP98	11	3744435	C	G
OGDHL_10_50950976_G/A	OGDHL	10	50950976	G	A
OLFM1_9_138011540_T/C	OLFM1	9	138011540	T	C

PABPC3_13_25670868_G/A	PABPC3	13	25670868	G	A
PABPC3_13_25670877_G/A	PABPC3	13	25670877	G	A
PABPC3_13_25670955_C/T	PABPC3	13	25670955	C	T
PABPC3_13_25671015_A/G	PABPC3	13	25671015	A	G
PABPC3_13_25671195_A/G	PABPC3	13	25671195	A	G
PAK2_3_196529902_G/C	PAK2	3	196529902	G	C
PANK3_5_167986134_T/C	PANK3	5	167986134	T	C
PANK3_5_167988433_T/A	PANK3	5	167988433	T	A
PAPPA2_1_176679244_G/T	PAPPA2	1	176679244	G	T
PCDHA9_5_140228164_C/A	PCDHA9	5	140228164	C	A
PEX6_6_42935117_G/A	PEX6	6	42935117	G	A
PHACTR1_6_13283706_G/A	PHACTR1	6	13283706	G	A
PHKB_16_47732476_C/T	PHKB	16	47732476	C	T
PIEZO1_16_88787673_G/A	PIEZO1	16	88787673	G	A
PIEZO2_18_10731428_C/T	PIEZO2	18	10731428	C	T
PIK3C2G_12_18649057_C/T	PIK3C2G	12	18649057	C	T
PIK3C2G_12_18650667_A/T	PIK3C2G	12	18650667	A	T
PKHD1L1_8_110457064_G/T	PKHD1L1	8	110457064	G	T
PLCG2_16_81888178_C/T	PLCG2	16	81888178	C	T
PLEC_8_144995494_C/T	PLEC	8	144995494	C	T
PLVAP_19_17471595_T/G	PLVAP	19	17471595	T	G
POTED_21_14987871_G/T	POTED	21	14987871	G	T
POU2F1_1_167343528_G/A	POU2F1	1	167343528	G	A
PPIAL4G_1_143767513_A/T	PPIAL4G	1	143767513	A	T
PPIAL4G_1_143767544_T/A	PPIAL4G	1	143767544	T	A
PPIAL4G_1_143767547_G/A	PPIAL4G	1	143767547	G	A
PPP1R2_3_195269788_T/C	PPP1R2	3	195269788	T	C
PPP1R9A_7_94540527_G/A	PPP1R9A	7	94540527	G	A
PRKRA_2_179300979_A/T	PRKRA	2	179300979	A	T
PSAPL1_4_7435721_C/T	PSAPL1	4	7435721	C	T
PSMD9_12_122353796_A/G	PSMD9	12	122353796	A	G
RAB26_16_2203334_G/A	RAB26	16	2203334	G	A
RAB40B_17_80615774_T/G	RAB40B	17	80615774	T	G
RAG1_11_36597313_A/G	RAG1	11	36597313	A	G
RC3H1_1_173952595_C/T	RC3H1	1	173952595	C	T
RIMS1_6_73016976_A/T	RIMS1	6	73016976	A	T
RNF123_3_49759490_G/A	RNF123	3	49759490	G	A
RPL19_17_37360863_A/T	RPL19	17	37360863	A	T
RRAS_19_50140130_G/A	RRAS	19	50140130	G	A
RRN3_16_15162102_G/A	RRN3	16	15162102	G	A
RSPH4A_6_116950734_G/A	RSPH4A	6	116950734	G	A
RYR3_15_33954652_C/T	RYR3	15	33954652	C	T
SACS_13_23905771_C/A	SACS	13	23905771	C	A
SALL2_14_21991626_C/G	SALL2	14	21991626	C	G

SBNO1_12_123805023_C/A	SBNO1	12	123805023	C	A
SCN2A_2_166245924_G/C	SCN2A	2	166245924	G	C
SCN4A_17_62041068_T/C	SCN4A	17	62041068	T	C
SDR16C5_8_57228812_G/A	SDR16C5	8	57228812	G	A
SERPINB10_18_61600384_C/T	SERPINB10	18	61600384	C	T
SERPINB8_18_61654463_A/G	SERPINB8	18	61654463	A	G
SETD8_12_123889492_A/C	SETD8	12	123889492	A	C
SLC25A5_X_118604006_A/G	SLC25A5	X	118604006	A	G
SLC25A5_X_118604467_C/T	SLC25A5	X	118604467	C	T
SLC25A5_X_118604911_C/A	SLC25A5	X	118604911	C	A
SLC25A5_X_118604935_T/C	SLC25A5	X	118604935	T	C
SLC25A5_X_118605017_C/T	SLC25A5	X	118605017	C	T
SLC35E2_1_1666175_C/T	SLC35E2	1	1666175	C	T
SLC39A12_10_18270341_A/G	SLC39A12	10	18270341	A	G
SLCO5A1_8_70617423_C/G	SLCO5A1	8	70617423	C	G
SNCAIP_5_121761114_C/T	SNCAIP	5	121761114	C	T
STAB2_12_104048454_C/A	STAB2	12	104048454	C	A
SYT6_1_114641758_A/G	SYT6	1	114641758	A	G
SYT8_11_1857751_C/G	SYT8	11	1857751	C	G
TAS2R31_12_11183066_A/T	TAS2R31	12	11183066	A	T
TAS2R46_12_11214025_A/T	TAS2R46	12	11214025	A	T
TCF3_19_1650228_A/G	TCF3	19	1650228	A	G
TEKT4_2_95541427_G/T	TEKT4	2	95541427	G	T
TEKT4_2_95541447_C/T	TEKT4	2	95541447	C	T
TGM1_14_24729863_G/A	TGM1	14	24729863	G	A
TH_11_2190951_C/T	TH	11	2190951	C	T
TIAM2_6_155561796_C/T	TIAM2	6	155561796	C	T
TIMM23_10_51620361_G/C	TIMM23	10	51620361	G	C
TIMM23_10_51623147_C/T	TIMM23	10	51623147	C	T
TLR2_4_154625951_C/A	TLR2	4	154625951	C	A
TMEM74_8_109796955_G/A	TMEM74	8	109796955	G	A
TMPRSS13_11_117789345_G/C	TMPRSS13	11	117789345	G	C
TP53_17_7577139_G/A	TP53	17	7577139	G	A
TP53_17_7579472_G/C	TP53	17	7579472	G	C
TPD52L3_9_6328947_T/C	TPD52L3	9	6328947	T	C
TPTE_21_10943003_C/T	TPTE	21	10943003	C	T
TSPAN31_12_58139552_G/T	TSPAN31	12	58139552	G	T
TSTA3_8_144697051_T/C	TSTA3	8	144697051	T	C
TTPAL_20_43117986_C/T	TTPAL	20	43117986	C	T
TXNRD2_22_19907099_C/A	TXNRD2	22	19907099	C	A
TYR_11_89017961_G/A	TYR	11	89017961	G	A
USP32_17_58285542_G/A	USP32	17	58285542	G	A
VANGL2_1_160388913_G/A	VANGL2	1	160388913	G	A
WDR62_19_36577616_G/C	WDR62	19	36577616	G	C

WDR72_15_53907948_G/A	WDR72	15	53907948	G	A
WNK2_9_96021312_G/A	WNK2	9	96021312	G	A
WNT16_7_120969745_G/T	WNT16	7	120969745	G	T
YLPM1_14_75248652_C/G	YLPM1	14	75248652	C	G
ZCWPW1_7_100017260_T/C	ZCWPW1	7	100017260	T	C
ZNF404_19_44377669_G/A	ZNF404	19	44377669	G	A
ZNF544_19_58774094_C/T	ZNF544	19	58774094	C	T
ZNF880_19_52888071_G/T	ZNF880	19	52888071	G	T
ZP3_7_76071228_A/G	ZP3	7	76071228	A	G

Table 5 – Single nucleotide variants exclusive to the non-responders

Annotation	Gene	Chromosome	Location	Substituted Amino Acid	New Amino Acid
A4GALT_22_43089654_C/T	A4GALT	22	43089654	C	T
ABCA13_7_48390326_G/A	ABCA13	7	48390326	G	A
ABCC3_17_48761053_G/A	ABCC3	17	48761053	G	A
ACAA1_3_38167095_A/G	ACAA1	3	38167095	A	G
ACACB_12_109650663_A/G	ACACB	12	109650663	A	G
ACAD11_3_132338346_T/G	ACAD11	3	132338346	T	G
ACADL_2_211060050_T/G	ACADL	2	211060050	T	G
ACE_17_61568577_C/T	ACE	17	61568577	C	T
ACTN2_1_236902618_G/A	ACTN2	1	236902618	G	A
ADAMTS1_21_28212761_G/A	ADAMTS1	21	28212761	G	A
ADNP2_18_77895325_T/G	ADNP2	18	77895325	T	G
AGXT_2_241808314_C/T	AGXT	2	241808314	C	T
AK2_1_33478931_G/C	AK2	1	33478931	G	C
ALG1_16_5128817_G/A	ALG1	16	5128817	G	A
ALPP_2_233243586_C/T	ALPP	2	233243586	C	T
ALPPL2_2_233271669_C/T	ALPPL2	2	233271669	C	T
AMY2A_1_104163266_G/A	AMY2A	1	104163266	G	A
ANKRD36_2_97860487_T/C	ANKRD36	2	97860487	T	C
APOBEC3G_22_39482396_C/A	APOBEC3G	22	39482396	C	A
ATP6V0D2_8_87151837_A/T	ATP6V0D2	8	87151837	A	T
BMP2K_4_79832411_A/G	BMP2K	4	79832411	A	G
C18orf25_18_43796346_G/C	C18orf25	18	43796346	G	C
C1QTNF9_13_24895805_G/A	C1QTNF9	13	24895805	G	A
C2orf43_2_20974689_C/T	C2orf43	2	20974689	C	T
C3orf39_3_43121884_G/C	C3orf39	3	43121884	G	C
CACNA1H_16_1254369_C/T	CACNA1H	16	1254369	C	T
CCBL2_1_89448608_G/A	CCBL2	1	89448608	G	A
CDC27_17_45214523_A/C	CDC27	17	45214523	A	C
CDC27_17_45214531_G/A	CDC27	17	45214531	G	A
CDC27_17_45214551_G/A	CDC27	17	45214551	G	A
CDC27_17_45214615_G/C	CDC27	17	45214615	G	C
CDC27_17_45214617_G/C	CDC27	17	45214617	G	C
CDC27_17_45214623_G/A	CDC27	17	45214623	G	A
CDC27_17_45219296_G/C	CDC27	17	45219296	G	C
CDC27_17_45219332_T/G	CDC27	17	45219332	T	G
CDC27_17_45247298_A/G	CDC27	17	45247298	A	G
CDC27_17_45247301_A/G	CDC27	17	45247301	A	G
CDC27_17_45258951_A/G	CDC27	17	45258951	A	G
CDC27_17_45258954_A/G	CDC27	17	45258954	A	G

CDH8_16_61859047_T/C	CDH8	16	61859047	T	C
CEP135_4_56819375_A/G	CEP135	4	56819375	A	G
CFTR_7_117188750_C/T	CFTR	7	117188750	C	T
CHRNE_17_4806020_G/A	CHRNE	17	4806020	G	A
CHST15_10_125769672_G/A	CHST15	10	125769672	G	A
CLCN4_X_10176599_T/C	CLCN4	X	10176599	T	C
CLCNKB_1_16371067_G/T	CLCNKB	1	16371067	G	T
CNGA4_11_6265242_G/C	CNGA4	11	6265242	G	C
CNN2_19_1036211_C/T	CNN2	19	1036211	C	T
COL15A1_9_101778346_C/G	COL15A1	9	101778346	C	G
COL18A1_21_46911188_C/G	COL18A1	21	46911188	C	G
COL6A2_21_47551942_G/A	COL6A2	21	47551942	G	A
COSM45060_17_7577581_A/G	COSM45060	17	7577581	A	G
CTBP2_10_126681824_G/A	CTBP2	10	126681824	G	A
CTBP2_10_126681831_C/G	CTBP2	10	126681831	C	G
CTBP2_10_126681838_C/G	CTBP2	10	126681838	C	G
CTBP2_10_126681848_T/A	CTBP2	10	126681848	T	A
CTBP2_10_126683235_C/A	CTBP2	10	126683235	C	A
CTBP2_10_126691552_T/G	CTBP2	10	126691552	T	G
CTDSP2_12_58217698_G/T	CTDSP2	12	58217698	G	T
CTDSP2_12_58217770_G/T	CTDSP2	12	58217770	G	T
CYP4F2_19_15989696_G/C	CYP4F2	19	15989696	G	C
DISP1_1_223116472_G/A	DISP1	1	223116472	G	A
DNA2_10_70191724_C/G	DNA2	10	70191724	C	G
DNAH17_17_76456017_C/G	DNAH17	17	76456017	C	G
DOCK7_1_62993881_T/C	DOCK7	1	62993881	T	C
DROSHA_5_31508739_C/T	DROSHA	5	31508739	C	T
DSG1_18_28909921_G/T	DSG1	18	28909921	G	T
DUOX2_15_45392075_G/A	DUOX2	15	45392075	G	A
DUOX2_15_45393014_G/C	DUOX2	15	45393014	G	C
EME1_17_48457758_C/G	EME1	17	48457758	C	G
EMR2_19_14875388_G/A	EMR2	19	14875388	G	A
ENOX2_X_129837156_G/A	ENOX2	X	129837156	G	A
ESPNL_2_239039981_A/G	ESPNL	2	239039981	A	G
EXTL3_8_28575417_T/C	EXTL3	8	28575417	T	C
FAM126A_7_23016393_C/G	FAM126A	7	23016393	C	G
FAM8A1_6_17606159_C/A	FAM8A1	6	17606159	C	A
FANCA_16_89857935_G/A	FANCA	16	89857935	G	A
FCGBP_19_40376675_G/A	FCGBP	19	40376675	G	A
FES_15_91433090_A/G	FES	15	91433090	A	G
FGFR3_4_1806629_C/T	FGFR3	4	1806629	C	T
FNDC1_6_159655103_T/G	FNDC1	6	159655103	T	G
FOXN4_12_109725707_G/A	FOXN4	12	109725707	G	A
FRG1_4_190876196_G/A	FRG1	4	190876196	G	A
FRG1_4_190876293_C/A	FRG1	4	190876293	C	A

FRG1_4_190883039_T/C	FRG1	4	190883039	T	C
FUT3_19_5843784_A/T	FUT3	19	5843784	A	T
GDNF_5_37816112_G/A	GDNF	5	37816112	G	A
GLB1_3_33138549_G/A	GLB1	3	33138549	G	A
GLIS2_16_4385158_A/G	GLIS2	16	4385158	A	G
GLOD4_17_685752_G/A	GLOD4	17	685752	G	A
GPATCH2_1_217604654_T/C	GPATCH2	1	217604654	T	C
GSTT1_22_24379402_T/G	GSTT1	22	24379402	T	G
HEXDC_17_80391684_A/G	HEXDC	17	80391684	A	G
HRAS_11_533880_G/A	HRAS	11	533880	G	A
IL3RA_X_1471083_C/G	IL3RA	X	1471083	C	G
INF2_14_105180785_C/T	INF2	14	105180785	C	T
IQSEC3_12_247544_C/T	IQSEC3	12	247544	C	T
IRX4_5_1878325_C/T	IRX4	5	1878325	C	T
IRX6_16_55362942_T/C	IRX6	16	55362942	T	C
KCNG4_16_84256410_C/T	KCNG4	16	84256410	C	T
KCNH6_17_61615545_A/G	KCNH6	17	61615545	A	G
KCNJ12_17_21319087_G/A	KCNJ12	17	21319087	G	A
KCNJ12_17_21319523_C/T	KCNJ12	17	21319523	C	T
KCNJ12_17_21319786_G/A	KCNJ12	17	21319786	G	A
KIAA0753_17_6513329_G/A	KIAA0753	17	6513329	G	A
KIAA1958_9_115422069_G/A	KIAA1958	9	115422069	G	A
KIF24_9_34254413_G/C	KIF24	9	34254413	G	C
KLK10_19_51519365_C/G	KLK10	19	51519365	C	G
KRAS_12_25398284_C/A	KRAS	12	25398284	C	A
KRT18_12_53343209_G/A	KRT18	12	53343209	G	A
KRT18_12_53343225_C/T	KRT18	12	53343225	C	T
KRT18_12_53343231_G/C	KRT18	12	53343231	G	C
KRT32_17_39619115_G/A	KRT32	17	39619115	G	A
KRT36_17_39643340_T/G	KRT36	17	39643340	T	G
KRT40_17_39135089_G/A	KRT40	17	39135089	G	A
KRT40_17_39137154_C/G	KRT40	17	39137154	C	G
KRT40_17_39137387_C/T	KRT40	17	39137387	C	T
LDHAL6B_15_59500180_C/G	LDHAL6B	15	59500180	C	G
LRP1B_2_141459344_C/T	LRP1B	2	141459344	C	T
LRRC17_7_102574920_G/C	LRRC17	7	102574920	G	C
LYPD2_8_143833856_C/T	LYPD2	8	143833856	C	T
MATN2_8_98943447_G/C	MATN2	8	98943447	G	C
MDGA2_14_47770622_G/A	MDGA2	14	47770622	G	A
MGAT2_14_50089014_A/C	MGAT2	14	50089014	A	C
MINK1_17_4797305_G/A	MINK1	17	4797305	G	A
MLL2_12_49430947_T/C	MLL2	12	49430947	T	C
MLL3_7_151927021_C/A	MLL3	7	151927021	C	A
MLL3_7_151927067_T/C	MLL3	7	151927067	T	C
MLL3_7_151935910_C/T	MLL3	7	151935910	C	T

MLL5_7_104717522_A/G	MLL5	7	104717522	A	G
MPPED1_22_43831057_G/T	MPPED1	22	43831057	G	T
MSR1_8_16026181_T/C	MSR1	8	16026181	T	C
MTCH2_11_47663948_C/T	MTCH2	11	47663948	C	T
MTCH2_11_47663951_A/G	MTCH2	11	47663951	A	G
MUC4_3_195495916_G/C	MUC4	3	195495916	G	C
MUC6_11_1027811_C/T	MUC6	11	1027811	C	T
MYH3_17_10542257_A/G	MYH3	17	10542257	A	G
MYH4_17_10355371_C/T	MYH4	17	10355371	C	T
MYO1H_12_109872909_C/T	MYO1H	12	109872909	C	T
MYOM3_1_24409191_C/T	MYOM3	1	24409191	C	T
MZT2B_2_130948087_C/T	MZT2B	2	130948087	C	T
NCOA1_2_24888632_G/A	NCOA1	2	24888632	G	A
NCOR1_17_16097870_C/A	NCOR1	17	16097870	C	A
NHLRC1_6_18122258_C/T	NHLRC1	6	18122258	C	T
NIN_14_51202311_G/C	NIN	14	51202311	G	C
NPBWR1_8_53852871_A/T	NPBWR1	8	53852871	A	T
OR51G1_11_4945199_C/T	OR51G1	11	4945199	C	T
PABPC1_8_101725003_C/A	PABPC1	8	101725003	C	A
PABPC1_8_101727714_G/A	PABPC1	8	101727714	G	A
PABPC1_8_101727716_C/T	PABPC1	8	101727716	C	T
PABPC1_8_101730043_G/C	PABPC1	8	101730043	G	C
PABPC1_8_101730064_G/A	PABPC1	8	101730064	G	A
PABPC1_8_101730110_A/C	PABPC1	8	101730110	A	C
PAK2_3_196509577_C/G	PAK2	3	196509577	C	G
PARN_16_14576574_A/C	PARN	16	14576574	A	C
PCDHB3_5_140480852_G/A	PCDHB3	5	140480852	G	A
PCDHB4_5_140502343_C/T	PCDHB4	5	140502343	C	T
PCDHB4_5_140502344_C/T	PCDHB4	5	140502344	C	T
PCDHB8_5_140558628_T/C	PCDHB8	5	140558628	T	C
PCDHGB6_5_140788491_T/G	PCDHGB6	5	140788491	T	G
PHF11_13_50095041_A/G	PHF11	13	50095041	A	G
PIEZO1_16_88791458_G/A	PIEZO1	16	88791458	G	A
PIGT_20_44048972_A/C	PIGT	20	44048972	A	C
PLEKHG2_19_39913519_C/G	PLEKHG2	19	39913519	C	G
POU4F2_4_147561758_C/T	POU4F2	4	147561758	C	T
PPL_16_4935985_C/G	PPL	16	4935985	C	G
PRDM7_16_90126993_A/G	PRDM7	16	90126993	A	G
PRKRA_2_179309165_G/A	PRKRA	2	179309165	G	A
PRR23C_3_138762854_G/T	PRR23C	3	138762854	G	T
PRSS3_9_33797951_A/C	PRSS3	9	33797951	A	C
PRUNE2_9_79320847_G/C	PRUNE2	9	79320847	G	C
PTPRS_19_5258067_C/T	PTPRS	19	5258067	C	T
RANBP2_2_109382348_T/C	RANBP2	2	109382348	T	C
RASA4_7_102235769_T/C	RASA4	7	102235769	T	C

RBBP5_1_205068225_T/C	RBBP5	1	205068225	T	C
RBMX_X_135958704_G/C	RBMX	X	135958704	G	C
SDK2_17_71426656_G/T	SDK2	17	71426656	G	T
SEC14L3_22_30864610_A/G	SEC14L3	22	30864610	A	G
SERPINB10_18_61582751_T/G	SERPINB10	18	61582751	T	G
SETD8_12_123892186_T/C	SETD8	12	123892186	T	C
SIGLEC11_19_50463982_T/G	SIGLEC11	19	50463982	T	G
SIPA1L1_14_72054755_C/A	SIPA1L1	14	72054755	C	A
SKIV2L_6_31931747_G/A	SKIV2L	6	31931747	G	A
SLC15A1_13_99337138_A/G	SLC15A1	13	99337138	A	G
SLC25A5_X_118603958_G/A	SLC25A5	X	118603958	G	A
SLC25A5_X_118604030_T/C	SLC25A5	X	118604030	T	C
SLC25A5_X_118604399_C/G	SLC25A5	X	118604399	C	G
SLC25A5_X_118604428_T/C	SLC25A5	X	118604428	T	C
SLC2A1_1_43393457_T/C	SLC2A1	1	43393457	T	C
SLC44A4_6_31846741_C/A	SLC44A4	6	31846741	C	A
SLC45A4_8_142228160_C/T	SLC45A4	8	142228160	C	T
SLC46A3_13_29292117_C/T	SLC46A3	13	29292117	C	T
SLC6A7_5_149578877_C/T	SLC6A7	5	149578877	C	T
SMPD4_2_130930380_A/G	SMPD4	2	130930380	A	G
SOX7_8_10683685_A/G	SOX7	8	10683685	A	G
SPNS1_16_28990588_G/A	SPNS1	16	28990588	G	A
SREK1IP1_5_64020269_T/C	SREK1IP1	5	64020269	T	C
SRMS_20_62174830_C/T	SRMS	20	62174830	C	T
SRPK3_X_153047251_A/G	SRPK3	X	153047251	A	G
STK17A_7_43659260_T/C	STK17A	7	43659260	T	C
TAS2R46_12_11214080_G/A	TAS2R46	12	11214080	G	A
TBX10_11_67402362_T/G	TBX10	11	67402362	T	G
TCF7_5_133451683_C/A	TCF7	5	133451683	C	A
TFAP2A_6_10410556_C/T	TFAP2A	6	10410556	C	T
TGM4_3_44929287_G/C	TGM4	3	44929287	G	C
TMEM41B_11_9308058_A/G	TMEM41B	11	9308058	A	G
TNFRSF14_1_2488153_A/G	TNFRSF14	1	2488153	A	G
TNRC6A_16_24834859_T/C	TNRC6A	16	24834859	T	C
TNS1_2_218713282_G/A	TNS1	2	218713282	G	A
TNXB_6_32010272_T/A	TNXB	6	32010272	T	A
TPSD1_16_1306986_C/T	TPSD1	16	1306986	C	T
TROAP_12_49724370_G/A	TROAP	12	49724370	G	A
TRPM2_21_45825813_G/C	TRPM2	21	45825813	G	C
TRPV5_7_142625304_C/T	TRPV5	7	142625304	C	T
TSPAN32_11_2325427_T/C	TSPAN32	11	2325427	T	C
USP40_2_234394477_A/G	USP40	2	234394477	A	G
VWA3B_2_98928429_C/G	VWA3B	2	98928429	C	G
VWF_12_6128067_G/A	VWF	12	6128067	G	A
WDR33_2_128525866_A/G	WDR33	2	128525866	A	G

WNT10B_12_49364239_C/T	WNT10B	12	49364239	C	T
WWC3_X_10090689_G/T	WWC3	X	10090689	G	T
ZBTB9_6_33423004_C/G	ZBTB9	6	33423004	C	G
ZNF717_3_75790837_C/A	ZNF717	3	75790837	C	A
ZNF717_3_75790880_A/G	ZNF717	3	75790880	A	G
ZNF730_19_23329194_A/G	ZNF730	19	23329194	A	G
ZNF813_19_53995266_C/T	ZNF813	19	53995266	C	T

Table 6 – Single nucleotide variants present in paired samples and exclusive to the responders

Annotation	Gene	Chromosome	Location	Substituted Amino Acid	New Amino Acid
A2M_12_9262564_G/T	A2M	12	9262564	G	T
ABCA7_19_1045173_G/A	ABCA7	19	1045173	G	A
ACTN2_1_236911005_G/A	ACTN2	1	236911005	G	A
ADCY2_5_7789872_C/A	ADCY2	5	7789872	C	A
BRAF_7_140453136_A/T	BRAF	7	140453136	A	T
C1orf109_1_38151996_A/C	C1orf109	1	38151996	A	C
CDAN1_15_43020983_G/A	CDAN1	15	43020983	G	A
CDC27_17_45214648_G/C	CDC27	17	45214648	G	C
CDC27_17_45214654_C/T	CDC27	17	45214654	C	T
CTDSP2_12_58220784_A/T	CTDSP2	12	58220784	A	T
CTDSP2_12_58220811_G/T	CTDSP2	12	58220811	G	T
EPB41L3_18_5398020_C/G	EPB41L3	18	5398020	C	G
KRAS_12_25398284_C/T	KRAS	12	25398284	C	T
LAMB1_7_107594098_C/A	LAMB1	7	107594098	C	A
LGALS3_14_55604935_C/A	LGALS3	14	55604935	C	A
MAP2K3_17_21207834_C/T	MAP2K3	17	21207834	C	T
MEOX2_7_15725874_C/G	MEOX2	7	15725874	C	G
MYO5A_15_52664445_C/T	MYO5A	15	52664445	C	T
NOS1_12_117669907_G/A	NOS1	12	117669907	G	A
NRP2_2_206610510_G/A	NRP2	2	206610510	G	A
PABPC3_13_25671015_A/G	PABPC3	13	25671015	A	G
PANK3_5_167988433_T/A	PANK3	5	167988433	T	A
PAPPA2_1_176679244_G/T	PAPPA2	1	176679244	G	T
PHACTR1_6_13283706_G/A	PHACTR1	6	13283706	G	A
PIK3C2G_12_18650667_A/T	PIK3C2G	12	18650667	A	T
PKHD1L1_8_110457064_G/T	PKHD1L1	8	110457064	G	T
PLCG2_16_81888178_C/T	PLCG2	16	81888178	C	T
PPIAL4G_1_143767513_A/T	PPIAL4G	1	143767513	A	T
RIMS1_6_73016976_A/T	RIMS1	6	73016976	A	T
RRAS_19_50140130_G/A	RRAS	19	50140130	G	A
SCN2A_2_166245924_G/C	SCN2A	2	166245924	G	C
SCN4A_17_62041068_T/C	SCN4A	17	62041068	T	C
SDR16C5_8_57228812_G/A	SDR16C5	8	57228812	G	A
SLC25A5_X_118604911_C/A	SLC25A5	X	118604911	C	A
SLC25A5_X_118604935_T/C	SLC25A5	X	118604935	T	C
SLCO5A1_8_70617423_C/G	SLCO5A1	8	70617423	C	G
TAS2R31_12_11183066_A/T	TAS2R31	12	11183066	A	T
TIMM23_10_51623147_C/T	TIMM23	10	51623147	C	T

TSPAN31_12_58139552_G/T	TSPAN31	12	58139552	G	T
TTPAL_20_43117986_C/T	TTPAL	20	43117986	C	T
VANGL2_1_160388913_G/A	VANGL2	1	160388913	G	A
WDR62_19_36577616_G/C	WDR62	19	36577616	G	C
WNK2_9_96021312_G/A	WNK2	9	96021312	G	A

Table 7 – Single nucleotide variants present in paired samples and exclusive to the non-responders

Gene	Chromosome	Location	Substituted Amino Acid	New Amino Acid
ABCA13_7_48390326_G/A	7	48390326	G	A
ACAA1_3_38167095_A/G	3	38167095	A	G
C1QTNF9_13_24895805_G/A	13	24895805	G	A
CDC27_17_45214551_G/A	17	45214551	G	A
CDC27_17_45258951_A/G	17	45258951	A	G
CDC27_17_45258954_A/G	17	45258954	A	G
COL18A1_21_46911188_C/G	21	46911188	C	G
CTDSP2_12_58217698_G/T	12	58217698	G	T
KRAS_12_25398284_C/A	12	25398284	C	A
KRT18_12_53343209_G/A	12	53343209	G	A
KRT32_17_39619115_G/A	17	39619115	G	A
KRT40_17_39137387_C/T	17	39137387	C	T
MDGA2_14_47770622_G/A	14	47770622	G	A
MINK1_17_4797305_G/A	17	4797305	G	A
MTCH2_11_47663948_C/T	11	47663948	C	T
NCOA1_2_24888632_G/A	2	24888632	G	A
PCDHB8_5_140558628_T/C	5	140558628	T	C
PIGT_20_44048972_A/C	20	44048972	A	C
PRSS3_9_33797951_A/C	9	33797951	A	C
SIPA1L1_14_72054755_C/A	14	72054755	C	A
SLC45A4_8_142228160_C/T	8	142228160	C	T
TCF7_5_133451683_C/A	5	133451683	C	A
TRPV5_7_142625304_C/T	7	142625304	C	T

Appendix 2

Genetic variants in colorectal cancer identified by next generation sequencing studies

Paper	Number of Patients	Comparing	Identified Variants	Summary
The Cancer Genome Atlas Network Nature, 2012	276	Tumour and normal mucosa	ACVR2A, APC, TGFBR2, BRAF, MSH3, MSH6, MYO1B, TCF7L2, CASP8, CDC27, FZD3, MIER3, TCERG1, MAP7, PTPN12, P53, KRAS, TTN, PIK3CA, FBXW7, SMAD4, NRAS, FAM123B, SMAD2, CTNNB1, KIAA1804, SOX9, ACVR1B, GPC6, EDNRB	Implicated pathways included WNT, RAS-MAPK, PI3K, TGF-B, P53, and DNA mismatch repair.
The consensus coding sequences of human breast and colorectal cancers Science, 2006	11	Tumour and normal mucosa	ABCA1, ACSL5, ADAM29, ADAMTS15, ADAMTS18, ADAMTSL3, APC, C10orf137, C15orf2, C6orf29, CD109, CD248, CHL1, CNTN4, CSMD3, EPHA3, EPHB6, ERCC6, EVL, EYA4, FBXW7, GALNS, GNAS, GUCY1A2, HAPLN1, HIST1H1B, K6IRS3, KCNQ5, KIAA1409, KRAS, LGR6, LMO7, LOC157697, LRP2, MAP2, MCP, MGC33407, MKRN3, MLL3, MMP2, NF1, OBSCN, P2RX7, P2RY14, PHIP, PKHD1, PKNOX1, PRKD1, PTPRD, PTPRU, RET, RUNX1T1, SCN3B, SDBCAG84, SEC8L1, SFRS6, SLC29A1, SMAD2, SMAD3, SMAD4, SYNE1, TBX22, TCF7L2, TGFBR2, TP53, TTLL3, UHRF2, UQCRC2, ZNF442	Sanger sequencing study identifying 189 genes, most of which not known to be implicated in carcinogenesis
Patterns of somatic mutation in human cancer genomes Nature, 2007	28	Tumour and normal mucosa	TTN, BRAF, ATM, TAF1L, ERN1, MAP2K4, SHUK, FGFR2, NTRK3, MGC42105, TGFBR2, EPHA6, FLJ23074, ITK, DCAMKL3, STK11, PAK7, STK6, BRD2, RPS6KA2	44 mutations identified, many of which were protein kinases
Somatic mutation profiles of MSI and MSS colorectal cancer identified by whole exome next generation sequencing and bioinformatics analysis PLOS One, 2010	2 (1 MSI-S, 1 MSI-H)	Tumour and normal mucosa	FRAP1, FAM5B, RGS16, RCOR3, ATF3, C1orf201, C1orf91, RLF, ZNF691, ALX3, COPA, TRIM17, CNR2, WDTC1, FOXJ3, PTPRF, GATAD2B, USP21, IPO9, MTR, CSMD2, DNALI1, MYCL1, SYT6, CD2, PRCC, NR1I3, FCGR2A, KIF14, PLXNA2, PTPN14, CDC42BPA, ZMYM4, STK40, HPS1, TACC2, ITIH2, CEP55, RRP12, FAM171A1, PTER, SVIL, PFKP, LRRTM3, HERC4, TCF7L2, C10orf119, FGFR2, BICC1, IDE, PNLIPRP1, TIAL1, FRMD4A, BMPR1A, SORBS1, PGR, CUL5, RBM7, UBE4A, NCAPD3, NAV2, PAX6, DDB1, NRXN2, MTMR2, BUD13, HYOU1, HINFP, MADD, CTR9, POU2AF1, TECTA, NUP160, SF1, ATG2A, NUMA1, CWF19L2, VWA5A, COPB1, AHNAK, RAB6A, FBXW8, ERC1, RECQL, CPNE8, MFSD5, IPO8, SFRS2IP, MAP3K12, DDX23, GPR84, ITGA7, LRP1, UBE3B,	MSI List: 359 significant mutations for the MSI tumour and 45 for the MSS, all with predicted altered protein function

			MED13L, DHX37, SLC39A5, ALG5, CARS2, WASF3, UBL3, RAB2B, EXDL2, PCNX, KCNK10, C14orf102, ADCY4, NIN, PTPN21, TDP1, CPSF2, CTSG, CDKN3, SIX6, SLC10A1, FLVCR2, SSTR1, ACTR10, RDH12, MLH3, SPG11, GLDN, SNX1, OCA2, GJD2, ALDH1A2, MYO1E, KIAA1024, C15orf29, INO80, DMXL2, RORA, ARNT2, DNAJA3, LONP2, GRIN2A, NUP93, GAN, ZNF597, C16orf62, SEZ6L2, RBL2, RFWD3, BCAR1, TLK2, ALDH3A1, OR1A1, ZNF403, ETV4, CA10, MTMR4, APPBP2, ELAC2, PRPF8, FBXL20, CACNG4, TMEM104, DRG2, PIGS, PLXDC1, SPAG9, COIL, KCTD2, DOK6, TXNL1, ROCK1, WDR7, ZADH2, ANGPTL6, CREB3L3, ZNF569, LENG8, ARHGEF18, COPE, STXBP2, RNASEH2A, TSSK6, C19orf47, HAS1, SF4, IL1A, DHRS9, ITGAV, TRAK2, MAP2, HDAC4, AGXT, MAPRE3, EHD3, FSHR, MGAT4A, GLI2, MBD5, SCN3A, SSFA2, NRP2, GALNT14, WDR33, UGCGL1, ACVR2A, LRP2, RBM45, DYSF, CNNM4, CHRNA1, MARCH4, SPHKAP, SPTBN1, SMEK2, C20orf6, TNNC2, SLC2A10, TSHZ2, NCOA6, GMEB2, ACSS1, JAG1, FLRT3, SEC23B, CSE1L, DSCR3, DYRK1A, ERG, FAM3B, PCNT, USP25, KIAA0179, HMGXB4, TMPRSS6, SULT4A1, CYTSA, RBM5, ALAS1, CCDC37, SUCNR1, FNDC3B, OSBPL10, CTNNB1, C3orf23, HYAL2, TBC1D23, HRH1, TIPARP, LARS2, WDR6, NFKBIZ, UROC1, SLC25A38, CXCR6, PRKCD, PHF17, GRIA2, KDR, PCDH18, CCRN4L, GABRB1, COX18, MTTP, MANBA, MFSD8, GALNT7, IRF2, WDFY3, LMNB1, PCDHB3, LARP1, GABRA6, PCDH24, ADAMTS12, DMGDH, CSPG2, MAN2A1, TRIM36, SIL1, GRM6, PARP8, WDR55, POU4F3, C5orf42, ACOT12, ALDH7A1, LAMA4, ROS1, ENPP3, TAAR2, TAAR1, IL20RA, CNPY3, PLA2G7, POPDC3, TULP4, ZNF318, RP3-337H4.1, CDC2L6, AIG1, ITPR3, ZFAND3, FRS3, MEP1A, IGF2R, TFAP2B, SLC17A5, PRSS35, MAP3K7, PLOD3, BRAF, PDIA4, TRA2A, AEBP1, GRM3, MCM7, STAG3, RELN, LAMB4, GLI3, DDX56, PCOLCE, SMURF1, C8orf41, CNGB3, HTRA4, ASPH, SULF1, ANXA13, RB1CC1, ARFGEF1, CSMD3, NOV, PPM2C, LAPTM4B, UGCG, UNC13B, RORB, KIF12, GLE1, NUP214, DBC1, ENDOG, ADAMTS13, SNAPC3, EXOSC2, SLC24A2, L1CAM, KIF4A,	

			ABCB7, GPR174, GABRE, NHS, PRICKLE3, DMD	
Somatic mutation profiles of MSI and MSS colorectal cancer identified by whole exome next generation sequencing and bioinformatics analysis PLOS One, 2010	2 (1 MSI-S, 1 MSI-H)	Tumour and normal mucosa	PLA2G2D, MEF2D, AKR7A3, WDTC1, IL12RB2, ARHGAP21, SUPV3L1, BMPR1A, CTR9, MLL, DAGLA, MICAL2, TNKS1BP1, RCOR2, PRICKLE1, KRAS, MTERFD3, DAO, FREM2, UGCGL2, SETDB2, RBBP6, TP53, KCNJ12, ADNP2, CD22, NUP62, STAT1, PNPT1, GPR45, EHD3, ATP9A, USP13, PLD1, ITGA9, DNAH5, SNX18, TNFRSF21, ASCC3, THEM2, HCRTR2, SRRT, CREB3L2, HOXA1, ABRA	MSS List: 359 significant mutations for the MSI tumour and 45 for the MSS, all with predicted altered protein function
Exome capture sequencing of adenoma reveals genetic alterations in multiple cellular pathways at the early stage of colorectal tumorigenesis PLOS One, 2013	1	Tumour, adenoma and normal mucosa	OR6X1, SLC15A3, KRTHB4, RBFOX1, LAMA3, CDH20, BIRC6, APC, NMBR, GLCCI1, EFR3A, FTHL17, , PGM1, DTL, PPP1R3C, OR51E2, RRP8, NARS2, FAM109A, FAM181A, NRXN3, KIAA1409, TGM7, CORO1A, KRTHA1, GNAL, PPAP2C, FLJ37549, RYR1, GSK3A, ATF2, AFP36L2, NFATC2, ZFP64, GRIK1, KRTAP19-7, DESK1, KLHL22, ALPK1, FBXW7, APC, POU4F3, FLT4, FAM54A, KIF25, SDK1, TRF2, CUX1, NRG1, OR13J1, COL4A6, WDR44	12 variants were identified in the adenoma and 42 in the adenocarcinoma
Chromothripsis is a common mechanism driving genomic rearrangements in primary and metastatic colorectal cancer Genome Biology, 2011	4	Primary tumour, normal mucosa, liver metastasis and liver parenchyma	APC, DDR2, KRAS, PTPRF, SMAD2, SMAD4, TP53, MLL3, PART14, PIK3CA, KDR, PRKCD, RFC1, EXOC4, TSC1, FGFR2, NUP98, ERBB3, RASA3, DNAH9, TAOK1, ATRX, TTN, EPHA4	24 genes suggesting the relevance of chromothripsis to metastagenesis
Genomic sequencing of colorectal adenocarcinomas identifies a recurrent VTI1A-TCF7L2 fusion	9	Tumour and normal mucosa	TARDBP, INADL, CFH, CYS1, RASGRP3, CCDC88A, C2orf78, FER1L5, TTN, IGFBP5, RAF1, LTF, PPP2R3A, PCCB, KLHL6, PAK2, SLC10A7, ACSL1, CMYA5, FAM81B, APC, APC, PCDHGC3, DHX16, SYNGAP1, C6orf204, POT1, GRM8, DMRT1, KIAA1539, ECM2, BAAT, ABL1, SEC16A, ITIH5, ITPRIP, IRF7, TRIM6-TRIM34, IPO7, ANO3, OR8H2, CEP164, CASC1, KRAS, DDX11, PUS7L, PAN2,	Eleven rearrangements encode predicted in-frame fusion proteins, including a fusion of TVI1A and TCF7L2 found in 3 out of 9 patients

Nature Genetics, 2011			ZFP106, BBS4, UBFD1, TP53, MAP2K3, TOP2A, TRIM47, FAM38B, ROCK1, NFATC1, OR10H3, TMEM147, SAE1, PPP2R1A, GZF1, PTPRT, CASS4, GTPBP5, CHAF1B, LCA5L, CHEK2, FAM47A, FAM123B, CACNA1S, C1orf107, TAF5L, C2orf78, FIGN, COBLL1, GLB1, TOPBP1, KCNAB1, TMPRSS11F, RGMB, APC, APC, OPRM1, PCLO, AKAP9, PRKAR2B, PLXNA4, FOXD4, C9orf95, CYLC2, TAF3, C10orf82, OR51B4, C11orf65, WNK1, KRAS, MDM1, CLLU1, DNAH10, DHX37, KIAA1409, RYR3, PLIN1, OR4F15, NSMCE1, HYDIN, ZNF521, EMR1, OR7E24, KIAA1683, ZNF761, EYA2, UBASH3A, MXRA5, FAM47C, TBC1D8B, CHD5, CSMD2, PODN, NTNG1, HAO2, SEMA6C, SLC27A3, DHX9, HHIPL2, SUSD4, ABCG8, SCN1A, TTN, TTN, MYO1B, COL6A3, FLNB, STXBP5L, PCOLCE2, P2RY12, MED12L, DCAF4L1, FAM13A, DCHS2, CYP4V2, FYB, PCDHGA6, CSF1R, SNCB, TBC1D9B, HIST1H1D, ZNF323, NKAIN2, PLG, SP4, RABGEF1, CYP3A43, DGKI, OR2A5, TM7SF4, CSMD3, TG, DMRT3, PDCD1LG2, GABBR2, JMJD1C, ANXA11, GRID1, SORCS1, PRMT3, RAG1, ATG2A, GPR83, NCAM1, DSCAML1, OR8D1, NDUFA9, ADAMTS20, KRT76, NBEA, SIAH3, ATP7B, SCEL, RTN1, ALDH6A1, NRXN3, SERPINA1, DICER1, RYR3, CYP1A2, DNAH3, SCNN1G, MYH3, ATPAF2, PNMT, ASB16, USH1G, ASXL3, SMAD4, ABCA7, SEMA6B, EMR1, SYDE1, PSG3, LILRB3, CYP2D6, FLJ44635, MAGEE2, MAGEA11, SYTL1, PHACTR4, KIAA0467, C8A, PTPRC, CAPN2, PLB1, CTNNA2, SNRNP200, LRP2, HAT1, TTN, HECW2, CADPS, CADPS, PVRL3, UROC1, NFXL1, RNF150, C5orf44, SLCO6A1, APC, PCDHA3, PCDHGA7, FAT2, TBC1D9B, TRIM26, MUC21, BAT2, PI16, MDGA1, TCTE1, PGK2, ASCC3, RBM16, IGF2R, C6orf118, C6orf118, ISPD, ADCY1, IMMP2L, ZNF425, ADRA1A, MMP16, DEPDC6, EPPK1, AK3, TAF1L, FANCG, DAPK1, DBC1, CDK5RAP2, LRIT2, CSRP3, PDHX, OR4D9, HSPA8, WNK1, C3AR1, PHC1, PDZRN4, C12orf56, TMCC3, CUX2, FLT1, FARP1, HDC, TMOD3, IREB2, ACAN, RBBP6, TAT, PHF23, TP53, EFCAB5, BPTF, TCEB3CL, ARHGEF18, CACNA1A, LAIR1, HM13, B4GALT5, SLC9A8, KRTAP6-2, PRAME, MYO18B, RANGAP1, ATP6AP2,	

			USP9X, UBE4B, NRAS, USH2A, OBSCN, XDH, VRK2, ANKRD36B, LIPT1, TTN, TTN, ICA1L, SCN10A, PCBP4, DZIP3, PIK3CA, HTT, ANK2, PRSS48, CDH12, IL31RA, TNPO1, APC, SLC27A6, HIST1H2AJ, BRD2, COL12A1, EPM2A, SYNE1, MRPS17, PTPN12, AKAP9, SSPO, DLC1, SLC7A2, PREX2, FLJ43860, EPPK1, GLT6D1, NEBL, PTCHD3, ANK3, C10orf4, TCF7L2, TUB, BTBD10, LDHA, OR4C13, OR8K3, OR1S2, TMEM218, CACNA1C, PIK3C2G, LRRK2, PDZRN4, ZFC3H1, ZNF84, PCDH17, SIPA1L1, SPTLC2, EFTUD1, C15orf32, SYNM, TP53, ABCA10, OTOP2, ZNF750, CXXC1, CPAMD8, ZNF568, ZNF569, SYNGR4, ZNF578, KIR2DL1, TSHZ2, ADAMTS5, COL4A5, KIAA1210, EIF4G3, SFRS4, HDAC1, LPHN2, LCE4A, GREB1, SCLT1, APC, SRA1, CRIP3, HCRTR2, AKD1, RP1L1, TRPA1, ZFHX4, OR1L4, KCNT1, PNPLA7, CNTN5, KRAS, FLT3, DCLK1, ADPRHL1, WWP2, CDC27, SCN4A, SMAD4, MUC16, GPR32, MAGEC1, SLITRK2, VPS13D, NRAS, DDR2, PRG4, SRBD1, UXS1, PTPN4, LRP1B, GAD1, TTN, ITGAV, NOP58, DNAJB2, PDCD6IP, DCLK3, SCN11A, BOC, STXBP5L, ENOPH1, C4orf31, FBXW7, PPWD1, APC, APC, RBM27, PEG10, PSMC2, BCAP29, PLXNA4, CSMD3, CSMD3, FLJ46321, BAT2L, C9orf96, CARD9, FRMD4A, PTER, CUBN, CACNB2, SVIL, PCBD1, EXOC6, DMBT1, GRIK4, KRT1, DNAJC14, ESYT1, KCNMB4, PPP1R12A, ANKS1B, ACACB, PDS5B, SLITRK5, HECTD1, RHOJ, SFRS5, FAM181A, HERC1, MFGE8, NLRC5, COG4, TP53, SLFN5, GAS2L2, FBXO47, NPEPPS, TXNDC2, SMAD2, MBD1, GRWD1, FPR2, NLRP9, NLRP4, FRMPD4, TRO, FAM70A, HSPG2, GMEB1, TNNI3K, EPS8L3, ARNT, SHC1, KIF14, BTG2, ANGEL2, TARBP1, APOB, USP34, FAM136A, TBR1, COL6A3, MYRIP, CD200R1L, C4orf49, GALNTL6, SORBS2, MTRR, FBXL7, OSMR, C7, RASA1, MEP1A, PTP4A1, PHIP, HTR1E, C6orf167, FAM184A, GRM1, VSTM2A, C7orf42, CCDC146, DOCK4, ST7, UBE2H, MGAM, DLC1, KIAA1967, NRG1, UBR5, MTSS1, COL22A1, DNTT, GSTO2, MUC2, FOLH1, NUMA1, PCF11, FAT3, CUL5, OR10G7, PRMT8, KCNA6, KCNA1, KRAS, OVCH1, SFRS2IP, DDX23, ANKRD33, HELB, NAV3, C12orf51, RPL6, SACS,	

			FNDC3A, KPNA3, TDRD3, FAM155A, OR4K14, PNN, FBN1, SLC27A2, VPS13C, TP53, KCNJ12, RAB11FIP4, NFE2L1, TLK2, ABCA9, PTPRM, HNRNPM, ZNF667, ZNF329, ITCH, ELFN2, SAMM50, ESPN, MTHFR, PPT1, ZCCHC11, DPT, FAM129A, HMCN1, HMCN1, NFASC, CENPF, PRSS38, ARID4B, RYR2, OR14C36, C2orf71, EHBP1, TEX261, FER1L5, CNTNAP5, TLK1, ALS2CR11, CXCR2, TMBIM1, COL4A4, COL6A3, OR6B2, USP19, TOPBP1, EPHB1, LEKR1, APBB2, REST, RAPGEF2, WDR17, CDH9, ZFYVE16, ST8SIA4, APC, APC, KIF3A, ATP10B, C5orf41, CAPN11, GABRR2, WBSCR17, SEMA3C, STAG3, TFR2, LRRN3, CPA5, MGAM, GIMAP8, PXDNL, RP1, NCOA2, CA2, FBXO43, RANBP6, ACO1, FAM189A2, GABBR2, OR13D1, FAM129B, NTNG2, MAMDC4, C10orf18, PRKCQ, USP6NL, C10orf140, KIAA1462, GJD4, CSGALNACT2, RTKN2, CHUK, PKD2L1, SHOC2, ATRNL1, BNIP3, OR52A5, CCKBR, DENND5A, SAA2, NAV2, C11orf49, OR4C11, GLYATL1, FAM111B, FAT3, BCL9L, FLI1, GLB1L2, AKAP3, NOP2, A2M, DUSP16, RERGL, KRAS, KRT75, KRT2, OR6C2, TIMELESS, APAF1, CKAP4, RNFT2, CLIP1, FLJ10357, ZNF219, SPTB, NDN, RTF1, PML, SNX33, UNC45A, C16orf38, DCI, STX1B, CHD9, CCDC135, TSNAXIP1, SLC12A4, DHX38, CBFA2T3, ZNF778, SHBG, KRT12, GPATCH8, SPATA20, TEX14, C18orf34, MYO9B, WDR88, HRC, C20orf12, RALGAPA2, WFDC3, C20orf108, UCKL1, PRPF6, IGSF5, CCT8L2, GAB4, MCAT, CELSR1, ARSH, TLR8, PHEX, TCEAL3, COL4A5	
Exome sequencing reveals frequent inactivating mutations in ARID1A, ARID1B, ARID2 and ARID4 in microsatellite unstable colorectal cancer International Journal of	21	Tumour and normal mucosa	ARID1A, ARID1B, ARID2, ARID3A, ARID4A, ARID4B, ARID5A, JARID2, KDM5A, KDM5B, KDM5C, KDM5D	Analysis focussed to ARID genes only which were frequently mutated (13-39%)

Cancer, 2013				
Comprehensive genomic analysis of a metastatic colon cancer to the lung by whole exome sequencing and gene expression analysis International Journal of Oncology, 2014	1	Metastatic lung tumour and normal lung	ADCY2, ADCY9, APC, GNB5, KRAS, LRP6, HDAC6, ARHGEF17	8 of the 71 variants identified pertain to the 'metastatic colorectal cancer signalling' or 'phospholipase C signalling' pathways
Targeted sequencing of cancer related genes in colorectal cancer using next generation sequencing PLOS One, 2013	60	Tumour and normal mucosa	AATK, ABL1, ABL2, ACVR2A, AKT1, AKT2, ALK, APC, ATM, AXIN2, BCL2, BCL9, BLM, BMPR1A, BRCA1, BRAF, BRCA2, BUB1B, BCL10, BRIP1, CARD11, CBL, CCND1, CDH1, CDK4, CDK6, CDKN1B, CDKN2A, CDX2, CEBPA, CHEK2, CREB1, CREBBP, CSF1, CSF1R, CSMD3, CTNNB1, CYLD, DCC, EGFR, ELK1, ELN, ENG, EP300, EPHA1, EPHB1, EPM2A, ERBB2, ERCC1, ERCC2, ERCC3, ERCC4, ERCC5, EWSR1, EXT1, EXT2, EZH2, FANCA, FANCC, FANCE, FANCF, FGFR1, FGFR3, FGFR2, FLI1, FLT3, FBXW7, FOXN1, FOXL2, GATA1, GATA2, GATA3, GNAS, GPC3, HIP1, HNF1A, HRAS, IDH1, IL21R, IL6ST, ITK, JAK1, JAK2, JAK3, KIT, KRAS, LCK, MAF, MAFB, MAP2K4, MDM2, MEN1, MET, MLH1, MLH3, MLL, MMP14, MPL, MSH2, MSH6, MUTYH, MUSK, MYC, MYCN, MYH11, MYH9, NEK11, NF1, NF2, NFKB2, NOTCH1, NPM1, NRAS, NTRK1, NTRK3, OBSCN, PALB2, PARP1, PDGFRA, PDGFRB, PHOX2B, PIK3CA, PIK3R1, PIM1, PLAG1, PML, PMS1, PMS2, PRDM16, PRKAR1A, PTGS2, PTEN, PTPN11, PTK7, RAD51L1, RAF1, RARA, RASSF1, RB1, RECQL4, REL, RET, ROR1, ROS1, RUNX1, RYR1, SH3GL1, SMAD2, SMAD4, SMARCB1, SMO, SPP1, SPTAN1, SRC, STAT1, STAT3, STK11, STK11IP, SUFU, SYK, TAF15, TAF1L, TEK, TGFBR1, TGFBR2, TGFA, TLX1, TLX3, TOP1, TOP2A, TP53, TRRAP, TSC1, TSC2, TTN, VHL, VEGFA, WAS, WHSC1, WRN, WT1, XPA, XPC	183 genes selected for analysis from COSMIC database (study designed to validate new platform)

Appendix 3

Proteomic comparison of metastatic tumour and normal adjacent liver parenchyma

Accession Number	Name	p Value	Log2 Fold Change (Metastasis/Parenchyma)
P09210	Glutathione S-transferase A2	3.92E-09	-5.472
P23141	Liver carboxylesterase 1	5.38E-09	-5.215
Q68CK6	Acyl-coenzyme A synthetase ACSM2B, mitochondrial	1.10E-10	-5.201
P11509	Cytochrome P450 2A6	9.30E-08	-5.094
Q93088	Betaine--homocysteine S-methyltransferase 1	6.84E-10	-5.021
P09110	3-ketoacyl-CoA thiolase, peroxisomal	1.19E-10	-4.897
P10632	Cytochrome P450 2C8	2.59E-08	-4.883
P00367	Glutamate dehydroge0se 1, mitochondrial	6.38E-11	-4.759
P16662	UDP-glucuronosyltransferase 2B7	4.67E-08	-4.733
P45954	Short/branched chain specific acyl-CoA dehydroge0se, mitochondrial	8.59E-12	-4.690
Q16822	Phosphoenolpyruvate carboxyki0se [GTP], mitochondrial	8.59E-11	-4.683
P30039	Phe0zine biosynthesis-like domain-containing protein	1.44E-07	-4.662
Q9UJM8	Hydroxyacid oxidase 1	1.46E-09	-4.651
P50440	Glycine amidinotransferase, mitochondrial	5.74E-10	-4.582
P28845	Corticosteroid 11-beta-dehydroge0se isozyme 1	2.94E-11	-4.552
P05091	Aldehyde dehydroge0se, mitochondrial	2.66E-11	-4.547
P11712	Cytochrome P450 2C9	7.21E-08	-4.523
P21549	Serine--pyruvate aminotransferase	6.46E-10	-4.497
Q3LXA3	Bifunctio0l ATP-dependent dihydroxyacetone ki0se/FAD-AMP lyase (cyclizing)	4.01E-08	-4.489
Q00796	Sorbitol dehydroge0se	9.97E-09	-4.479
Q08426	Peroxisomal bifunctio0l enzyme	5.57E-10	-4.474
P00352	Reti0l dehydroge0se 1	4.66E-09	-4.468
O95954	Formimidoyltransferase-cyclodeami0se	2.03E-09	-4.437
P00325	Alcohol dehydroge0se 1B	2.72E-07	-4.425
P07099	Epoxide hydrolase 1	1.68E-09	-4.398
P55157	Microsomal triglyceride transfer protein large subunit	1.45E-09	-4.386
P00480	Ornithine carbamoyltransferase, mitochondrial	1.55E-11	-4.383
P30084	Enoyl-CoA hydratase,	1.00E-09	-4.341

	mitochondrial		
P08684	Cytochrome P450 3A4	9.61E-09	-4.333
P24752	Acetyl-CoA acetyltransferase, mitochondrial	2.54E-10	-4.315
P42765	3-ketoacyl-CoA thiolase, mitochondrial	7.98E-11	-4.304
P54868	Hydroxymethylglutaryl-CoA synthase, mitochondrial	8.37E-09	-4.299
P33121	Long-chain-fatty-acid--CoA ligase 1	9.84E-10	-4.269
P07327	Alcohol dehydroge0se 1A	5.89E-07	-4.240
P00966	Argininosucci0te synthase	2.59E-09	-4.227
Q14749	Glycine N-methyltransferase	1.88E-08	-4.213
P05089	Argi0se-1	1.88E-10	-4.202
P16152	Carbonyl reductase [0DPH] 1	8.85E-11	-4.163
Q9P0Z9	Peroxisomal sarcosine oxidase	9.10E-10	-4.145
P10620	Microsomal glutathione S-transferase 1	9.58E-08	-4.141
P30046	D-dopachrome decarboxylase	2.87E-07	-4.117
P80404	4-aminobutyrate aminotransferase, mitochondrial	4.38E-11	-4.083
P04040	Catalase	1.11E-09	-4.064
P52895	Aldo-keto reductase family 1 member C2	7.97E-06	-4.055
P30038	Delta-1-pyrroline-5-carboxylate dehydroge0se, mitochondrial	9.86E-10	-4.039
P05062	Fructose-bisphosphate aldolase B	7.22E-09	-4.038
P00326	Alcohol dehydroge0se 1C	2.73E-07	-4.016
O75521	Enoyl-CoA delta isomerase 2, mitochondrial	7.57E-10	-4.013
P00505	Aspartate aminotransferase, mitochondrial	1.50E-10	-4.004
Q9UBQ7	Glyoxylate reductase/hydroxypyruvate reductase	3.57E-09	-4.004
Q7Z4W1	L-xylulose reductase	2.61E-08	-3.962
Q9UI17	Dimethylglycine dehydroge0se, mitochondrial	1.26E-08	-3.958
P23378	Glycine dehydroge0se [decarboxylating], mitochondrial	4.07E-06	-3.956
P20132	L-serine dehydratase/L-threonine deami0se	3.70E-03	-3.955
P16930	Fumarylacetoacetase	3.06E-09	-3.899
Q14032	Bile acid-CoA:amino acid N-acyltransferase	5.92E-07	-3.896
P21695	Glycerol-3-phosphate dehydroge0se [0D+], cytoplasmic	2.35E-06	-3.893

P16219	Short-chain specific acyl-CoA dehydroge0se, mitochondrial	1.07E-08	-3.877
P35914	Hydroxymethylglutaryl-CoA lyase, mitochondrial	1.89E-09	-3.849
O75452	Retinol dehydroge0se 16	4.42E-08	-3.837
O75891	Cytosolic 10-formyltetrahydrofolate dehydroge0se	3.31E-09	-3.825
P05181	Cytochrome P450 2E1	1.95E-06	-3.820
P30042	ES1 protein homolog, mitochondrial	3.84E-08	-3.818
P00167	Cytochrome b5	5.81E-10	-3.811
P32754	4-hydroxyphenylpyruvate dioxyge0se	2.86E-09	-3.800
P34896	Serine hydroxymethyltransferase, cytosolic	9.55E-09	-3.796
P22307	Non-specific lipid-transfer protein	5.34E-11	-3.769
P11310	Medium-chain specific acyl-CoA dehydroge0se, mitochondrial	2.06E-07	-3.769
P30086	Phosphatidylethanolamine-binding protein 1	8.69E-09	-3.766
P52758	Ribonuclease UK114	1.92E-09	-3.762
P22310	UDP-glucuronosyltransferase 1-4	1.07E-08	-3.762
P51648	Fatty aldehyde dehydroge0se	1.15E-08	-3.756
P49419	Alpha-aminoadipic semialdehyde dehydroge0se	1.78E-10	-3.721
P49189	4-trimethylaminobutyraldehyde dehydroge0se	2.60E-09	-3.702
P27338	Amine oxidase [flavin-containing] B	4.97E-09	-3.685
P30613	Pyruvate ki0se isozymes R/L	1.47E-06	-3.670
P51857	3-oxo-5-beta-steroid 4-dehydroge0se	3.04E-06	-3.654
P54855	UDP-glucuronosyltransferase 2B15	8.05E-07	-3.630
P04424	Argininosucci0te lyase	2.90E-10	-3.624
Q06520	Bile salt sulfotransferase	3.44E-07	-3.615
P40939	Trifunctio0l enzyme subunit alpha, mitochondrial	3.25E-09	-3.612
P34913	Epoxide hydrolase 2	3.16E-08	-3.610
P48735	Isocitrate dehydroge0se [0DP], mitochondrial	1.57E-07	-3.600
P28332	Alcohol dehydroge0se 6	9.97E-07	-3.599
A6NLP5	Tetratricopeptide repeat protein 36	2.67E-08	-3.599
Q02252	Methylmalo0te-semialdehyde dehydroge0se [acylating], mitochondrial	1.62E-08	-3.590

Q16851	UTP--glucose-1-phosphate uridylyltransferase	1.76E-09	-3.589
Q9H8H3	Methyltransferase-like protein 7A	1.19E-08	-3.582
P31513	Dimethylaniline monooxyge0se [N-oxide-forming] 3	1.08E-06	-3.581
Q6YN16	Hydroxysteroid dehydroge0se-like protein 2	6.56E-09	-3.578
Q00266	S-adenosylmethionine synthase isoform type-1	3.32E-07	-3.550
Q14117	Dihydropyrimidi0se	2.73E-09	-3.527
Q9H2M3	Betaine--homocysteine S-methyltransferase 2	2.25E-07	-3.521
Q02928	Cytochrome P450 4A11	9.11E-08	-3.515
P11498	Pyruvate carboxylase, mitochondrial	9.27E-07	-3.513
P11182	Lipoamide acyltransferase component of branched-chain alpha-keto acid dehydroge0se complex, mitochondrial	7.68E-09	-3.512
P25705	ATP synthase subunit alpha, mitochondrial	3.70E-08	-3.508
Q16762	Thiosulfate sulfurtransferase	5.35E-09	-3.500
Q13228	Selenium-binding protein 1	3.18E-10	-3.499
Q16698	2,4-dienoyl-CoA reductase, mitochondrial	2.60E-08	-3.484
Q13011	Delta(3,5)-Delta(2,4)-dienoyl-CoA isomerase, mitochondrial	1.34E-10	-3.483
P36871	Phosphoglucomutase-1	1.80E-08	-3.462
P23786	Carnitine O-palmitoyltransferase 2, mitochondrial	8.17E-08	-3.457
Q6IB77	Glycine N-acyltransferase	2.04E-07	-3.439
P38117	Electron transfer flavoprotein subunit beta	4.54E-09	-3.429
Q9Y2P5	Bile acyl-CoA synthetase	3.49E-08	-3.426
P06737	Glycogen phosphorylase, liver form	2.48E-08	-3.421
P35573	Glycogen debranching enzyme	1.53E-08	-3.418
Q93099	Homogentisate 1,2-dioxyge0se	4.25E-07	-3.413
P26440	Isovaleryl-CoA dehydroge0se, mitochondrial	2.95E-09	-3.412
Q02338	D-beta-hydroxybutyrate dehydroge0se, mitochondrial	1.37E-08	-3.400
Q9H2X3	C-type lectin domain family 4 member M	7.42E-06	-3.400
P46952	3-hydroxyanthranilate 3,4-dioxyge0se	8.79E-08	-3.373
P51649	Succi0te-semialdehyde dehydroge0se, mitochondrial	3.03E-08	-3.371

Q9H2A2	Aldehyde dehydroge0se family 8 member A1	3.59E-07	-3.368
Q96HR9	Receptor expression-enhancing protein 6	3.51E-08	-3.360
Q16836	Hydroxyacyl-coenzyme A dehydroge0se, mitochondrial	1.24E-09	-3.341
P13804	Electron transfer flavoprotein subunit alpha, mitochondrial	1.98E-09	-3.335
Q9UNU6	7-alpha-hydroxycholest-4-en-3-one 12-alpha-hydroxylase	1.27E-07	-3.332
Q9BRX8	Redox-regulatory protein PAMM	7.44E-10	-3.311
O14975	Very long-chain acyl-CoA synthetase	1.38E-07	-3.304
Q7Z5P4	17-beta-hydroxysteroid dehydroge0se 13	8.32E-07	-3.299
P49327	Fatty acid synthase	5.55E-06	-3.286
P22033	Methylmalonyl-CoA mutase, mitochondrial	1.53E-07	-3.279
Q6UX53	Methyltransferase-like protein 7B	7.92E-08	-3.274
A2VDF0	Fucose mutarotase	1.39E-06	-3.257
O95563	Brain protein 44	2.57E-07	-3.254
P36537	UDP-glucuronosyltransferase 2B10	4.92E-06	-3.249
P30041	Peroxiredoxin-6	9.49E-08	-3.246
Q9UBR1	Beta-ureidopropio0se	1.38E-06	-3.237
Q9UJS0	Calcium-binding mitochondrial carrier protein Aralar2	1.86E-07	-3.236
P13929	Beta-enolase	1.04E-03	-3.232
Q9NR77	Peroxisomal membrane protein 2	9.39E-07	-3.229
P09467	Fructose-1,6-bisphosphatase 1	6.65E-06	-3.215
P24298	Alanine aminotransferase 1	3.13E-08	-3.204
P21399	Cytoplasmic aconitate hydratase	1.49E-07	-3.193
Q06278	Aldehyde oxidase	2.66E-07	-3.173
Q96DG6	Carboxymethylenebutenolidase homolog	4.86E-09	-3.161
O75874	Isocitrate dehydroge0se [0DP] cytoplasmic	9.23E-08	-3.159
P00918	Carbonic anhydrase 2	2.26E-07	-3.148
P47989	Xanthine dehydroge0se/oxidase	2.52E-07	-3.139
O14756	17-beta-hydroxysteroid dehydroge0se type 6	1.23E-06	-3.129
P11168	Solute carrier family 2, facilitated glucose transporter member 2	9.98E-07	-3.126
P42330	Aldo-keto reductase family 1	2.49E-04	-3.116

	member C3		
P13716	Delta-aminolevulinic acid dehydratase	3.83E-08	-3.114
P07954	Fumarate hydratase, mitochondrial	1.87E-09	-3.112
Q14914	Prostaglandin reductase 1	7.04E-07	-3.111
P50226	Sulfotransferase 1A2	1.56E-03	-3.104
P11586	C-1-tetrahydrofolate synthase, cytoplasmic	1.85E-07	-3.080
Q96I99	Succinyl-CoA ligase [GDP-forming] subunit beta, mitochondrial	9.26E-10	-3.064
O95154	Aflatoxin B1 aldehyde reductase member 3	5.86E-07	-3.061
P07237	Protein disulfide-isomerase	2.25E-08	-3.053
Q9BWD1	Acetyl-CoA acetyltransferase, cytosolic	1.03E-06	-3.042
P50053	Ketohexoki0se	7.29E-07	-3.031
Q86WU2	Probable D-lactate dehydroge0se, mitochondrial	3.30E-05	-3.020
Q86WA6	Valacyclovir hydrolase	2.42E-06	-3.020
O60701	UDP-glucose 6-dehydroge0se	9.44E-08	-3.008
Q96DC8	Enoyl-CoA hydratase domain-containing protein 3, mitochondrial	1.88E-05	-2.983
O76054	SEC14-like protein 2	4.38E-07	-2.948
Q9BPW8	Protein NipS0p homolog 1	1.57E-07	-2.911
P32929	Cystathionine gamma-lyase	1.46E-05	-2.905
P55084	Trifunctio0l enzyme subunit beta, mitochondrial	7.96E-09	-2.898
Q9BY49	Peroxisomal trans-2-enoyl-CoA reductase	3.21E-07	-2.897
P31937	3-hydroxyisobutyrate dehydroge0se, mitochondrial	1.10E-05	-2.895
O43175	D-3-phosphoglycerate dehydroge0se	1.09E-07	-2.884
O95831	Apoptosis-inducing factor 1, mitochondrial	1.39E-09	-2.882
Q86TX2	Acyl-coenzyme A thioesterase 1	3.06E-08	-2.867
O00264	Membrane-associated progesterone receptor component 1	2.65E-07	-2.864
Q96AB3	Isochorismatase domain-containing protein 2, mitochondrial	3.75E-07	-2.856
P25325	3-mercaptopyruvate sulfurtransferase	1.71E-07	-2.852
Q9H0W9	Ester hydrolase C11orf54	1.90E-06	-2.847
Q15166	Serum paraoxo0se/lacto0se 3	9.24E-06	-2.843
Q9UI32	Glutami0se liver isoform, mitochondrial	6.92E-04	-2.832

Q96EY8	Cob(I)yrinic acid a,c-diamide adenosyltransferase, mitochondrial	2.64E-07	-2.822
Q4G0N4	0D ki0se domain-containing protein 1	3.97E-08	-2.822
Q9Y281	Cofilin-2	3.80E-08	-2.820
Q16134	Electron transfer flavoprotein-ubiquinone oxidoreductase, mitochondrial	6.80E-07	-2.818
P51659	Peroxisomal multifunctio0l enzyme type 2	1.58E-10	-2.813
P35520	Cystathionine beta-synthase	1.72E-07	-2.807
Q92947	Glutaryl-CoA dehydroge0se, mitochondrial	2.16E-07	-2.805
Q9Y2Q3	Glutathione S-transferase kappa 1	1.13E-06	-2.800
P49638	Alpha-tocopherol transfer protein	1.58E-06	-2.782
Q9UL12	Sarcosine dehydroge0se, mitochondrial	4.04E-08	-2.781
P30048	Thioredoxin-dependent peroxide reductase, mitochondrial	2.83E-08	-2.781
Q15067	Peroxisomal acyl-coenzyme A oxidase 1	7.92E-06	-2.780
P37059	Estradiol 17-beta-dehydroge0se 2	1.62E-04	-2.769
Q08AH3	Acyl-coenzyme A synthetase ACSM2A, mitochondrial	6.28E-05	-2.761
Q6NVY1	3-hydroxyisobutyryl-CoA hydrolase, mitochondrial	1.23E-05	-2.760
P06576	ATP synthase subunit beta, mitochondrial	2.78E-06	-2.759
Q13576	Ras GTPase-activating-like protein IQGAP2	1.09E-06	-2.759
P27144	Adenylate ki0se isoenzyme 4, mitochondrial	1.33E-07	-2.752
Q86VD7	Solute carrier family 25 member 42	3.76E-05	-2.748
Q53FZ2	Acyl-coenzyme A synthetase ACSM3, mitochondrial	5.86E-07	-2.716
O43708	Maleylacetoacetate isomerase	3.64E-04	-2.702
P22760	Arylacetamide deacetylase	2.37E-04	-2.700
Q99424	Peroxisomal acyl-coenzyme A oxidase 2	1.17E-06	-2.687
P48449	Lanosterol synthase	8.01E-08	-2.687
Q86YB7	Enoyl-CoA hydratase domain-containing protein 2, mitochondrial	1.96E-06	-2.677
O15229	Kynurenine 3-monooxyge0se	1.52E-05	-2.674
Q99714	3-hydroxyacyl-CoA dehydroge0se type-2	5.39E-10	-2.664
Q9ULD0	2-oxoglutarate dehydroge0se-	9.73E-07	-2.649

	like, mitochondrial		
P54840	Glycogen [starch] synthase, liver	2.50E-06	-2.625
Q9BX68	Histidine triad nucleotide-binding protein 2, mitochondrial	3.45E-07	-2.622
P42126	Enoyl-CoA delta isomerase 1, mitochondrial	2.11E-10	-2.598
Q08257	Quinone oxidoreductase	3.53E-06	-2.590
P34897	Serine hydroxymethyltransferase, mitochondrial	5.12E-10	-2.588
Q9NQR4	Omega-amidase NIT2	1.53E-06	-2.581
O00748	Cocaine esterase	2.83E-06	-2.574
P06133	UDP-glucuronosyltransferase 2B4	7.26E-08	-2.570
P20815	Cytochrome P450 3A5	2.61E-02	-2.565
P05177	Cytochrome P450 1A2	1.09E-04	-2.564
Q13423	0D(P) transhydroge0se, mitochondrial	4.39E-07	-2.561
Q96CN7	Isochorismatase domain-containing protein 1	1.50E-08	-2.558
P28288	ATP-binding cassette sub-family D member 3	1.46E-05	-2.557
P17174	Aspartate aminotransferase, cytoplasmic	1.91E-05	-2.536
Q96LJ7	Dehydroge0se/reductase SDR family member 1	8.40E-06	-2.527
Q9NQ94	APOBEC1 complementation factor	8.17E-06	-2.491
Q969Z3	MOSC domain-containing protein 2, mitochondrial	3.12E-05	-2.468
P14550	Alcohol dehydroge0se [0DP+]	1.42E-06	-2.466
Q709F0	Acyl-CoA dehydroge0se family member 11	2.26E-04	-2.458
P43155	Carnitine O-acetyltransferase	1.14E-05	-2.433
Q9NPJ3	Acyl-coenzyme A thioesterase 13	5.53E-06	-2.428
P17516	Aldo-keto reductase family 1 member C4	1.52E-05	-2.420
P31040	Succi0te dehydroge0se [ubiquinone] flavoprotein subunit, mitochondrial	7.73E-08	-2.395
Q03154	Aminoacylase-1	1.15E-05	-2.393
Q96GK7	Fumarylacetoacetate hydrolase domain-containing protein 2A	1.34E-06	-2.388
O14832	Phytanoyl-CoA dioxyge0se, peroxisomal	4.37E-06	-2.369
P30043	Flavin reductase (0DPH)	1.32E-05	-2.355
Q8NBX0	Saccharopine dehydroge0se-like oxidoreductase	1.46E-06	-2.351

Q9NPD5	Solute carrier organic anion transporter family member 1B3	1.02E-03	-2.336
Q9Y6B6	GTP-binding protein SAR1b	5.38E-07	-2.335
Q96I15	Selenocysteine lyase	5.78E-06	-2.327
P49326	Dimethylaniline monooxyge0se [N-oxide-forming] 5	1.57E-05	-2.322
P54819	Adenylate ki0se 2, mitochondrial	7.53E-06	-2.321
Q8WW59	SPRY domain-containing protein 4	8.13E-07	-2.319
P16083	Ribosyldihydronicoti0mide dehydroge0se [quinone]	8.43E-04	-2.314
Q15493	Regucalcin	1.13E-05	-2.314
Q96KP4	Cytosolic non-specific dipeptidase	8.57E-07	-2.312
O75356	Ectonucleoside triphosphate diphosphohydrolase 5	3.11E-07	-2.310
Q9Y2S2	Lambda-crystallin homolog	3.52E-06	-2.310
P21953	2-oxoisovalerate dehydroge0se subunit beta, mitochondrial	6.02E-05	-2.308
P09417	Dihydropteridine reductase	1.09E-04	-2.307
Q96EK6	Glucosamine 6-phosphate N-acetyltransferase	7.81E-05	-2.300
P11766	Alcohol dehydroge0se class-3	2.22E-06	-2.297
P49748	Very long-chain specific acyl-CoA dehydroge0se, mitochondrial	1.59E-06	-2.296
Q96NU7	Probable imidazolonepropio0se	1.04E-05	-2.294
Q9UBM7	7-dehydrocholesterol reductase	6.33E-06	-2.288
Q9H9B4	Sideroflexin-1	3.37E-05	-2.285
P05166	Propionyl-CoA carboxylase beta chain, mitochondrial	7.36E-07	-2.285
Q969I3	Glycine N-acyltransferase-like protein 1	5.84E-04	-2.275
P48047	ATP synthase subunit O, mitochondrial	4.80E-06	-2.266
P21397	Amine oxidase [flavin-containing] A	1.57E-04	-2.264
P23434	Glycine cleavage system H protein, mitochondrial	1.11E-04	-2.259
Q8N0X4	Citrate lyase subunit beta-like protein, mitochondrial	1.73E-08	-2.257
P16435	0DPH--cytochrome P450 reductase	1.95E-07	-2.245
Q9UP52	Transferrin receptor protein 2	1.63E-04	-2.236
Q9NUI1	Peroxisomal 2,4-dienoyl-CoA reductase	4.41E-06	-2.225
Q6NUM9	All-trans-retinol 13,14-	7.29E-05	-2.223

	reductase		
Q7L5Y1	Mitochondrial enolase superfamily member 1	1.18E-02	-2.221
Q96IU4	Abhydrolase domain-containing protein 14B	1.64E-05	-2.208
O95479	GDH/6PGL endoplasmic bifunctio0l protein	5.60E-04	-2.205
O75964	ATP synthase subunit g, mitochondrial	2.24E-05	-2.201
Q96RQ3	Methylcrotonoyl-CoA carboxylase subunit alpha, mitochondrial	2.07E-05	-2.183
Q9Y2T3	Guanine deami0se	6.65E-07	-2.178
P78417	Glutathione S-transferase omega-1	4.80E-05	-2.177
Q6NUN0	Acyl-coenzyme A synthetase ACSM5, mitochondrial	3.48E-05	-2.177
P04179	Superoxide dismutase [Mn], mitochondrial	9.69E-04	-2.176
P30040	Endoplasmic reticulum resident protein 29	3.30E-08	-2.153
P00441	Superoxide dismutase [Cu-Zn]	3.61E-04	-2.150
P07306	Asialoglycoprotein receptor 1	1.11E-03	-2.137
P78329	Leukotriene-B(4) omega-hydroxylase 1	3.44E-06	-2.128
P51570	Galactoki0se	5.10E-06	-2.123
P21964	Catechol O-methyltransferase	1.93E-04	-2.110
P21912	Succi0te dehydroge0se [ubiquinone] iron-sulfur subunit, mitochondrial	4.42E-07	-2.105
O43772	Mitochondrial carnitine/acylcarnitine carrier protein	2.43E-04	-2.092
Q5R3I4	Tetratricopeptide repeat protein 38	1.13E-05	-2.053
Q9NRV9	Heme-binding protein 1	3.48E-06	-2.029
P40925	Malate dehydroge0se, cytoplasmic	3.88E-06	-2.019
Q16719	Kynureni0se	1.50E-05	-2.019
P36269	Gamma-glutamyltransferase 5	2.46E-04	-2.005
P04208	Ig lambda chain V-I region WAH	1.44E-03	2.013
P24158	Myeloblastin	9.71E-03	2.019
P60903	Protein S100-A10	8.84E-04	2.022
P35555	Fibrillin-1	3.19E-03	2.029
P55011	Solute carrier family 12 member 2	2.51E-03	2.050
Q96PD5	N-acetylmuramoyl-L-alanine amidase	2.83E-03	2.060
P02647	Apolipoprotein A-I	9.89E-04	2.107
P05546	Heparin cofactor 2	3.09E-02	2.109

P07195	L-lactate dehydroge0se B chain	1.01E-03	2.132
P05155	Plasma protease C1 inhibitor	1.77E-03	2.148
Q01105	Protein SET	3.17E-03	2.151
P30740	Leukocyte elastase inhibitor	1.57E-04	2.155
P68032	Actin, alpha cardiac muscle 1	1.06E-02	2.171
P98095	Fibulin-2	2.33E-05	2.204
P00751	Complement factor B	3.50E-04	2.208
P62328	Thymosin beta-4	1.40E-02	2.211
P01766	Ig heavy chain V-III region BRO	5.99E-04	2.213
P37802	Transgelin-2	3.13E-05	2.214
Q14126	Desmoglein-2	7.40E-06	2.233
P00736	Complement C1r subcomponent	7.20E-03	2.247
Q12805	EGF-containing fibulin-like extracellular matrix protein 1	2.55E-04	2.254
P25311	Zinc-alpha-2-glycoprotein	9.84E-04	2.260
P63104	14-3-3 protein zeta/delta	1.35E-05	2.262
P23528	Cofilin-1	1.79E-05	2.267
P43652	Afamin	1.74E-03	2.297
O14791	Apolipoprotein L1	5.69E-03	2.308
P06331	Ig heavy chain V-II region ARH-77	2.62E-03	2.309
P04003	C4b-binding protein alpha chain	2.59E-03	2.357
P04217	Alpha-1B-glycoprotein	3.39E-02	2.364
Q9H299	SH3 domain-binding glutamic acid-rich-like protein 3	1.44E-04	2.376
P01023	Alpha-2-macroglobulin	4.31E-03	2.378
P16070	CD44 antigen	2.35E-04	2.379
Q16363	Laminin subunit alpha-4	3.26E-07	2.395
Q16819	Meprin A subunit alpha	2.64E-02	2.424
P01024	Complement C3	1.76E-03	2.443
Q9UM07	Protein-arginine deimi0se type-4	1.04E-02	2.454
P21333	Filamin-A	4.40E-06	2.457
Q9UGI8	Testin	4.34E-03	2.459
P19827	Inter-alpha-trypsin inhibitor heavy chain H1	1.84E-04	2.469
P01591	Immunoglobulin J chain	9.02E-04	2.470
P16402	Histone H1.3	3.73E-03	2.473
P02786	Transferrin receptor protein 1	1.93E-03	2.499
P01717	Ig lambda chain V-IV region Hil	5.64E-03	2.507
P07585	Decorin	4.01E-04	2.535
P01859	Ig gamma-2 chain C region	2.23E-03	2.553
P35749	Myosin-11	9.25E-05	2.590

P13671	Complement component C6	3.09E-02	2.609
P01008	Antithrombin-III	3.76E-02	2.619
P00734	Prothrombin	4.60E-03	2.623
P50454	Serpin H1	3.39E-06	2.629
P01876	Ig alpha-1 chain C region	3.84E-04	2.672
P04114	Apolipoprotein B-100	1.99E-03	2.688
P16401	Histone H1.5	2.34E-03	2.690
Q9BXN1	Asporin	2.88E-03	2.728
P08670	Vimentin	2.57E-04	2.763
P01011	Alpha-1-antichymotrypsin	4.90E-03	2.766
P0CG05	Ig lambda-2 chain C regions	4.52E-05	2.785
P01033	Metalloprotei0se inhibitor 1	7.08E-04	2.804
P02763	Alpha-1-acid glycoprotein 1	4.18E-03	2.805
P02749	Beta-2-glycoprotein 1	5.44E-04	2.808
P80188	Neutrophil gelati0se-associated lipocalin	5.35E-03	2.827
P07355	Annexin A2	3.16E-05	2.829
P05452	Tetranectin	5.28E-05	2.829
P51888	Prolargin	2.00E-04	2.836
P12429	Annexin A3	2.65E-05	2.841
P01833	Polymeric immunoglobulin receptor	1.50E-02	2.847
Q15113	Procollagen C-endopeptidase enhancer 1	3.66E-03	2.847
O00560	Syntenin-1	1.32E-02	2.848
Q01995	Transgelin	4.97E-04	2.854
P01042	Kininogen-1	2.29E-04	2.860
Q08380	Galectin-3-binding protein	9.63E-06	2.868
P02750	Leucine-rich alpha-2-glycoprotein	1.27E-02	2.869
P02790	Hemopexin	9.56E-04	2.890
P01743	Ig heavy chain V-I region HG3	4.13E-04	2.909
P12532	Creatine ki0se U-type, mitochondrial	2.69E-03	2.928
P07358	Complement component C8 beta chain	7.16E-04	2.933
P04075	Fructose-bisphosphate aldolase A	7.57E-08	2.947
P01764	Ig heavy chain V-III region VH26	1.02E-03	2.962
P17096	High mobility group protein HMG-I/HMG-Y	2.03E-03	3.007
B9A064	Immunoglobulin lambda-like polypeptide 5	1.83E-04	3.007
P80511	Protein S100-A12	9.60E-04	3.013
P04083	Annexin A1	1.85E-05	3.045
P35900	Keratin, type I cytoskeletal 20	2.34E-05	3.045

P54709	Sodium/potassium-transporting ATPase subunit beta-3	1.76E-05	3.057
P35858	Insulin-like growth factor-binding protein complex acid labile subunit	8.85E-03	3.082
P06396	Gelsolin	4.81E-06	3.084
P00747	Plasminogen	3.27E-04	3.100
Q12864	Cadherin-17	6.88E-04	3.109
P02649	Apolipoprotein E	1.21E-03	3.120
P08603	Complement factor H	2.60E-05	3.129
P06454	Prothymosin alpha	2.30E-02	3.130
P17931	Galectin-3	1.88E-05	3.130
P36955	Pigment epithelium-derived factor	1.94E-06	3.146
Q8WVV4	Protein POF1B	2.45E-04	3.166
P16444	Dipeptidase 1	5.43E-05	3.169
Q7Z406	Myosin-14	6.83E-06	3.177
P02452	Collagen alpha-1(I) chain	1.33E-04	3.178
P00450	Ceruloplasmin	3.16E-04	3.191
O15551	Claudin-3	7.97E-03	3.200
P07357	Complement component C8 alpha chain	4.67E-03	3.209
P02743	Serum amyloid P-component	4.14E-04	3.246
P02671	Fibrinogen alpha chain	9.40E-04	3.256
P10643	Complement component C7	6.01E-03	3.263
P26447	Protein S100-A4	6.37E-05	3.265
O00299	Chloride intracellular channel protein 1	9.57E-06	3.304
P07996	Thrombospondin-1	2.81E-06	3.327
Q92598	Heat shock protein 105 kDa	2.91E-06	3.337
P19823	Inter-alpha-trypsin inhibitor heavy chain H2	6.42E-05	3.346
P02788	Lactotransferrin	1.15E-03	3.377
P02787	Serotransferrin	8.27E-05	3.408
P09211	Glutathione S-transferase P	4.77E-08	3.439
P06314	Ig kappa chain V-IV region B17	5.25E-05	3.485
P21810	Biglycan	5.67E-06	3.547
P02774	Vitamin D-binding protein	1.07E-05	3.566
P55058	Phospholipid transfer protein	5.77E-05	3.571
P01857	Ig gamma-1 chain C region	2.10E-05	3.574
P01871	Ig mu chain C region	1.55E-04	3.600
P40121	Macrophage-capping protein	3.63E-08	3.651
P08123	Collagen alpha-2(I) chain	3.43E-05	3.656
P02766	Transthyretin	2.21E-03	3.669
P02765	Alpha-2-HS-glycoprotein	2.16E-05	3.674

P01861	Ig gamma-4 chain C region	1.69E-02	3.679
P13688	Carcinoembryonic antigen-related cell adhesion molecule 1	6.13E-03	3.681
P02679	Fibrinogen gamma chain	1.02E-03	3.710
Q8NFJ5	Retinoic acid-induced protein 3	5.13E-04	3.712
Q14764	Major vault protein	3.73E-09	3.752
P06727	Apolipoprotein A-IV	2.88E-05	3.799
P02652	Apolipoprotein A-II	5.84E-05	3.813
P31949	Protein S100-A11	3.50E-08	3.869
Q15582	Transforming growth factor-beta-induced protein ig-h3	7.34E-06	3.893
P24821	Te0scin	1.54E-07	3.927
P14618	Pyruvate ki0se isozymes M1/M2	5.51E-09	3.927
Q9H444	Charged multivesicular body protein 4b	4.25E-06	3.937
P31947	14-3-3 protein sigma	9.06E-04	3.946
P07360	Complement component C8 gamma chain	1.04E-03	3.970
P06702	Protein S100-A9	8.84E-05	3.971
P06703	Protein S100-A6	6.13E-06	3.993
P11166	Solute carrier family 2, facilitated glucose transporter member 1	5.16E-03	3.995
P05107	Integrin beta-2	2.63E-03	4.036
P02751	Fibronectin	1.68E-08	4.059
P59665	Neutrophil defensin 1	1.22E-03	4.069
P08727	Keratin, type I cytoskeletal 19	2.77E-06	4.077
P51884	Lumican	7.04E-06	4.097
P25815	Protein S100-P	1.36E-04	4.127
P02675	Fibrinogen beta chain	1.20E-04	4.128
P05109	Protein S100-A8	4.42E-04	4.202
P01009	Alpha-1-antitrypsin	6.42E-04	4.293
P02748	Complement component C9	1.66E-04	4.363
P11215	Integrin alpha-M	6.70E-04	4.400
P05164	Myeloperoxidase	5.23E-04	4.425
Q8IUX7	Adipocyte enhancer-binding protein 1	6.98E-08	4.429
P35442	Thrombospondin-2	5.61E-08	4.620
O95994	Anterior gradient protein 2 homolog	9.84E-06	4.621
Q6UX06	Olfactomedin-4	4.59E-05	4.640
Q9H3R2	Mucin-13	5.42E-07	4.643
P01031	Complement C5	8.03E-05	4.708
P16422	Epithelial cell adhesion molecule	3.64E-06	4.751

P04004	Vitronectin	3.43E-05	4.790
P10909	Clusterin	8.79E-05	4.928
P19075	Tetraspanin-8	1.49E-03	4.960
P06731	Carcinoembryonic antigen-related cell adhesion molecule 5	5.12E-07	5.132
Q99715	Collagen alpha-1(XII) chain	9.58E-09	5.181
Q15063	Periostin	2.53E-08	5.322
P21926	CD9 antigen	7.72E-06	5.684

Appendix 4

Proteomic comparison of responders and non-responders in the primary tumour

Accession Number	Name	P Value	Log2 Fold Change (Responder/Non-Responder)
Q04695	Keratin, type I cytoskeletal 17	3.71E-02	-165.421
O95831	Apoptosis-inducing factor 1, mitochondrial	1.37E-04	-13.086
O00217	NADH dehydrogenase [ubiquinone] iron-sulfur protein 8, mitochondrial	2.13E-03	-12.553
P13804	Electron transfer flavoprotein subunit alpha, mitochondrial	1.72E-03	-12.381
Q07812	Apoptosis regulator BAX	2.07E-03	-11.959
P08729	Keratin, type II cytoskeletal 7	1.25E-02	-11.876
Q08426	Peroxisomal bifunctional enzyme	2.33E-04	-9.918
P15559	NAD(P)H dehydrogenase [quinone] 1	2.64E-04	-9.918
O75494	Serine/arginine-rich splicing factor 10	1.50E-05	-9.448
P30101	Protein disulfide-isomerase A3	2.10E-03	-9.063
P05091	Aldehyde dehydrogenase, mitochondrial	1.18E-02	-9.063
P50225	Sulfotransferase 1A1	1.29E-02	-7.781
P05783	Keratin, type I cytoskeletal 18	2.35E-02	-7.727
P36952	Serpin B5	1.58E-02	-7.111
Q9HCY8	Protein S100-A14	1.70E-03	-6.916
Q12788	Transducin beta-like protein 3	3.30E-03	-6.727
P58107	Epiplakin	4.30E-05	-6.277
O43704	Sulfotransferase family cytosolic 1B member 1	4.09E-02	-6.233
P08727	Keratin, type I cytoskeletal 19	1.41E-02	-5.856
P36776	Lon protease homolog, mitochondrial	1.72E-03	-5.657
Q9NUV9	GTPase IMAP family member 4	3.06E-03	-5.579
Q00266	S-adenosylmethionine synthase isoform type-1	2.19E-02	-5.426
Q9Y6N5	Sulfide:quinone oxidoreductase, mitochondrial	4.74E-04	-5.278
P22695	Cytochrome b-c1 complex subunit 2, mitochondrial	4.27E-03	-5.098
P49411	Elongation factor Tu, mitochondrial	1.18E-02	-5.098
Q15084	Protein disulfide-isomerase A6	1.62E-02	-5.063
O00515	Ladinin-1	2.93E-02	-5.028
Q9BW92	Threonyl-tRNA synthetase, mitochondrial	4.75E-03	-4.724
Q15477	Helicase SKI2W	2.09E-02	-4.691

P63151	Serine/threonine-protein phosphatase 2A 55 kDa regulatory subunit B alpha isoform	9.31E-03	-4.659
P09327	Villin-1	2.32E-02	-4.659
P49748	Very long-chain specific acyl-CoA dehydrogenase, mitochondrial	1.25E-02	-4.595
P35900	Keratin, type I cytoskeletal 20	2.16E-02	-4.469
P20339	Ras-related protein Rab-5A	3.00E-02	-4.469
P42765	3-ketoacyl-CoA thiolase, mitochondrial	1.81E-03	-4.438
P41240	Tyrosine-protein kinase CSK	2.84E-04	-4.228
Q56VL3	OCIA domain-containing protein 2	1.39E-02	-4.170
P30039	Phenazine biosynthesis-like domain-containing protein	7.25E-04	-4.141
P05026	Sodium/potassium-transporting ATPase subunit beta-1	4.09E-04	-4.056
Q9NX46	Poly(ADP-ribose) glycohydrolase ARH3	5.11E-04	-4.028
P24666	Low molecular weight phosphotyrosine protein phosphatase	2.93E-02	-4.000
P12532	Creatine kinase U-type, mitochondrial	8.75E-03	-3.945
O15438	Canalicular multispecific organic anion transporter 2	4.04E-05	-3.918
Q16836	Hydroxyacyl-coenzyme A dehydrogenase, mitochondrial	1.96E-03	-3.681
P09110	3-ketoacyl-CoA thiolase, peroxisomal	2.84E-03	-3.605
P13667	Protein disulfide-isomerase A4	2.07E-02	-3.555
Q99959	Plakophilin-2	2.05E-02	-3.506
Q99623	Prohibitin-2	1.07E-03	-3.482
P62424	60S ribosomal protein L7a	1.52E-02	-3.482
Q6UX53	Methyltransferase-like protein 7B	2.86E-02	-3.434
P26373	60S ribosomal protein L13	1.46E-03	-3.411
Q9BRX8	Redox-regulatory protein PAMM	2.12E-02	-3.411
P20810	Calpastatin	2.48E-02	-3.364
P15924	Desmoplakin	8.44E-04	-3.340
Q6YN16	Hydroxysteroid dehydrogenase-like protein 2	4.58E-03	-3.294
Q15067	Peroxisomal acyl-coenzyme A oxidase 1	2.15E-02	-3.294

Q27J81	Inverted formin-2	8.85E-03	-3.249
Q13523	Serine/threonine-protein kinase PRP4 homolog	2.10E-04	-3.204
P16219	Short-chain specific acyl-CoA dehydrogenase, mitochondrial	1.41E-02	-3.182
Q8NE62	Choline dehydrogenase, mitochondrial	3.82E-04	-3.010
O60218	Aldo-keto reductase family 1 member B10	1.08E-03	-2.928
P14324	Farnesyl pyrophosphate synthase	3.17E-02	-2.908
Q9NYK5	39S ribosomal protein L39, mitochondrial	1.48E-02	-2.888
Q9UM54	Myosin-VI	2.04E-02	-2.888
P07332	Tyrosine-protein kinase Fes/Fps	1.07E-03	-2.868
O95487	Protein transport protein Sec24B	8.33E-04	-2.848
Q7Z406	Myosin-14	1.95E-02	-2.848
P98170	Baculoviral IAP repeat-containing protein 4	1.44E-02	-2.828
P56134	ATP synthase subunit f, mitochondrial	1.79E-02	-2.789
P21912	Succinate dehydrogenase [ubiquinone] iron-sulfur subunit, mitochondrial	1.84E-02	-2.789
Q9H4G0	Band 4.1-like protein 1	7.41E-03	-2.770
Q9UHG3	Prenylcysteine oxidase 1	3.59E-02	-2.770
Q9NX40	OCIA domain-containing protein 1	2.18E-03	-2.676
Q99523	Sortilin	1.34E-02	-2.676
Q9Y394	Dehydrogenase/reductase SDR family member 7	1.65E-04	-2.639
O14936	Peripheral plasma membrane protein CASK	7.48E-04	-2.621
Q9BRP8	Partner of Y14 and mago	3.54E-02	-2.621
O95571	Protein ETHE1, mitochondrial	3.68E-04	-2.567
P07355	Annexin A2	4.91E-02	-2.567
Q9UBF2	Coatomer subunit gamma-2	2.16E-02	-2.532
O75795	UDP-glucuronosyltransferase 2B17	1.86E-04	-2.497
Q9Y446	Plakophilin-3	8.78E-03	-2.497
Q15149	Plectin	1.33E-02	-2.497
Q6NUK1	Calcium-binding mitochondrial carrier protein SCaMC-1	1.94E-02	-2.445
P06753	Tropomyosin alpha-3 chain	3.27E-02	-2.412
P07954	Fumarate hydratase,	1.04E-02	-2.395

	mitochondrial		
O14896	Interferon regulatory factor 6	1.79E-02	-2.395
Q9NVS9	Pyridoxine-5'-phosphate oxidase	2.00E-02	-2.395
Q00610	Clathrin heavy chain 1	2.75E-02	-2.378
P30153	Serine/threonine-protein phosphatase 2A 65 kDa regulatory subunit A alpha isoform	3.68E-03	-2.362
Q14764	Major vault protein	7.77E-03	-2.362
Q8N1S5	Zinc transporter ZIP11	2.24E-02	-2.282
P45880	Voltage-dependent anion-selective channel protein 2	4.92E-02	-2.282
Q12962	Transcription initiation factor TFIID subunit 10	5.44E-03	-2.250
Q16718	NADH dehydrogenase [ubiquinone] 1 alpha subcomplex subunit 5	2.06E-03	-2.219
O43491	Band 4.1-like protein 2	1.81E-02	-2.204
P05141	ADP/ATP translocase 2	2.20E-02	-2.204
Q8WUM4	Programmed cell death 6-interacting protein	4.71E-03	-2.173
P24539	ATP synthase subunit b, mitochondrial	8.16E-03	-2.158
P38117	Electron transfer flavoprotein subunit beta	1.29E-02	-2.158
Q9BTZ2	Dehydrogenase/reductase SDR family member 4	1.77E-02	-2.144
A5YKK6	CCR4-NOT transcription complex subunit 1	6.41E-03	-2.114
Q02318	Sterol 26-hydroxylase, mitochondrial	6.70E-03	-2.114
P35232	Prohibitin	3.53E-03	-2.099
P30040	Endoplasmic reticulum resident protein 29	2.40E-02	-2.099
Q9Y2S2	Lambda-crystallin homolog	3.25E-03	-2.085
Q6NUM9	All-trans-retinol 13,14-reductase	4.99E-02	-2.085
P45974	Ubiquitin carboxyl-terminal hydrolase 5	6.28E-03	-2.056
O95168	NADH dehydrogenase [ubiquinone] 1 beta subcomplex subunit 4	4.86E-02	-2.056
P51659	Peroxisomal multifunctional enzyme type 2	2.65E-02	-2.042
Q9UNZ2	NSFL1 cofactor p47	2.50E-02	-2.028
Q9NPJ3	Acyl-coenzyme A thioesterase 13	1.40E-03	2.014

Q9BVP2	Guanine nucleotide-binding protein-like 3	1.15E-03	2.042
P63208	S-phase kinase-associated protein 1	4.18E-02	2.071
Q13451	Peptidyl-prolyl cis-trans isomerase FKBP5	2.86E-02	2.085
Q6NYC8	Phostensin	2.41E-02	2.114
Q4VC31	Coiled-coil domain-containing protein 58	7.64E-03	2.129
Q9ULC4	Malignant T cell-amplified sequence 1	3.02E-02	2.173
P17931	Galectin-3	5.40E-03	2.219
P49591	Seryl-tRNA synthetase, cytoplasmic	1.51E-02	2.362
P42345	Serine/threonine-protein kinase mTOR	3.09E-03	2.395
Q96IJ6	Mannose-1-phosphate guanyltransferase alpha	4.98E-03	2.428
Q13315	Serine-protein kinase ATM	1.55E-02	2.462
Q15181	Inorganic pyrophosphatase	4.43E-02	2.479
Q08945	FACT complex subunit SSRP1	4.70E-02	2.532
P61970	Nuclear transport factor 2	6.29E-03	2.657
P04003	C4b-binding protein alpha chain	4.76E-02	2.676
O00505	Importin subunit alpha-3	2.00E-04	2.751
O43708	Maleylacetoacetate isomerase	2.73E-02	2.751
Q96CW1	AP-2 complex subunit mu	4.68E-03	2.828
P07686	Beta-hexosaminidase subunit beta	2.26E-02	2.828
P29622	Kallistatin	2.85E-02	2.888
Q5SSJ5	Heterochromatin protein 1-binding protein 3	4.86E-02	2.928
P04083	Annexin A1	2.96E-02	2.969
P48643	T-complex protein 1 subunit epsilon	1.20E-02	3.010
P27169	Serum paraoxonase/arylesterase 1	6.80E-03	3.031
P01903	HLA class II histocompatibility antigen, DR alpha chain	1.33E-02	3.117
P28845	Corticosteroid 11-beta-dehydrogenase isozyme 1	8.77E-04	3.182
Q06323	Proteasome activator complex subunit 1	3.88E-04	3.272
P04899	Guanine nucleotide-binding protein G(i) subunit alpha-2	1.92E-03	3.411

P62917	60S ribosomal protein L8	8.21E-04	3.434
P56199	Integrin alpha-1	1.04E-03	3.458
Q14019	Coactosin-like protein	2.49E-02	3.458
P05388	60S acidic ribosomal protein P0	4.43E-02	3.555
P62701	40S ribosomal protein S4, X isoform	1.94E-02	3.655
P11387	DNA topoisomerase 1	4.28E-02	3.811
P04216	Thy-1 membrane glycoprotein	1.52E-02	3.837
P31513	Dimethylaniline monooxygenase [N-oxide-forming] 3	2.00E-02	3.864
Q12805	EGF-containing fibulin-like extracellular matrix protein 1	1.30E-03	3.891
Q9C005	Protein dpy-30 homolog	2.71E-02	4.028
O75874	Isocitrate dehydrogenase [NADP] cytoplasmic	3.10E-03	4.347
P21953	2-oxoisovalerate dehydrogenase subunit beta, mitochondrial	1.32E-03	4.563
P21980	Protein-glutamine gamma-glutamyltransferase 2	2.99E-03	4.595
Q9Y6D6	Brefeldin A-inhibited guanine nucleotide-exchange protein 1	7.37E-03	4.595
O94826	Mitochondrial import receptor subunit TOM70	3.15E-03	4.857
P40227	T-complex protein 1 subunit zeta	1.93E-02	5.063
P50135	Histamine N-methyltransferase	1.82E-04	5.618
P07339	Cathepsin D	6.55E-04	5.657
P16662	UDP-glucuronosyltransferase 2B7	2.29E-02	5.657
Q8TEX9	Importin-4	5.29E-03	5.816
Q99536	Synaptic vesicle membrane protein VAT-1 homolog	1.85E-02	5.856
P09417	Dihydropteridine reductase	1.40E-02	6.021
Q9H1E5	Thioredoxin-related transmembrane protein 4	3.43E-02	6.190
P12111	Collagen alpha-3(VI) chain	4.77E-02	6.409
P24752	Acetyl-CoA acetyltransferase, mitochondrial	9.73E-03	8.282
Q05707	Collagen alpha-1(XIV) chain	2.32E-02	8.694
P06733	Alpha-enolase	7.48E-03	8.754
P11586	C-1-tetrahydrofolate synthase, cytoplasmic	1.73E-05	15.242
P13760	HLA class II histocompatibility antigen, DRB1-4 beta chain	5.91E-03	88.035

Q16822	Phosphoenolpyruvate carboxykinase [GTP], mitochondrial	3.11E-05	194.012

Appendix 5

Supporting Publications, Presentations, Prizes and Grants

Manuscripts Accepted

The use of a tissue stabilization gel (Allprotect^{TM}) to facilitate clinical sampling in translational surgical trials. Sutton, Jones, Morrison, Goldring, Palmer, Park, Malik, Vimalachandran, Kitteringham. Accepted by the British Journal of Surgery.

Predicting response to neoadjuvant treatment in advanced colorectal cancer – A review of relevant mechanisms and potential biomarkers. P A Sutton, R P Jones, J P Evans, C Goldring, D Palmer, N Kitteringham, D Vimalachandran, H Z Malik. Accepted by Colorectal Cancer.

Hepatic activation of irinotecan predicts tumour response in patients with colorectal liver metastases treated with DEBIRI: exploratory findings from a phase II study. Jones, Sutton, Greensmith, Santoyo-Castelazo, Carr, Jenkins, Rowe, Hamlett, Park, Terlizzo, O'Grady, Ghaneh, Fenwick, Malik, Poston, Kitteringham. Cancer Chemotherapy and Pharmacology. 2013. 72(2):359-68.

Manuscripts In Preparation

Exome sequencing of synchronously resected primary and metastatic colorectal tumours. Sutton, Puthen, Jones, Evans, Goldring, Palmer, Park, Malik, Vimalachandran, Kitteringham.

Proteomic profiling of primary and metastatic colorectal cancers identifies NQO1 as a potential response biomarker and therapeutic target. Sutton, Jones, Evans, Andrews, Terlizzo, Hamlett, Jenkins, Puthen, Goldring, Palmer, Park, Malik, Vimalachandran, Kitteringham.

Proteomic analysis to identify biomarkers in the primary tumour which predict response to neoadjuvant chemotherapy in liver metastases

Paul Sutton, Jonathan Evans, Robert Jones, Hassan Malik, Dale Vimalachandran, Daniel Palmer, Chris Goldring, Neil Kitteringham

Abstract to be published in The Lancet

Academy of Medical Science – 02/15 [Poster]

NQO1 expression in the primary colorectal tumour is a predictive biomarker and therapeutic target for the neoadjuvant treatment of metastatic colorectal cancer

Paul Sutton, Rob Jones, Jonathan Evans, Chris Goldring, Daniel Palmer, Neil Kitteringham, Dale Vimalachandran, Hassan Malik

Published in the meeting proceedings

Liverpool and North West Society of Surgeons Annual Meeting – 12/14 [Oral Plenary]

High NQO1 expression in primary colorectal cancer predicts chemoresistance in colorectal liver metastases

Sutton, Jones, Jenkins, Vimalachandran, Goldring, Kitteringham, Malik, Palmer

European Journal of Surgical Oncology, 2014. 40(11)S50-51.

BASO-ESSO Annual Meeting – 11/14 [Oral]

High expression of acid ceramidase confers radioresistance in rectal cancer

Sutton, Bowden, Jithesh, Hamid, Abbott, Palmer, Goldring, Kitteringham, Vimalachandran

European Journal of Surgical Oncology, 2014. 40(11)S99-100.

BASO-ESSO Annual Meeting – 11/14 [Poster]

Exome sequencing of synchronously resected primary colorectal cancer and colorectal liver metastases to identify novel response biomarkers and drug targets

Sutton, Jithesh, Jones, Vimalachandran, Goldring, Kitteringham, Malik, Palmer

European Journal of Surgical Oncology, 2014. 40(11)S21-22.

BASO-ESSO Annual Meeting – 11/14 [Oral]

Proteomic profiling of the diagnostic tumour biopsy to predict response to neoadjuvant chemoradiotherapy in rectal cancer

Sutton, Jones, Goldring, Malik, Vimalachandran, Kitteringham, Palmer

Journal of Clinical Oncology, 2014. 32(suppl; abstr e14579)

American Society of Clinical Oncology – 06/14 [Poster]

Proteomic analysis of primary colorectal cancer to generate response biomarkers for liver metastases

Sutton, Jones, Goldring, Malik, Vimalachandran, Kitteringham, Palmer

Journal of Clinical Oncology, 2014. 32(suppl; abstr e14535)

American Society of Clinical Oncology – 06/14 [Poster]

Phenotypic analysis of primary colorectal cancer to inform the management of metastatic disease

Sutton, Jones, Jithesh, Andrews, Park, Malik, Kitteringham, Vimalachandran

Colorectal Disease, 2014. 16(s2) p1-226

Tripartite Colorectal Meeting – 06/14 [Oral]

Temporal phenotypic profiling of rectal cancer to predict response to neoadjuvant chemoradiotherapy

Sutton, Jithesh, Bowden, Abbott, Hamid, Jenkins, Palmer, Goldring, Vimalachandran

Colorectal Disease, 2014. 16(s2) p1-226

Tripartite Colorectal Meeting – 06/14 [Oral]

Evaluation of a tissue stabilization gel to facilitate clinical sampling for translational research in colorectal cancer

Sutton, Jones, Morrison, Goldring, Kitteringham, Palmer, Vimalachandran

Colorectal Disease, 2014. 16(s2) p1-226

Tripartite Colorectal Meeting – 06/14 [Lunchtime Poster]

Evaluation of a tissue stabilisation gel to facilitate clinical sampling in translational surgical trials

Sutton, Jones, Malik, Vimalachandran, Kitteringham

Published in the meeting proceedings

ASGBI – 04/14 [Poster]

Phenotypic analysis of primary colorectal cancer to inform the management of metastatic disease

Sutton, Jones, Malik, Jenkins, Vimalachandran, Goldring, Palmer, Kitteringham

The Lancet, 2014. 383, pS98

Academy of Medical Science – 02/14 [Poster]

Phenotypic analysis of primary colorectal cancer to inform the management of metastatic disease

Sutton, Jones, Malik, Jenkins, Vimalachandran, Goldring, Palmer, Kitteringham

British Journal of Surgery, 2014. 101(s4) p11

Society of Academic and Research Surgery – 01/14 [Oral]

Validation of Allprotect^{TM} – a commercially available tissue stabilisation gel

Sutton, Goldring, Palmer, Kitteringham, Vimalachandran

Colorectal Disease, 2013. 15(s1) p1-65

Association of Coloproctology of Great Britain and Ireland – 07/13 [Poster]

A strategy for identifying novel therapeutic targets in the management of colorectal liver metastases

Sutton, Goldring, Palmer, Kitteringham, Vimalachandran

Colorectal Disease, 2013. 15(s1) p1-65

Association of Coloproctology of Great Britain and Ireland – 07/13 [Poster]

A global proteomic assessment to compare biological characteristics of primary and metastatic colorectal cancer

Sutton, Goldring, Palmer, Kitteringham, Vimalachandran

Colorectal Disease, 2013. 15(s1) p1-65

Association of Coloproctology of Great Britain and Ireland – 07/13 [Poster]

Prizes

Roger Croton Prize for Best Oral Presentation

Mersey Deanery Regional Meeting – 09/14

ASiT Annual Travelling Fellowship

Association of Surgeons in Training – 08/14

Royal College of Surgeons of England Travelling Fellowship

Royal College of Surgeons of England – 01/14

European Society of Surgical Oncology Travelling Fellowship

European Society of Surgical Oncology – 01/14

Ronald Raven Prize

British Association of Surgical Oncology – 11/13

Cancer Research UK (Liverpool Centre) Travel Award

Cancer Research UK – 11/13

Niru Goenka Research Prize

Countess of Chester Hospital/University of Chester – 06/13

The travelling fellowships were awarded for a visit to the colorectal/surgical oncology units at the Cleveland Clinic, Cleveland OH and Mayo Clinic, Rochester MN in May-June 2014.

Grants

Arising from and for the continuation of work presented in this thesis.

Wellcome Trust (2013)	**£2000**
Clatterbridge Centre for Oncology (2013)	**£20000**
Cancer Research UK (2014)	**£3000**
NHS Health Education North West Madel Fellowship (2014)	**£80000**
Bowel Disease Research Federation (2014)	**£12400**

The Madel Fellowship was awarded to a Mersey surgical trainee for the continuation of the work presented in Chapter 5 - A global proteomic assessment of serial rectal tumour biopsies.